Basement and climate controls on proximal depositional systems in continental settings

Dario Ventra

UTRECHT STUDIES IN EARTH SCIENCE

Mededelingen van de

Faculteit Geowetenschappen

Universiteit Utrecht

N. 4

Members of the dissertation committee:

Prof. dr. Steven M. de Jong,
Faculty of Geosciences,
Utrecht University, the Netherlands

Prof. dr. Adrian J. Hartley,
Department of Geology and Petroleum Geology,
University of Aberdeen, UK

Prof. dr. Salomon B. Kroonenberg,
Department of Geotechnology,
Technische Universiteit Delft, the Netherlands

Dr. Gary J. Nichols,
Department of Earth Sciences,
Royal Holloway University of London, UK

Dr. Henk van Steijn,
Faculty of Geosciences,
Utrecht University, the Netherlands

Prof. dr. Jutta Winsemann,
Institut für Geologie,
Leibniz Universität Hannover, Germany

This study was supported by the Netherlands Council for Earth and Life Sciences (ALW) with financial aid from the Netherlands Organization for Scientific Research (NWO).

Research was carried out at the Sedimentology Group,
Department of Earth Sciences, Utrecht University,
Budapestlaan 4, 3584CD, Utrecht (the Netherlands).

ISBN/EAN : 978-90-6266-285-2

Basement and climate controls on proximal depositional systems in continental settings

De controle van basement en klimaat over proximale afzettingsmilieus in continentale systemen

(met een samenvatting in het Nederlands)

Controlli climatici e di substrato sui sistemi deposizionali prossimali in ambienti continentali

(con un riassunto in italiano)

Proefschrift

ter verkrijging van de graad van doctor aan de Universiteit Utrecht
op gezag van de rector magnificus, prof.dr. G.J. van der Zwaan,
ingevolge het besluit van het college voor promoties
in het openbaar te verdedigen
op vrijdag 2 december 2011 des ochtends te 10.30 uur

door

Dario Ventra

geboren op 6 augustus 1969
te San Paolo Belsito (Italië)

Promotor: Prof. dr. P.L. de Boer

Co-promotor: Dr. F.J. Hilgen

CONTENTS

"*In walking across one of these large fans along the path, which is usually made in a curve somewhere between the arc and the chord, one is apt to be continually expecting in a few steps to arrive at the summit of the slope; but again and again is one disappointed, new portions of the cone intervening in succession, until the central radius is reached*."

Frederic Drew, 1873
Quarterly Journal of the Geological Society

Chapter 1

Introduction and conceptual framework

1.1 THE OVERLOOKED PROXIMAL DOMAIN: WHERE IT ALL STARTS…

Countless introductory textbooks on geology and sedimentology feature classic panoramas of the Earth's surface, most likely inspired by the suggestive 'fresco' that opens Rigby & Hamblin's (1972) *Recognition of Ancient Sedimentary Environments* (Fig. 1). Even in times of Google Earth, such an extraordinary variety of environments all visible from a single perspective is no match for the real world. The most enthusiastic Earth scientist would be hard pressed to find any corners of the planet in which all possible environmental settings are so neatly aligned next to each other, along a continuum stretching from the steepest highlands to the deep oceanic realm. In spite of their somewhat excessive idealization of geomorphic reality, these images have earned their presence in numerous publications because of their undisputed didactic value. The student gains an instant bird's-eye view over the diversity of environments characterizing the Earth's surface, and immediately acquires a feeling for the large-scale, 'megageomorphic' controls on their distribution. In particular, the student quickly learns that the origin and recognition of most such environments are tied to understanding how loose materials are transported and distributed from one kind of setting to another. In other words, to sedimentary processes.

Taking one step forward, from observation to interpretation, our classic panoramic view can be considered a graphic rendition of the unified chain of dispersal of clastic sediments. The receiving end of the system, in the foreground, is represented by coastal and marine environments, artfully veiled by a curtain of blueish seawater and invariably comprising a thick submarine fan fed by subaqueous sediment gravity flows. Research in the 80's (Normark, 1985; Bouma *et al.*, 1985; Mutti & Normark, 1987) was quickly faced with the realization that turbidity currents were not as well-behaved as most process and facies models would let us believe, and that in most instances 'submarine fans' hardly turned out to be fan-shaped at all. Yet the name stuck and is still widely in use both in industry and academia. We now know that manifold combinations of sediment transport processes and sea-bottom topographies can produce endless geometries and architectures for accumulations of sand and mud, but in marine sedimentology a deep-sea fan remains a fan even when it's actually not a fan!

At the opposite end of the clastic chain, in the background of our panoramic images, farther from a viewer's attention, are those geomorphic systems that first receive sediments directly from relief sources. Alluvial fans, high-gradient streams, and the occasional glacial terraces and moraines are usually drawn in the distance, shrunk by perspective necessity. That such landforms even exist is an immediate hint to the fact that sediment does not travel quickly and continuously towards final depositional basins, but is frequently stored along the way, even right after its first mobilization from bedrock and soils. To Rigby and Hamblin's credit, the original figure in that special publication actually shows a number of very large fans. However,

Figure 1 *- Rigby & Hamblin's (1972) pictorial panorama of continental, coastal and marine depositional environments. Alluvial fans are visible on the right, adjacent to highland areas (from SEPM Special Publication 16, Recognition of Ancient Sedimentary Environments).*

their number and suspiciously oversized appearance probably resulted from the need to honour what became the very first review article on alluvial fans (Bull, 1972), hosted in their edited publication. In successive versions of that figure, through the years, those fans have shrunk in size and significantly gone down in numbers.

Be that as it may, by far most research on clastic sedimentology nowadays is carried out on processes and environments somewhere in the foreground of the panorama. Low-gradient sedimentary environments span the widest extent at the Earth's surface, and lay down deposits with the highest preservation potential in the long term. Those are the environments that geologists most frequently encounter in the rock record, and that industry most commonly explores in the subsurface. Proximal environments, on the other hand, have long remained in the background of research, just as in our classic figure. The term 'proximal' is used here to denote depositional systems in direct proximity to high-relief terrigenous sources, commonly along subaerial basin margins, and most frequently (but not only) in tectonically active regions. The most representative of such environments, and possibly the most misunderstood, are alluvial fans, which many sedimentologists and geomorphologists often consider an odd end-member along the spectrum of fluvial typologies. Proximal fluvial systems in high-gradient settings are also commonly overlooked in the literature. The Cenozoic record of many continental basins comprises great volumes of coarse, poorly organized deposits from scarcely integrated drainage networks with ephemeral discharge. Small river systems active mainly through infrequent or catastrophic hydrologic events are abundant throughout present landscapes but definitely not in the literature, where they are usually misidentified as alluvial fans. Mountain slopes, the basic landscape elements by which we define the very concept of relief (Davis, 1898; Twidale, 1959), are the second most widespread depositional systems in continental settings after alluvial floodplains. Yet, they have been almost completely ignored so far because of their apparently chaotic deposits and scarce accessibility, leaving a major gap in our knowledge of sedimentary environments right there where it all starts, where sediment routing begins.

1.2 ALLUVIAL FANS: WHAT'S IN A NAME…

Alluvial fans are the most important depositional landforms along tectonically active basin margins, and more generally at topographic transitions between highlands and low-lying areas. Most commonly, one may encounter a passing definition of alluvial fans that roughly sounds like: "…cone-shaped accumulation of sediments at the base of a mountain front, where a stream emerges from the uplands." The disarming truth and simplicity of these words have been echoed repeatedly over a few tens of years of publications but are quickly muted in the face of nature's complexity, and especially by the loud arguments of a few scientists in serious disagreement. In stark contrast with submarine turbidite systems, for alluvial researchers a fan is not necessarily a fan even when indeed it looks like a fan! The writer himself holds his own opinions on the matter of how we should define alluvial fans, but will mercifully not claim to have found the ultimate key to the problem. (Although he might commonly suggest that careful reconsideration of the word 'stream' would bring us way closer to a solution…)

In spite of their relatively simple geometry and architecture (Fig. 2), alluvial fans have been described from a great variety of environmental and climatic settings where they are produced by a wide range of sedimentary processes. This diversity of context and processes probably lies at the roots of the difficulty in finding a commonly agreed definition for these depositional systems. Studies on alluvial fans have been classically split into two main lines of research, one focused on Quaternary systems and climate controls, and the other on the ancient stratigraphic record, with a main view to tectonic contexts and controls. The two subfields are characterized by rather separate perspectives, and especially by the dominant opinions of different experts. To date, the available literature starts to be considerable, although it remains well below the critical mass reached for other depositional systems, such as rivers, turbidite systems or glaciers. The split personality of alluvial-fan research, however, lingers on.

Figure 2 *- A typical alluvial fan sloping down from highland sources into the distal floodbasin (Central Depression, Atacama Desert, northern Chile).*

The basic traits of fan geomorphology were already described in the late 18th and 19th centuries by European and American naturalists at disparate world locations (Saussure, 1796; Surrell, 1870; Drew, 1873; Dutton, 1880; Gilbert, 1882; Conway, 1893; Davis, 1898). The striking point in common to most of these otherwise disconnected observations was the recognition of alluvial fans as landforms typical of high-relief settings, and characterized by infrequent high-energy processes that transport coarse-grained sediment. Indeed, it can hardly pass unnoticed that the fundamental trigger for fan sedimentation has been forever captured in its unpleasant essence by a news piece of the 18th century, going by the most British title of "*Dreadful storm in Cumberland*" (Smith, 1754). This article probably represents the very first account of alluvial-fan activity.

The historical core of fan research was developed in the United States during the first half and middle of the 20th century. Though not particularly numerous, various seminal papers, still widely cited today, were

written by geographers and geomorphologists who worked in the semiarid southwestern states. Particular attention was paid to the significance of Quaternary to present-day alluvial fans for general theories of landscape evolution, a topic then at the forefront of geoscientific research. Despite the ultimate geomorphic objectives, the nature of alluvial-fan processes inevitably implied that several such works also count among the very first sedimentological and hydrological discussions of subaerial debrisflows (Blackwelder, 1928; Fryxell & Horberg, 1941; Sharp, 1942; Sharp & Nobles, 1953; Hooke, 1967), hyperconcentrated flows (Bull, 1963) and desert floods (Pack, 1923; Chawner, 1935; Davis, 1938; Krumbein, 1942; Rahn, 1967). Contemporaneous and later studies of alluvial fans in other locations around the world (Mason & Foster, 1956; Hoppe & Eckman, 1964; Winder, 1965; Legget *et al*., 1966; Waldron, 1967; Broscoe & Thomson, 1969; Johnson & Rahn, 1970; Ryder, 1971; Prior & Stephens, 1972; Wasson, 1977, 1979; Rachocki, 1990; Derbyshire & Owen, 1990; Darby *et al*., 1990) were and still are poorly referred to today. Next to many valuable observations of present environments, the geographic imbalance of early alluvial-fan research toward the southwestern USA inevitably caused the long-standing misconception of alluvial fans as characteristic landforms of dryland settings. Recent review articles (Blair & McPherson, 1994a; Harvey *et al*., 2005; Dorn, 2009) emphasise that such a fan-climate connection is disproven by many case studies available today, but an introductory treatment of alluvial fans in many textbooks on general sedimentology and geomorphology is still presented in chapters dedicated to desert environments. By reflection, the same kind of reasoning was applied to debrisflow processes and deposits, which automatically started to be linked to the same specific climate framework (e.g. Blissenbach, 1954).

The first of two dominant trends in alluvial-fan studies, mentioned above, is possibly inherited from these early research efforts and consists in the analysis of causal and temporal linkages between alluvial fan development and climate change. It can be confidently stated that most recent research articles on alluvial fans still explicitly examine climate as the dominant or most likely control factor (e.g. Harvey, 1987; Frostick & Reid, 1989; Nemec & Postma, 1993; Roberts, 1995; Kochel *et al*., 1997; Pope & Millington, 2000; Harvey & Wells, 2003; Harvey *et al*., 2003; Zanchetta *et al*., 2004; Hartley *et al*., 2005; Waters *et al*., 2010). The close spatial and process relationships between alluvial fans and their catchments render these systems particularly useful to examine landscape evolution driven by exogenous processes. Alluvial fans are products of the direct physical coupling of relief and erosion/denudation on one hand, and of variations in depositional processes on the other.

Whereas old ideas on fan-climate relationships paved the way, the recent literature explosion has been spurred mainly by the parallel development of dating and paleoclimatology in Quaternary science. The complementary results are that: 1) many studies of landscape evolution and climate change carry Quaternary alluvial fans as their prominent evidence; and 2) studies on Quaternary to Recent alluvial fans almost inevitably discuss regional climate change on multiple time scales in order to rationalize geomorphic and sedimentologic observations. Although many valuable contributions have been made, an early tendency to search for general models of fan-climate relationships has left room for the sober realization that fan processes and dynamics are also strictly dependent on catchment properties and geological context. Every fan system most likely follows its own evolution course (see section 1.4). Classical field-based studies are

nowadays integrated by great advances in dating techniques, which consent to overcome the typical absence of dateable material in coarse-grained fan deposits. Conceptual progress in studies of catchment hydrology and geomorphology will also help to frame alluvial-fan evolution into a more solid theory of landscapes in the future.

Figure 3 *- Recent debrisflow deposits in the proximal, upslope reaches of a thickly forested alluvial fan near Whistler, Cascade Range, British Columbia, Canada (view upfan, author for scale); note complete scouring of bark off the tree on the left, and damming effects of fallen trunks on flow runout, as indicated by distribution of coarse-grained deposits.*

A more properly geological approach to alluvial fans as recognizable environments in the ancient rock record and to long-term controls on their processes and stratigraphy came later, and was strongly driven by the need to evaluate recent and ancient fan deposits as aquifers, hydrocarbon reservoirs and hosts for minerals. Many important studies in this period are represented by public reports from government agencies (Bull, 1964; Denny, 1965; Lustig, 1965; McGowen & Groat, 1971; McGowen, 1979). The number of works in this research thread grew very slowly and today remains distinctly subordinate to the geomorphologic-climatic trend. The adoption of a geologic perspective however has induced its own bias in terms of scale and of interpretive framework. Most studies concern successions dating from a wide range of time periods in Earth's history, commonly much older than Quaternary systems and in much thicker exposures. They are often discussed in terms of tectonic controls. A number of classical studies belonging to this research framework dates mainly from the 60's to the 80's (Bull, 1964; Hooke, 1972; Steel *et al*., 1977; Heward, 1978; Gloppen & Steel, 1981; Anadón *et al*., 1986; Hirst & Nichols, 1986; DeCelles *et al*., 1987; Nichols, 1987; DeCelles *et al*., 1991), characterized by a notable emphasis on petrography, regional geology, and

especially on process sedimentology. Whereas the birth of sedimentology as a discipline was almost entirely focused on carbonates and sandstones, many fundamental ideas on the transport and deposition of coarse-grained debris have been first exposed in articles dealing with alluvial fans and fan-deltas (Sharp, 1942; Sharp & Nobles, 1953, Bull, 1963; Hooke, 1967; Broscoe & Thomson, 1969; Nemec & Muszynski, 1982; Wells, 1984; Balance, 1984; Massari, 1984; Postma, 1984; Nemec *et al.*, 1984; Wells & Dohrenwend, 1985; Flint & Turner, 1988; Postma & Cruickshank, 1988; Todd, 1989; Nemec, 1990a; Sohn *et al.*, 1999).

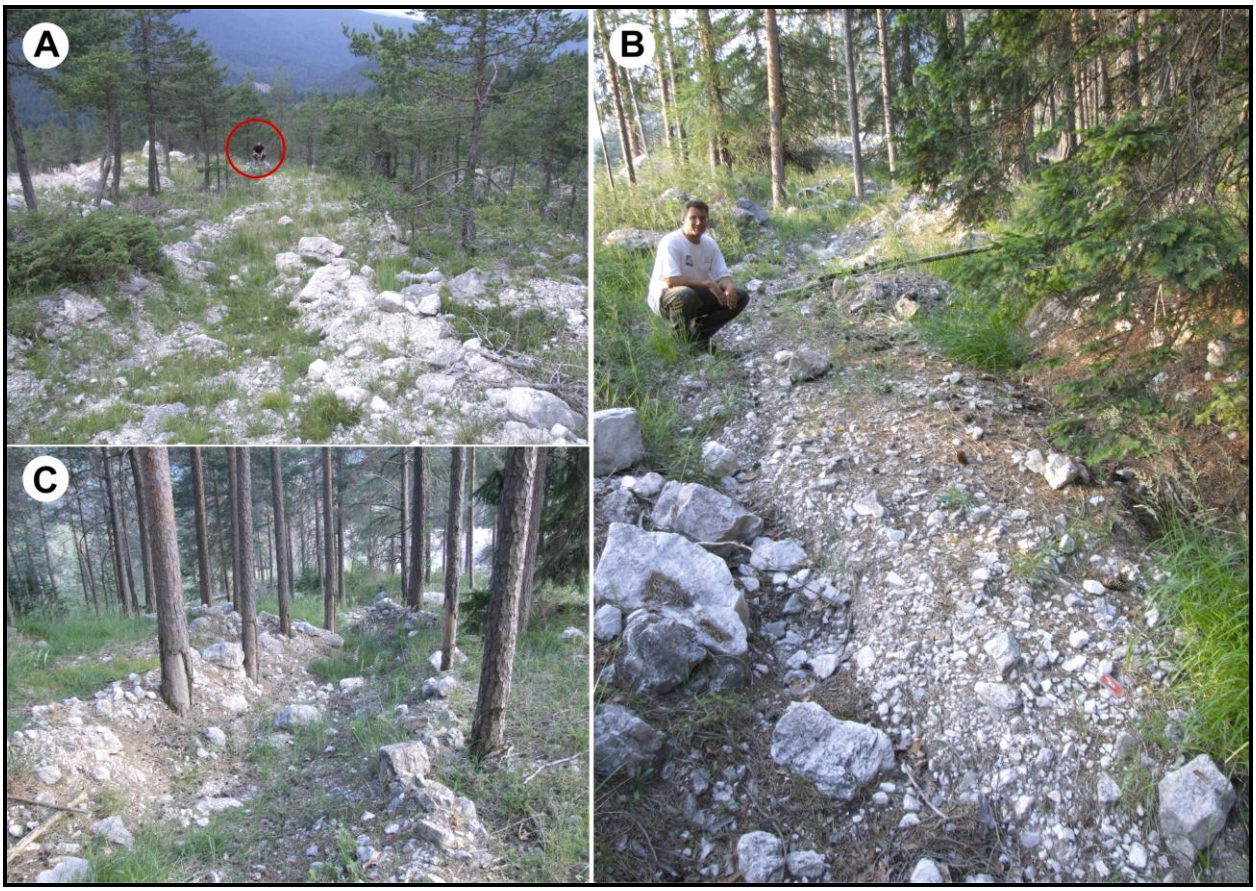

Figure 4 *- Debris-flow sedimentation on alluvial fans of the eastern Italian Alps (medial and distal segments of Aquabona and Pezie fans, Cortina d'Ampezzo). (A) Superposition of coarse-grained levees from different events (author for scale circled in red). (B) Abrupt termination of a clast-poor mudflow tongue (author for scale). (C) Downfan view of debrisflow levees and frontal termination; note bark scours with upfan orientation and uniform height.*

Research on alluvial fans has thus reached an appreciable degree of maturity, although still riddled with open questions and a few old misconceptions. Generalized models of alluvial-fan stratigraphy have not yet been developed, most likely due to the strong individuality of these depositional systems, depending on regional geologic context and catchment characters. Significant volumes of fan deposits are created only through a persistent, long-term combination of abundant sediment sources, topographic gradients and localized subsidence. Hence, both accommodation and sediment supply for long-lived alluvial fans strongly depend on local patterns of active tectonics. Past conceptual models relating upward-coarsening and upward-fining fan successions to active or receding tectonics (e.g. Bull, 1977; Steel & Wilson, 1975; Steel *et*

al., 1977; Heward, 1978; Nilsen, 1982; Galloway & Hobday, 1996) have been proven simplistic and not generally applicable in the view of recent refinements of our knowledge of subsidence patterns and structural geometry at the active margins of sedimentary basins (Jordan *et* al., 1981; Blair & Bilodeau, 1988; Crews & Ethridge, 1993). Another common assumption on alluvial fans concerns the supposed downslope-fining of sediment texture, accompanied by changes in dominant processes and facies, from mass flows in the proximal fan domain to water flows in the distal one. Although intuitively sensible, this simplistic reference model has been confirmed only by a minor number of published case studies. The generalization was inspired by research on the Trollheim fan (western USA; Hooke, 1967, 1987) which was successively proven flawed (Blair & McPherson, 1992). Conglomerates in the distal fan domain, originally interpreted as waterflow deposits, were found out to be reworked debrisflow deposits at the fan surface; stratigraphic sections confirmed the abundance of matrix-rich, debrisflow facies as the main constructive deposits in the distal fan segments. The basic problem with this invalid generalization is that the significant differences in runout potential and loss of capacity between mass flows (typically debris flows) and exceptional water flows are not fully expressed over high-gradient fan surfaces of only a few hundred of meters to a few kilometers in radius. The frequently adopted climatic classification of alluvian fans as 'humid' or 'arid' (e.g. Bull, 1972, 1977; Schumm, 1977; Gloppen & Steel, 1981; Nilsen, 1982; Hooke, 1987; Stanistreet & McCarthy, 1993) also led to misinterpretations of fan sedimentology, with significant implications for paleoclimatology and for regional landscape history. The recent expansion of published research to domains outside the classic American southwest has brought the sobering realization that sedimentary processes on alluvial fans are in most respects azonal (Blair & McPherson, 1994a; Dorn, 2009).

The writer had occasion to visit several active fan systems in different climate settings, from tropical hyperarid (Coastal Cordillera, northern Chile), to arid subtropical (Andean piedmont, central Argentina), temperate wet (Cascade Range and Rocky Mountains, British Columbia and Alberta, Canada), Mediterranean (northern Apennines, Tuscany) and seasonal alpine (Alps, northeastern Italy and central Switzerland) (Figs. 3 to 6). In all cases, it was clear that precipitation patterns, vegetation types and soil development did not significantly affect the dominant types of sedimentary processes. These could be examined from recent deposits over the active fan surfaces and from stratigraphic exposures. In particular, coarse-grained debrisflow levees and snouts have been recognized in all conditions, from the barren, Mars-like surfaces of the Atacama Desert fans to the thickly forested fan slopes of British Columbia and on the Alps. Whereas the frequency of events and their initiation are indeed variable, fan deposits demonstrate that these systems have all been constructed by statistically 'catastrophic' mass flows, hyperconcentrated flows and sheetfloods.

The different geomorphic contexts of the visited locations converge toward the observation that alluvial fans develop downslope of catchments with relatively reduced areal extent, high internal relief and poorly integrated drainage networks with low-order streams. More commonly, bedrock or hillslope hollows act as main drainage pathways, rather than actual stream channels. Such catchments are generally: a) activated mainly by severe precipitation events; b) prone to flash floods and hydrographs with sharp peaks, irrespective of the climate setting; c) sources of sediment-water output in which the second component is

frequently subordinate to the first, by volume. Surveys conducted in most of the catchments did not show any evidence for active streams. Elevated sediment-water ratios are generally conducive to cohesive mass flows (mostly debrisflows, and occasionally landslides), hyperconcentrated flows, and shallow distributive or unconfined runoff patterns (sheetflows or sheetfloods; Hogg, 1982).

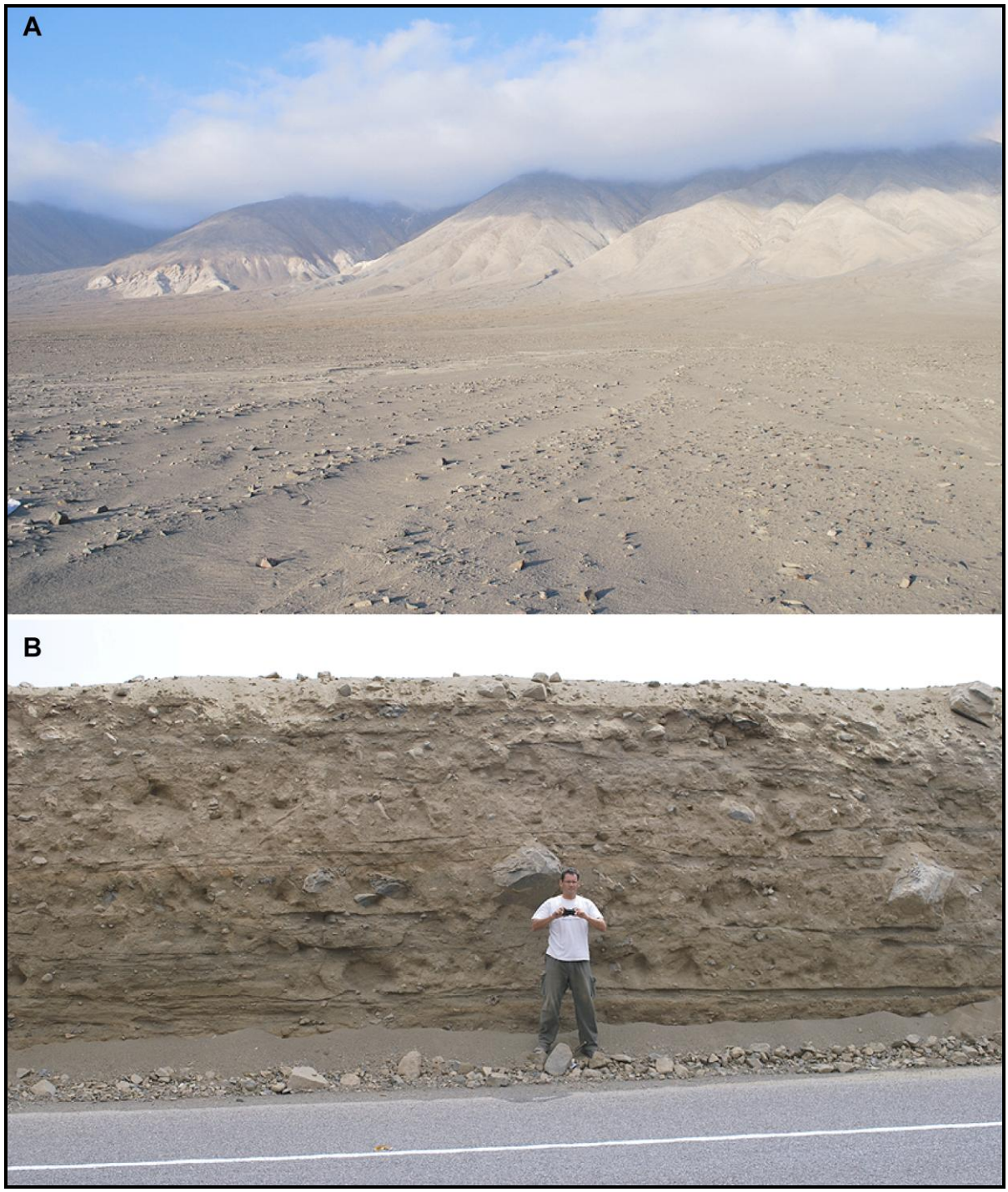

Figure 5 *- Alluvial fan along the Pacific coast of the Atacama Desert (north of Antofagasta, Chile). (A) Surface morphology, with debrisflow lobes partially buried by a thin eolian cover. (B) Distal, cross-fan stratigraphic section, showing evidence for debris flows as main constructive processes, accompanied by thin sheetflood interbeds (author for scale).*

Figure 6 *- Debrisflow levees on a vegetated alluvial fan near Allmendhubel, central Alps, Switzerland (author for scale); note colonization of coarse sediment by low vegetation at an incipient stage in fore- and middleground, and at an almost complete stage in background.*

Fan surfaces with entrenched channels occupied by actively flowing streams were observed only in southwestern Canada, and can be considered an interesting confirmation of the considerations reported here. Most of these fans are fed by downslope wasting of relict glacial deposits from higher altitudes, dating from the last Wisconsinan glacial phase (Wilford, pers. com.; Wilford *et al.*, 2005; see also Church & Ryder, 1972). As high volumes of unstable relict sediments were initially available, fan construction proceeded through dominant mass flows. Sediment sources were not continuously replenished by active tectonics, and their gradual depletion in the Holocene caused progressive catchment expansion and a concomitant reduction in available debris volumes. Nowadays, most runoff issued by catchments upslope is not able to mobilize the more stable, residual fraction of original glacial deposits, if not during particularly severe meteorologic events or protracted humid periods. Most present-day runoff thus flows over fan surfaces which are inactive, and reworks them forming incised channels. The fans themselves are therefore early postglacial relicts (*paraglacial* in the terminology of Church & Ryder, 1972), no longer depositionally active. The history of fan construction and deactivation has been determined by trends of increasing and successively decreasing sediment-water ratios.

The ultimate problem in alluvial fan research is represented, paradoxically, by uncertainty on what we should refer to as 'alluvial fans' at all. This issue was raised by Blair and McPherson (1994a, 1994b;

McPherson & Blair, 1993) with a lack of scientific diplomacy that was not welcome by many researchers in the field, but that certainly contributed to revive the interest on alluvial fans and to fine-tune the scope of later work. In the closing paragraph of the introduction to their flagship article, Blair and McPherson (1994a) stated: "On the basis of an extensive study of modern alluvial fans in a variety of global settings, we conclude, *counter to contemporary thought but consistent with early scientists* [added italics], that there is a fundamental and natural distinction between fans and other sedimentary environments, including gravel-bed rivers. This distinction is reflected, and readily determined by, the morphology, hydraulic and sedimentary processes, and resultant facies and facies assemblages of alluvial fans. The uniqueness of the facies assemblages also facilitates the clear and simple differentiation of fans even in settings where the geomorphic context is lost, including in the stratigraphic record."

The issue had been indirectly presaged by a closely related terminological controversy in the literature, just a few years before, on what should be the most appropriate definition and application of the term 'fan delta' (Nemec & Steel, 1988; Nemec, 1990b; McPherson *et al.*, 1987, 1988). The parallel discussion on alluvial fans however caught much more attention in the scientific community. Whereas some experts in the field followed up in explicit agreement with Blair & McPherson (e.g. Nichols & Hirst, 1998; Smith, 2000; Moscariello, 2005), the majority actually minced no words in protest on what was perceived as an unjustified semantic restriction. Two discussions and replies were published on the *Journal of Sedimentary Research* after publication of the controversial review. In keeping with the long-lived dichotomic subdivision of alluvial fan research, most of the authors in disagreement with Blair and McPhersons's views were those active in geomorphology and Quaternary geology, but protest came basically from all camps. The most fervent discussion soon focused on whether many river systems should be formally excluded from the alluvial-fan category even in the presence of fan-shaped

(distributive) plan-view patterns of alluvial deposition. The Kosi River of northern India, cited countless times as the most extensive alluvial fan in the world, is the textbook example of these systems. An authoritative classification of these sedimentary systems into debrisflow-dominated and fluvial-dominated fans, published shortly before Blair and McPherson's paper (Stanistreet & McCarthy, 1993), became the reference frame for critics (Fig. 7). Interestingly, to date the question remains unresolved in the literature, but most people involved with fan research will informally assert to have the solution and to be standing in the right conceptual camp. Potential approaches to the solution linger between the lines of the recent research revival on the geologic significance of distributive fluvial systems (Hartley *et al.*, 2010; Weissmann et al., 2011) and on the renewed interest on 'fluvial fans'.

Having said that, where does the writer stand in all of this? The impression is that a certain degree of approximation has characterized the literature for too long. Careful reading of many articles suggests that too many fluvial deposits, especially ephemeral fluvial systems at basin margins, have been discussed as alluvial fans, often applying the same misconceptions as in the classic fan literature of a few decades ago. The proper identification of depositional systems has important implications for a correct framing of facies analysis, for the prediction of facies architectures and palaeogeography, and for the interpretation of regional tectonics. Interestingly, the opposite mistake has been very rarely observed: very few articles have

been encountered discussing generic 'fluvial' deposits that one could arguably reinterpret as alluvial-fan successions. In this respect, it seems that Blair and McPherson's (1994a; McPherson & Blair, 1993) opinions on the general confusion in the literature are definitely right. The frequent dismissal of the issue as a merely semantic one is not acceptable, since scientific research advances through the communication and discussion of complex concepts which are ever more numerous and interrelated; the application of an unambiguous terminology lies at the base of good communication. A cursory look at the professional medical literature and its complex jargon should demonstrate the importance of an accurate terminology. That the intricacies of such a jargon remain cryptic to the layman is no reason to underestimate its practical importance to those who apply it, and especially to those who benefit from it.

Nonetheless, scientific terminology should ideally reflect the true character of natural entities, and not our state of doubt. As mentioned above, there is as yet no general consensus on the application of the term 'alluvial fan'. Its usage to denote a supposed end-member along a continuum of 'fluvial' phenomena (e.g. Schumm, 1977; Miall, 1996; Bridge, 2003) is clearly misleading, since there are no documented depositional systems in the literature with characteristics intermediate between alluvial fans and rivers. As discussed by Blair and McPherson, the contrast in hydrological and sedimentary processes between the two kinds of depositional systems is very strong, and it bears on distinctive morphologies and stratigraphic signatures. The term 'alluvial' (from the Latin *alluvium*) is generally adopted to indicate material transported and redeposited by surface runoff, and it therefore stresses a process inference. The term 'fan', on the other hand, highlights the morphologic outcome of areally distributed sediment transport from a fixed source area. The unfortunate choice of 'alluvial fan' thus couples a very generic process, which takes place in countless settings on Earth, to a morphologic trait which can result from many process combinations. If one opted for a strictly etymological constraint, indeed a great variety of subaerial landforms and depositional systems would fall under the 'alluvial fan' catch-all. Historically, however, the term was applied to systems with distinctly high gradients, dominated by flood hydrological processes and by sedimentation from unconfined to poorly confined events where sediment-water ratios forced mass-flows to be the most frequent trasport mechanism. That no exact numbers have yet been established to formally delimit the morphologic and hydrological boundaries of such systems is no valid excuse to ignore their distinctive character. If we stick to the original usage, there can hardly be any doubts on what active systems should be identified as alluvial fans at the Earth's surface today.

Alluvial fans are conical, high-gradient piedmont landforms developed through deposition mainly from mass flows and unconfined floods issued by point sources in correspondence of major topographic breaks. (And the Kosi River should probably be viewed just for what it's called: a river…)

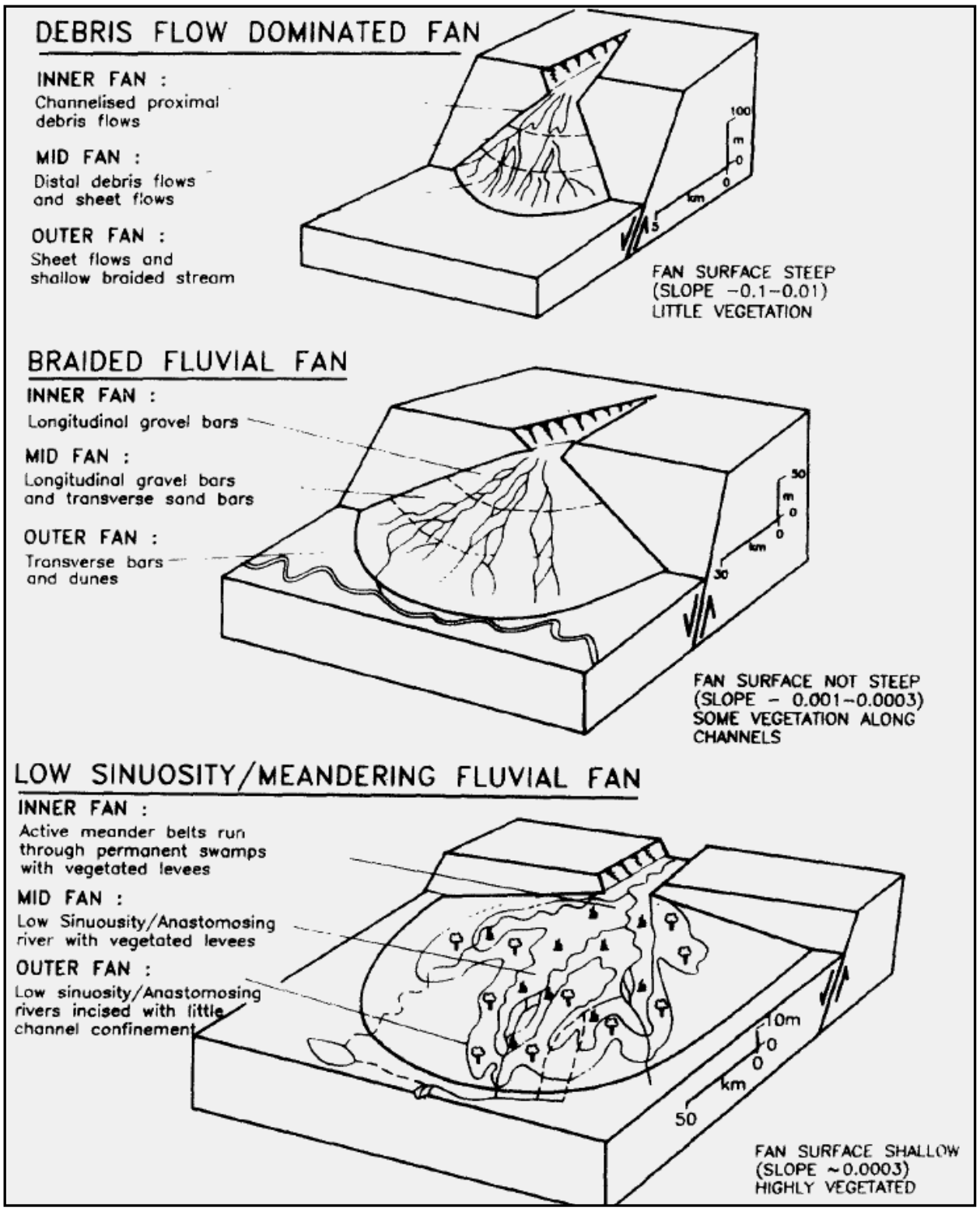

Figure 7 *- Stanistreet and McCarthy's (1993) classification of subaerial fan systems. For a simple example of one of the classical wrong points with this conceptual scheme, compare "little vegetation" in the surface description of debris-flow-dominated fans (at top) with figures 3, 4 and 6. This kind of classification is fundamentally flawed in that it considers development of a distributive pattern of sediment transport and deposition as a basic, distinctive surface process, instead of a topographically forced result of sediment and water supply from a single source, relatively stable through time.*

1.3 COLLUVIAL DEPOSITIONAL SYSTEMS: THE LAST FRONTIER?

The origin, evolution and geometric configuration of mountain slopes have been among the most important questions to be first approached by scientific geomorphology. The existing literature on the subject is chronologically biased toward the middle half of the 20th century, when the first models of slope evolution were tentatively developed under the conviction that either climate-related processes (Fenneman, 1908; Lawson, 1932; Peltier, 1950) or geological time (Davis, 1909; Wood, 1942; Savigear, 1952; Penck, 1953; King, 1957, 1967) could be the main driving factors. Admittedly, there is as yet no strong consensus on whether general models of hillslope formation and evolution have been achieved, but geomorphologists are still actively pursuing this question, slopes being by definition one of the basic landform elements to shape our landscapes.

By contrast, a complementary sedimentological perspective on slope studies has developed very late, and has started gaining some ground in the scientific literature only over the last fifteen-twenty years. One might as well consider, from a more reductionist stance, that understanding slope morphology is closely tied to understanding the processes and patterns of regolith transport and distribution (Fig. 8) over slopes under variable environmental conditions. No surprise therefore that geomorphic lines of inquiry have often come to a theoretical *impasse* without the support of well-grounded ideas on the basic active processes of slope (re)sedimentation.

TYPICAL CHARACTERISTICS	colluvial fan	alluvial fan
Geomorphic setting:	mountain slope and its base (slope fan)	mountain footplain or broad valley floor (footplain fan)
Catchment:	mountain-slope ravine	intramontane valley or canyon
Apex location:	high on the mountain slope (at the base of ravine)	at the base of mountain slope (valley/canyon mouth)
Depositional slope:	35-45° near the apex, to 15-20° near the toe	seldom more than 10-15° near the apex, often less than 1-5° near the toe
Plan-view radius:	less than 0.5 km, rarely up to 1-1.5 km	commonly up to 10 km, occasionally more than 100 km
Sediment:	mainly gravel, typically very immature	gravel and/or sand, immature to mature
Grain-size trend:	coarsest debris in the lower/toe zone	coarsest debris in the upper/apical zone
Depositional processes:	avalanches, including rockfall, debrisflow and snowflow; minor waterflow, with streamflow chiefly in gullies	debrisflow and/or waterflow (braided streams)
EXAMPLES	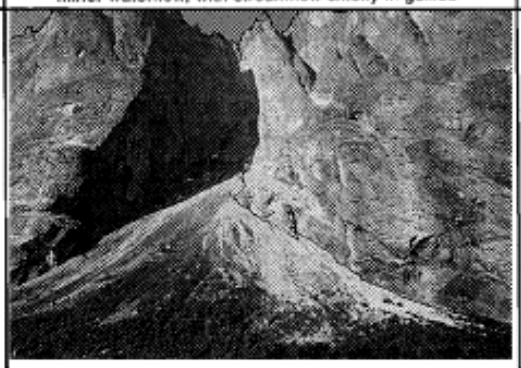 The Brotfonna colluvial fan, Trollvegen near Romsdal, Norway; one of the world's largest colluvial fans, with a height of 830 m and a plan-view radius of 1.5 km.	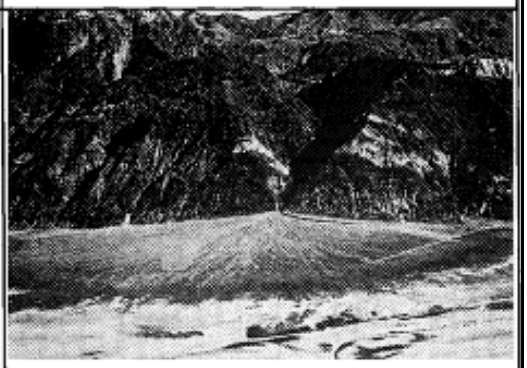 The Badwater alluvial fan, eastern side of Death Valley, California; a modest fan, with a radius of c. 6 km.

Figure 8 *- Fundamental geomorphic and sedimentological distinctions between colluvial fans and alluvial fans, the main depositional systems in piedmont settings (from Blikra & Nemec, 1998).*

Traditionally, clastic sedimentologists have not been very attracted by deposits accumulated along piedmont systems. Reasons for this have been commonly ascribed to a combination of extreme textural immaturity and lack of organization which would make most slope successions unapproachable in terms of process sedimentology and architectural facies models. Although such reasons are more supposed than real, the myth has lingered on. An accompanying, partly more correct observation has often been that slope deposits have very little preservation potential, being intrinsically related to environmental settings with high relief and dominant erosion on geological time scales. In other words, if they are not there, why bother… In the end, the expected absence of slope sediments from the stratigraphic record of ancient sedimentary basins has been gradually revealed to be more of a self-fulfilling prophecy than a fact by a growing body of observations in the literature (e.g. Bryhni, 1978; Choe & Chough, 1988; Higgs, 1990; Tanner & Hubert, 1991; Dávila & Astini, 2003; Wilmsen *et al.*, 2009) (Fig. 9). A glaring lack of ideas on the part of their colleague geomorphologists on how hillslopes would develop through time probably also didn't help to spur the interest of sedimentologists.

Several authors have recently stated that the analysis of slope depositional systems represents the last open frontier for clastic sedimentology (Imeson *et al.*, 1980; Blikra & Nemec, 1998; Turner & Makhlouf, 2002), and that time has come to start filling the gaps on a setting that can provide much information once a substantial body of basic knowledge has been created. Although slope deposits do not figure among the major types of hydrocarbon reservoirs, it is reasonable to expect that any major discovery of this type in the future would significantly support research on these depositional environments. The pressing need for hazard prevention in highland settings is also an important motivation to improve our understanding of stratigraphic event records in these systems.

Most early sedimentological observations in slope settings were actually reported by geomorphologists (e.g. White, 1949; Rapp, 1960; Selby, 1971; Clark *et al.*, 1972; Kirkby & Statham, 1975), who applied a process-oriented perspective to the analysis of surface features, but not on stratigraphic products. A true renaissance in slope sedimentology has been recently revived by the work of a few dedicated authors. Although not the first sedimentologist to stand fearless in the face of mountain rubble, Wojtek Nemec's voluminous papers from the late 90's (Blikra & Nemec, 1998; Nemec & Kazanci, 1999) are the ones that most effectively brought the subject to the attention of international readers. Others had started to explore the complexity of these sedimentary environments more or less in the same years, especially from the point of view of process-facies relationships (Van Steijn *et al.*, 1984; Pérez, 1989; Luckman, 1988, 1992; Hétu, 1990, 1995; Hinchliffe *et al.*, 1998; Jomelli, 1999). The topic has only just started to be explored by advanced sedimentological research, as testified by uncertainties in the terminology to be adopted for scientific communication. The traditional terms *colluvium*, *talus* and *scree* are commonly used in a broad sense to denote both depositional landforms along slopes and the constituent deposits, irrespective of genetic processes (Blikra & Nemec, 1998). Some authors however are starting to invoke a higher level of semantic rigour (e.g. Turner, 1996; Sanders, 2010), suggesting that *colluvium* be restricted to sediment transported by runoff processes, whereas *scree* and *talus* should be reserved respectively to coarse-grained deposits from rockfall and grainflow processes and to their steep, cone-shaped accumulations. Given the high heterogeneity of slope processes, it will be difficult to

apply formal terminological requirements in detailed sedimentological analyses, and it might be more productive to adopt the traditional general usage for now, as more research is in progress.

Figure 9 *- Crudely stratified Miocene colluvial deposits onlapping the original paleorelief of the Cretaceous basement (eastern margin of the Teruel Basin, near Riodeva, Spain).*

Some research trends are already discernible in colluvial sedimentology. Since the most abundant and complete stratigraphic successions are from Quaternary to Recent piedmonts, a dominant tendency to analyze such deposits in terms of climate forcing has already gained a relatively broad stage. This approach naturally results from the fact that Quaternary sediments are the most amenable to high-resolution dating and to comparison with reliable palaeoclimatic records. In fact, several articles have convincigly demonstrated a close link between chronological changes in slope processes and architectures on one hand, and independently constrained time-series of palaeoclimate proxies on the other (e.g. Blikra & Nemec, 1998; Blikra & Selvik, 1998; Nemec & Kazanci, 1999; Hinchliffe, 1999; Hétu & Gray, 2000; Pederson *et al.*, 2000; Texier & Meireles, 2003; Pawelec, 2006; Sletten & Blikra, 2007). Advances and arising questions in the separate field of palaeoseismology have helped to open a parallel line of inquiry into the significance of slope deposits to unravel palaeotectonic patterns of relief evolution (Nelson, 1992; Arrowsmith *et al.*, 1996; Porat *et al.*, 1996; McCalpin & Nishenko, 1996; Kozhurin *et al.*, 2006). By far the greatest volume of work on slope sedimentology however has been carried out on paraglacial and periglacial (high-altitude and/or high-

latitude) environments (e.g. Rapp, 1960; Chandler, 1973; Francou, 1990; Gardner *et al.*, 1991; Pérez, 1993; Bertran & Texier, 1994; Bertran *et al.*, 1995; Kotarba, 1997; Blikra & Nemec, 1998; Blikra & Selvik, 1999; Jomelli, 1999; Hétu & Gray, 2000; Curry, 2000; Zurawek *et al.*, 2005; Sletten & Blikra, 2007; Sanders, 2010), to the effect that colluvial sedimentology is often automatically related to 'cold' settings, unless otherwise specified. The scarcity of soils and vegetation in alpine and subpolar environments certainly offers good access to piedmont surfaces and transects. Most likely, however, the prevalence of studies in such settings is due to their extreme climate conditions, which make them very susceptible to transitions in geomorphic thresholds due to environmental fluctuations. The climatic school of thought thus makes its presence felt in this growing discipline not only in terms of research goals, but also in providing a growing bias of case studies based within a limited range of environmental conditions. Confirmation can be obtained by a careful scrutiny of reference lists in the very first review articles on slope sedimentology (Van Steijn *et al.*, 1995; Van Steijn, 2011). In this respect, an interesting parallel can be drawn with the first decades of alluvial-fan research, in which studies of dryland fans set the trend for such systems to be viewed as typical for arid regions.

To date, case studies of slope sedimentology carried out in temperate to warm-arid settings remain a minority (Gerson, 1982; Abrahams *et al.*, 1985; Friend *et al.*, 2000; Turner & Makhlouf, 2002; Nichols *et al.*, 2005; Gernon *et al.*, 2009), and will therefore contribute to expand the scope of the discipline. The application of new techniques, such as ground penetrating radar and electrical tomography, expanded the spatial scale of slope sedimentology, allowing comparative analyses of broad piedmont systems and particularly of thick colluvial successions not entirely accessible in stratigraphic exposures (Berthling *et al.*, 2000; Sass *et al.*, 2007; Sass & Krautblatter, 2007; Scapozza *et al.*, 2011). Interestingly, the latter works have offered a broad outlook over the internal architecture of colluvial deposits, and have inspired the first conceptual models of colluvial genetic stratigraphy (Sass & Krautblatter, 2007; Sanders *et al.*, 2009; Sanders, 2010). Needless to say, these studies remain restricted to alpine and periglacial settings, and we are not yet able to compare ideas on the large-scale geometry and evolution of piedmont depositional systems with similar datasets from temperate or arid environments.

1.4 CATCHMENT GEOLOGY AND GEOMORPHOLOGY: PRIME MOVERS…

From the previous sections, an interesting parallel stands out between the present growth of research in colluvial sedimentology and the coming of age of alluvial fan research in the late 20th century. In both fields, the starting phase was strongly dominated by observations focused on sedimentary processes and geomorphology within specific environments (drylands of the American southwest for fans, and alpine to periglacial 'cold' settings for slope deposits). As the number of case studies increased, focus shifted to a larger-scale perspective on causal relations between depositional patterns and allogenic factors. In particular, a rising attention to climate as a dominant driver of sedimentary processes developed in both fields, probably steered by advances in Quaternary geoscience. Various kinds of climate inferences and interpretations, therefore, continuously stand behind research programs on these proximal depositional

environments at basin margins. In parallel with the history of alluvial fan research, this trend was not always a source of progress and actually led to a few possible misconceptions in the literature (see section 1.2.).

In colluvial sedimentology, the most recent research trend is typified by works which succesfully relate past variations in sedimentary processes with Quaternary climate changes. Considering the morphological context in which these depositional systems develop, however, one cannot ignore that not only their very existence, but their dynamics must be closely influenced also by local relief. In spite of an overwhelming literature on cold-regional colluvial deposits, the few studies conducted in other settings show that the basic nature of sediment gravity flows is azonal with respect to climate. Sediment-gravity flows and debris falls are the primary constructive processes in talus cones and colluvial aprons; their mechanics are closely controlled by slope topographic profiles and by the granulometry and mineralogy of resedimented debris. The presence of fines, and the amount of clay minerals in particular, significantly influence the stability and yield properties of regolith in the presence of different possible triggers of slope failure. For example, the effectiveness of direct mechanical destabilization (earthquake agitation, superimposed shear, basal slope steepening, etc.) is generally reduced in the presence of abundant interstitial fines. Interstitial overpressures during major precipitations and wet periods, on the other hand, are the most frequent cause of slope failure, and preferentially take place within mud-rich regoliths and soils of low permeability. Once initiated, regolith failures have the potential to turn into various kinds of sediment transport processes downslope, and one of the main controls on flow properties and transformations again will be exerted by the original composition of the resedimented material. The occurrence of long-runout debrisflows for example depends on the volume of mud in the mixture. Although the intensity of chemical weathering is regulated by climate, lithotypes such as dolostones and quartzites will generally not produce any fines or clay minerals, whereas many low-grade, basic metamorphic rocks, marlstones and mudstones will produce high amounts of clay under virtually any weathering regime. For non-cohesive processes of resedimentation (grainflows, debris falls) the geometric configuration of slopes along the pathway of descent is a fundamental determinant of process mechanics. Whereas debris fall involves clasts falling downslope without mutual interaction, grainflow processes are related to the volume concentration of clasts, and thus the potential for clasts to interact during fall. Slope concavities and hollows tend to force falling particles through a confined volume, favoring grainflow over debris-fall processes. Surface hydrology is another important player in the picture. Besides dominant sediment-gravity flows, colluvial deposits can be characterized by waterlain sediments. The morphology of slope surfaces and of higher bedrock walls controls the efficiency of piedmont sectors in collecting and transferring runoff downslope. The distribution of waterlain deposits thus will follow lateral variations in piedmont morphology, and not necessarily record the timing and intensity of past pluvial phases.

Despite its intuitive importance, the role of relief morphology and geology in controlling the production and resedimentation of colluvial material has been taken into some consideration only in a few case studies so far (Welch, 1970; Gardner, 1980; Matsuoka & Sakai, 1999; Nemec & Kazanci, 1999; Zurawek *et al.*, 2005; Pawelec, 2006). Slope deposits are associated with geomorphic settings of dominant long-term erosion, and the original geomorphic context will most likely not be preserved or will be greatly modified. It is thus

inherent to these settings that stratigraphic analyses of ancient colluvial deposits cannot fully constrain the role of primary relief. The implications for climate interpretations of slope deposits are potentially significant. Reliable palaeoclimate inferences should be warranted only in the presence of high-resolution dating and of a regional database of palaeoclimate proxies for cross-reference.

Similar considerations apply to alluvial fans, although these depositional systems extend over larger surfaces and result from a time-integrated sediment transfer out of proper hydrologic catchments, and not from the direct, short-range relocation of debris downslope of local sources. In spite of considerable attention to climate and tectonics in controlling fan successions (section 1.2), several recent case studies have indirectly or intentionally shown how fan sedimentary processes vary in conjunction with catchment lithologies and tectonic deformation (Fig. 10). For instance, Blair (1999a) carried out comparative sedimentological studies between Quaternary fans in Death Valley, and found consistent relations between the production of fines from catchment bedrock and the role of debrisflows in fan construction, along similar principles to those exposed above for slope deposystems. A few similar cases have been described from various locations by other authors (Kostaschuk *et al.*, 1986; Webb & Fielding, 1999; Levson & Rutter, 2000; Moscariello *et al.*, 2002; Hartley *et al.*, 2005; Welsh & Davies, 2010). It is interesting to note that these examples have been restricted to the Quaternary, probably because catchment accessibility is the only way to constrain a direct link between fan sedimentation and catchment processes. The only studies fully demonstrating catchment-fan sedimentological coupling in the ancient stratigraphic record have been presented by Nichols and Thompson (2005) from the Miocene of the northern Ebro Basin (Spain) and by Wagreich and Strauss (2005) from the Miocene of the intermontane Fohnsdorf Basin (eastern Alps). In the first case, partial preservation of the original basement relief was due to a combination of endorheic drainage and foreland tectonics. Continuous internal aggradation within an endorheic basin allowed gradual onlap of the basin margin and long-term preservation of the original relief. The foreland basin setting allowed for later exhumation of basement lithotypes by thrust faults, and thus the possibility to reconstruct the stratigraphic column that originally outcropped in highland catchments. Traditionally, studies on ancient alluvial fan successions have recognized the imprint of catchment geology in 'vertical' changes in the petrography of fan sediments, following progressive basement unroofing (e.g. Mack & Rasmussen, 1984; DeCelles *et al.*, 1987; Mellere, 1993; Sohn *et al.*, 1999). Such information has been considered of primary importance to trace regional palaeotectonic histories and landscape evolution.

The realisation that variable source lithologies can directly influence the nature of sedimentary processes at basin margins has fundamental implications for more than just reconsidering some palaeoclimatic interpretations. Highland areas are increasingly occupied by human settlements and infrastructures of various kinds, and obviously subject to frequent landscape instability. Hazard prediction depends also on the ability to foresee the mechanics and extent of sedimentary events. In terms of resource exploration, the evaluation of alluvial fans as potential aquifers or subsurface reservoirs depends on facies prediction and on a good understanding of system-scale architecture. If relationships between catchment geology and fan processes were better explored by basic research, knowledge of the regional geology and basement stratigraphy along ancient basin margins could prove fundamental to predictions of fan depositional

processes, and thus of the expected facies types. In areas of poor subsurface data coverage this approach can provide a starting reference framework, all the more so considering that an understanding of large-scale depositional architectures in alluvial fans is still lacking (section 1.2).

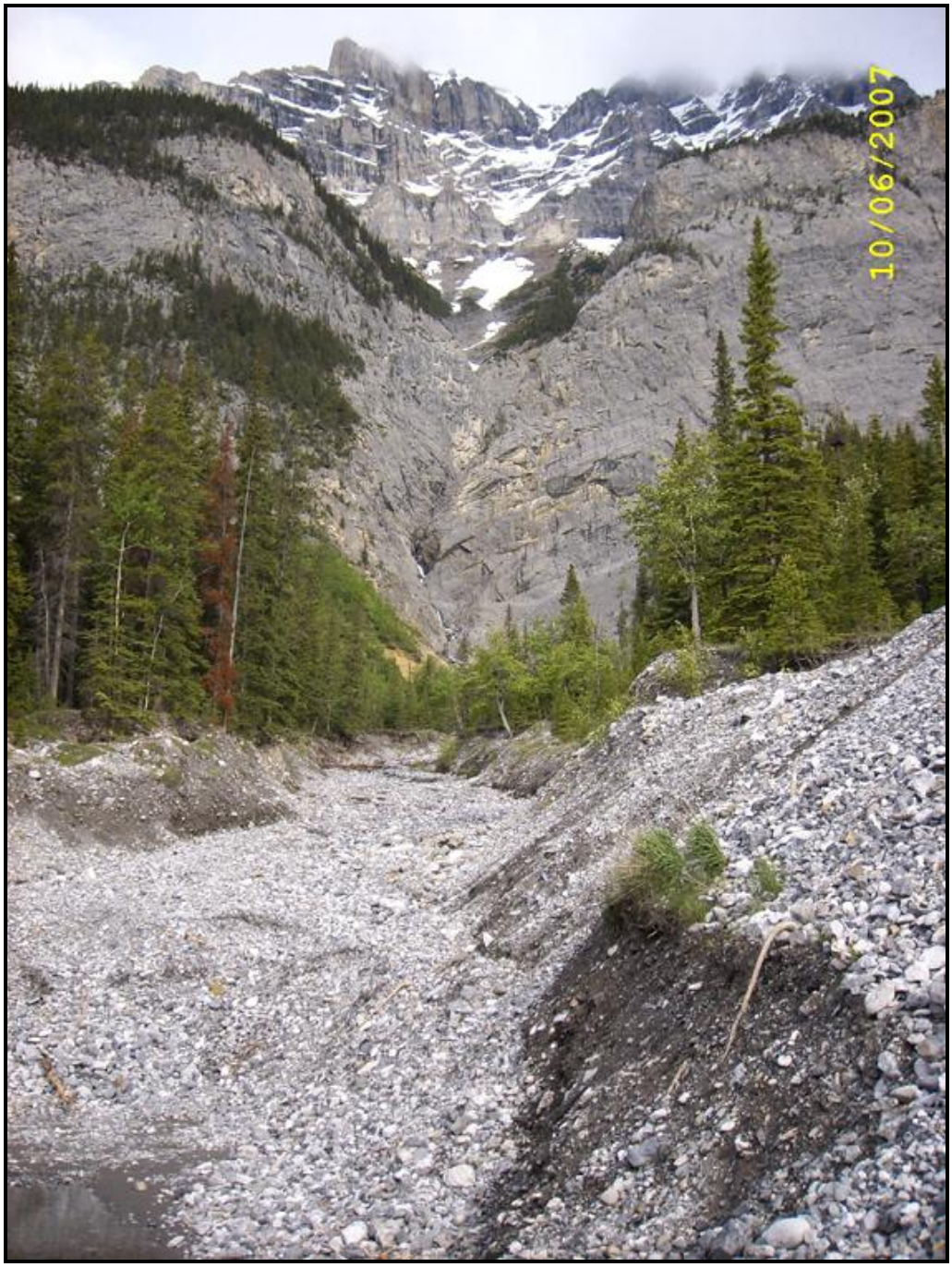

Figure 10 *- View upslope from the most proximal reaches of an alluvial fan (Rocky Mountains, Alberta, Canada); the catchment is a deep gorge eroded in Paleozoic limestones and shales.*

1.5 THE BROADER PERSPECTIVE: A VIEW BASINWARD…

The stratigraphic importance of subaerial depositional systems at basin margins lies in their role as gateways and buffers for clastic sediments on their way to longer-term deposition in distal environments. In the analysis of sedimentary successions the sequence stratigraphic paradigm has come to represent a powerful framework for weighing the role of allogenic factors and to predict large-scale depositional patterns. Base level, tectonics and climate are the three controls on sedimentation traditionally considered in basin analysis. Much progress in the geology of clastic sediments has been made thanks to this well-established conceptual approach. However, a fourth big player has appeared in the game lately: sediment supply (Jones & Frostick, 2002; Allen, 2008; Leeder, 2011). Sediment flux to basins is increasingly recognized as a first-order control on facies patterns and far-field dispersal. From the perspective of the sediment routing system (section 1.1), basin fills can be viewed as the final, integrated result of temporally and spatially variable sediment flux. Hinterland drainage systems and depositional landforms constitute the first stepping stones along the routing system, and an understanding of their dynamics is fundamental not only for the interpretation of stratigraphic data, but increasingly for prediction and modelling of basin fills (Hovius, 1998; Paola, 2000; Jones & Frostick, 2002; Carvajal & Steel, 2006; Carroll *et al*., 2006).

Variable rates of sediment yield and transfer to, and through, sedimentary basins are difficult to quantify within present landscapes, and even harder to evaluate from ancient stratigraphic successions. In the first case, we can observe present events but we miss their long-term significance due to a necessarily limited temporal perspective. In the second case, we cannot reconstruct the exact sequence of processes from source to sink lying at the origin of specific volumes of sediment. Studies of landscape evolution in tectonically active regions provide insights on how geomorphic processes and variables provide their source input to the stratigraphic machine. Such studies are carried out by geophysical methods, remote sensing, numerical modelling and geochemical proxies (see Leeder, 2011 and references therein), but they offer only a large-scale view, integrated over long times and on a regional to subcontinental basis. The significance of single, local events is lost in this perspective. The direct analysis of proximal depositional systems thus remains the most reliable key to infer which triggers and physical processes act on landscape change and sediment routing in the most proximal tracts of clastic dispersal (e.g. André, 1986; Eaton *et al*., 2003; Lancaster & Casebeer, 2007). The stratigraphic record, after all, is still the best way to find out what has actually been going on (Miall, 1995).

Depositional landforms such as talus cones, colluvial aprons, and especially alluvial fans, which are the largest and longest-lived, represent sediment traps in the immediate proximity of highland sources (Fig. 11). In geomorphic terms, the common trait to these depositional systems is given by their occurrence at transitions between two principal landscape zones, where the general conditions for sediment transport change abruptly (Harvey, 2010). The competence and capacity of transport processes are strongly reduced at topographic boundaries between steep mountain slopes and flatter footslopes and at the unconfinement of channel/canyon systems issued from highlands over valley floors. Sediment storage generally involves the coarsest fractions, but a few examples of alluvial fans built by significant or prevalent mud-grade deposits are reported in the literature (e.g. Legget *et al*, 1966; Wasson, 1977; Nakayama, 1999). The efficiency of

sediment storage within these zones affects also processes and morphologies that take place farther downstream or downslope. In general, under conditions of excess power for sediment transport (Bull, 1979), sediment tends to bypass or to be removed from proximal depositional systems, which are thus directly coupled with more distal components in the chain of clastic dispersal (Harvey 1992, 1997; Brunsden, 2001; Macklin & Lewin, 2003; Larsen *et al.*, 2004). This translates into faster and potentially less selective sediment supply basinward, at least through part of the system, and in a closer reflection of quantities (and changes) in sediment yield from hinterland sources. This sediment input signal is of great importance if one considers that bedrock and small drainage basins in highland regions are much more efficient in yielding sediment than larger basins (Fournier, 1960; Leeder, 1991; Milliman & Syvitski, 1992). By contrast, under conditions of reduced power or of increased sediment availability, prevalent deposition takes place in proximal depositional systems, which thus function as local buffers to the chain of dispersal. On geologic time scales, relief is gradually eroded, coarse-clastic sediment supply is reduced or shut down, and catchment expansion and integration can shift local sedimentary dynamics toward those typical of fluvial systems (lower sediment-water ratios). Locations that once hosted mountain-front alluvial fans can thus become river-dominated, eventually joining an integrated river network.

Catchment size and geology and the general geomorphic framework regulate the volume and dynamics of colluvial and fan systems, and thus their efficiency and persistence as buffers to sediment dispersal. For large alluvial fans, volumes of stored sediment are elevated enough to preserve long records of environmental change in catchment/highland regions. As mentioned in section 1.2, the challenge for the interpretation of these records lies in our not yet clear picture of how alluvial fans
respond to local tectonics and to climate change. For systems developed in proximity to marine or lacustrine basins (coastal fans and fan deltas), base-level changes add to the possible allogenic controls. The difference between measured sediment delivery to ocean basins and estimated upland denudation has been ascribed partly to differences in techniques of data generation, to long-term sediment trapping in large floodplain systems and delta tops (Milliman & Meade, 1983; Hovius, 1998; Stanley & Hait, 2000), but recently also to sediment storage along areas of gradient change between hinterlands and lowlands, whether or not actively subsiding (Leeder, 1991; Allen, 2008). A potential problem in modelling sediment transport and landscape evolution in such areas, for example, is due to the adoption of linear diffusive processes to represent rates of sediment transfer (Flemings & Jordan, 1989; Leeder, 1991; Paola *et al.*, 1992; Paola, 2000). Equations are usually based on the assumption that deposition is governed by relations between changing slope gradients and laws of sediment transport or hydraulic settling for bedload and washload in channels. Modelling by means of the diffusion equation, in particular, has been assumed both theoretically and experimentally to be a valid first-order approximation for the time-averaged behaviour of alluvial rivers (e.g. Paola *et al.*, 1992), which are considered to carry out most of the geomorphic work on sediments in simulations of large continental basins and basin margins. However, sediment transport in proximal basinal settings generally occurs through environments which have nothing much to do with ordinary 'rivers', and through processes commonly unrelated to turbulent channel flows. Consequently, we have not really adequately integrated these initial tracts of the sediment routing system into general basin models. Even the rates of sediment

yield from small mountain catchments cannot be considered linear, since they are often controlled by irregular processes dependent on specific geomorphic thresholds (e.g. Ohmori & Shimazu, 1994; Allen & Hovius, 1998; Blair, 1999b). Furthermore, in consideration of what has been discussed in section 1.4, it should be considered that the mechanics and frequency of sedimentary events in proximal depositional systems vary irregularly with the nature of catchment bedrock. For all these reasons, the incorporation of alluvial fans and slope systems into large-scale models of basin evolution faces particular challenges which still need to be qualitatively addressed.

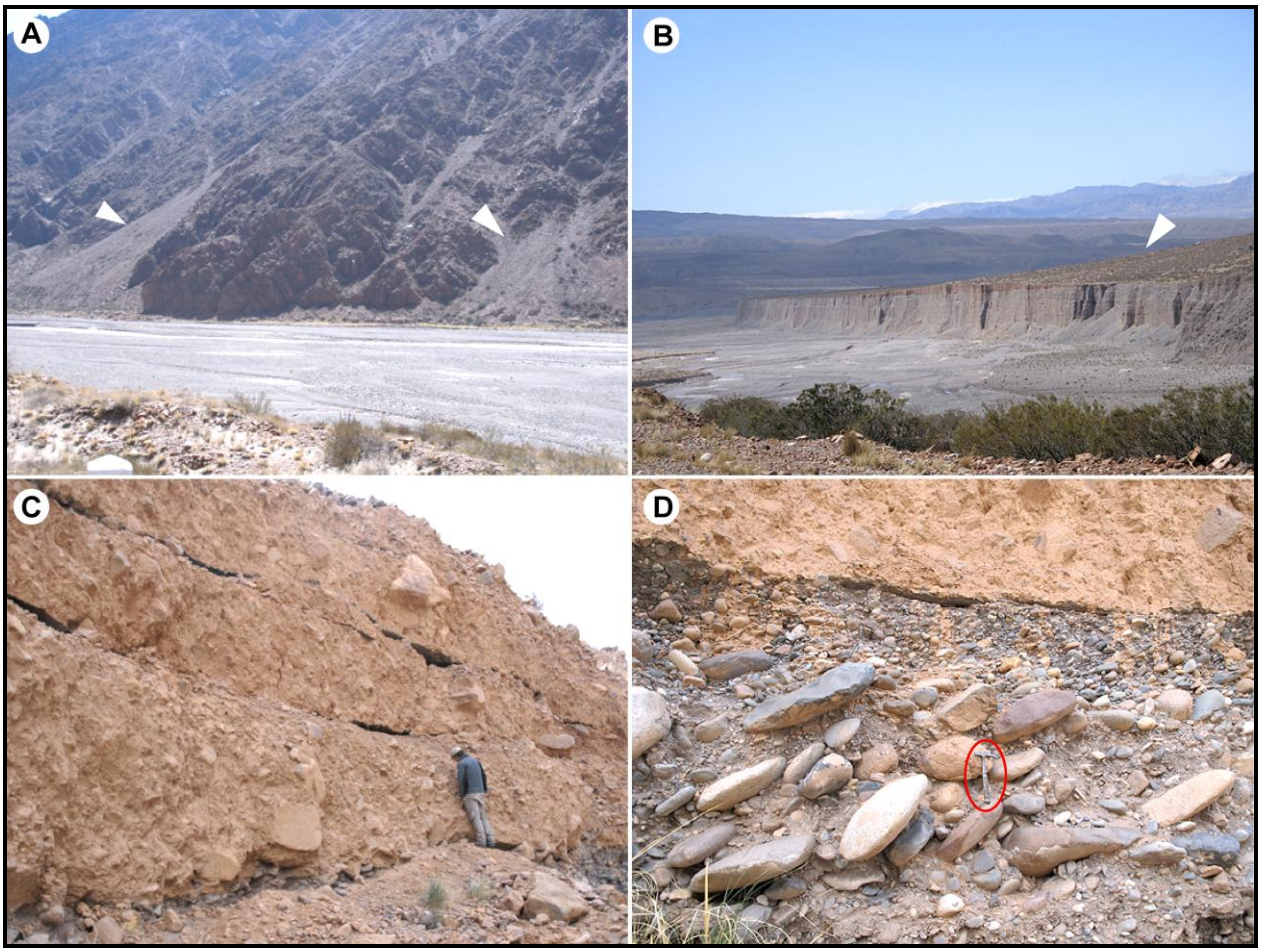

Figure 11 *- Small- and large-scale interactions in the clastic routing system; Mendoza River Valley, central Cordillera Frontal, Argentina. The Mendoza River is sourced by an Andean catchment, joins the Desaguadero River downstream and finally drains to the Atlantic margin of South America.(A) Gravelly talus cones (white pointers) retain coarse sediment at the topographic confluence between the channel belt and confining bedrock slopes. (B) The high course of the Mendoza River is laterally confined by alluvial fans (white pointer), which control the river position and the rate of sediment input from lateral highland sources. (C) Mass-flow deposits exposed laterally to the channel belt (M. Cartigny for scale). (D) Imbricated fluvial gravel (hammer for scale) overlain by debris-flow deposits of an alluvial fan prograding from the valley side.*

1.6 THESIS OUTLINE

The intended purpose of this research program was to explore alluvial-fan and colluvial depositional systems at the margins of continental basins in order to gain insights into the relative importance of allogenic controls on sedimentation and local geologic context. The chosen examples are widely distributed along the geochronological scale, ranging from Late Miocene to Quaternary and still presently active. This broad chronological perspective offers a good balance between observations carried out in settings where the original geomorphic context is partly lost, and where the available database spans long time intervals, and settings where it is possible to gain basically only a snapshot of presently active processes, but with high confidence to link them to local geological conditions.

Most of this thesis is based on field observations. There are still relevant gaps in our knowledge of alluvial fans and colluvial systems. This is due both to the relatively little work carried out in these settings, and especially to the frequent development of general 'theories' on such systems, which has often steered past research along paths later revealed poorly productive, or too generalistic. The amount of numerical modelling done on alluvial fans is minimal, since we do not yet have a critical mass of observations to produce reliable digital landscapes and derived stratigraphies. In fact, part of the stratigraphic data contained here will be used to calibrate a digital stratigraphic model of catchment denudation and alluvial-fan development, in order to verify its accuracy prior to the systematic exploration of further numerical scenarios. Research on colluvial sedimentology is at a beginning stage, and fieldwork is thus the indicated approach to contribute fundamental ideas.

The starting motivation for this work was offered by preliminary field observations in the Teruel Basin (central Spain), according to which stratal architectures in alluvial-fan conglomerates along the basin margin might be characterized by a Milankovitch-controlled stratigraphic pattern. **Chapter 2** consists of work carried out in cooperation with H. Abels, H. Abdul Aziz and F. Hilgen (Utrecht University), exploring the fundamental hypothesis that orbitally forced climate change governed hydrologic processes and sedimentation in the area. A clear relationship between facies cycles in distal mudflat to shallow lacustrine domains (*Prado Section*) and wet/dry climate phases was to be ascertained in order to understand the local palaeoenvironmental context, before applying it to interbedded distal-fan units.

Chapter 3 presents a detailed discussion of the regular facies relationships between distal alluvial-fan sedimentation and stratal patterns within the lower Prado Section, in collaboration with H. Abels, F. Hilgen and P. De Boer (Utrecht University). The conceptual premise is based on the common observation that patterns of sedimentation in alluvial fans are usually not regular, since they are related to a stochastic combination of catchment denudation rates and high-magnitude meteorological events. The many geomorphic thresholds inherent to fan-catchment systems generally do not consent the development of a highly predictable, organized stratigraphy. The information gathered from the Prado Section provides a rare opportunity to view recurrent facies relationships between fan strata and distal deposits in a chronological and palaeoclimatic framework of high-resolution for the Late Miocene. A conceptual model of climate-driven sedimentation can thus be extended from basinal environments to a more proximal domain.

Chapter 4, co-authored by G. Chong Díaz (Universidad Catolica del Norte, Antofagasta) and P. De Boer (Utrecht University), explores the complexity and heterogeneity of an extensive colluvial apron in the coastal piedmont of the Atacama Desert, northern Chile. The potential of the study area was noticed during field surveys in search of possible fan systems to associate to the Teruel case. The unusual opportunity to analyze these slope sediments was given by an abandoned roadcut that stretches along the entire studied piedmont. This provided full accessibility to slope surfaces and vertical stratigraphic exposures at footslopes. Coupled observations of active slope processes and morphology and of the resultant facies associations consented to define distinct slope sectors, and to derive a general model for morphologically controlled colluvial sedimentation. The additional value of this study is given by the notable rarity of detailed published research on colluvial sedimentation in arid environments. The great diversity of processes and facies associations encountered in the different slope sectors offers the possibility to apply selected observations from this study to similar depositional settings developed in dry highlands under a variety of morphological contexts.

Chapter 5 returns to the Teruel Basin and offers a zoomed-in analysis on the sedimentary dynamics of the alluvial fan discussed in chapter 3 from a climate perspective. The bipartite stratigraphic architecture of the alluvial fan suggests a possible relationship between the time succession of dominant depositional processes and unroofing of the palaeocatchment, whose stratigraphy is still partially accessible in outcrops on the adjacent basin margin. Whereas sedimentary signatures described in chapter 3 clearly show a climate imprint, this study explores the hypothesis that catchment geology is the ultimate control on which particular processes will take place and on what kinds of strata will carry the possible allogenic signatures.

Chapter 6 offers a coupled sedimentological and taphonomic analysis of the Collecurti paleontological site (Colfiorito Basin, central Italian Apennines) conducted in cooperation with P. Mazza (Universitá degli Studi di Firenze). This bonebed achieved the status of a fundamental marker for the Middle Pleistocene macrofaunal turnover in the Mediterranean. Its importance is due to the concentration and excellent preservation of various mammalian taxa in a piedmont setting where fossilization would commonly be a rare occurrence. An analysis of process sedimentology in the stratigraphic interval of the bonebed considers the hypothesis that a debrisflow might have transported disconnected bones from an upslope catchment, while quickly burying several other carcasses that were already lying on site. If the ultimate controls on the sedimentary event were related to the general geology and palaeogeography of the basin margin, it should be possible to predict the occurrence of analogue bonebeds elsewhere in similar intermontane troughs of the Apennines.

The final **chapter 7** provides an integrated overview of individual chapter conclusions and offers some general insights derived from this thesis which might be applied in forthcoming research.

REFERENCES

Abrahams, A.D., Parsons, A.J. and **Hirsh, P.J.** (1985) Hillslope gradient – particle size relations: evidence for the formation of debris slopes by hydraulic processes in the Mojave Desert. *Journal of Geology*, **93**, 347-357.

Allen, P.A. (2008) Time scales of tectonic landscapes and their sediment routing systems. In: *Landscape Evolution: Tectonics over Different Time and Space Scales* (Eds. K. Gallagher, S.J. Jones and J. Wainwright), Geological Society of London Special Publication, **296**, 7-28.

Allen, P.A. and **Hovius, N.** (1998) Sediment supply from landslide-dominated catchments: implications for basin-margin fans. *Basin Research*, **10**, 19-35.

Anadón, P., Cabrera, L., Colombo, F., Marzo, M. and **Riba, O.** (1986) Syntectonic intraformational unconformities in alluvial fan deposits, eastern Ebro Basin margins (NE Spain). In: *Foreland Basins* (Eds. P.A. Allen and P. Homewood), IAS Special Publication, **8**, 259-271.

André, M.-F. (1986) Dating slope deposits and estimating rates of rock wall retreat in northwest Spitsbergen by lichenometry. *Geografiska Annaler, ser. A*, **68**, 65-75.

Arrowsmith, J.R., Pollard, D.D. and **Rhodes, D.D.** (1996) Hillslope development in areas of active tectonics. *Journal of Geophysical Research*, **101, B3**, 6255-6275.

Ballance, P.F. (1984) Sheet-flow-dominated gravel fans of the non-marine middle Cenozoic Simmler Formation, central California. *Sedimentary Geology*, **38**, 337-359.

Berthling, I., Etzelmüller, B., Isaksen, K. and **Sollid, J.L.** (2000) Rock glaciers on Prins Karls Forland. II: GPR soundings and the development of internal structures. *Permafrost and Periglacial Processes*, **11**, 357-369.

Bertran, P. and **Texier, J.-P.** (1994) Structures sédimentaires d'un cone de flots de débris (Vars, Alpes Françaises Méridionales). *Permafrost and Periglacial Processes*, **5**, 155-170.

Bertran, P., Francou, B. and **Texier, J.-P.** (1995) Stratified slope deposits: the stone-banked sheets and lobes model. In: *Steepland Geomorphology* (Ed. O. Slaymaker), pp. 147-169, John Wiley & Sons Ltd.

Blackwelder, E. (1928) Mudflow as a geologic agent in semi-arid mountains. *Geological Society of America Bulletin,* **39**, 465-484.

Blair, T.C. (1999a) Cause of dominance by sheetflood vs. debris-flow processes on two adjoining alluvial fans, Death Valley, California. *Sedimentology*, **46**, 1015-1028.

Blair, T.C. (1999b) Alluvial fan and catchment initiation by rock avalanching, Owens Valley, California. *Geomorphology*, **28**, 201-221.

Blair, T.C. and **Bilodeau, W.L.** (1988) Development of tectonic cyclothems in rift, pull-apart and foreland basins: sedimentary response to episodic tectonism. *Geology*, **16**, 517-520.

Blair, T.C. and **McPherson, J.G.** (1992) The Trollheim alluvial fan and facies model revisited. *Geological Society of America Bulletin*, **104**, 762-769.

Blair, T.C. and **McPherson, J.G.** (1994a) Alluvial fans and their natural distinction from rivers based on morphology, hydraulic processes, sedimentary processes, and facies assemblages. *Journal of Sedimentary Research*, **A64**, 450-489.

Blair, T.C. and **McPherson, J.G.** (1994b) Alluvial Fan Processes and Forms. In: *Geomorphology of Desert Environments* (Eds A.D. Abrahams and A.J. Parsons), pp. 354-402, Chapman & Hall, London.

Blikra, L.H. and **Nemec, W.** (1998) Postglacial colluvium in western Norway: depositional processes, facies and palaeoclimatic record. *Sedimentology*, **45**, 909-959.

Blikra, L.H. and **Selvik, S.F.** (1998) Climatic signals recorded in snow avalanche-dominated colluvium in western Norway: depositional facies successions and pollen records. *The Holocene*, **8**, 631-658.

Blissenbach, E. (1954) Geology of alluvial fans in semiarid regions. *Geological Society of America Bulletin*, **65**, 175-190.

Bouma, A.H., Normark, W.R. and **Barnes, N.E.** (1985) COMFAN: Needs and Initial Results. In: *Submarine Fans and Related Turbidite Systems* (Eds. A.H. Bouma, W.R. Normark and N.E. Barnes), pp. 7-11, Springer-Verlag, New York.

Bridge, J.S. (2003) *Rivers and Floodplains: Forms, Processes and Sedimentary Record*. Blackwell Publishing, Oxford.

Broscoe, A.J. and **Thomson, S.** (1969) Observations on an alpine mudflow, Steele Creek, Yukon. *Canadian Journal of Earth Sciences*, **6**, 219-229.

Brunsden, D. (2001) A critical assessment of the sensitivity concept in geomorphology. *Catena*, **42**, 99-123.

Bryhni, I. (1978) Flood deposits in the Hornelen Basin, west Norway (Old Red Sandstone). *Norsk Geologisk Tidskkrift*, 58, 273-300.

Bull, W.B. (1963) Alluvial-fan deposits in western Fresno County, California. *Journal of Geology*, **71**, 243-251.

Bull, W.B. (1964) *Alluvial Fans and Near-Surface Subsidence in Western Fresno County, California.* US Geological Survey Professional Paper, 437-A.

Bull, W.B. (1972) Recognition of alluvial fan deposits in the stratigraphic record. In: *Recognition of Ancient Sedimentary Environments* (Eds. Rigby, J.K. and Hamblin, W.K.), pp. 63-83, SEPM Special Publication, 16, Tulsa (OK).

Bull, W.B. (1977) The alluvial-fan environment. *Progress in Physical Geography*, **1**, 63-83.

Bull, W.B. (1979) Threshold of critical power in streams. *Geological Society of America Bulletin*, **90**, 453-464.

Carroll, A.R., Chetel, L.M. and **Elliot Smith, M.** (2006) Feast to famine: sediment supply control on Laramide basin fill. *Geology*, **34**, 197-200.

Carvajal, C.R. and **Steel, R.J.** (2006) Thick turbidite successions from supply-dominated shelves during sea-level highstand. *Geology*, **34**, 665-668.

Chandler, R.J. (1973) The inclination of talus, arctic talus terraces, and other slopes composed of granular materials. *Journal of Geology*, **81**, 1-14.

Chawner, W.D. (1935) Alluvial fan flooding, the Monrose, California flood of 1934. *Geographical Review*, **25**, 77-88.

Choe, M.Y. and **Chough, S.K.** (1988) The Hunghae Formation, SE Korea: Miocene debris aprons in a back-arc intraslope basin. *Sedimentology*, **35**, 239-255.

Church, M. and **Ryder, J.M.** (1972) Paraglacial sedimentation: A consideration of fluvial processes conditioned by glaciation. *Geological Society of America Bulletin*, **83**, 3059-3072.

Clark, S.H.B., Foster, H.L. and **Bartsch, S.R.** (1972) Growth of a talus cone in the western Chugach Mountains, Alaska. *Geological Society of America Bulletin*, **83**, 227-230.

Conway, W.M. (1893) Exploration in the Mustagh Mountains. *Geographical Journal*, **2**, 289-303.

Crews, S.G. and **Ethridge, F.G.** (1993) Laramide tectonics and humid alluvial fan sedimentation, NE Uinta Uplift, Utah and Wyoming. *Journal of Sedimentary Petrology*, **63**, 420-436.

Darby, D.A., Whittecar, G.R., Barringer, R.A. and **Garrett, J.R.** (1990) Alluvial lithofacies recognition in a humid-tropical setting. *Sedimentary Geology*, **67**, 161-174.

Davis, W.M. (1898) *Physical Geography*. Ginn & Co., Boston & London, 428 pp.

Davis, W.M. (1938) Sheet floods and streamfloods. *Geological Society of America Bulletin*, **49**, 1337-1416.

Dávila, F.M. and **Astini R.A.** (2003) Early Middle Miocene broken foreland development in the southern Central Andes: evidence for extension prior to regional shortening. *Basin Research*, **15**, 379-396.

DeCelles, P.G., Gray, M.B., Ridgway, K.D., Cole, R.B., Pivnik, D.A., Pequera, N. and **Srivastava, P.** (1991) Controls on synorogenic alluvial-fan architecture, Beartooth Conglomerate (Palaeocene), Wyoming and Montana. *Sedimentology*, **38**, 567-590.

DeCelles, P.G., Tolson, R.B., Graham, S.A., Smith, G.A., Ingersoll, R.V., White, J., Schmidt, C.J., Rice, R., Moxon, I., Lemke, L., Handschy, J.W., Follo, M.F., Edwards, D.P., Cavazza, W., Caldwell, M. and **Bargar, E.** (1987) Laramide thrust-generated alluvial-fan sedimentation, Sphinx Conglomerate, southwestern Montana. *AAPG Bulletin*, **71**, 135-155.

Davis, W.M. (1909) *Geographical Essays*. University of Michigan Library.

Denny, C.A. (1965) *Alluvial Fans in the Death Valley Region, California and Nevada.* US Geological Survey Professional Paper, 466.

Derbyshire, E. and **Owen, L.A.** (1990) Quaternary Alluvial Fans in the Karakoram Mountains. In: *Alluvial Fans: A Field Approach* (Eds. A.H. Rachocki and M. Church), pp. 27-53, John Wiley & Sons.

Dorn, R.I. (2009) The Role of Climatic Change in Alluvial Fan Development. In: *Geomorphology of Desert Environments* (Eds A.J. Parsons and A.D. Abrahams), 2nd Edition, Springer Science, pp. 723-742.

Drew, F. (1873) Alluvial and lacustrine deposits and glacial records of the Upper Indus Basin. *Quarterly Journal of the Geological Society of London*, **29**, 441-471.

Dutton, C.E. (1880) *Report on the Geology of the High Plateaus of Utah*. U.S. Government Printing Office, Washington (D.C.).

Eaton, L.S., Morgan, B.A., Kochel, R.C. and **Howard, A.D.** (2003) Role of debris flows in long-term landscape denudation in the central Appalachians of Virginia. *Geology*, 31, 339-342.

Fenneman, N.M. (1908) Some features of erosion by unconcentrated wash. *Journal of Geology*, 16, 746-754.

Flemings, P.B. and **Jordan, T.E.** (1989) A synthetic stratigraphic model of foreland basin development. *Journal of Geophysical Research*, B94, 3851-3866.

Flint, S. and **Turner, P.** (1988) Alluvial fan and fan-delta sedimentation in a forearc extensional setting: the Cretaceous Coloso Basin of northern Chile. In: *Fan Deltas: Sedimentology and Tectonic Settings* (Eds. W. Nemec and R.J. Steel), pp. 387-398, Blackie & Son, Glasgow.

Fournier, F. (1960) *Climat et erosion: la relation entre l'erosion du sol par l'eau et les precipitations atmospheriques.* Presses Universitaire de France, Paris.

Francou, B. (1990) Stratification mechanisms in slope deposits in high subequatorial mountains. *Permafrost and Periglacial Processes*, **1**, 249-253.

Friend, D.A., Phillips, F.M., Campbell, S.W., Liu, T. and **Sharma, P.** (2000) Evolution of desert colluvial boulder slopes. *Geomorphology*, **36**, 19-45.

Frostick, L.E. and **Reid, I.A.N.** (1989) Climatic versus tectonic controls on fan sequences: lessons from the Dead Sea, Israel. *Journal of the Geological Society of London*, **146**, 527-538.

Fryxell, F.M. and **Horberg, L.** (1943) Alpine mudflows in Grand Teton National Park, Wyoming. *Geological Society of America Bulletin*, **54**, 457-472.

Galloway, W.E. and **Hobday, D.K.** (1996) *Terrigenous Clastic Depositional Systems*, Springer-Verlag, Berlin.

Gardner, J.S. (1980) Frequency, magnitude, and spatial distribution of mountain rockfalls and rockslides in the Highwood Pass area, Alberta, Canada. In: *Thresholds in Geomorphology* (Eds. D.R. Coates and J.D. Vitek), pp. 267-295, Allen & Unwin, London.

Gardner, T.W., Ritter, J.B., Shuman, C.A., Bell, J.C., Sasowsky, K.C. and **Pinter, N.** (1991) A periglacial stratified slope deposit in the Valley and Ridge Province of central Pennsylvania, USA: sedimentology, stratigraphy and geomorphic evolution. *Permafrost and Periglacial Processes*, **2**, 141-162.

Gernon, T.M., Field, M. and **Sparks, R.S.J.** (2009) Depositional processes in a kimberlite crater: the Upper Cretaceous Orapa South Pipe (Botswana). *Sedimentology*, **56**, 623-643.

Gerson, R. (1982) Talus relicts in deserts: a key to major climatic fluctuations. *Israel Journal of Earth Sciences*, **31**, 123-132.

Gilbert, G.K. (1882) Contributions to the History of Lake Bonneville. *U.S. Geological Survey, Second Annual Report*, pp. 167-200.

Gloppen, T.G. and **Steel, R.J.** (1981) The deposits, internal structure and geometry in six alluvial fan – fan delta bodies (Devonian, Norway) – a study in the significance of bedding sequences in conglomerates. In: *Recent and Ancient Nonmarine Depositional Environments: Models for Exploration* (Eds. F.G. Ethridge and R.M. Flores), SEPM Special Publication, **31**, 49-69.

Hartley, A.J., Mather, A.E., Jolley, E. and **Turner, P.** (2005) Climatic controls on alluvial-fan activity, Coastal Cordillera, northern Chile. In: *Alluvial Fans: Geomorphology, Sedimentology, Dynamics* (Eds. A.M. Harvey, A.E. Mather and M. Stokes), Geological Society of London Special Publication, **251**, 95-115.

Hartley, A.J., Weissmann, Go.S., Nichols, G.J. and **Warwick, G.L.** (2010) Large distributive fluvial systems: characteristics, distribution, and controls on development. *Journal of Sedimentary Research*, **80**, 167-183.

Harvey, A.M. (1987) Patterns of Quaternary aggradational and dissectional landform development in the Almeria region, southeast Spain: a dry-region, tectonically active landscape. *Die Erde*, **118**, 193-215.

Harvey, A.M. (1992) Process interactions, temporal scales and the development of gully systems: Howgill Fells, northwest England. *Geomorphology*, **5**, 323-344.

Harvey, A.M. (1997) Coupling between hillslope gully systems and stream channels in the Howgill Fells, northwest England: temporal implications. *Geomorphology; Relief, Processes, Environment*, **1**, 3-20.

Harvey, A.M. (2003) The Response of Dry-Region Alluvial Fans to Quaternary Climatic Changes. In: *Desertification in the Third Millennium* (Eds. A.S. Alsharhan, W.W. Wood, A.S. Goudie, A. Fowler and E.M. Abdellatif), pp. 75-90, Swets & Zeitlinger Publishers, Lisse, the Netherlands.

Harvey, A.M. (2010) Local Buffers to the Sediment Cascade: Debris Cones and Alluvial Fans. In: *Sediment Cascades: An Integrated Approach* (Eds. T. Burt and R. Allison), pp. 153-180, John Wiley & Sons.

Harvey, A.M. and **Wells, S.G.** (2003) Late Quaternary variations in alluvial fan geomorphic and sedimentologic processes, Soda Lake basin, eastern Mojave Desert, California. In: *Paleoenvironments and Paleohydrology of the Mojave and southern Great Basin Deserts* (Eds Y. Enzel, S.G. Wells and N. Lancaster), GSA Special Paper, **368**, 207-230.

Harvey, A.M., Mather, A.E. and **Stokes, M.** (2005) Alluvial fans: geomorphology, sedimentology, dynamics – introduction. A review of alluvial-fan research. In: *Alluvial Fans: Geomorphology, Sedimentology, Dynamics* (Eds. A.M. Harvey, A.E. Mather and M. Stokes), Geological Society of London Special Publication, **251**, 1-7.

Heward, A.P. (1978) Alluvial fan sequence and megasequence models: with examples from Westphalian D – Stephanian B coalfields, northern Spain. In: *Fluvial Sedimentology* (Ed. A.D. Miall), Canadian Society of Petroleum Geologists Memoir, **5**, 669-702.

Hétu, B. (1990) Évolution récente d'un talus d'éboulis en milieu forestier, Gaspésie, Québec. *Géographie physique et Quaternaire*, **44**, 199-215.

Hétu, B. (1995) Le litage des éboulis stratifiés cryoniveaux en Gaspésie (Quebec, Canada): Role de la sédimentation nivéo-éolienne et des transits supraniveaux. *Permafrost and Periglacial Processes*, **6**, 147-171.

Hétu, B. and **Gray, J.T.** (2000) Effects of environmental change on scree slope development throughout the postglacial period in the Chic-Choc Mountains in the northern Gaspésie Peninsula, Québec. *Geomorphology*, **32**, 335-355.

Higgs, R. (1990) Sedimentology and tectonic implications of Cretaceous fan-delta conglomerates, Queen Charlotte Islands, Canada. *Sedimentology*, **37**, 83-103.

Hinchliffe, S. (1999) Timing and significance of talus slope reworking, Trotternish, Skye, northwest Scotland. *The Holocene*, **9**, 483-494.

Hinchliffe, S., Ballantyne, C.K. and **Walden, J.** (1998) The structure and sedimentology of relict talus, Trotternish, northern Skye, Scotland. *Earth Surface Processes and Landforms*, **23**, 545-560.

Hirst, J.P.P. and **Nichols, G.J.** (1986) Thrust tectonic controls on alluvial sedimentation patterns, southern Pyrenees. In: *Foreland Basins* (Eds. P.A. Allen and P. Homewood), IAS Special Publication, **8**, 153-164.

Hogg, S.E. (1982) Sheetfloods, sheetwash, sheetflow, or...? *Earth Science Reviews*, **18**, 59-76.

Hooke, R., LeB. (1967) Processes on arid-region alluvial fans. *Journal of Geology*, **75**, 438-460.

Hooke, R., LeB. (1972) Geomorphic evidence for Late-Wisconsin and Holocene Tectonic Deformation, Death Valley, California. Geological Society of America Bulletin, **83**, 2073-2098.

Hooke, R.LeB. (1987) Mass-movements in semiarid environments and the morphology of alluvial fans. In: *Slope Stability* (Eds. M.G. Anderson and K.S. Richards), pp. 505-529, John Wiley & Sons.

Hoppe, G. and Eckman, S. (1964) A note on the alluvial fans of Lattjovagge, Swedish Lapland. *Geografiska Annaler*, **46**, 338-342.

Hovius, N.H. (1998) Controls on sediment supply by large rivers. In: *Relative Role of Eustasy, Climate and Tectonism in Continental Rocks* (Eds. K.W. Shanley and P.J. McCabe), SEPM Special Publication, **59**, 3-16.

Imeson, A.C., Kwaad, F.J.P.M. and **Mücher, H.J.** (1980) Hillslope processes and deposits in forested areas of Luxembourg. In: *Timescales in Geomorphology* (Eds. R.A. Cullingford, D.A. Davidson and J. Lewin), pp. 31-42. John Wiley & Sons, Chichester.

Johnson, A.M. and **Rahn, P.H.** (1970) Mobilization of debris flows. *Zeitschrift für Geomorphologie, Supplementband*, **9**, 168-186.

Jomelli, V. (1999) Dépots d'avalanches dans les Alpes Françaises: géométrie, sédimentologie et géodynamique dpuis le petit age glaciaire. *Géographie physique et Quaternaire*, **53**, 199-209.

Jones, S.J. and **Frostick, L.E.** (2002) Introduction. In: *Sediment Flux to Basins: Causes, Controls and Consequences* (Eds. S.J. Jones and L.E. Frostick) Geological Society of London Special Publications, **191**, 1-4.

Jordan, T.E. (1981) Thrust loads and foreland basin evolution, Cretaceous, western United States. *AAPG Bulletin*, **65**, 2506-2520.

King, L.C. (1957) The uniformitarian nature of hillslopes. *Transactions of the Royal Geological Society of Edinburgh*, **17**, 81-102.

King, L.C. (1967) *The Morphology of the Earth*. 2nd edition, Oliver & Boyd, Glasgow.

Kirkby, M.J. and **Statham, I.** (1975) Surface stone movement and scree formation. *Journal of Geology*, **83**, 349-362.

Kochel, R.C., Miller, J.R. and **Ritter, D.F.** (1997) Geomorphic response to minor cyclic climate changes, San Diego County, California. *Geomorphology*, **19**, 277-302.

Kostaschuk, R.A., MacDonald, G.M. and **Putnam, P.E.** (1986) Depositional process and alluvial fan – drainage basin morphometric relationships near Banff, Alberta, Canada. *Earth Surface Processes and Landforms*, **11**, 471-484.

Kotarba, A. (1997) Formation of high-mountain talus slopes related to debris-flow activity in the High Tatra Mountains. *Permafrost and Periglacial Processes*, **8**, 191-204.

Kozhurin, A., Acocella. V., Kyle, P.R., Lagmay, F.M., Melekestsev, I.V., Ponomareva, V., Rust, D., Tibaldi, A., Tunesi, A., Corazzato, C., Rovida, A., Sakharov, A., Tengonciang, A. and **Uy, H.** (2006) Trenching studies of active faults in Kamchatka, eastern Russia: Palaeoseismic, tectonic and hazard implications. *Tectonophysics*, **417**, 285-304.

Krumbein, W.C. (1942) Flood deposits of Arroyo Seco, Los Angeles County, California. *Geological Society of America Bulletin*, **53**, 1355-1402.

Lancaster, S.T. and **Casebeer, N.E.** (2007) Sediment storage and evacuation in headwater valleys at the transition between debris-flow and fluvial processes. *Geology*, **35**, 1027-1030.

Larsen, I.J., Schmidt, J.C. and **Martin, J.A.** (2004) Debris-fan reworking during low-magnitude floods in the Green River canyons of the eastern Unita Mountains, Colorado and Utah. *Geology*, **32**, 309-312.

Lawson, A.C. (1932) Rainwash erosion in humid regions. *Geological Society of America Bulletin*, **43**, 703-724.

Leeder, M.R. (1991) Denudation, vertical crustal movements and sedimentary basin infill. *Geologische Rundschau*, **80**, 441-458.

Leeder, M.R. (2011) Tectonic sedimentology: sediment systems deciphering global to local tectonics. *Sedimentology*, **58**, 2-86.

Legget, R.F., Brown, R.J.E. and **Johnston, G.H.** (1966) Alluvial fan formation near Aklavik, Northwest Territories, Canada. *Geological Society of America Bulletin*, **77**, 15-30.

Levson, V.M. and **Rutter, N.W.** (2000) Influence of bedrock geology on sedimentation in Pre-Late Wisconsinan alluvial fans in the Canadian Rocky Mountains. *Quaternary International*, **68-71**, 133-146.

Luckman, B.H. (1988) Debris accumulation patterns on talus slopes in Surprise Valley, Alberta. *Géographie physique et Quaternaire*, **42**, 247-278.

Luckman, B.H. (1992) Debris flows and snow avalanche landforms in the Lairig Ghru, Cairngorn Mountains, Scotland. *Geografiska Annaler, ser. A*, **74**, 109-121.

Lustig, L.K. (1965) *Clastic Sedimentation in Deep Springs Valley California*. US Geological Survey Professional Paper, 352-F.

Mack, G.H. and **Rasmussen, K.A.** (1984) Alluvial-fan sedimentation of the Cutler Formation (Permo-Pennsylvanian) near Gateway, Colorado. *Geological Society of America Bulletin*, **95**, 109-116.

Macklin, M.G. and **Lewin, J.** (2003) River sediments, great floods and centennial-scale Holocene alluvial fan systems. *Journal of Quaternary Science*, **18**, 102-105.

Mason, A.C. and **Foster, H.L.** (1956) Extruded mudflow hills of Nirasaki, Japan. *Journal of Geology*, **64**, 74-83.

Massari, F. (1984) Resedimented conglomerates of a Miocene fan-delta complex, southern Alps, Italy. In: *Sedimentology of Gravels and Conglomerates* (Eds. W. Nemec and R.J. Steel), Canadian Society of Petroleum Geologists Memoir, **10**, 259-278.

Matsuoka, N. and **Sakai, H.** (1999) Rockfall activitiy from an alpine cliff during thawing periods. *Geomorphology*, **28**, 309-328.

McCalpin, J.P. and **Nishenko, S.P.** (1996) Holocene paleoseismicity, temporal clustering, and probabilities of future large (M>7) earthquakes on the Wasatch fault zone, Utah. *Journal of Geophysical Research*, **101, B3**, 6233-6253.

Mc Gowen, J.H. (1979) Alluvial Fan Systems. In: *Depositional and Groundwater Flow Systems in the Exploration for Uranium* (Eds. W.E. Galloway, C.W. Kreitler and J.H. McGowen), pp. 43-79, Texas Bureau of Economic Geology.

McGowen, J.H. and **Groat, C.G.** (1971) *Van Horn Sandstone, West Texas: An Alluvial Fan Model for Mineral Exploration*. Texas Bureau of Economic Geology Report, 72.

McPherson, J.G. and **Blair, T.C.** (1993) Alluvial Fans: Fluvial or Not? Abstracts and Keynote Addresses, 5th International Conference of Fluvial Sedimentology, Brisbane, Australia, pp. K33-K41.

McPherson, J.G., Shanmugam, G. and **Moiola, R.J.** (1987) Fan-deltas and braid deltas: Varieties of coarse-grained deltas. *Geological Society of America Bulletin*, **99**, 331-340.

McPherson, J.G., Shanmugam, G. and **Moiola, R.J.** (1988) Fan deltas and braid deltas: conceptual problems. In: *Fan Deltas: Sedimentology and Tectonic Settings* (Eds. W. Nemec and R.J. Steel), pp. 14-22, Blackie and Son, Glasgow.

Mellere, D. (1993) Thrust-generated, back-fill stacking of alluvial fan sequences, south-central Pyrenees, Spain (La Pobla de Segur Conglomerates). In: *Tectonic Controls and Signatures in Sedimentary Successions* (Eds. L.E. Frostick and R.J. Steel), IAS Special Publication, **20**, 259-276.

Miall, A.D. (1995) Whither Stratigraphy? *Sedimentary Geology*, **100**, 5-20.

Miall, A.D. (1996) *The Geology of Fluvial Deposits: Sedimentary Facies, Basin Analysis, and Petroleum Geology*. Springer, New York.

Milliman, J.D. and **Meade, R.H.** (1983) World-wide delivery of river sediment to the oceans. *Journal of Geology*, **91**, 1-21.

Milliman, J.D. and **Syvitski, J.P.M.** (1992) Geomorhic/tectonic control of sediment discharge to the ocean: the importance of small mountainous rivers. *Journal of Geology*, **100**, 525-544.

Moscariello, A. (2005) Exploration potential of the mature southern North Sea basin margins: some unconventional plays based on alluvial fan and fluvial fan sedimentation models. In: *Petroleum Geology:*

North-West Europe and Global Perspectives – Proceedings of the 6th Petroleum Geology Conference (Eds. A.G. Doré and B.A. Vining), pp. 595-605, The Geological Society, London.

Moscariello, A., Marchi, L., Maraga, F. and **Mortara, G.** (2002) Alluvial fans in the Italian Alps: sedimentary facies and processes. In: *Flood and Megaflood Processes and Deposits: Recent and Ancient Examples* (Eds I.P. Martini, V.R. Baker and G. Garzón), IAS Special Publication, **32**, 141-166.

Mutti, E. and **Normark, W.R.** (1987) Comparing Examples of Modern and Ancient Turbidite Systems: Problems and Concepts. In: *Marine Clastic Sedimentology* (Eds. J.K. Leggett and G.G. Zuffa), pp. 1-38, Graham & Trotman Publishers, UK.

Nakayama, K. (1999) Sand- and mud-dominated alluvial-fan deposits of the Miocene Seto Porcelaine Clay Formation, Japan. In: *Fluvial Sedimentology VI* (Eds. N.D. Smith and J. Rogers), IAS Special Publication, **28**, 393-407.

Nelson, A.R. (1992) Lithofacies analysis of colluvial sediments – An aid in interpreting the recent history of Quaternary normal faults in the Basin and Range province, western United States. *Journal of Sedimentary Petrology*, **62**, 607-621.

Nemec, W. (1990a) Aspects of sediment movement on steep delta slopes. In: *Coarse-Grained Deltas* (Eds A. Colella and D.B. Prior), IAS Special Publication, **10**, 29-73.

Nemec, W. (1990b) Deltas – remarks on terminology and classification. In: *Coarse-Grained Deltas* (Eds A. Colella and D.B. Prior), IAS Special Publication, **10**, 3-12.

Nemec, W. and **Kazanci, N.** (1999) Quaternary colluvium in west-central Anatolia: sedimentary facies and palaeoclimatic significance. *Sedimentology*, **46**, 139-170.

Nemec, W. and **Muszynski, A.** (1982) Volcaniclastic alluvial aprons in the Tertiary of Sofia District (Bulgaria). *Annales Societatis Geologorum Poloniae*, **52**, 239-303.

Nemec, W. and **Postma, G.** (1993) Quaternary alluvial fans in southwestern Crete: sedimentation processes and geomorphic evolution. In: *Alluvial Sedimentation* (Eds. M. Marzo and C. Puigdefabregas), IAS Special Publication, **17**, 235-276.

Nemec, W. and **Steel, R.J.** (1988) What is a fan delta and how do we recognize it? In: *Fan Deltas: Sedimentology and Tectonic Settings* (Eds. W. Nemec and R.J. Steel), pp. 3-13, Blackie and Son, Glasgow.

Nemec, W., Steel, R.J., Porebski, S.J. and **Spinnangr, A.** (1984) Domba Conglomerate, Devonian, Norway: Process and lateral variability in a mass flow-dominated lacustrine fan-delta. In: *Sedimentology of Gravels and Conglomerates* (Eds. W. Nemec and R.J. Steel), Canadian Society of Petroleum Geologists Memoir, **10**, 279-294.

Nichols, G.J. (1987) Syntectonic alluvial fan sedimentation, southern Pyrenees. *Geological Magazine*, **124**, 121-133.

Nichols, G.J. and **Hirst, J.P.P.** (1998) Alluvial fans and fluvial distributary systems, Oligo-Miocene, northern Spain: contrasting processes and products. *Journal of Sedimentary Research*, **68**, 879-889.

Nichols, G. and **Thompson, B.** (2005) Bedrock lithology control on contemporaneous alluvial fan facies, Oligo-Miocene, southern Pyrenees, Spain. *Sedimentology*, **52**, 571-585.

Nichols, K.K., Bierman, P.R., Eppes, M.C., Caffee, M., Finkel, R. and **Larsen, J.** (2005) Late Quaternary history of the Chemehuevi Mountain piedmont, Mojave Desert, deciphered using ^{10}Be and ^{26}Al. *American Journal of Science*, **305**, 345-368.

Nilsen, T.H. (1982) Alluvial fan deposits. In: *Sandstone Depositional Environments* (Eds P.A. Scholle and P. Spearing), AAPG Memoir, **31**, 49-86.

Normark, W.R. (1985) Local morphologic controls and effects of basin geometry on flow processes in deep marine basins. In: *Provenance of Arenites* (Ed. G.G. Zuffa), pp. 47-63, Reidel Publishing Company, Dordrecht, the Netherlands.

Ohmori, H. and **Shimazu, H.** (1994) Distribution of hazard types in a drainage basin and its relation to geomorphological setting. *Geomorphology*, **10**, 95-106.

Pack, F.J. (1923) Torrential potential of desert waters. *Pan-American Geologist*, **40**, 349-356.

Paola, C. (2000) Quantitative models of sedimentary basin filling. *Sedimentology*, **47** (supplement), 121-178.

Paola, C., Heller, P.L. and **Angevine, C.L.** (1992) The large-scale dynamics of of grain size variation in alluvial basins. 1. Theory. *Basin Research*, **4**, 73-90.

Pawelec, H. (2006) Origin and palaeoclimatic significance of the Pleistocene slope covers in the Cracow Upland, southern Poland. *Geomorphology*, **74**, 50-69.

Pederson, J., Pazzaglia, F. and **Smith, G.** (2000) Ancient hillslope deposits: missing links in the study of climate controls on sedimentation. *Geology*, **28**, 27-30.

Peltier, L.C. (1950) The geographic cycle in periglacial regions as it is related to climatic geomorphology. *Annals of the American Association of Geographers*, **40**, 214-236.

Penck, W. (1953) *The Morphological Analysis of Landforms*. Macmilla & Co. Ltd.

Pérez, F.L. (1989) Talus fabric and particle morphology on Lassen Peak, California. *Geografiska Annaler, ser. A*, **71**, 43-57.

Pérez, F.L. (1993) Talus movement in the high equatorial Andes: a synthesis of ten years of data. *Permafrost and Periglacial Processes*, **4**, 199-215.

Pope, R.J.J. and **Millington, A.C.** (2000) Unravelling the patterns of alluvial fan development using mineral magnetic analysis: examples from the Sparta Basin, Lakonia, southern Greece. *Earth Surface Processes and Landforms*, 25, 601-615.

Porat, N., Wintle, A.G., Amit, R. and **Enzel, Y.** (1996) Late Quaternary earthquake chronology from luminescence dating of colluvial and alluvial deposits of the Arava Valley, Israel. *Quaternary Research*, 46, 107-117.

Postma, G. (1984) Mass-flow conglomerates in a submarine canyon: Abrioja fan-delta, Pliocene, southeast Spain. In: *Sedimentology of Gravels and Conglomerates* (Eds. W. Nemec and R.J. Steel), Canadian Society of Petroleum Geologists Memoir, **10**, 237-257.

Postma, G. and **Cruickshank, C.** (1988) Sedimentology of a late Weichselian to Holocene, terraced fan delta, Varangerfjord, northern Norway. In: *Fan Deltas: Sedimentology and Tectonic Settings* (Eds. W. Nemec and R.J. Steel), pp. 144-157, Blackie & Son, Glasgow.

Prior, D.B. and **Stephens, N.** (1972) Some movement patterns of temperate mudflows: examples from north-eastern Ireland. *Geological Society of America Bulletin*, **83**, 2533-2543.

Rachocki, A.H. (1990) The Leba River Alluvial Fan and its Palaeogeomorphological Significance. In: *Alluvial Fans: A Field Approach* (Eds. A.H. Rachocki and M. Church), pp. 305-317, John Wiley & Sons.

Rahn, P.H. (1967) Sheetfloods, streamfloods, and the formation of pediments. *Annals of the Association of American Geographers*, **57**, 593-604.

Rapp, A. (1960) Recent development of mountain slopes in Kärkevagge and surroundings, northern Scandinavia. *Geografiska Annaler*, 42, 65-200.

Rigby, J.K. and **Hamblin, W.K.** (1972) *Recognition of Ancient Sedimentary Environments*. SEPM Special Publication, 16, Tulsa (OK).

Ritter, J.B., Miller, J.R. and **Husek-Wulforst, J.** (2000) Environmental controls on the evolution of alluvial fans in Buena Vista Valley, north central Nevada, during late Quaternary time. *Geomorphology*, **36**, 63-87.

Roberts, N. (1995) Climatic forcing of alluvial fan regimes during the late Quaternary in the Konya Basin, south central Turkey. In: *Mediterranean Quaternary River Environments* (Eds. J. Lewin, M.G. Macklin and J.C. Woodward), pp. 207-217, Balkema, Rotterdam.

Ryder, J.M. (1971) Some aspects of the morphometry of paraglacial alluvial fans in south-central British Columbia. *Canadian Journal of Earth Sciences*, **8**, 1252-1264.

Sanders, D. (2010) Sedimentary facies and progradational style of a Pleistocene talus-slope succession, Northern Calcareous Alps, Austria. *Sedimentary Geology*, **228**, 271-283.

Sanders, D., Ostermann, M. and **Kramers, J.** (2009) Quaternary carbonate-rocky talus slope successions (Eastern Alps, Austria): sedimentary facies and facies architecture. *Facies*, **55**, 345-373.

Sass, O. and **Krautblatter, M.** (2007) Debris flow-dominated and rockfall-dominated talus slopes: genetic models derived from GPR measurements. *Geomorphology*, **86**, 176-192.

Sass, O., Krautblatter, M. and **Morche, D.** (2007) Rapid lake infill following major rockfall (bergsturtz) events revealed by ground-penetrating radar (GPR) measurements, Reintal, German Alps. *The Holocene*, **17**, 965-976.

Savigear, R.A. (1952) Some observations on slope development in South Wales. *Transactions of the Institute of British Geographers*, **18**, 31-51.

Saussure, H.B., De (1796) *Voyages Dans les Alpes; Précédes d'un Essai sur l'Historie Naturelle des Environs de Genéve*. Lous Fauche-Borel, Neuchatel, 594 pp.

Scapozza, C., Lambiel, C., Baron, L., Marescot, L. and **Reynard, E.** (2011) Internal structure and permafrost distribution in two alpine periglacial talus slopes, Valais, Swiss Alps. *Geomorphology*, **132**, 208-221.

Schumm, S.A. (1977) *The Fluvial System*. John Wiley & Sons, New York, 338 pp.

Selby, M.J. (1971) Slopes and their development in an ice-free, arid area of Antarctica. *Geografiska Annaler*, **53**, 235-245.

Sharp, R.P. (1942) Mudflow levees. *Journal of Geomorphology*, **5**, 222-227.

Sharp, R.P. and **Nobles, L.H.** (1953) Mudflow of 1941 at Wrightwood, southern California. *Geological Society of America Bulletin*, **64**, 547-560.

Sletten, K. and **Blikra, L.H.** (2007) Holocene colluvial (debris-flow and water-flow) processes in eastern Norway: stratigraphy, chronology and palaeoenvironmental implications. *Journal of Quaternary Science*, **22**, 619-635.

Smith, G. (1754) Dreadful storm in Cumberland. *Gentleman's Magazine*, **24**, 464-467.

Smith, G.A. (2000) Recognition and significance of streamflow-dominated piedmont facies in extensional basins. *Basin Research*, **12**, 399-411.

Sohn, Y.K., Rhee, C.W. and **Kim, B.C.** (1999) Debris flow and hyperconcentrated flood-flow deposits in an alluvial fan, northwestern part of the Cretaceous Yongdong Basin, central Korea. *Journal of Geology*, **107**, 111-132.

Stanistreet, I.G. and **McCarthy, T.S.** (1993) The Okavango Fan and the classification of subaerial fan systems. *Sedimentary Geology*, **85**, 115-133.

Stanley, D.J. and **Hait, A.K.** (2000) Deltas, radiocarbon dating, and measurements of sediment storage and subsidence. *Geology*, **28**, 295-298.

Steel, R.J. and **Wilson, A.C.** (1975) Sedimentation and tectonism (?Permo-Triassic) on the margin of the North Minch Basin, Lewis. *Journal of the Geological Society of London*, **131**, 183-200.

Steel, R.J., Mæhle, S., Nilsen, H., Røe, S.L. and **Spinnangr, A.** (1977) Coarsening-upward cycles in the alluvium of the Hornelen Basin (Devonian) Norway: Sedimentary response to tectonic events. *Geological Society of America Bulletin*, **88**, 1124-1134.

Surrell, A. (1870) *Etude sur les Torrentes des Hautes-Alpes*. Imprimerie Cusset, Paris, 2nd Edition.

Tanner, L.H. and **Hubert, J.F.** (1991) Basalt breccias and conglomerates in the Lower Jurassic McCoy Brook Formation, Fundy Basin, Nova Scotia: differentiation of talus and debris-flow deposits. *Journal of Sedimentary Petrology*, **61**, 15-27.

Texier, J.-P. and **Meireles, J.** (2003) Relict mountain slope deposits of northern Portugal: facies, sedimentogenesis and environmental implications. *Journal of Quaternary Science*, **18**, 133-150.

Todd, S.P. (1989) Stream-driven, high-density gravelly traction carpets: possible deposits in the Trabeg Conglomerate Formation, SW Ireland and some theoretical considerations of their origin. *Sedimentology*, **36**, 513-530.

Turner, A.K. (1996) Colluvium and Talus. In: *Landslides – Investigation and Mitigation* (Eds. A.K. Turner and R.L. Schuster), pp. 525-554, National Academy Press.

Turner, B.R. and **Makhlouf, I.** (2002) Recent colluvial sedimentation in Jordan: fans evolving into sand ramps. *Sedimentology*, **49**, 1283-1298.

Twidale, C.R. (1959) Some problems of slope development. *Australian Journal of Earth Sciences*, **6**, 131-147.

Van Steijn, H. (2011) Stratified slope deposits: periglacial and other processes involved. In: *Ice-Marginal and Periglacial Processes and Sediments* (Eds. I.P. Martini, H.M. French and A. Pérez-Alberti), Geological Society of London Special Publication, **354**, 213-226.

Van Steijn, H., Van Brederode, L.E. and **Goedheer, G.J.** (1984) Stratified slope deposits of the gréze-litée type in the Ardéche Region in the south of France. *Geografiska Annaler, ser. A*, **66**, 295-305.

Van Steijn, H., Bertran, P., Francou, B., Hétu, B. and **Texier, J.-P.** (1995) Models for the genetic and environmental interpretation of stratified slope deposits: review. *Permafrost and Periglacial Processes*, **6**, 125-146.

Wagreich, M. and **Strauss, P.E.** (2005) Source area and tectonic control on alluvial-fan development in the Miocene Fohnsdorf intramontane basin, Austria. In: *Alluvial Fans: Geomorphology, Sedimentology, Dynamics* (Eds. A.M. Harvey, A.E. Mather and M. Stokes), Geological Society of London Special Publication, **251**, 207-216.

Waldron, H.H. (1967) Debris flow and erosion control problems caused by ash eruptions of Irazu volcano, Costa Rica. *US Geological Survey Bulletin*, 1241-I.

Wasson. R.J. (1977) Last-glacial alluvial fan sedimentation in the Lower Derwent Valley, Tasmania. *Sedimentology*, **24**, 781-799.

Wasson, R.J. (1979) Sedimentation history of the Mundi Mundi alluvial fans, western New South Wales. *Sedimentary Geology*, **22**, 21-51.

Waters, J.V., Jones, S.J. and **Armstrong, H.A.** (2010) Climatic controls on late Pleistocene alluvial fans, Cyprus. *Geomorphology*, **115**, 228-251.

Webb, J.A. and **Fielding, C.R.** (1999) Debris Flow and Sheetflood Fans of the Northern Prince Charlers Mountains, East Antarctica. In: *Varieties of Fluvial Form* (Eds. A.J. Miller and A. Gupta), pp. 317-341, John Wiley & Sons Ltd.

Weissmann, G.S., Hartley, A.J., Nichols, G.J., Scuderi, L.A., Olson, M.E., Buehler, H.A. and **Massengill, L.C.** (2011) Alluvial facies distributions in continental sedimentary basins – Distributive fluvial systems. In: *From River to Rock Record* (Eds S.K. Davidson, S. Leleu and C.P. North), SEPM Special Publication, **97**, 327-356.

Welch, D.M. (1980) Substitution of space for time in a study of slope development. *Journal of Geology*, 78, 234-239.

Wells, N.A. (1984) Sheet debris flow and sheetflood conglomerates in Cretaceous cool-maritime alluvial fans, South Orkney Islands, Antarctica. In: *Sedimentology of Gravels and Conglomerates* (Eds. W. Nemec and R.J. Steel), Canadian Society of Petroleum Geologists Memoir, **10**, 133-146.

Wells, S.G. and **Dohrenwend, J.C.** (1985) Relict sheetflood bed forms on late Quaternary alluvial-fan surfaces in the southwestern United States. *Geology*, **13**, 512-516.

Welsh, A. and **Davies, T.** (2010) Identification of alluvial fans susceptible to debris-flow hazards. *Landslides*, **8**, 183-194.

White, S.E. (1949) Processes of erosion on steep slopes of Oahu, Hawaii. *American Journal of Science*, **247**, 168-186.

Wilford, D.J., Sakals, M.E., Innes, J.L. and **Sidle R.C.** (2005) Fans with forests: contemporary hydrogeomorphic processes on fans with forests in west central British Columbia, Canada. In: *Alluvial Fans: Geomorphology, Sedimentology, Dynamics* (Eds. A.M. Harvey, A.E. Mather and M. Stokes), Geological Society of London Special Publication, **251**, 25-40.

Wilmsen, M., Fürsich, F.T. and **Taheri, J.** (2009) The Shemshal Group (Lower Middle Jurassic) of the Binalud Mountains, NE Iran: stratigraphy, depositional environments and geodynamic implications. In:

South Caspian to Central Iran Basins (Eds. M.-F. Brunet, M. Wilmsen and J.W. Granath), Geological Society of London Special Publication, **312**, 175-188.

Winder, C.G. (1965) Alluvial cone construction by alpine mudflow in a humid temperate region. *Canadian Journal of Earth Sciences*, **2**, 270-277.

Wood, A. (1942) The development of hillside slopes. *Proceedings of the Geological Association of London*, **53**, 128-140.

Zanchetta, G., Sulpizio, R. and **Di Vito, M.A.** (2004) The role of volcanic activity and climate in alluvial fan growth at volcanic areas: an example from southern Campania (Italy). *Sedimentary Geology*, **168**, 249-280.

Zurawek, R., Zyszkowski, E. and **Górecki, A.** (2005) Topographic control of periglacial slope covers, Slęza Massif, southwest Poland: a statistical approach. *Permafrost and Periglacial Processes*, **16**, 241-248.

"*The scientist, by the very nature of his committment,*
creates more and more questions, never fewer.
Indeed the measure of our intellectual maturity, one philosopher suggests,
is our capacity to feel less and less satisfied with our answers to better problems. "

G.W. Allport,
Becoming, 1955

Chapter 2

Orbital climate forcing in mudflat to marginal lacustrine deposits in the Miocene Teruel Basin (northeast Spain)

H.A. Abels, H. Abdul Aziz, D. Ventra & F.J. Hilgen

ABSTRACT

Upper Miocene mudflat and marginal lacustrine sediments were deposited on the fringes of an alluvial-fan system in the low-gradient, endorheic southern Teruel Basin, northeast Spain. The 147-m-thick Prado succession consists of 55 meter-scale sedimentary cycles displaying clastic-rich and a carbonate-rich intervals. The clastic-rich parts are weakly pedogenically modified, red to yellow-orange mudstones and are interpreted as deposits of a well-drained mudflat. The carbonate-rich sediments consist of calcretes, marls, and muddy limestones. The calcretes range from dispersed nodules to massive nodular and are interpreted to be of pedogenic or phreatic origin. The marls and muddy limestones are light- to dark-gray and rich in organic matter, shell fragments, and gastropods. They are interpreted as ephemeral pond to marginal lacustrine deposits. A composite sedimentary cycle model is presented summarizing the different facies and their vertical distribution throughout the Prado area. On a 10 m scale, distinct stratigraphic intervals show lithologic trends representing alternating wetter and drier paleoenvironments. Cycle characteristics are laterally consistent, whereby limestone beds pinch out towards the basin margin and thicken towards the central parts of the 10-km-wide and 20-km-long sub-basin.

The high-resolution magnetostratigraphy resolves four normal-polarity and four reversed-polarity intervals that are straightforwardly correlated to chron interval C5n.2n to C5Ar.1r in the ATNTS04 time scale. The resulting age control indicates a duration of 19 to 23 kyr for the meter-scale facies cycles, suggesting control by precession-driven climate change. An astronomical tuning is established by correlating each cycle to the La2004 precession curve using recently recalibrated ages for the polarity reversals as a starting point. The resulting astronomical ages for the reversals in the Prado section are consistent with the astronomically calibrated magnetostratigraphy and cyclostratigraphy of the marine Monte dei Corvi section in Italy. At Prado, three intervals with thicker-than-average cycle thickness most likely reflect obliquity influence during 405 kyr eccentricity minima when precession amplitudes are low. This corroborates the orbital forcing hypothesis of the lithofacies cycles and the astronomical tuning of the Prado succession. The combined magnetostratigraphy and cyclostratigraphy method applied in this study shows the high potential of this method for detecting orbital climate forcing in continental successions.

2.1. INTRODUCTION

The recognition of astronomically forced sedimentary cyclicity in continental basin fills can considerably enhance both relative and absolute age control (Kent & Olsen, 1999; Hinnov, 2000), understanding of the sedimentology (Meyers *et al.*, 2001; Weedon, 2003), quantification of rates and duration of sedimentary, climatic, and paleontological processes (Fischer & Roberts, 1991; Meyers *et al.*, 2001), and possibilities for correlation within and beyond the basin (Van Vugt *et al.*, 1998). The influence of astronomical climate forcing has now been demonstrated and suggested for various types of lacustrine successions with different geological ages (Bradley, 1929; Eardley *et al.*, 1973; Olsen, 1986; Astin, 1990; Fischer & Roberts, 1991; Abdul Aziz *et al.*, 2000; Reinhardt & Ricken, 2000; Luzón *et al.*, 2002). The detection of astronomical cyclicity requires sufficiently long sediment records (Olsen, 1986; Abdul Aziz *et al.*, 2003) or a first-order reliable age control, that can be magnetostratigraphic (Van Vugt *et al.*, 2001; Kruiver *et al.*, 2002; Abdul Aziz *et al.*, 2004) or radiometric dating of ash layers intercalated within the sediment record (Pietras & Carroll, 2006; Meyers & Sageman, 2007; Machlus *et al.*, 2008). The geomagnetic polarity time scales of the Neogene, and recently the Paleogene, have been considerably improved by astronomically calibrated ages for polarity reversals (Lourens *et al.*, 2004; Pälike *et al.*, 2006; Westerhold *et al.*, 2008). These improved ages allow detection of orbital climate forcing in continental sediment records and construction of astrochronologies in even relatively short sedimentary successions (Van Vugt *et al.*, 1998; Steenbrink *et al.*, 1999; Abdul Aziz *et al.*, 2004; Abels *et al.*, 2009), thus avoiding statistical analyses that are reported to often contain a certain degree of subjectivity (Wilkinson *et al.*, 2003; Meyers & Sageman, 2007; Bailey & Smith, 2008).

The Upper Miocene Cascante section in the southern Teruel Basin (NE Spain) displays very regular, meter-scale cyclicity of alternating red-brown, distal-alluvial-fan mudstones and palustrine to shallow lacustrine limestones. High-resolution magnetostratigraphic age control, substantiated by mammal biostratigraphy, revealed that this meter-scale cyclicity is related to the climatic precession cycle (Abdul Aziz *et al.*, 2004). Carbonate microfacies analysis of limestone beds of successive meter-scale cycles revealed the additional presence of larger-scale lake-level variations that are related to the short and long eccentricity cycles. These results allowed construction of an astrochronology for this part of the basin (Abels *et al.*, 2009). Roughly time-equivalent deposits are present in the Prado area, 6.5 kilometers NNW of the Cascante section and located in the same structural segment of the Teruel Basin, but at the opposite basin margin.

The succession at Prado shows different lithological characteristics than the succession in the Cascante area, being dominated by yellow-orange to red-brown mudstones and calcretes from (relatively) well-drained mudflats and marginal lacustrine calcareous mudstones and muddy limestones. In analogy with the Cascante section, the Prado section is characterized by meter-scale, mudstone - limestone cycles over its whole stratigraphic extent, but with a higher variability in sedimentological characteristics, both laterally and vertically. On a larger scale, stratigraphic intervals dominated by limestones or calcareous mudstones alternate with intervals characterized by prevalent mudstone deposits. The rough time equivalence with the Cascante succession is known from formation-scale correlations in the relatively small basin and from preliminary small-mammal biostratigraphic results. A direct, bed-to-bed, lithological correlation to the Cascante section can, however, not be achieved, either physically or by matching lithological characteristics.

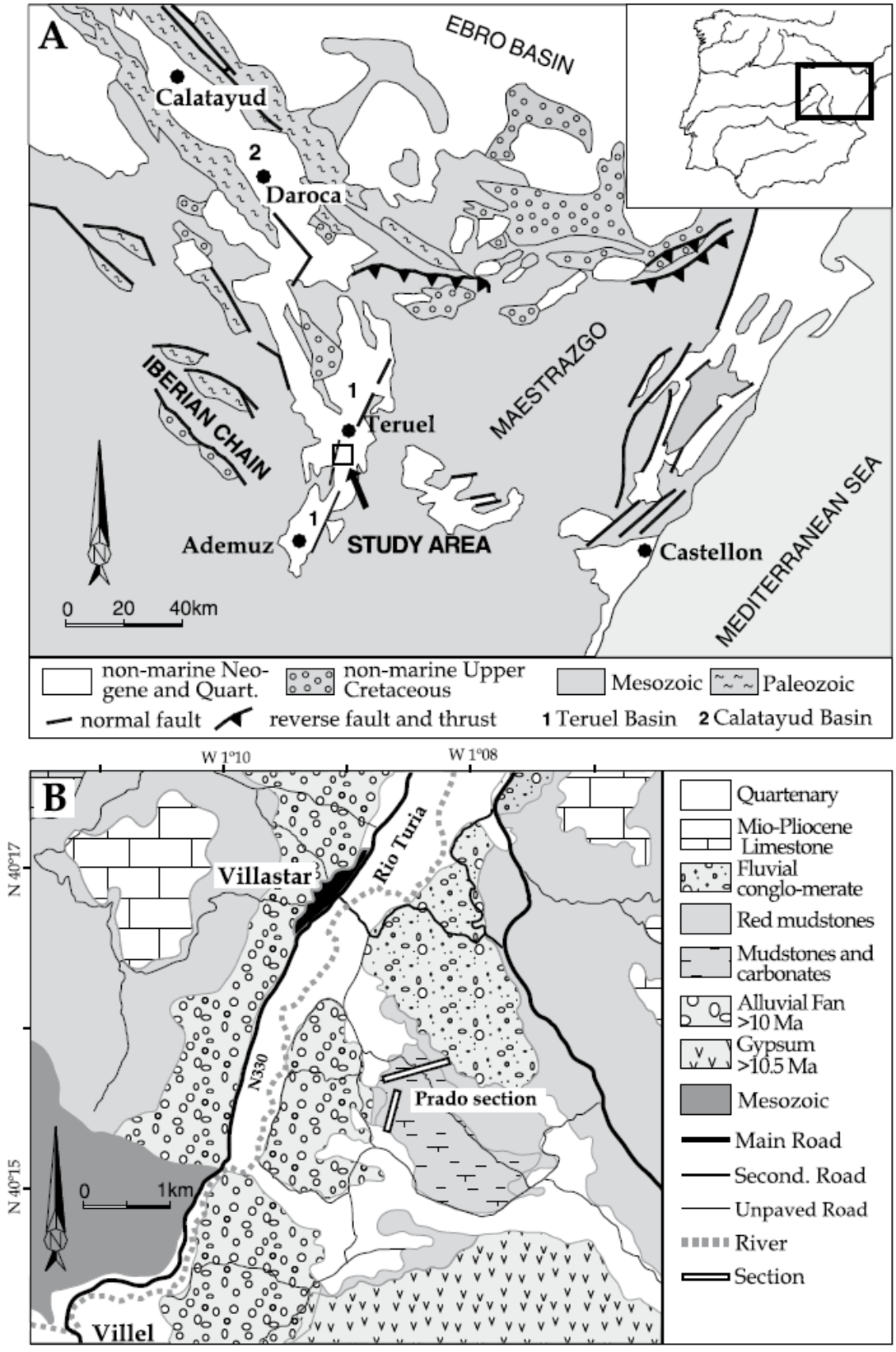

Figure 1 *- Geographic location of the Prado area within (A) Spain and (B) the southern part of the Teruel Basin. (C) Schematic geological map of the Prado area; the position and extent of the two transects making up the sedimentary log of the Prado Section are indicated.*

Therefore, detailed magnetostratigraphic sampling has been carried out to obtain a first-order age control that allows detecting orbital forcing within the Prado section, and, subsequently, constructing an independent astrochronological framework for this part of the Teruel Basin. The vertically and laterally more complex meter-scale cyclicity and dominant long-term changes in the sedimentary successions of the Prado area are expected to possibly reflect processes other than orbital forcing. Therefore, the construction of a high-resolution age model is essential to further investigate this possibility.

2.2. GEOLOGICAL SETTING

The Teruel Basin (Comunidad de Aragón, Teruel Province, NE Spain; Fig. 1) is a complex of axially linked, NNE-SSW oriented half grabens developed on top of the Central Iberian Range. After the main Paleogene constructive phases of the Iberian Range, the Teruel Basin formed as a result of reactivation of Mesozoic tectonic lineaments during E-W extension that started in the Early Miocene (Anadón & Moissenet, 1996). The Teruel Basin is approximately 100 km long and 15 km wide, and the main phase of deposition took place between Early Miocene and Late Pliocene (Anadón & Moissenet, 1996). Sedimentation occurred in an internally drained, semiarid, continental setting dominated by marginal to axial alluvial systems as well as lacustrine-palustrine domains of variable depth and extent (Broekman, 1983; Kiefer, 1988; Anadón *et al*., 1997). The basin fill is characterized by large-scale (> 40 m) alternations of red, alluvial siliciclastics and lacustrine carbonates or evaporites (Broekman *et al*., 1983; Kiefer, 1988; Anadón *et al*., 1997; Alonso-Zarza & Calvo, 2000). Both the Cascante and the Prado areas are located in the southern part of the Teruel Basin in the Teruel-Ademuz Sub-Basin (Fig. 1). This sub-basin is approximately 35 km long and 15 km wide and is flanked by a Mesozoic basement, composed of Triassic fine-grained siliciclastic and evaporitic rocks and Jurassic limestones. Miocene alluvial-fan conglomerates and breccias dominate along the basin margin and grade laterally, within a few kilometers, into fine-grained distal fan to mudflat and shallow lacustrine deposits in the more central part of this relatively small sub-basin (Kiefer, 1988). The Prado area is accessible from the N-330 from Teruel to Ademuz, via a dirt road east of Villastar (040°12′18″ N, 001°07′22″ W).

In the Prado area (~5 km^2), a dominantly siliciclastic succession is situated stratigraphically between the top of the Libros Gypsum Unit exposed in the southern part of the area (Anadón *et al*., 1997; Ortí *et al*., 2003), with an approximate age of 11 Ma (Abdul Aziz *et al.*, 2004), and a red mudstone unit with intercalated fluvial conglomerates in the northeast (Fig. 1). The sediments of the succession consist of red to yellow-orange mudstones, calcretes, and shallow lacustrine to palustrine limestones. The lateral continuity of exposures allows us to trace individual carbonate beds and mudstone color patterns over hundreds of meters from the northwest to the southeast across the area, while lateral trends from northeast to southwest can be studied over only tens of meters (Fig. 1). To the west, conglomerates and sandstones that were sourced by an adjacent alluvial fan along the western basin margin interfinger with the lower part of the stratigraphic succession in Prado. Paleocurrent directions indeed indicate a western to northwestern source. The fluvial conglomerates delimiting the top of the Prado section instead indicate a source in the north.

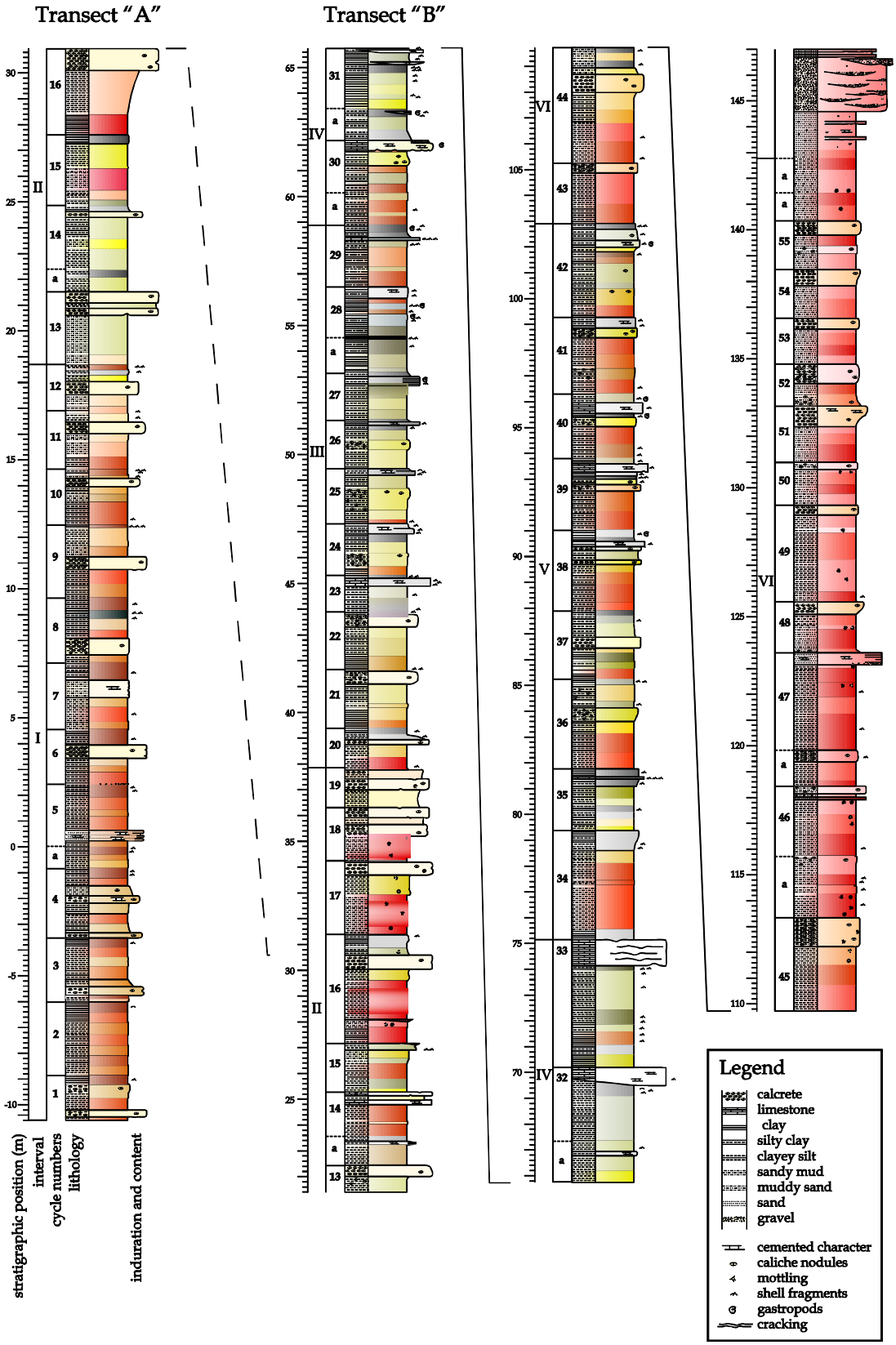

Figure 2 *- Detailed lithological log of the Prado Section along transects A and B (Fig. 1C). Stratigraphic positions, interval numbering and and cycle numbers are indicated; the dashed line indicates the correlation between the two transects; solid lines indicate continuation of the log.*

2.3. METHODS

2.3.1 General Methods

Stratigraphic thickness was measured by a Jacob's Staff. The lithological colors in this study comprise brownish black (7.5YR 3/1), dark red (10R 3/4-6), red (10R 4-5/6-8), (light) orange (2.5YR 6-7/6-8), pale orange (5YR 8/4), yellow orange (10YR 7-8/8), light-yellow orange (10YR 8/3-4), pale yellow (2.5Y 8/3-4), gray (5Y 4-6/1), and light gray (2.5Y 7-8/1) (Munsell, 1999). The qualifier *centimeter-scale* refers to a size between 1 and 3 cm, *millimeter-scale* to between 1 and 10 mm, and *sub-millimeter-scale* to less than 1 mm. Calcrete classification follows Machette (1985), as also applied by Wright and Tucker (1991). No petrographic tools were used to further distinguish between calcrete origins. Approximately 30 thin sections of palustrine limestones were studied for microfacies analysis.

2.3.2 Magnetostratigraphic Methods

The Prado section was sampled at average stratigraphic intervals of 35 cm (range 10 cm to 1 m). Samples were drilled using a water-cooled, electric drill powered by a portable generator. The characteristic remanent magnetization (ChRM) was determined by thermal demagnetization, using incremental heating steps of 20 and 30°C, carried out in a laboratory-built shielded furnace. The natural remanent magnetization (NRM) of 170 samples was measured on a vertically oriented 2G Enterprises DC SQUID cryogenic magnetometer (noise level 10^{-7} A/m) in a magnetically shielded room at the Niederlippach paleomagnetic laboratory of *Ludwig-Maximilians University* Munich, Germany. The NRM of the other 204 samples were measured on a horizontal 2G Enterprises DC SQUID cryogenic magnetometer (noise level 3 x 10^{-12} A/m) at the Paleomagnetic Laboratory Fort Hoofddijk, *Utrecht University*, the Netherlands, following the same analytical procedure. Demagnetization results are plotted on orthogonal vector diagrams (Zijderveld, 1967), and ChRM directions are calculated using principal component analysis (Kirschvink, 1980).

2.4. SEDIMENTOLOGY

2.4.1. The Prado Section

A continuous sedimentary log of the Prado Section (hereafter, PS; Figs. 1, 2) was recorded. Due to the structural dip towards the NNE, the section is a composite of two transects; the lower transect "A" trends laterally towards the ENE, and the upper transect "B" to the north (Fig. 1). The overall section is 155 m thick, and its base (040° 15′ 17″ N 001° 08′ 45″ W) is located about 730 meters SW from its top (040° 15′ 47″ N 001° 08′ 12″ W). The log represents the complete stratigraphy in the Prado area, which has been cross-checked by several logs in lateral transects. Moreover, the outcrops are excellently exposed, allowing intervals to be traced laterally over hundreds of meters.

Based on distinct facies associations, the section was subdivided into six intervals, labeled I to VI (Fig. 2). In total, 55 lithofacies cycles were counted and numbered from bottom to top (Fig. 2). Ten additional cycles were counted, with less distinct lithological characteristics; these are coded with an additional "a" following

the number of the cycle they are in. The sedimentological characteristics of each interval (I to VI) are reported below.

2.4.1.1. Interval I - Cycles 1 - 12

This interval is characterized mainly by dark red to red (clayey) siltstones with meter-scale intercalations of carbonate-enriched beds, with a few orange sandy and dark-red clayey mudstone horizons. The dark red to red clayey siltstones have a homogeneous character, commonly display millimeter to centimeter gray mottling, and occasionally show vague yellow-orange mottling. Dispersed millimeter-scale carbonate nodules occur. Gradual as well as sharp transitions occur to the meter-scale intercalations of the dark-red clayey mudstone horizons. These occur at a relatively regular basis every 2.5 to 3 meters and contain small (< 2 mm), thin-walled shell fragments. In most cases, the mudstones display sparse millimeter-scale, and occasionally centimeter-scale, gray and infrequently yellow-orange mottles and contain few, dispersed carbonate nodules.

The carbonate-enriched beds (in cycles 1, 3, 4a, 6, and 8 to 12; Fig. 2) are between 20 and 60 cm thick and are mainly pale-orange to orange with few light-gray mottles and have a dominantly silty matrix. These are relatively indurated, massive nodular beds that are occasionally horizontally brecciated at their tops. To the top of this interval, these beds are light-yellow-orange and have more frequently a very-fine sand matrix. We interpret these beds as calcretes that resemble Stage II and III calcretes according to the classification of Machette (1985). Levels slightly enriched in carbonate occur between these calcretes, with caliche nodules ranging from 5 to 20 mm in size, located just below or above the calcretes, but also as individual levels within the clayey siltstones. The carbonate-enriched beds, and to a lesser extent the calcretes, present a high lateral variability, changing in thickness over tens of meters or disappearing completely, suggesting a possible relation with grain-size distribution or indicating lateral variability of the paleoenvironment.

In the logged transect, two pale-orange, calcareous, fine-grained sandstones occur that have a clearly defined bottom and top and internally a thinner-bedded, centimeter-scale planar structure (cycles 5 and 7; Fig. 2). These sandstones are enriched in carbonate and appear as indurated levels. Here, the complete stratigraphic framework of this interval has not been worked out, because it is beyond the purpose of this study. Also, their occasional occurrence does not seem to have a consistent relation with the cyclic sedimentary dynamics observed.

Dark-red and, in cycle 8, gray mudstones with shell fragments occur regularly at an average stratigraphic distance of 2.5 m. In the lower part of interval I, these cycles are around 3 m thick, while in the upper part their thickness is less than 2.5 m. Calcretes and carbonate-enriched beds in the lower part of this interval do not reveal a consistent stratigraphic relation with these cycles. Higher up, above cycle 9, calcretes occur directly below the dark-red or gray clay layers. Lithofacies cycles in interval I were counted on the basis of the occurrence of dark-red mudstones.

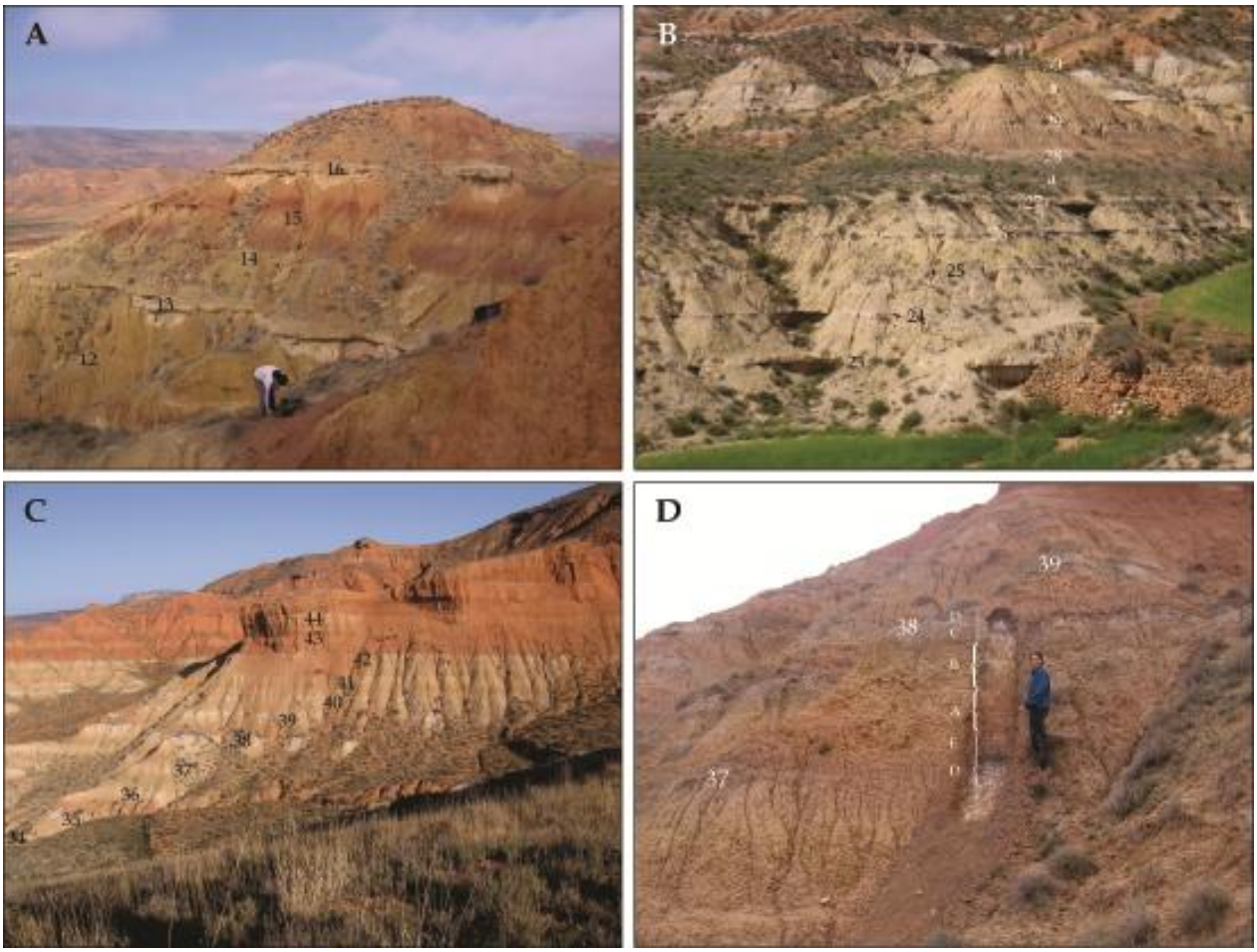

Figure 3 *- Photographs of the Prado section along the logged transects; see Figure 2 for scales. Cycle numbers are positioned on the most indurated layers, all carbonate-rich lithologies. (A) Cycles 12 to 16 in the top of the "A" transect. (B) Cycles 23 to 30 in the "B" transect. (C) Cycles 34 to 44 (with cycles 45 and 46 vaguely visible to the right) of the "B" transect. Above cycle 42, the second shift to well-drained floodplain sediments is visible. On top, an angular unconformity with Pleistocene conglomerates is present. (D) Cleaned surface across cycle 38 in the "B" transect as part of Part B. Lithologies A to E are indicated (Fig. 4).*

2.4.1.2. Interval II - Cycles 13 – 19

This interval includes the overlap between the "lower" and "upper" sub-logs that comprises cycles 13 to 16 (Figs. 3A, 2). Interval II is characterized by cycles consisting of red, orange, and light-yellow-orange, occasionally sandy, siltstones; light-gray, calcareous, clayey siltstones; limestones 20 to 80 cm thick; and gray to light-gray silty claystones.

The red sandy siltstones display sparse millimeter-scale light-gray and some orange-yellow mottling. The clayey siltstones below the limestone beds display variable thickness and show millimeter- to centimeter-scale yellow-orange mottling, which can intensify closer to the limestones. Limestone beds occur as nodular massive, relatively smooth calcretes. These have a light-yellow-orange color and display a relatively gradual base, which occasionally undulates smoothly, and a sharp(er) top. The matrix consists of silt- to sand-size grains, as well as one thin pebble layer in the bed of cycle 13. This bed is traced as the lateral equivalent of a thick conglomerate bed. Yellow centimeter-size mottling is common, and occasionally red millimeter-size spots occur. Also, more tabular limestone beds occur with sharp bases and tops. These tabular beds display

silt-size matrix, yellow mottles, and have abundant vertically oriented rhizocretions. These beds resemble palustrine limestones. Above the limestones, fining-upward trends from siltstone to silty claystone occur, accompanied by more gray colors and an increase in organic-matter content, yellow millimeter-scale mottles, and occasionally millimeter-scale shell fragments.

This interval comprises 10 or 11 lithofacies cycles, consisting of a mudstone and a limestone or calcareous part. Cycle thickness varies from 0.9 m (cycle 13a) to 4.2 m (cycle 16), with an average of 2.5 m.

2.4.1.3. Interval III - Cycles 20 - 29

This interval is characterized by light-gray to light-yellow-orange mudstones with sparse yellow-orange mottling and meter-scale intercalations of calcrete beds and light-gray marls and silty limestones (Fig. 3C). The calcretes are 20 to 50 cm thick and light-yellow-orange in color, with yellow-orange mottles in a silty matrix (cycles 20 to 22 and 24 to 26; Fig. 2). Their appearance varies from a dispersed and cemented nodular to nodular massive character with more gradual bases and relatively sharp tops. They reach Stage I to III according to the calcrete classification of Machette (1985). Laterally, calcrete beds grade from loose nodule layers to cemented beds, and reverse.

Calcretes in the lower part of this interval (cycles 19 to 22; Fig. 2) are directly overlain by brownish-black calcareous mudstones that contain millimeter-scale to centimeter-scale shell fragments. These mudstones are in turn overlain by the light-yellow-orange mudstone. Higher up in this interval (cycles 23 to 26), the first 50 to 75 cm above the calcretes is characterized by light-gray marls and (light-gray) silty carbonates. Above cycle 26, calcretes are absent, and thicker (up to 40 cm), gray marls or light-gray muddy carbonates occur (cycles 26 to 29), rich in shell fragments and often complete gastropods. The muddy carbonates are soft, dusty, and poorly lithified, and display sparse millimeter-scale yellow-orange mottling, ranging in thickness between 10 and 40 cm. The thicker beds (e.g., cycles 23 and 27) also show vertically oriented, centimeter-scale root traces and, especially at their tops, horizontal cracks. Tens of meters eastwards from the logged transect, the limestone beds of cycles 23, 26, 27, 29 and 30 are much thicker, reaching up to 60 cm. These limestones occur stratigraphically associated with intervals of shell-bearing, light-gray calcareous siltstones. Above these limestones, pale-yellow siltstones occur with red mudstones within centimeters above the carbonate interval in cycles 20, 24, 25, 28, 29.

Ten or eleven regular lithological repetitions occur within Interval III, on average every 2.0 m (range 1.6 to 2.5 m). As described above, the position of the calcretes within the lithofacies cycles changes trough the interval. Cycle boundaries are defined at the tops of the gray, shell-fragment-rich siltstones or carbonates.

2.4.1.4. Interval IV - Cycles 29a – 33

In interval IV, light-gray mudstones prevail, with varying amounts of yellow-orange mottling and meter-scale intercalations of gastropod-rich, light-gray, muddy limestones and (dark-)gray marls. Light-gray mudstones display millimeter-scale yellow-orange mottling that increases in intensity and size (up to centimeter scale) just above the gray marls and limestones (cycles 28a, 28, 26a, 26).

The limestones range from 10 cm up to 1 m in thickness, and pinch out over a distance of a few meters, mainly towards the basin margin in the west and locally in other directions as well. Towards the basin center in the east, most limestone and stratigraphically associated (dark-)gray marl intervals become thick and prominent limestone beds. In the logged transect, the basal and top transitions of the beds are rather sharp. Mostly, they show gentle centimeter-scale undulations both at the bases and within the beds, and, locally, centimeter-scale bedding. Bed tops commonly feature horizontal cracks. The beds are soft and porous, with relatively much organic matter, and often full of complete and fragmented gastropod remains. Sparse millimeter-scale yellow-orange mottling and locally centimeter-scale root traces are present. The limestone beds are stratigraphically associated with (dark-) gray marls that are rich in very fine-grained organic matter, most probably plant debris, and fragmented and complete gastropod shells. The organic-rich levels in interval IV are occasionally rich in small-mammal remains, and sparse large-mammal remains have been found.

In this interval, cycle boundaries are defined at the top of the gray mudstone or limestone beds. Cycle thickness varies between 3.3 to 5.0 m for the 4 well-defined cycles (cycles 30, 31, 32, 33). In between these cycles, three less clear cycles are present (cycles 29a, 30a, and 31a; Fig. 2).

2.4.1.5. Interval V - Cycles 34 - 42

Interval V is dominantly characterized by red mudstones with intercalations of between 75 and 150 cm of light-yellow-orange calcretes, (dark-)gray calcareous mudstones, and light-gray limestones on meter scale (Figs. 3B, D). The red mudstone displays sparse millimeter-scale yellow-orange and light-gray mottling and occasionally millimeter-scale dispersed caliche nodules. The basal part of this mudstone is often dark red changing upwards to red, while more intense yellow-orange mottling usually increases towards the top, resulting in orange colors.

The intercalations generally start with a calcrete bed, 20 to 50 cm thick, that varies between loose nodule levels to more cemented nodule levels, and occasionally massive nodular beds. The calcretes are light yellow to yellow, have a silty to muddy matrix, occasionally display vertical arrangement of nodules resembling root morphologies, and show relatively gradual bases and sharp tops and upward-increasing carbonate content. Nodules vary in size from sub-millimeter to centimeter scale and are subspherical. The calcretes reach Stage II to III (cycles 36 to 41; Fig. 2) according to the calcrete classification of Machette (1985).

The calcretes are followed by a (dark-)gray calcareous mudstone with sparse shell fragments. In some cycles, a (dark-)gray marl rich in shell fragments occurs, with local intercalations of a light-gray limestone (cycles 34, 35, 38 to 40, and 42). The thickness of the gray calcareous mudstone ranges between 20 and 125 cm. The intercalated limestone beds range in thickness between 10 and 40 cm, are light gray, have undulating bases, and contain shell fragments and infrequently complete gastropod shells. The limestone beds in this interval have sedimentological characteristics similar to the limestones of cycles 30 to 33 in interval IV, though the latter are thicker. Locally, the limestone pinches out or increases in thickness laterally over a few meters towards the east as well as west.

Interval V comprises nine sedimentary cycles with an average thickness of 3.3 m, and ranging between 2.4 and 4.3 m in thickness. The repetitive pattern of sediments is very regular in this interval, and cycle boundaries are easily defined at the bases of the red mudstones.

2.4.1.6. Interval VI - Cycles 43 - 55

A distinct change occurs above interval V (cycle 42; Figs. 2, 3B), from dominant (light-yellow-)orange and red mudstones with intercalated gray mudstones and limestones, to dominant orange silty and sandy mudstones (Fig. 3B). This transition was traced laterally from east to west over a distance of 0.5 km, which is the limit of the outcrop exposures.

The interval above this shift, interval VI, is characterized by dominance of orange, fine-sandy siltstone and light-orange, silty, fine sandstone. Sparse, millimeter-scale light-gray mottling occurs, with occasional levels of centimeter-scale light-gray mottling and sparse millimeter- to centimeter-scale carbonate nodules. On meter scale, intercalations of calcrete beds 40 to 120 cm thick and fine to pebbly sandstones occur.

The calcrete beds have a silty to fine sandy matrix and millimeter-scale (light-)yellow-orange mottling, and are usually poorly cemented loose nodule levels and occasionally better-cemented nodular beds. In poorly cemented nodule layers, a dark red matrix with millimeter-scale yellow mottling occurs, especially near the tops of the beds. In redder intervals, millimeter- to centimeter-scale light-gray mottling occurs. The bases of the beds are gradual, and their tops are relatively sharp. According to the calcrete classification, these calcretes represent Stage 1 to 2 (Machette, 1985).

In cycle 44, the calcrete is covered by a gray, organic-rich, fine-sandy mudstone, while in other cycles (cycles 43, 45, 46, and 48) calcretes are followed by red sandy siltstones occasionally displaying sparse millimeter-scale shell fragments.

The fine-sandy to pebbly intercalations are cemented by carbonate and fine slightly upward. At the base of the sandstone bed in cycle 47, a 50-cm-thick conglomeratic lobe pinches out within 10 meters both to the east and to the west. This conglomerate is characterized by a clast-supported fabric of subrounded pebbles and rare cobbles, a poorly sorted muddy to coarse sandy matrix, and a relatively high matrix-to-clasts ratio. The associated sandstone beds consists of poorly sorted, fine to very coarse sand with plane-parallel lamination and sparse, floating pebbles.

Above interval VI, a coarsening-upward towards a conglomerate 2 to 5 m thick is present. Locally, the base of the conglomerate incises up to 3 meters in the sandy interval below. The conglomerate consists of several ~ 30-cm-thick fining-upward beds. The pebble clasts vary in size from 1 to 30 cm, with an average of 4 cm. The subrounded clasts are densely packed in a fine to very coarse sand matrix.

Cycles in interval VI have an average thickness of 2.9 m but show a wide range from 1.6 to 5.2 m. Depending on two less well defined cycles (45a and 46a), 13 to 15 cycles are present excluding the two potential cycles above cycle 55. The lower part of this interval consists of relatively thick cycles thicker than 3 m (cycles 44 to 47, and 49), while towards the top the average cycle thickness is only 1.8 m (cycles 50, and 52 to 55).

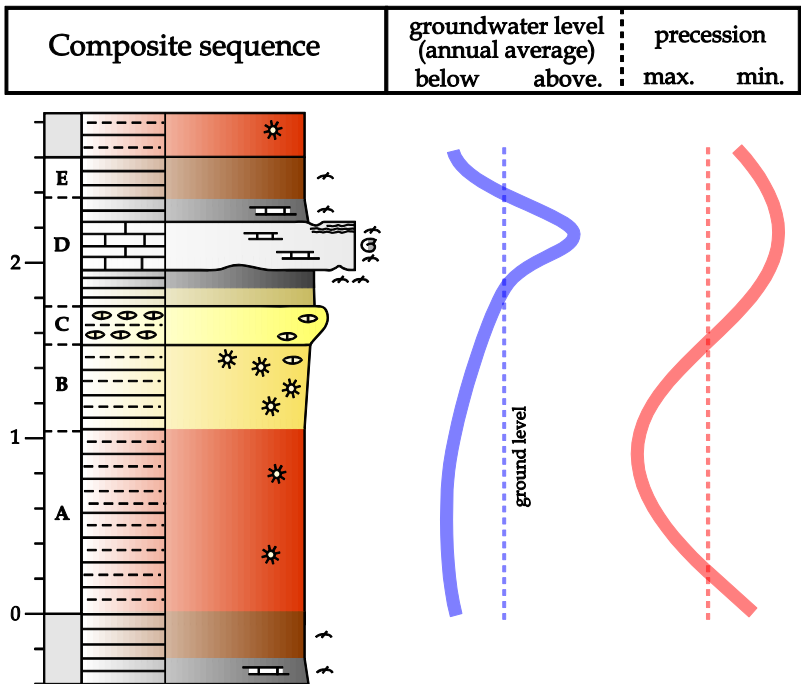

Figure 4 *- Lithological characteristics of the composite lithofacies cycle in the Prado section (see Fig. 2 for legend and the section 4.2 on description and interpretation of facies A to E). Scale is in meters. To the right, interpretation in terms of local, relative annual averaged groundwater level and the precession cycle are given. In print version, color codes are given; rd for red, gy for gray, or for orange, d for dark, and l for light.*

2.4.2. Composite Sedimentary Cycle

The persistent, meter-scale lithofacies cycles in the Prado section generally consist of a red and/or (light-) yellow-orange mudstone part, mainly encompassing the lower, thicker fraction of the cycle, and a carbonate-rich part (Figs. 4, 3D) represented by light-yellow-orange calcretes and gray organic-matter-rich muddy limestones, or marls. Cycle boundaries were consistently placed at the transition from dominantly calcareous to dominantly siliciclastic intervals (see above for details). In total, 55 cycles show a well-defined lithofacies transition at their tops (solid lines in Fig. 2), while 10 additional cycles show more diffuse transitions or less distinct lithologies (dotted lines in Fig. 2). The average thickness of a sedimentary cycle in the Prado section is 2.6 meters, with a standard deviation of 0.9 meters and extremes ranging from 1.2 to 5.2 meters. Three intervals with thick cycles (> 3.5 m) occur in the section: cycles 16 and 17 in interval II, cycles 30 to 33 in interval IV, and cycles 46, 47, and 49 in interval VI (Fig. 2). In order to facilitate interpretation and discussion of facies and the variable sedimentological expressions of stratigraphic intervals, an idealized composite lithofacies cycle was constructed (facies A to E; Figs. 4, 3D). This cycle consists of five distinct facies, superimposed according to their recurrent vertical transitions in the different types of cycles discussed above. This composite cycle is thus not found as a real stratigraphic unit at outcrop, but it reliably represents the overall facies variability, and especially facies transitions, which are recognized consistently throughout the section.

2.4.2.1. Facies A

Description. The composite cycle starts with a red, occasionally orange or dark-red, massive and homogeneous silty mudstone (Fig. 4), displaying different amounts of sparse light-gray, millimeter- to centimeter-scale mottling. Rare millimeter-scale carbonate nodules are found. Infrequent millimeter-scale shell fragments occur, especially at the bases of the mudstone beds. The mudstones lack primary depositional structures, well-developed pedologic (soil) horizons and structures, and internal discontinuities and erosional features at their bases and tops. Lithological transitions at their bases are usually relatively sharp, whereas transitions to overlying lithologies are more gradual.

Interpretation. The massive and homogeneous red mudstones display the characteristics of a well drained mudflat deposit with very weak pedogenic overprint (Kraus & Hasiotis, 2006). The sparse, light-gray mottling indicates weakly reducing conditions due to short periods of seasonal wetting (Kraus, 2002; Kraus & Hasiotis, 2006) or localized biological activity. The scarce rhizocretions and the absence of bioturbation point to poor colonization by vegetation or other organisms (Huerta & Armenteros, 2005). The rare carbonate nodules, interpreted as incipient caliche, indicate precipitation of calcium carbonate in the Bk horizon of a calcic soil profile (Retallack, 2001). Lack of well-developed soil profiles and structures indicate only minor pedogenesis within the deposit. A semiarid climate could have been a significant cause of poor pedogenesis, although the overall homogeneity of facies vertically through the beds also suggests that time was a significant factor. The slow development of a mature soil profile was probably hindered by continuous, relatively high aggradation rates (Buurman, 1980). Incipient pedoturbation, desiccation, and compaction possibly removed any original structures (cf. Wright & Marriott, 2007). The fine-grained sediments were probably deposited by distal sheetwash during waning-flow stages of major flood events from the adjacent basin margin where these lost capacity over the flat, sparsely vegetated distal surfaces (Abels *et al.*, 2009).

2.4.2.2. Facies B

Description. The transition from facies A to B is usually gradual. Facies B consists of orange to light-yellow-orange, massive, silty to sandy mudstones. These mudstones display abundant centimeter-scale yellow-orange mottling, minor millimeter-scale light-gray mottling, and a generally higher content in dispersed carbonate nodules and rhizocretions than in facies A. In some cycles, the sediment is rather uniform in color, whereas in others it has a multi-colored, patchy appearance with red, yellow-orange, light-yellow-orange, and light-gray mottling. The abundance of millimeter- to centimeter-scale carbonate nodules and intense yellow-orange mottling tends to increase towards the top of facies B. Similarly to facies A, facies B is also characterized by internal homogeneity and the absence of primary sedimentary structures at outcrop scale. The boundary between facies A and B is defined arbitrarily within the composite cycle, whereas in the field it is usually diffuse over an interval with characteristics intermediate between A and B.

Interpretation. The sedimentary processes by which facies B was formed are interpreted as fairly similar to those for A. The most significant difference is the slightly coarser grain size and slightly higher carbonate and rhizocretion content in facies B, accompanied by a greater size and color intensity of mottled domains,

and the general occurrence of (light-)yellow-orange mottling. The upward increase of yellow-orange mottles from the red mudstones of facies A to the orange mudstones of facies B is interpreted as an increase of (seasonal) wetting of the soil profile (Kraus, 2002; Kraus & Hasiotis, 2006; PiPujol & Buurman, 1997). The slightly coarser grain size and increased carbonate content and pedogenesis might be indicative of a more frequent or persistent availability of water. The prevalence of Jurassic and Cretaceous carbonate formations in the Mesozoic catchment areas led to a high availability of dissolved carbonates in both surface runoff and groundwater. The increase in overall carbonate content from facies A to facies B might thus be related to rising availability of water via groundwater and/or runoff. Towards the top of facies B, these (seasonally regulated) soil-forming processes were further enhanced. The presence of yellow-brown colors in red soils and the dispersed presence of carbonate nodules suggest moderately well-drained conditions with a short period of seasonal wetting (Kraus & Hasiotis, 2006).

2.4.2.3. Facies C

Description. Above facies B, calcrete beds 20 to 60 cm thick occur that display gradual bases and relatively sharp tops. The beds are commonly light-yellow-orange with yellow-orange and occasionally light-gray mottles. Beds vary from noncemented carbonate nodule levels, to better cemented nodular levels, and finally to indurated massive nodular beds with a smooth appearance.

Weakly-cemented nodule levels display (dark-)red matrix and millimeter-scale to centimeter-scale light-gray mottling with sparse yellow-orange mottling. Better-cemented beds dominantly display centimeter-scale yellow-orange mottling with infrequent millimeter-scale light-gray mottles. The matrix is usually silty to, infrequently, fine sandy. Carbonate nodules are millimeter- to centimeter-scale and subspherical, and may display a vertical arrangement resembling root morphologies. At the tops of the beds, horizontal structures may be present, either as millimeter-scale cracks in cemented beds or as horizontally oriented nodules in less-cemented beds. Laterally, less-cemented beds may grade into more indurated beds and vice versa. Also, the stratigraphic thickness of individual beds may vary laterally, including smooth undulation of the bases of the beds. According to the calcrete classification of Machette (1985) as followed by Wright and Tucker (1991), the calcrete characteristics would fit Stage I or II for the incipient weakly cemented nodule levels to between Stage III and IV for well-cemented massive nodular beds. No horizontal platy, tabular structures characteristic of a full Stage IV calcrete are observed.

Interpretation. Carbonate precipitation in the Stages I to IV calcretes likely occurred due to calcium-carbonate saturation in the capillary fringe zone above the groundwater table or in the Bk horizon of a calcic soil profile or due to a mix of these pedogenic and phreatic processes (Alonso-Zarza, 2003; Huerta & Armenteros, 2005; Retallack, 2001; Wright & Tucker, 1991). Climate was semiarid and seasonally dry with an annual precipitation estimated between 500 to 550 mm (Van Dam, 2006), supporting the occurrence of pedogenic calcretes; however, other climate(s) are reported to support calcrete formation as well. The original red mudstone matrix and the occasional lateral gradual changes from weakly cemented to more indurated beds suggest that the (facies C) calcretes did not (principally) originate from calcretized lacustrine or palustrine carbonates (Huerta & Armenteros, 2005; Wright & Tucker, 1991). Nevertheless, the carbonate-

rich basin margins and underlying lithology suggests that dissolved carbonate was abundantly present in the Prado paleoenvironment. Also, the relatively impermeable sub-surface, due to the presence of multiple well-cemented calcretes in the Prado succession and the gypsum formation below, may have resulted in a relatively poor drainage, giving evapo(transpi)ration a significant role, thereby redistributing the abundant dissolved carbonate and facilitating relatively rapid calcrete development (Wright & Tucker, 1991). The availability of water instead of time or (dissolved) carbonate might have been the critical factor in controlling carbonate deposition in calcrete beds in the Prado paleoenvironment. We interpret the gradual change from facies A to B and finally to C as a gradual increase in water saturation of the soil profile, in accordance with a lateral facies model of Huerta & Armenteros (2005) for Miocene sediments in the Duero basin. In their model, lateral coexistence of reddish-brown mudstones, scattered carbonate nodules, nodular calcrete facies, and massive calcrete is shown in a transect from well-drained distal alluvial floodplain, to less well-drained distal floodplain, and finally to more inundated areas near the lake margin.

2.4.2.4. Facies D

Description. The lower portion of facies D, over a variable thickness between 0 and 60 cm, represents characteristics transitional from facies C. This transitional interval constitutes gray calcareous mudstones with light-orange-yellow mottling. This interval is covered by dominantly light- to dark-gray marls and muddy limestones, locally intercalated with 20-cm-thick light-gray limestone beds that have a maximum thickness of 1 m. Mudstones and marls contain abundant millimeter- to centimeter-scale shell fragments and complete gastropod remains. Thin (< 10 cm) organic-rich layers are present, usually containing coarse plant debris and remains of small mammals, and occasionally large mammals.

The intercalated light-gray limestone beds have sharp undulating bases, are weakly indurated, and contain a relatively high amount of fine siliciclastic components. In many cycles, the limestones are rich in dispersed organic matter and intact or fragmented gastropod remains. Besides the undulating bases, slightly undulating internal surfaces are locally evident within the limestone beds, especially in the thicker ones. Some beds pinch out laterally over distances of a few meters, but usually they extend over 50 meters at outcrop, and some are traceable over hundreds of meters towards the more central parts of the basin, farther east from Prado. The tops of the limestone beds usually feature horizontal cracks, while sparse rhizoturbation is present throughout the beds, and more frequently within their upper parts.

Interpretation. Deposition of gray, gastropod-rich, calcareous mudstones and marls indicates rising groundwater levels and occasional ponding of the surface. These conditions rapidly halted calcrete development, and caused fine clastic sedimentation to alternate with (biochemical) carbonate precipitation. Temporary reduced oxygenation is indicated by preservation of abundant organic matter, including gastropod and mammal remains, and by light-gray colors indicating the remobilization of iron (Kraus & Hasiotis, 2006). Intercalated, undulating, light-gray limestones are interpreted as the result of carbonate deposition in very shallow and relatively wide, elongated depressions through which sluggish surface waters were slowly directed towards the basin center, or to local small ponds on the mudflat. Thicker limestone beds, laterally continuous over long (> 500 m) distances, are interpreted as pond and marginal lacustrine

deposits. The absence of extensive palustrine features within and on top of limestones beds suggests that their deposition rates were relatively fast, leaving no significant time for reworking at the sediment-water interface in shallow-water conditions. Palustrine features are reported to develop rapidly in freshwater limestones (Alonso-Zarza, 2003), while desiccation is particularly expected in very shallow-water environments in a semiarid, seasonal climate (Van Dam, 2006).

2.4.2.5. Facies E

Description. The topmost facies within the composite lithofacies cycle is represented by a dark-red to brownish-black, massive silty clay containing dispersed millimeter-scale shell fragments. Millimeter-scale, yellow-orange and red mottling is present. No primary sedimentary structures are evident at outcrop.

Interpretation. The dark mudstones are interpreted as mudflat deposits, analogous to those of facies A and B. Environmental conditions did not allow more than weak pedogenesis keeping pace with aggradation of the surface. Mild pedoturbation disrupted any primary sedimentary structures but did not reach a full stage of soil formation. The vague reddish and occasionally yellow-orange mottles characterizing facies E probably indicate a return to more oxygenated conditions of the floodplain, related to a gradual shift from a poorly drained (facies D) to a well-drained (facies A) mudflat environment (Kraus & Hasiotis, 2006). Within the interpretive framework of our representative sedimentary cycle, facies E is regarded as a transitional facies between D and A.

2.4.3. Depositional Model

The representative facies succession A to E in the meter-scale lithofacies cycles in Prado are interpreted as deepening-upwards sedimentary sequences due to variations in relative groundwater level at the site of deposition. Groundwater level and/or water availability was low on a well-drained mudflat during deposition of facies A. The subsequent rise of the water table resulted in more effective pedogenic processes, produced facies B, and eventually led to the development of calcic soil profiles or phreatic calcretes (facies C). The further rise of groundwater levels resulted in more persistent saturation up to the ground surface, with temporary development of poorly oxygenated wet mudflat environment of facies D, in which sluggish elongated, low-energy channel bodies and small ponds developed. Occasionally, this rise led to the development of marginal lacustrine environments, especially towards the center of the basin. Finally, a lowering of groundwater level resulted in a stratigraphically rapid return to the well-drained, dry mudflat environment represented by facies A, with facies E as a transitional stage. In the composite sedimentary cycle, the facies A and B, related to groundwater-level lowstands, are referred to as the “dry” part of the cycle. Conversely, facies C, D, and E, which are related to groundwater-table highstands, are referred to as the “wet” part of the cycle. Note that with the “wet” and with the “dry” part of the cycle we refer only to the relative groundwater table in the sediment at the site of deposition and we do not insinuate any mechanism behind these changes.

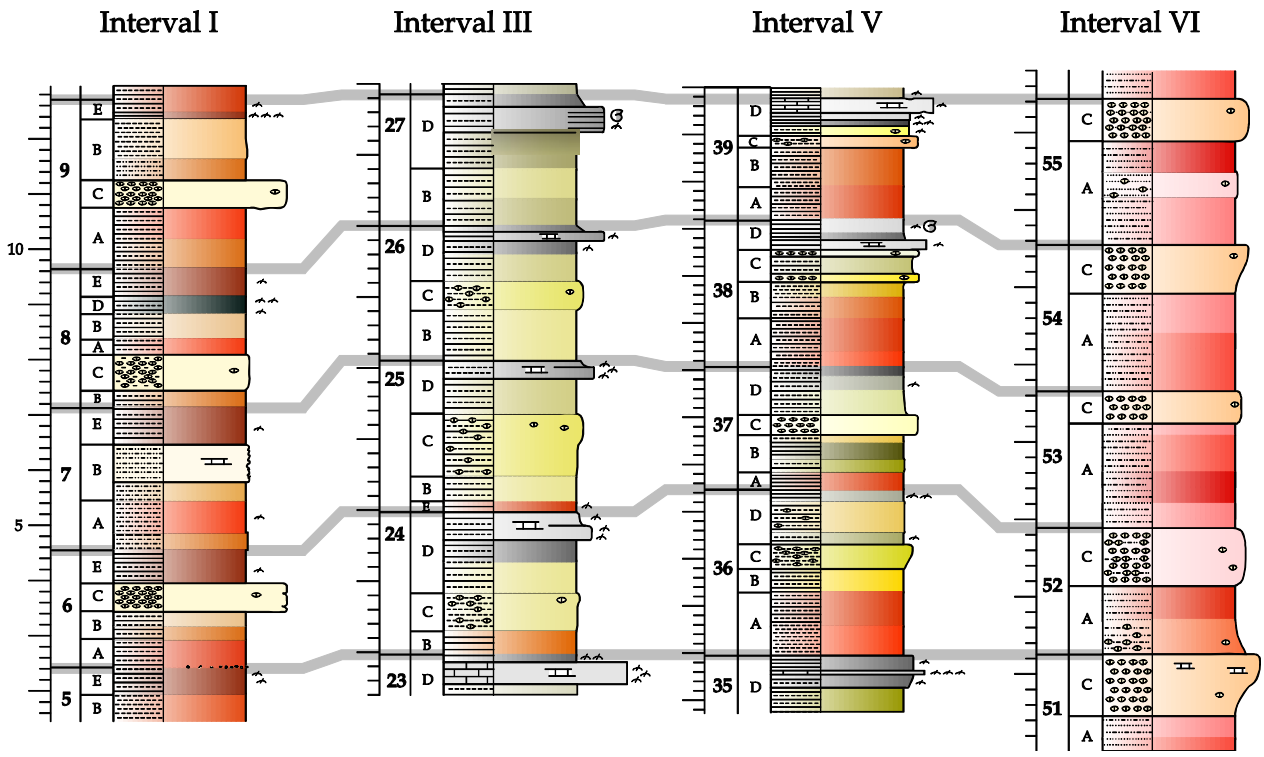

Figure 5 *- Detailed comparison of the four distinct stratigraphic intervals in the Prado section, which reveal regular meter-scale lithofacies cycles. The well-drained red mudstone facies gradually disappears from interval I to III but reappears in two steps from III to V and from V to VI (see section 2.6.5).*

2.4.4. Large-Scale Changes

Throughout the Prado section, intervals I to VI all show different facies characteristics that are variations of the composite cycle. Four characteristic intervals (part of intervals I, III, V, and VI) are compared (Fig. 5), in order to illustrate these major sedimentary signatures and paleoenvironmental changes. The sediments of the other two intervals, II and IV, are not elaborated here because they represent transitional intervals with thicker-than-average cycle thicknesses including less well-defined cycles. Gray lines in Figure 5 indicate cycle boundaries and thus the transition from the "wet" to the "dry" parts of the cycles. In the basal part of interval I, the stratigraphic log is composed mainly of facies A, B, E, and occasionally C. In interval III, cycles are composed dominantly of facies C, D, and only rarely E, while facies A and B are absent. Higher up, in interval V, facies A and B reappear and the cycles closely resemble the composite sedimentary cycle model, displaying the whole facies spectrum from A to E. With a sharp transition above cycle 42, cycles in interval VI are again dominated only by facies A and B, with thin intercalations of facies C. The main differences between intervals I and VI are the absence of facies E and the higher lateral continuity of carbonate-rich beds in VI. Interpretations in terms of local, relative hydrological balance suggest a progressively rising groundwater table from interval I to III, followed by a subsequent lowering in two main steps: at the transition from interval IV to V (above cycle 33), and at the transition from interval V to VI (above cycle 42). Above interval VI, the Prado section is topped by tens of meters of red, weakly pedogenically modified mud deposits with minor sandstone sheets and conglomeratic channel fills in single and multiple stories. On a decimeter to meter scale, the mudstones present rhythmic facies transitions similar to facies A and B. The

lateral continuity of these deposits is occasionally interrupted by the erosional bases of coarse-clastic channel bodies and associated sandstone splays. This overlying succession is interpreted as being deposited in a poorly confined, ephemeral fluvial system sourced from the north, which is along the strike of the basin. The greatest volume of sediments is represented by overbank fines grading laterally to shallow, isolated channels that are locally filled by much coarser and poorly organized sediment, in correspondence of major floods. The presence of these erosional channels suggests higher gradient within the basin that is related to increased accumulation rates. The end of the endorheic configuration of the basin is discarded here, in as much as clearly endorheic lacustrine sediments are present up to the Pliocene in the basin.

2.5. MAGNETOSTRATIGRAPHY

A detailed magnetostratigraphic age model was established to test whether the regular occurrence of meter-scale lithofacies cycles is related to orbital climate forcing. First-order age control is derived from lithostratigraphic correlation to the well-dated time-equivalent Cascante section (Abels *et al.*, 2009), where the magnetostratigraphy was tied to the geomagnetic time scales using biostratigraphy of small-mammal faunas (Abdul Aziz *et al.*, 2004). The presence of the top of the Libros Gypsum Unit (Anadón *et al.*, 1997; Ortí *et al.*, 2003) below both the Cascante and the Prado sections indicates that they are roughly time-equivalent, which is confirmed by preliminary mammal biostratigraphic results (J. Van Dam, personal communication, 2008).

2.5.1. Results

The results of the thermal demagnetization for the Prado samples are of good quality (Figs. 6A-D). Initial NRM intensities vary according to facies (Fig. 7), with highest NRM intensities (7.8 to 95.4 mA/m) in the red mudstones and siltstones of facies A and E that typically dominate in intervals I, II, and VI. The lowest intensities (0.04 to 7.8 mA/m) are found in facies B and D, which contain more carbonate and dominate intervals III and IV. The calcretes of facies C show a wider range of NRM intensities varying between 0.07 and 87.3 mA/m, with highest values corresponding to the lithologies from interval VI (cycles 43-55) (Fig. 7). The Zijderveld diagrams and thermal decay curves show that the total remanent magnetic signal consists of three components. The first is a randomly oriented component that is removed between temperatures of 100ºC and 120ºC, and represents a laboratory-induced magnetization related to storage. The second component is removed between 210ºC and 270ºC; however, in a few samples this component is removed up to temperatures of 390ºC (especially in cycles 49 to 51; Fig. 6C). This component has a normal polarity and is interpreted to represent a viscous overprint by the present-day Earth's magnetic field. The third component displays dual polarities and is interpreted as the characteristic remanent magnetization (ChRM) of the sediment. Three unblocking temperatures of the ChRM can be distinguished in the Prado section. The ChRM of ~ 60% of the samples is fully demagnetized at temperatures from 600ºC up to 700ºC, indicating unblocking temperatures for (fine-grained) hematite (Figs. 6A, C, E). Samples with these unblocking temperatures are mostly from lithologies A and B (and E), i.e., from the well-drained-mudflat deposits. The

ChRM of ~ 35% of the samples is removed between 520ºC and 600ºC, which is a typical unblocking temperature range for magnetite (Figs. 6B, D). Samples with this temperature range include all facies A to E.

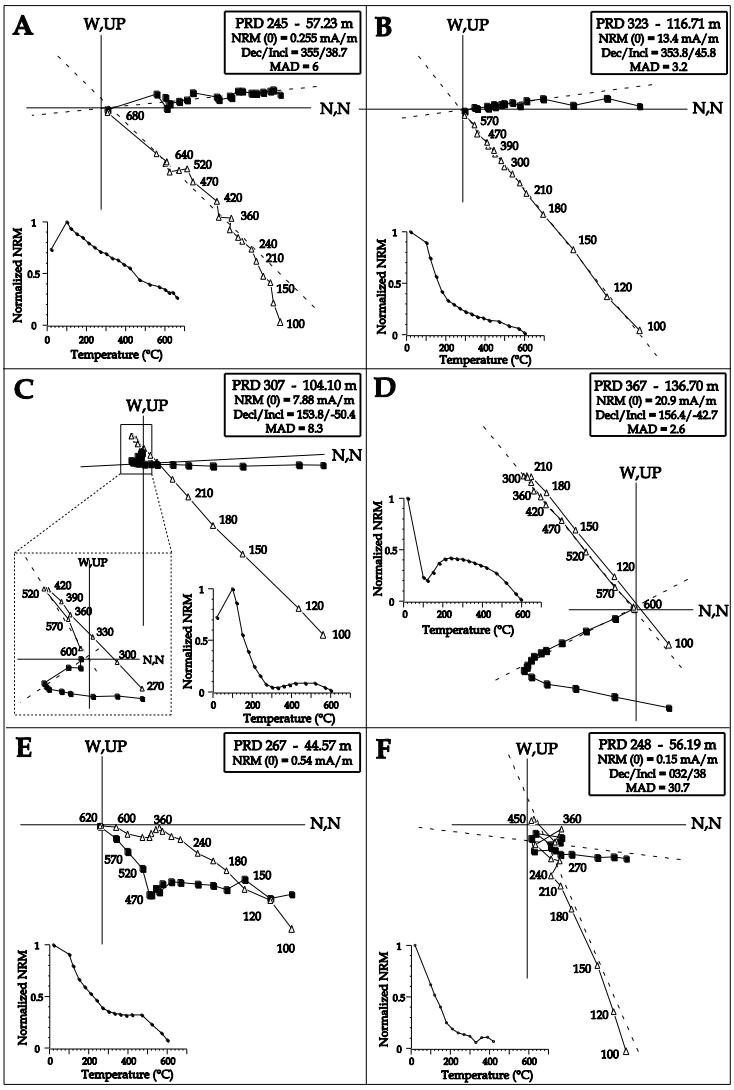

Figure 6 *- Thermal demagnetization diagrams and decay curves (inset) of selected samples from the Prado section. Open (closed) symbols denote projection on the vertical (horizontal) scale. Numbers along demagnetization trajectories indicate temperature steps in °C. Dashed lines are the interpreted declination and inclination direction of the characteristic remanent demagnetization (ChRM). MAD denotes the maximum average deviation of the interpreted ChRM direction. See text for details on A-E. Figure 6F denotes an example with unresolved polarity.*

The remaining 5% of the samples have unblocking temperatures between 390ºC and 480ºC, suggesting iron sulfides as the main carrier of the ChRM (Fig. 6F). Most of these samples belong to carbonate-rich mudstones of facies D. Susceptibility measurements indicate stable values for the samples with high unblocking temperatures (570ºC and higher) with no significant change in mineral composition during the thermal demagnetization. The samples from the calcareous gray mudstones of facies D show a distinct increase of susceptibility values from temperatures around 360ºC and higher, probably due to the oxidation of the iron sulfides.

The ChRM directions were calculated for more than five temperature steps in the range 270 to 700°C. The quality of the measurements and the line fitting were evaluated by visual inspection of Zijderveld diagrams and by calculating the maximum angular deviation (MAD). The magnetic polarity record of the Prado section was interpreted using MAD values smaller than 20º as cutoff. Values larger than 20º and non-interpretable samples are indicated in Figure 7 by open circles and crosses, respectively.

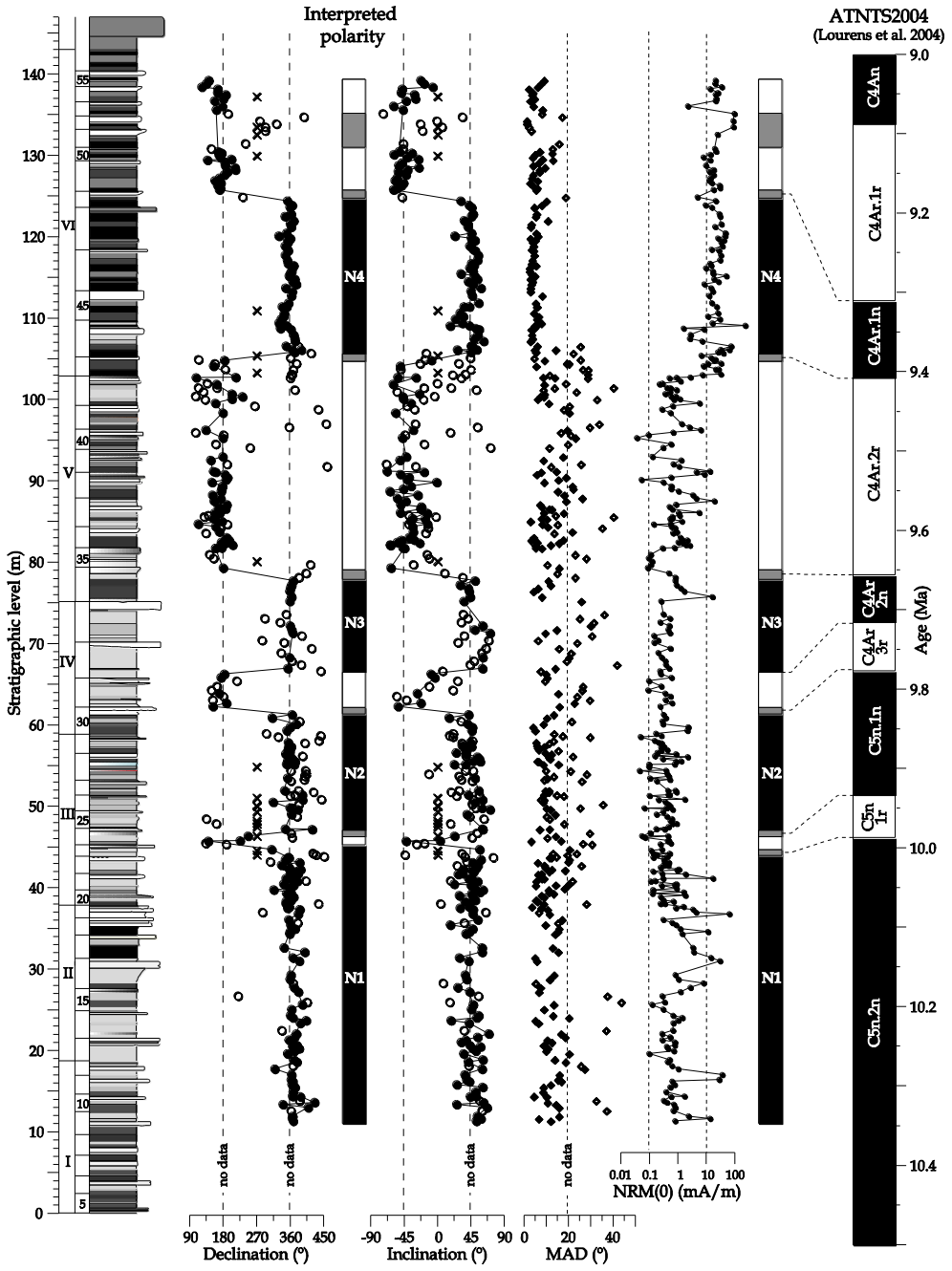

Figure 7 *- Declination, inclination, and interpreted polarity for the Prado magnetostratigraphy. To the left, a schematic column of the section is given, including stratigraphic position, and interval and cycles numbers. Black, white, and gray colors in the interpreted polarity column respectively indicate normal, reversed, and non-resolved polarity. The graphs to the right show the maximum average deviation (MAD), initial natural remanent magnetization (NRM), and the correlation of the interpreted polarity record at Prado to the ATNTS04 of Lourens et al. (2004).*

2.5.2. Correlation to the ATNTS2004

Declination and inclination data are plotted in stratigraphic order and reveal seven polarity reversals, with gray colors indicating the uncertainty intervals of the reversal level (Fig. 7). The established lithostratigraphic and time-equivalent relationships between the Prado and Cascante sections allow a straightforward correlation of the Prado polarity record to the ATNTS04 (Lourens *et al*., 2004). Starting from the base of the Prado section, the long normal-polarity interval N1 is correlated to chron C5n.2n. The subsequent three normal-polarity intervals N2, N3, and N4 are correlated to chrons C5n.1n, C4Ar.2n and C4Ar.1n, respectively. The correlation of the Prado magnetostratigraphy to the ATNTS04 of Lourens *et al*. (2004) reveals a complete polarity record ranging from chron C5n.2n to C4Ar.1r and covering a time span of more than 1 million years, i.e., from ~ 10.3 to 9.2 Ma.

2.6. CYCLOSTRATIGRAPHY

2.6.1. Orbital Forcing

Correlation of the magnetostratigraphy with the ATNTS2004 time scale (Lourens *et al*., 2004) provides a detailed age model for the Prado section. In the time interval considered, the astronomical ages for polarity reversals in the ATNTS2004 were derived from astronomically tuned sapropel patterns in the deep marine Monte dei Corvi section in northern Italy (Hüsing *et al*., 2007). In Figure 8, the magnetostratigraphy of the Prado section is compared to the recently improved astronomically dated ages of polarity reversals in this deep marine section. Gray bars represent ranges of uncertainty in depth at Prado and time at Monte dei Corvi.

In the magnetic-polarity interval between the reversals at the top of chron C5n.1r and the top of C4Ar.1n, there are 24 well-defined lithofacies cycles in the Prado section with an uncertainty of half a cycle in both directions. Additionally, there are five less well-defined “a” cycles in this interval, making a total of 29 ± 0.5 cycles (Fig. 8). In the Monte dei Corvi section, the time between the two reversals is 626 ± 9 kyr (Hüsing *et al*., 2007). This results in a period between 25.1 and 27.0 kyr for a well-defined lithofacies cycle, and between 20.9 and 22.3 kyr when the “a” cycles are included. The latter period is suggestively close to the duration of a *climatic* precession cycle with main periods of 18.9, 22.2, and 23.5 kyr (Laskar *et al*., 2004). The suggestion by the age control that the meter-scale lithofacies cyclicity may be driven by precession is further elucidated.

2.6.2. Precession Phase Relation

In the depositional model presented in Figure 4, the paleoenvironmental interpretation of the sedimentary cycles was formulated in terms of local, relative hydrological balance. Inasmuch as precession forcing is suggested by the age model, meter-scale sedimentary rhythms controlled by groundwater levels then must be related to precession. The phase relation between changes in the regional water table and precession remains, however, unknown. The phase relation relates to two elements: the relationship between groundwater level (and, consequently, sedimentology) and local climate, and the link between local climate and precession.

The relation between groundwater table (and sedimentological processes) and local climate can be straightforward. Lower groundwater tables inferred from the development of well-drained floodplains in facies A and B ("dry" part of the cycle) might indeed relate to decreased precipitation rates, and vice versa. However, increased sedimentation rates caused by increased precipitation could have a similar effect. According to the latter hypothesis, waterlogged environments could then occur during times of sediment starvation due to decreased precipitation. These processes might have a different effect on different parts of the basin (Picard & High, 1981). Increased seasonality with a short wet season is suggested by yellow-orange mottling in facies B with respect to facies A (see interpretation in the section 4.2.2; Kraus, 2002; Kraus & Hasiotis, 2006).

Abels *et al.* (2009) elaborated on the link between local climate and precession, when trying to solve the same problem for the sedimentary cycles in the nearby, time-equivalent Cascante section in the Teruel Basin. Geological data as well as climate modeling of precession extremes indicated that winter precipitation increased significantly during precession minima (and related boreal summer insolation maxima), while increased summer precipitation is cancelled by high summertime evaporation rates during these times (Abels *et al.*, 2009). In their climate model, increased winter precipitation is due to elevated Mediterranean Sea temperatures and resulting cloud formation. Consequently, precession minima most likely resulted in a significant increase in the net water budget for the Teruel Basin. Following this reasoning, precession minima should be correlated with increased winter precipitation and lake-level highstands, and vice versa, in agreement with previous studies (Sierro *et al.*, 2000; Kruiver *et al.*, 2002; Abdul Aziz *et al.*, 2003; Abels *et al.*, 2009). Enhanced seasonality is suggested by increased color mottling in facies A to B in the meter-scale lithofacies cycles. Most probably the "wet" part (facies C, D, and E; see section 2.4.3) of the lithofacies cycles and related groundwater table highstands in Prado relate to precession minima and association summer insolation maxima. The remaining uncertainties, however, lead us to consider both phase relations in the established astronomical tuning (Fig. 8).

2.6.3. Astronomical Tuning

Starting from the polarity reversals, the astronomical tuning of the Prado section is based on the correlation of successive lithofacies cycles to consecutive precession cycles (Fig. 8). The tuning of the "wet" part (see section 2.4.3) of the cycles to precession minima and 65° N summer insolation maxima is shown, as well as the alternative tuning following the opposite phase relation (Fig. 8). Solid lines in the Figure 8 are used when only one possible correlation exists, primarily due to the position and age of polarity reversals. Dotted lines instead indicate that the suggested correlation is the most probable, but an alternative correlation is possible with one precession cycle upwards or downwards. The resulting astronomical ages for the polarity reversals in the Prado section fall within the uncertainty intervals of the ages in the Monte dei Corvi section (Fig. 8). This implies that similar numbers of lithofacies cycles are present in the same intervals in both sections constrained by their independent, high-resolution magnetostratigraphy.

An uncertainty of one cycle exists in the tuning of this interval, which increases downwards to an uncertainty of two cycles. Therefore, the tuning is presented only for the "B" transect of the Prado section

and not extended downwards to include the "A" transect. To solve the tuning of the cycles in transect "A" requires additional (magneto-)stratigraphic constraints, that have to come from locating of two cryptochrons of the long chron C5n.2n (Evans *et al.*, 2007) in this lower part of the Prado section.

The astronomical tuning from cycles 13 to 30 is rather straightforward. The tuning in this interval depends on counting cycle 30 as a single or double cycle. If that cycle is considered as a double cycle, the tuning would shift one precession cycle downwards. In this case, the reversed chron found in cycles 23 and 24 still matches the ages for chron C5n.1r (Fig. 8; Hüsing *et al.*, 2007). In addition, the match of the closely spaced cycles 18 and 19 with two closely spaced precession cycles at 10.05 Ma makes the presented tuning even more likely.

From cycle 30 to 34 and from cycle 45 to 49, the precise tuning of individual lithofacies cycles to precession is less uncertain. Here again, low eccentricity modulates precession, permitting an interplay between precession and obliquity. Nevertheless, cycles 34 to 45 are well constrained by the polarity reversals and the tuning seems to be correct. The tuning reveals that the three intervals with thicker-than-average sedimentary cycles (cycles 16 and 17 in interval II, cycles 30 to 33 in interval IV, and cycles 46, 47, and 49) fall in 405 kyr eccentricity minima (Fig. 8). Such minima display reduced amplitudes of precession due to low eccentricity, thus allowing the 41 kyr obliquity cycle to interfere with precession. Consequently, the thickest cycles (14, 16, 17, 30 to 34, 46, 47, and 49; most including an "a" cycle and indicated by "!" in Fig. 8) may represent obliquity cycles, each comprising two precession cycles. This suggests that the "a" cycles should indeed be regarded as full precession cycles. Also, some of them may represent the longest or most extreme precession minima (or, oppositely, maxima).

The constructed astro-magnetostratigraphic age model for the Prado section thus provides a strong indication that the meter-scale lithofacies cycles are forced by climate variations dominantly driven by the *climatic* precession cycle. Additionally, the astronomical tuning reveals the imprint of periods of low 405 kyr eccentricity by reducing the amplitude of precession. In these periods, obliquity interferes with precession or even might dominate the climate forcing (Abdul Aziz *et al.*, 2003; Hüsing *et al.*, 2007). Astronomical forcing of sedimentation processes recorded in the Prado section is therefore regarded to be the most likely hypothesis underlying the three superimposed scales of lithofacies cyclicity.

2.6.4. Precession – Obliquity Interference Patterns

In Mediterranean deep-marine successions, distinct sedimentary patterns often show a close match with patterns in the summer insolation curve for 65° N (Lourens *et al.*, 2001; Hüsing *et al.*, 2007). The 65° N summer insolation curve is used here, because this target curve best reflects the Mediterranean marine sedimentary cycle patterns in the Neogene (Hilgen *et al.*, 2000; Sierro *et al.*, 2000; Lourens *et al.*, 2001; Hilgen *et al.*, 2003; Hüsing *et al.*, 2007). In times of 405 kyr eccentricity minima the relative influence of obliquity on insolation becomes more prominent, and consequently obliquity can interfere with precession. The resulting distinct patterns in insolation curves are used to evaluate the match with sedimentary cycle patterns (Lourens et al. 2001). In the interval between 9.65 and 9.45 Ma in the Cascante section, the sedimentary record shows a distinct precession – obliquity interference pattern that approximately matches

the P-0.5T (precession minus half obliquity) target curve (Abels *et al.*, 2009), which is similar to the 65° N summer insolation curve. The evaluation of the tuning of the Prado cycles below suggests that a different target curve might be needed for sedimentary cycles in the Iberian Peninsula.

In the Prado section, alternating thick and thin "dry" parts of the cycle (i.e., facies A and B corresponding to groundwater-table lowstands) occur in the same time interval as in Cascante, confirming the presence of an obliquity – precession interference pattern in the stratigraphic column at Prado. However, the thick "dry" parts (cycles 34, 36, 38, 39, 41; Fig. 8) do not specifically match with extreme insolation minima, and thin "dry" parts do not match with relatively high insolation minima. On the contrary, a good pattern match is achieved when the opposite phase relation is regarded (Fig. 8), i.e., the "dry" part corresponding to precession minimum. At present, it is not possible to use this thickness mismatch with insolation as proof of an opposite phase relation because of the remaining uncertainties in the relation between local groundwater fluctuations and local climate and between local climate and precession, as discussed above. Moreover, it can be argued whether sedimentary cycles should be tuned to the 65° N summer insolation or a to different target curve.

2.6.5. Large-Scale Trends

Most large-scale paleoenvironmental shifts in the Prado section occur in intervals of 405 kyr eccentricity minima. The first shift is the change from well-drained mudflat environments in intervals I and II to more persistently waterlogged environments of intervals III and IV, at ~ 10.05 Ma. The reverse environmental change occurs in two steps. The first occurs at 9.65 Ma, from interval IV to V, in which well-drained environments re-enter the stratigraphy. This drying trend culminates in a second one occurring at 9.44 Ma, from interval V to VI, where well-drained mudflat to floodplain environments dominate. The relation between large-scale trends and 405 kyr eccentricity is suggestive, but the time span comprised by the sedimentary record in Prado is regarded to be too short to directly relate such paleoenvironmental shifts to eccentricity. Furthermore, while the 405 kyr minima at 9.35 Ma and 10.15 Ma are related to thick well-drained mudstones, the 405 kyr minimum at 9.7 Ma is related to thick waterlogged mudstones. This suggests that throughout the Prado section the sedimentary paleoenvironments would have reacted differently to long-eccentricity minima. It is then also plausible that other forcing mechanisms played a role, which may include tectonics, non-orbital climate variations, climate variations related to orbital cycles of longer periodicity (Abels *et al.*, 2009), or a geomorphologic shift of the lacustrine environment.

2.7. DISCUSSION

Orbital climate forcing is shown to be the most plausible driver of paleoenvironmental change and therefore of local patterns in sedimentation in the Prado area, by using an integrated stratigraphic and sedimentologic methodology. In addition, the cyclostratigraphic approach enables to establish a high-resolution magneto-astro-chronological framework and analyze the meaning and architecture of facies variability at a temporal scale of 10^3 to 10^5 yr, which is usually hard to attain in ancient continental successions.

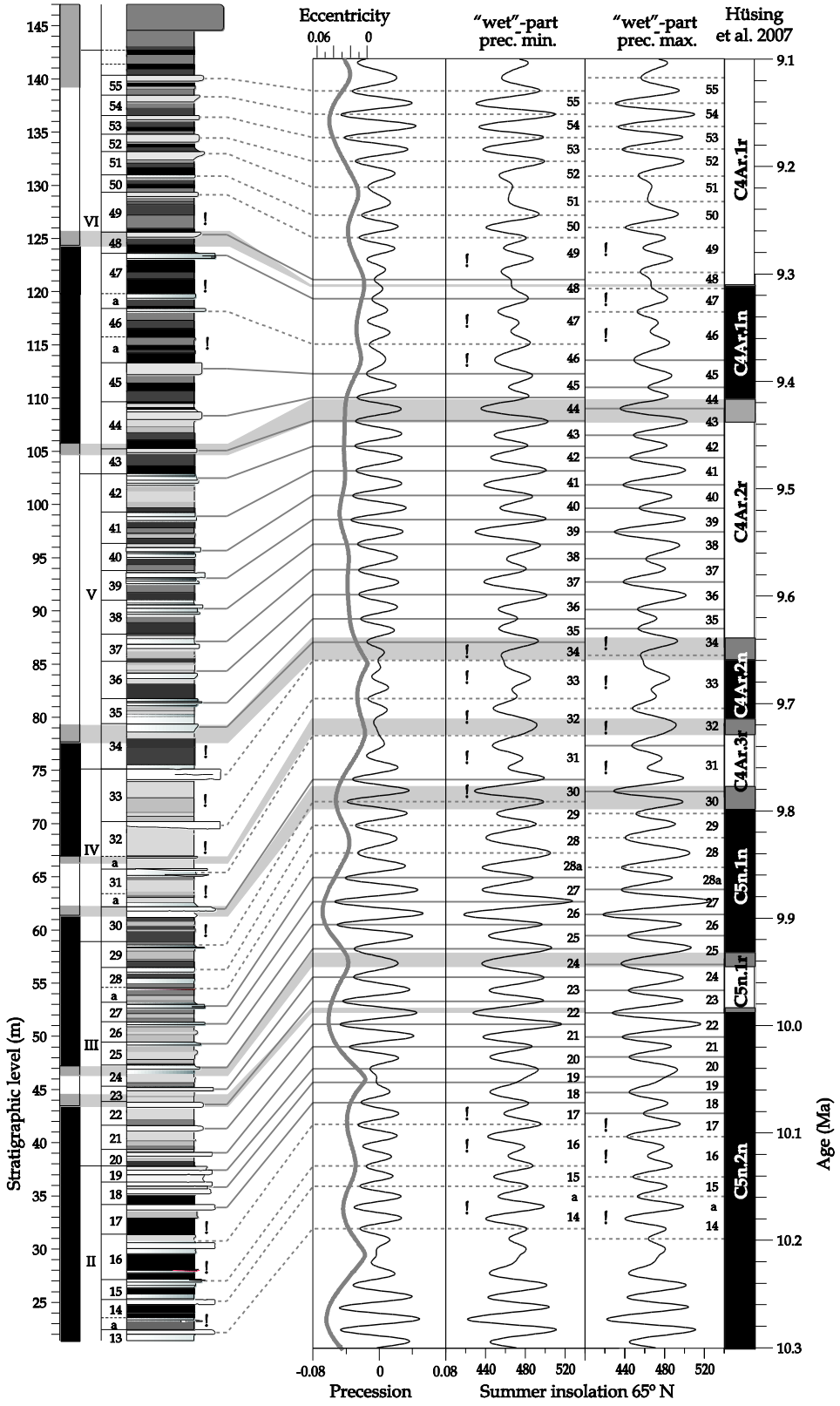

Figure 8 *- Astronomical calibration of the lithofacies cycles in Prado to precession and insolation target curves of Laskar et al. (2004), according to the two phase relations discussed in the text. To the left, a schematic log of the Prado section is shown, including the interpreted polarity results, and interval and cycle numbers. Cycle numbers are also indicated along the insolation curves. Thick cycles are indicated by "!" and occur during long, 405 kyr eccentricity minima. Gray-shaded bands indicate the correlation of polarity reversals and their respective uncertainty intervals in the Prado section to the astronomically calibrated reversals of the Monte dei Corvi in Italy (Hüsing et al., 2007).*

The Miocene facies organization on a meter scale in Prado is dominantly controlled by the climatic precession cycle, with a recognizable imprint by long, 405 kyr eccentricity and by obliquity on stratigraphic scales variable from meters to tens of meters. The influence of the precession cycle on the climate of the Iberian Peninsula and its signature in the geologic record has previously been identified in the Late Cenozoic Spanish sedimentary record (Abdul Aziz *et al.*, 2000; Sierro *et al.*, 2000; Krijgsman *et al.*, 2001; Sierro *et al.*, 2001; Kruiver *et al.*, 2002; Luzón *et al.*, 2002; Abdul Aziz *et al.*, 2004). Some of these studies also confirmed the concomitant role of obliquity and short and long eccentricity in coupling longer-term climate change to sedimentation (Krijgsman *et al.*, 1994; Barberà *et al.*, 1996; Sierro *et al.*, 2000; Abdul Aziz *et al.*, 2003; Abels *et al.*, 2009).

Orbital forcing in the Prado section is demonstrated with the use of polarity-reversal ages that have been calculated by astronomical tuning of sapropel patterns in the Miocene Monte dei Corvi section, in northern Italy (Hüsing *et al.*, 2007). Our reasoning thus highly depends on such astronomically tuned sedimentary successions that have a reliable magnetostratigraphy. The astronomical control of sedimentary cyclicity at Monte dei Corvi was confirmed by the astronomically tuned sapropels at Monte Gibliscemi (Hilgen *et al.*, 2000; Hilgen *et al.*, 2003). Further corroboration comes from the $^{40}Ar/^{39}Ar$ dating of biotites from two intercalated ash layers that indicate an average periodicity close to 20 kyr for basic cycles, of ~ 40 kyr for intermediate cycles, and of ~ 100 and ~ 400 kyr for the larger-scale cycles in the interval bracketed by the ash layers (Cleaveland *et al.*, 2002; Hilgen *et al.*, 2003). It must be noted that using astronomically calibrated ages for polarity reversals to construct an age model in an independent section is not equivalent to importing orbital cycle frequencies recognized in the section from which these ages were derived. This is because reversals of the Earth's magnetic field occur independently of orbital climate forcing. The results from the Prado section can rather be regarded as a corroboration of the constructed time scale and astronomical forcing hypothesis for the Monte dei Corvi section, similar to the corroboration based on comparing sapropel patterns of Monte dei Corvi and Monte Gibliscemi (Hilgen *et al.*, 2003). The three cyclostratigraphic studies were carried out independently, even though Monte dei Corvi reversal ages were used as first-order age control for the Prado stratigraphy. The three sedimentary systems of these sections developed totally independently in separate marine environments and in the continental realm.

The cyclostratigraphy method applied in this study has a high potential for detecting orbital climate forcing in continental successions. Importing astronomically calibrated ages of reversal boundaries does not imply that the age model of the studied succession is biased towards astronomical forcing. Instead, if the astronomical time scale is correctly calibrated, then potentially the best possible detailed age model is used (Van Vugt *et al.*, 1998; Kruiver *et al.*, 2002; Abels *et al.*, 2009). Also, the method avoids demonstration of astronomical forcing by comparing the lithofacies cyclicity with orbital cycle ratios derived from statistical analysis (Wilkinson *et al.*, 2003; Meyers & Sageman, 2007; Bailey & Smith, 2008). Future statistical analysis of a sound, well-defined proxy record for water availability in the Prado paleoenvironment would, however, make the astronomical forcing hypothesis of this study stronger.

2.8. CONCLUSIONS

Astronomical climate forcing of facies organization is demonstrated in the continental Prado section as part of the Upper Miocene fill of the endorheic, low-gradient southern Teruel Basin (Northeast Spain). Detailed sedimentological logging coupled to stratigraphic analysis allowed the recognition of a meter-scale, composite lithofacies cycle. This cycle consists of an alternation of predominantly fine clastic and carbonate or carbonate-rich facies, and is interpreted in terms of relative variations through time of local groundwater level. The detailed magnetostratigraphic age model provided for the Prado section suggests that the meter-scale cyclicity is regulated by the climatic precession cycle. An astrochronology is established by correlating the individual meter-scale cycles to successive precession cycles. The resulting astronomical ages for polarity reversals at Prado are within the uncertainties of the time scale used. The age framework shows the superimposed imprint of long eccentricity and obliquity in modulating precession-scale cyclicity in three stratigraphic intervals. Uncertainties remain regarding the exact phase relation of groundwater to local climate and local climate to precession. Nevertheless, the astronomical tuning clearly reveals that orbital forcing was the prevailing forcing mechanism in the Prado mudflat to marginal lacustrine paleoenvironments at 10^3 yr to 10^5 yr time scales. This study shows that using astronomically calibrated ages for reversal boundaries is a useful method for demonstrating orbital forcing in nonmarine successions.

ACKNOWLEDGEMENTS

Jan van Dam, Liesbeth Jasperse, Karel Steensma, and Anne van der Weerd are thanked for field assistance. Uwe Kircher (LMU Munich, Germany) is thanked for assistance with palaeomagnetic measurements. José Pedro Calvo (IGME, Spain) is thanked for fruitful sedimentological discussions in the field. Poppe de Boer (Utrecht University, Netherlands) is thanked for constructive remarks on earlier versions of the manuscript. Fieldwork permits in this protected area are kindly supplied by the Instituto Aragonés de Gestión Ambiental (INAGA). Hemmo Abels and Dario Ventra acknowledge the financial support of the Dutch Science Foundation (NWO).

REFERENCES

Abdul Aziz, **H., Hilgen, F.J., Krijgsman, W., Sanz, E.** and **Calvo, J.P.** (2000) Astronomical forcing of sedimentary cycles in the middle to late Miocene continental Calatayud Basin (NE Spain). *Earth and Planetary Science Letters*, **177**, 9-22.

Abdul Aziz, H., Krijgsman, W., Hilgen, F.J., Wilson, D.S. and **Calvo, J.P.** (2003) An astronomical polarity timescale for the late Middle Miocene based on cyclic continental sequences. *Journal of Geophysical Research*, **108 B3**, doi: 10.1029/2002JB001818.

Abdul Aziz, H., Van Dam, J.A., Hilgen, F.J. and **Krijgsman, W.** (2004) Astronomical forcing in Upper Miocene continental sequences: implications for the Geomagnetic Polarity Time Scale. *Earth and Planetary Science Letters*, **222,** 243-258.

Abels, H.A., Abdul Aziz, H., Calvo, J.P. and **Tuenter, E.** (2009) Shallow lacustrine carbonate microfacies documents orbitally paced lake-level history in the Teruel Basin (NE Spain). *Sedimentology*, **56**, 399-419.

Alonso-Zarza, A.M. (2003) Palaeoenvironmental significance of palustrine carbonates and calcretes in the geological record. *Earth-Science Reviews*, **60**, 261-298.

Alonso-Zarza, A.M. and **Calvo, J.P.** (2000) Palustrine sedimentation in an episodically subsiding basin: the Miocene of the northern Teruel Graben (Spain). *Palaeogeography, Palaeoclimatology, Palaeoecology*, **160**, 1-21.

Anadón, P. and **Moissenet, E.** (1996) Neogene basins in the eastern Iberian range. In: *Tertiary Basins of Spain – The Stratigraphic Record of Crustal Kinematics* (Eds. P.F. Friend and C.J. Dabrio), pp. 68-71, Cambridge University Press, Cambridge, UK.

Anadón, P., Ortí, F. and **Rosell, L.** (1997) Unidades evaporíticas de la zona de Libros-Cascante (Mioceno, Cuenca de Teruel): Características estratigráficas y sedimentológicas. *Cuadernos de Geología Ibérica*, **22**, 283-304.

Astin, T.R. (1990) The Devonian lacustrine sediments of Orkney, Scotland; implications for climate cyclicity, basin structure and maturation history. *Journal of the Geological Society of London*, **147**, 141-151.

Bailey, R.J. and **Smith, D.G.** (2008) Quantitative tests for stratigraphic cyclicity. *Geological Journal*, **43**, 431-446.

Barberà, X., Cabrera, L., Marzo, M. and **Ripepe, M.** (1996) Sedimentación lacustre y ciclicidad: las sucesiones fluvio-lacustres del Oligoceno superior del sector SE de la cuenca del Ebro. *Geogaceta*, **20**, 1072-1073.

Bradley, W.H. (1929) *The varves and climate of the Green River epoch*. U.S. Geological Survey, Professional Paper **158-E**, p. 87-110.

Broekman, J.A. (1983) Environments of deposition, sequences and history of Tertiary continental sedimentation in the Basin of Teruel-Ademuz (Spain). *Proceedings of the Koninklijke Nederlandse Academie van Wetenschappen*, Series B, **86**, 25-37.

Broekman, J.A., Besems, R.E., Van Daalen, P. and **Steensma, K.** (1983) Lithostratigraphy of Tertiary continental deposits in the Basin of Teruel-Ademuz (Spain). *Proceedings of the Koninklijke Nederlandse Academie van Wetenschappen*, Series B, **86**, 1-16.

Buurman, P. (1980) Paleosols in the Reading Beds (Paleocene) of Alum Bay, Isle of Wight, U.K. *Sedimentology*, **27**, 593-606.

Cleaveland, L., Jensen, J., Goese, S., Bice, D.M. and **Montanari, A.** (2002) Cyclostratigraphic analysis of pelagic carbonates at Monte dei Corvi (Ancona, Italy) and astronomical calibration of the Serravallian - Tortonian boundary. *Geology*, **30**, 931-934.

Eardley, A.J., Shuey, R.T., Gvosdetsky, V., Nash, W.P., Picard, M.D., Gray, D.C. and **Kukla, G.J.** (1973) Lake cycles in the Bonneville Basin, Utah. *Geological Society of America Bulletin*, **84**, 211-216.

Evans, H.F., Westerhold, T., Paulsen, H. and **Channell, J.E.T.** (2007) Astronomical ages for Miocene polarity chrons C4Ar-C5r (9.3-11.2 Ma), and for three excursion chrons within C5n.2n. *Earth and Planetary Science Letters*, **256**, 455-465.

Fischer, A.G. and **Roberts, L.T.** (1991) Cyclicity in the Green River Formation (lacustrine Eocene) of Wyoming. *Journal of Sedimentary Petrology*, **61**, 1146-1154.

Hilgen, F.J., Abdul Aziz, H., Krijgsman, W., Raffi, I. and **Turco, E.** (2003) Integrated stratigraphy and astronomical tuning of the Serravallian and lower Tortonian at Monte dei Corvi (Middle-Upper Miocene, northern Italy). *Palaeogeography, Palaeoclimatology, Palaeoecology*, **199**, 229-264.

Hilgen, F.J., Krijgsman, W., Raffi, I., Turco, E. and **Zachariasse, W.J.** (2000) Integrated stratigraphy and astronomical calibration of the Serravallian/Tortonian boundary section at Monte Gibliscemi (Sicily, Italy). *Marine Micropaleontology*, **38**, 181-211.

Hinnov, L.A. (2000) New perspectives on orbitally forced stratigraphy. *Annual Reviews of Earth and Planetary Sciences*, **28**, 419-475.

Huerta, P. and **Armenteros, I.** (2005) Calcrete and palustrine assemblages on a distal alluvial-floodplain: A response to local subsidence (Miocene of the Duero basin, Spain). *Sedimentary Geology*, **177**, 253-270.

Hüsing, S.K., Hilgen, F.J., Abdul Aziz, H. and **Krijgsman, W.** (2007) Completing the Neogene geological time scale between 8.5 and 12.5 Ma. *Earth and Planetary Science Letters*, **253**, 340-358.

Kent, D.V. and **Olsen, P.E.** (1999) Astronomically tuned geomagnetic polarity timescale for the Late Triassic. *Journal of Geophysical Research*, **104, B6**, 12831-12841.

Kiefer, E. (1988) Facies development of a lacustrine tecto-sedimentary cycle in the Neogene Teruel-Ademuz Graben (NE Spain). *Neues Jahrbuch für Geologie und Paläontologie*, **6**, 327-360.

Kirschvink, J.L. (1980) The least-squares line and plane and the analysis of paleomagnetic data. *Geophysical Journal of the Royal Astronomical Society*, **62**, 699-718.

Kraus, M.J. (2002) Basin-scale changes in floodplain paleosols: implications for interpreting alluvial architecture. *Journal of Sedimentary Research*, **72**, 500-509.

Kraus, M.J. and **Hasiotis, S.T.** (2006) Significance of different modes of rhizolith preservation to interpreting paleoenvironmental and paleohydrologic settings: examples from Paleogene paleosols, Bighorn Basin, Wyoming, U.S.A.. *Journal of Sedimentary Research*, **76**, 633-646.

Krijgsman, W., Fortuin, A.R., Hilgen, F.J. and **Sierro, F.J.** (2001) Astrochronology for the Messinian Sorbas basin (SE Spain) and orbital (precessional) forcing for evaporite cyclicity. *Sedimentary Geology*, **140**, 43-60.

Krijgsman, W., Langereis, C.G., Daams, R. and **Van der Meulen, A.J.** (1994) Magnetostratigraphic dating of the middle Miocene climate change in the continental deposits of the Aragonian type area in the Calatayud - Teruel basin (Central Spain). *Earth and Planetary Science Letters*, **128**, 513-526.

Kruiver, P.P., Krijgsman, W., Langereis, C.G. and **Dekkers, M.J.** (2002) Cyclostratigraphy and rock-magnetic investigation of the NRM signal in late Miocene palustrine-alluvial deposits of the Librilla section (SE Spain). *Journal of Geophysical Research*, **107, B12**, doi 10.1029/2001JB000945.

Laskar, J., Robutel, P., Joutel, F., Gastineau, M., Correia, A.C.M. and **Levrard, B.** (2004) A long term numerical solution for the insolation quantities of the Earth. *Astronomy and Astrophysics*, **428**, 261-285.

Lourens, L.J., Hilgen, F.J., Shackleton, N.J., Laskar, J. and **Wilson, D.S.** (2004) The Neogene Period. In: *A Geologic Time Scale 2004* (Eds. F.M. Gradstein, J.M. Ogg and A. Smith), pp. 405-440, Cambridge University Press, Cambridge, UK.

Lourens, L.J., Wehausen, R. and **Brumsack, H.-J.** (2001) Geological constraints on tidal dissipation and dynamical ellipticity of the Earth over the past three million years. *Nature*, **409**, 1029-1033.

Luzón, A., González, A., Muñoz, A. and **Sánchez-Valverde, B.** (2002) Upper Oligocene-Lower Miocene shallowing-upward lacustrine sequences controlled by periodic and non-periodic processes (Ebro Basin, northeastern Spain). *Journal of Paleolimnology*, **28**, 441-456.

Machette, M.N. (1985) Calcic soils of the southwestern United States. In: *Soils and Quaternary Geology of the Southwestern United States* (Ed. D.L. Weide), Geological Society of America Special Paper, *203*, 1-21.

Machlus, M.L., Olsen, P.E., Christie-Bick, N. and **Hemming, S.R.** (2008) Spectral analysis of the Lower Eocene Wilkins Peak Member, Green River Formation, Wyoming: Support for Milankovitch cyclicity. *Earth and Planetary Science Letters*, **268**, 64-75.

Meyers, S.R. and **Sageman, B.B.** (2007) Quantification of deep-time orbital forcing by average spectral misfit. *American Journal of Science*, **307**, 773-792.

Meyers, S.R., Sageman, B.B. and **Hinnov, L.A.** (2001) Integrated quantitative stratigraphy of the Cenomanian-Turonian Bridhe Creek Limestone Member using evolutive harmonic analysis and stratigraphic modeling. *Journal of Sedimentary Research,* **71**, 628-644.

Munsell, R.A. (1999) *Munsell Soil Color Charts*. M. C. Company, Maryland, Macbeth Division of Kollmorgen.

Olsen, P.E. (1986) A 40-million-year lake record of early Mesozoic orbital climate forcing. *Science*, **234**, 842-848.

Ortí, F., Rosell, L. and **Anadón, P.** (2003) Deep to shallow lacustrine evaporites in the Libros Gypsum (southern Teruel Basin, Miocene, NE Spain): an occurence of pelletal gypsum rhythmites. *Sedimentology*, **50**, 361-386.

Pälike, H., Norris, R.D., Herrle, J.O., Wilson, P.A., Coxall, H.K., Lear, C.H., Shackleton, N.J., Tripati, A.K. and **Wade, B.S**. (2006) The heartbeat of the Oligocene climate system. *Science*, **314**, 1894-1898.

Picard, M.D. and **High, L.R.** (1981) Physical stratigraphy of ancient lacustrine deposits. In: *Recent and Ancient Nonmarine Depositional Environments* (Eds. F.G. Ethridge and R.M. Flores), SEPM Special Publication, **31**, 233-259.

Pietras, J.T. and **Carroll, A.R.** (2006) High-resolution stratigraphy of an underfilled lake basin: Wilkins Peak Member Eocene Green River Formation, Wyoming, U.S.A.. *Journal of Sedimentary Research*, **76**, 1197-1214.

PiPujol, M.D. and **Buurman, P.** (1997) Dynamics of iron and calcium carbonate redistribution and palaeohydrology in middle Eocene alluvial paleosols of the southeast Ebro Basin margin (Catalonia, northeast Spain). *Palaeogeography, Palaeoclimatology, Palaeoecology*, **134**, 87-107.

Reinhardt, L. and **Ricken, W.** (2000) The stratigraphic and geochemical record of Playa Cycles: monitoring a Pangaean monsoon-like system (Triassic, middle Keuper, S. Germany). *Palaeogeography, Palaeoclimatology, Palaeoecology*, **161**, 205-227.

Retallack, G.J. (2001) *Soils of the Past - an Introduction to Paleopedology*. Blackwell Science Ltd., Oxford, UK, 404 p.

Sierro, F.J., Hilgen, F.J., Krijgsman, W. and **Flores, J.A.** (2001) The Abad composite (SE Spain): a Messinian reference section for the Mediterranean and the APTS. *Palaeogeography, Palaeoclimatology, Palaeoecology*, **168**, 141-169.

Sierro, F.J., Ledesma, S., Flores, J.-A., Torrescusa, S. and **Martínez del Olmo, W.** (2000) Sonic and gamma-ray astrochronology: cycle to cycle calibration of Atlantic climatic records to Mediterranean sapropels and astronomical oscillations. *Geology*, **28**, 695-698.

Steenbrink, J., Van Vugt, N., Hilgen, F.J., Wijbrands, J.R. and **Meulenkamp, J.E.** (1999) Sedimentary cycles and volcanic ash beds in the Lower Pliocene lacustrine succession of Ptolemais (NW Greece): discrepancy between $^{49}Ar/^{39}Ar$ and astronomic ages. *Palaeogeography, Palaeoclimatology, Palaeoecology*, **152**, 283-303.

Van Dam, J.A. (2006) Geographic and temporal patterns in the late Neogene (12–3 Ma) aridification of Europe: The use of small mammals as paleoprecipitation proxies. *Palaeogeography, Palaeoclimatology, Palaeoecology*, **238**, 190-218.

Van Vugt, N., Langereis, C.G. and **Hilgen, F.J.** (2001) Orbital forcing in Pliocene-Pleistocene Mediterranean lacustrine deposits: dominant expression of eccentricity versus precession. *Palaeogeography, Palaeoclimatology, Palaeoecology*, **172**, 193-205.

Van Vugt, N., Steenbrink, J., Langereis, C.G., Hilgen, F.J. and **Meulenkamp, J.E.** (1998) Magnetostratigraphy-based astronomical tuning of the early Pliocene lacustrine sediments of Ptolemais (NW Greece) and bed-to-bed correlation with the marine record. *Earth and Planetary Science Letters*, **164**, 535-551.

Weedon, G.P. (2003) *Time-Series Analysis and Cylostratigraphy - Examining Stratigraphic Records of Environmental Cycles*. Cambridge University Press, Cambridge, UK, 274 p.

Westerhold, T., Röhl, U., Raffi, I., Fornaciari, E., Monechi, S., Reale, V., Bowles, J. and **Evans, H.F.** (2008) Astronomical calibration of the Paleocene time. *Palaeogeography, Palaeoclimatology, Palaeoecology*, **257**, 377-403.

Wilkinson, B.H., Merrill, G.K. and **Kivett, S.J.** (2003) Stratal order in Pennsylvanian cyclothems. *Geological Society of America Bulletin*, **115**, 1068-1087.

Wright, P.V. and **Marriott, S.B.** (2007) The dangers of taking mud for granted: Lessons from Lower Old Red Sandstone dryland river systems of South Wales. *Sedimentary Geology*, **195**, 91-100.

Wright, V.P. and **Tucker, M.E.** (1991) Calcretes: an introduction. In: *Calcretes* (Eds. V.P. Wright and M.E. Tucker), IAS Reprint Series, **2**, 1-22.

Zijderveld, J.D.A. (1967) A.C. demagnetization of rocks: analysis of results. In: Developments in Solid Earth Geoscience Methods in Palaeomagnetism (Eds. D.W. Collinson, K.M. Creer and S.K. Runcorn), pp. 254-286, Elsevier Publishing Company, Amsterdam, the Netherlands.

"*The important thing in science is not so much to obtain new facts, as to discover new ways of thinking about them.*"

William L. Bragg

Chapter 3

Orbitally controlled sedimentation in a Miocene alluvial fan (Teruel Basin, Spain)

D. Ventra, H.A. Abels, F.J. Hilgen & P.L. de Boer

ABSTRACT

The role of climate change in driving alluvial-fan sedimentation proves hard to assess, especially in pre-Quaternary successions for which detailed chronologies and climate records cannot be easily established. In the central Teruel Basin (Spain), a high-resolution chronology and paleoclimate information were derived by orbital tuning of Late Miocene mudflat to ephemeral lake deposits. The semiarid paleoclimatic setting made this low-gradient, basinal environment particularly sensitive to thresholds in local hydrological balance. Basic facies rhythms have been attributed to alternating, relatively humid/arid phases controlled by the climatic precession cycle. The lower stratigraphic interval of this reference section is interfingered by distal, coarse-clastic beds from a coeval alluvial fan. The regular occurrence of debrisflow units in correspondence of distal strata indicative of arid-humid climate transitions shows that fan sedimentation was regulated by climate cyclicity. The highest volumes of clastic transfer to basinal mudflats from the adjacent fan domain correspond to relatively humid periods with more pronounced seasonality during precession minima. Distal to medial sections within alluvial-fan outcrops also feature prominent alternations of coarse and fine clastic packages, laterally continuous at the scale of the whole depositional system. This high degree of architectural organization, uncommon in fan successions, suggests the influence of a periodic and persistent forcing mechanism which, as evidenced by the stratigraphic relationships with the reference section, must have been been orbitally controlled climate change.

3.1. INTRODUCTION

Alluvial fans and their catchments are geomorphic entities of restricted area, and therefore potentially able to respond in relatively short times to allogenic forcing. However, the concomitant occurrence of autogenic processes and feedbacks makes alluvial fans very complex systems, in spite of their apparently simple geometry and organization, and general models for their stratigraphic evolution are still in debate (Lecce, 1990; Blair & McPherson, 1994; Harvey *et al.*, 2005; Harvey, 2010). Idealized models of fan sedimentation and dynamics are particularly elusive because of the great variety of geologic and climatic settings in which alluvial fans can develop, even within a single region (e.g. Harvey *et al.*, 1999; Blair, 1999; Mather *et al.*, 2005; Dühnforth *et al.*, 2008).

In particular, the role of climate change in fan evolution is hard to decipher, both for the Quaternary and in the ancient stratigraphic record (Bull, 1991; Dorn, 1994, 1996). Tectonics, as the direct control on fan

location, sediment supply and accommodation, has traditionally overshadowed the climatic factor in the interpretation of alluvial-fan successions over geologic timescales (e.g., Bull, 1977; Heward, 1978; North *et al*., 1989; De Celles *et al*., 1991; Fraser & De Celles, 1992; Liu & Yang, 2000; Harvey *et al*., 2005; Leleu *et al.*, 2009). On the other hand, interpretations of fan deposits in terms of climate have long been considered subject to potential flaws because primary sedimentary processes in alluvial fans are triggered by intense, episodic meteorological events that cannot be uniquely and unambiguously ascribed to any specific long- or medium-term climate phase (Dorn, 1994, 2009; Blair & McPherson, 1994). A common lack of high-resolution chronological control and paleoclimate proxies in coarse-clastic successions makes it hard to link the inferred processes to possible environmental controls within a reliable time framework. Direct assessment of relations between specific sediment packages in fan deposits and the associated climate context is thus rare in pre-Quaternary studies. Several recent studies emphasize the importance of climate with respect to more classic tectonic interpretations (e.g. De Boer *et aI*., 1991; Ritter *et al*., 1995; Reheis *et al*., 1996; Mack & Leeder, 1999; Ritter *et aI.*, 2000; Singh *et al*., 2001; Harvey, 2004; Quigley *et al*., 2007), usually from a geomorphic perspective rather than a stratigraphic one, and often limited to the Quaternary (Harvey *et al*., 2005; Dorn, 2009).

This study presents a new approach to address fan-climate relationships in pre-Quaternary successions, based on the stratigraphic record of the western margin of the Tertiary Teruel Basin (central Spain). Here, extensive outcrops in facies successions of low-energy environments have provided high-resolution chronological and paleoenvironmental information by the integration of different stratigraphic methods (Krijgsman *et al.*, 1994, 1997; Van Dam, 1997; Abdul Aziz *et al*., 2004; Abels *et al*., 2009a), mainly magnetostratigraphy and cyclostratigraphy. The opportunity to physically correlate these successions with adjacent exposures of coarse-clastic systems along the basin margin allows direct comparisons between very different, coeval depositional systems that developed under the same paleoenvironmental conditions.

3.2. GEOLOGICAL SETTING AND STUDY AREA

The Teruel Basin (Spain; Fig. 1) is a Neogenic tectonic depression developed through the axial linkage of NNE-SSW-oriented half grabens (Anadon *et al*., 1990; Guimerà, 1997) over the central Iberian Range. With a length of approximately 115 km and a variable width of 15-20 km, the basin started opening from the early Miocene as part of the Western European Rift System (Anadón *et al*., 1990; Roca & Guimerà, 1992; Lewis *et al*., 2000), by extensional reactivation of pre-Tertiary tectonic lineaments of the Iberian Range (Anadon & Moissenet, 1996). The main depositional history of the Teruel Basin ranges from the early Miocene up to late Pliocene-early Pleistocene, with various phases of tectonic reactivation which delimited a topographically enclosed endorheic depression.

The basin fill comprises coarse and fine alluvial clastics and terrestrial carbonates and evaporites, with a facies distribution typical of continental grabens and half grabens (Leeder & Jackson, 1993; Gawthorphe & Leeder, 2000). Coarse-clastic sedimentation took place in alluvial fans and ephemeral fluvial systems along the basin margins (Broekman, 1983; Kiefer, 1988; Anadón *et al*., 2000; Alonso-Zarza & Calvo, 2000; Abels *et aI.*, 2009a; Ventra, 2009). Lacustrine-palustrine and mudflat environments occupied the central, low-relief

areas of the basin, with deposition of continental carbonates and fine-grained clastics. The stability of these central environments was favored by protracted conditions of internal drainage, which led to a low topography within the basin and continuous aggradation.

In the middle to late Miocene, the Teruel Basin was located slightly south of its present latitude, with a highly seasonal, semiarid Mediterranean climate (Van Dam & Weltje, 1999; Alcalá *et al.*, 2000; Van Dam, 2006). As a topographically isolated endorheic trough, its environments and sedimentary processes were highly sensitive to changes in the regional hydrological balance, driven by climate variations. Tertiary lacustrine and alluvial successions in the Teruel and adjacent Calatayud basins have yielded abundant proof of climate control (Alonso-Zarza & Calvo, 2000; Anadón *et al.*, 2000; Ortí *et al.*, 2003), orbital forcing in particular (Abdul Aziz *et al.*, 2000, 2004; Abels *et al.*, 2009a, 2009b), contributing with a substantial extension to the Astronomically Tuned Neogene Time Scale (ATNTS; Abdul Aziz *et al.*, 2003).

The study area is located directly south of Villastar (Fig. 2), in the central segment of the basin, approximately 12 km south of Teruel. A continuous stratigraphic record is exposed in the badlands of the *Prado* area, where coarse-clastic units of an alluvial fan interfinger with the late-Miocene aggradational succession of mudflat to ephemeral lacustrine facies known as *Prado Section* (Abels *et al.*, 2009b). The local Mesozoic basement, accessible on the highlands between Villastar and Villel (Fig. 1), consists of folded Triassic continental to paralic mudstones, unconformably overlain by a thick sequence of Cretaceous alluvial-eolian mudstones and sandstones and marine carbonates. Tectonic subsidence and relief along the western boundary of the basin, now partly onlapped by Tertiary deposits, provided local topographic gradients, debris sources from the exposed Mesozoic basement, and accommodation. The alluvial-fan outcrops in close proximity of Villastar are the best exposed of several clastic systems along the local basin margin. The Villastar Fan prograded to the SE with a minimum radial extension of approximately 4 km; the most proximal portions of the fan and its catchment are presently onlapped by younger Tertiary sediments. General morphology and facies associations reflect a classic high-gradient, mass-flow-dominated alluvial fan (Blair & McPherson 1994).

The present-day physiography of the study area is characterized by low relief to the east and southeast, where fine-grained clastics and continental carbonates of the *Prado Section* are exposed in deeply dissected *badlands* (Figs. 3A, B). Coarse alluvial-fan deposits form prominent steep hills farther to the west (Fig. 3C). This study focuses on stratigraphic relationships between the two adjacent paleodepositional systems. The relevant stratigraphic evidence is accessible in gullies and hillsides along the original eastern fan fringe (Figs. 2, 3C); the southern fan fringe, which probably also interfingers with low-gradient basinal environments, is not exposed. A detailed chronological and paleoenvironmental context for this area has been established by integrated stratigraphy of the *Prado Section* in a previous paper (Abels *et al.*, 2009b), and is briefly summarized in the following section.

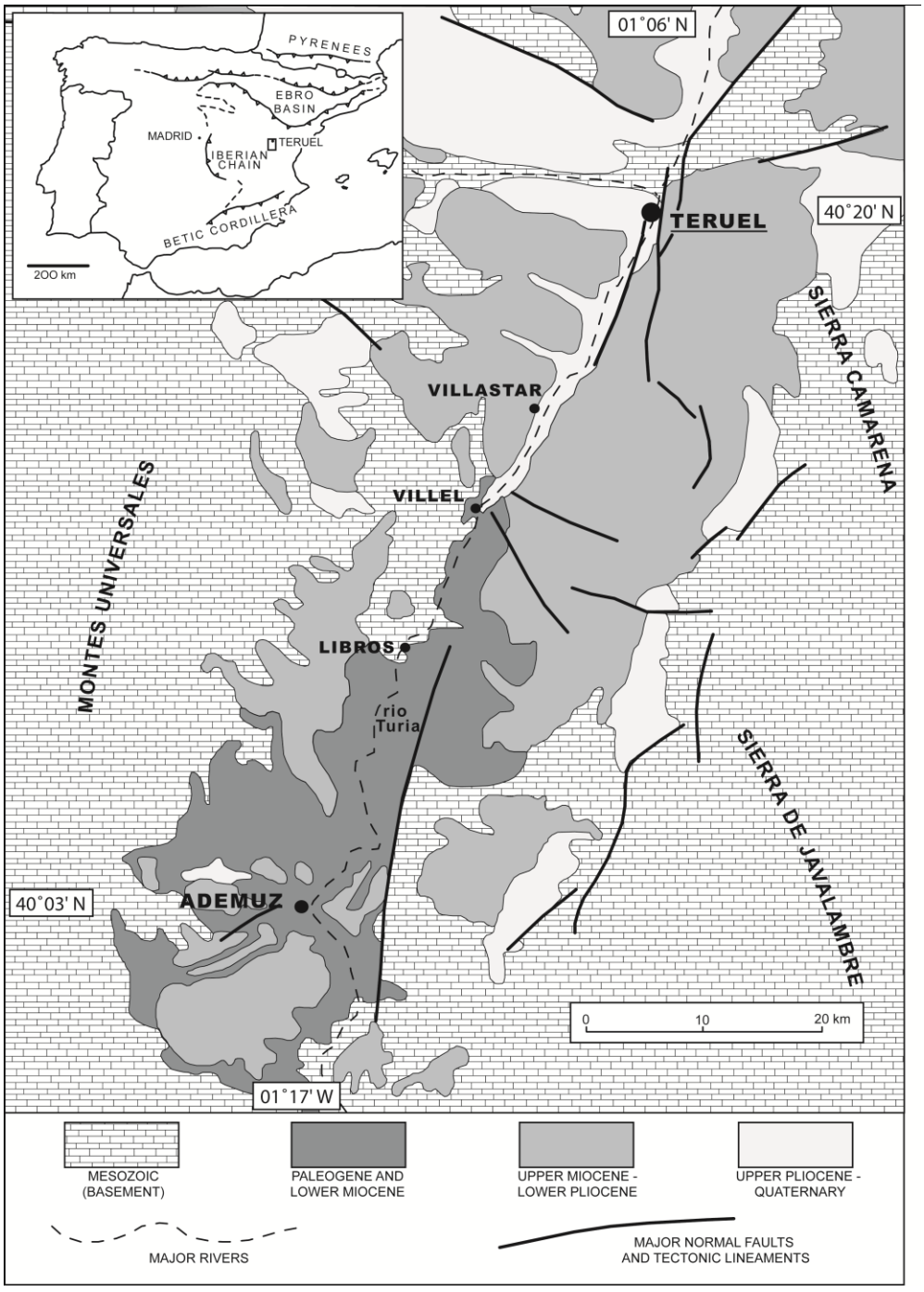

Figure 1 *- Geological map of the Teruel Basin; inset shows location in Spain.*

3.3.THE PRADO SECTION

3.3.1. Stratigraphic Framework

The *Prado Section* (PS), described by Abels *et al.* (2009b), comprises approximately 150 m of fine clastic and carbonate sediments dating from ~10.5 to ~9 Ma (Tortonian/Vallesian, late Miocene). The succession lies in stratigraphic continuity above the Libros Gypsum Unit (Fig. 2; Anadón *et al.*, 1997; Ortí *et al.*, 2003), outcropping south of the study area, and below a thick clastic unit of ephemeral alluvial origin, outcropping in hills to the east.

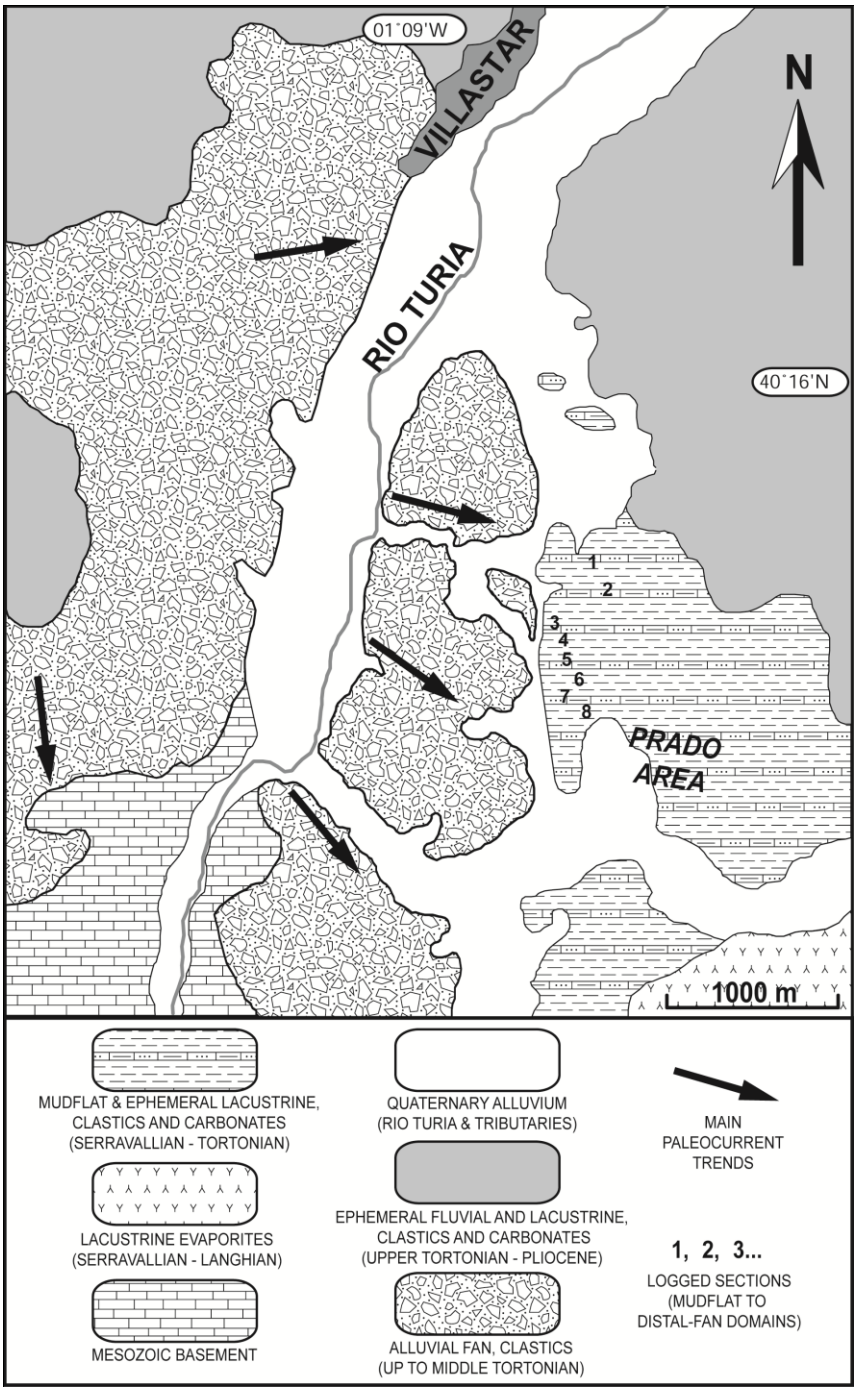

Figure 2 *- Geological map of the study area. Neogene deposits are mapped according to facies and paleoenvironmental criteria. Numbers correspond to the location of logs in Fig. 5.*

The PS features a prominent vertical organization of facies transitions on different scales (Fig. 4). The basal portion comprises mainly red to orange, pedogenically modified alluvial mudstones with interspersed, carbonate-rich horizons and incipient calcretes. This lower part grades upward into an extensive interval of increased lithological variability, with a reduced volume of mudstones and a notable increase in calcic horizons and especially limestones of palustrine and marginal lacustrine origin. The uppermost interval of the PS consists again of dominant, alluvial fine-grained clastics, with rare interbedded carbonate-rich units (Abels *et al.*, 2009b).

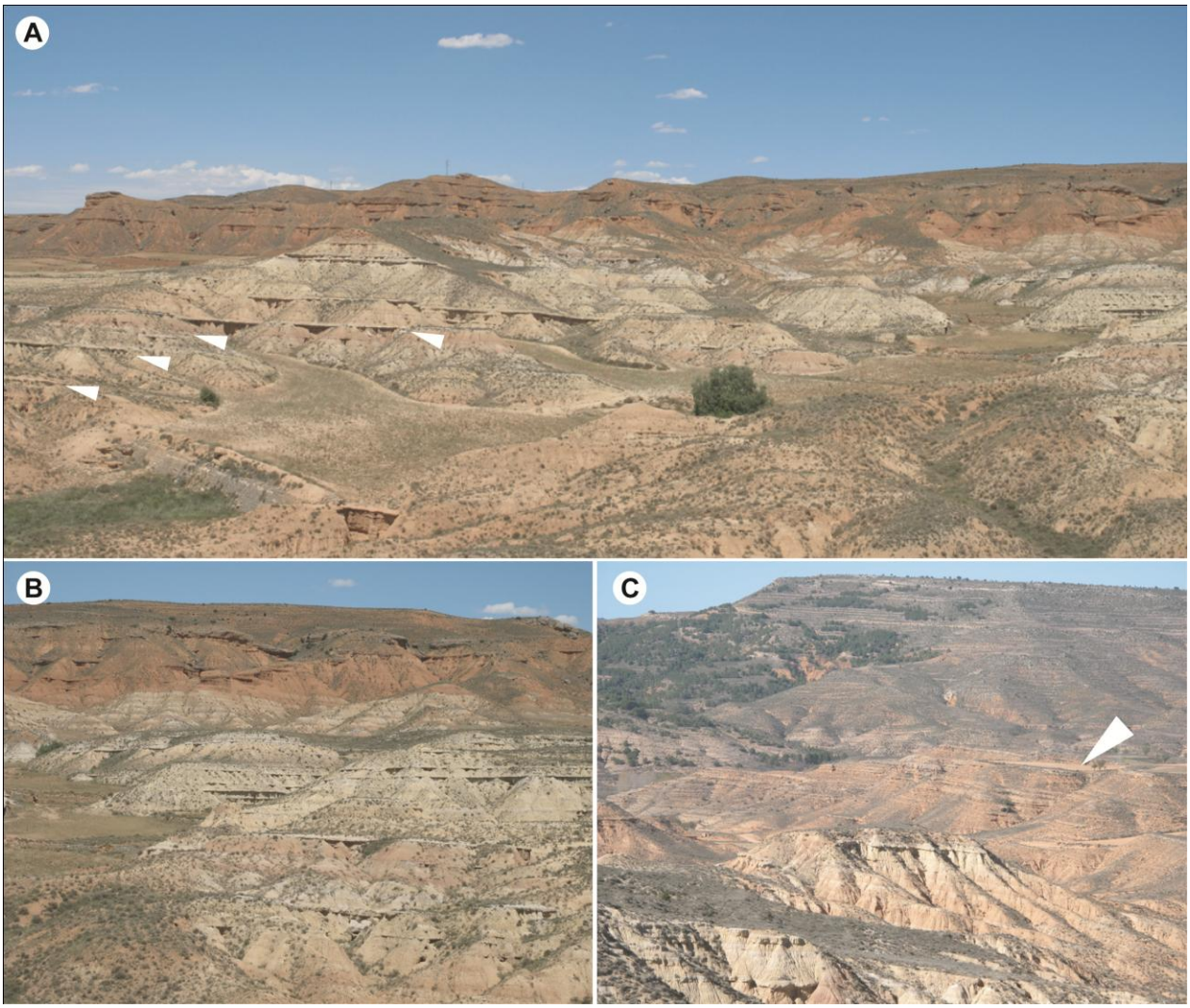

Figure 3 *- (A) Panoramic eastward view of the Prado Section, highlighting the lateral continuity of prominent calcic horizons (white pointers) in the basal interval. (B) View towards the distal domain of the Prado Section, in the southeast.* ***(****C) Westward view to the proximal domain of the Prado Section; note alluvial-fan strata (white pointer) dipping east toward the Prado Section.*

Superimposed on this large-scale trend, the section presents smaller-scale metric alternations of dominantly fine clastic deposits and $CaCO_3$-rich or carbonate facies. Cycle thicknesses vary between 1 and 5 m, with an average of 2.6 m. The lithological composition of single cycles varies depending on its position within the larger-scale domains of the PS. An ideal sedimentary rhythm was therefore described by Abels *et al*. (2009b) as reference for a depositional model relating sedimentation to environmental change.

Lithofacies cycles have been interpreted in terms of variations in groundwater level and, more generally, water availability at the depositional surface. Reduced water availability and low groundwater tables led to a well-drained, low-relief mudflat environment with poorly structured, pedogenically modified muds. Interbedded, incipient calcic horizons correspond to phases of increased water availability and/or temporarily reduced sediment supply, with prolonged surface stability. Gradually rising groundwater levels and occasional flooding resulted in poorly drained mudstone facies and the establishment of shallow ponds or marginal lacustrine conditions, with deposition of extensive (bio)chemical limestone beds.

Detailed magnetostratigraphy and preliminary mammal biostratigraphy, consented the definition of magnetopolarity intervals in the PS (Abels *et al*., 2009b), spanning from chron C5n.2n to C4Ar.1r. An age model was then derived by correlation with the ATNTS (Lourens *et al.*, 2004), for which polarity reversals in this time interval have been recently dated by astronomical tuning of deep marine deposits in the Monte dei Corvi section in Italy (Hüsing *et al.*, 2007). This high-resolution age control allowed Abels *et al.* (2009b) to show that stratigraphic thickness and facies composition of basic, meter-scale facies rhythms were controlled by climatic precession cycles, with an average periodicity of 21 kyr (Abels *et al.*, 2009b, based on the astronomical solution by Laskar *et al.*, 2004). Modulation over longer timescales was observed to occur by the long eccentricity cycle (405 kyr) and by the obliquity cycle (41 kyr). Clearly, orbital climate forcing is the most probable control on paleoenvironmental change driving the development of the basic facies succession within each cycle. Subsequently, an astronomical tuning of meter-scale cycles in the PS to Laskar *et al*.'s (2004) numerical solution was constructed (Fig. 4).

The causal relationship between regional hydrology and astronomically forced paleoclimate cycles was interpreted in terms of significantly increased winter precipitation during precession minima, corresponding to boreal summer insolation maxima (Abels *et al.*, 2009b). Climate modeling of precession extremes indicated that high insolation in Mediterranean summers would have raised sea-surface temperatures and led to enhanced atmospheric moisture budget during Mediterranean winter, leading to a higher annual positive hydrological budget for the Teruel Basin (Abels *et al.*, 2009a). In environmental terms, precession minima, and related maxima in winter precipitation, would have enhanced runoff, groundwater and lake-level highstands. The related sedimentological and pedological responses were increased mottling and Ca mobilization/precipitation within pedogenic mudstones, and increased deposition of palustrine - marginal lacustrine carbonate facies. Precession maxima corresponded to phases of minimal insolation and a markedly negative hydrological budget. Previous stratigraphic and sedimentological studies conducted in the region support this model (Sierro *et al*., 2000; Kruiver *et al*., 2002; Abdul Aziz *et al*., 2003; Abels *et al*., 2009a).

3.3.2. Methodology and Objectives

Eight stratigraphic sections were logged in the lowest interval of the PS (Fig. 5), extending ascertained stratigraphy and correlations of the PS towards the western margin of the Prado area. Here, the prograding alluvial fan merged distally with mudflat and marginal lacustrine subenvironments, as shown by interbedded coarse-clastic units in the recurrent mudstone-carbonate cycles of the PS. Excellent exposures of the lower PS along variously intersecting gullies allowed optimal access to local stratigraphy and detailed correlations (Figs. 3, 6). Partial overlap between sections allowed control on lateral facies variability as well as correlation across the few, small post-depositional faults.

Extension of chronological control downward in the stratigraphy of the PS was attempted by high-resolution core sampling for magnetostratigraphy (~20 cores/m). Abels *et al*. (2009b) found the basal portion of the PS to be entirely comprised within the normal C5n.2n geopolarity subchron, with a duration of approximately 1 My (Cande & Kent, 1995; Hilgen *et al*., 1995; Lourens *et al.*, 2004), which prevents the construction of a more

detailed age model for this stratigraphic interval. Cryptochrons that have been reported for this long interval of normal polarity (Evans *et al.*, 2007) were not found. In spite of the limited age control, direct stratigraphic continuity with the overlying PS and full analogy in terms of facies characterization and rhythmicity, consent to interpret local sedimentary rhythms as the expression of the same precessional climate controls. Distal-fan deposits can thus be interpreted within the same paleoclimatic and paleoenvironmental context as reconstructed for the complete Prado Section.

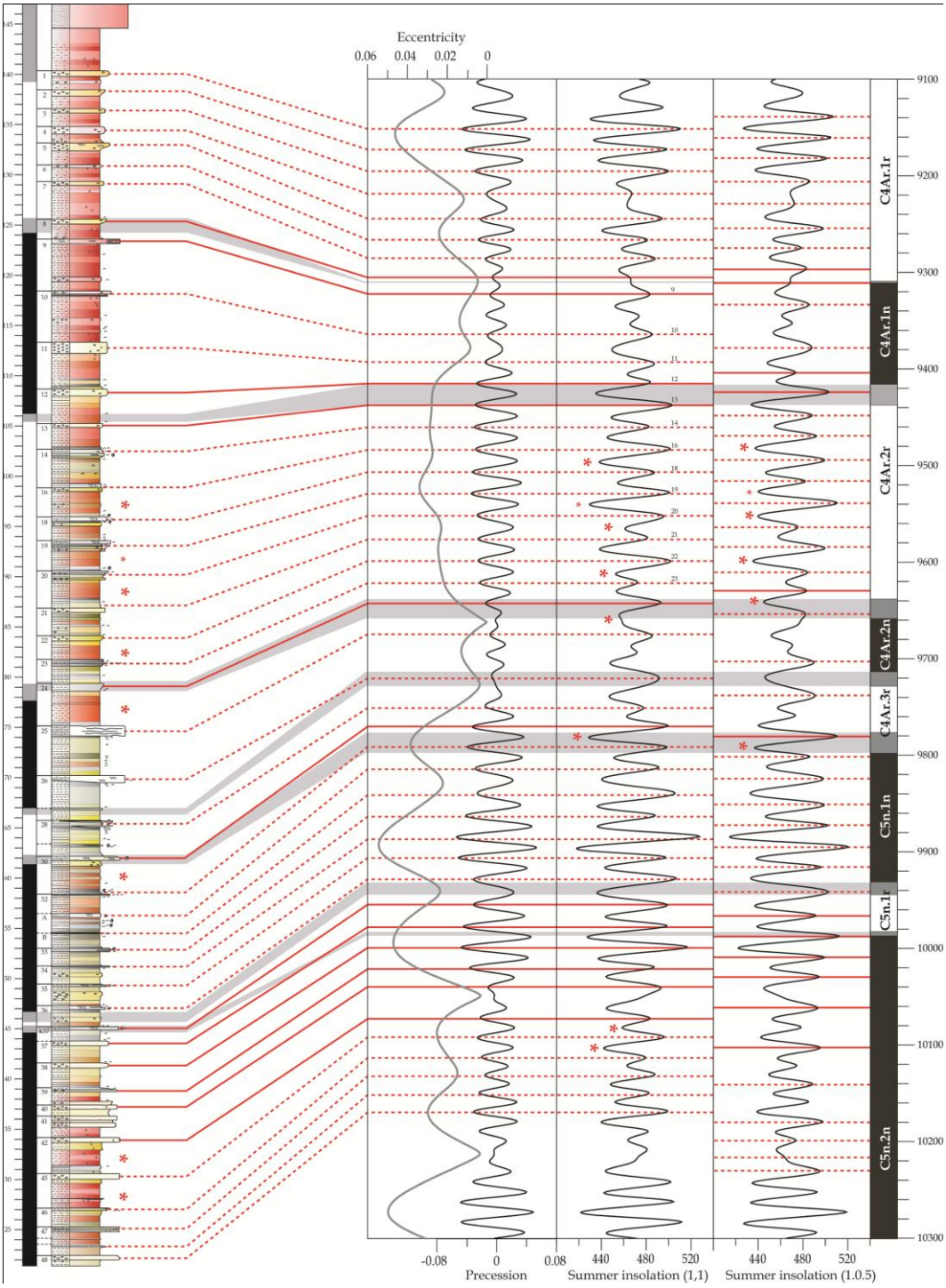

Figure 4 *- Astronomical tuning of stratigraphy in the Prado Section (left column) with the orbital precession cycle, and calculation of associated values of summer insolation according to Laskar et al.'s (2004) numerical solutions. Magnetopolarity shown on the right column.*

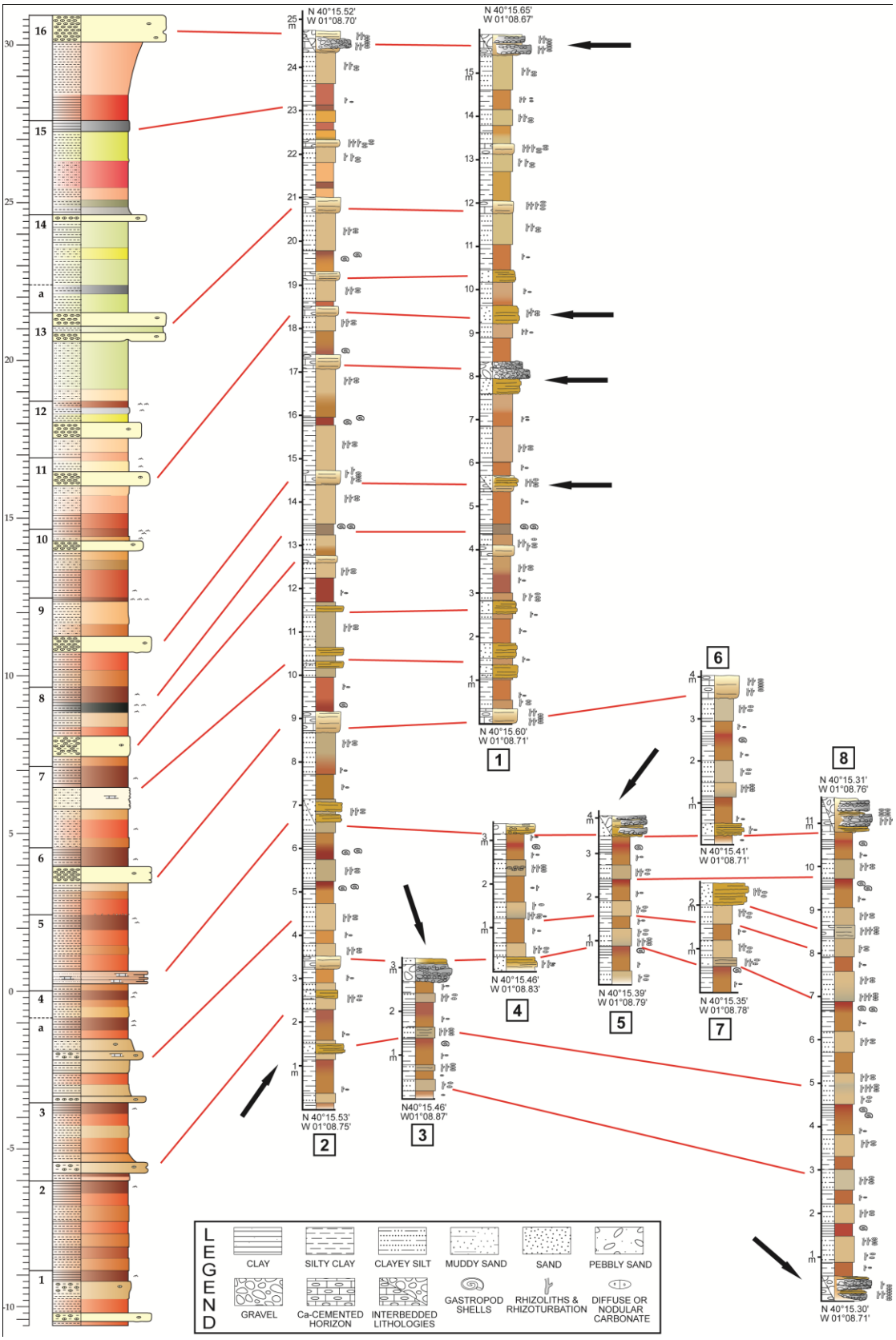

Figure 5 *- Stratigraphic logs measured along the transitional belt between the basinal domain, with mudflat and ephemeral lacustrine deposits (Prado Area), and the distal-fan domain. Black arrows point to the most prominent and continuous clastic units of fan provenance; log numbers correspond to those shown in Figure 2. Partially overlapping stratigraphy from Abels et al. (2009b) shown on the left, for comparison.*

3.4. SEDIMENTOLOGY

3.4.1. Basinal Facies Cycles

Facies A (silty claystones) - Facies A comprises the greatest volume of sediments in the lower part of the PS, and consists of massive, red (reddish orange to dark red) claystones and silty claystones (Figs. 7B, 8A). No primary structures or distinct pedological horizons are evident at outcrop or in hand samples. Weak pedogenic modification is represented by sparse, millimetric carbonate nodules; isolated, mm- to cm-scale grey mottles, usually of equant shape and irregular margins; rare millimetric to centimetric rhizotubules and drab haloes. No other mesoscopic pedological features, such as slickensides or ped structures, are recognizable. Macroscopic bioturbation is not evident. Contacts with coarser facies B mudstones are always planar and laterally continuous, commonly expressed by a gradual transition in color and grain size, but occasionally abrupt and characterized by a sharp color contrast.

Red claystones of facies A reflect alluvial deposition over a low-gradient mudflat environment with weak pedogenic modification. Massive clay and silty clay were probably carried as suspended load by occasional, distal sheetflow events from the adjacent highlands and alluvial fan (Bull, 1977; Hubert & Hyde, 1982; Demicco & Gierlowski-Kordesch, 1986; Hill, 1989; Pimentel, 2002). Deposition took place from suspension settling after local flow expansion and ponding over the low-gradient mudflat. Tractive transport in the form of coarse-silt to sand-sized mud aggregates cannot be excluded (Gierlowski-Kordesch & Gibling, 2002; Wright & Marriott, 2007; Schieber *et al.*, 2007). Sand fractions are almost absent in these deposits.

The scarcity and generally small size of mottled domains and carbonate nodules, together with the lack of soil structures and mature profiles, point to weak pedogenic modification of the primary deposit (Kraus, 1999; Huerta & Armenteros, 2005; Kraus & Hasiotis, 2006). This might be due to a combination of steady aggradation, preventing full development of distinct pedogenic horizons (Buurman, 1980; Kraus, 1999; Daniels, 2003), and prominent semiarid conditions. Low groundwater levels and circulation likely maintained a generally oxidizing environment in the upper sedimentary column and hindered solute mobilization in the soil. Scarcity of bioturbation and vegetation remnants, with only sparse, small rhizoconcretions and drab haloes confirm this. The absence of slickensides, in spite of clay being the dominant component in this facies, also indicates a poor hydrological contrast between seasons and no effective wet-dry cycles (Yaalon & Kalmar, 1978; Zaleha, 1997; Kraus, 2002; Hillier *et al.*, 2010).

Facies B (clayey sandy siltstones) - Facies B consists of massive beds of light orange to yellow-brown, clayey sandy siltstones and sandy siltstones(Figs. 7C, 8B). As in facies A, no primary sedimentary structures or distinct pedogenic horizons are visible at outcrop. Beds are homogeneous, except for an occasional vertical increase in secondary pedogenic features. Carbonate is distinctly more abundant than in facies A, represented by mm- to cm-scale nodules and frequent, grey to yellow-grey rhizoliths, usually preserved as single, rounded or tubular nodules, occasionally clustered in vague branching patterns. Mottled domains also occupy a larger part of the sediment than in facies A, usually as irregular, centimetric, yellow-orange to grey patterns. Besides abundant rhizoliths, no other biogenic structures or fossil remains were observed. Facies B is also characterized by a higher content of fine sand, usually dispersed in the ground mass, and

occasionally represented by thin, interbedded sandstones (facies E) or sparse, small lenses of silty, fine sandstone, a few mm thick and rarely up to a few cm in width.

The amount of carbonates, mottling and rhizoconcretions often presents a gradual increase upward within beds. It rises from a minimum above contacts with the underlying facies A, to a maximum toward the top, where some beds have a multicolored appearance in fresh exposures. Transitions with the overlying facies C are commonly gradual. The abundance of pedogenic carbonate and mottled domains tends to be distinctly higher in facies B beds which are overlain by thick, well-developed facies C beds. Transitions upward to facies A beds, on the other hand, are simply represented by a diminution of secondary pedogenic features and a more or less gradual change in overall color and grain size.

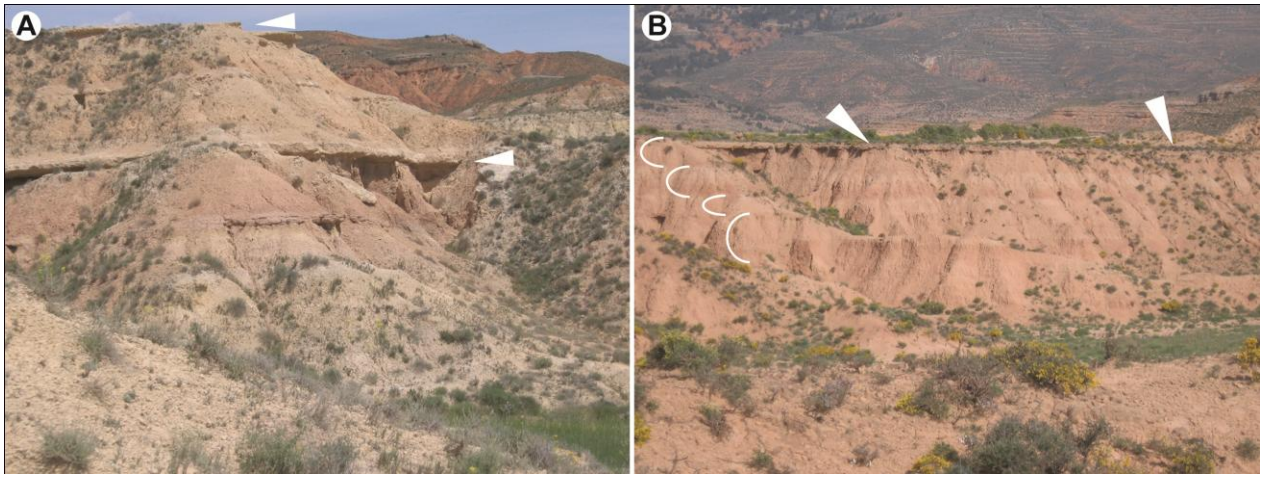

Figure 6 *- Tabular, laterally continuous stratification in basinal deposits of the Prado Area. (A) Prominent calcic horizons (facies C) in the mudstone-dominated middle part of the Prado Section. (B) Broad outcrop view of cyclic alternations (white arches to the left) of red claystones (facies A) and light brown siltstones (facies B) in the lower part of the Prado Section. Note lateral continuity of amalgamated sandstone beds on top of the section (white pointers).*

Homogeneous sandy siltstones of facies B are interpreted as pedogenically modified distal alluvium laid down on a low-gradient mudflat (Talbot *et al.*, 1994; Jorgensen & Fielding, 1996), by analogy with facies A. Absence of primary sedimentary structures is related to biotic and pedogenic activity. The lack of well-organized soil horizons is probably due to a relatively high rate of aggradation relative to effective pedogenic processes in a semiarid environment (Kraus, 1999; Daniels, 2003; Hampton & Horton, 2007). However, the relative abundance of biogenic and pedogenic features compared to facies A points to a more effective modification of the depositional surface. Larger and widespread rhizoconcretions and reprecipitated carbonates, as well as larger mottled domains indicate higher availability of water and probably more prolonged seasonal wetting of soil profiles. The potential to transfer and deposit solutes within the incipient soil was greater than in facies A (Kraus, 2002; Kraus & Hasiotis, 2006). The coarser grain size of facies B siltstones and of the interbedded sandstone facies relates to times of enhanced surface runoff and sediment transport. Scattered lenses of silt and fine sand represent remnants of ephemeral rill systems at the paleosurface.

Weak, incipient pedogenesis of fine-grained alluvium in a semiarid environment developed during more pronounced seasonal wetting and colonization of the depositional surface by sparse vegetation than in facies A. Dominant yellow-brown colors reflect a stronger hydrological cycle and possibly temporary waterlogging relative to well-drained mudflat deposits of facies A (Kraus & Hasiotis, 2006; Abels *et al*., 2009b). The poor permeability of underlying, dominantly clayey facies A horizons would have favored a relatively prolonged water retention and circulation at the top sedimentary column during facies B deposition.

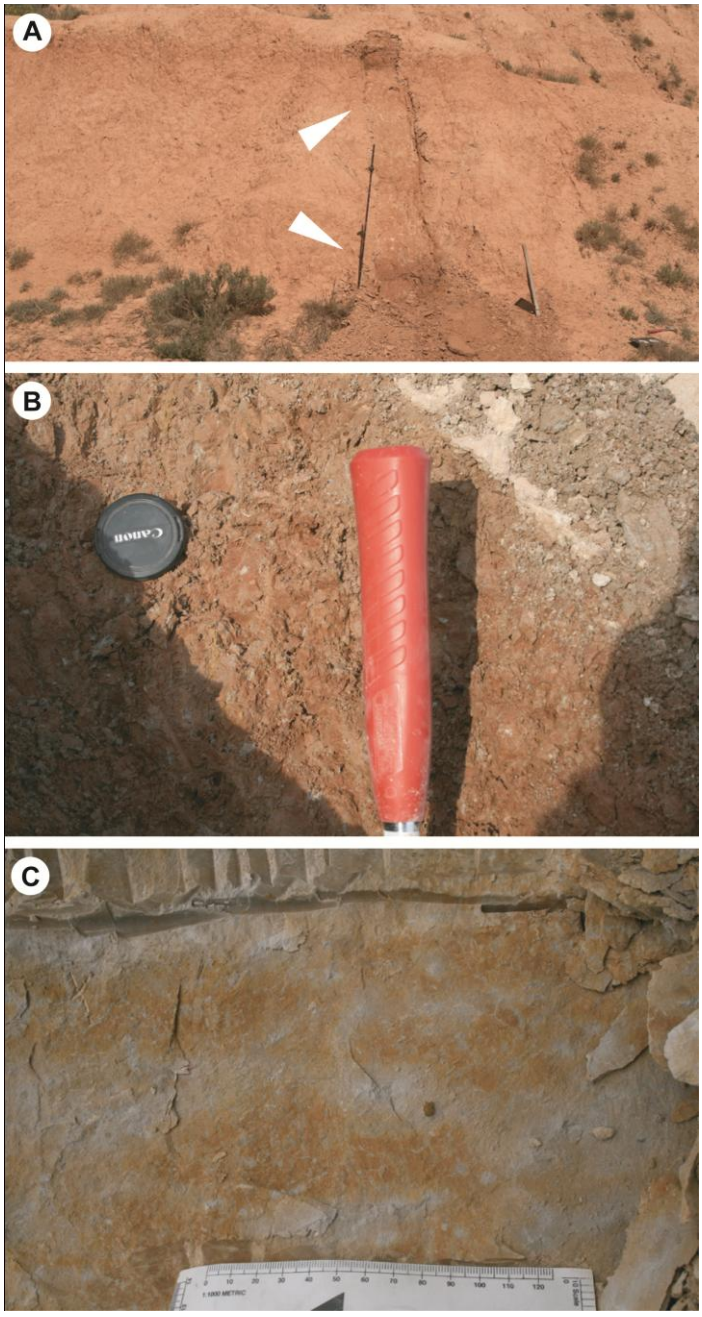

Figure 7 *- (A) Shallow trench to access unweathered deposits, lower Prado Section. Note the differences in tone and visibility between red mudstones (facies A, white pointers) at outcrop and in the trenched exposure. (B) Clayey mudstones of facies A, with minor pedogenic modification; hammer for scale is 35 cm long. (C) Silty mudstones of facies B, with pervasive pedogenic features; note size and abundance of drab haloes; hammer for scale is 35 cm long.*

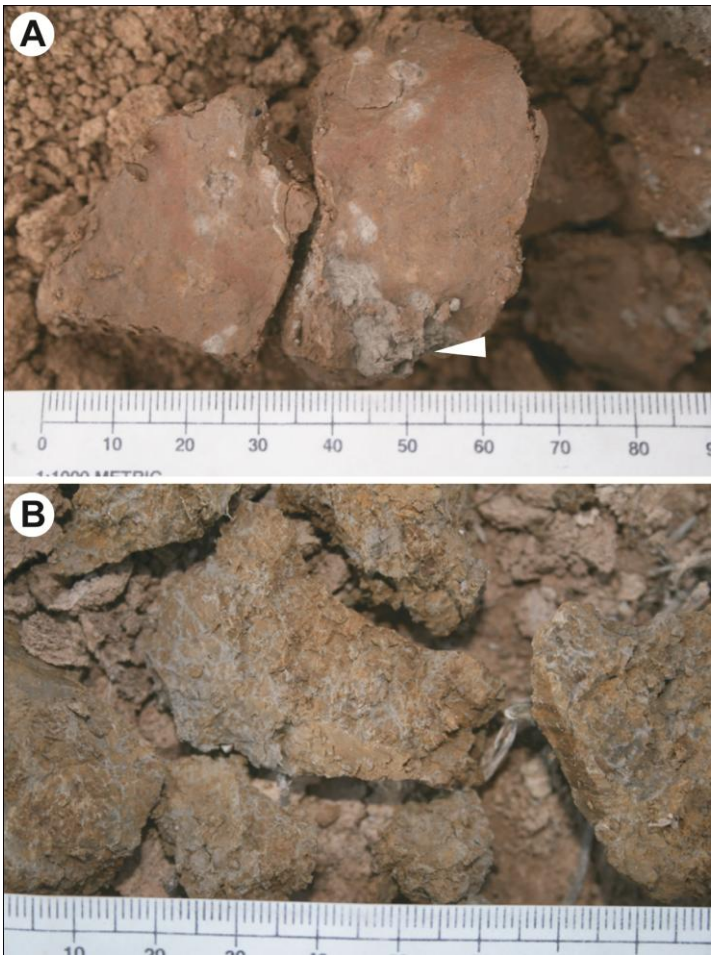

Figure 8 *- Samples of dominant mudstone facies in the Prado Section; scale is in centimeters and millimeters. (A) Facies A claystones; note relatively scarce pedogenic alteration consisting of red mottles, one rhizoconcretion (white pointer), and millimetric carbonate nodules. (B) Facies B siltstones; note pervasiveness of yellow to orange mottling, rhizohaloes and high carbonate content.*

Facies C (calcic horizons) - Facies C is stratigraphically superposed to facies B through gradual or abrupt contacts, and overlain by facies A through abrupt contacts. Facies characters vary from carbonate-rich siltstones to incipient calcrete horizons, ~20 to 60 cm thick, displaying prominent lateral continuity over the entire outcrop belt (Fig. 9A).

Units with the lowest carbonate content are light orange to yellowish, and consist of a silty to fine sandy matrix with abundant millimetric to rarely centimetric carbonate nodules and carbonate-filled fractures, distributed throughout the sediment and occasionally concentrated in horizontal levels. Gray to yellow-orange mottling is also abundant in millimetric to centimetric domains, and rhizoliths are frequent as isolated or clustered carbonate-rich tubules. With higher carbonate content, better cemented and indurated beds present a massive and compact appearance. The silty-sandy matrix is more cemented, and domains of coalesced nodules are present (Fig. 9B). Beds are light yellow to gray and show pervasive, centimetric, yellow to gray mottling. Bed tops are locally characterized by more distinct structural features such as incipient or horizontally oriented cracks; vague, diffuse banding; and preferential alignments of carbonate nodules in relatively less cemented units.

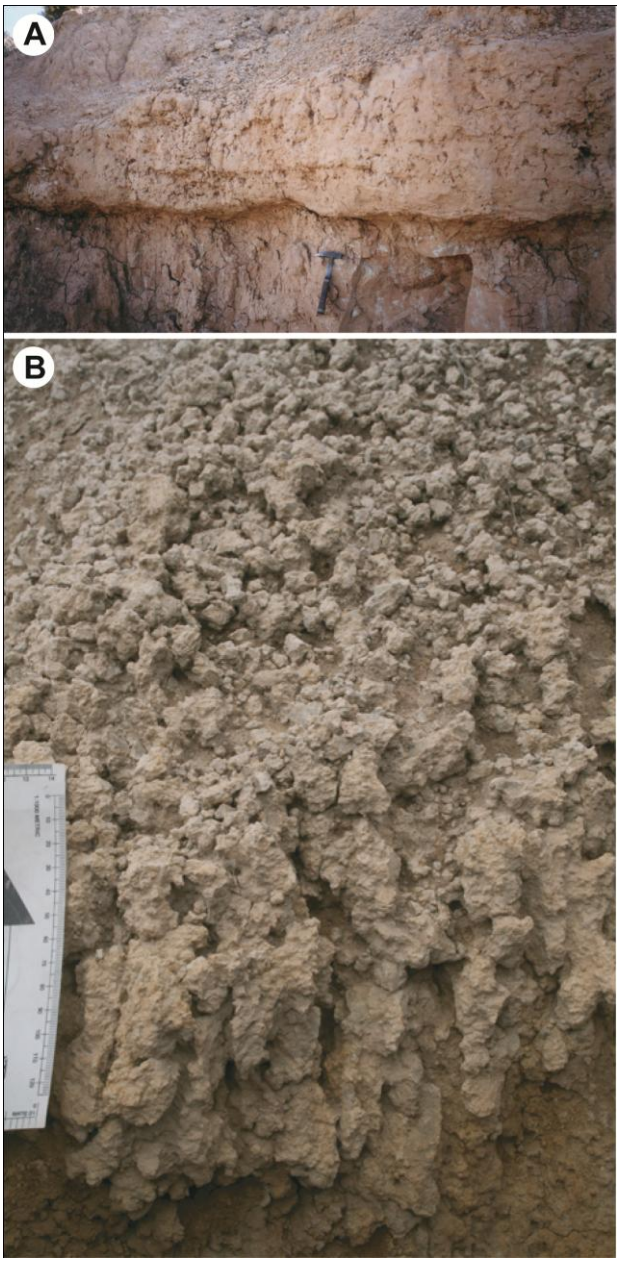

Figure 9 *- Calcic horizons in the Prado Section (facies C). (A) Massive, prominent Ca-cemented horizon with abrupt contact to underlying siltstones of facies B; hammer for scale is 32 cm. (B) Close-up of weathered calcic horizon, showing distinctly nodular structure and tubular features, probably rhizoconcretions, along the basal transition to underlying facies B (lower margin of photo); scale to the left is in centimetres and millimetres.*

Facies C presents variable characteristics, from Ca-rich pedogenic horizons to incipient calcretes, corresponding to development stages I-III (Machette, 1985; Wright & Tucker, 1991; Retallack, 2001). The semiarid climate with pronounced dry seasons in the Teruel Basin favored calcrete formation (Alcalá *et al.*, 2000; Alonso-Zarza & Calvo, 2000; Van Dam, 2006). Dominant limestones and dolostones in the nearby Mesozoic basement acted as local sources of calcium carbonate dissolved in surface runoff and groundwater. Solute mobilization and precipitation within the fine clastic matrix occurred at times of relatively more frequent precipitation and water circulation near the depositional surface. Considering the dominance of

claystones and interbedded $CaCO_3$-cemented horizons in the lower stratigraphic column of the Prado area, the sedimentary substrate must have been relatively impermeable and the depositional interface poorly drained, as still evident today. Variations in groundwater content were probably represented by an ephemeral water table controlled by seasonality of the local hydrological balance, and by the evapotranspiration regime of local vegetation. In semiarid climates, the depth of calcrete formation varies from a few decimeters to not more than 1 m below the surface (Royer, 1999; Retallack, 2005), in accordance with thicknesses of facies C beds. Given the availability of dissolved carbonates, the critical variables for incipient calcrete formation must have been surface and groundwater circulation, and the duration of exposure of the depositional surface (Wright, 1990; Wright & Tucker, 1991; Lang, 1993). The striking abundance of rhizoliths and mottled features in this facies, compared to A and B mudstone facies, indeed suggests deposition and pedogenic modification at times of more active hydrological cycle. The attainment of only partial stages of calcretization (stage IV calcrete units have not been observed) confirms the dominant effect of continued aggradation preventing exposure of the depositional surface for long enough, as observed in facies A and B (Wright, 1990; Kraus, 1999).

Facies D (organic-rich claystones) - Facies D comprises a minor volume of sediments in the lower Prado Section and does not occur in every cycle. It consists of centimetric, commonly dark red to dark grey beds of poorly indurated clay; where present, silt is a minor component, whereas coarser clastic particles are absent. Upper and lower stratigraphic contacts are abrupt, characterized by a planar, non-erosive geometry and are laterally continuous at outcrop. Beds are internally structureless and homogeneous, and stand out with respect to the dominant facies A and B for their lack of carbonate segregations and rhizoliths. Mottling is very sparse and represented by yellow to orange millimetric domains; in thicker beds, mottling is confined mainly to the topmost portions. The most distinctive trait of this facies however is the frequent occurrence of fragmented or almost complete gastropod shells, commonly scattered in the sediment, and occasionally concentrated along specific levels within thicker beds.

Facies D differs from other deposits in its almost purely clayey texture, scarcity of secondary pedogenic features, and especially in the relative abundance of gastropod remains. The very fine grain size, lack of sedimentary structures and the lateral continuity of beds suggest deposition from waning flow and suspension fallout into shallow ponds developed over an extensively flooded mudflat (Hubert & Hyde, 1982; Beer & Jordan, 1989; Saez *et al.*, 2007; Hampton & Horton, 2007). Flooding of the mudflat was probably of relatively short duration as testified by the reduced thicknesses of facies D. Development of shallow-water bodies however was probably uninterrupted by desiccation events, given the high textural homogeneity of beds, and especially the absence of sedimentary indicators of surface exposure and repeated flooding, such as mudcrack molds, mud intraclasts, and eolian adhesion structures (e.g. Hubert & Hyde, 1982; Reinhardt & Ricken, 2000; Hampton & Horton, 2007). The depositional environment was therefore closer to marginal lake conditions than to a clay playa or temporarily flooded mudflat (Tunbridge, 1984; Mertz & Hubert, 1994). The longer submersion of the depositional interface is confirmed by the scarcity of pedogenic features and root structures. The relatively humid environment was probably colonized by invertebrates, as evident from

the marked abundance of gastropod shells and especially the diffuse presence of organic matter, which gives some clay beds a distinctly darker color. Sparse, millimetric mottled domains within the top few centimeters of most beds indicate a reprise of pedogenic alteration upon return to subaerial conditions.

Depositional architecture and environmental controls - The lower part of the PS is organized in distinct facies cycles (Abels *et al*., 2009b). Regular alternations of facies A and B mudstones, with variable thickness, represent the basic cycle that dominates the succession (Fig. 6A). Carbonate-rich beds of facies C do not occur in every cycle, but where present they always overlie facies B siltstones. The upward transition to facies C is marked by a progressive increase in carbonate content, pedogenic features, and rhizoconcretions in the upper levels of facies B. Like facies C, facies D claystones are not present in every cycle, but where present they are usually in direct stratigraphic contact with calcic horizons of facies C. The four facies stack vertically with high lateral continuity, and are correlatable at outcrop over hundreds of meters.

The architecture and sedimentology of the lower PS point to the low-gradient, featureless depositional topography of a mudflat. Substantial runoff events in dryland environments with flat topography can distribute clastic sediment over broad areas, as reflected by the great spatial extent and continuity of facies (e.g. Hubert & Hyde, 1982; Beer & Jordan, 1989; Hampton & Horton, 2007). Runoff tends to develop as unconfined overland flow, and its spreading and shallowing favors deposition rather than erosion, resulting in conformable facies contacts and a good preservation potential.

Due to the absence of direct topographic controls and the episodicity of precipitation, the primary character of clastic facies in mudflats is commonly overprinted by concurrent climatic, hydrological and pedogenic factors (Smoot, 1983; Demicco & Gierlowski-Kordesch, 1986; Reinhardt & Ricken, 2000; Pimentel, 2002). Facies cyclicity in the lower part of the PS thus is related to changes in local hydrology and pedogenic processes driven by cyclic climate control. The substantial homogeneity and amalgamation of fine clastic deposits indicates poor variation of depositional processes through time, and constant aggradation that prevented the full development of pedogenic profiles. Prevailing aggradation is confirmed by the almost total absence of scour features and of reworked calcrete and mud intraclasts, which are commonly recognizable in successions from low-gradient, distal floodplain settings (Reinhardt & Ricken, 2000; Marriott & Wright, 1996, 2004).

Under this regime, transitions between facies A, B, C, and D represent periodic variations in shallow groundwater level. Facies A corresponds to times of reduced hydrological activity on a dominantly dry and well-drained mudflat. A low or only temporary groundwater table slowed down chemical processes under a desiccated, well-oxygenated surface, and prevented the establishment of dense vegetation. The relative abundance of clay could have been enhanced by selective deflation of less cohesive, silty to fine-sand fractions. At times of increased runoff, the mudflat shifted to a more positive hydrological balance; facies B and C accumulated coarser sediments, and groundwater recharge sustained a denser vegetation and enhanced (bio)chemical activity. The evidence of more pervasive pedogenic modification in facies B units, compared to facies A, is related to this shift in surface hydrology. Carbonate-rich facies C indicates periods of maximum hydrological activity in the semiarid context of the Prado area, when relatively abundant

groundwater and dissolved carbonates were distributed over wide mudflat areas by enhanced seasonal runoff. Given the constant aggradation of the depositional surface and the permanent presence of $CaCO_3$ sources in the area, water availability and evapotranspiration rates were the dominant constraints on the formation of pedogenic carbonate horizons and incipient calcretes, instead of the duration of surface exposure (Wright, 1990; Strong *et al.*, 1992; Glover & Powell, 1996; Abels *et al.*, 2009b). Occasional deposition of thin facies D units is the expression of short periods of maximum hydrological balance on the mudflat and establishment of shallow ponds.

The lateral homogeneity of facies and the lateral continuity of their vertical transitions over the whole study area support environmental change as a causal factor, rather than differential runoff distribution and sediment supply shifting over specific active sectors of the mudflat. The interpretation of gradual facies changes as a result of variable water saturation at the depositional interface is supported also by comparison with models of lateral facies transitions in Cenozoic basins of Portugal and Spain (e.g. Pimentel, 2002; Huerta & Armenteros, 2005), in which coeval distal-floodplain deposits present lateral gradients of pedogenic modification and carbonate precipitation, controlled by their positions from well-drained to frequently inundated areas.

3.4.2. Coarse-grained interbeds

Facies S (muddy sandstones) - Facies S consists of centimetric beds of moderately sorted, fine to medium clayey sandstone, single or in amalgamated associations of 2-4 beds (Fig. 10A). Sandstone beds do not show primary sedimentary structures, but crude normal grading and scattered granules and pebbles are recognizable in some units (Fig. 10B) Sparse, millimetric to centimetric carbonate nodules, orange to yellow mottling and calcite-filled fractures are the most salient internal structures. The fine grain size and abundant clay and silt matrix confer sandstones a relatively smooth appearance both at outcrop an on fractured sample surfaces. Massive sandstones are stratigraphically associated with pedogenized siltstones of facies B, usually at their tops. Contacts are sharp, defined by differences in grain size and cementation, and basal surfaces are commonly planar to very gently undulating, non-erosive to weakly erosive. Beds are traceable up to a few hundred meters, but their distribution is limited to the western Prado area, with pinch-out terminations to the east and southeast.

The massive structure, poor sorting and broad outcrop extent of this lithofacies suggest deposition from relatively competent unconfined flows carrying high sediment concentrations (Tunbridge, 1984; Fisher *et al.*, 2008). Flow expansion and deceleration took place over the proximal mudflat, favored by loss of gradient and possibly by the interference of sparse vegetation. Rapid waning and high sediment load prevented substrate erosion and the development of tractive bedforms (Lowe, 1988; Arnott & Hand, 1989). Abundant clayey to silty matrix indicate high volumes of suspended fines, which damped turbulence and raised competence, as demonstrated by lack of structures and by the presence of floating granule- to pebble-sized clasts (Baas & Best, 2002; Baas *et al.*, 2009). Some flows probably showed a clay-modulated behavior transitional to laminar as concentrated slurries that expanded over the surface (Wasson, 1979; Wells & Harvey, 1987; Stokes & Mather, 2000). The presence of sandstone strata in the western belt of the study area

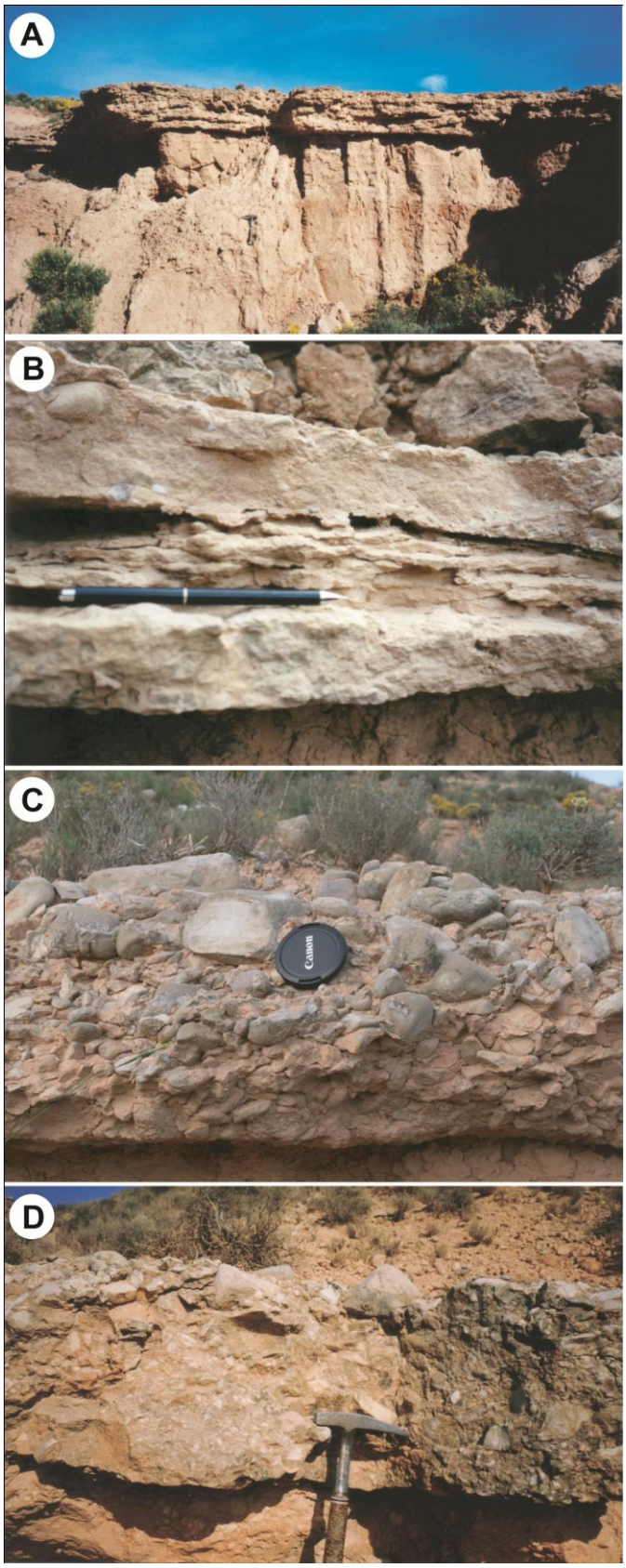

Figure 10 *- Clastic facies of distal-fan provenance within the Prado Section. (A) Tabular sandstone beds with planar contact over underlying mudstones; hammer for scale is 32 cm long. (B) Detail of well-bedded, massive sandstones (facies S); pencil for scale is 14 cm long. Note floating pebbles and granules within top and basal parts of topmost bed. (C) and (D) Debris-flow beds (facies G) with distinct inverse grading, poorly erosive bases and clast to matrix suport; lens cap is ~10 cm in diameter and hammer is 32 cm long.*

indicates local provenance from the adjacent alluvial-fan system, with flow gradually waning towards the eastern distal domain, where beds pinch out.

Facies G (conglomerates) - Facies G consists of extensive, tabular beds of poorly sorted, well to moderately rounded pebble to fine boulder gravel. Beds vary in thickness from 10-15 to 70 cm, and are internally massive, clast- to matrix-supported and commonly ungraded, or inversely graded with cobbles and boulders concentrated at bed tops (Figs. 10C, D) The matrix consists of poorly sorted sandy to granule-bearing claystone. Except for one case, basal surfaces are crudely planar and non-erosive.

Most gravel beds are laterally continuous over tens of meters, but not as extensive over the whole area as finer-grained facies. As with the sandstones, their distribution is limited to the western portion of the study area. Terminations towards the east are represented by a gradual pinch-out of conglomerates, frequently followed by a lateral transition to tabular, centimetric beds of structureless, pebbly, muddy sandstones, often associated with pebble stringers (Fig. 11). Stratigraphically, facies G is consistently associated with incipient calcretes or Ca-rich horizons of facies C. Gravel beds pinch out into relatively thick calcrete units. Distal pebble stringers and sandstone beds can be followed at outcrop to extend over several meters into calcic horizons (Fig. 11), of which they thus form a coarse-clastic division.

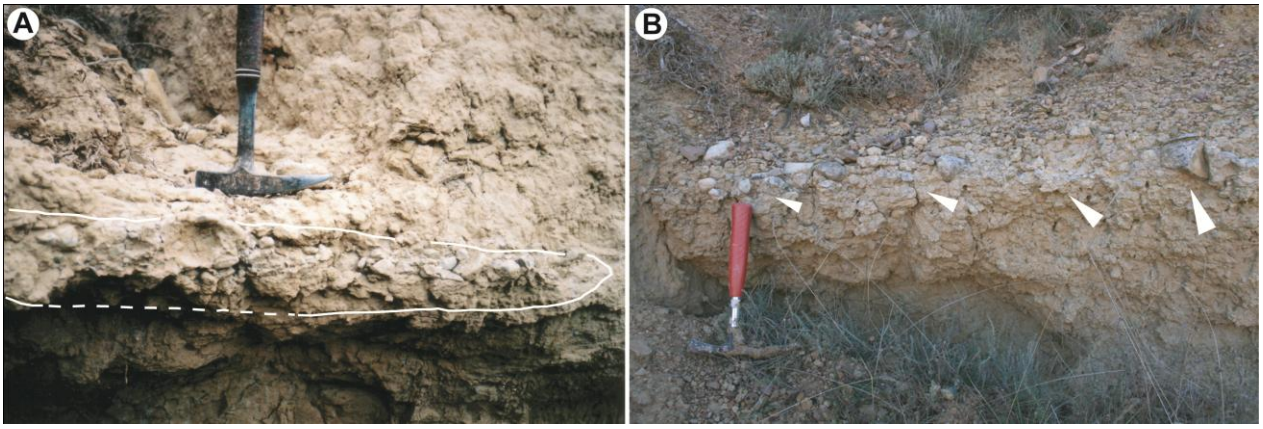

Figure 11 *- (A) Distal, thin termination of a debris-flow bed (highlighted in white) into a calcic horizon of facies C; paleoflow direction to the right; hammer is 32 cm. Note inverse grading of thin frontal lobe, and pedogenic modification of the fine-grained matrix. (B) Distal fining and thinning of a debris-flow bed into an incipient calcrete (white pointers indicate more visible coarse fraction of the flow unit); paleoflow to the left; hammer for scale is 35 cm long.*

Poorly sorted gravelly textures associated with abundant clay-rich matrix, floating outsized clasts, the absence of internal structures and abrupt distal terminations all indicate deposition from competent, cohesive mass flows with probable plastic or pseudoplastic rheology (Johnson, 1970, 1984; Nemec & Steel, 1984; Pierson & Costa, 1987; Blair & McPherson, 1998). The abundant clayey matrix supported gravel clasts through buoyancy and maintaining excess fluid pressure in the granular mixture. Lack of erosion along the basal surfaces points to an essentially laminar flow regime.

The character of facies G thus points to debris-flow events with western provenance, from the adjacent alluvial fan, extending their runout eastward onto the distal mudflat, where they came to a halt.

Deceleration was caused by the sudden reduction of internal shear once the flows reached the essentially nil gradient of the mudflat. Amalgamated gravel beds probably represent emplacement from flow surges in close succession within a single event (Major, 1997; Major & Iverson, 1999). Associations of gravel beds separated by discontinuous, centimetric remnants of muddy sediments instead suggest distinct debris-flow events within a relatively close time span, alternating with low-energy sheetflow sedimentation. Finer, pebbly sandstone beds pinching and fining out beyond gravel units represent overpassing by more fluid flow tails, which gradually lost competence over the mudflat (Pierson & Scott, 1985; Meyer & Wells, 1997; Blair & McPherson, 1998; Matthews *et al.*, 1999).

Stratigraphic relationships with basinal sediments - Conglomerate and sandstone beds have non-erosive bases. Their intercalations with the mudflat succession therefore do not disrupt the stratigraphic continuity, and bed terminations can be traced distally, indicating the exact time of occurrence of each coarse-clastic event in the context of the paleoenvironmental cyclicity of the lower PS. Coarse-clastic beds occur at stratigraphic positions which distally merge with facies B and C. Conglomerates occur in correspondence to facies C as lateral equivalents or pinching out into it (Fig. 5).

Single and amalgamated sandstone beds (facies S) merge distally into facies B siltstones and facies C calcic horizons. Contacts with the surrounding sediments are always sharp and laterally continuous, highlighted by the coarser texture and minor pedogenic modification of sandstones due to very rapid emplacement as compared with the slow aggradation of mudflat siltstones. Facies G conglomerates stand out in the mud- to carbonate-dominated Prado outcrops, and consistently merge laterally into calcic horizons C. In only one case the basal surface of a conglomerate shows significant erosional topography (Fig. 5, conglomerate at top log 3). In general, the distal correlation into calcic horizons is clearly marked by the pinch-out of gravel beds, and of their equivalent pebbly sandstones into facies C.

As discussed above, sedimentary cycles within the basinal Prado Section were shown to be controlled by climate change related to orbital precession. The stratigraphic interval studied here is comprised within the lower part of the PS; here, sedimentary characters change gradually from the base towards the top, with a gradual increase in calcic horizons (facies C) and in organic-rich mudstones (facies D). These two facies characterize the sedimentary rhythmicity in the well-dated, upper part of the PS, and their stratigraphic spacing with facies A and B in the lower PS is similar to the precession-controlled thickness observed in the upper PS. Therefore, the most plausible origin for this rhythmicity in the lower PS remains orbital forcing, with precession as driver of the basic sedimentary cycles. The phase-relation of sedimentary cycles to orbitally forced climate variability remains uncertain, due to uncertainties on the exact climatic impact of precession on the local water budget of the Miocene Teruel Basin (Abels *et al.*, 2009a, 2009b). However, as discussed above, precession minima most likely relate to positive hydrological balance due to enhanced winter precipitation and runoff, and therefore to relatively wetter paleoenvironments (Abels *et al.*, 2009a, 2009b). The calcic horizons of facies C are interpreted to represent a protracted, relatively wet climate phase, since in the most favorable conditions several hundreds to a few thousands of years are required to mobilize and reprecipitate sufficient solutes to form incipient calcrete horizons (Machette, 1985; Wright,

1990, 2007; Candy & Black, 2009). This inference is confirmed by the correspondence of their position within sedimentary cycles with that of shallow lacustrine carbonates in cycles of the upper PS, and by the lateral grading of come calcis horizons into more distal lacustrine carbonates farther to the east and southeast (Abels *et al.*, 2009b). The regular occurrence of coarse-clastic beds of debris-flow origin in stratigraphic correspondence to calcic horizons of the distal mudflat domain thus indicates that sediment shedding from the fan catchment reached its maxima not in coincidence of precession minima, but during times immediately preceding precession minima; or in paleoclimatic and paleohydrologic terms, during times of progressively increasing seasonality in regional climate and of growing water availability.

3.5. DISTAL-FAN SEDIMENTOLOGY AND ARCHITECTURE

The distribution of coarse-clastic units in the western Prado area and their eastward terminations clearly point to an origin as episodic, high-energy events from the Villastar fan along the nearby western basin margin. The alluvial fan is fully exposed along slopes and ravines in the hills that border the Prado *badlands* to the west, bordering the Mesozoic basement. The sharp increase in conglomerate and sandstone beds immediately west of Prado and their accompanying increase in stratal dip indicate the tipically abrupt physiographic transition between an alluvial-fan and the adjacent, lower-gradient environment (Blair & McPherson, 1994; Anderson & Cross, 2001).

The lower PS lies entirely within the normal C5n.2n subchron, and the absence of magnetic reversals in the stratigraphic interval prevents the establishment of detailed chronological tie-points. However, the direct, exposed transition in facies associations between the two domains, the absence of large-scale faults along their contact, and the possibility to correlate one conglomerate bed through the hills across the two domains (from west to east, coordinates 40°15,73'N 01°09,10'W – 40°15,79'N 01°09,23'W – 40°15,66'N 01°08,73'W – 40°15,61'N 01°08,78'W), all confirm the physical continuity and age equivalence of the two paleoenvironments.

Distal to medial fan segments are organized in tabular, alternating coarse and fine clastic packages (Fig. 12), an unusual architecture for alluvial-fan successions. Clastic units extend over more than one kilometre along depositional dip, and are conformably stacked into a regularly aggrading wedge. No major incised channel remnants or erosional surfaces are evident on a scale of meters to tens of meters. This indicates that the fan system never underwent significant incision and did not feature well-developed surface channel networks or an incised fanhead trench. The system was instead characterized by a strongly depositional regime and dominant aggradation.

Fine-clastic packages in the distal to medial fan consist of massive, weakly pedogenized sandy mudstones in laterally continuous units varying in thickness from a few tens of centimeters to over 1 m. Distinct bedding and sedimentary structures are commonly absent, and pedogenic features are limited to sparse rhizoliths and rare mottling patterns. Locally, a crude layering is given by discontinuous color banding parallel to the depositional paleosurface (dipping eastward), represented by alternating dark red and orange colors. This color pattern however is not traceable farther than a few meters, and tends to merge laterally into uniformly colored mudstones. Extensive beds of structureless sandstones and pebbly sandstones are normally part of

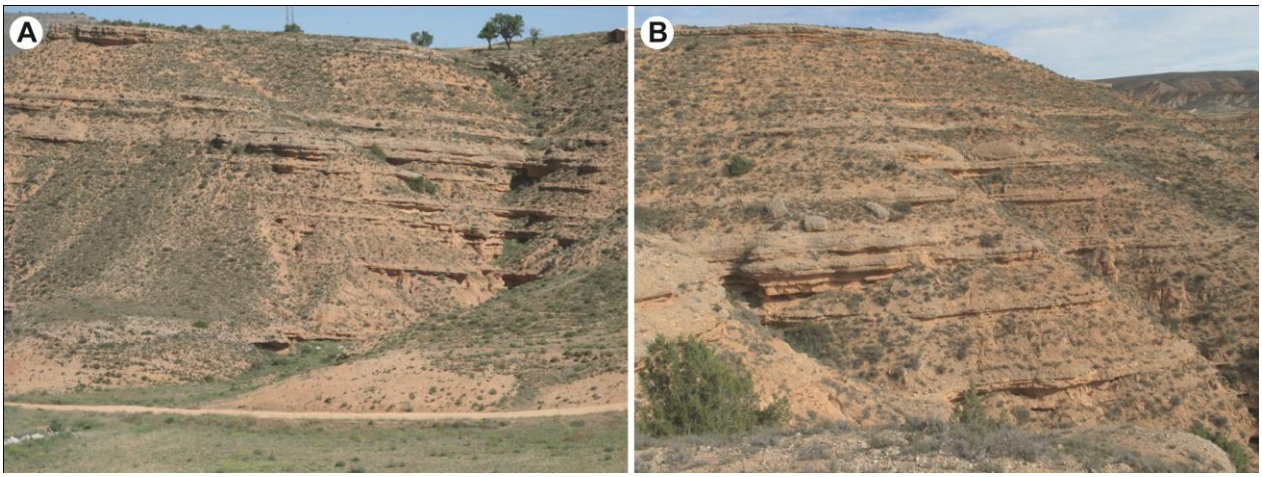

Figure 12 *- Distal-fan outcrops immediately to the west of the Prado Area. (A) Outcrop view with distinct alternation of tabular coarse- and fine-clastic units; tallest tree on top is ~7 m. (B) Closer view of outcrop face in A. Note associated conglomerates and sandstones in coarse-clastic units; shrub vegetation follows the lateral continuity of mudstone units.*

thick mudstone-dominated intervals. Commonly a few cm thick sandstones are continuous at outcrop as single or amalgamated beds, locally grading laterally into small lenses of pebble gravel.

Coarser clastic packages are lithologically more uniform and comprise a lower volume of sediment (~20-30%) than the dominant mudstones. They consist of single or more commonly amalgamated pebble to coarse cobble gravels, up to ~1.5 m thick, traceable over hundreds of metres at outcrop and accompanied by cm-thick interbeds of structureless, pebbly muddy sandstones. Gravel beds are massive, poorly sorted, matrix- to locally clast-supported, and are commonly characterized by a high volume of clay-rich, muddy sandy matrix. Clast fabrics are weak to absent. Basal contacts of both gravel and sandstone beds are commonly non-erosive to weakly erosive, with basal topography up to a few centimetres. These coarse-clastic units are the proximal equivalents of cohesive debris-flow beds and unconfined sheetflood to hyperconcentrated-flow sandstones in the mudflat succession. The absence of erosive geometries in the fan succession and the great lateral extent of gravel and sandstone beds allow to relate their origin to distinct sedimentation events when mass flows and sheetfloods affected large portions of the fan surface. Extensive tabular beds of the same facies interfingering with the lower PS imply events that mobilized particularly high volumes of sediment, bypassing the active fan surface and coming to a halt after the main slope-break between the alluvial fan and the mudflat.

The dominant volume of massive red mudstones indicates that the prevalent mode of aggradation over most of the distal fan surface was by unconfined or poorly channelized runoff events with low-energy and/or minor coarse sediment load. Although rare, similar mud-dominated alluvial fan systems have been described from the Quaternary record (e.g. Wasson, 1977; Nakayama, 1999) in regions with significant sources of fine-grained sediments. Along the western margin of the Teruel Basin near Villastar, major clay- and silt-sized sediment sources lie in the Late–Triassic and Early-Cretaceous formations that comprise thick, tectonized successions of red mudstones from alluvial and paralic environments, with intercalated gypsum and minor sandstones (Godoy *et al.*, 1983).

In the proximal fan domain, the general coarse sediments and frequent amalgamation of beds do not consent tracing coarse- and fine-clastic packages updip. The dominance of high-energy processes in the proximal area and a steeper depositional surface probably reduced mudstone deposition, and favored sediment bypass towards more distal fan settings. The mudflat environment of the Prado Section was the ultimate collector of fine clastic sediment in the system.

3.6. CONTROLS ON ALLUVIAL-FAN SEDIMENTATION

The architecture of the Villastar fan consists of conformably stacked, laterally continuous, tabular packages of coarse and fine clastic sediment. Absence of erosive features and inset geometries at the scale of the whole fan, and the rarity of channel fills and scours at metric scale, indicate that the system did not develop proximal fanhead trenches and that local incisions and channels were also not common over the active fan surface (e.g. Balance, 1984; Horton, 1998; Nichols & Thompson, 2005). Conditions of prevailing aggradation in alluvial fans can occur in internally drained basins, such as the Teruel Basin was in the Late Miocene. Endorheic conditions within a topographically confined depression force sediment to accumulate until aggradation reaches a threshold height at basin margin, enabling sediment export externally to the basin (Viseras & Fernandez, 1992; Nichols, 2004, 2005). As long as the endorheic conditions persist, the alluvial base level is forced to rise until it coincides with the ultimate base level, represented by the lowest topographic barriers at basin margins. Internal accommodation is thus maintained positive (Shanley & McCabe, 1994; Holbrook *et al.*, 2006), and sedimentation is favored over incision and bypass also in high-gradient alluvial settings.

Forced aggradation implies a generally subdued internal topography in endorheic basins. In the absence of sediment bypass to external depocenters, internal gradients tend to be compensated by alluvial, eolian and/or lacustrine deposition. The Neogene of the Teruel Basin is consequently dominated by an essentially layer-cake stratigraphy of mudflat and shallow-lacustrine sediments (Kiefer, 1988; Alonso-Zarza & Calvo, 2000; Abels *et al.*, 2009a, 2009b). In such continental settings the development of facies successions is highly sensitive to climate change, which directly controls interactions between sediment supply, pedogenesis and geochemical processes over extensive areas (e.g. Smoot & Olsen, 1985; Reinhardt & Ricken, 2000; Abdul Aziz *et al.*, 2003b; Alonso-Zarza *et al.*, 2009). The process model developed here for the lower PS is based on this principle, and accounts for periodic supply of coarse-grained sediments from the adjacent Villastar fan. The hydrological coupling between alluvial fans and their distal environments has been recognized both in present environments (e.g. Laymon *et al.*, 1998; Woods *et al.*, 2006) and in the stratigraphic record (Walker, 1967; Dorsey & Roberts, 1996; Hillier *et al.*, 2010). The high-gradient fan surface is maintained well-drained above the local water table and contributes surficial runoff and sediment supply to the distal fan fringe, where waterlogging and pedogenic conditions are regulated by the hydrological balance.

Relationships with the PS indicate enhanced distal-fan activity mainly in times immediately preceding the wettest climate phase, which is here correlated to precession minima. Numerical models of orbital control on Spanish climate (Abels *et al.*, 2009a) have shown increased winter runoff at precession minima, whereas summer precipitations and runoff are nearly zero in both extremes of the precession cycle. This indicates a

condition of very high seasonality in the yearly distribution of precipitation, although the model cannot exactly characterize whether precipitation occurred in extreme events or it was equally distributed during the winter season.

Considering the phase relationship between facies rhythms of the PS and Earth's orbital periods, the stratigraphic correlation of coarse-grained beds of fan provenance to Prado facies C can hardly be explained in terms of alternative tectonic or autogenic hypotheses. The topmost depositional units in the Villastar fan, laterally correlatable to the lower PS, do not show any detectable unconformities, indicating the absence of significant tectonics during this stage of fan activity. The regime of forced aggradation in the endorheic Teruel Basin prevented the autogenic incision/aggradation cycles characteristic of fan systems (Schumm *et al.*, 1987; Fraser & DeCelles, 1992; Kim & Muto, 2007) due to the distally rising base level (Nichols, 2004). The lack of cross-cutting stratal geometries between and within clastic units, and the lack of internal reactivation surfaces such as terraces and trenching, indicate the near absence of autogenic patterns of avulsion and switch for depositionally active fan lobes (Denny, 1965; DeCelles *et al*., 1991; Galloway & Hobday, 1996). The absence of proximal incision and fanhead trenching promoted widespread sediment distribution and aggradation over the whole fan surface ('*fan resurfacing*') on much shorter time scales than in cases where sediment is preferentially routed along feeder channels. In the Quaternary record, it has been possible to estimate that complete fan resurfacing by debris flows took place over a very few thousands of years in untrenched fans (Dühnforth *et al*., 2007). The characteristic architecture of the Villastar fan, with laterally continuous but sedimentologically well-differentiated clastic packages, can thus be interpreted as deposition by well distinct processes which tended to dominate aggradation over most of the fan surface during specific time intervals.

By contrast, climate controls on the PS and the interbedded debris-flow deposits point to a regular pattern of geomorphic dynamics in the fan catchment. The mud-dominated lower PS and distal- to medial-fan deposits were fed by the Late-Triassic and Early-Cretaceous claystones and siltstones. The carbonate lithologies of debris-flow conglomerates correspond to Cretaceous micritic and platform limestones and dolostones which were the only gravel source in the drainage system. The sedimentology and stratigraphy of conglomerates in the PS indicate the occurrence of catastrophic mass flows in single or closely spaced events, involving sufficient volumes of coarse and fine sediment to bypass the entire fan surface and extend for hundreds of meters over the distal mudflat. However, proximal fan outcrops show a prevalence of debris-flow deposits at all stratigraphic levels, implying that debris flows represented the dominant depositional process in the proximal fan domain over the whole time interval. The distinctiveness of distal debris-flow units in the lower PS, therefore, lies not so much in their occurrence, but rather in the particularly elevated volumes of sediment that were available at certain times.

Numerous studies on Quaternary and Recent piedmont settings demonstrate that major phases of geomorphic instability and sediment mobilization are closely related to climatic transitions. Geomorphic activity has been observed to be effectively coupled to climate change taking place on variable time scales, from multiannual to millennial (Gerson, 1982; Mayer *et al.*, 1984; Bull, 1991; Nemec & Postma, 1993; Evans & Clague, 1994; Berrisford & Matthews, 1997; Kochel *et al*., 1997; Hinderer, 2001; Van der Zwan, 2002; Viles &

Goudie, 2003; Thomas, 2003, 2004; Molnar, 2004). Debris flows are among the most widespread geomorphic processes in highland settings. Contrary to other mechanisms of subaerial sediment transport in which particles are entrained by moving fluids as a distinct dispersed phase, in debris flows sediment is saturated with interstitial water, and both components move downslope as a single phase with viscoplastic behavior (Johnson, 1970; Iverson, 1997). Their occurrence is therefore tied to the availability of abundant loose regolith, to its water saturation during exceptional precipitations or protracted antecedent rainfall (Wieczorek & Glade, 2005), and to high-gradient settings where gravity can directly entrain the sediment-water mixtures. The relationship between extreme precipitations and debris-flow events is well established, both from studies of recent and historical events (e.g. Wieczorek, 1987; Kochel, 1987; Zimmermann & Haeberli, 1992; Scott, 2000; Griffiths *et al*., 2004) and in the Quaternary stratigraphic record (e.g. Kochel & Johnson, 1984; Grosjean *et al*., 1997; Yafyazova, 2003; Keefer *et al*., 2003; Sletten & Blikra, 2007). Extreme meteorological events also trigger bedrock and colluvial landslides (Starkel, 1976; Selby, 1976; Crozier, 1997; Trustrum *et al*., 1999; Beylich & Sandberg, 2005) which are subject to rapid reworking in highland catchments and drastically increase sediment yield (Markham & Day, 1994; Allen & Hovius, 1998; Hovius *et al*., 2000).

At system scale, climate drives alluvial-fan dynamics by shifting the interplay between sediment yield from catchments, the frequency of effective floods, and their critical power. In geomorphic and stratigraphic terms this determines whether fan evolution will be dominated by aggradation, dissection, progradation, or protracted inactivity (Harvey, 2004, 2010). Long-term variations in sediment yield can be viewed in terms of interrelations between topography, precipitation and vegetation (Schumm, 1968; Tucker & Slingerland, 1997; Hooke, 2000), this latter two factors strictly related to climate. The debate on climate control of fan systems has been centered on Late Quaternary successions, due to stratigraphic completeness and abundant climate proxies. Divergent schools of thought, mainly focused on geomorphology, have traditionally attributed dominant fan aggradation to either relatively humid or relatively arid periods, and *viceversa* for degradation (see reviews in Dorn, 1994, 2009, and Harvey, 2004). Investigations aimed at longer, geological time scales have focused more on tectonics, also because of inherent difficulties in extracting paleoclimate information from fan sequences. Modelling studies, however, show a clear sensitivity of alluvial-fan systems to climate forcing. Koltermann and Gorelick (1992) reproduced a layered fan system with a 'synthetic stratigraphy' consisting of alternating coarse and fine units, by application of climate forcing at orbital frequencies, based on glacial-deglacial cycles in the southwestern United States. Allen and Densmore (2000) carried out numerical experiments on the response of catchment-fan systems along rifted basin margins. Tectonic signals were recognizable on long time scales and featured considerable lag times, whereas high-frequency climate change generated direct responses in the geomorphic system, amenable to be recorded in stratigraphy. In analogy with the observations reported here, sediment yield rapidly increased during transitions to wet conditions, whereas rapid catchment depletion resulted in a successive decrease in fan sedimentation, dependent on catchment recharge time. In conformity with modelling studies, the most plausible mechanism to explain the observed stratigraphic relationships in the Prado Section lies in the long-term destabilization of colluvial slopes within the fan catchment during initial phases of increased

seasonality in precipitation and enhanced winter storminess, but in advance of the establishment of a relative wet climate phase, during which fully forested highland catchments would have been stable and characterized by relative minima in sediment yield (Schumm, 1968; Hooke, 2000). Regardless of absolute precipitation amounts, the fundamental trigger of geomorphic instability and increased sediment yield would have been the progressive enhancement of seasonality in precipitation driven by approaching phases of precession minima. This is corroborated by recent research showing that correlations between total annual rainfall and sediment production in modern continental settings are poor, whereas rainfall seasonality is a much more accurate predictor of sediment yield (Wilson, 1973; Ziegler *et al.*, 1987; Hooke, 2000; Van der Zwan, 2002; Cecil & Dulong, 2003; Cecil *et al.*, 2003).

A number of studies on the Quaternary record attribute enhanced alluvial-fan aggradation to wet periods (e.g. Dorn, 1988; Maizels, 1990; Nanson *et al.*, 1992; Al Farraj & Harvey, 2004; DeLong & Arnold, 2007; Dühnforth *et al.*, 2007), whereas the evidence pointing to more specific dry-to-humid transitions has been presented in a few cases (Roberts & Barker, 1993; Jain & Tandon, 2003; Frankel *et al.*, 2007). Alluvial-fan deposits with a similar, coarse- and fine-grained bipartite architecture to the one described here were described from the Plio-Pleistocene of the Rio Grande Rift (Mack & Leeder, 1999), and tentatively attributed to Milankovitch cycles based on estimated average thicknesses of facies cycles compared to the thickness of deposits comprised within magnetopolarity intervals.

3.7. CONCLUSIONS

Late Miocene stratigraphy near Villastar (central Teruel Basin, Spain) bears a clear imprint of orbitally controlled climate on its facies successions. The Prado Section is characterized by distinct facies rhythms demonstrating repeated shifts from a dry to poorly drained mudflat environment, with occasional establishment of shallow ephemeral ponds. Pedogenic modification in this low-gradient environment was maintained at an incipient stage by continuous aggradation, but shows variable characters depending on the variable activity of local hydrological cycle and vegetation. Orbital tuning of the Praso Section and climate modelling show that relatively humid phases allowed solute transport and distribution during in correspondence of precession minima, due to an enhanced hydrological cycle. This favored the formation of Ca-rich horizons and incipient calcretes in dominantly muddy sediments of the Prado Section.

This mudflat succession is regularly interfingered by debris-flow units provenant from an alluvial fan at the adjacent basin margin. Single and amalgamated coarse-clastic beds can be traced distally into calcic horizons, and their emplacement can thus be related to phases of increased seasonality and runoff while reaching an orbital configuration of precession minimum. This suggests a linkage between catchment geomorphology and fan sedimentology, in which higher sediment yield occurred during gradual rises in regional humidity, which permitted major runoff events to destabilize catchment colluvium not yet protected by a full vegetative mantle. Considering the limited spatial and temporal resolution of climate models, and the impossibility to resolve sedimentation and climate control at a scale of single transport events, the proximate control can be be hypothesized at system scale to be the variable coupling of weathering rates (sediment production), stability of colluvial mantles and vegetation density in the

catchment (sediment yield), tied to varying seasonal distribution of precipitation. It is commonly and correctly assumed that alluvial-fan construction depends on stochastic, catastrophic events (Blair & McPherson, 1994), resulting in poorly structured successions. Nonetheless, fan processes may closely follow climate variability over geological timescales in suitable settings. An integrated stratigraphic analysis of ancient alluvial fan successions, especially adopting cyclostratigraphy, can shed light on the long-term stratigraphic effects of the centennial- to millennial-scale processes which have been found to control alluvial fans in Late Quaternary to Holocene successions. In the case at hand, sedimentation in the endorheic Teruel Basin resulted in construction of a fan system with fewer degrees of freedom in its geomorphic, and consequently stratigraphic dynamics. Forced base-level rise produced a fully aggradational succession that cannot be directly compared to Quaternary case studies in terms of fan dynamics, but that preserves an essentially complete record of sedimentary events at an approximate time resolution of 10^4 y.

ACKNOWLEDGEMENTS

This work was financially supported by the the National Science Foundation of The Netherlands (NWO), project ALW 815.01.012. We are grateful to Jan van Dam and Hayfaa Abdul-Aziz for field cooperation and discussions on regional geology. Gary A. Smith and David M. Miller provided constructive comments on a preliminary manuscript.

REFERENCES

Abdul Aziz, H., Hilgen, F.J., Krijgsman, W., Sanz, E. and **Calvo, J.P.** (2000) Astronomical forcing of sedimentary cycles in the middle to late Miocene continental Calatayud Basin (NE Spain). *Earth and Planetary Science Letters*, **177**, 9-22.

Abdul Aziz, H., Krijgsman, W., Hilgen, F.J., Wilson, D.S. and **Calvo, J.P.** (2003a) An astronomical polarity timescale for the late middle Miocene based on cyclic continental sequences. *Journal of Geophysical Research*, **108 B3**, DOI: 10.1029/2002JB001818.

Abdul Aziz, H., Sanz-Rubio, E., Calvo, J.P., Hilgen, F.J. and **Krijgsman, W.** (2003b) Palaeoenvironmental reconstruction of a middle Miocene alluvial fan to cyclic shallow lacustrine depositional system in the Calatayud Basin (NE Spain). *Sedimentology*, **50**, p. 211-236.

Abdul Aziz, H., Van Dam, J., Hilgen, F.J. and **Krijgsman, W.** (2004) Astronomical forcing In Upper Miocene continental sequences: implications for the Geomagnetic Polarity Time Scale. *Earth And Planetary Science Letters*, **222**, 243-258.

Abels, H.A., Abdul Aziz, H., Calvo, J.P. and **Tuenter, E.** (2009a) Cyclostratigraphic application of carbonate petrography in a Miocene lacustrine-siliciclastic succession (Teruel Basin, Spain): Implications for lake level, orbital phase relations and astronomical tuning. *Sedimentology*, **56**, 399-419.

Abels, E.A., Abdul Aziz, H., Ventra, D. and **Hilgen, F.J.** (2009b) Astronomical forcing of mudflat-lacustrine successions in the Prado Section, Teruel Basin, Spain. *Journal of Sedimentary Research*, **79**, 831-847.

Alcalá, L., Alonso-Zarza, A.M., Alvarez Sierra, M.A., Azanza, B., Calvo, J.P., Cañaveras, J.C., Van Dam, J.A., Garcés, M., Krijgsman, W., Van Der Meulen, A.J., Morales, J., Pelaéz-Campomanes, P., Pérez González, A., Sancho, R. and **Sanz Rubio, E.** (2000) El Registro Sedimentario Y Faunístico de las Cuencas de Calatayud-Daroca y Teruel. Evolución Paleoambiental y Paleoclimática Durante el Neógeno. *Revista de la Sociedad Geologica de España*, **13**, 323-343.

Al Farraj, A. and **Harvey, A.M.** (2004) Late Quaternary interactions between aeolian and fluvial processes: a case study in the northern UAE. *Journal of Arid Environments*, **56**, 235-248.

Allen, P.A. and **Hovius, N.** (1998) Sediment supply from landslide-dominated catchments: implications for basin margin fans. *Basin Research*, **10**, 19-35.

Allen, P.A. and **Densmore, A.L.** (2000) Sediment flux from an uplifting fault block. *Basin Research*, **12**, 367-380.

Alonso-Zarza, A.M. and **Calvo, J.P.** (2000) Palustrine sedimentation in an episodically subsiding basin: the Miocene of the northern Teruel Graben (Spain). *Palaeogeography, Palaeoclimatology, Palaeoecology*, **160**, 1-21.

Alonso-Zarza, A.M., Zhao, Z., Song, C.H., Li, J.J., Zhang, J., Martín-Pérez, A., Martín-García, R., Wang X.X., Zhang, Y. and **Zhang, M.H.** (2009) Mudflat/distal fan and shallow lake sedimentation (upper Vallesian-Turolian) in the Tianshui Basin, Central China: Evidence against the late Miocene eolian loess. *Sedimentary Geology*, **222**, 42-51.

Anadón, P. and **Moissenet, E.** (1996) Neogene basins in the Eastern Iberian Range. In: *Tertiary Basins of Spain – The Stratigraphic Record of Crustal Kinematics* (Eds. P.F. Friend and C.J. Dabrio), pp. 68-76, Cambridge University Press, Cambridge, UK.

Anadón, P., Moissenet, E. and **Simón, J.L.** (1990) The Neogene Grabens of the Eastern Iberian Chain (Eastern Spain). In: *Iberian Neogene Basins* (Eds. J. Agustí and J. Martinell), Field Guidebook Paleontologia i Evolución, Memoria Especial, **2**, 97-130.

Anadón, P., Orti, F. and **Rosell, L.** (1997) Unidades evaporiticas de la zona de Libros-Cascante (Mioceno, Cuenca de Teruel): Caracteristicas estratigráficas y sedimentológicas. *Cuadernos de Geologia Ibérica*, **22**, 283-304.

Anadón, P., Orti, F. and **Rosell, L.** (2000) Neogene Lacustrine Systems of the Southern Teruel Graben (Spain). In: *Lake Basins Through Space and Time* (Eds. E.H. Gierlowski-Kordesch and K.R. Kelts), AAPG Studies in Geology, **46**, 497-504.

Anderson, D.S. and **Cross, T.A.** (2001) Large-scale cycle architecture in continental strata, Hornelen Basin (Devonian), Norway. *Journal of Sedimentary Research*, **71**, 255-271.

Arnott, R.W.C. and **Hand, B.M.** (1989) Bedforms, primary structures and grain fabric in the presence of suspended sediment rain. *Journal of Sedimentary Petrology*, **59**, 1062-1069.

Ballance, P.F. (1984) Sheetflow-dominated gravel fans of the nonmarine middle Cenozoic Simmler Formation, central California. *Sedimentary Geology*, **38**, 337-359.

Baas, J.H. and **Best, J.L.** (2002) Turbulence modulation in clay-rich sediment-laden flows and some implications for sediment deposition. *Journal of Sedimentary Research*, **72**, 336-340.

Baas, J.H., Best, J.L., Peakall, J. and **Wang, M.** (2009) A phase diagram for turbulent, transitional, and laminar clay suspension flows. *Journal of Sedimentary research*, **79**, 162-183.

Beer, J.A. and **Jordan, T.E.** (1989) The effects of Neogene thrusting on deposition in the Bermejo Basin, Argentina. *Journal of Sedimentary Petrology*, **59**, 330-345.

Berrisford, M.S. and **Matthews, J. O.** (1997) Phases of enhanced rapid mass movement and climatic variation during the Holocene: a synthesis. In: *Rapid Mass Movement as a Source of Climatic Evidence for the Holocene* (Ed. B. Frenzel), Paläoklimaforschung Series, **19**, 409-440.

Beylich, A.A. and **Sandberg, O.** (2005) Geomorphic effects of the extreme rainfall event of 20-21 July, 2004 in the Latnjavagge catchment, northern Swedish Lapland. *Geografiska Annaler*, **87 A**, 409-419.

Blair, T.C. (1999) Cause of dominance by sheetflood vs. debris-flow processes on two adjoining alluvial fans, Death Valley, California. *Sedimentology*, **46**, 1015-1028.

Blair, T.C. and **McPherson, J.G.** (1994) Alluvial fan processes and forms. In: *Geomorphology of Desert Environments* (Eds. A.D. Abrahams and A.J. Parsons), pp. 354-402, Chapman & Hall, London.

Blair, T.C. and **McPherson, J.G.** (1998) Recent debris-flow processes and resultant form and facies of the Dolomite alluvial fan, Owens Valley, California. *Journal of Sedimentary Research*, **68**, 800-818.

Broekman, J.A. (1983) Environments of deposition, sequences and history of Tertiary continental sedimentation in the Basin of Teruel-Ademuz (Spain). *Proceedings of the Royal Dutch Academy of Sciences*, **B86**, 25-37.

Broekman, J.A., Besems, R.E., Van Daalen, P. and **Steensma, K.** (1983) Lithostratigraphy of Tertiary continental deposits in the Basin of Teruel-Ademuz (Spain). *Proceedings of the Royal Dutch Academy of Sciences*, **B86**, 1-16.

Bull, W.B. (1977) The alluvial-fan environment. *Progress in Physical Geography*, **1**, 222-269.

Bull, W.B. (1991) *Geomorphic Responses to Climate Change*. Oxford University Press, New York, USA.

Buurman, P. (1980) Paleosols in the Reading Beds (Palaeocene) of Alum Bay, Isle of Wight, U.K. *Sedimentology*, **27**, 593-606.

Cande, S.C. and **Kent, D.V.** (1995) Revised calibration of the geomagnetic polarity timescale for the late Cretaceous and Cenozoic. *Journal of Geophysical Research*, **100**, 6093-6095.

Candy, I. and **Black, S.** (2009) The timing of Quaternary calcrete development in semi-arid southeast Spain: investigating the role of climate on calcrete genesis. *Sedimentary Geology*, **218**, 6-15.

Cecil, C.B. and **Dulong, F.T.** (2003) Precipitation models for sediment supply in warm climates. In: *Climate Controls on Stratigraphy* (Eds. C.B. Cecil and N.T. Edgar), SEPM Special Publication, **77**, 21-27.

Cecil, C.B., Dulong, F.T., Harris, R.A., Cobb, J.C., Gluskoter, H.G. and **Nugroho, H.** (2003) Observations on climate and sediment discharge in selected tropical rivers, Indonesia. In: *Climate Controls on Stratigraphy* (Eds. C.B. Cecil and N.T. Edgar), SEPM Special Publication, **77**, 29-50.

Clarke, L., Quine, T.A. and **Nicholas, A.** (2010) An experimental investigation of autogenic behaviour during alluvial fan evolution. *Geomorphology*, **115**, 278-285.

Crozier, M.J. (1997) The climate landslide couple: a southern hemisphere perspective. In: *Rapid Mass Movement as a Source of Climatic Evidence for the Holocene* (Ed. B. Frenzel), Paläoklimaforschung Series, **19**, 333-354.

Daniels, M.J. (2003) Floodplain aggradation and pedogenesis in a semiarid environment. *Geomorphology*, **56**, 225-242.

De Boer, P.L., Pragt, J.S.J. and **Oost, A.P.** (1991) Vertically persistent sedimentary facies boundaries along growth anticlines and climate-controlled sedimentation in the thrust-sheet-top South Pyrenean Tremp-Graus Foreland Basin. *Basin Research*, **3**, 63-78.

DeCelles, P.G., Gray, M.B., Ridgway, K.D., Cole, R.B., Pivnik, D.A., Pequera, N. and **Srivastava, P.** (1991) Controls on synorogenic alluvial-fan architecture, Beartooth Conglomerate (Palaeocene), Wyoming and Montana. *Sedimentology*, **38**, 567-590.

Delong, S.B. and **Arnold, L.J.** (2007) Dating alluvial deposits with optically stimulated luminescence, AMS C-14 and cosmogenic techniques, western Transverse Ranges, California, USA. *Quaternary Geochronology*, **2**, 129-136.

Demicco, R.V. and **Gierlowski-Kordesch, E.** (1986) Facies sequences of a semi-arid closed basin: the Lower Jurassic East Berlin Formation of the Hartford Basin, New England, U.S.A. *Sedimentology*, **33**, 107-118.

Denny, C.S. (1965) *Alluvial fans in the Death Valley region, California and Nevada*. United States Geological Survey Professional Paper **466**.

Dorn, R.I. (1988) A rock varnish interpretation of alluvial-fan development in Death Valley, California. *National Geographic Research*, **4**, 56-73.

Dorn, R.I. (1994) The Role of Climatic Change in Alluvial Fan Development. In: *Geomorphology of Desert Environments* (Eds. A.D. Abrahams and A.J. Parsons), pp. 354-402, Chapman & Hall, London.

Dorn, R.I. (1996) Climatic Hypotheses of Alluvial-fan Evolution in Death Valley Are Not Testable. In: *The Scientific Nature of Geomorphology* (Eds. B.L. Rhoads and C.E. Thorn), pp. 191-220, Proceedings of the 27th Binghamton Symposium in Geomorphology. John Wiley & Sons, New York.

Dorn, R.I. (2009) The Role of Climatic Change in Alluvial Fan Development. In: *Geomorphology of Desert Environments*, 2nd ed. (Eds. A.J. Parsons and A.D. Abrahams), pp. 723-742, Springer Science.

Dorsey, R.J. and **Roberts, P.** (1996) Evolution of the Miocene north Whipple basin in the Aubrey Hills, western Arizona, upper plate of the Whipple detachment fault. In: *Reconstructing the History of Basin and Range Extension Using Sedimentology and Stratigraphy* (Ed. K.K. Beratan), pp. 127-146, Geolocial Society of America Special Paper, **303**, 127-146.

Dühnforth, M., Densmore, A.L., Ivy-Ochs, S. and **Allen, P.A.** (2008) Controls on sediment evacuation from glacially modified and unmodified catchments in the eastern Sierra Nevada, California. *Earth Surface Processes and Landforms*, **33**, 1602-1613.

Dühnforth, M., Densmore, A.L., Ivy-Ochs, S., Allen, P.A. and **Kubik, P.W.** (2007) Timing and patterns of debris flow deposition on Shepherd and Symmes creek fans, Owens Valley, California, deduced from cosmogenic ^{10}Be. *Journal of Geophysical Research*, **112**, F03S15, doi: 10.1029/2006JF000562.

Evans, S.G. and **Clague, J.J.** (1994) Recent climatic change and catastrophic geomorphic processes in mountain environments. *Geomorphology*, **10**, 107-128.

Fisher, J.A., Krapf, C.B.E., Lang, S.C., Nichols, G.J. and **Payenberg, T.H.D** (2008) Sedimentology and architecture of the Douglas Creek terminal splay, Lake Eyre, central Australia. *Sedimentology*, **55**, 1915-1930.

Frankel, K.L., Brantley, K.S., Dolan, J.F., Finkel, R.C., Klinger, R.E., Knott, J.R., Machette, M.N., Owen, L.A., Phillips, F.M., Slate, J.L. and **Wernicke, B.P.** (2007) Cosmogenic Be^{10} and Cl^{36} geochronology of offset alluvial fans along the northern Death Valley fault zone: implications for transient strain the eastern California shear zone. *Journal of Geophysical Research, Solid Earth*, **112**, B06407.

Fraser, G.S. and **DeCelles, P.G.** (1992) Geomorphic controls on sediment accumulation at margins of foreland basins. *Basin Research*, **4**, 233-252.

Galloway, W.E. and **Hobday, D.K.** (1996) *Terrigenous Clastic Depositional Systems*. Springer-Verlag, Berlin, 489 p.

Gawthorpe, R.L. and **Leeder, M.R.** (2000) Tectono-sedimentary evolution of active extensional basins. *Basin Research*, **12**, 195-218.

Gerson, R. (1982) Talus relicts in deserts: a key to major climatic fluctuations. *Israel Journal of Earth Sciences*, **31**, 123-132.

Gierlowski-Kordesch, E.H. and **Gibling, M.R.** (2002) Pedogenic mud aggregates, in rift sedimentation. In: *Sedimentation in Continental Rifts* (Eds. R.W. Renaut and G.M. Ashley), pp. 195-206, SEPM Special Publication, **73**, 195-206.

Glover, B.W. and **Powell, J.H.** (1996) Interaction of climate and tectonics upon alluvial architecture: Late Carboniferous – Early Permian sequences at the southern margin of the Pennine Basin, UK. *Palaeogeography, Palaeoclimatology, Palaeoecology*, **121**, 13-34.

Godoy, A., Olivé, A. and **Moissenet, E.** (Eds.) (1983) *La Puebla de Valverde*. Explanatory notes, Sheet 590 (27-23), Mapa Geologico de España, 68 p.

Griffiths, P.G., Webb, R.H. and **Melis, T.S.** (2004) Frequency and initiation of debris flows in Grand Canyon, Arizona. *Journal of Geophysical Research*, **109**, F04002, doi:10.1029/2003JF000077.

Grosjean, M., Nuñez, L., Cartajena, I. and **Messerli, B.** (1997) Mid-Holocene climate and culture change in the Atacama Desert, northern Chile. *Quaternary Research*, **48**, 239-246.

Guimerá, J. (1997) Las fosas neógenas de Teruel y el Jiloca: su relación con la estructura cortical. In: *Avances en el Conocimiento del Terciario Ibérico* (Eds. J.P. Calvo and J. Morales), pp. 105-108, Museo Nacional de Ciencias Naturales, Madrid.

Hampton, B.A. and **Horton, B.K.** (2007) Sheetflow fluvial processes in a rapidly subsiding basin, Altiplano Plateau, Bolivia. *Sedimentology*, **54**, 1121-1147.

Harvey, A.M. (1997) The role of alluvial fans in arid zone fluvial systems. In: *Arid Zone Geomorphology* (Ed. D.S.G. Thomas), pp. 231-259, John Wiley & Sons, Chichester.

Harvey, A.M. (2004) The response of dry-region alluvial fans to late Quaternary climatic change. In: *Desertification in the Third Millennium* (Eds. A.S. Alsharhan, W.W. Wood, A S. Goudie, A. Fowler, and E.M. Abdellatif), pp. 83-98, Balkema, Rotterdam.

Harvey, A.M. (2010) Local Buffers to the Sediment Cascade: Alluvial Fans and Debris Cones. In: *Sediment Cascades: an Integrated Approach* (Eds. T. Burt and R. Allison), pp. 153-180, John Wiley & Sons Ltd..

Harvey, A.M., Wigand, P.E. and **Wells, S.G.** (1999) Response of alluvial fan systems to the late Pleistocene to Holocene climatic transition: contrasts between the margins of pluvial Lakes Lahontan and Mojave, Nevada and California, USA. *Catena*, **36**, 255-281.

Harvey, A.M., Mather, A.E. and **Stokes, M.** (2005) Alluvial fans: geomorphology, sedimentology, dynamics - introduction. A review of alluvial-fan research. In: *Alluvial Fans: Sedimentology, Geomorphology, Dynamics* (Eds. A.M. Harvey, A.E. Mather, and M. Stokes), pp. 1-17, Geological Society of London Special Publication, **251**, 1-7.

Heward A.P. (1978) Alluvial fan sequence and megasequence models. In: *Fluvial Sedimentology* (Ed. A.D. Miall), Canadian Society of Petroleum Geologists Memoir, **5**, 669-702.

Hilgen, F.J., Krijgsman, W., Langereis, C.G., Lourens, L.J., Santarelli, A. and **Zachariasse, W.J.** (1995) Extending the astronomical (polarity) time scale into the Miocene. *Earth and Planetary Science Letters*, **136**, 495-510.

Hill, G. (1989) Distal alluvial fan sediments from the Upper Jurassic of Portugal: controls on their cyclicity and channel formation. *Journal of the Geological Society of London*, **146**, 539-555.

Hillier, R.D., Waters, R.A., Marriott, S.B. and **Davies, J.R.** (2010) Alluvial fan and wetland interactions: evidence of seasonal slope wetlands from the Silurian of south central Wales, UK. *Sedimentology*, **58**, 831-853.

Hinderer, M. (2001) Late Quaternary denudation of the Alps, valley and lake fillings and modern river loads. *Geodinamica Acta*, **14**, 231-263.

Holbrook, J., Scott, R.W. and **Oboh-Ikuenobe, F.E.** (2006) Base-level buffers and buttresses: A model for upstream versus downstream control on fluvial geometry and architecture within sequences. *Journal of Sedimentary Research*, **76**, 162-174.

Hooke, R. LeB. (2000) Toward a uniform theory of clastic sediment yield in fluvial systems. *Geological Society of America Bulletin*, **112**, 1778-1786.

Horton, B.K. (1998) Sediment accumulation on top of the Andean orogenic wedge: Oligocene to late Miocene basins of the Eastern Cordillera, southern Bolivia. *Geological Society of America Bulletin*, **110**, 1174-1192.

Hovius, N., Stark, C.P., Hao-Tsu, C. and **Jiun-Chan, L.** (2000) Supply and removal of sediment in a landslide-dominated mountain belt: Central Range, Taiwan. *Journal of Geology*, **108**, 73-89.

Hubert, J.F. and **Hyde, M.G.** (1982) Sheet-flow deposits of graded beds and mudstones on an alluvial sandflat-playa system: Upper Triassic Blomidon redbeds, St. Mary's Bay, Nova Scotia. *Sedimentology*, **29**, 457-475.

Huerta, P. and **Armenteros, I.** (2005) Calcrete and palustrine assemblages on a distal alluvial-floodplain: A response to local subsidence (Miocene of the Duero Basin, Spain). *Sedimentary Geology*, **177**, 253-270.

Iverson, R.M. (1997) The physics of debris flows. *Reviews of Geophysics*, **35**, 245-296.

Jain, M. and **Tandon, S.J.** (2003) Fluvial response to Late Quaternary climate changes, western India. *Quaternary Science Reviews*, **22**, 2233-2235.

Johnson, A.M. (1970) *Physical Processes in Geology*. San Francisco, Freeman, Cooper & Co., 576 p.

Johnson, A.M. (1984) Debris flow. In: *Slope Instability* (Eds. D. Brunsden and D.B. Prior), pp. 257-361, John Wiley & Sons, New York.

Keefer, D.K., Moseley, M.E. and **DeFrance, S.D.** (2003) A 38000-year record of floods and debris flows in the Ilo region of southern Peru and its relation to El Niño events and great earthquakes. *Palaeogeography, Palaeoclimatology, Palaeoecology*, **194**, 41-77.

Kiefer, E. (1988) Facies development of a lacustrine tecto-sedimentary cycle in the Neogene Teruel-Ademuz Graben (NE Spain). *Neues Jahrbuch für Geologie und Paläontologie*, **6**, 327-360.

Kim, W. and **Muto, T.** (2007) Autogenic response of alluvial-bedrock transition to base-level variation: Experiment and theory. *Journal of Geophysical Research*, **112**, F03S14, doi:10.1029/2006JF00056.

Kochel, R.C. (1987) Holocene debris flows in central Virginia. In: *Debris Flows/Avalanches – Process, Recognition and Mitigation* (Eds. J.E. Costa and G.F. Wieczorek), Geological Society of America, Reviews in Engineering Geology, **7**, 139-155.

Kochel, R.C. and **Johnson, R.A.** (1984) Geomorphology and sedimentology of humid-temperate alluvial fans, central Virginia. In: *Sedimentology of Gravels and Conglomerates* (Eds. E.H. Koster and R.J. Steel), Canadian Society of Petroleum Geologists Memoir, **10**, 109-122.

Kochel, R.C., Miller, J.R. and **Ritter, D.F.** (1997) Geomorphic response to minor cyclic climate changes, San Diego County, California. *Geomorphology*, **19**, 277-302.

Koltermann, C.E. and **Gorelick, S.M.** (1992) Paleoclimatic signature in terrestrial flood deposits. *Science*, **256**, 1775-1781.

Kostaschuk, R.A., Macdonald, G.M. and **Putnam, P.E.** (1986). Depositional process and alluvial fan-drainage basin morphometric relationships near Banff, Alberta, Canada. *Earth Surface Processes and Landforms*, **11**, 471-484.

Kraus, M.J. (1999) Paleosols in clastic sedimentary rocks: their geologic applications. *Earth Science Reviews*, **47**, 41-70.

Kraus, M.J. (2002) Basin-scale changes in floodplain paleosols: implications for interpreting alluvial architecture. *Journal of Sedimentary Research*, **72**, 500-509.

Kraus, M.J. and **Hasiotis, S.T.** (2006) Significance of different modes of rhizolith preservation to interpreting paleoenvironmental and paleohydrologic settings: examples from Paleogene paleosols, Bighorn Basin, Wyoming, U.S.A. *Journal of Sedimentary Research*, **76**, 633-646.

Krijgsman, W., Langereis, C.G., Daams, R. and **Van Der Meulen, A.J.** (1994) Magnetostratigraphic dating of the middle Miocene climate change in the continental deposits of the Aragonian type area in the Calatayud-Teruel basin (central Spain). *Earth and Planetary Science Letters*, **128**, 513-526.

Krijgsman, W., Delahaije, W., Langereis, C.G. and **De Boer, P.L.** (1997) Cyclicity and NRM acquisition in the Armantes section (Miocene, Spain): Potential for an astronomical polarity time scale for the continental record. *Geophysical Research Letters*, **24**, 1027-1030.

Kruiver, P.P., Krijgsman, W., Langereis, C.G. and **Dekkers, M.J.** (2002) Cyclostratigraphy and rock-magnetic investigation of the NRM signal in late Miocene palustrine-alluvial deposits of the Librilla section (NE Spain). *Journal of Geophysical Research*, **107**, **B12**, DOI: 10-1029/2001JB000945.

Lang, S.C. (1993) Evolution of Devonian alluvial systems in an oblique-slip mobile zone – an example from the Broken River Province, northeastern Australia. *Sedimentary Geology*, **85**, 501-535.

Laskar, J., Robutel, P., Joutel, F., Gastineau, M., Correia, A.C.M. and **Levrard, B.** (2004) A long term numerical solution for the insolation quantities of the Earth. *Astronomy and Astrophysics*, **428**, 261-285.

Laymon, C., Quattrocchi, D., Malek, E., Hipps, L., Boettinger, J. and **McCurdy, G.** (1998) Remotely-sensed regional-scale evapotranspiration of a semi-arid Great Basin desert and its relationship to geomorphology, soils, and vegetation. *Geomorphology*, **21**, 329-349.

Lecce, S.A. (1990) The Alluvial Fan Problem. In: *Alluvial Fans: A Field Approach* (Eds. A.H. Rachocki and M. Church), pp. 3-24, John Wiley & Sons, New York.

Leeder, M.R. and **Jackson, J.A.** (1993) The interaction between normal faulting and drainage in active extensional basins, with examples from the western United States and central Greece. *Basin Research*, **5**, 79-102.

Leleu, S., Ghienne, J.-F. and **Manatschal, G.** (2009) Alluvial fan development and morphotectonic evolution in response to contractional fault reactivation (Late Cretaceous – Palaeocene), Provence, France. *Basin Research*, **21**, 157-187.

Lewis, C.J., Vergés, J. and **Marzo, M.** (2000) High mountains in a zone of extended crust: Insights into the Neogene-Quaternary topographic development of northeastern Iberia. *Tectonics*, **19**, 86-102.

Liu, S. and **Yang, S.** (2000) Upper Triassic - Jurassic sequence stratigraphy and its structural controls in the western Ordos Basin, China. *Basin Research*, **12**, 1-18.

Lourens, L.J., Hilgen, F.J., Shackleton, N.J., Laskar, J. and **Wilson, D.S.** (2004) The Neogene Period. In: *A Geologic Time Scale 2004* (Eds. F.M. Gradstein, J.M. Ogg and A. Smith), pp. 405-440, Cambridge University Press, UK.

Lowe, D.R. (1988) Suspended-load fallout rate as an independent variable in the analysis of current structures. *Sedimentology*, **35**, 765-776.

Machette, M.N. (1985) Calcic soils of the southwestern United States. In: *Soils and Quaternary Geology of the Southwestern United States* (Eds D.L. Weide), Geological Society of America Special Paper, **203**, 1-21.

Mack, G.H. and **Leeder, M.R.** (1999) Climatic and tectonic controls on alluvial-fan and axial-fluvial sedimentation in the Plio-Pleistocene Palomas half graben, southern Rio Grande rift. *Journal of Sedimentary Research*, **69**, 635-652.

Maizels, J.L. (1990) Long-term paleochannel evolution during episodic growth of an exhumed alluvial fan, Oman. In: *Alluvial Fans: A Field Approach* (Eds. A.H. Rachocki and M. Church), pp. 271-304, Wiley, Chichester.

Major, J.J. (1997) Depositional processes in large-scale debris-flow experiments. *Journal of Geology*, **105**, 345-366.

Major, J.J. and **Iverson, R.M.** (1999) Debris-flow deposition: Effects of pore-fluid pressure and friction concentrated at flow margins. *Geological Society of America Bulletin*, **111**, 1424-1434.

Markham, A. and **Day, G.** (1994) Sediment transport in the Fly River Basin, Papua New Guinea. In: *Variability in Stream Erosion and Sediment Transport* (Eds. L.J. Olive, R.J. Loughran and J.A. Kesby), International Association of Hydrological Sciences Publication, **224**, 233-239.

Marriott, S.B. and **Wright, V.P.** (1996) Sediment recycling on Siluro-Devonian floodplains. *Journal of the Geological Society of London*, **153**, 661-664.

Marriott, S.B. and **Wright, V.P.** (2004) Mudrock deposition in an ancient dryland system: Moor Cliffs Formation, Lower Old Red Sandstone, southwest Wales, UK. *Geological Journal*, **39**, 277-298.

Matthews, J.A., Shakesby, R.A., McEwen, L.J., Berrisford, M.S., Owen, G. and **Bevan, P.** (1999) Alpine debris-flows in Leirdalen, Jotunheimen, Norway, with particular reference to distal fans, intermediate-type deposits, and flow types. *Arctic, Antarctic and Alpine Research*, **31**, 421-435.

Mayer, L., Gerson, R. and **Bull, W.B.** (1984) Alluvial gravel production and deposition: A useful indicator of Quaternary climatic changes in deserts. *Catena Supplement Band*, **5**, 137-151.

Mertz, K.A. and **Hubert, J.F.** (1990) Cycles of sand-flat sandstone and playa-lacustrine mudstone in the Triassic-Jurassic Blomidon redbeds, Fundy Rift Basin, Nova Scotia: implications for tectonic and climatic controls. *Canadian Journal of Earth Sciences*, **27**, 442-451.

Meyer, G.A. and **Wells, S.G.** (1997) Fire-related sedimentation events on alluvial fans, Yellowstone National Park, U.S.A. *Journal of Sedimentary Research*, **67**, 776-791.

Molnar, P. (2004) Late Cenozoic Increase in Accumulation Rates of Terrestrial Sediment: How Might Climate Change Have Affected Erosion Rates? *Annual Review of Earth and Planetary Science*, **32**, 67-89.

Nakayama, K. (1999) Sand- and mud-dominated alluvial-fan deposits of the Miocene Seto Porcelain Clay Formation, Japan. In: *Fluvial Sedimentology VI* (Eds. N.D. Smith and J. Rogers), International Association of Sedimentologists Special Publication, **28**, 393-407.

Nanson, G.C., Price, D.M. and **Short, S.A.** (1992) Wetting and drying of Australia over the past 300 ka. *Geology*, **20**, 791-794.

Nemec, W. and **Postma, G.** (1993) Quaternary alluvial fans in southwestern Crete: sedimentation processes and geomorphic evolution. In: *Alluvial Sedimentation* (Eds. M. Marzo and C. Puigdefabregas), International Association of Sedimentologists Special Publication, **17**, 235-276.

Nemec, W.J. and **Steel, R.J.** (1984) Alluvial and coastal conglomerates: Their significant features and some comments on gravelly mass-flow deposits. In: *Sedimentology of Gravels and Conglomerates* (Eds. E.H. Koster and R.J. Steel), Canadian Society of Petroleum Geologists Memoir, **10**, 1-31.

Nichols, G.J. (2004) Sedimentation and base level in an endorheic basin: the early Miocene of the Ebro Basin, Spain. *Boletín Geológico y Minero*, **115**, 427-438.

Nichols, G.J. (2005) Tertiary alluvial fans at the northern margin of the Ebro Basin: a review. In: *Alluvial Fans: Sedimentology, Geomorphology, Dynamics* (Eds. A.M. Harvey, A.E. Mather and M. Stokes), Geological Society of London Special Publication, **251**, 187-206.

Nichols, G. and **Thompson, B.** (2005) Bedrock lithology control on contemporaneous alluvial fan facies, Oligo-Miocene, southern Pyrenees, Spain. *Sedimentology*, **52**, 571-585.

North, C.P., Todd, S.P. and **Turner, J.P.** (1989) Alluvial fans and their tectonic controls. *Journal of the Geological Society of London*, **146**, 507-508.

Pierson, T.C. and **Costa, J.E.** (1987) A rheologic classification of subaerial sediment-water flows. In: *Debris Flows/Avalanches – Process, Recognition, and Mitigation* (Eds. J.E. Costa and G.F. Wieczorek), Geological Society of America Reviews in Engineering Geology, **7**, 1-12.

Pierson, T.C. and **Scott, K.M.** (1985) Downstream dilution of a lahar; Transition from debris flow to hyperconcentrated streamflow. *Water Resources Research*, **21**, 1511-1524.

Pimentel, N.L.V. (2002) Pedogenic and early diagenetic processes in Palaeogene alluvial fan and lacustrine deposits from the Sado Basin (S Portugal). *Sedimentary Geology*, **148**, 123-138.

Quigley, M.C., Sandiford, M. and **Cupper, M.** (2007) Distinguishing tectonic from climatic controls on range-front sedimentation. *Basin Research*, **19**, 491-505.

Reheis, M.C., Slate, J.L., Throckmorton, C.K., McGeehin, J.P., Sarna-Wojcicki, A.M. and **Dengler, L.** (1996) Late Quaternary sedimentation on the Leidy Creek fan, Nevada-California: geomorphic responses to climate change. *Basin Research*, **12**, 279-299.

Reinhardt, L. and **Ricken, W.** (2000) The stratigraphic and geochemical record of Playa Cycles: monitoring a Pangaean monsoon-like system (Triassic, Middle Keuper, S. Germany). *Palaeogeography, Palaeoclimatology, Palaeoecology*, **161**, 205-227.

Retallack, G.J. (2001) *Soils of the Past. An Introduction to Paleopedology*. Blackwell Science, Oxford, UK, 404 p.

Retallack, G.J. (2005) Pedogenic carbonate proxies for amount and seasonality of precipitation in paleosols. *Geology*, **33**, 333-336.

Ritter, J.B., Miller, J.R. and **Husek-Wulforst, J.** (2000) Environmental controls on the evolution of alluvial fans in Buena Vista Valley, North Central Nevada, during late Quaternary time. *Geomorphology*, **36**, 63-87.

Ritter, J.B., Miller, J.R., Enzel, Y. and **Wells, S.G.** (1995) Reconciling the roles of tectonism and climate in Quaternary alluvial fan evolution. *Geology*, **23**, 245-248.

Roberts, N. and **Barker, P.** (1993) Landscape stability and biogeomorphic response to past and future climatic shifts in intertropical Africa. In: *Landscape Sensitivity* (Eds. D.S.G. Thomas and R.J. Allison), pp. 65-82, Wiley, London.

Roca, E. and **Guimerá, J.** (1992) The Neogene structure of the eastern Iberian margin: structural constraints on the crustal evolution of the Valencia trough (western Mediterranean). *Tectonophysics*, **203**, 203-218.

Royer, D.L. (1999) Depth to pedogenic carbonate horizons as a paleoprecipitation indicator? *Geology*, **20**, 331-334.

Sáez, A., Anadón, P., Herrero, M.J. and **Moscariello, A.** (2007) Variable style of transition between Palaeogene fluvial fan and lacustrine systems, southern Pyrenean foreland, NE Spain. *Sedimentology*, **54**, 367-390.

Schieber, J., Southard, J. and **Thaisen, K.** (2007) Accretion of Mudstone Beds from Migrating Floccule Ripples. *Science*, **318**, 1760-1763.

Schumm, S.A. (1968) Speculations concerning paleohydrologic controls on terrestrial sedimentation. *Geological Society of America Bulletin*, **79**, 1573-1588.

Schumm, S.A., Mosley, M.P. and **Weaver, W.E.** (1987) *Experimental Fluvial Geomorphology*. John Wiley & Sons, New York.

Scott, K.M. (2000) Precipitation-triggered debris flow at Casita Volcano, Nicaragua: Implications for mitigation strategies in volcanic and tectonically active steeplands. In: *Debris-Flow Hazards Mitigation: Mechanics, Prediction, and Assessment* (Eds. G.F. Wieczorek and N.D. Naeser), pp. 3-13, Balkema, Rotterdam.

Selby, M.J. (1976) Slope erosion due to extreme rainfall: A case study from New Zealand. *Geografiska Annaler*, **58**, 131-138.

Shanley, K.W. and **McCabe, P.J.** (1994) Perspectives on the sequence stratigraphy of continental strata. *AAPG Bulletin*, **78**, 544-568.

Sierro, F.J., Ledesma, S., Flores, J.-A., Torrescusa, S. A. and **Martiné Del Olmo, W.** (2000) Sonic and gamma-ray astrochronology: cycle to cycle calibration of Atlantic climatic records to Mediterranean sapropels and astronomical oscillations. *Geology*, **28**, 695-698.

Singh, A.K., Parkash, B., Mohindra, R., Thomas, J.V. and **Singhvi, A.K.** (2001) Quaternary alluvial fan sedimentation in the Dehradun valley piggyback basin, NW Himalaya: tectonic and paleoclimatic implications. *Basin Research*, **13**, 449-471.

Sletten, K. and **Blikra, L.H.** (2007) Holocene colluvial (debris-flow and water-flow) processes in eastern Norway: stratigraphy, chronology and palaeoenvironmental implications. *Journal of Quaternary Science*, **22**, 619-635.

Smoot, J.P. (1983) Depositional subenvironments in an arid closed basin; the Wilkins Peak Member of the Green River Formation (Eocene), Wyoming, U.S.A. *Sedimentology*, **30**, 801-827.

Smoot, J.P. and **Olsen, P.E.** (1985) Massive mudstone in basin analysis and paleoclimatic interpretation of the Newark Supergroup. In: *Proceedings 2nd USGS Workshop on the Early Mesozoic Basins of the Eastern United States* (Eds. G.P. Robinson and A.J. Froelich), pp. 29-33, USGS Circular 946.

Starkel, L. (1976) The role of extreme (catastrophic) meteorological events in the contemporaneous evolution of slopes. In: *Geomorphology and Climate* (Ed. E. Derbyshire), pp. 203-246, John Wiley & Sons, London.

Stokes, M. and **Mather A.E.** (2000), Response of Plio-Pleistocene alluvial systems to tectonically induced base-level changes, Vera basin, SE Spain. *Journal of the Geological Society of London*, **157**, 303-316.

Strong, G.E., Giles, J.R. and **Wright, V.P.** (1992) A Holocene calcrete from North Yorkshire, England: implications for interpreting palaeoclimates using calcretes. *Sedimentology*, **39**, 333-347.

Thomas, M.F. (2003) Late Quaternary sediment fluxes from tropical watersheds. *Sedimentary Geology*, **162**, 63-81.

Thomas, M.F. (2004) Landscape sensitivity ro rapid environmental change – a Quaternary perspective with examples from tropical areas. *Catena*, **55**, 107-124.

Trustrum, N.A., Gomez, B., Page, M.J., Reid, L.M. and **Hicks, D.M.** (1999) Sediment production, storage and output: the relative role of large magnitude events in steepland catchments. *Zeitschrift für Geomorphologie*, **115**, 71-86.

Tucker, G.E. and **Slingerland, R.** (1997) Drainage basin responses to climate change. *Water Resources Research*, **33**, 2031-2047.

Tunbridge, I.P. (1984) Facies model for a sandy ephemeral stream and clay playa complex; the Middle Devonian Trentishoe Formation of North Devon, U.K. *Sedimentology*, **31**, 697-715.

Van Dam, J.A. (1997) The small mammals from the upper Miocene of the Teruel-Alfambra region (Spain): paleobiology and paleoclimatic reconstructions. *Geologica Ultraiectina*, **156**, 204 p.

Van Dam, J.A. (2006) Geographic and temporal patterns in the late Neogene (12-3 Ma) aridification of Europe: The use of small mammals as paleoprecipitation proxies. *Palaeogeography, Palaeoclimatology, Palaeoecology*, **152**, 283-303.

Van Dam, J.A. and **Weltje, G.J.** (1999) Reconstruction of the Late Miocene climate of Spain using rodent paleocommunity successions: an application of end-member modelling. *Palaeogeography, Palaeoclimatology, Palaeoecology*, **151**, 267-305.

Van Der Zwan, C.J. (2002) The impact of Milankovitch-scale climatic forcing on sediment supply. *Sedimentary Geology*, **147**, 271-294.

Ventra, D. (2009) Ephemeral alluvial systems of the Teruel Basin (Miocene, Spain): Basinal and climatic controls. *Acta Geologica Lilloana*, **21**, 67-68.

Viles, H.A. and **Goudie, A.S.** (2003) Interannual, decadal and multidecadal scale climatic variability and geomorphology. *Earth Science Reviews*, **61**, 105-131.

Viseras, C. and **Fernandez, G.** (1992) Sedimentary basin destruction inferred from the evolution of drainage systems in the Betic Cordillera, southern Spain. *Journal of the Geological Society of London*, **149**, 1021-1029.

Walker, T.R. (1967) Formation of red beds in ancient and modern deserts. *Geological Society of America Bulletin*, **78**, 353-368.

Wasson, R.J. (1977) Last-glacial alluvial fan sedimentation in the Lower Derwent Valley, Tasmania. *Sedimentology*, **24**, 781-799.

Wasson, R.J. (1979) Sedimentation history of the Mundi Mundi alluvial fans, western New South Wales. *Sedimentary Geology*, **22**, 21-51.

Wells, S.G. and **Harvey, A.M.** (1987) Sedimentologic and geomorphic variations in storm-generated alluvial fans, Howgill Fells, northwest England. *Geological Society of America Bulletin*, **98**, 182-198.

White, K., Drake, N., Millington, A. and **Stokes, S.** (1996) Constraining the timing of alluvial fan response to Late Quaternary climatic changes, southern Tunisia. *Geomorphology*, **17**, 295-304.

Wieczorek, G.F. (1987) Effect of rainfall intensity and duration on debris flows in central Santa Cruz Mountains, California. In: *Debris Flows/Avalanches – Process, Recognition, and Mitigation* (Eds. J.E. Costa and G.F. Wieczorek), Geological Society of America Reviews in Engineering Geology, **7**, 93-104.

Wieczorek, G.F. and **Glade, T.** (2005) Climatic factors influencing occurrence of debris flows. In: *Debris-flow Hazards and Related Phenomena* (Eds. M. Jakob M. and O. Hungr), pp. 325-362, Springer, Berlin.

Wilson, L. (1973) Variations in sediment yield as a function of mean annual precipitation. *American Journal of Science*, **273**, 335-349.

Woods, S.W., Macdonald, L.H. and **Westbrook, C.J.** (2006) Hydrologic interactions between an alluvial fan and a slope wetland in the central Rocky Mountains, USA. *Wetlands*, **26**, 230-243.

Wright, V.P. (1990) Estimating rates of calcrete formation and sediment accretion in ancient alluvial deposits. *Geological Magazine*, **127**, 273-276.

Wright, V.P. (2007) Calcrete. In: *Geochemical Sediments and Landscapes* (Eds. D.J. Nash and S.J. McLaren), pp. 10-45, Blackwell Publishing, Oxford, UK.

Wright, V.P. and **Tucker, M.E.** (1991) Calcretes: an Introduction. In: *Calcretes* (Eds. V.P. Wright and M.E. Tucker), International Association of Sedimentologists Reprint Series, **2**, 1-22.

Wright, V.P. and **Marriott, S.B.** (2007) The dangers of taking mud for granted: lessons from Lower Old Red Sandstone dryland river systems of South Wales. *Sedimentary Geology*, **195**, 91-100.

Yaalon, D.H. and **Kalmar, D.** (1978) Dynamics of cracking and swelling clay soils: displacement of skeletal grains, optimum depth of slickensides, and rate of intra-pedonic turbation. *Earth Surface Processes*, **3**, 31-42.

Yafyazova, R.K. (2003) Influence of climate change on mudflow activity on the northern slope of the Zailiysky Alatau Mountains, Kazakhstan. In: *Debris-flow Hzards Mitigation: Mechanics, Prediction and Assessment* (Eds. D. Rickenmann and C.L. Chen), pp. 199-204, Millpress, Rotterdam.

Zaleha, M.J. (1997) Siwalik paleosols (Miocene, northern Pakistan): Genesis and controls on their formation. *Journal of Sedimentary Research*, **67**, 821-839.

Ziegler, A.M., Raymond, A.L., Gierlowski, T.C., Horrell, M.A., Rowley, D.B. and **Lottes, A.L.** (1987) Coal climate and terrestrial productivity: the present and early Cretaceous compared. In: *Coal and Coal-Bearing Strata: Recent Advances* (Ed. A.C. Scott), Geological Society of London Special Publication, **32**, 25-49.

Zimmermann, M. and **Haeberli, W.** (1992) Climatic change and debris flow activity in high mountain areas: A case study in the Swiss Alps. *Catena Supplementband*, **22**, 59-72.

"*Physical geography and geology,*
are inseparable scientific twins."

Sir Roderick Impey Murchison

Chapter 4

Colluvial sedimentation in a hyperarid setting (Atacama Desert, northern Chile): geomorphic controls and stratigraphic facies variability

D. Ventra, G. Chong Díaz & P.L. de Boer

ABSTRACT

Colluvial depositional systems have been recently analysed with emphasis on periglacial and alpine settings, and on relationships between Quaternary slope stratigraphy and climate change. This study examines the role of variable slope morphology, surface hydrology and microclimate in controlling colluvial sedimentation along a tract of the Coastal Cordillera in the hyperarid Atacama Desert of northern Chile. Slope accessibility along this piedmont is accompanied by continuous stratigraphic exposures, consenting direct comparisons between active surface processes and the resulting sedimentary record. The combination of active tectonic setting and hyperarid climate offers morphologically varied slope subenvironments within a relatively restricted area, and prevents interference from differential distribution of vegetation and pedogenic cover.

Five piedmont sectors are identified, based on slope morphology, surface processes and sedimentary signatures, ranging from steep talus cones, to debrisflow- and eolian-dominated colluvial ramps, to an alluvial fan. Colluvial sedimentation is controlled by complex interactions of slope gradients and profiles, bedrock lithology, exposure to dominant wind, and potential runoff pathways. Facies associations and architectures at outcrop present extremely diversified characters in each sector. The general sedimentary processes do not differ fundamentally from those reported in periglacial and alpine colluvial settings. Major distinctions consist in the importance of aeolian processes; the role of aeolian deposits in controlling dominant types of sediment gravity flows; the absence of clay minerals and of pedogenic activity. Discrepancies are also evident between active processes and some of the stratigraphic features; for example, preservation of alluvial and aeolian facies in stratigraphic sections does not exactly correspond to the dominant processes over active slopes. Furthermore, this comparative analysis of several facies associations from an arid piedmont setting highlights the importance of considering subtle differences in local geomorphology and autogenic processes in the interpretation of colluvial stratizgraphy.

4.1. INTRODUCTION

Sediment accumulations along and at the base of slopes are referred to as *colluvium* when transported by dominant aqueous processes, and *scree* or *talus* when resulting mainly from rockfall and sediment-gravity processes (Bates & Jackson, 1984; Turner, 1996; Neuendorf *et al.*, 2005). More commonly, the three terms are used interchangeably in geomorphic and sedimentological literature to denote slope deposits in general, irrespective of genetic processes (Fairbridge, 1968; Ritter *et al.*, 1995; Blikra & Nemec, 1998; Van Steijn, 2011). Colluvial systems are often considered particularly complex, due to the high textural immaturity and architectural heterogeneity of their deposits. Studies of slope deposits are therefore relatively rare in the literature, representing one of the last frontiers of clastic sedimentology (Imeson *et al.*, 1980; Blikra & Nemec, 1998; Turner & Makhlouf, 2002).

Being intrinsically related to high-relief settings with low preservation potential, slope deposits are marginal components of ancient continental basin-fills, with few examples in the literature (e.g., Veevers & Roberts, 1966; Porter, 1987; Tanner & Hubert, 1991; Pederson *et al.*, 2001), due mainly to poor recognition. However, their ubiquity in terrestrial settings with significant topographic gradient offers ample opportunities to couple process sedimentology with Quaternary climate and neotectonic archives. Recent studies demonstrate that careful analysis of piedmont environments and slope deposits may contribute to understand regional climate variability and tectonics, especially where reliable dating methods can be applied (Gerson, 1982; Nelson, 1992; Blikra & Longva, 1995; Blikra & Nemec, 1998; Nemec & Kazanci, 1999; Pederson *et al.*, 2000; Clarke *et al.*, 2003; Pawelec, 2006). Major emphasis has been given to interpret climate signatures from the internal heterogeneities of colluvial aprons, in recognition of variable regolith production and resedimentation through time. This kind of research has been carried out mostly in periglacial and cold temperate settings (e.g. Jahn, 1960; Wasson, 1979; Van Steijn *et al.*, 1995; Pérez, 1998; Blikra & Nemec, 1998; Nemec & Kazanci, 1999; Matsuoka & Sakai, 1999; Hètu & Gray, 2000; Van Steijn, *et al.*, 2002; Texier & Meireles, 2003; Pawelec, 2006; Hinchcliffe & Ballantyne, 2009; Wilson, 2009; Sanders *et al.*, 2009), whereas case studies from arid settings are limited (Gerson, 1982; Friend *et al.*, 2000; Turner & Makhlouf, 2002).

In spite of such advances, few studies on comparative slope sedimentology (Gardner, 1980; Blikra & Nemec, 1998; Matsuoka & Sakai, 1999; Sass & Krautblatter, 2007) help to validate inferences based on the analysis of fossil colluvium. Variable sedimentary styles are commonly ascribed to allogenic forcing, but the importance of local topographic constraints remains difficult to assess in colluvial stratigraphy (Luckman, 1976; Statham & Francis, 1986; Texier & Meireles, 2003; Pawelec, 2006; Sass & Krautblatter, 2007).

This study discusses the sedimentology of present-day colluvial aprons along the hyperarid coast of the Atacama Desert, northern Chile (Fig. 1). Different process associations and facies architectures are identified along a continuous coastal stretch characterized by significant topographic variability over relatively short distances. Slope deposits are accessible both over the active surface and in stratigraphic sections, which allows to constrain modern processes and relate them to the corresponding stratigraphic products. A comparative analysis of the distinct slope sectors allows us further to discuss a wide range of facies models

for arid colluvium in relation to local geomorphic factors, as well as the implications for colluvial stratigraphy.

4.2. GEOLOGICAL AND CLIMATIC SETTING

4.2.1. Coastal escarpment

The Pacific coast of Chile (Fig. 1) stretches along the active subduction boundary between the oceanic Nazca Plate and the continental South American Plate. The tectonic regime is one of uplift, in response to crustal thickening and plate convergence (Armijo & Thiele, 1990; Delouis *et al.*, 1998). The northern Chilean coast is characterized by a prominent, continuous escarpment, extending over more than 800 km with elevations up to 600-1000 m above sea level, locally indented by marine planation surfaces. It is generally referred to as c*oastal cliff* or c*oastal scarp* (Mortimer & Saric, 1972; Hartley & Jolley, 1995; Hartley *et al.*, 2005b; Cembrano *et al.*, 2007). The prevailing lithologies comprise volcanic andesites of Jurassic age and granitoids of Jurassic and Cretaceous age (Fig. 2; Ferraris & Di Biase, 1978; Charrier *et al.*, 2007). Jurassic sedimentary rocks of marine origin and Paleozoic metamorphic rocks occur locally (Boric *et al.*, 1990). As a morphotectonic feature of continental scale, this escarpment represents the internal, subaerial boundary of the present Chile Trench (Allmendinger *et al.*, 2005), and the western margin of the Coastal Cordillera (Cembrano *et al.*, 2007; Charrier *et al.*, 2007; Hartley & Evenstar, 2010). Its morphology, however, has been defined by a permanent, steep cliffline along the Pacific coast since approximately the Miocene (Mortimer & Saric, 1972; Hartley & Jolley, 1995). Besides rare outcrops of Cenozoic shallow-marine deposits (Hartley & Jolley, 1995), sedimentary systems along the coastal scarp are represented by alluvial and colluvial fans, locally accompanied by aeolian deposits, and rare coarse-grained deltas constructed by ephemeral streams.

Most of northern Chile is occupied by the Atacama Desert. Climate varies from arid to hyperarid, with several localities recording no precipitation for many consecutive years (Miller, 1976; Vargas *et al.*, 2000). This regional aridity has persisted since the late Mesozoic or early Cenozoic (Miller, 1976; Houston & Hartley, 2003; Hartley *et al.*, 2005a; Clarke, 2006) due to a combination of: 1) the region's persistent location within the southern tropical belt of high atmospheric pressure; 2) the predominance of easterly wind patterns over tropical South America, with Atlantic oceanic moisture severely depleted over the continent before reaching the Pacific margin; 3) the onset of significant Andean uplift since the Miocene (Isacks, 1988; Hartley, 2003), considerably enhancing the rain shadow to the west; 4) the local oceanic circulation involving cold subantarctic Humboldt Current, which depresses regional temperatures relative to global colatitudinal values and strongly reduces evaporation. Relatively more abundant precipitations occur in El Niño years and during maxima in the Pacific Decadal Oscillation (PDO) index (Vuille, 1999; Vargas *et al.*, 2000; Houston & Hartley, 2003; Keefer *et al.*, 2003; Houston, 2006).

4.2.2. Study area

The study area stretches over ~5 km along the coastal escarpment, south of the city of Antofagasta, between 23°46,55' and 23°48' S, corresponding respectively to the beach locality of *Caleta Coloso* and the promontories north of *Caleta Bolfin* (Figs. 1, 3). It is characterized by steep slopes with basal terminations

represented by promontories of fractured bedrock along the steepest reaches, and well-delimited gravelly pocket beaches (Fig. 4A). Relief ranges from an average of ~250 m above sea level (asl) along the northernmost sector to a maximum of 938 m asl (*Cerro Coloso*) along the southern one.

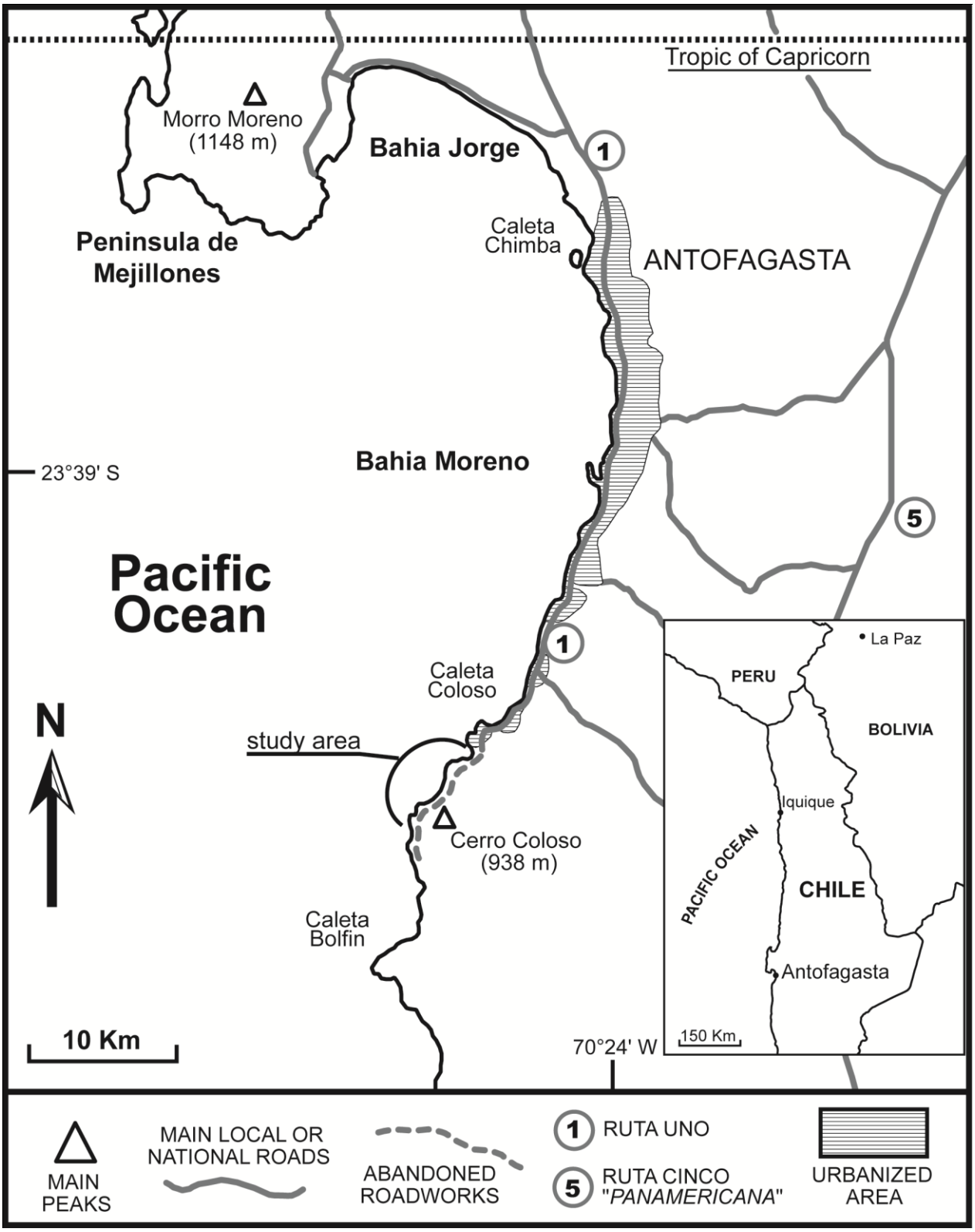

Figure 1 *- Location map of the study area, south of Antofagasta, northern Chile.*

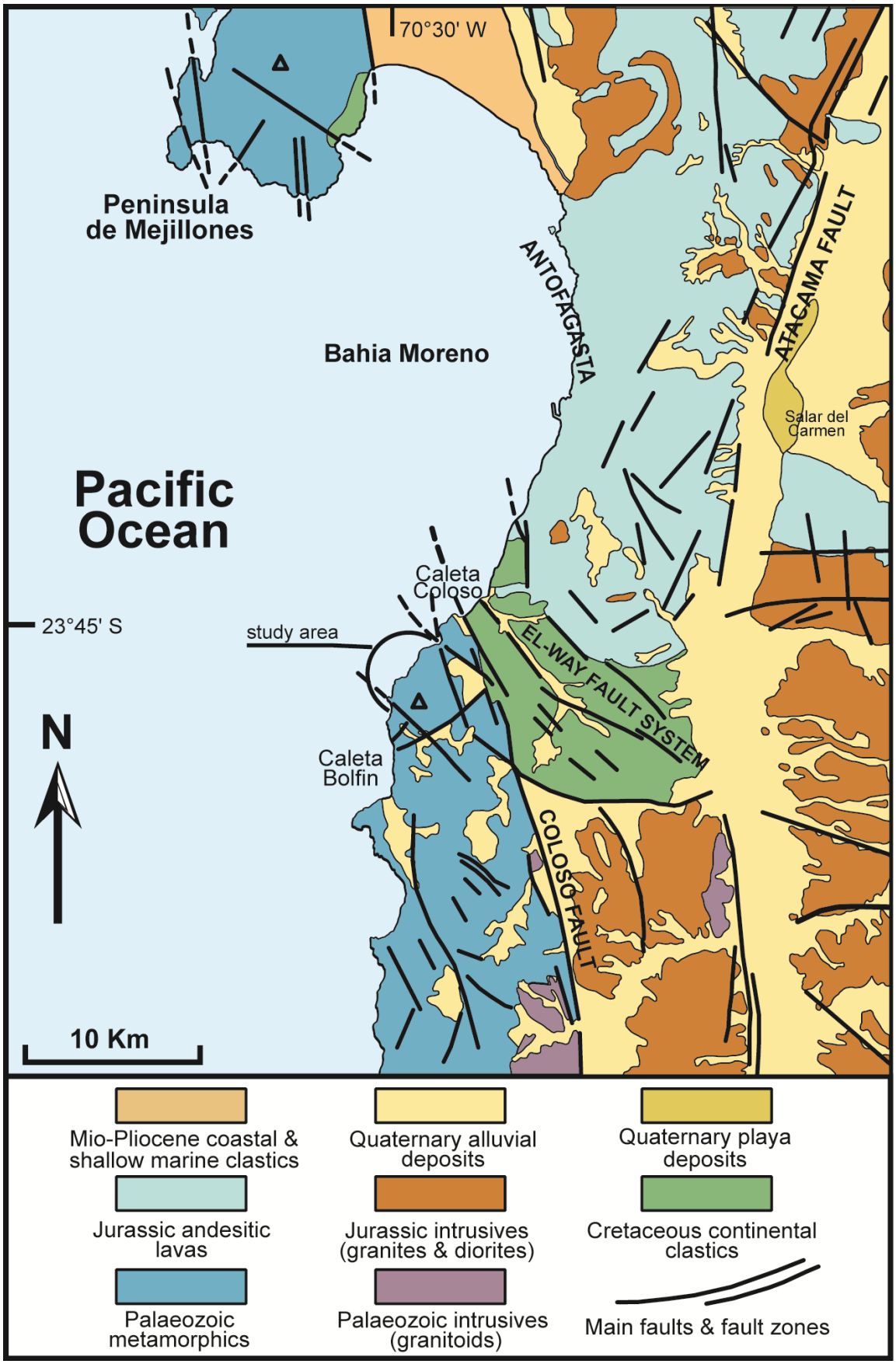

Figure 2 - *Geological map of the coastal region of Antofagasta (modified after Ferraris & Di Biase, 1978).*

The area shows lithological uniformity, represented by a suite of Palaeozoic, metamorphic granulites and amphibolites of the Bolfin Formation (Fig. 3; Ferraris & Di Biase, 1978; Lucassen & Franz, 1992), accompanied by a delimited mafic intrusion. Lithological uniformity reduces the influence of differential bedrock properties and weathering between different slope sectors.

Two regional fault systems strike at high angle towards the coast (Fig. 2): the Coloso Fault System, a lateral branch of the continental Atacama Fault Zone; and the El-Way Fault System, one of the vertical extensional fault zones cross-cutting the Coastal Cordillera (Scheuber & Andriessen, 1990). These fracture zones converge along a narrow fractured belt that runs approximately NW immediately landward of the study area, intersecting the coast at its northern limit. Structural control determines the presence of a distinctly incised catchment that slopes down northwards from Cerro Coloso (Figs. 3, 4B). The western boundary of this catchment is delimited by a small topographic divide that gradually lowers northward and opens towards the coast, merging with the fracture zone. The northernmost slope sectors in the area (sectors 4 and 5; Figs. 3, 4B) can thus be affected by significant runoff conveyed by the catchment during occasional precipitations, whereas southern slopes are largely shielded from runoff (Fig. 4B).

Annual temperature ranges in the region are characterized by narrow seasonal variability (Miller, 1976), with a yearly average of 17.0° (GHCN, 2008a), and extremely low precipitations average 3.5 mm per year (GHCN, 2008b). Several consecutive years occur without any precipitation at all. The major supply of humidity at low heights along the coast is represented by the *camanchacas,* persistent coastal fogs produced by condensation from subsiding warm air along the eastern margin of the SE Pacific Anticyclone interacting with the cold Humboldt Current at sea level (Aravena *et al.*, 1989; Marchant *et al.*, 2007). Macroscopic vegetation is absent over the whole study area. Persistent cold winds vary seasonally with directions to north and northeast, depending on the position of the South Pacific Anticyclone (Tomczak & Godfrey, 1994; Muñoz *et al.*, 2007). Wave climate impacts the slope bases with average wave heights of 2-3 m during the year (Maul, 2005).

Next to direct slope accessibility, an abandoned roadcut provides continuous stratigraphic exposures along the basal slope reaches (Figs. 4A, B), and the possibility to compare them with active morphological features. Almost all small- and large-scale surface features find equivalents in specific facies traits and architectures at corresponding locations along the stratigraphic exposures. The observed surface therefore can be considered fully representative of the colluvial stratigraphy along the roadcut. No chronological data are available, but the very slow rates of geomorphic processes in the Atacama (Dunai *et al.*, 2005; Nishiizumi *et al.*, 2005; Hartley *et al.*, 2005b), the low frequency of major depositional events in the region (Vargas *et al.*, 2000; Hartley *et al.*, 2005b), and the surficial position of the exposed stratigraphic column indicate a late Quaternary to recent age for the studied sediments.

4.3. METHODS

Five piedmont sectors are distinguished in the study area (Fig. 3), based on slope morphology, active processes and sedimentary signatures (Table 1). Bedrock morphologies and colluvial cover vary from steep,

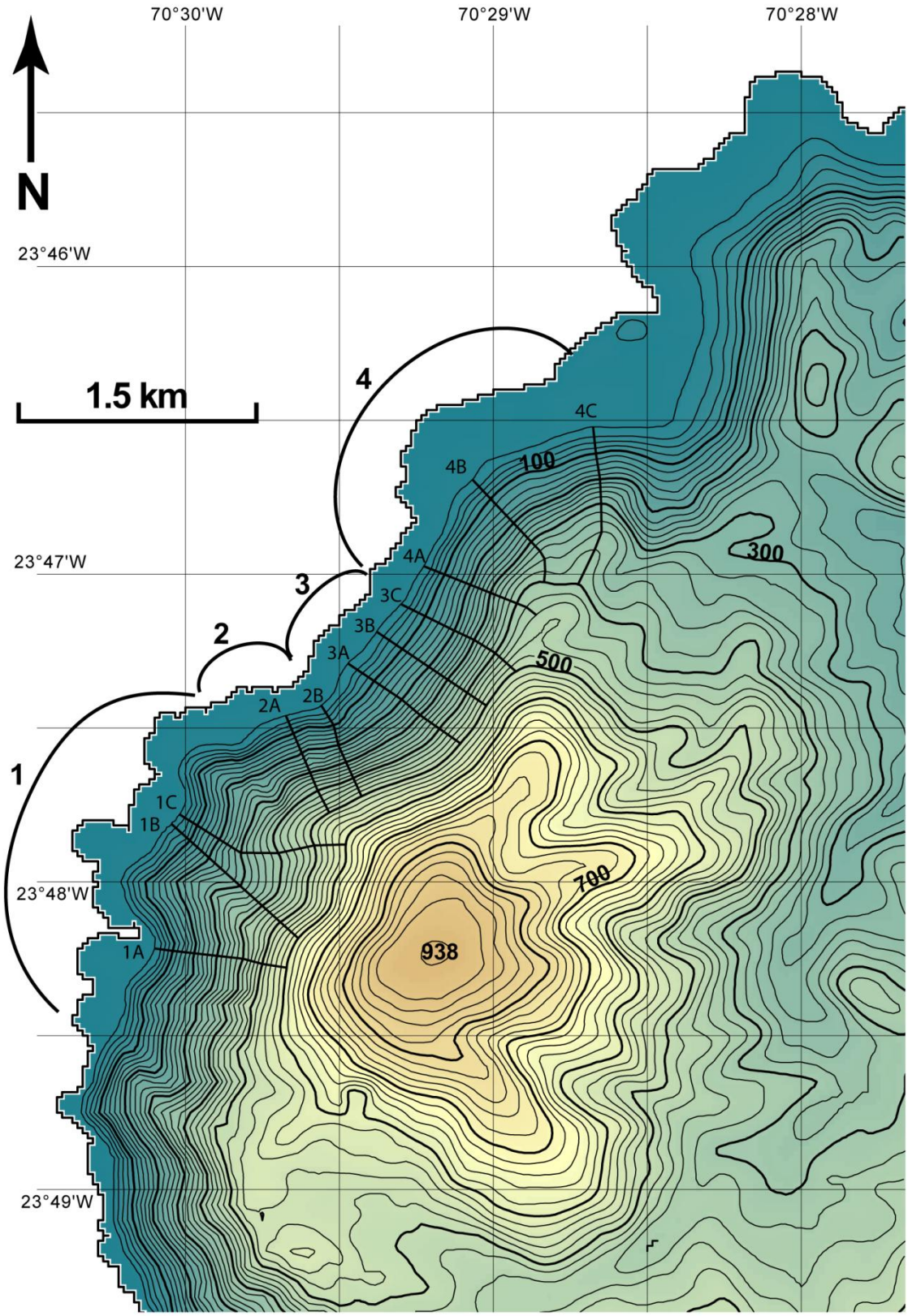

Figure 3 *- Topography of the study area (GIS elaboration of ASTER GDEM dataset, METI-NASA project; 20 m contours), showing the position and extent of piedmont sectors 1 to 4, the adjacent alluvial fan, and the orientation of topographic profiles illustrated in Fig. 5.*

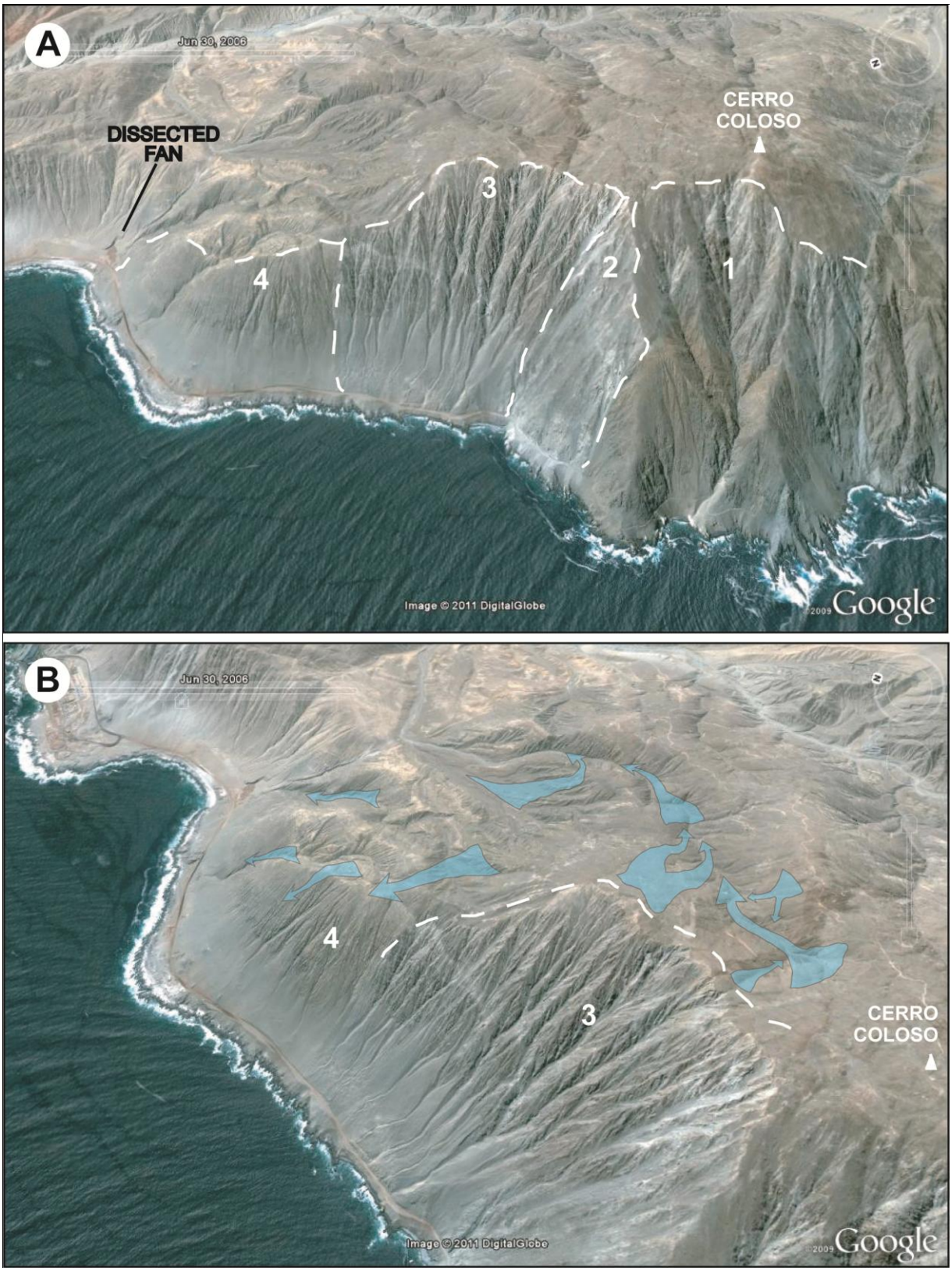

Figure 4 *- Panoramic images (Google Earth®) of the study area. (A) East-oriented panoramic, highlighting the extent of slope sectors, and the alluvial fan at the northern margin of the area. (B) Northeast-oriented view of sectors 3 and 4, highlighting main drainage pathways over the surface; note the bedrock divide (white stippled line) that isolates sector 3 slopes from runoff, and concentration of drainage to the north of Cerro Coloso into the incised catchment feeding the alluvial fan in the north. In both images, note basal roadcut running parallel to slope bases.*

gravity-dominated sectors in the south to more subdued relief in the north, with an increasing influence of associated alluvial and aeolian processes. Slope morphology, active processes and sedimentary facies have been described and quantified by field reconnaissance. A digital topographic model has been generated (~1:20000, contour interval 20 m; Fig. 3) by elaborating ASTER GDEM datasets (ASTER Global Digital Elevation Model project, coordinated by METI and NASA; ground resolution 1-by-1 arcsecond; downloaded November 2009 at http://www.gdem.aster.ersdac.or.jp/). A plan-view distortion of digital topography appears below 10 m asl and at the coastline, due to absent ASTER data coverage of the ocean surface. This information gap causes erroneous altitude-distance interpolations in GIS elaboration along the lowermost, western boundary of the dataset. This however does not influence our analysis, since the studied slopes rise sufficiently far from the shoreline in the north of the area and at altitudes above 15-20 m in the south. The whole study area is visible at high resolution on GoogleEarth® by zooming in at the specified latitudes along the Chilean coast.

Quantification of slope morphology (Fig. 5) was carried out on digital topographic data and by direct field positioning with a portable GPS unit (Garmin Geko 301). Slope angles were measured in the field with a Brunton clinometer, averaging three readings within a circle of 1m radius for every point of measurement. The talus maturity index, being the dimensionless ratio of talus or colluvial mantle height to overall relief height, was calculated in conformity with Statham (1976) and Hinchcliffe *et al.* (1998).

Standard granulometric analyses (laser diffraction, Sysmex® Malvern Master Sizer) have been carried out on fine aeolian and sheetflood deposits, as well as on the matrix of mass-flow deposits. Textural terminology for gravel-sized materials follows Blair & McPherson's (1999) extension of the Udden-Wentworth granulometric scale (Wentworth, 1922; Folk, 1954). Sedimentary fabrics are described according to Harm *et al.*'s (1975) notation, where long and intermediate clast axes are referred to respectively as *a* and *b*, and indices (*p*), (*t*) and (*i*) indicate respectively parallel or transverse orientation to flow and clast axis imbrication. Process terminology follows Blikra & Nemec's (1998) proposal to write 'debrisflow' and 'debrisfall' as single words, by semantic analogy with other process-related terms, such as grainflow.

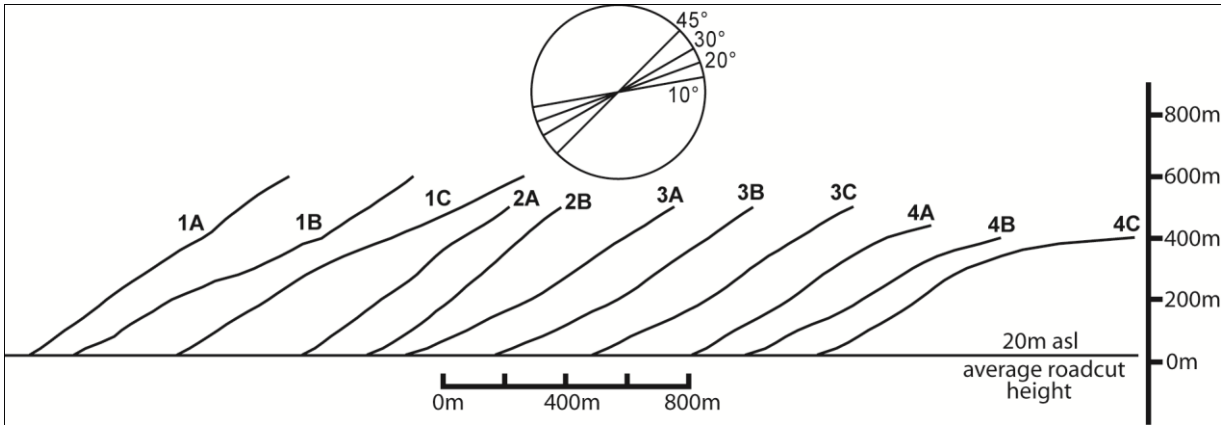

Figure 5 *- Selected topographic profiles for slope sectors 1 to 4 (no vertical exaggeration; see Fig. 3 for profile location). Note general northward decrease in gradient and steepness and increase in concavity from sectors 1 to sector 4, with exception of profiles 2A and 2B (see text for discussion).*

	LATITUDINAL EXTENT	MORPHOLOGY (max. height asl; colluvium height asl; talus maturity index; gradient range)	ACTIVE PROCESSES	MAIN SURFACE FEATURES	OUTCROP DEPOSITS
SLOPE SECTOR 1	23°48,06' - 23°47,55' S	938 - 840 m 100 - 195 m 0.14 - 0.23 40-45° to 15-20°	Rockfall & debrisfall supply; extensive grainflow & minor debris-creep resedimentation; major aeolian deflation; interstitial aeolian deposition	Bedrock-dominated; steep gravelly cones & aprons; isolated sediment pockets	Dominant rock- & debrisfall gravel; interlayered grainflow lobes; debris-creep lobes
SLOPE SECTOR 2	23°47,55' - 23°47,39' S	840 - 800 m 125 - 195 m 0.15 - 0.24 > 45° to 35°	Debrisfall supply; minor grainflow resedimentation; major aeolian deflation	Bedrock-dominated; steep talus cones	Dominant rock- & debrisfall gravel; minor interlayered grainflow lobes
SLOPE SECTOR 3	23°47,39' - 23°47,02' S	800 - 480 m 230 - 270 m 0.35 - 0.47 30-35° to 15-20°	Debrisflow & local aeolian supply; minor rock-/debrisfall & grainflow supply and resedimentation; deflation	High talus cones; extensive aeolian-debrisflow apron with ridge & chute topography; abundant debrisfall gravel over the surface	Dominant debrisflow lobes; interlayered aeolian wedges; minor grainflow & debrisfall gravel
SLOPE SECTOR 4	23°47,02' - 23°46,53' S	450 - 300 m 120 - 150 m 0.37 - 0.50 32-35° to < 10-15°	Aeolian & minor debrisflow supply; extensive sheetflood & debrisflow resedimentation	Aeolian ramp; minor debrisfall gravel at surface and buried debrisflows	Dominant debrisflow sheets; interlayered hyperconc.-flow deposits

Table 1 *- Summary of morphological features, active surface processes and main sedimentary products for each slope sector.*

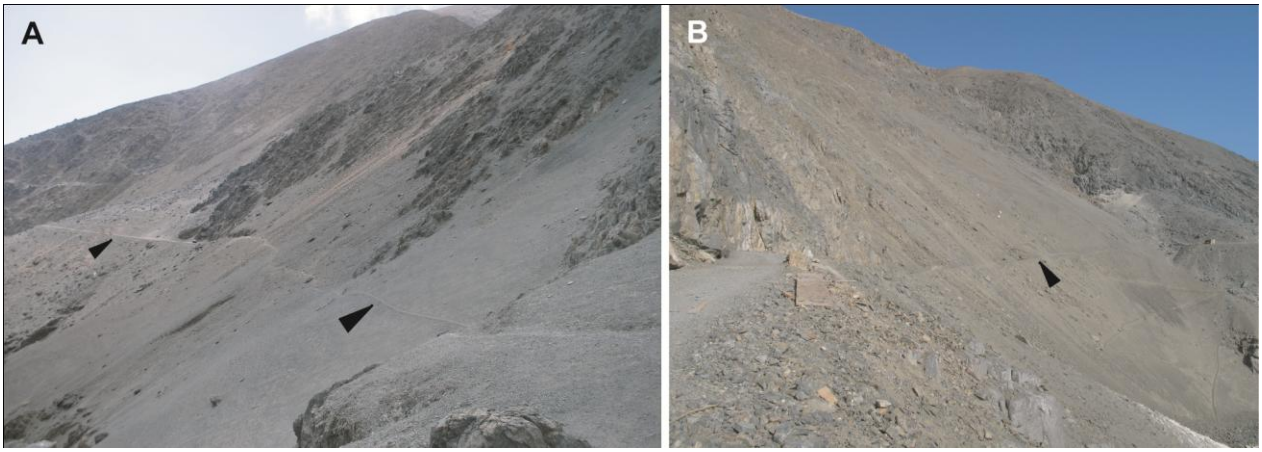

Figure 6 *- Sector 1, panoramic views of colluviated slope reaches; higher bedrock slopes in background rise to the top of Cerro Coloso. (A) Note major depositional domains with steep, wide colluvial cones and aprons, separated by protruding bedrock ridges and outliers. Footpath width (black pointers) varies from 1 to 2 m. (B) Close-up of a steep, broad talus cone delimited by bedrock outliers.*

4.4. SECTOR 1

4.4.1. Geomorphology

Piedmont sector 1 (Fig. 6) is located at the southern margin of the study area, and is characterized by the highest relief, comprising the western slopes of Cerro Coloso (938 m asl). Altitudes range from 938 m to ~840 m at the transition with sector 2. Local bedrock is uniform and consists of coarse crystalline granulites. Bedrock joints and fractures are densely spaced, from several decimetres down to centimetres (Figs. 7A, B, D), and surficial weathering produces high amounts of *grus* and pebble to cobble gravel (Fig. 7C).

Slope profiles (Fig. 5, profiles 1A to C) are rectilinear to convex, with higher angles (40-45° to 31-35°) in basal and medial reaches, dominated by recessive erosion and sediment removal by coastal processes. Bare rocky promontories towards the basal parts of slopes attain the highest angles,and delimit steep talus cones. The gradient gradually decreases upslope to 20° and less, towards the plateau top of Cerro Coloso. Overall slope morphology is characterized by steep, fractured bedrock ridges and 'noses', a few metres to tens of metres wide, alternating with inset depositional domains including isolated talus cones and talus aprons hundreds of metres wide (Fig. 6). Isolated rockfall events were heard and observed continuously during field surveys, especially towards headwalls upslope, and along the steepest reaches of unconsolidated talus. Shallow-marine erosion and sediment remobilization are instrumental in determining which slope tracts are continuously subject to basal erosion and oversteepening, and which accumulate a basal platform of coarse sediments above which talus aprons can prograde and are relatively stable. The talus maturity index (dimensionless ratio of talus or colluvial mantle height to overall relief height; Statham, 1976; Hinchcliffe *et al.*, 1998) for this sector ranges between very low values, from 0.14 to 0.23.

4.4.2. Facies and processes

Facies At

Description. Facies At is widespread on bedrock-dominated tracts of sector 1,and forms small pods or mounds entrapped over partially protected bedrock outliers and bedrock terracettes (Figs. 8A, B). The geometry of the deposit thus varies with local bedrock configuration. It consists of very poorly sorted, non-stratified, coarse-clastic mixtures, varying from sandy pebble to boulder gravel, to granule-rich sand with pebbles and cobbles. Sand fractions are irregularly distributed over the bedrock surface, tending to grow thicker towards adjacent bedrock walls and in the lee of larger clast mounds. On exposed terraces, the deposits wedge out towards the seaward margin. Where medium to very coarse sand is abundant, its volume is inversely related to local wind exposure; sand partially buries gravel fractions, but small pebbles and fine cobbles are scattered over the sandy surface. Where sand is a minor component, coarse clasts are randomly distributed and occasionally assume unstable positions.

Interpretation. Very poor sorting, absence of structures and the precarious position of facies At on restricted bedrock surfaces point to a local origin and practically no preservation potential. Pebble to boulder fractions are deposited by individual rockfall events. The mixture of fresh and highly weathered clasts suggests incremental accumulation rather than mass deposition from large events (Fig. 7C). Coarser clasts are preferentially entrapped on the most confined bedrock ledges. Clasts in unstable positions were probably emplaced by recent events, not yet remobilized by wind gusts or subsequent rockfall impacts.

Most of the sand is probably of local derivation, since bedrock weathering produces high amounts of *grus*. Sector 1 is located on a coastal promontory exposed to strong southerly winds (Tomczak & Godfrey, 1994). Most fines are mobilized by coastal winds, and only a small amount is trapped locally on well-enclosed bedrock terraces, preferentially in the lee of larger clast mounds (Fig. 7A). Finer gravel on top of sandy surfaces indicates that smaller clasts, upon falling, do not carry enough momentum to partially bury themselves in the sand.

This facies is not recognizable in any stratigraphic section, even those reaching down to the bedrock surface. This confirms the low preservation potential, and a higher likelihood for remobilization (as confining bedrock weathers away, or by mass flows from above) and the small volume of these deposits.

Facies Rf

Description. Facies Rf is volumetrically dominant in sector 1, where its deposits determine the gradient of talus cones and aprons. It is poorly organized, lacking distinct depositional units over the active surface (Figs. 6, 8) and lacking discernible bedding and structures in stratigraphic exposures (Figs. 9, 10A,C).

Facies Rf consists of very angular to subrounded, moderately sorted, clast-supported, fine pebble to cobble gravel with granules and boulders (Fig. 9C). Openwork cobble to boulder gravel dominates the lower reaches of talus cones, whereas fine cobble to pebble gravel with patchy sand-granule matrix is common towards higher slope tracts. Downslope coarsening occurs along active surfaces, whereas weak normal grading is occasionally visible in stratigraphy. Disorganized fabrics characterize granule and fine pebble classes, whereas *a(t)* and *a(t)b(i)* orientations prevail for cobbles and prolate boulders both over the surface and at downslope terminations. Oblate and bladed boulders assume flat, slope-parallel positions both at the surface and in stratigraphy (Figs. 7A, 8A,C, 9A, 10B). Equant and prolate cobbles and boulders are most abundant at talus base, whereas oblate and bladed outsized clasts are more common upslope. Stratigraphic contacts with facies Gf and Dc deposits show irregular bases, conformable to the underlying topography, and a common truncation of the top surface by overlying deposits.

Interpretation. Facies Rf represents primary rockfall events from bedrock walls (Rapp, 1960; Statham, 1976; Statham & Francis, 1986; Nemec, 1990; Bertran *et al.*, 1997) or secondary debrisfalls from remobilization of unstable regolith (Blikra & Nemec, 1998). The mixture of fresh and variably weathered amphibolite clasts attests to a mixed debrisfall origin. Transport and deposition take place as isolated fragments or in well-dispersed assemblages with minimal or no clast interaction (*debris fall* of Nemec, 1990, and Sohn & Chough, 1993). Momentum is transferred and maintained directly by single particles in motion (Campbell & Gong, 1986; Campbell, 1990) and dissipated by inelastic to quasi-elastic collisions with the surface. Downslope momentum flux is also referred to as *streaming mode* in studies of granular dispersions with low clast concentrations (Campbell, 1990; Nemec, 1990).

The absence of bedding and structure is related to single- to multi-particle events, in which individual clast behaviour and deposition are not influenced by the presence and transport history of other clasts, and flow mediation by fluids does not occur (interaction with the atmospheric medium is negligible; Campbell, 1990; Sohn & Chough, 1993).

Transport is rather influenced by particle weight and shape, and by topographic factors such as gradient and slope roughness (Statham, 1976; Parsons & Abrahams, 1987; Blikra & Nemec, 1998), defined as the ratio of moving clast diameter to the representative diameter of clasts at slope surface. Coarser clasts, thus, relatively unhindered by surface microtopography (Kirkby & Statham, 1975; Statham, 1976; Nemec, 1990), easily bypass the entire slope length and occur mainly downslope. Smaller clasts instead are more likely to be interlocked and trapped upslope over the irregular surface. Higher momentum for larger clasts also

favours their segregation downslope (Kim *et al.*, 1995; Sohn *et al.*, 1997; Blikra & Nemec, 1998). This holds also for falling assemblages of clasts, since in a sufficiently dispersed state each particle would be independently driven downslope by its own momentum (Nemec, 1990).

Fabric a(t) and *a(t)b(i)* and the abundance of equant and prolate clasts downslope are due to their final rolling motion, relatively unhindered by surface roughness (Bertran *et al.*, 1997). Bladed and oblate boulders frequently lie flat upslope because their shape maximises friction with scree elements. Random fabrics for granule- to pebble-sized clasts are related to final emplacement by variable interlocking with local microtopography (Bertran *et al.*, 1997). Talus infill by finer *grus* probably is due to *in situ* weathering and aeolian infiltration (Nemec & Kazanci, 1999). Irregular basal contacts express conformable deposition over the underlying surface, since individual grainfall events do not generally erode the substrate, unless this is already unstable.

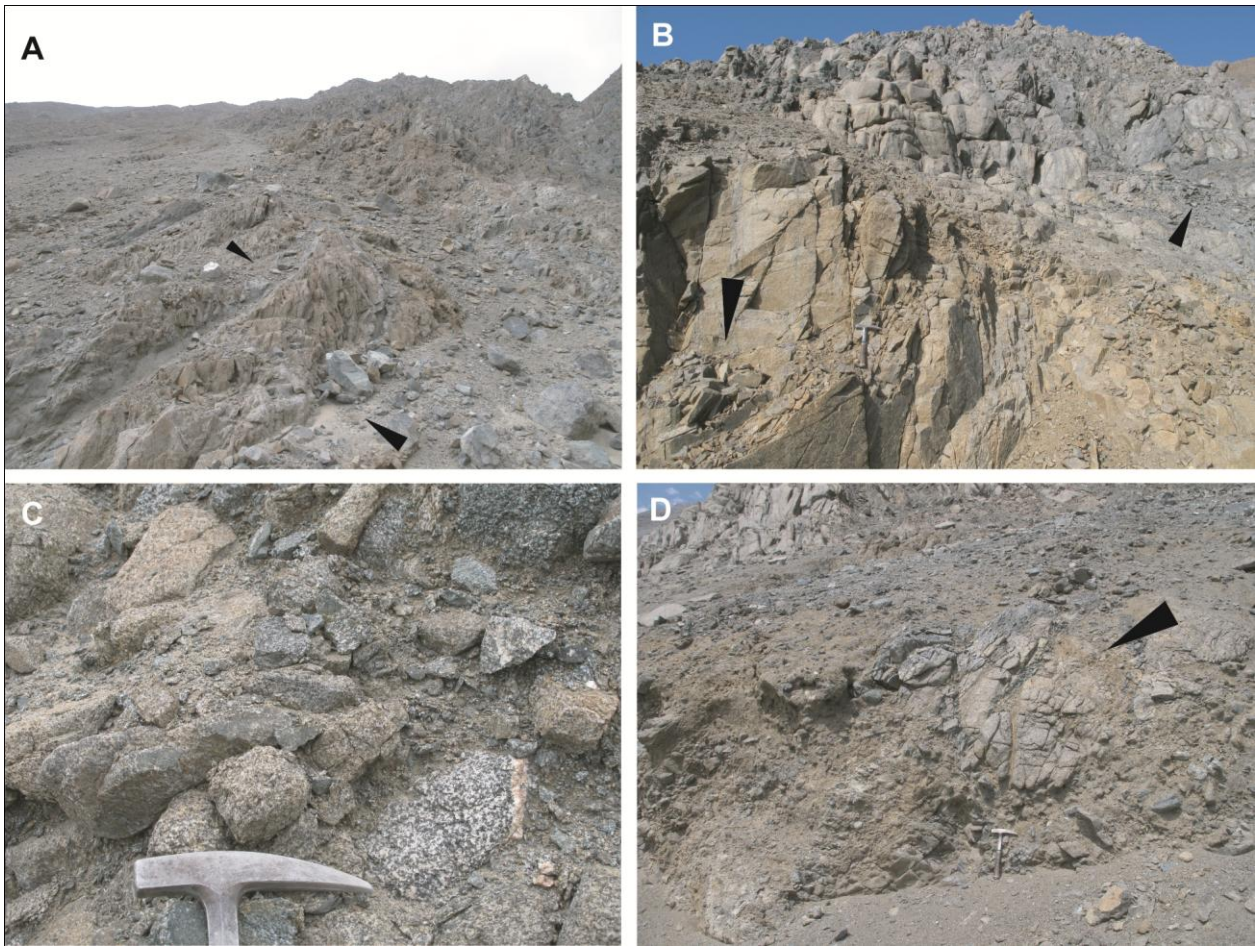

Figure 7 *- Sector 1, morphology and sedimentary facies; hammer is 32 cm long. Note dense fracture patterns in bedrock exposures. (A) High bedrock slopes at ~300 m asl, with mixed rockfall-aeolian pockets of facies At and Rf (black pointers) and high scree cone (higher upslope, top left corner). (B) Narrow bedrock ledges shaped by jointing and topple processes, hosting perched pockets of facies At (black pointers). (C) Detail from a partially failed talus cone, with monomictic clast composition and variable stages of weathering and grusification; note abundant production of coarse sand between clasts, and its scarcity at the exposed top of the deposit. (D) Facies Dc deposits at the base of a small talus cone; note bedrock boulder (black pointer) splitting along original jointing.*

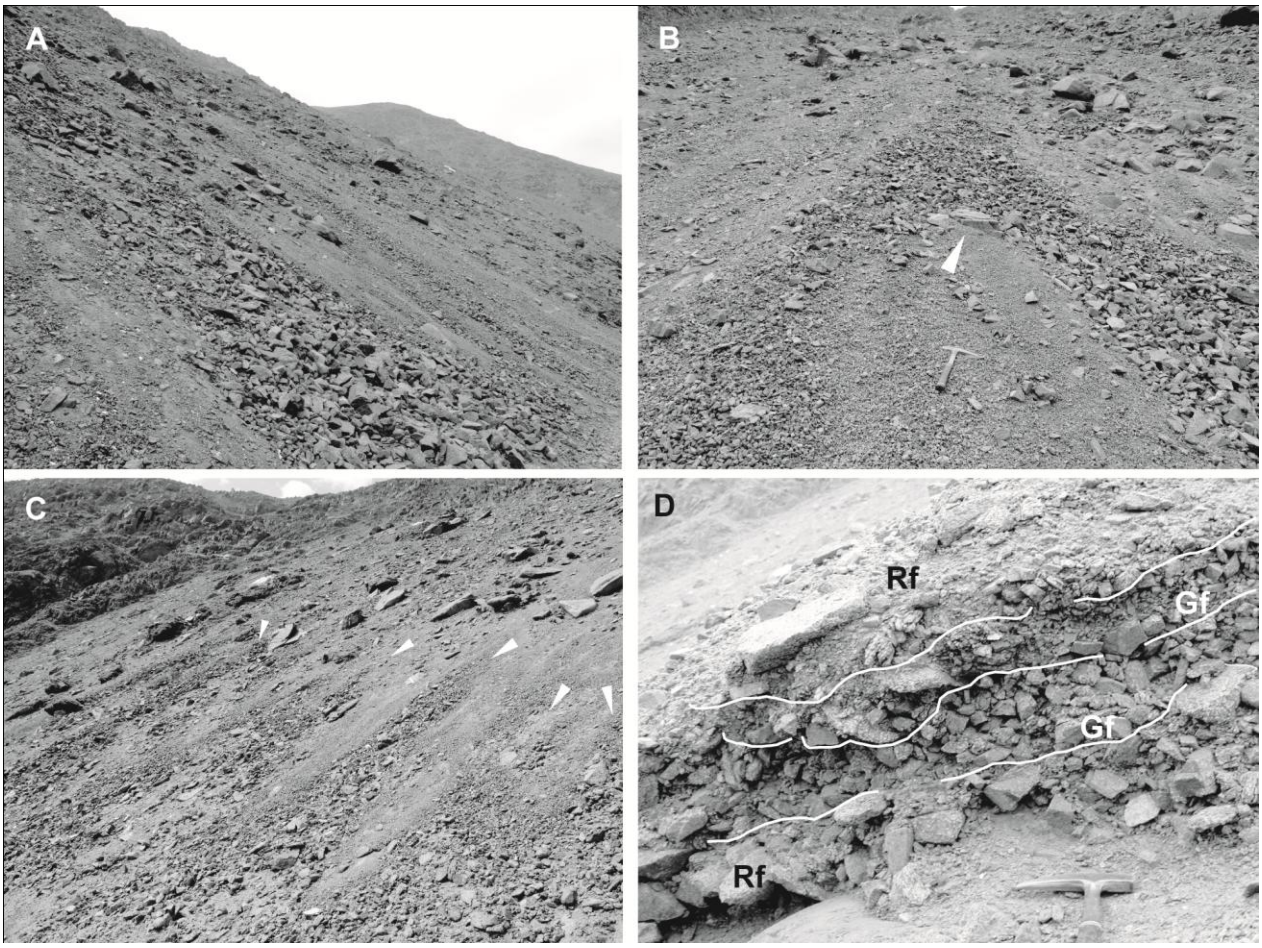

Figure 8 *- Sector 1, active talus surfaces; hammer is 32 cm long. (A) Grainflow lobe gently scouring the underlying scree surface; note upslope fining and tapering of the grainflow lobe deposit, and oblate and bladed boulders stranded higher upslope. (B) Scree surface gently scoured by a grainflow lobe which bifurcates around an obstacle boulder (white pointer). (C) Unstable surface on high talus cone (~ 300 m asl) with frequent small-scale grainflow resedimentation (white pointers; note stranded, oblate and bladed boulders towards the top. (D) Stratigraphic view through partially failed talus cone, with two openwork, well-sorted grainflow deposits (Gf) comprised between poorly sorted, more weathered rock- and debrisfall deposits (Rf).*

Facies Gf

Description. This facies is widespread on and within talus cones dominated by facies Rf. It consists of moderately to well-sorted lobes of angular to subrounded, clast-supported, fine pebbles to coarse cobbles (Figs. 8A,B,C) with rare associated boulders. Individual lobes extend downslope for 2-4 m and up to 20 m, fanning out at their terminations, which are commonly a few clasts thick. Lobe tails upslope taper laterally and merge indistinctly with the surrounding scree (Fig. 8B). Some lobes split and bifurcate around large obstacles (Fig. 9B). Depositional units present variable mixtures of both fresh (light-toned) and weathered (reddish-toned) granulite clasts.

In stratigraphy (Figs. 8D, 9, 10A,C), facies Gf lobes are commonly a few centimetres up to a few decimetres thick, and taper distinctly upslope. Basal surfaces vary from planar to irregular; some lobes have cleared their way into the talus surface, partially embedding within it (Figs. 8, 10A) especially at their downslope end. Granulometry features a distinct downslope coarsening (Figs. 8, 9, 10C). In section, coarse and outsized clasts form short, discontinuous stringers detached from the lobe terminus (Fig. 9A). Weak to distinct

vertical inverse grading is common in stratigraphic sections, but normal grading and inverse-to-normal grading are also observed. Elongate clasts present *a(p)* fabric within lobe bodies, but usually *a(t)* or *a(t)b(i)* orientation at lobe fronts, with b-axis imbrication commonly oriented upslope. Disorganized fabrics are frequent in equant gravel.

Interpretation. Facies Gf shares many characteristics with Rf (moderate sorting, clast support, downslope coarsening, fabrics), implying a related origin. Noncohesive clast dispersions due to gravity can change flow regime from *streaming* (see facies Rf) to a *collisional* mode with increasing concentration (Campbell & Gong, 1986; Nemec, 1990; Sohn & Chough, 1993). Frequent interparticle collisions dominate momentum transfer, as is typical for grainflows (Nemec, 1990; Kim *et al.*, 1995).

Clast segregation in grainflows produces inverse grading and downslope coarsening, because larger particles concentrate towards the top of the active flow, which attains a higher velocity (Nemec, 1990; Sohn & Chough, 1993; Sohn *et al.*, 1997). Inverse grading in cohesionless clast dispersions is classically attributed to dispersive pressure (Bagnold, 1954; Lowe, 1976). This view is recently being reconsidered (Hunter, 1985; Straub, 2001; Legros, 2002) in favour of geometric mechanisms inherent to sheared granular flows, such as kinetic sieving (Middleton, 1970; Savage & Lun, 1988), by which small particles in a dilated granular dispersion tend to infiltrate between the large ones, and thus reach lower flow layers. Frictional interlocking and framework effects will preserve this dynamic layering at flow cessation. Normal and inverse-to-normal grading are due to delayed emplacement of a trailing tail of finer gravel over coarser outrunners (Van Steijn *et al.*, 1995; Sohn *et al.*, 1997).

Frequent *a(p)* fabrics relate to clast shearing at last flow stages, as the still mobile dispersion acquired higher concentration (Rees, 1968). Outsized clasts roll ahead due to their high inertia (Kim *et al.*, 1995; Sohn *et al.*, 1997), producing frontal cobble stringers with *a(t)* or *a(t)b(i)* fabrics. Upslope imbrication is the most stable position for gravel halting against obstacle clasts. Gentle basal scours indicate mobilization of unstable scree by grainflows over steep surfaces. In the presence of particularly massive obstacles, some grainflows split into separate flow units (Fig. 8B). Grainflows probably originated from localized failure of unconsolidated talus due to depositional oversteepening, rockfall overload or seismic shaking. Thorough mixing of freshly and deeply weathered clasts points to their separate origin from bedrock walls.

Facies Dc

Description. This facies is interlayered with Rf and Gf deposits (Fig. 10C) and associated with the upslope presence of broad bedrock ledges hosting relatively large volumes of facies At (Figs. 7D, 10B). It consists of elongate tongues of very poorly sorted silty, sandy, pebble to boulder gravel. Thickness ranges from a few decimetres up to a couple of metres; width reaches no more than 2-3 m. Lobes are several metres long and form asymmetrical mounds with a pronounced head downslope, and an elongate tail upslope. Old lobes are partially buried by rockfall and grainflow scree, whereas recent ones are visible at the surface, where they have partially displaced gravel along their path.

In the only two available stratigraphic exposures, the internal structure is chaotic, with clast- and matrix-supported domains of pebble to cobble gravel in a medium to very coarse, granule-rich sand matrix. The

matrix is cohesive due to intermixed silt and pervasive salt cementation. Crude internal layering is locally defined by coarser clasts with long axes oriented parallel to slope or imbricated upslope (Figs. 10B,C). Basal contacts are planar to gently erosive. Outsized cobbles and boulders are concentrated or perched at the top, especially at downslope terminations (Fig. 10B)

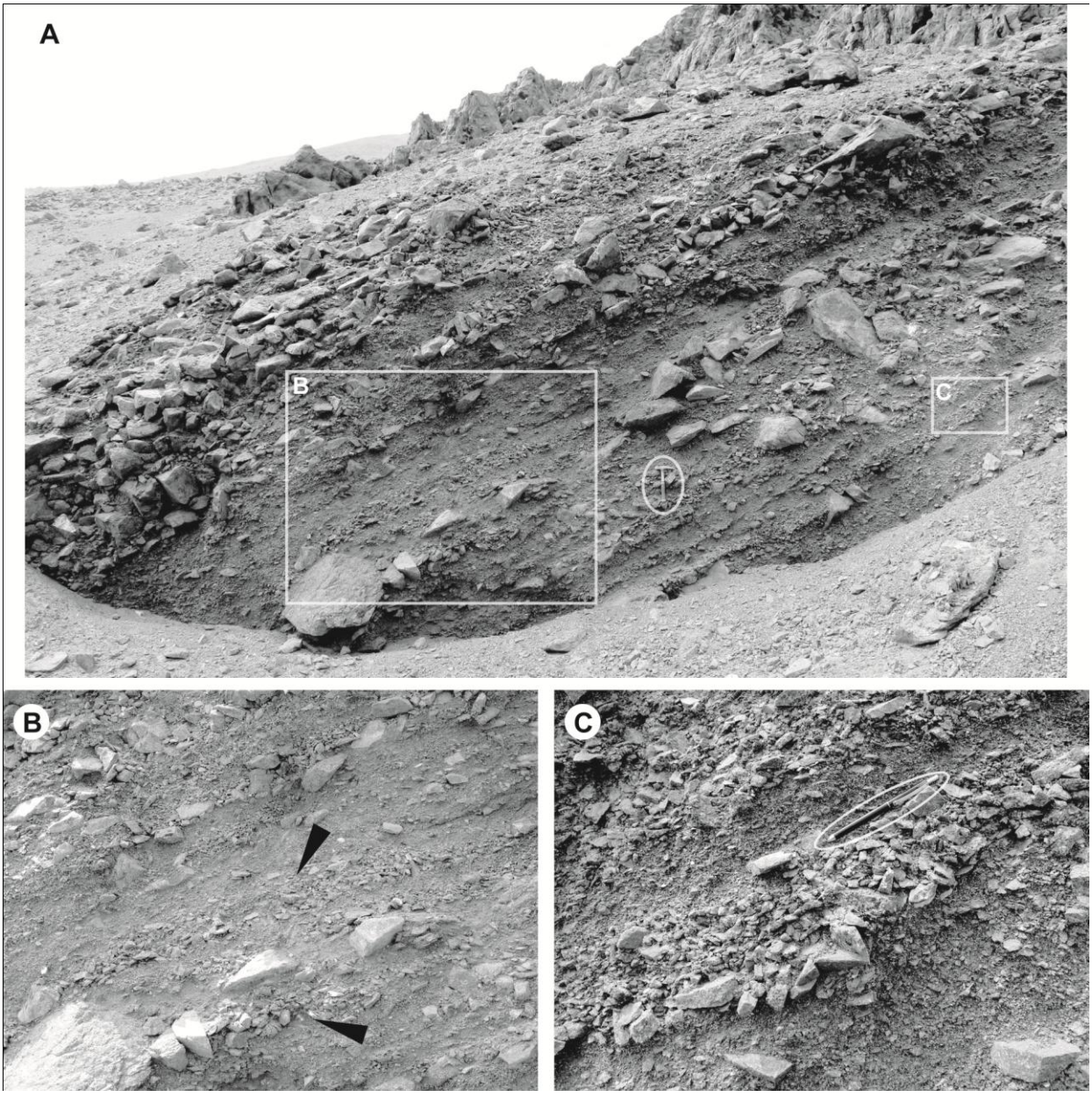

Figure 9 *- Sector 1, stratigraphic exposure through partially failed talus cone; hammer is 32 cm long; pencil 15 cm long. (A) Dip-oriented section at ~90 m asl. Note generally poor organization, but distinct, steeply inclined layering parallel to the active surface; dominant rock- and debrisfall gravel with intercalated beds and lenses of grainflow deposits; larger cobbles and boulders rest flat over both present and paleo-depositional surfaces. (B) Detail of lobe-shaped, cobbly, distal terminations of small grainflow deposits (black pointers); note lobes tapering upslope and terminations against a larger outrun clast (higher lens) and a probable rockfall boulder (lower lens). (C) Detail of centimetric, well-sorted lenses of grainflow origin (see fig. 9C); note frequent a(p)a(i) pebble orientations and distinct normal grading in the lower unit; inverse to normal grading in the upper one.*

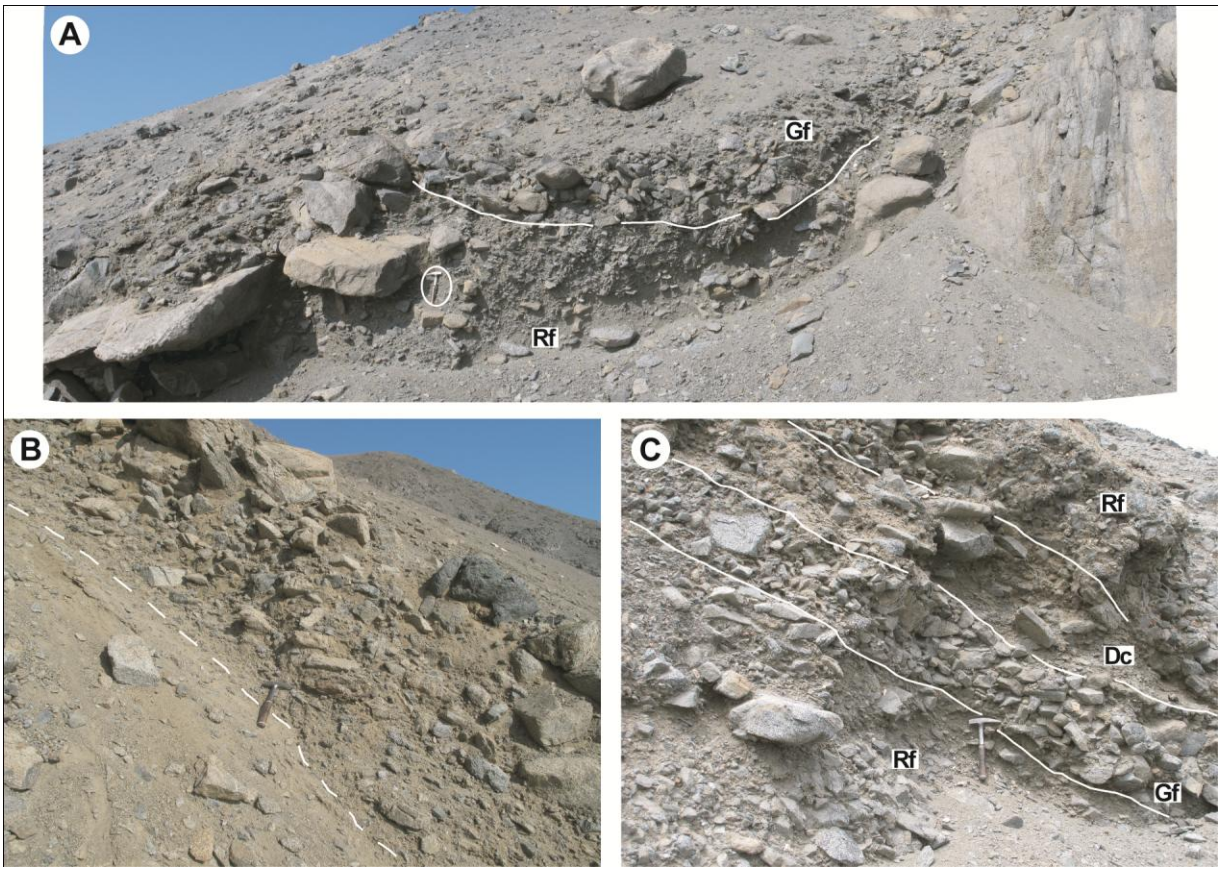

Figure 10 *- Sector 1, shallow stratigraphic exposures through talus deposits; hammer is 32 cm long. (A) Bedrock-confined scree cone with poorly sorted, rockfall- and debrisfall-dominated gravel (Rf) deeply scoured by a coarse-grained grainflow lens (Gf). (B) Partially failed colluvial mantle exposing debris-creep deposits (above white stippled line) resting over a bedrock surface; note steep depositional gradient, high volume of sand to granule matrix, and elongate and oblate clasts oriented parallel to the slope or imbricated upslope. (C) Stratigraphic view through basal talus cone; dominant rockfall scree (Rf) intercalated by probable grainflow deposits (Gf; note moderate to good sorting, inverse grading and downslope coarsening), and probable debris-creep deposits (Dc; note abundant matrix and sheared, a(p) to ap)a(i) fabrics of larger clasts).*

.Interpretation. The very poorly sorted and structureless nature of Dc deposits and their downslope extension point to mass-flow processes (Iverson, 2003). Sediment gravity flows are traditionally categorized on the basis of flow mechanics and sediment-support mechanisms (Dott, 1963; Lowe, 1979; Nemec, 1990), although it is well known that such categories actually span a process continuum (Martinsen, 1994; Iverson, 2003). At one end of the process spectrum, the unconsolidated mass is subject to very low shear rates with only incipient mobilization, slow deformation and substantial preservation of coherence and internal structure (creep, sliding). At progressively greater shear rates, the sediment mass can be fully dispersed, with complete loss of its initial structure and attainment of new particle distributions. Debrisflows span an intermediate position within this process range (Nemec, 1990; Iverson, 1997). They are mixtures of granular material and ambient fluid where solids are concentrated enough to generate elevated frictional and cohesive resistance to shearing and dispersion. Initial remoulding of the static mass proceeds through internal reorganization under the effects of particle-particle and particle-fluid interactions (Pierson, 1986; Iverson, 1997; Iverson & Vallance, 2001).

Facies 1D presents internal reorganization and clast segregation, as highlighted by coarse clast fabrics and outsized cobbles and boulders concentrated to the front. Mobilization is also attested by gently scoured basal contacts and lateral displacement of adjacent scree. Pronounced lobe fronts suggest inertial deformation of a sufficiently coherent upper surface during downslope motion. All of these characters correspond to debrisflow deposits. The extremely steep slopes and coarse sandy matrix indeed would imply low ability to maintain cohesion under high momentum. Attainment of a high velocity can be excluded because of the unconsolidated substrate close to yield angle, since overriding fast flows would have triggered talus failure and flow continuation, rather than emplacement. Momentum must have been high enough on occasions when coarser clasts, with higher inertial mass, were transferred towards the flow front. However, coarse clasts concentrated on the top and front of lobes would easily be destabilized downslope if such flows attained significant speed. Furthermore, sustained debrisflows do not normally come to rest over gradients in excess of 30°. It is therefore inferred that these chaotic deposits result from processes of debris creep (Van Steijn *et al.*, 1995; Pérez, 1998; Blikra & Nemec, 1998) and intermittent sliding, at the limit of incipient debrisflows.

Triggering events with the potential to overcome the yield strength of poorly sorted regolith would be followed by slow, quasi-static internal deformation, and occasional faster advancement. In the hyperarid, tectonically active Atacama piedmont colluvial mobilisation can be induced by dynamic loading from massive debris falls or grainfalls, and by seismic agitation, extremely common in the region (Armijo & Thiele, 1990; Comte *et al.*, 1992).

Some of the large clasts lying flat on lobe tops are probably rockfall products being passively rafted downslope, since such effective clast segregation towards the flow top would not be possible without elevated shear rates (Takahashi, 1980; Davies, 1986; Suwa, 1988). Their precarious position confirms that these sediment bodies never attain high speed. Direct occurrence downslope of large bedrock ledges accumulating At and Rf deposits suggests remobilisation of sediments enriched in aeolian and weathering fines, which provide moderate cohesion.

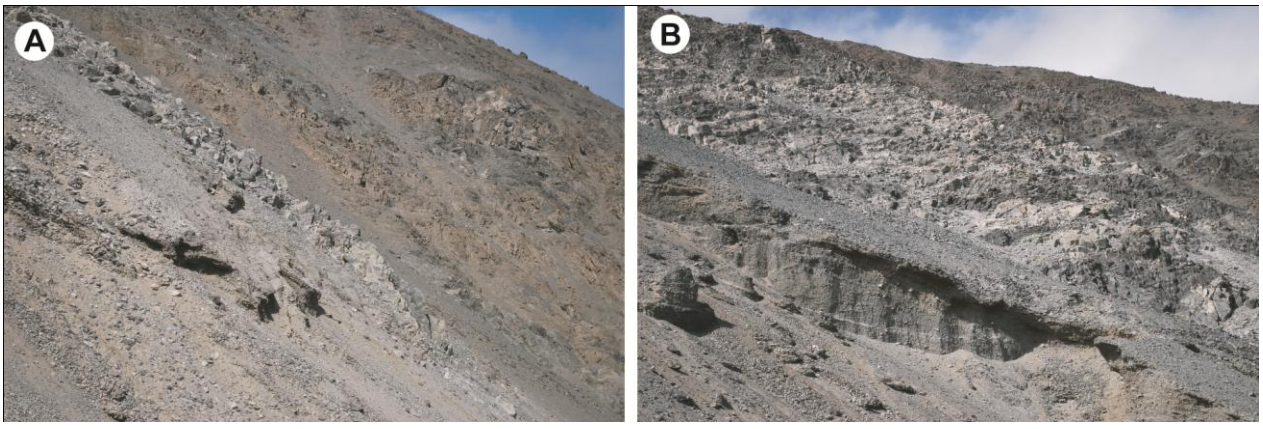

Figure 11 *- Sector 2 slopes. (A) Bedrock ridge and thin, marginal talus cover at ~90 m asl; note colour contrast of bedrock lithologies between sector 2 (foreground) and sector 1 (background slopes). (B) Bedrock surfaces and incised talus cone with secondary talus ramp; sector 2 footslope.*

4.5. SECTOR 2

4.5.1. Geomorphology

Sector 2 is the narrowest in extent, stretching over only 600 m, (Figs. 3, 4A) along the northwestern slopes of Cerro Coloso. It presents the steepest morphology (Figs. 11A, 12A), with bedrock walls reaching up to ~850 m asl and gradients ranging between 40 and 45°. Slope profiles are rectilinear and locally convex up to about 800 m asl (Fig. 5, profiles 2A and B), where they abruptly flatten connecting to the top of Cerro Coloso. This extreme morphology is probably related to lithostructural control along the outcrop extent of a gabbroic intrusion (Lucassen & Franz, 1992) with widely spaced fracture patterns, competent appearance, and lower weathering grade than surrounding metamorphics (Figs. 4A, 11).

Talus cones occupy a reduced fraction of slopes in the lower 100-200 m, separated by wide bedrock cliffs and outliers terminating at high angle to sea level. The talus maturity index ranges from 0.15 to 0.24. Talus angles vary from over 40° in unstable accumulations upslope, down to about 25-30° or less where some cones toe out to the roadcut. Roadworks in this sector partially exposed the outer margins of these basal talus aprons, producing good vertical exposures (Figs. 11B, 12B). Rockfall and debrisfall events have been observed to take place with a frequency of several per hour during field surveys. Stabilization of colluvial aprons has been prevented by high-angle slope terminations to a linear coastline, which favour basal wave action, and by maximum exposure to local winds.

4.5.2. Facies and processes

Facies At occurs in very small volumes owing to low 'accommodation' on steep, resistant bedrock slopes with very few available ledges. Associated aeolian fines are scarce since this piedmont tract is the most exposed to strong winds. Facies Rf is volumetrically more dominant than in sector 1 (Fig. 13). Rockfall gravel at the surface includes lesser amounts of interstitial fines than in sector 1, but buried rockfall deposits, accessible in stratigraphy, comprise relatively higher amounts of coarse sand and granules. This is probably due to strong deflation at the surface, and to the high resistance of gabbroic lithology to disintegration upon weathering with thus a reduced production of fines; buried deposits, on the other hand, protected by overlying scree, gradually disaggregate and retain their finer (pseudo)matrix (Figs. 13, 14C,D).

A markedly reduced volume of facies Gf grainflow deposits is present in sector 2 (Figs. 13, 14), as evidenced by the rarity of distinct lobate, downslope-coarsening depositional units in stratigraphic sections. Grainflow deposits are relatively more abundant at the base of scree cones (Fig. 14A), in bedrock chutes and along lateral confluences of adjacent talus cones. In the latter position, grainflow lobes have a concave-up lensoidal geometry that conforms to the underlying surface (Fig. 14D), as well as a distinctly coarser texture along the lobe axis, fining out laterally.

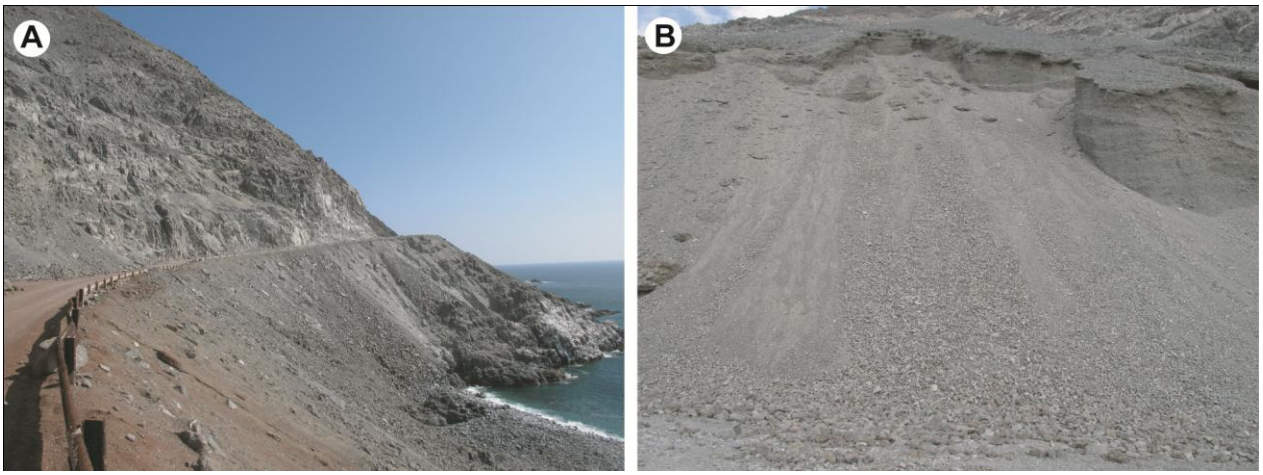

Figure 12 *- Sector 2 slopes. (A) Steep gradients in bedrock slopes terminating at high angle to sea level; view from abandoned roadcut. (B) Rockfall and grainflow deposits forming a high-angle, secondary talus ramp after destabilization of natural talus cone (higher up in the photo) by roadworks.*

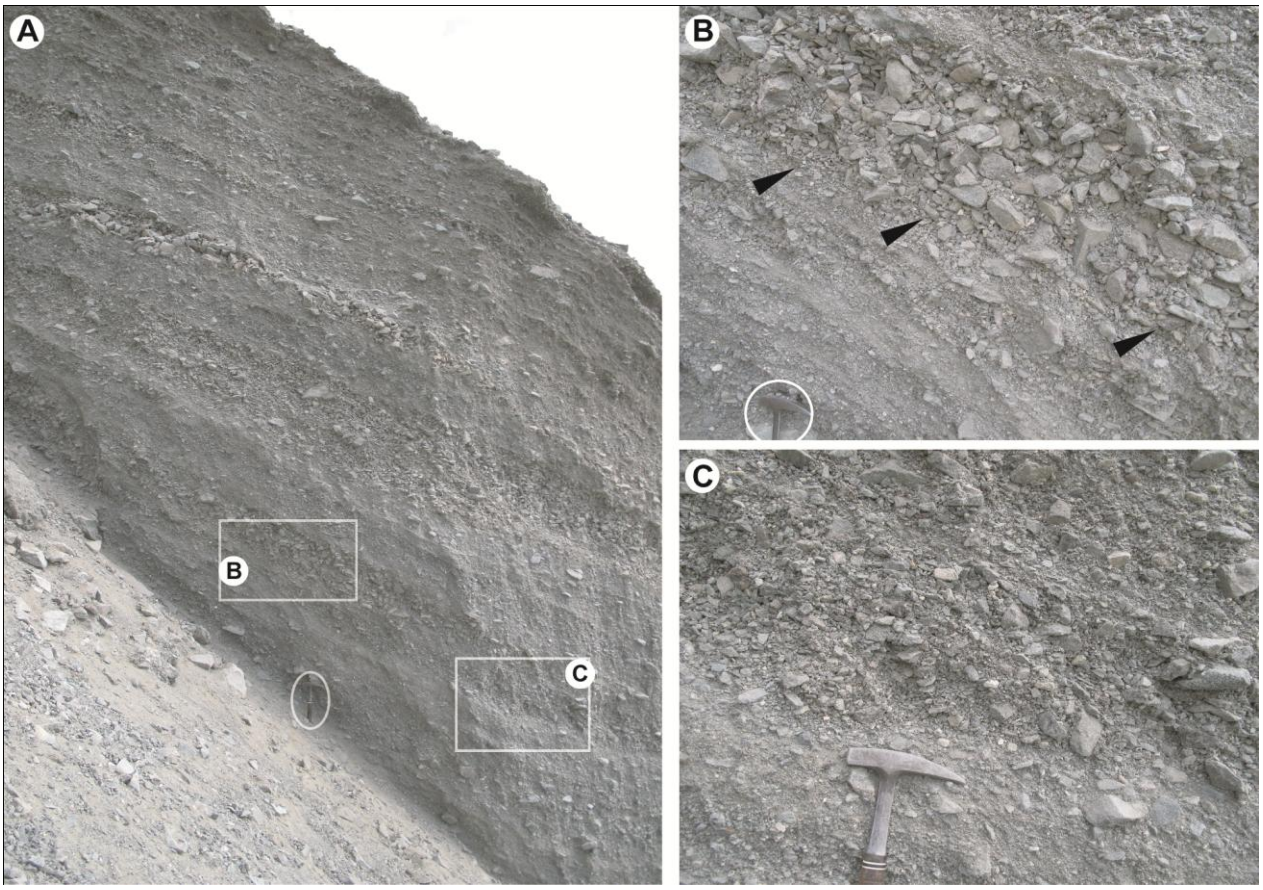

Figure 13 *- Sector 2, talus stratigraphy; hammer is 32 cm long. (A) Steeply dipping stratification, following the original depositional gradient; note coarser-grained, better-sorted grainflow and debrisfall intercalations within finer, 'background' rockfall gravel. (B) Detail of openwork, moderately sorted, inversely to normally graded pebble to cobble gravel from probable grainflow (black pointers along basal surface); note dominant a(p) and a(p)a(i) fabric of elongated and oblate clasts. (C) Detail of crude layering in poorly sorted, granule to cobble rockfall and debrisfall gravel (facies Rf). Fine-poor deposits in the upper half of the photo correspond to a possible period of fast deposition with reduced surface exposure, weathering and deflation.*

This difference in grainflow abundance and distribution between sectors 1 and 2 is probably due to slope morphology. Bedrock chutes along Sector 2 slopes offer a higher gradient than the surrounding rockfaces, enhancing local talus instability and focusing sediment transport downslope. The dynamic distinction between *streaming* debrisfall avalanches and *collisional* grainflows is related to particle concentration during flow events (see facies Rf and Gf in *Sector 1*). In case of scree failure, falling particle assemblages can maintain a highly dispersed state over high-gradient, planar or convex slope surfaces (Sohn & Chough, 1993), explaining the dominance of rockfall and debrisfall facies in Sector 2. On the other hand, lateral confinement in chutes constrains clast dispersions within a limited space, forcing flow dynamics into a collisional regime (Nemec, 1990; Sohn & Chough, 1993). Furthermore, chute flanks converge towards a central axis, driving falling clasts to bounce and roll not only downslope, but also along their axis. This effect, more pronounced for larger particles, results in gravel lenses with coarse clasts distributed at their center, and with finer lateral 'wings'. The same mechanism applies to clasts falling in isolation.

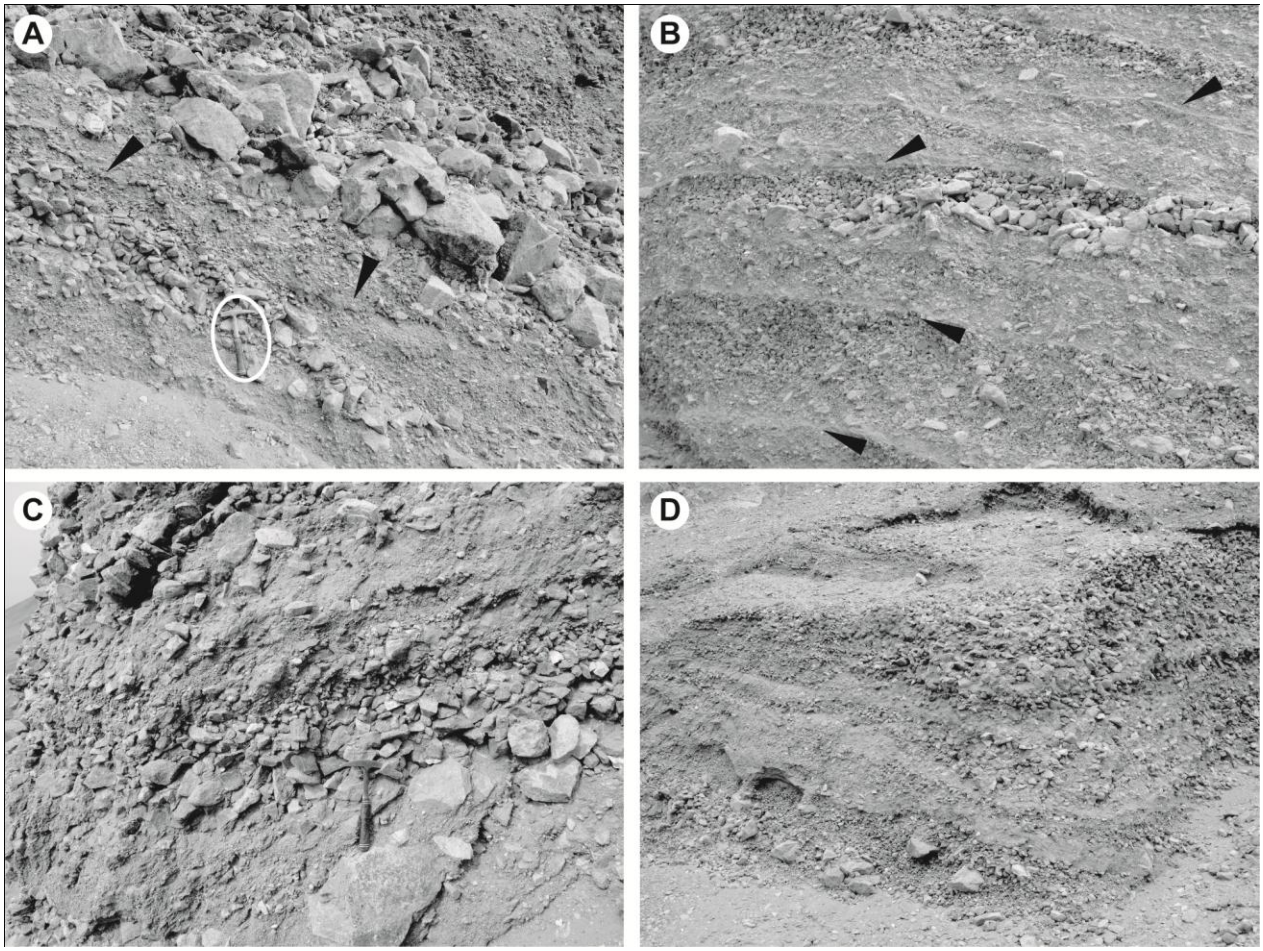

Figure 14 *- Sector 2, talus stratigraphy; hammer is 32 cm long. (A) to (C) Openwork lenses of cobble to fine boulder gravel from debrisfalls and grainflows within finer 'background' rockfall deposits. Note weakly cemented surfaces (black pointers) representing probable intervals of inactivity and exposure. (D) Moderately to well-sorted cobble gravel at the confluence between two small, converging talus cones, forming a coarse, laterally confined gully fill.*

4.6. SECTOR 3

4.6.1. Geomorphology

Sector 3 stretches over 900 m with relatively more subdued relief than sectors 1 and 2 (Figs. 3, 4A). Altitudes gradually drop from ~730 m asl at the southern limit to ~480 m asl northward. Gradients are distinctly bipartite, from 30-35° on upper slopes, and locally steeper along rockwalls, decreasing abruptly to 20-25° and less at 180-200 m asl (Figs. 5, 15). Markedly concave topographic profiles feature rectilinear to gently convex upper segments, with a kinked connection (Fig. 16A) to gently concave lower segments. Bare rockwalls are indented by deep gullies and hollows (Figs. 4A, 15, 16A), the widest of which (~4-6 m width) contain abundant regolith and aeolian sand. Sector 3 slopes connect upward to the northern flank of Cerro Coloso via a narrow divide that stretches along the whole sector (Fig. 4B). With a relative elevation of 10-15 m over the adjacent northern flanks of Cerro Coloso, the divide effectively shields Sector 3 from surface runoff (Fig. 4B).

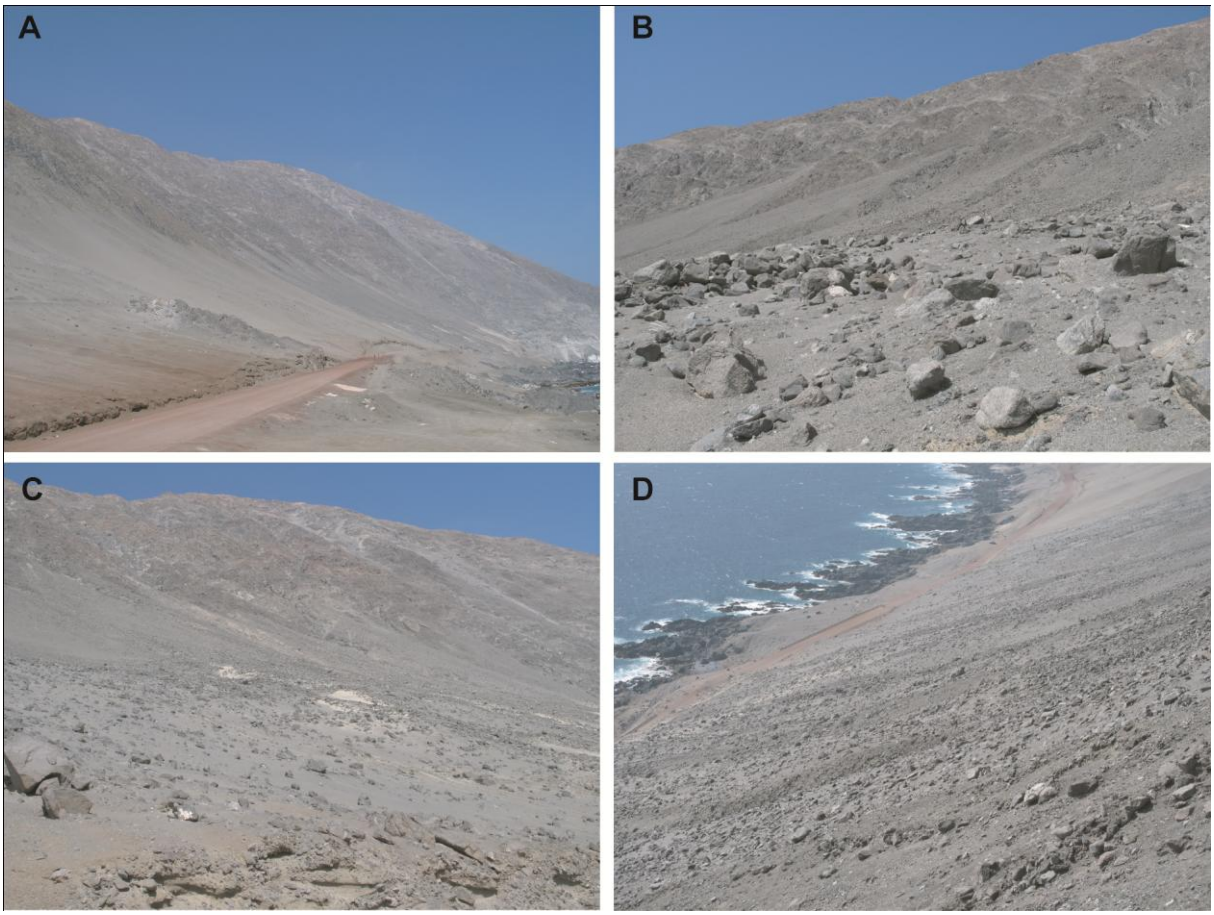

Figure 15 *- Sector 3 slopes, panoramic views. (A) View over the entire sector (central-right portion of photo) with clearly bipartite architecture of upper, high-gradient bedrock cliffs and lower-gradient colluvial apron. (B) and (C) Views over higher slopes at the northern margin of sector 3; high, laterally truncated talus cones and indented topography of bedrock cliffs. (D) Lower slopes of sector 3; colluvial apron that gradually connects down to sealevel. Note the complex architecture of alternating gravel lobes, low-relief sandy surfaces, and scattered coarse debris.*

Figure 16 *- Sector 3, high talus cones. (A) Surface and stratigraphic expression of gradient knickpoint (black pointer) between a proximal talus cone and the upper portions of the colluvial ramp; youngest units of the scree cone 'downlap' over sandy-gravelly units deposited by mixed debrisflow and aeolian processes. (B) Interbedded, very coarse Rf and Gf gravel in talus cone; outcrop exposure is ~ 4 m high.*

The talus maturity index along this sector (0.35 to 0.47) is considerably higher than along the southern piedmont; the colluvial apron is well developed, and mantles lower slopes with a complex morphology. The higher portions, above 170-200 m asl, consist of steep (up to 35-40°) talus cones directly abutting bare bedrock walls (Figs. 15B,C, 16A) and laterally truncated (Figs. 16A,B) in correspondence of major bedrock gullies. A sharp drop in gradient around 180 m asl marks the transition from upper, bedrock- and talus-dominated slopes to lower colluvial slopes (Figs. 15, 16A). These consist of an extensive sedimentary apron with irregular topography. Relief features rise commonly less than 1-2 m above the average surface (Figs. 15D, 17A, 18) and are composed of poorly sorted, sandy, pebble to boulder gravel ridges, elongate downslope and with prominent terminations. When partly buried by other deposits, they appear as irregular, subdued mounds. Some elongate gravel ridges extend downslope in parallel pairs separated by sand-filled throughs (Figs. 17A, 18; see facies 3A).

Negative topography between gravel lobes is partly to entirely filled by fine to medium sand upslope, and medium to very coarse sand downslope (Fig. 18), with associated thin discontinuous layers of granules to fine pebbles and scattered cobbles or boulders (Figs 18). Chutes show several stages of infill, from incipient, with northward-dipping sand wedges attached to the lee (northern) side of gravel ridges (Figs. 18A,B,C), to advanced (Fig. 18C), to complete (Fig. 18D). In the incipient stage, the next ridge to the north is usually not subject to sand deposition and is exposed (Figs. 17A, 18B). Sandy surfaces feature discontinuous trains of wind ripples and deflation moats around obstacle clasts (Figs. 18C,D, 21). Ripple trains transverse to the chute axes or gradually curved around protruding obstacles (Fig. 18C). Together with the south- to westward orientation of obstacle scours, they point to prevalent seawinds blowing to the north and northeast.

On a higher level in sector 3 morphology, gravel ridges radiate mainly from point sources in correspondence of headwall gullies and lateral incisions in talus cones. Gravel lobes therefore extend downslope along preferential zones, stacking vertically and laterally into composite mounds at the foot of slopes (Figs. 15D,

17A,B,C). The lower colluvial apron is also abundantly strewn with cobbles and boulders, isolated or in clusters, whose average sizes markedly coarsen downslope.

Slope terminations in sector 3 connect to the shore at a lower angles than in Sectors 1 and 2 (Fig. 5). The shore profile is gently arcuate to rectilinear, and forms a wide embayment to the north of Cerro Coloso. Consequently, sector 3 is exposed to a less energetic wave climate than sectors 1 and 2, and features gravelly beaches and a thicker colluvial apron. Partially protection in the lee of Cerro Coloso reduces deflation, and favours local sand deposition. Field surveying has been accompanied by continuous sandblasting and observation of intermittent clouds of saltating sand.

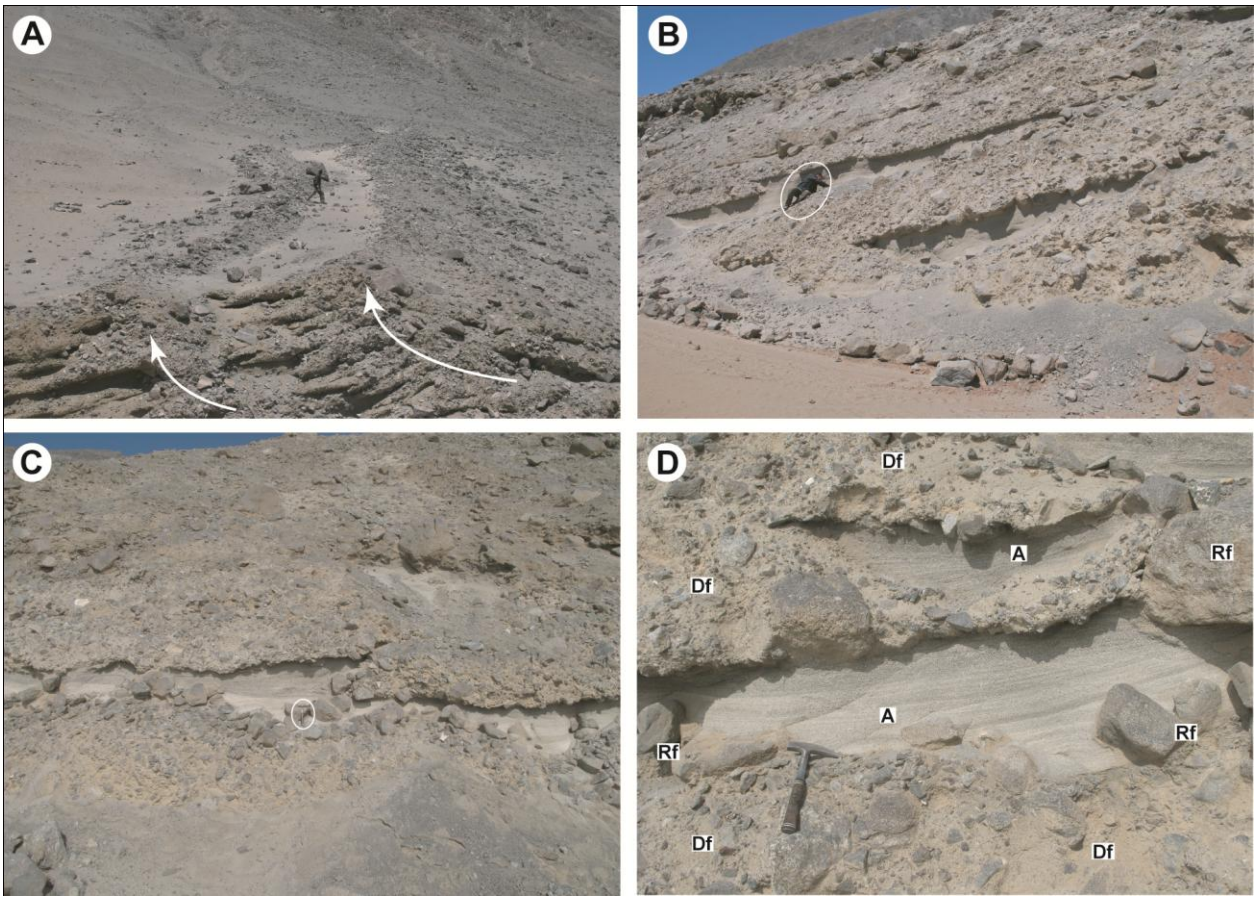

Figure 17 *- Sector 3, dominant facies architecture in the lower colluvial apron, roadcut outcrops. In all photos, north (downwind) is to the left; first author for scale is 1.85 m; hammer is 32 cm. (A) Distal debrisflow mound composed of stacked levee-lobe units sidestepping northward, and interbedded aeolian sand. Note topmost deposits in stratigraphy corresponding to the most recent debrisflow event, still fully exposed over the active surface as paired levees with trapped aeolian sand. Note also exposed surface of gravel mound in deflation upwind, whereas the downwind side is partly covered by aeolian sand. (B) Northern margin of a distal debrisflow mound, with aggrading and sidestepping debrisflow units and interbedded aeolian sand. (C) Vertically aggrading debrisflow lenses, with associated aeolian lenses and sparse debrisfall boulders. (D) Close-up of two aeolian-sand wedges (facies A) delimited by debrisflow lenses (facies Df); note inclined sand lamination prograding downwind (towards left in the photo). Scattered boulders (Rf) are probable secondary debrisfalls from coeval, surrounding debrisflow lobes (see Figs 18A and B).*

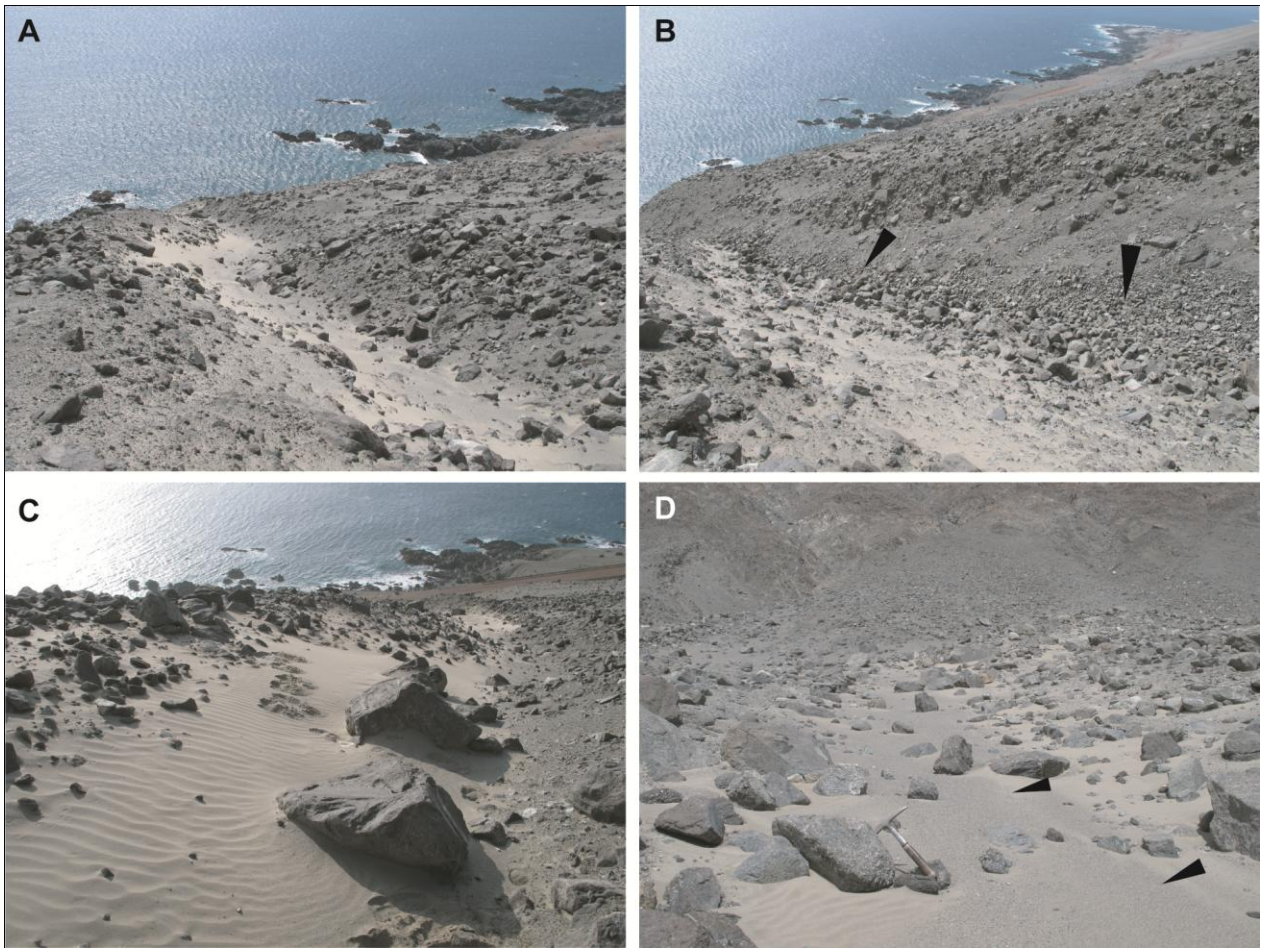

Figure 18 *- Progressive stages of aeolian aggradation between debrisflow lobes, from incipient (A) to complete (D); in pictures (A) to (C), north (downwind) is to the right. In B, note slope-parallel alignment of cobbles and boulders (black pointers) gradually released by deflation of the overlying debrisflow ridge. In (D), note surficial, granule to fine pebble blow-out lag (black pointers) between weathering gravel lobes.*

4.6.2. Facies and processes

Facies Df

Description. These deposits dominate sector 3 both over active slopes and in stratigraphy. They consist of structureless, very poorly sorted, pebble to medium boulder gravel in a matrix of silty, granule-rich, fine to medium sand, with local clast-supported domains (Figs. 17, 18A,B, 19A). Depositional geometries consist of downslope-elongate mounds forming conspicuous relief elements (Figs. 15D, 17A, 18A,B), up to a few meters wide in the lowest slope reaches, commonly tapering upslope, and varying in thickness from a few decimetres to 1.5-2 m. Two morphological styles dominate: laterally extensive, matrix-supported gravel mounds; and paired, narrow clast-supported ridges extending downslope with sinuous trajectories (Fig. 17A), with distinct coaresning-outward texture especially in the outer bends. As noted above, gravel lobes radiate downslope from large bedrock gullies and extend over specific slope areas. Distally, they therefore aggrade into terminal mounds up to several metres thick, composed of vertically and laterally stacked gravel lenses (Figs. 17A,B).

In stratigraphy, facies Df is represented by amalgamated lenses (Figs. 17C,D, 19A) with sharp contacts to sandy facies A. Basal surfaces are weakly to non-erosive, locally underlain facies Ad deformed laminasets

(Fig. 22). A basal, millimetric to centimetric division can be present, as distinctly well-sorted, coarse sand analogue to underlying facies A (Fig. 22). Gravel fabrics are weak, except for *a(p)* orientation of bladed and oblate clasts. Grading varies from absent to inverse, with cobbles and boulders concentrated towards the lens tops and margins. Outsized boulders can be present long basal or top surfaces, isolated or in clusters (Fig. 17C and D).

Interpretation. Facies Df presents typical traits of debrisflows, such as massive structure, very poor sorting, matrix support, weak clast fabrics and sharp stratigraphic contacts with poorly or non-erosive base (Smith & Lowe, 1991; Blair & McPherson, 1998; Blikra & Nemec, 1998). Preferential deposition downslope of major bedrock gullies points to these as sources of loose regolith (Reneau & Dietrich, 1987; Innes, 1993), which included significant amounts of windblown fine sand trapped in protected hollows upslope and favouring development of plastic gravity flows (e.g. Bowman *et al.*, 1996). Flows gain further cohesion through bulking additional fine and medium sand over the colluvial mantle, as testified by thin, sand-enriched divisions along the base of distal lobes (Fig. 22). The process was probably enhanced by the presence of water in the flow. Given the hyperarid climate and absence of clay, cohesion was thus provided by minor silt and abundant fine to medium aeolian sand; clast support was aided by temporary excess pore pressures and framework effects (Iverson, 1997). The relatively low volume of gravel and its poor segregation in distal debrisflow lenses suggest scarce clast interactions during flow, but paired gravel ridges upslope imply construction of coarse-grained levees through lateral segregation of coarse clast (Suwa, 1988; Blair & McPherson, 1998). Conformable to gently disturbed basal contacts indicate laminar flows.

Most debrisflows came to a halt over the reduced gradients of lower slopes, which are thus dominated by gravel ridges. Point sources upslope forced flow paths to be maintained over fixed runout zones. Consequently, emplacement consisted in progressive lobe stacking and sidestepping for long-runout events, building up the distal mounds. Small, asymmetric mounds (Figs. 17A,B) result from aggradation of relatively few flow units. The larger ones comprise numerous lobes stacking with opposite vergence. Repeated aggradation in the presence of growing mounds forced successive flows to change stacking vergence, following the lowest available topography.

Facies A

Description. Facies A is the second most abundant in sector 3, distributed as a discontinuous mantle upslope and in discrete lenses delimited by gravel ridges downslope (Figs. 17B,D, 19). It consists of moderately to very well sorted, coarse to very coarse, granule-rich sand downslope, with a distinct fining trend to medium-fine sand upslope (see Fig. 27B). Roadcut outcrops are thus invariably dominated by very coarse sand, with finer sand only in intercalated facies Am (see below).

This facies shows planar to slightly concave-up, millimetric sand laminae (Figs. 19B,C) with inclination ranging from subhorizontal to 10-15°, invariably dipping northward. Lamination is defined by fine alternations of different grain sizes and by segregations of monomineralic grains that confer the deposit a distinctly striped appearance. Laminae form dm-thick sets (Figs. 17D, 19A,B) separated by second-order, planar to gently curved bounding surfaces. In stratigraphy, several laminasets form wedge-shaped units

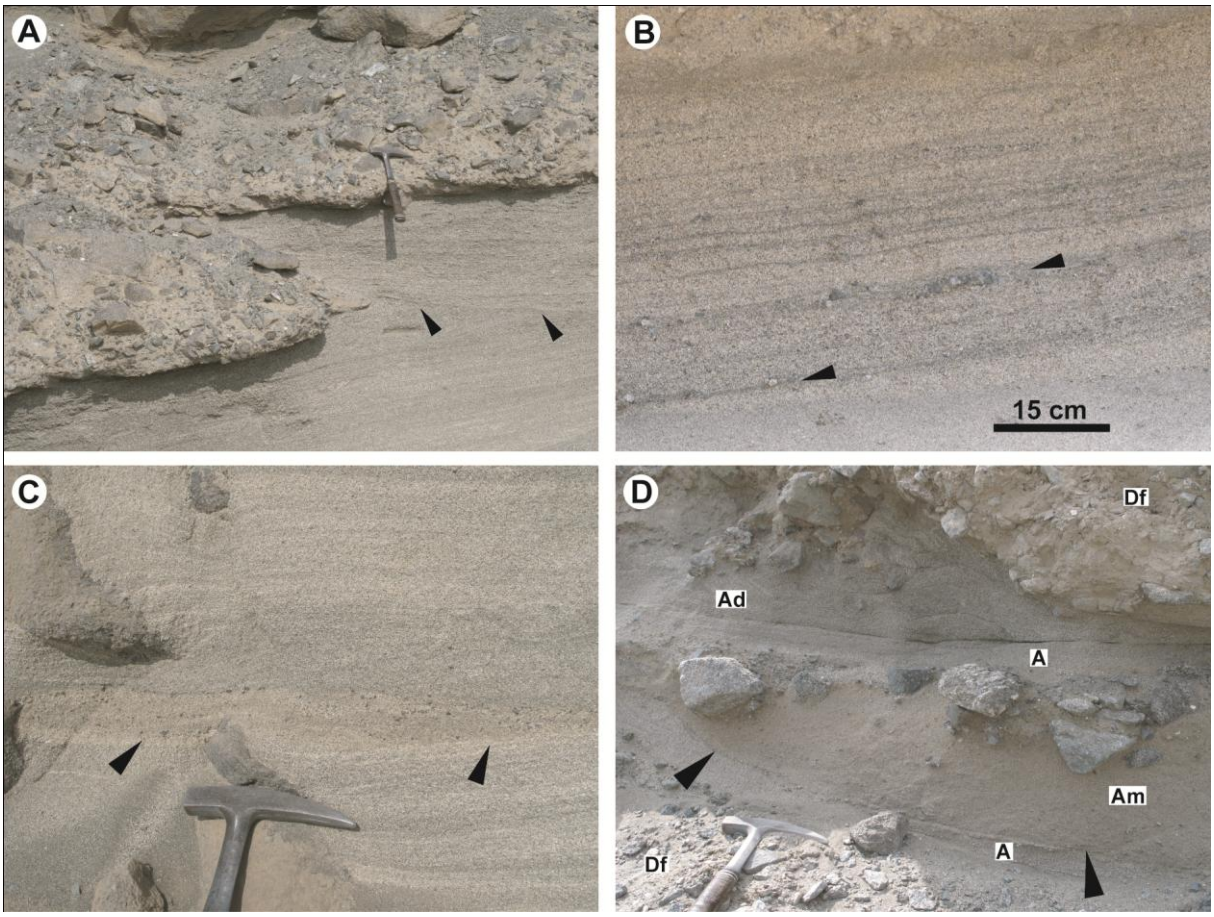

Figure 19 *- Sector 3, stratigraphic facies details, roadcut outcrops. In all pictures, north (downwind) is to the left; hammer for scale is 32 cm long. (A) Overlapping aeolian lenses delimited by debrisflow lobes and separated by a reactivation surface (black pointers). (B) Pin-stripe lamination in facies A, and interlayered Ac lags (black pointers). (C) and (D) Facies Am massive sand lenses (black pointers indicate lower boundaries) within aeolian sands. Note embedded cobbles at lens top in (D). Note also a thin layer of deformed aeolian sand (facies Ad) at the base of the debrisflow (Df) in (D), separated by a sharp shear surface from underlying aeolian deposits (A).*

Figure 20 *- Incipient 'clast ghost' after long exposure and grusification at the surface of sector 3, illustrating the virtual absence of precipitation; hammer head is 16 cm long.*

delimited by debrisflow lenses (Figs. 17B,C,D, 19A). Subordinate, discontinous layers of granules and fine pebbles are intercalated between laminasets and along second-order surfaces. Lamination thickens locally to centimetres, with distinct inverse grading.

Interpretation. Stratigraphic facies and comparisons with the active surface consent to interpret facies A as aeolian deposits. The irregular topography represents a roughness element for the generally strong winds, promoting deflation over relief features and deposition in topographic lows. Sandy laminasets are interpreted as low-angle grainfall strata due to flow separation of north- to northeastbound wind in the lee of debrisflow mounds (Hesp, 1981; Clemmensen 1986). Lamina segregation by grainsize and composition is due to fluctuations in wind strength (Fryberger *et al.*, 1979). Grainfall accretion is followed by continuous reworking of the depositional surface by strongly channeled winds into flat, millimetric laminae (Hunter, 1977; Kocurek & Dott, 1981; Clemmensen & Abrahamsen, 1983). Small, structureless sand rims at the base of isolated pebbles represent the infill of obstacle scours (small scour-and-fill structures; *sensu* Clemmensen, 1986), and are also evidence of aeolian reworking. Isolated occurrences of slightly thicker laminasets with inverse grading (Fig. 19B) represent pin-stripe lamination produced by wind ripples (Hunter, 1977). Their rarity is probably due to the generally high wind speed.

Laminasets with variable northward to subhorizontal inclination indicate different stages of progressive aeolian infill of negative topography between gravel ridges. As observed over the surface (Fig. 18), aeolian accumulation generally starts with inclined sand wedges abutting the leeward margin behind debrisflow ridges. Truncation surfaces indicate major episodes of deflation or reactivation due to changes in wind direction, windstorms or periods of reduced sand supply. This is testified by granule and pebble lags prevalently distributed along second-order surfaces. Similar facies have been identified in sand-sheet deposits (Fryberger *et al.*, 1979; Kocurek, 1986; Lea, 1990; Halsey & Catto, 1994; Williams, 1998) and low-angle aeolian stratasets from periglacial settings (Hétu, 1995; Hétu & Gray, 2000). In this setting, preservation as isolated sand lenses is due to the irregular topography of debrisflow deposits ('wind-shadow deposits'; Hesp 1981; Clemmensen, 1986). Common bypass of mass flows over higher slope segments determines a flatter, more regular topography, where a thin aeolian mantle gains more lateral continuity, but also reduced preservation potential.

Facies Ad

Description. Facies Ad forms isolated lenses between and specifically below debrisflow deposits. It presents identical texture and primary structure to facies A, but differs in being gently to pervasively folded and microfaulted, with convolutions and truncation of laminasets and bounding surfaces (Figs. 19D, 22). The primary lamination however is generally well preserved on a microscale.

Interpretation. Texture and structures identical to facies A suggest an origin by deformation of aeolian sand strata. Deformation of unlithified to weakly cohesive aeolian sand occurs through various combinations of trigger mechanisms (Owen, 1987; Collinson, 1994). Internal folding points to loss of frictional strength and possible temporary liquefaction. However, the subaerial location in a hyperarid setting and the surficial position within the thin colluvium exclude permanent saturation by a water table. Liquefaction by complete

water saturation would result in rapid water expulsion, with pervasive disruption of original fabric and lamination, and formation of dewatering structures. Such features were not observed. Deformed sand units are invariably positioned directly underneath debrisflow lobes, which can have reached lower slopes only during significant precipitation. Aeolian sands were probably deformed through a combination of rapid, partial saturation by rain infiltration and internal shear by superposed debrisflows over the high-gradient surface. Shearing would have favoured temporary overpressure from water and air trapped in the sand, leading to density instability (De Boer, 1979). Local shear planes and microfaulting parallel to debrisflow bases (Fig. 22) confirm the causal link. Analogue combinations of sediment-water interaction and loading effects have been inferred for deformed aeolian bedsets in ancient and modern deposits (Jones, 1972; Doe & Dott, 1981; Loope *et al.*, 1999). Permanent coastal fogs, common in the region, may enhance sand competence and susceptibility to transient saturation, as observed on the hyperarid coasts of Namibia (Walter, 1979, cit. Doe & Dott, 1980). Although similar instances of aeolian sand deformation have been associated to water saturation during exceptional floods (Hurst & Glennie, 1998), this hypothesis is discounted by the absence of pervasive reworking or erosive surfaces in distal Sector 3 deposits. Moreover, isolated gullies upslope cannot collect significant runoff.

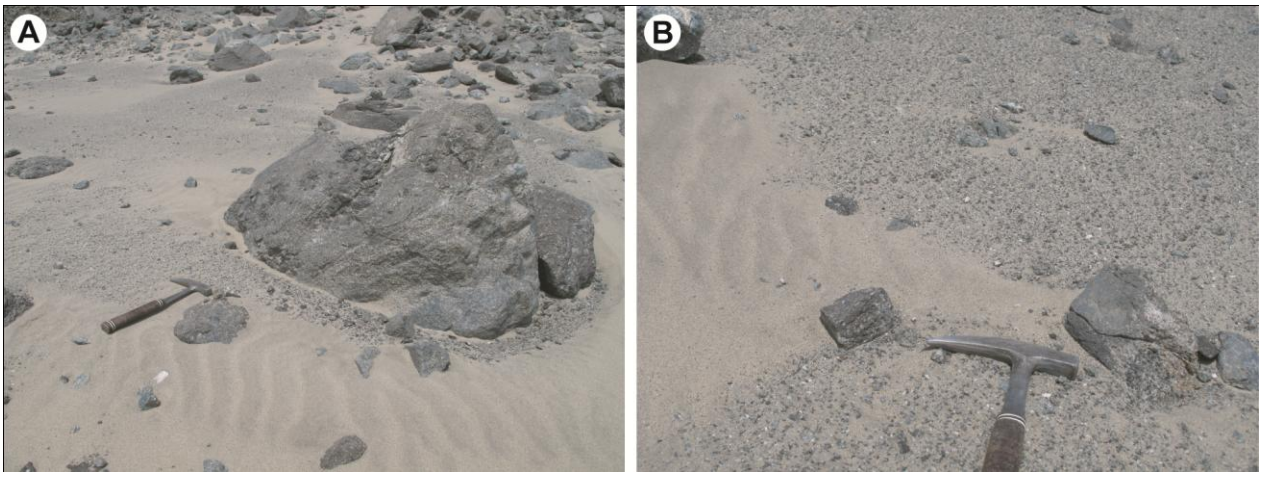

Figure 21 *- Aeolian blow-out lags over the lower surface of sector 3; north (downwind) is to the left, and hammer is 32 cm long. (A) Exposed boulder sourcing thin layer of granules and fine pebbles, fining downwind. (B) Wind-shadow effect in the lee of an exposed cobble; the sandy surface directly in the lee of the obstacle is shielded from the advancement of windblown grus.*

Facies Am

Description. This facies occurs exclusively as isolated, centimetric lenses within aeolian sand wedges of facies A (Figs. 19C,D). It consists of moderately to well sorted, medium to very coarse, granule-rich massive sand, ungraded or inversely graded. A larger-scale example is represented by a trough-shaped unit, ~1 m wide and ~25 cm thick, with pebbles and fine to medium cobbles confined at the top (Fig. 19D). Basal surfaces are flat to slightly convex, whereas the top is typically convex. Am lenses are easily distinguished from surrounding aeolian strata by their poorer sorting and massive structure.

Interpretation. Texture, sorting and massive structures suggest an origin from small grainflow lobes over the steep aeolian surface (Hunter, 1977; Kocurek & Dott, 1981; Turner & Makhlouf, 2002). Finer textures than the

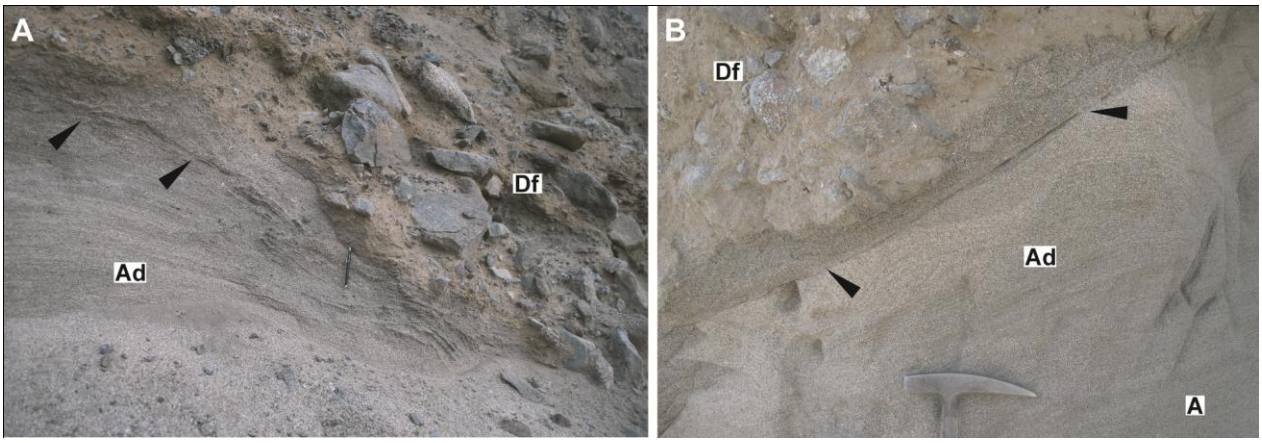

Figure 22 *- Sector 3, roadcut outcrops. (A) and (B) Deformed aeolian deposits (facies Ad) below large debrisflow lenses (Df); folding and microfaulting in aeolian deposits are highlighted by the geometry of laminae. Note shear surfaces (black pointers) and partial bulking of coarse aeolian sand into debrisflow bases. In (B), note transition from highly deformed aeolian deposits (facies Ad) at the center, gradually downward to almost undisturbed aeolian lamination (facies A).*

encasing facies A indicate upslope provenance, where aeolian sand is mainly finer. Absent fabrics and structures imply very brief flow durations, with no time for internal clast segregation. Conformable to gently erosive base indicates scarce sediment entrainment from the runout surface. The larger lens in fig. 19D, markedly scoured at base and with gravel at its top, represents an event with sufficient mass and runout to destabilize the underlying surface. Grainflows have been generated during field surveys by walking along the steepest reaches of sand-filled chutes; such events are probably generated by frequent rockfalls and seismic shaking. The rare occurrence of facies Am is certainly due to continuous aeolian reworking of the active surface.

Facies Ac

Description. This rare facies occurs as discontinuous layers of granules and fine pebbles within aeolian sand wedges, especially along second-order reactivation surfaces. Lateral extent reaches up to a few tens of cm and thickness is defined by the largest pebble or granule concentrations. Some layers are laterally graded, with the largest pebbles at the southern (windward) end, fining northward (downwind) into granules or very coarse sand. Such thin coarse interlayers are always perfectly conformable to sandy laminae, distinguishable by the sharp textural contrast.

Interpretation. By comparison with active surface processes, facies Ac interlayers are interpreted as blow-out lags. Reconnaissance along sector 3 has shown numerous clasts exposed at the aeolian surfaces in various stages of weathering (Figs. 20, 21A), from surficial fracturing and spalling to complete disaggregation into *grusy* clast 'ghosts'. Small clast fragments have been observed to be entrained by strong wind gusts. Mobility is mainly controlled by particle size and shape. Fine lithic pebbles are blown away probably only during severe windstorms (Selby *et al.*, 1974; Sakamoto-Arnold, 1981; Hétu, 1991; Hétu & Gray, 2000; Van Steijn *et al.*, 2002), especially if they acquired platy shapes, with high surface/weight ratios, from the original metamorphic texture. Sand and granules instead are deflated more continuously. Such thin blow-out lags are seen exclusively downwind of exposed cobbles and/or boulders (Figs. 18D, 21), extending up 1-3 m

downwind of large clusters of exposed gravel only. Origin by deflation is frequently confirmed by the surface distribution of *grus*, that clearly traces the wind path between and around large obstacle clasts (Fig. 21).

Facies Rf and Gf

Gravelly facies Rf and Gf in sector 3 are abundant upslope in high talus cones developed below rockwalls (Figs 16A,B). Interstitial fine to medium sand is much more abundant than in sectors 1 and 2, and contributes to stabilize these scree cones. Isolated and clustered clasts occur also in the colluvial apron over lower slopes, where they halted upslope or rolled down preferentially along distal sandy chutes, because of topographic channeling and the low surface roughness of aeolian sand. The typical coarsening-downslope trend in these facies is due to the fundamental control of momentum on clast runout distance. At outcrop, rockfall gravel is thus present mainly as cobbles and boulders within aeolian sand wedges, where lamination is disrupted by loading effects. More localized rockfall sources are represented by debrisflow lobes, which shed clasts directly into the adjacent chutes as deflation gradually erodes the matrix (Figs. 18A,B).

4.7. SECTOR 4

4.7.1. Geomorphology

Sector 4 extends over the northernmost piedmont tract with the most subdued morphology (Figs. 3, 4A, 23A,B,C). Heights gradually descend from 450 in the south to 310 m asl at the northward intersection with the incised canyon along Coloso Fault System. Gradients vary from 32-35° proximally to ~15° at distal terminations (Fig. 5), with gently concave profiles and no slope breaks. Short steep segments upslope thus connect to an extensive, low-gradient basal ramp (Fig. 24). The colluvial mantle extends up to 130-160 m asl and covers the largest part of slope surface compared to other sectors (Figs. 23A,B,C). The talus index varies between 0.37 and 0.50. Slope tops open landwards onto a small catchment, partly delimited to the east by the bedrock ridge that connects to Cerro Coloso (Figs. 4A and B). Smooth bedrock walls are intersected by a dense network of shallow rills and incisions, and by one major gully issuing from the perched catchment upslope (Fig. 4A).

The colluvial mantle is characterized by a continuous, featureless sandy apron (Figs. 15A, 23A,B,C, 25C). It is composed of moderately to well sorted, massive to rarely plane-laminated, fine to medium sand upslope, and medium to coarse sand downslope, a few centimetres thick along the lowest slope segments (Fig. 25D), and a few decimetres thick at intermediate heights. Further upslope, the sandy apron thickens into discontinuous mounds that lap onto the base of bedrock cliffs (Figs. 25A,B). The surface is flat or gently undulated, covered by a discontinuous lag of coarse sand and granules (Fig. 25D), locally hardened by salt crusts. Trains of aeolian ripples are rare (Fig. 25C) and ephemeral. They were observed to form and disappear on a daily basis. The topography is locally modified only by rare concentrations of fine gravel with very low relief, almost completely buried in sand (Figs. 23C, 25B). Scattered rockfall gravel is far less abundant than over the adjacent sector 3.

The colluvial surface presents typical traits of a *aeolian ramp*, consisting mainly of sand banked against local relief that acted as an obstacle to wind transport (Lancaster & Tchakerian, 1996; Thomas *et al.*, 1997). Fine and medium sand bypass the intensely deflated sectors to the south and are temporarily deposited along sector 4, partially protected in the lee of Cerro Coloso. The distinctly concave slopes offer an ideal topographic trap for aeolian deposition. Aeolian sand ramps typically occupy great portions of the piedmont surface (Lancaster & Tchakerian, 1996). This explains the limited bedrock exposure in Sector 4, and the scarcity of rockfall gravel at the surface.

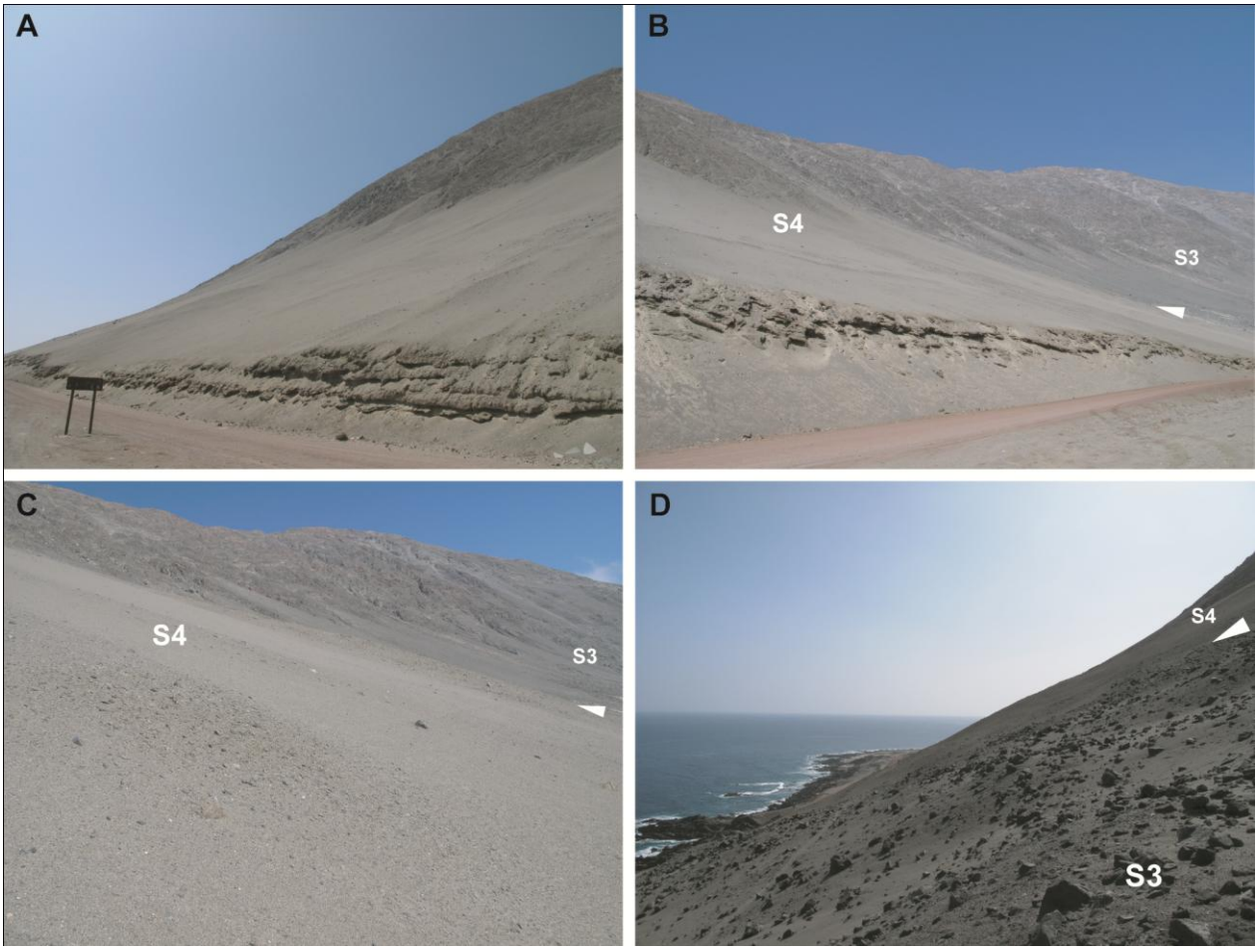

Figure 23 *- Sector 4, panoramic views of the active surface. (A) View upslope, showing relatively subdued relief with smoothly concave gradient; a featureless sandy apron climbing up to bedrock cliffs, and basal sections through sedimentary deposits. (B) and (C) Views of transitional area between slope sectors 3 (S3, right) and 4 (S4, left); note gradually decreasing relief and the sharp textural transition (white pointers) from gravelly colluvium over sector 3 to the sand-dominated apron of sector 4. In (C), note gravelly mudflow remnant almost completely buried in sand. (D) Contour-parallel, northward view of abruptly changing slope surface (white pointer) from the northern limit of sector 3 (boulder-strewn surface in foreground) to the smooth sandy surface of sector 4 (background).*

Figure 24 *- Northward view (from sector 2) of distal terminations of sectors 3 and 4 (S3 and S4); truck for scale. Note tangential downslope connection of sector 4 to sea level with no break in slope.*

4.7.2. Facies and processes

Facies A is a minor component of the stratigraphy in sector 4, and represents sparse remnants of deposits observed in shallow trenches on the present aeolian surface (Fig. 25D). It consists of massive to crudely plane-laminated, moderately to well-sorted, medium to rarely coarse sand with scattered pebbles. Granule-rich interlayers indicate thin deflation lags formed at times of reduced sand supply. This facies occurs in centimetric beds or lenses commonly overlain by facies Df (Fig. 26A), but is continuous along the top of the outcrop, where it offers a vertical section through the thin aeolian ramp.

Debrisflow deposits of facies Df comprise approximately 60% of sector 4 outcrops, where they consist of very poorly sorted, matrix-supported lenses of massive, sandy pebble to cobble gravel, normally a few decimetres thick. Lenses extend laterally up to 2-3 m (Figs. 26A,B) with a planar architecture that conforms to the underlying flat surface and with frequent vertical and lateral amalgamation (Figs. 23A,B). Basal surfaces are mostly non-erosive. Compared with Df deposits of adjacent sector 3, the gravel fraction is less abundant and does not exceed fine cobbles; matrix is represented by a moderately to well sorted, silty, granule-bearing, medium to fine sand, texturally similar to local facies A (see Fig. 27). Contrary to distal mounds in sector 3, interference and topographic compensation between individual debrisflow units has been limited to lateral amalgamation. Such features point to an origin from dense flows issued by the catchment upslope, followed by bulking and transformation into debrisflows during runout over the aeolian ramp. Reduced gravel content relates to relatively high volumes of entrained aeolian fines. Low aspect ratios and planar geometry of debrisflows imply lateral expansion over the surface, since the small volume of gravel probably prevented formation of coarse levees (Blair & McPherson, 1998).

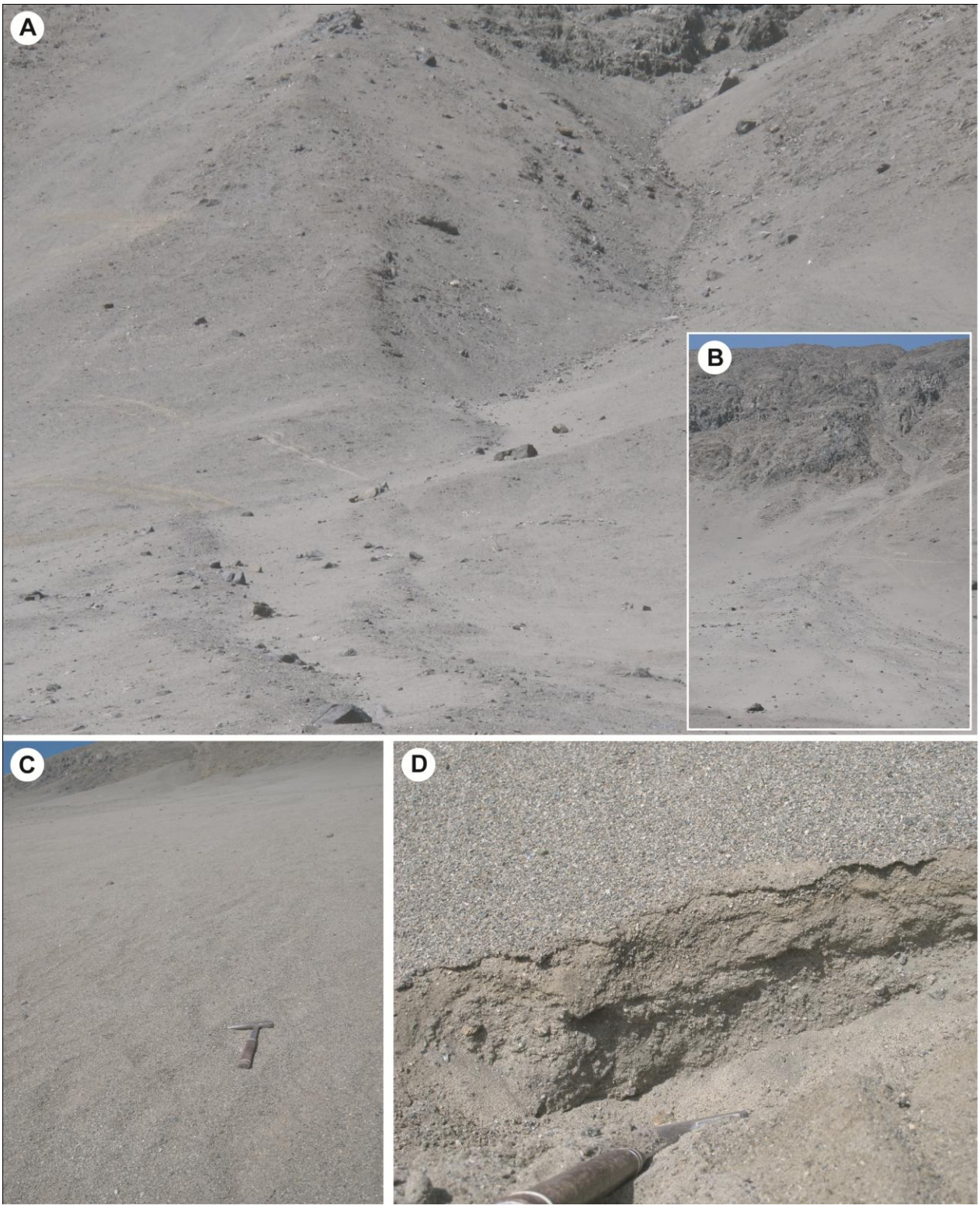

Figure 25 *- Sector 4, active surface; hammer is 32 cm long. (A) and (B) Upslope limit of aeolian ramp; sand mounds rising against bedrock cliffs, interrupted by bedrock gullies issuing occasional debrisflows. Note paired gravel levees with distinctly smaller grain-size and volume than those in Fig. 17A (sector 3). (C) Flat, featureless sandy surface with faint trains of aeolian ripples and almost complete absence of rockfall gravel. (D) Lower aeolian ramp, ~ 50 m asl; centimetric layer of massive, medium to coarse sand, overlain by a lag of very coarse sand and granules; below, granule-rich to pebbly coarse sands of sheetflood origin.*

Facies Hf

Description. This facies is ubiquitous along sector 4 outcrops, though subordinate in volume to Df. It is represented by moderately sorted, granule-rich, fine to very coarse sand (see Fig. 27C) in laterally continuous decimetric beds and lenses delimited by debrisflow lobes. Structure varies from crudely massive (Figs. 26B and D) to distinct plane-laminated at mm- to cm-scale (Fig. 26C), with alternations of granule to coarse-sandy layers and fine to medium sand layers (Fig 27C, samples 4.24 and 4.17). Some units appear massive, but an original lamination is recognizable from planar alignments of granules. Lensoidal, cm- to dm-wide scour fills are highlighted by textural variations. Bedform and sedimentary structures are absent. Thicker, massive units comprise scattered pebbles and fine cobbles with random fabrics; a(t) fabrics are usually associated with coarser laminae in more structured deposits.

Interpretation. Relatively good sorting, laterally extensive lamination, planar geometries with localized scour fills relate this facies to sheetfloods. Absence of tractive structures and poor textural segregation suggest rapid deposition from ephemeral hyperconcentrated flows (Nemec & Muszynski, 1982; Maizels, 1993; Kim *et al.*, 1997). Rapid loss of capacity was due to flow expansion and shallowing, probably accompanied by partial inflitration into the sandy substrate. Turbulence in thin runoff sheets would have been partly suppressed by high sediment concentration, and massive units probably indicate flow regime transitional to laminar. Sediment was rapidly dumped through a phase of concentrated dispersion above the substrate, preventing traction of single particles (Arnott & Hand, 1989; Smith & Lowe, 1991). Sand-granule couplets indicate fluctuations in flow stability and velocity. Discontinuous lenses and scour fills are due to recessional flood stages, as runoff separated into distinct paths over the irregular microtopography. Flat bedding and lamination might be upper-stage plane beds, but the relatively high gradient (10-15°) would have favoured erosion or bypass rather than deposition from a supercritical flow. Associated fine gravel commonly does not present tractive fabrics, which confirms transport within sediment-water mixtures occasionally dense enough to carry fine pebbles by buoyancy and inertial effects, rather than traction. The ubiquitous presence of this facies along the whole outcrop belt, coupled with the virtual absence of aeolian facies in stratigraphy, suggest periodic stripping of the sand ramp by flash floods issued from the catchment above.

4.8. ALLUVIAL FAN

4.8.1. Morphology

A small alluvial fan occupies the northernmost piedmont sector, where the Coloso Fault System intersects the coast (Figs. 4A, 28A) forming a deeply incised catchment along a sharp transition from granulites to amphibolites in the metamorphic basement. The fan has been almost completely excavated for aggregate extraction (Fig. 28B); only the proximal and medial portions are exposed in broad outcrops. The apex (23°46,54' S - 70°28,41' W) corresponds to the convergence of two catchment canyons (Figs. 4A, 28A). The radius is estimated around 700 m, with the present-day shoreline as distal limit.

Fan outcrops show a distinct bipartite architecture. A seaward-dipping prism of crudely tabular units represents the main fan body, aggrading without internal discontinuities to a thickness of ~15 m at the highest available exposure (Figs. 28B, 29). Depositional dip ranges from 5° to 8° seaward. More proximally

and at outcrop tops, a distinct facies assemblage is separated from the main fan body by a marked erosional surface dipping seaward and extending over ~20 m across fan, probably representing an incised fan channel. The system architecture suggests a protracted phase of fan aggradation, followed by incision. This might have been related to local base-level fall along the uplifting coast, or to progressive catchment expansion and integration, with consequent increased water discharges in relation to sediment loads.

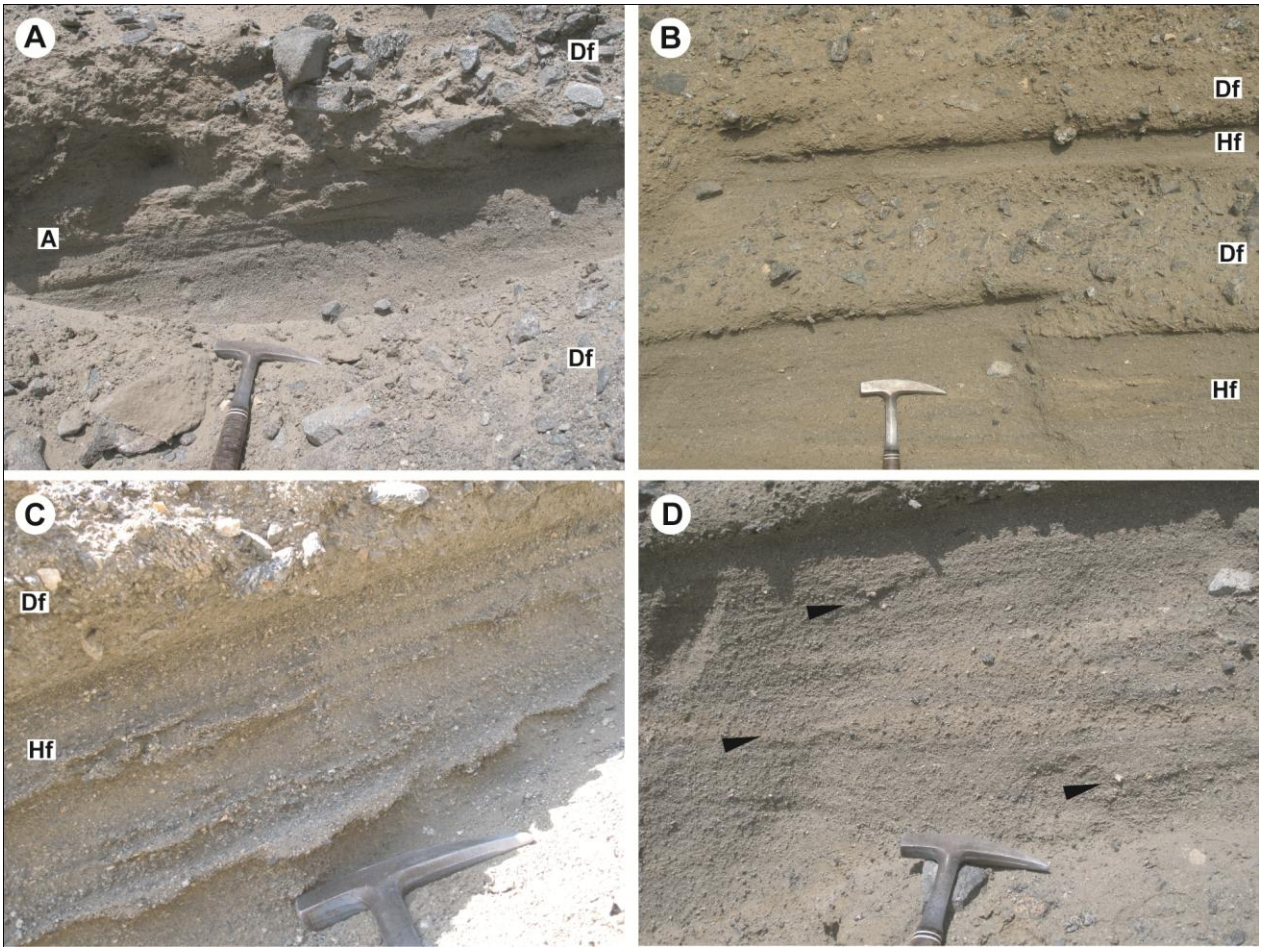

Figure 26 *- Sector 4, roadcut outcrops; hammer is 32 cm long. (A) Debrisflow deposits (facies Df) with underlying well-sorted, massive to crudely bedded sands of probable aeolian origin (facies A). (B) Intercalation of essentially flat-based mudflow lobes (Df) and sheetflood alluvium (Hf). (C) Laterally continuous to discontinuous planar lamination in facies Hf. (D) Hyperconcentrated flow deposits comprised between two mudflow lobes; note lenticular alternation of finer, poorly sorted silty sands and coarser, moderately sorted, granule-bearing to pebbly sands; note also cm-scale scours (black pointers) and lags along facies partings.*

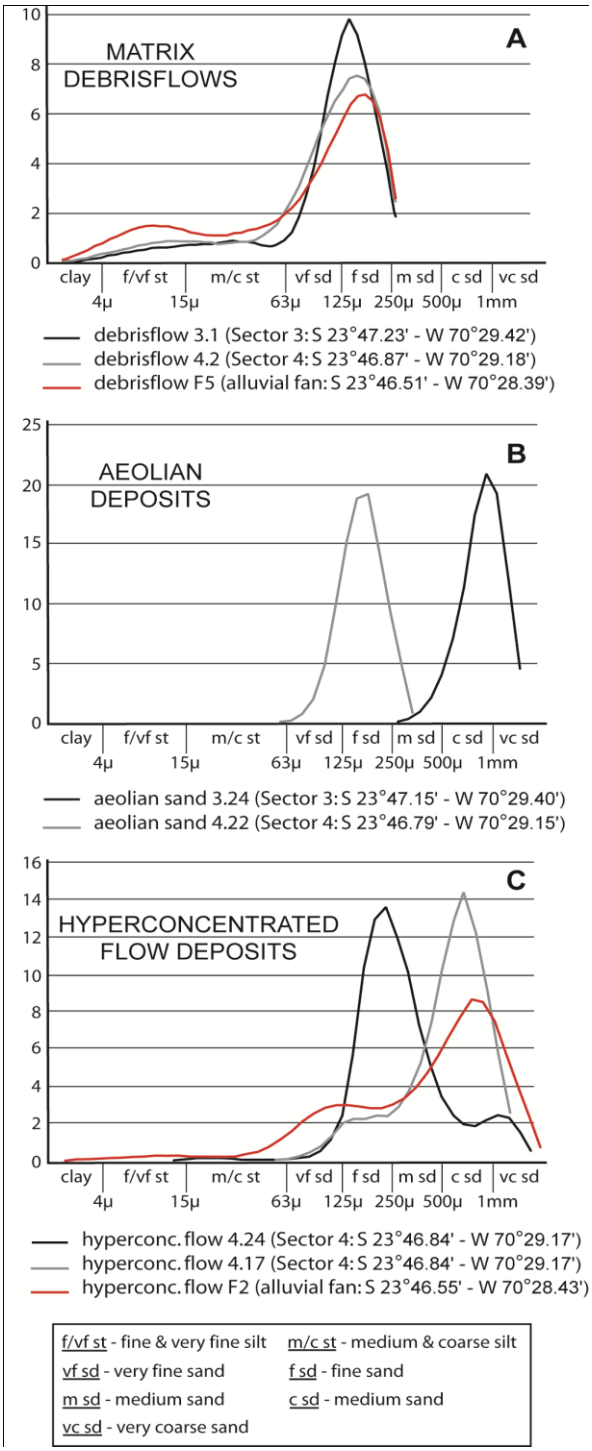

Figure 27 *- Grain-size distributions for representative samples of fine-grained deposits. On the horizontal axis, granulometry; on the vertical axis, individual weight % for each size class. (A) Silty, sandy matrix of debrisflows; note good sorting of matrix sands in sectors 3 and 4, due to bulking of well-sorted, fine aeolian sands at slope tops (compare identical modes for samples 4.2 in A, and 4.22 in B). Note also greater skewness toward finer components in alluvial-fan debrisflow (red), due probably to longer regolith maturation, absent deflation and pervasively sheared bedrock in the large catchment of tectonic origin. (B) Aeolian sands from footslopes of sectors 3 and 4; note net decrease in modal grain size from sector 3, upwind, to 4, downwind. (C) Granulometric curves for coarse (grey) and fine (black) laminae in crudely bedded hyperconcentrated flows of facies Hf in Sector 4; compare good overall sorting, by entrainment of aeolian sands, to the poor sorting of hyperconcentrated-flow facies in the alluvial fan (red).*

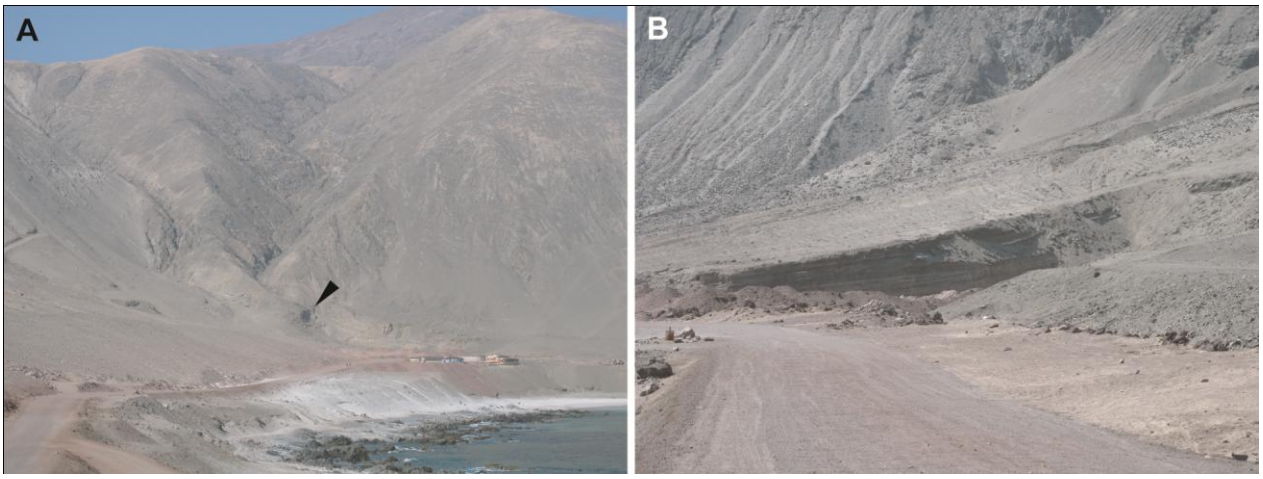

Figure 28 *- Alluvial fan. (A) Panoramic view of the northern slopes of Cerro Coloso (highest massif in background), with two descending catchment canyons feeding the fan (black pointer indicates northern outcrop shown in panel B). (B) Wedge-shaped, downdip section of the alluvial fan, northern outcrop; note relatively low-gradient profile sloping seawards; most proximal outcrop face is ~15 m high.*

4.8.2. Facies and processes

Two main facies associations are distinguished. One constitutes the main fan body and comprises facies Df, Dfr and Hf (Figs. 29, 30); the other, limited to the incised channel, includes facies Hf, E, Wp, Wc and Wb (Fig. 31).

Debrisflow deposits (facies Df) dominate the main fan body, and particularly the lower two thirds of the stratigraphy (Figs. 29, 30A,B,C). Facies Hf is volumetrically dominant at the top of the main fan body (Fig. 29) and in incised-channel deposits (Fig. 31A). Distinctly coarser-grained and less sorted than its equivalent in sector 4, it ranges from pebbly, granule-bearing coarse sands to silty, pebbly, sandy granules (Fig. 27C). Beds are occasionally massive, but more commonly a crude layering (Figs. 30C,D, 31A) is defined by alternating, normally graded, coarse-fine planar laminae, and by discontinuous trains of granules and fine pebbles (Figs. 30C,D) with weak *a(t)* and *a(t)a(i)* fabrics. Gravel assumes prevalent *a(p)* or *a(p)a(i)* orientations in massive beds. Basal contacts are gently erosive, and tractive structures are absent. Centimetric scour fills are locally evidenced by the curved geometry of coarse-grained laminae or the dip of gravel clusters. By analogy with sector 4, this facies is interpreted as deposits of ephemeral hyperconcentrated flows. Forced clast interactions in a concentrated dispersion and rapid deposition prevented bedform development and sorting at final flow stages (Smith & Lowe, 1991; Maizels, 1993). Plane-laminated units with crude normal grading usually present coarse-fine couplets with tractive *a(t)* gravel fabrics, showing a degree of flow organization and sediment segregation in waning flows. Massive, poorly sorted units with *a(p)* fabrics indicate poor interparticle mobility and strong interactions in highly concentrated dispersions (Rees, 1968). Fine gravel trains indicate transient instability in flow structure and competence (Kim *et al.*, 1997).

Aeolian facies A is limited to a 2.8 m-thick sandbody in the incised channel sequence (Fig. 31D), wedging out distally beneath an erosive surface. It consists of millimetric laminae of very well-sorted, medium-coarse sanD which form cross-cutting sets with a dominant N-NE dip. The position in the proximal channel-fill and

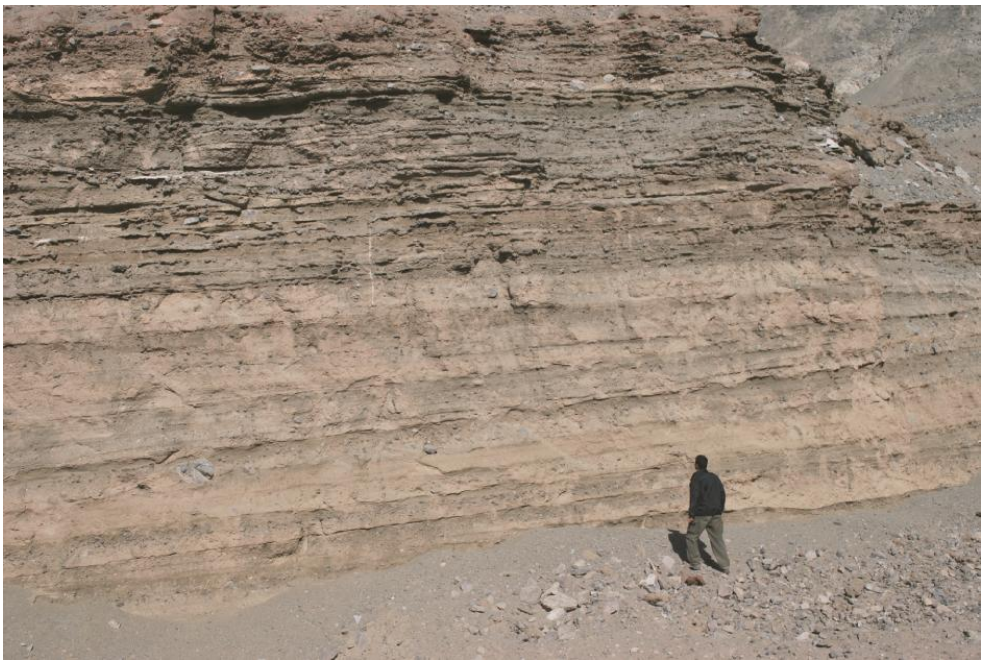

Figure 29 *- Strike-oriented, distal end of northern fan outcrop in Fig. 30B; geologist is 1.85 m tall; note conformable aggradation and transition from dominant debrisflow-dominated deposits at the base, to hyperconcentrated-flow-dominated deposits to the top.*

orientation of laminasets suggest a phase of aeolian deposition by prevalent longshore winds to NNE in the lee of the channel margin, during prolonged fan inactivity.

Facies Dfr

Description. This facies is exclusively present as discontinuous layers on top of Df deposits (Fig. 30B). It consists of moderately sorted granule to medium cobble gravel, massive to crudely laminated, with moderate *a(t)* or *a(t)b(i)* fabrics; coarser clasts show *a(p)* fabrics. Thickness varies from a few clasts to 10-15 cm, and bases are weakly erosive into underlying debrisflow beds. Sorting and fabric are relatively better developed where the facies occurs as lenses rather than in extensive layers.

Interpretation. The superposed position to debrisflow beds, weakly erosive bases and gravel fractions texturally equivalent to underlying beds suggest post-depositional winnowing and scouring of debrisflows by recessional runoff, or by successive precipitation (Blair & McPherson, 1994, 1998). Selective transport of the fine-grained components left a moderately sorted gravel lag with local tractive fabrics. Cobbles and boulders with *a(p)* or random orientations were probably exposed by progressive erosion of the debrisflow body, but too massive to be reoriented. Variable sorting and fabrics probably relate to runoff intensity and duration, or to the number of reworking events, depending on the duration of debrisflow exposure at the fan surface.

Facies Wp

Description. This facies occurs within incised channel deposits. It consists of normally graded gravel couplets with planar to gently concave-up geometry (Figs. 33B,C). The lower, centimetric divisions are clast-supported, fine pebble to fine cobble gravel, openwork to matrix-rich, moderately to well sorted, with

a(t)a(i) fabric; the matrix consists of sand and granules. Upper divisions, 2-5 cm thick, consist of moderately sorted, sandy, fine pebble to granule gravel, massive to normally graded, with *a(t)* or *a(t)a(i)* fabrics. Couplets extend downdip over several metres and are stacked with a comformable geometry.

Interpretation. Good sorting, open frameworks, tractive fabrics and normal grading point to deposition from bedload sheets (Bristow *et al.*, 1999; Kim *et al.*, 2009) or low-amplitude gravel bedforms (Lunt & Bridge, 2007) in ephemeral floods. Rapid aggradation prevented full bedform development, but sufficient clast dispersion allowed hydraulic sorting. The coarse matrix infiltrated into lower divisions during deposition of upper divisions, but its general scarcity indicates a protracted phase of flow recession.

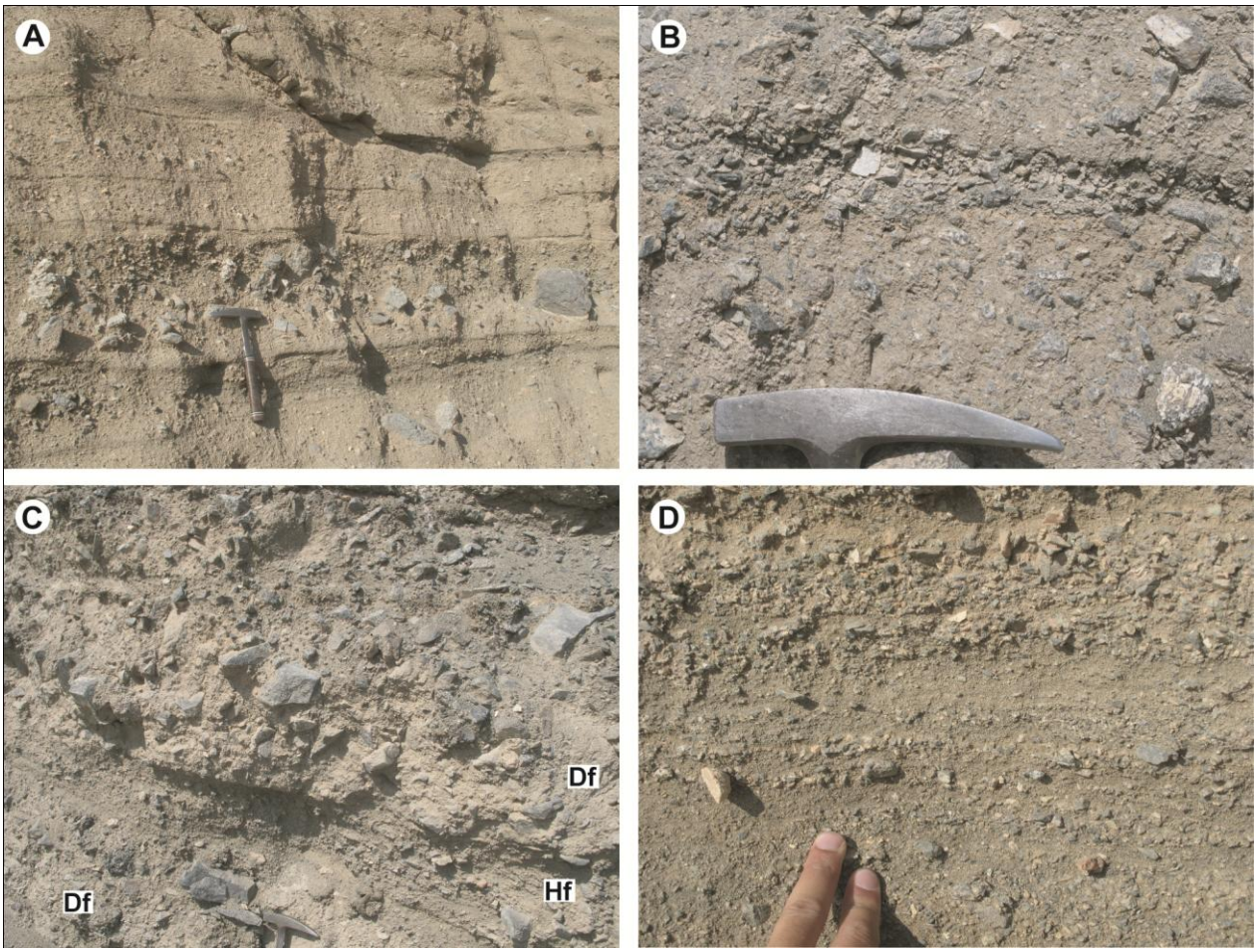

Figure 30 *- Fan outcrops, dominant facies; hammer is 32 cm long and points downcurrent. (A) Vertically stacked, partly amalgamated debrisflows. (B) Thin, openwork parting of reworked gravel between debrisflow beds (facies Dr). (C) Crudely laminated, poorly sorted, gravelly sands between debrisflow lobes (facies Hf). (D) Detail of facies Hf; paleoflow to the left.*

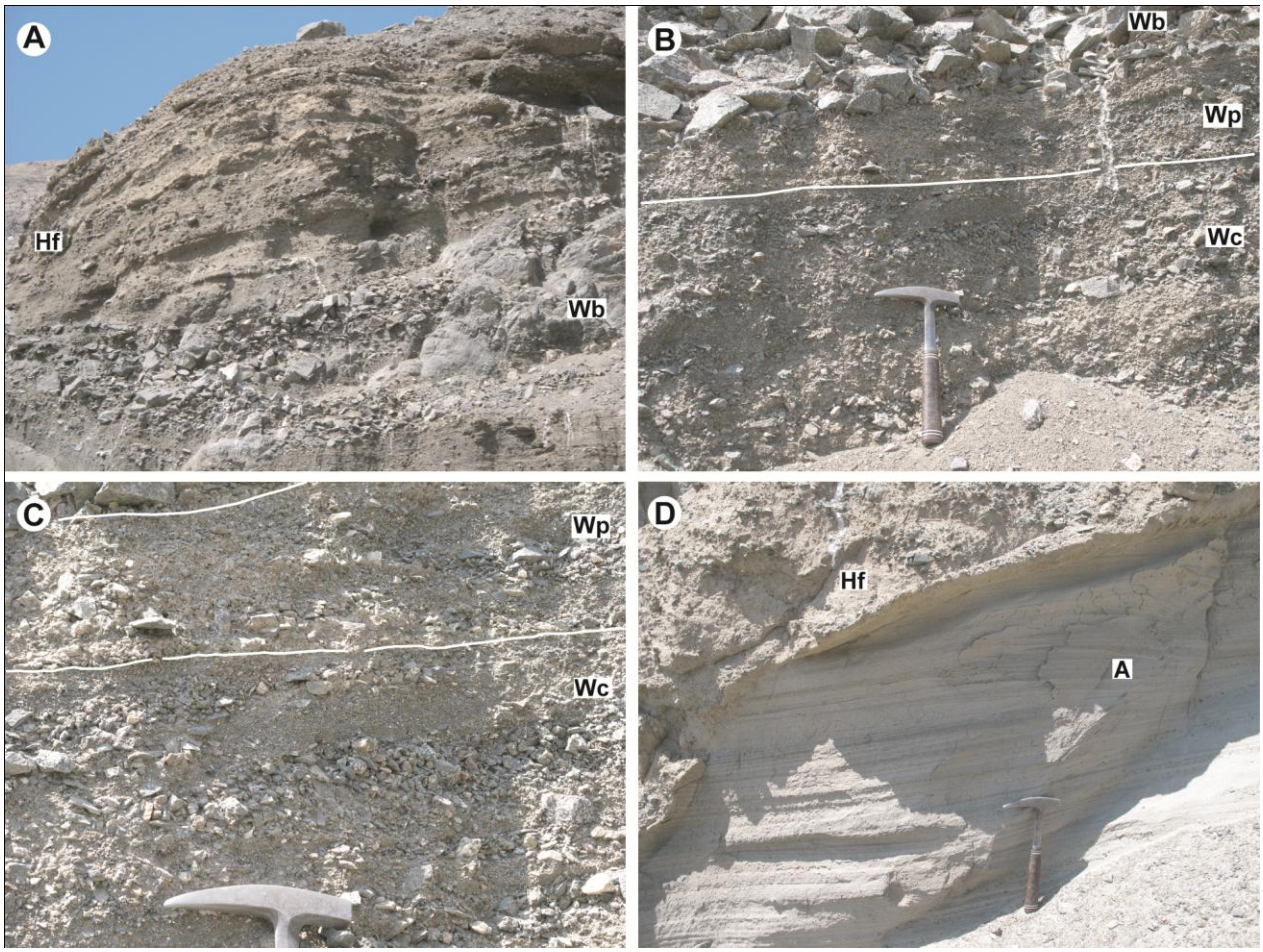

Figure 31 *- Incised-channel facies, top fan outcrops; hammer is 32 cm long and paleoflow to the left. (A) Boulder beds of facies Wb overlain by a thick package of confined hyperconcentrated-flow gravelly sands (Hf). (B) and (C) Views of incised-channel facies sequences from planar, inclined, coarse and fine gravel couplets of facies Wc, to planar, subhorizontal gravel couplets of facies Wp, up to coarse gravelly Wb deposits. (D) Well-stratified aeolian deposits (facies A) eroded and overlain by hyperconcentrated-flow deposits.*

Facies Wc

Description. This facies is present in the channel fill as a single, tabular, cross-stratified basal unit with bipartite plane laminae (Figs. 31B,C). Basal divisions are well-sorted, openwork pebbles to fine cobbles, 2-6 cm thick, with normally graded tops and *a(t) or a(t)a(i)* fabrics. Upper, fine divisions are massive, ungraded to normally graded, moderately sorted pebbly, sandy granule gravel. Sets dip at 8-12° with an angular contact to the channel base.

Interpretation. Sets of bipartite, inclined laminae point to traction and progressive accretion of low-relief bars or bedforms by frontal avalanching of coarse gravel and fine sediment overpassing during high flow stage, followed by fine gravel deposition at waning flow (Todd, 1996). Distinct cross-stratification implies deeper flows than for plane-stratified Wp deposits.

Facies Wb

Description. This facies is limited to the top portion of the channel fill, where it forms a lens-shaped, erosively based unit (Fig. 31A). It consists of three amalgamated beds, each 80-120 cm thick, of poorly sorted,

matrix- to clast-supported cobbles to fine boulders. The matrix is a poorly sorted sandy, pebbly granule gravel. Beds are normally graded, with a lower clast-supported, cobbly to bouldery division, passing upward into finer gravel. Fabrics are very poorly developed.

Interpretation. Pronounced basal erosion, normal grading, very coarse gravel and poor sorting and fabrics indicate powerful flash floods (Blair, 1987, 2002; Gutiérrez *et al.*, 1998; Moscariello *et al.*, 2002). Sediment was supported by high turbulence and clast interactions. The coarsest load was abruptly deposited during flow expansion or at a gradient transition, probably favoured by channel irregularities and bed roughness. Finer gravel was dumped during rapid flow recession, when the dispersion was still concentrated enough to prevent bedform development and clast segregation. The amalgamation of three similar depositional units suggests complex flood dynamics related to catchment hydraulic thresholds (Gutiérrez *et al.*, 1998; Blair, 2002), rather than repetition of identical events.

4.9. SLOPE SECTORS: DISCUSSION AND COMPARISON

The previous sections demonstrate the geomorphic and sedimentological variability of the studied piedmont. Five sectors are distinguished by sharp transitions in slope morphology, surface processes, and facies associations and architectures in stratigraphy. Tables 1 and 2 provide summaries of general morphology and facies distribution; most important factors and process interactions are systematically compared below. The alluvial fan is discussed as a depositional end-member of piedmont morphodynamics; its spatial continuity within the colluvial system allows a useful comparison of processes and causal relations.

	SLOPE SECTOR 1	SLOPE SECTOR 2	SLOPE SECTOR 3	SLOPE SECTOR 4	ALLUVIAL FAN
AEOLIAN FACIES	**At** perched windblown coarse sand & granules (mixed with rock- & debrisfall sediments)	**At** perched rock- & debrisfall gravel with minor aeolian admixtures	**A** laminated sand in lenses & wedges (with associated subfacies **Ad**, **Am**, **Ac**)	**A** massive to locally laminated, medium to coarse sand	**A** cross-bedded sand (local, within incised-channel deposits)
NON-COHESIVE MASS-FLOW FACIES	**Rf** rock- & debrisfall gravel in steep cones **Gf** grainflow gravel lenses & lobes	**Rf** rock- & debrisfall gravel in steep cones **Gf** grainflow gravel lenses & lobes	**Rf** & **Gf** rockfall & grainflow gravel as proximal talus cones and scattered clasts over distal apron		
COHESIVE MASS-FLOW FACIES	**Dc** matrix-supported gravel lobes from intermittent debris creep or incipient debrisflows		**Df** matrix-supported, debrisflow gravels in ridges & lobes	**Df** matrix-supported debrisflow lobes	**Df** clast-poor debrisflow lobes
HYPERCONC-FLOW FACIES				**Hf** mod. to poorly sorted, crudely bedded pebbly to granule-rich sands	**Hf** mod. to poorly sorted, crudely bedded pebbly to granule-rich sands
WATERFLOW FACIES					**Wc**, **Wp**, **Wb** poorly to well sorted, plane- to cross-bedded gravel **Dfr** thin gravel lags from reworked debrisflow lobes

Table 2 *- Stratigraphic facies distribution over different piedmont sectors in the study area.*

4.9.1. Sectors 1 and 2

Sectors 1 and 2 in the south present the most rugged relief and steepest gradients for both bedrock and talus slopes (Fig. 5). Very low values of the talus maturity index (0.14 to 0.24) indicate immature development of colluvial cover and low slope stability (Statham, 1976; Hinchcliffe *et al.*, 1998; Curry & Morris, 2004); in other words, scarce potential to preserve sediment of local provenance, in spite of abundant bedrock sources. Two factors contribute to minor talus development: the very high gradient of slopes over their whole vertical extent, down to sea level; and maximum exposure to winds due to a position on a coastal headland. High-energy processes along the steep, rocky shoreline prevent the formation of basal sediment ramps upon which further colluvium could be stabilized. Steep subaqueous slopes provide an accommodation excess, and a depositional 'graded profile' is therefore difficult to attain on lower slope segments. As a consequence, the higher slopes are also maintained as steep transport pathways, rather than depositional loci.

Interactions between structure and processes therefore stabilize a high-gradient relief and force sediment transport and reworking by frequent rockfalls and debrisfalls, and subordinately by grainflows and talus creep. Steep talus cones are relatively stable only in correspondence of structurally controlled bedrock and shoreline embayments, where partial protection from waves prevents basal erosion. Even so, as observed during surveys, deposits are very unstable and only temporary in what is essentially a clastic bypass system. The dynamics of cohesionless grainflows and debrisfalls determine which process will dominate on a local scale, depending on slope profile, gradient and lateral confinement. In this respect, differences in bedrock lithology and fracturing between sectors 1 and 2 are probably the main control on facies abundance.

Sporadic runoff probably plays a very minor role in both sectors due to the convex profiles of high mountain slopes. Convex surfaces imply runoff dispersion and consequent minor effects from potential floods. On the other hand, exposure to very strong winds is a fundamental factor. Fine sand and minor silt fractions are produced by bedrock weathering all along the studied piedmont (Fig. 7C), but their preservation over the surface is extremely limited, due to continuous deflation and to infiltration into openwork gravel. The coarse matrix abundant at depth in gravelly deposits is mainly derived from *in situ* weathering rather than from aeolian transport. The scarcity of fine matrix in surface deposits promotes the occurrence of rockfalls and grainflows over debrisflows (Statham & Francis, 1986; Iverson, 1997), favoured also by high gradients, which impose elevated shear rates on resedimented granular masses.

4.9.2. Sector 3

Central Sector 3 (Fig. 4A) presents notably reduced gradients and elevations compared to the southern sectors, as relief decreases northward of Cerro Coloso. It comprises an extensive colluvial apron of high complexity, although the talus index (0.35 to 0.47) still points to relative slope immaturity (Hinchcliffe *et al.*, 1998; Curry & Morris, 2004). Bedrock is more extensive than sedimentary surfaces. However, contrary to sectors 1 and 2, lower-slope gradients (15-20°; Fig. 5) and morphologies are largely unrelated to bedrock control, and regulated instead by the colluvial apron.

Aeolian deposition plays a significant role, since this area lies in the immediate lee of Cerro Coloso, partially protected from southerly winds. Favoured by reduced slope gradients, abundant coarse-grained aeolian

sediments contribute to the aggradation and stabilization of the colluvial mantle. The presence of a bedrock ridge along the top of sector 3 allows only very limited runoff downslope, mostly along the largest bedrock gullies, and thus enhances preservation of the distal colluvial apron.

The most elevated portion of the sedimentary apron consist of high scree cones abutting against rockwalls. Their lateral extent is limited by basal destabilization in correspondence of major gullies, where occasional runoff is focused and debrisflows are generated. The bases of talus cones are presently prograding over the lower colluvial apron, which consists of intercalated mass-flow and aeolian deposits. Bedrock gullies act as temporary reservoirs for local regolith and minor aeolian drift, occasionally mobilised by flash floods. Widespread debrisflow deposits however are probably related more to the role of the aeolian mantle in sediment bulking and flow transformation of flash floods. Upslope fining of the aeolian cover is a contributing factor, since fine sediments are more effective in promoting initial cohesion and buoyancy in waterflows, and help to maintaining excess pore pressures in the granular dispersion (Iverson, 1997; Major & Iverson, 1999). The plastic rheology and laminar regime of resulting debrisflows, in turn, reduce their erosive potential and contribute to the stability of the colluvial surface.

Debrisflows derive from mixtures characterized by yield strength, and thus by the tendency to build positive depositional morphologies. Debrisflow ridges and mounds significantly contribute to the surface roughness of the lower colluvial ramp, which is further enhanced by their preferential deposition downslope from main bedrock gullies. Large, composite mounds aggrade by superposition and sidestepping of debrisflow lobes that accumulate over restricted distal sectors (Figs. 17A,B). The rugged depositional morphology is crucial in promoting aeolian sedimentation. As observed both over the active surface and in stratigraphy, the greatest volumes of aeolian deposits consist of sand wedges that accumulate in protected depressions in the lee of debrisflow lobes. A complex alternation of debrisflow lobes and aeolian lenses is therefore both the proximate control, and the sedimentary result, of this feedback chain.

4.9.3. Sector 4

Sector 4 (Fig. 4A) presents the most subdued morphology, being the most distal along the descending northern flank of Cerro Coloso. As in Sector 3, the colluvial apron is uninterrupted over lower slope segments, and high bedrock cliffs comprise a much reduced extension as compared to other sectors. This is due to both the lower relief, and to the altitude reached by the colluvial cover. The talus maturity index is the highest in the study area (0.37 to 0.50), but only marginally higher than in sector 3: although the local colluvial apron occupies a relative majority of the piedmont surface, it extends to much lower altitude, maintaining the sediment/bedrock ratio essentially unchanged.

In analogy with sector 3, local surface processes are regulated by interactions of aeolian activity with rare runoff issued from a confined top catchment. Low gradients and arched piedmont configuration induce local entrapment of most aeolian drift as a thin, continuous mantle of medium-fine sand. Supply is continuous enough to feed the extensive sand ramp, but in the long term aeolian transport probably bypasses sector 4 and more permanent deposition occurs along NW-trending, wind-transverse cliffs to the north of the study area. The low volume of scattered rockfall and debrisfall gravel over the surface,

compared with sector 3, is due to the reduced exposure of bedrock cliffs. The great textural contrast between the two colluvial systems is evident from panoramic views (Figs. 4, 15A,D, 23), in which sector 3 appears dark and rugged due to abundant scattered debris, and the smooth, sandy surface of sector 4 has a lighter tone (Figs. 23, 25).

An aeolian ramp is the dominant depositional feature in sector 4, but there is practically no evidence for it in the corresponding stratigraphic exposures. Basal outcrops consist almost exclusively of laterally extensive debrisflow lenses and hyperconcentrated-flow facies. The former presence of aeolian deposits might be inferred by the unusual good sorting of sand fractions in the matrix of debrisflows. This morphostratigraphic gap in facies architecture is related to the bedrock catchment on top of sector 4, which can occasionally concentrate and redistribute sufficient runoff to entirely rework the aeolian apron. Deposits of facies Hf confirm the local importance of surface hydrology. Along sector 3, most rockwalls are incised by distinct, relatively deep gullies (Fig. 15) that concentrate runoff only over specific areas. To the contrary, sector 4 headwalls present a continuous series of closely spaced, shallow rills and gullies which can distribute runoff more extensively downslope. Thus not only discharge is potentially higher than in sector 3, due to a local catchment, but its effects are better distributed over the colluvial apron. The absence of soil and vegetation in the catchment contributes to the rapid concentration and transfer of runoff.

An additional positive feedback to this morphogenetic trend is given by interactions between aeolian deposits and debrisflow processes. As in sector 3, surface availability of aeolian fines is probably the key in triggering debrisflows. The different characteristics of runout surfaces, on the other hand, induce different flow geometry and spatial organization. At early flow stages, well-distributed source pathways over bedrock walls imply an even distribution also for debrisflow events over sector 4 colluvial slopes. The flat, featureless aeolian ramp downslope allows an unobstructed descent and lateral spreading of debrisflows. The volumetric dominance of aeolian fines in debrisflow mixtures further inhibits the development of levees and flow confinement. The architecture of debrisflow lobes in sector 4 in fact consists of wide lenses with low aspect ratios, conformable to the underlying topography. Debrisflows with low aspect ratios and even distribution contribute to the flat surface morphology, which in turn favours the areally widespread distribution of shallow runoff during effective precipitation.

The outcome of this feedback chain is a stratigraphic record represented mainly by sheetfloods and mass flows in sector 4, which do not reflect the dominant aeolian processes over the active surface. In the context of the whole study area, however, the importance of aeolian processes in piedmont aggradation is evident when comparing the talus maturity indexes for sectors 3 and 4. With combined values between 0.35 and 0.50 (Table 1), talus indexes for both domains indicate a relatively limited expansion of the colluvial cover over bedrock relief, far from full aggradation potential. In slope geomorphology (e.g. Hinchcliffe *et al.*, 1998; Bertran & Texier, 1999; Curry & Morris, 2004), a value of 0.57 is considered representative only of incipient colluvial development. Yet, considering the absolute extension of colluvial mantles over the entire study area, by far the largest one is in sector 3, rising up to 260-270 m asl. In fact, sector 3 is the only one in which aeolian deposition truly contributes to aggradation, as confirmed by the abundance of aeolian facies in

stratigraphic sections. Sector 4, on the other hand, has a distinctly lower volume and extension of colluvial cover, and is the only one subject to the erosional effects of significant runoff.

4.9.4. Alluvial fan

The northern piedmont sector is occupied by an alluvial fan, rather than by a colluvial system. Blikra & Nemec (1998) and Blair & McPherson (2009) recently highlighted the geomorphic and sedimentological distinctions between talus cones, colluvial fans and alluvial fans. The alluvial fan markedly differs from the various kinds of colluvial depositional systems in the area because of: 1) its lower gradient; 2) its sediment distribution, radiating from a point source; 3) its catchment being a wide, incised canyon with maximum efficiency in conveying waterflows (Fig. 28A), rather than a network of shallow, poorly integrated mountain ravines; and 4) its facies association, characterized by water- and debrisflow processes, and absence of primary rockfall and grainflow deposits.

The fan catchment is developed at the intersection of the Coastal Scarp with the Coloso Fault System, where bedrock erodibility is structurally enhanced. An additional factor is probably the adjacent lithological boundary between granulites and amphibolites, where the basement is weakened by differential weathering effects. In the context of the study area, relief in correspondence of the alluvial fan has the least potential energy and the highest surface stability. The fan is an end-member in a continuum of piedmont sedimentary systems. As catchments progressively expand and integrate, and relief is reduced, this continuum is expressed from south to north by a gradual transition from gravity-dominated to runoff-dominated domains (Blair & McPherson, 1994). The various depositional systems and landforms along this gradation may not always be formally defined as different (Brazier *et al.*, 1988; Selby, 1993), but the end-members possess clearly distinctive traits (Blikra & Nemec, 1998, Blair & McPherson, 2009). From a stratigraphic viewpoint, the alluvial fan represents the most stable kind of system, with the highest potential to be preserved in the rock record (Figs. 28B, 29).

4.10. IMPLICATIONS FOR COLLUVIAL STRATIGRAPHY

The studied piedmont illustrates the high complexity and spatial variability of colluvial depositional systems. The investigation of active surfaces and of the very recent sediments exposed along basal outcrops does not extend the analysis into a time perspective. The exact chronological evolution of the system remains hard to ascertain without more complete downdip exposures or extensive GPR surveying (e.g. Sanders, 2010; Sass & Krautblatter, 2007).

Evidence from all slope sectors reveals a common trend in spatial relationships of landforms and facies. Coarser, poorly organized rockfall deposits, and associated debris- and grainfall deposits, are emplaced proximally as steep, isolated or coalesced talus cones. Transport and deposition farther from headwalls reflect more complex flow processes, with sediment issued from catchments upslope, reworked from higher slope segments and supplied by the wind. Such processes build finer-grained colluvial aprons of lower gradient and wider extent more distally, which represent an intermediate step in the continuum from talus cones to alluvial fans. This trend is best exemplified in sector 3, and confirms a genetic-stratigraphic model

of large-scale colluvial architecture recently inferred from studies in alpine and post-glacial settings (Sanders *et al.*, 2009; Hinchcliffe & Ballantyne, 2009; Sanders, 2010). Proximal sedimentation adjacent to bedrock cliffs produces steep talus cones, which are gradually followed and 'onlapped' at their base by a lower-gradient, generally finer-grained distal colluvial apron. In turn, this distal apron provides a relatively stable surface upon which proximal talus units can accrete and 'downlap'. Morphological evidence of this evolution lies in the bipartite slope gradients of sector 3 (Figs. 5, 15C, 16A), where the distal toes of talus cones 'onlap' the most elevated segments of the lower colluvial apron producing a distinct topographic knickpoint (Fig. 16A). The topographic inflection thus marks the transition between two distinct sedimentary domains: rockfall- and grainflow-dominated above, and aeolian- to gravity-flow-dominated below. It appears therefore that also colluvial systems in a hyperarid setting can present a differentially graded topography, according to the locally dominant depositional processes. Blikra & Nemec (1998) observed that coeval colluvial fans dominated by different processes are characterized by distinctly different surface gradients, and segmentation of talus slopes has been noted so far especially in alpine and periglacial settings (Francou & Manté, 1990; Jomelli & Francou, 2000; Sanders *et al.*, 2009). A main difference in sediment redistribution to distal slopes between these climate settings is given by the predominance of aeolian activity in arid environments, and of snow avalanches in alpine and periglacial environments (Blikra & Nemec, 1998; Jomelli & Francou, 2000).

A general trend to morphological and sedimentary 'maturity' is evident from south to north in the study area, with gradually more subdued relief and increasing extent and complexity of the colluvial cover. Stratigraphic exposures extend only a few metres below the surface, implying a limited timespan and most likely a coeval history, well within the 'steady state equilibrium' time range (Schumm & Lichty, 1965; Ritter *et al.*, 1995). Interpretation of the stratigraphic record in terms of ancient landscapes and geomorphic causality commonly suffers from uncertainty in distinguishing the effects of long-term allogenic controls from local process variability (Hilton Johnson, 1982). In this study, the problem is overcome by the contemporaneity of observed surfaces and deposits, and by the direct correlation of active surface processes and features with the relative stratigraphic signatures. Notably, lateral transitions between different stratigraphic domains along the piedmont are abrupt, and exactly coincident with geomorphic transitions over the active surface. This consents to link variable traits of the colluvial aprons to the spatial variability in geological and geomorphic controls.

Studies of recent and ancient slope deposits demonstrate the potential of colluvial sediments for palaeoclimate and palaeotectonic reconstructions (Nelson, 1992; McCalpin *et al.* 1993; Blikra & Nemec, 1998; Nemec & Kazanci, 1999; Pederson *et al.*, 2000; Pawelec, 2006). Nonetheless, colluvial sediments are tied to high-relief settings with high morphological variability and rapid evolution (Hewitt, 1972; Gardner, 1980). As in other environments, geomorphic evolution will modify sedimentation patterns (e.g. Blair & McPherson, 1994; Einsele & Hinderer, 1998; Yoshida *et al.*, 2007), and subtle morphologic variability in space and time can affect colluvial sedimentation. The long-term evolution of slope morphology thus represents a fundamental factor (Meis & Moura, 1984; Blikra & Nemec, 1998; Sanders *et al.*, 2009; Hinchcliffe & Ballantyne, 2009). In this regard, the morphological maturity of slopes is commonly expected to increase

with time, rather than in space, an assumption that does not match with this study. The notable differences in the colluvial aprons described here depend not on age, but on local piedmont morphology. This highlights the necessity to carefully constrain the geomorphic context in colluvial stratigraphy, and suggests caution in adopting morphostratigraphic criteria to infer relative ages and landscape histories from slope sediments.

Geomorphic controls have been recognized in some studies of present and Quaternary slope sedimentology (Nemec & Kazanci, 1999; Friend *et al.*, 2000; Texier & Meireles, 2003; Sass & Krautblatter, 2007) or were mentioned as a cautionary note (Luckman, 1976; Van Steijn *et al.*, 1995; Blikra & Nemec, 1998; Pawelec, 2006), especially where it was possible to refer to present-day landscapes and high-resolution chronologies. Sedimentological analyses of slope deposits dating farther back in time face more uncertainties. Added complications are represented by equifinality (Van Steijn *et al.*, 2002; Wilson, 2009), and by frequent sediment reworking. For instance, the architecture of distal debrisflow mounds in sector 3 (Figs. 17A,B) is characterized by depositional units stacking with different vergence and inclination through time, due to local autogenic dynamics. In ancient or poorly exposed successions, the same architecture might be explained by syndepositional tectonics. In piedmont sector 4, the palaeoclimate significance of the aeolian sand ramp, as well as its influence on other processes, would be lost in stratigraphy due to almost complete reworking by sheetfloods. A more conservative interpretation as a runoff-dominated environment might seem obvious. Similarly, pebble lags in sector 3 (facies Ac) might be viewed as the product of sporadic runoff or aeolian deflation in ancient records. Observations of the active surface instead show them to be a distinct facies from active aeolian deposition (Figs. 20, 21).

Aeolian facies have been recognized from periglacial and high-latitude slope settings (e.g. Hétu & Vandelac, 1989; Hétu, 1991; Ballantyne, 1998), but their volumetric importance in colluvial deposits has not yet been observed in the few studies from arid, low-latitude environments (Turner & Makhlouf, 2002). The general role of aeolian processes in the development of slope deposits remains poorly studied (Van Steijn *et al.*, 2002). The above observations show that aeolian deposits may greatly contribute to the aggradation and stabilization of colluvial aprons in desert settings, and that preservation of the relative stratigraphic evidence is subject to control by the local surface hydrology. In contrast with cold environments, where aeolian sediments can be modified by interactions with snow accumulations (*nivaeo-aeolian deposits*; cf. Van Steijn *et al.*, 2002), the typical structures and architectures of aeolian deposits in warm arid environments appear more recognizable.

4.11. CONCLUSIONS

Sedimentological and geomorphic surveys along the Atacama Desert coast have shown a great spatial variability of coeval colluvial processes and sediments within short distances, directly tied to local differences in the morphology, hydrology and microclimate of the hosting piedmont. Nemec and Kazanci (1999) synthesized this property of colluvial successions as 'high entropy'. The strong dependence of slope depositional systems on local geomorphology is a potential source of misinterpretation for the stratigraphic record, and should be given careful consideration.

Three main types of facies associations and architectures have been recognized. High-gradient slope tracts tend to accumulate relatively low volumes of coarse-grained, poorly structured screes from rockfall, debrisfall and grainflow processes. Lower-relief areas with potential to convey significant runoff develop highly organized colluvial aprons dominated by complex interactions between debrisflows, occasional floods, and aeolian deposition.

The great variety of processes recognized in this hyperarid setting does not differ fundamentally from those observed in studies of alpine, periglacial and temperate settings, and confirms that slope sediment transport processes are fundamentally 'azonal' (Van Steijn, 2011). The coupling of slope segmentation and downslope changes in dominant processes also closely recalls observations from other climate settings. More specific traits, such as the scarcity of clay, the importance of well-stratified aeolian deposits, and the absence of pedogenic horizons, could help to infer an arid to hyperarid setting in the stratigraphic record. Aeolian signatures however can be expected to be very variable, and possibly not preserved at all, depending on local piedmont hydrology and exposure to dominant winds.

ACKNOWLEDGEMENTS

This research was financed by grant 815.01.012 of NWO (Netherlands Council for Scientific Research). Maarten Zeylmans van Emmickhoven advised on satellite datasets for GIS elaboration, and Ton Zalm carried out granulometric analyses. George Postma is thanked for his encouragement on colluvial sedimentology. We acknowledge the constructive comments of Wojtek Nemec and an anonymous reviewer, and the assistance of journal editors Paul Carling and Stephen Rice.

REFERENCES

Allmendinger, R.W., Gonzalez, G., Yu, J., Hoke, G. and **Isacks, B.** (2005) Trench-parallel shortening in the Northern Chilean Forearc: Tectonic and climatic implications. *Geological Society of America Bulletin*, **117**, 89-104.

Aravena, K., Suzuki, O. and **Pollastri, A.** (1989) Coastal fog and its relation to groundwater in the IV region of northern Chile. *Chemical Geology*, **79**, 83-91.

Armijo, R. and **Thiele, R.** (1990) Active faulting in northern Chile: ramp stacking and lateral decoupling along a subduction plate boundary. *Earth and Planetary Science Letters*, **98**, 40-61.

Arnott, R.W.C. and **Hand, B.M.** (1989) Bedforms, primary structures and grain fabric in the presence of suspended sediment rain. *Journal of Sedimentary Petrology*, **59**, 1062-1069.

Bagnold, R.A. (1954) Experiments on a gravity-free dispersion of large solid spheres in a Newtonian fluid under shear. *Proceedings of the Royal Society of London*, **A225**, 49-63.

Ballantyne, C.K. (1998) Aeolian deposits on a Scottish mountain summit: characteristics, provenance, history and significance. *Earth Surface Processes and Landforms*, **23**, 625-641.

Bates, R.L. and **Jackson, J.A.** (1984) *Dictionary of Geological Terms*, 3rd edition. Anchor Publishing, 567 p.

Bertran, P. and **Texier, J.P.** (1999) Sedimentation processes and facies on a semi-vegetated talus, Lousteau, southwestern France. *Earth Surface Processes and Landforms*, **24**, 177-187.

Bertran, P., Hétu, B., Texier, J.-P. and **Van Steijn, H.** (1997) Fabric characteristics of subaerial slope deposits. *Sedimentology*, **44**, 1-16.

Blair, T.C. (1987) Sedimentary processes, vertical stratification sequences, and geomorphology of the Roaring River alluvial fan, Rocky Mountain National Park, Colorado. *Journal of Sedimentary Petrology*, **57**, 1-18.

Blair, T.C. (2002) Alluvial-fan sedimentation from a glacial-outburst flood, Lone Pine, California, and contrasts with meteorological flood deposits. In: *Flood and Megaflood Processes and Deposits* (Eds. I.P.Martini, V.R.Baker and G. Garzón), IAS Special Publication, **32**, 113-140.

Blair, T.C. and **McPherson, J.G.** (1994) Alluvial fans and their natural distinction from rivers based on morphology, hydraulic processes, sedimentary processes, and facies assemblages. *Journal of Sedimentary Research*, **A64**, 450-489.

Blair, T.C. and **McPherson, J.G.** (1998) Recent debris-flow processes and resultant form and facies of the Dolomite alluvial fan, Owens Valley, California. *Journal of Sedimentary Research*, **68**, 800-818.

Blair, T.C. and **McPherson, J.G.** (1999) Grain-size and textural classification of coarse sedimentary particles. *Journal of Sedimentary Research*, **69**, 6-19.

Blair, T.C. and **McPherson J.G.** (2009) Processes and Forms of Alluvial Fans. In: *Geomorphology of Desert Environments*, 2nd ed. (Eds. A.J. Parsons and A.D. Abrahams), pp. 413-467, Springer Science, Berlin.

Blikra, L.H. and **Longva, O.** (1995) Frost-shattered debris facies of Younger Dryas age in the coastal sedimentary successions in western Norway: palaeoenvironmental implications. *Palaeogeography, Palaeoclimatology, Palaeoecology*, **118**, 89-110.

Blikra, L.H. and **Nemec, W.** (1998) Postglacial colluvium in western Norway: depositional processes, facies and palaeoclimatic record. *Sedimentology*, **45**, 909-959.

Boric, R., Díaz, F. and **Maksaev, V.** (1990) Geología y yacimientos metalíferos de la Región de Antofagasta. *Boletín de Servicio Nacional de Geología y Minería de Chile*, **40**.

Bowman, D., Karnieli, A., Issar, A. and **Bruins, H.J.** (1996) Residual colluvio-aeolian aprons in the Negev highlands (Israel) as a palaeo-climatic indicator. *Paleaogeography, Palaeoclimatology, Palaeoecology*, **56**, 89-101.

Brazier, V, Whittington, G. and **Ballantyne, C.K.** (1988) Holocene debris cone evolution in Glen Etive, Western Grampian Highlands, Scotland. *Earth Surface Processes and Landforms*, **13**, 525-531.

Bristow, C.S., Skelly, R.L. and **Ethridge, F.G.** (1999) Crevasse splays from the rapidly aggrading, sand-bed, braided Niobrara River, Nebraska: effect of base-level rise. *Sedimentology*, **46**, 1029-1047.

Campbell, C.S. (1990) Rapid Granular Flows. *Ann. Rev. Fluid Mech.*, **22**, 57-92.

Campbell, C.S. and **Gong, A.** (1986) The stress tensor in a two-dimensional granular shear flow. *Journal of Fluid Mechanics*, **164**, 107-125.

Cembrano, J., Lavenu, A., Yañez, G., Riquelme. R., Garcia, M., Gonzalez, G. and **Herail, G.** (2007) Neotectonics. In: *The Geology of Chile* (Eds. T. Moreno and W. Gibbons), pp. 231-261, The Geological Society, London.

Charrier, R., Pinto, L. and **Rodriguez, M.P.** (2007) Tectonostratigraphic evolution of the Andean Orogen in Chile. In: *The Geology of Chile* (Eds. T. Moreno and W. Gibbons), pp. 21-114, The Geological Society, London.

Clarke, J.D.A. (2006) Antiquity of aridity in the Chilean Atacama Desert. *Geomorphology*, **73**, 101-114.

Clarke, M.L., Vogel, J.C., Botha, G.A. and **Wintle, A.G.** (2003) Late Quaternary hillslope evolution recorded in eastern South African colluvial badlands. *Palaeogeography, Palaeoclimatology, Palaeoecology*, **197**, 199-212.

Clemmensen, L.B. (1986) Storm-generated eolian sand-shadows and their sedimentary structures, Veyers Strand, Denmark. *Journal of Sedimentary Petrology*, **56**, 520-527.

Clemmensen, L.B. and **Abrahamsen, K.** (1983) Aeolian stratification and facies association in desert sediments, Arran Basin (Permian), Scotland. *Sedimentology*, **30**, 311-339.

Collinson, J. (1994) Sedimentary deformational structures. In: *The Geological Deformation of Sediments* (Ed. A. Maltman), pp. 95-125, Chapman & Hall, London.

Comte, D., Pardo, M., Dorbath, L., Dorbath, C., Haessler, H., Rivera, L., Cisternas, A. and **Ponce, L.** (1992) Crustal seismicity and subduction morphology around Antofagasta, Chile: preliminary results from a microearthquake survey. *Tectonophysics*, **205**, 13-22.

Curry, A.M. and **Morris, C.J.** (2004) Lateglacial and Holocene talus slope development and rockwall retreat on Mynydd Du, UK. *Geomorphology*, **58**, 85-106.

Davies, T.R.H. (1986) Large debris flows: a macroviscous phenomenon. *Acta Mechanica*, **63**, 161-178.

De Boer, P.L. (1979) Convolute lamination in modern sands of the estuary of the Oosterschelde, the Netherlands, formed as the result of entrapped air. *Sedimentology*, **26**, 283-294.

Delouis, B., Philip, B., Dorbath, L. and **Cisternas, A.** (1998) Recent crustal deformation in the Antofagasta region (northern Chile) and the subduction process. *Geophysical Journal International*, **132**, 302-338.

Doe, T.W. and **Dott, R.H.** (1980) Genetic significance of deformed cross bedding – With examples from the Navajo and Weber Sandstones of Utah. *Journal of Sedimentary Petrology*, **50**, 793-812.

Dott, R.H. (1963) Dynamics of subaqueous depositional gravity processes. *AAPG Bulletin*, **47**, 104-128.

Dunai, T.J., Gonzalez-Lopez, G.A., Juez-Larre, J., and **Carrizo, D.** (2005) Preservation of (Early) Miocene landscapes in the Atacama Desert, northern Chile. *Geochimica and Cosmochimica Acta*, **69**, A161.

Einsele, G. and **Hinderer, M.** (1998) Quantifying denudation and sediment-accumulation systems (open and closed lakes): basic concepts and first results. *Palaeogeography, Palaeoclimatology, Palaeoecology*, **140**, 7-21.

Fairbridge, R.W. (1968) The Encyclopedia of Geomorphology. Reinhold Book Corporation, New York, 1295 p.

Ferraris, B.F. and **Di Biase, F.F.** (1978) *Explanatory Notes Sheet N.30 (1:250,000), Hoja Antofagasta, Carta Geologica de Chile*. El Instituto Nacional de Investigaciones Geologicas de Chile, Santiago, 48 p.

Folk, R.L. (1954) The distinction between grain size and mineral composition in sedimentary-rock nomenclature. *Journal of Geology*, **62**, 344-359.

Francou, B. and **Manté, C.** (1990) Analysis of the segmentation in the profile of Alpine talus slopes. *Permafrost and Periglacial Processes*, **1**, 53-60.

Friend, D.A., Phillips, F.M., Campbell, S.W., Liu, T. and **Sharma, P.** (2000) Evolution of desert colluvial boulder slopes. *Geomorphology*, **36**, 19-45.

Fryberger, S.G., Ahlbrandt, T.S. and **Andrews S.** (1979) Origin, sedimentary features, and significance of low-angle eolian "sand sheet" deposits, Great Sand Dunes National Monument and vicinity, Colorado. *Journal of Sedimentary Petrology*, **49**, 733-746.

Gardner, J.S. (1980) Frequency, magnitude, and spatial distribution of mountain rockfalls and rockslides in the Highwood Pass area, Alberta, Canada. In: *Thresholds in Geomorphology* (Eds. D. R. Coates and J. D Vitek), pp. 267-295, Allen & Unwin, London.

Gerson, R. (1982) Talus relicts in deserts: A key to major climatic fluctuations. *Israel Journal of Earth Sciences*, **31**, 123-132.

GHCN (Global Historical Climatology Network) (2008a) Data from weather station Antofagasta (23.43°S 70.40°W).

http://www.worldclimate.com/cgi-bin/data.pl?ref=S23W070+1102+85442W

(Last update, February 2009).

GHCN (Global Historical Climatology Network) (2008b) Data from weather station Antofagasta (23.43°S 70.40°W).

http://www.worldclimate.com/cgi-bin/data.pl?ref=S23W070+2100+85442W

(Last update, February 2009).

Gutiérrez, F., Gutiérrez, M. and **Sancho, C.** (1998) Geomorphological and sedimentological analysis of a catastrophic flash flood in the Arás drainage basin (Central Pyrenees, Spain). *Geomorphology*, **22**, 265-283.

Halsey, L.A. and **Catto R.** (1994) Geomorphology, sedimentary structures , and genesis of dome dunes in Western Canada. *Géographie Physique et Quaternaire*, **48**, 97-105.

Harms, J.C., Southard, J.B., Spearing, D.R. and **Walker, R.G.** (1975) *Depositional Environments as Interpreted from Primary Sedimentary Structures and Stratification Sequences.* Short Course Lecture Notes, **2**, Society of Economic Paleontolofists and Mineralogists, Tulsa (OK).

Hartley, A.J. (2003) Andean uplift and climate change. *Journal of the Geological Society of London*, **160**, 7-10.

Hartley, A.J. and **Evenstar, L.** (2010) Cenozoic stratigraphic development in the north Chilean forearc: Implications for basin development and uplift history of the Central Andean margin. *Tectonophysics*, **495**, 67-77.

Hartley, A.J. and **Jolley, E.J.** (1995) Tectonic implications of Late Cenozoic sedimentation from the Coastal Cordillera of northern Chile (22-24°S). *Journal of the Geological Society of London*, **152**, 51-63.

Hartley, A.J., Chong, G., Houston, J. and **Mather, A.** (2005a) 150 million years of climatic stability: evidence from the Atacama Desert, northern Chile. *Journal of the Geological Society of London*, **162**, 421-424.

Hartley, A.J., Mather, A.E., Jolley, E. and **Turner, P.** (2005b) Climatic controls on alluvial-fan activity, Coastal Cordillera, northern Chile. In: *Alluvial Fans: Geomorphology, Sedimentology, Dynamics* (Eds. A.M. Harvey, A.E. Mather. And M. Stokes), Geological Society London Special Publication, **251**, 95-115.

Hesp, P.A. (1981) The formation of shadow dunes. *Journal of Sedimentary Petrology*, **51**, 101-112.

Hétu, B. (1991) Éboulis stratifiés actif près de Manche – d'Épée, Gaspésie (Québec, Canada). *Zeitschrift für Geomorphologie, Neue Folge*, **35**, 439-461.

Hètu, B. (1995) Le Litage des Éboulis Stratifiés Cryonivaux en Gaspesié (Québec, Canada) : Rôle de la Sédimentation Nivéo-Éolienne et des Transits Supranivaux. *Permafrost and Periglacial Processes*, **6**, 146-171.

Hètu, B. and **Gray, J.T.** (2000) Effects of environmental change on scree slope development throughout the postglacial period in the Chic Choc Mountains in northern Gaspé Peninsula, Québec. *Geomorphology*, **32**, 335-355.

Hétu, B. and **Vandelac, P.** (1989) La dynamique des éboulis schisteux au cours de l'hiver, Gaspésie septentrionale, Québec. *Géographie Physique et Quaternaire*, **43**, 389-406.

Hewitt, K. (1972) The mountain environment and geomorphic processes. In: *Mountain Geomorphology* (Eds. O. Slaymaker and H.J. McPherson), pp. 17-36, Tantalus Research, Vancouver, B.C.

Hilton Johnson, W. (1982) Interrelationships among geomorphic interpretations of the stratigraphic record, process geomorphology and geomorphic models. In: *Space and Time in Geomorphology* (Ed. C.E. Thorn), Binghamton Symposia in Geomorphology Int. Series, **12**, 219-241, Allen & Unwin, London.

Hinchliffe, S. and **Ballantyne, C.K.** (2009) Talus structure and evolution on sandstone mountains in NW Scotland. *The Holocene*, **19**, 477-486.

Hinchliffe, S., Ballantyne, C.K. and **Walden, J.** (1998) The structure and sedimentology of relict talus, Trotternish, northern Skye, Scotland. *Earth Surface Processes and Landforms*, **23**, 545-560.

Houston, J. (2006) The great Atacama flood of 2001 and its implications for Andean hydrology. *Hydrological Processes*, **20**, 591-610.

Houston, J. and **Hartley, A.J.** (2003) The central Andean west-slope rainshadow and its potential contribution to the origin of hyper-aridity in the Atacama Desert. *International Journal of Climatology.*, **23**, 1453-1464.

Hunter, R.E. (1977) Basic types of stratification in small eolian dunes. *Sedimentology*, **24**, 361-387.

Hunter, R.E. (1985) Subaqueous sand-flow cross strata. *Journal of Sedimentary Petrology*, **55**, 886-894.

Hurst, A. and **Glennie, K.W.** (1998) Mass-wasting of ancient aeolian dunes and sand fluidization during a period of global warming and inferred brief high precipitation: the Hopeman Sandstone (late Permian), Scotland. *Terra Nova*, **20**, 274-279.

Imeson, A.C., Kwaad, F.J.P.M. and **Mücher, H.J.** (1980) Hillslope processes and deposits in forested areas of Luxembourg. In: *Timescales in Geomorphology* (Eds. R.A. Cullingford, D.A. Davidson and J. Lewin), pp. 31-42, John Wiley & Sons, Chichester.

Innes, J.L. (1993) Debris flows. *Progress in Physical Geography*, **7**, 469-501.

Isacks, B.L. (1988) Uplift of the Central Andean Plateau and bending of the Bolivian Orocline. *Journal of Geophysical Research*, **93**, 3211-3231.

Iverson, R.M. (1997) The physics of debris flows. *Reviews of Geophysics*, **35**, 245-296.

Iverson, R.M. (2003) Gravity-Driven Mass Flows. In: *Encyclopedia of Sediments and Sedimentary Rocks* (Ed. G.V. Middleton), pp. 347-353, Kluwer Academic Publishers, Dordrecht.

Iverson R.M. and **Vallance, J.W.** (2001) New views of granular mass flows. *Geology*, **29**, 115-118.

Jahn, A. (1960) Some remarks on evolution of slopes in Spitsbergen. *Zeitschrift für Geomorphologie, Supplement Band*, **1**, 49-58.

Jomelli, V. and **Francou, B.** (2000) Comparing the characteristics of rockfall talus and snow avalanche landforms in an Alpine environment using a new methodological approach: Massif des Encrins, French Alps. *Geomorphology*, **35**, 181-192.

Jones, B.G. (1972) Deformation structures in siltstone resulting from the migration of an Upper Devonian aeolian dune. *Journal of Sedimentary Petrology*, **42**, 935-940.

Keefer, D.K., Moseley, M.E. and **deFrance, S.D.** (2003) A 38000-year record of floods and debris flows in the Ilo region of southern Peru and its relation to el Niño events and great earthquakes. *Palaeogeography, Palaeoclimatology, Palaeoecology*, **194**, 41-77.

Kim, B.C., Yu, K.M., Chun, H.Y., Choi, S.J. and **Kim, Y.B.** (1997) The southeastern margin of the Cretaceous Yongdong Basin, Korea: a lacustrine fan-delta system. *Geoscience Journal*, **1**, 61-74.

Kim, S.B., Chough, S.K. and **Chun, S.S.** (1995) Bouldery deposits in the lowermost part of the Cretaceous Kyokpori Formation, SW Korea: cohesionless debris flows and debris falls on a steep-gradient delta slope. *Sedimentary Geology*, **98**, 97-119.

Kim, S.B., Kim, Y.G., Jo, H.R., Jeong, K.S. and **Chough, S.K.** (2009) Depositional facies, architecture and environments of the Siwha Formation (Lower Cretaceous), mid-west Korea with special reference to dinosaur eggs. *Cretaceous Research*, **20**, 100-126.

Kirkby, M.J. and **Statham, I.** (1975) Surface Stone Movement and Scree Formation. *Journal of Geology*, **83**, 349-362.

Kocurek, G. (1986) Origins of low-angle stratification in aeolian deposits. In: *Aeolian Geomorphology* (Ed. G. Nickling), pp. 177-211, Binghamton Symposia in Geomorphology, **7**.

Kocurek, G. and **Dott, R.H.** (1981) Distinctions and uses of stratification types in the interpretation of eolian sand. *Journal of Sedimentary Petrology*, **51**, 579-595.

Lancaster, N. and **Tchakerian, V.P.** (1996) Geomorphology and sediments of sand ramps in the Mojave Desert. *Geomorphology*, **17**, 151-165.

Lea, P.D. (1990) Pleistocene periglacial eolian deposits in southwestern Alaska: sedimentary facies and depositional processes. *Journal of Sedimentary Petrology*, **60**, 582-591.

Legros, F. (2002) Can dispersive pressure cause inverse grading in grain flows? *Journal of Sedimentary Research*, **72**, 166-170.

Loope, D.B., Mason, J.A. and **Dingus, L.** (1999) Lethal Sandslides from Eolian Dunes. *Journal of Geology*, **107**, 707-713.

Lowe, D.R. (1976) Grain flow and grain flow deposits. *Journal of Sedimentary Petrology*, **46**, 188-199.

Lowe, D.R. (1979) Sediment Gravity Flows: Their Classification and Some Problems of Application to Natural Flows and Deposits. In: *Geology of Continental Slopes* (Eds. L.J. Doyle and O.H. Pilkey), SEPM Special Publication, **27**, 75-82.

Lucassen, F. and **Franz, G.** (1992) Generation and metamorphism of new crust in magmatic arcs: a case study from northern Chile. *Terra Nova*, **4**, 41-52.

Luckman, B.H. (1976) Rockfalls and rockfall inventory data; some observations from Surprise Valley, Jasper National Park, Canada. *Earth Surface Processes and Landforms*, **1**, 287-298.

Lunt, I.A. and **Bridge, J.S.** (2007) Formation and preservation of open-framework gravel strata in unidirectional flows. *Sedimentology*, **54**, 71-87.

Maizels, J. (1993) Lithofacies variations within sandur deposits: the role of runoff regime, flow dynamics and sediment supply characteristics. *Sedimentary Geology*, **85**, 299-325.

Major, J.J. and **Iverson, R.M.** (1999) Debris-flow deposition: Effects of pore-fluid pressure and friction concentrated at flow margins. *Geological Society of America Bulletin*, **111**, 1424-1434.

Marchant, M., Cecioni, A., Figueroa, S., Gonzalez, H., Giglio, S., Hebbeln, D., Kaiser, J., Lamy, F., Mohtadi, M., Pineda, V. and **Romero, O.** (2007) Marine geology, oceanography and climate. In: *The Geology of Chile* (Eds. T. Moreno and W. Gibbons), pp. 289-308, The Geological Society, London.

Martinsen, O. (1994) Mass Movements. In: *The Geological Deformation of Sediments* (Ed. A. Maltman), pp. 127-165, Chapman & Hall, London.

Matsuoka, N. and **Sakai, H.** (1999) Rockfall activity from an alpine cliff during thawing periods. *Geomorphology*, **28**, 309-328.

Maul, G. (2005) Wave climate. In: *Encyclopedia of Coastal Science* (Ed. M. L. Schwartz), pp. 1049-1052, Springer, Dordrecht.

McCalpin, J.P., Zuchiewicz, W. and **Jones, L.C.A.** (1993) Sedimentology of fault-scarp derived colluvium from the 1983 Borah Peak rupture, central Idaho. *Journal of Sedimentary Petrology*, **63**, 120-130.

Meis, M.R.M. and **Moura, J.R.S.** (1984) Upper Quaternary sedimentation and hillslope evolution: southeastern Brazilian Plateau. *American Journal of Science*, **284**, 241-254.

Middleton, G.V. (1970) Experimental studies related to problems of flysch sedimentation. In: *Flysch Sedimentology in North America* (Ed. J. Lajoie), Geological Society of Canada Special Paper, **7**, 253-272.

Miller, A. (1976) The climate of Chile. In: *Climates of Central and South America* (Ed. W. Schwerdtfeger), pp. 113-145. Elsevier, Amsterdam.

Mortimer, C. and **Saric, N.** (1972) Landform evolution in the coastal region of Tarapaca Province. *Revue de Géomorphologie Dynamique*, **21**, 162-170.

Moscariello, A., Marchi, L., Maraga, F. and **Mortara, G.** (2002) Alluvial fans in the Italian Alps: sedimentary facies and processes. In: *Flood and Megaflood Processes and Deposits* (Eds. I.P.Martini, V.R.Baker and G. Garzón), IAS Special Publication, **32**, 141-166.

Muñoz, J.F., Fernandez, B., Varas, E., Pastén, P., Gomez, D., Rengifo, P., Muñoz, J., Atenas, M., and **Jofré, J.C.** (2007) Chilean water resources. In: *The Geology of Chile* (Eds. T. Moreno T. and W. Gibbons), pp. 215-230, The Geological Society, London.

Nelson, A.R. (1992) Lithofacies analysis of colluvial sediments – An aid in interpreting the recent history of Quaternary normal faults in the Basin and Range province, western United States. *Journal of Sedimentary Petrology*, **62**, 607-621.

Nemec, W. (1990) Aspects of sediment movement on steep delta slopes. In: *Coarse-Grained Deltas* (Eds. A. Colella and D.B. Prior), IAS Special Publication, **10**, 29-73.

Nemec, W. and **Kazanci, N.** (1999) Quaternary colluvium in west-central Anatolia: sedimentary facies and palaeoclimatic significance. *Sedimentology*, **46**, 139-170.

Nemec, W. and **Muszynski, A.** (1982) Volcaniclastic alluvial aprons in the Tertiary Sofia District (Bulgaria). Annales Societatis Geologiae Pololoniae, **52**, 239-303.

Neuendorf, K.K.E., Mehl Jr., J.P. and **Jackson, J.A.** (2005) *Glossary of Geology*, 5th ed. American Geological Institute, Alexandria (VA), 779 p.

Nishiizumi, K., Caffee, M.W., Finkel, R.C., Brimhall, G., and **Mote, T.** (2005) Remnants of a fossil alluvial fan landscape of Miocene age in the Atacama desert of northern Chile using cosmogenic nuclide exposure age dating. *Earth and Planetary Science Letters*, **237**, 499-507.

Owen, G. (1987) Deformation processes in unconsolidated sands. In: *Deformation of Sediments and Sedimentary Rocks* (Eds. M.E. Jones and R.M.F. Preston), Geological Society of London Special Publication, **29**, 11-24.

Parsons, A.J. and **Abrahams, A.D.** (1987) Gradient-particle Size Relations on Quartz Monzonite Debris Slopes in the Mojave Desert. *Journal of Geology*, **95**, 423-452.

Pawelec, H. (2006) Origin and palaeoclimatic significance of the Pleistocene slope covers in the Cracow Upland, southern Poland. *Geomorphology*, **74**, 50-69.

Pederson, J., Pazzaglia, F. and **Smith, G.** (2000) Ancient hillslope deposits: Missing links in the study of climate controls on sedimentation. *Geology*, **28**, 27-30.

Pederson, J., Smith, G. and **Pazzaglia, F.** (2001) Comparing the modern, Quaternary, and Neogene records of climate-controlled hillslope sedimentation in southeast Nevada. *Geological Society of America Bulletin*, **113**, 305-319.

Pérez, L. (1998) Talus fabric, clast morphology, and botanical indicators of slope processes on the Chaos Crags (California Cascades), U.S.A. *Geographie Physique et Quaternaire*, **52**, 1-22.

Pierson, T.C. (1986) Flow behavior of channelized debris flows, Mount St. Helens, Washington. In: *Hillslope Processes* (Ed. A.D. Abrahams), pp. 269-296, Allen and Unwin, Boston.

Porter, M.L. (1987) Sedimentology of an ancient erg margin: the Lower Jurassic Aztec Sandstone, southern Nevada and southern California. *Sedimentology*, **34**, 661-680.

Rapp, A. (1960) Recent developments of mountain slopes in Kärkevagge and surroundings, northern Scandinavia. *Geografiska Annaler*, **42**, 65-200,

Rees, A.I. (1968) The production of preferred grain orientation in a concentrated dispersion of elongated and flattened grains. *Journal of Geology*, **76**, 457-465.

Reneau, S.L. and **Dietrich, W.E.** (1987) The importance of hollows in debris flow studies; Examples from Marin County, California. In: *Debris Flows / Avalanches: Process, Recognition, and Mitigation* (Eds. J.E. Costa and G.F. Wieczorek), Geological Society of America Reviews in Engineering Geology, **7**, 165-180.

Ritter, D.F., Kochel, R.C. and **Miller, J.R.** (1995) *Process Geomorphology*, 3rd ed. W.M.C. Brown Publishers, Dubuque, 560 p.

Sakamoto-Arnold, C.M. (1981) Eolian features produced by the December 1977 windstorm, southern San Joaquin Valley, California. *Journal of Geology*, **89**, 129-137.

Sanders, D. (2010) Sedimentary facies and progradational style of a Pleistocene talus-slope succession, Northern Calcareous Alps, Austria. *Sedimentary Geology*, **228**, 271-283.

Sanders, D., **Ostermann, M.** and **Kramers, J.** (2009) Quaternary carbonate-rocky talus slope successions (Eastern Alps, Austria): sedimentary facies and facies architecture. *Facies*, **55**, 345-373.

Sass, O. and **Krautblatter, M.** (2007) Debris flow-dominated and rockfall-dominated talus slopes: Genetic models derived from GPR measurements. *Geomorphology*, **86**, 176-192.

Savage, S.B. and **Lun, C.K.** (1988) Particle size segregation in inclined chute flow of dry cohesionless granular solids. *Journal of Fluid Mechanics*, **189**, 311-335.

Scheuber, E. and **Andriessen, P.A.M.** (1990) The kinematic and geodynamic significance of the Atacama fault zone, northern Chile. *Journal of Structural Geology*, **12**, 243-257.

Schumm, S.A. and **Lichty, R.W.** (1965) Time, space, and causality in geomorphology. *American Journal of Science*, **263**, 110-119.

Selby, M.J. (1993) Rock-slope Processes. In: *Hillslope Material and Processes*, Ch. 15, pp. 320-355. Oxford University Press, Oxford, 2nd ed.

Selby, M.J., Rains, M.B. and **Palmer, R.W.P.** (1974) Eolian deposits of the ice-free Victoria Valley, southern Victoria Land, Antarcica. *New Zealand Journal of Geology and Geophysics*, **17**, 543-562.

Smith, G.A. and **Lowe, D.R.** (1991) Lahars: volcano-hydrologic events and deposition in the debris flow – hyperconcentrated flow continuum. In: *Sedimentation in Volcanic Settings* (Eds. R.V. Fisher and G.A. Smith), SEPM Special Publication, **45**, 59-70.

Sohn, Y.K. and **Chough, S.K.** (1993) The Udo tuff cone, Cheju Island, South Korea: transformation of pyroclastic fall into debris fall and grain flow on a steep volcanic cone slope. *Sedimentology*, **40**, 769-786.

Sohn, Y.K., Kim, S.B., Hwang, I.G., Bahk, J.J., Choe, M.Y. and **Chough, S.K.** (1997) Characteristics and depositional processes of large-scale gravelly Gilbert-type foresets in the Miocene Doumsan fan delta, Phang Basin, SE Korea. *Journal of Sedimentary Research*, **67**, 130-141.

Statham, I. (1976) A scree-slope rockfall model. *Earth Surface Processes*, **1**, 43-62.

Statham, I. and **Francis, S.C.** (1986) Influence of scree accumulation and weathering on the development of steep mountain slopes. In: *Hillslope Processes* (Ed. A.D. Abrahams), pp. 245-267, Allen & Unwin, London.

Straub, S. (2001) Bagnold revisited: implications for the rapid motion of high-concentration sediment flows. In: *Particulate Gravity Currents* (Eds. W.D. McCaffrey, B.C. Kneller and J. Peakall), IAS Special Publication, **31**, 91-109.

Suwa, H. (1988) Focusing mechanism of large boulders to a debris-flow front. *Transactions of the Japanese Geomorphological Union*, **9**, 151-178.

Takahashi, T. (1980) Debris flow on prismatic open channel. *Journal of the Hydraulics Division, American Society of Civil Engineering*, **106**, 381-396.

Tanner, L.H. and **Hubert, J.F.** (1991) Basalt breccias and conglomerates of the Lower Jurassic McCoy Brook Formation, Fundy Basin, Nova Scotia: differentiation of talus and debris-flow deposits. *Journal of Sedimentary Petrology*, **61**, 15-27.

Texier, J.P. and **Meireles, J.** (2003) Relict mountain slope deposits of northern Portugal: facies, sedimentogenesis and environmental implications. *Journal of Quaternary Science*, **18**, 133-150.

Thomas, D.S.G., Bateman, M.D., Mehrshabi, D. and **O'Hara, S.L.** (1997) Development and Environmental Significance of an Eolian Sand Ramp of Last-Glacial Age, Central Iran. *Quaternary Research*, **48**, 155-161.

Todd, S.P. (1996) Process Deduction from Fluvial Sedimentary Structures. In: *Advances in Fluvial Dynamics and Stratigraphy* (Eds. P.A Carling and M.R. Dawson), pp. 299-350, John Wiley & Sons, Chichester.

Tomczak, M. and **Godfrey, J.S.** (1994) *Regional Oceanography: An Introduction*. Pergamon Press, London, 432 p.

Turner, B.R. and **Makhlouf, I.** (2002) Recent colluvial sedimentation in Jordan: fans evolving into sand ramps. *Sedimentology*, **49**, 1283-1298.

Van Steijn, H. (2011) Stratified slope deposits: periglacial and other processes involved. In: *Ice-Marginal and Periglacial Processes and Sediments* (Eds. I.P. Martini, H.M. French and A. Pérez-Alberti). Geological Society of London Special Publication, **354**, 213-226.

Van Steijn, H., Bertran, P., Francou, B., Hétu, B. and **Texier, J.** (1995) Models for the genetic and environmental interpretation of stratified slope deposits: Review. *Permafrost and Periglacial Processes*, **6**, 125-146.

Van Steijn, H., Boelhouwers, J., Harris, S. And **Hétu, B.** (2002) Recent research on the nature, origin and climatic relations of blocky and stratified slope deposits. *Progress in Physical Geography*, **26**, 551-575.

Vargas, G., Ortlieb, L. and **Rutllant, J.** (2000) Aluviones históricos en Antofagasta y su relación con eventos El Niño/Oscilación del Sur. *Revista Geologica de Chile*, **27**, 157-176.

Veevers, J.J. and **Roberts, J.** (1966) Littoral talus breccia and probable beach rock from the Visean of the Bonaparte Gulf Basin. *Australian Journal of Earth Sciences*, **13**, 387-403.

Vuille, M. (1999) Atmospheric circulation over the Bolivian Altiplano during dry and wet periods and extreme phases of the Southern Oscillation. *International Journal of Climatology*, **19**, 1579-1600.

Wasson, R.J. (1979) Stratified debris deposits in the Hindu Kush, Pakistan. *Zeitschrift für Geomorphologie, Neue Folge*, **23**, 301-320.

Wentworth, C.K. (1922) A scale of grade and class terms for clastic sediments. *Journal of Geology*, **30**, 377-392.

Williams, G.E. (1998) Late Neoproterozoic periglacial aeolian sand sheet, Stuart Shelf, South Australia. *Australian Journal of Earth Sciences*, **45**, 733-741.

Wilson, P. (2009). Rockfal talus slopes and associated talus-foot features in the glaciated uplands of Great Britain and Ireland: periglacial, paraglacial or composite landforms? In: *Periglacial and Paraglacial Processes and Environments* (Eds. J. Knight and S. Harrison), Geological Society of London Special Publication, **320**, 133-144.

Yoshida, S., Steel, R.J., and **Dalrymple, R.W.** (2007) Changes in depositional processes – An ingredient in a new generation of sequence-stratigraphic models. *Journal of Sedimentary Research*, **77**, 447-460.

"Apart from its healthful mental training as a branch of ordinary education, geology as an open-air pursuit affords an admirable training in habits of observation, furnishes a delightful relief from the cares and routine of everyday life, takes us into the open fields and the free fresh face of nature, leads us into all manner of sequestered nooks, whither hardly any other occupation would be likely to send us, sets before us problems of the highest interest regarding the history of the ground beneath our feet, and thus gives a new charm to scenery which may be already replete with attractions."

Sir Archibald Geikie

Chapter 5

Catchment control on sedimentary processes and stratigraphic architecture in a Miocene alluvial fan (Teruel Basin, Spain)

D. Ventra

ABSTRACT

Recent studies on Quaternary and present-day alluvial fans have highlighted the role of catchment geology in controlling fan sedimentology. Here, an example is discussed from the Neogene Teruel Basin (Spain), where excellent exposures provide the full record of sedimentological and architectural evolution of an alluvial fan along the western basin margin. The fan developed as a fully aggradational clastic wedge without significant unconformities or major incisions, due to forced positive accommodation in an endorheic setting. The spatial and temporal record of fan processes is thus completely preserved. The system is composed of two distinct clastic packages with a sharp, areally traceable transition. The Lower Fan Unit is dominated by conglomerates in extensive sheets and broad lenses, mainly from hyperconcentrated sheetfloods and sheetwash during early fan development. A sandstone-rich interval marks the vertically abrupt transition to the Upper Fan Unit, made of alternating coarse and fine clastic packages continuous over hundreds of meters. Dominant transport processes in this unit are modulated by the abundance of clay, varying from rheologically plastic debrisflows to pseudoplastic, clay-rich slurries and hyperconcentrated flows. Clast composition and analyses of colluvium from basement outcrops demonstrate that the development of fan processes and architecture in time is related to the successive denudation of the Mesozoic stratigraphy in the basement. Here, thick Triassic claystones of distal alluvial origin are overlain by sand-rich, paralic and shallow-marine deposits and a Cretaceous succession of platform to basinal dolostones and limestones. The sharp rheological and sedimentological transition from dominant water flows and hyperconcentrated flows to frequent cohesive debrisflows dispersed within great volumes of muddy alluvium is dictated by catchment incision and liberation of abundant clay sources. Two perfectly conformable clastic units with totally different sediments and architectures form the stratigraphic record of a single alluvial-fan system.

5.1. INTRODUCTION

Alluvial fans are the principal depositional landforms along tectonically active basin margins in continental settings. They typically develop at the transition between relief areas, which act as major clastic sources, and adjacent lowlands through which sediment is redistributed basinwards (Blair & McPherson, 1994). As such, alluvial fans control the patterns and mechanisms of initial sediment routing to more distal environments (Harvey, 2010). The sedimentary dynamics of fan systems are increasingly integrated into studies and theoretical modelling in basin analysis (Allen & Hovius, 1998; Frostick & Jones, 2002; Clevis *et al.*, 2004; Allen, 2008), but a major challenge is still given by the lack of general models of fan stratigraphic development in response to allogenic factors.

In spite of their relatively simple geometry and dynamics, the small size of catchment- fan systems makes them highly sensitive to tectonic, climatic and base-level forcing. Classical 'models' of fan development in relation to external controls are considered applicable only to limited instances. Such is the case for the concept of tectonically driven, coarsening- and fining-upward fan 'megasequences' (e.g. Heward, 1978; Rust, 1979; Steel *et al.*, 1977), and for the wet/dry dichotomy in climate-driven fan sedimentation (Bull, 1972; Nilsen, 1982; Hooke, 1987). Active tectonics is a necessary prerequisite for the formation and preservation of thick fan successions, but in the early decades of alluvial fan research tectonics was almost invariably considered also the primary control on fan processes and architecture (Beaty, 1961; Hooke, 1972; Steel, 1974; Heward, 1978). Advances in dating methods and palaeoclimatology promoted a gradual shift to viewing climate change as a more direct control on the style and timing of fan sedimentation. This has caused a major bias toward numerous Quaternary case studies, due to better chronological and palaeoclimatic information regarding that period (e.g. Wasson, 1977a, 1979; Nemec & Postma, 1993; Harvey, 1996; Reheis *et al.*, 1996; Harvey *et al.*, 1999; Ritter *et al.*, 2000; Hartley *et al.*, 2005; Dorn, 2009). This trend has been reinforced by case studies which demonstrated that climate variations were accompanied by base-level changes as additional control on fans and fan-deltas (Harvey *et al.*, 1999; Harvey, 2002; Viseras *et al.*, 2003; García & Stokes, 2006; Stokes & García, 2009). Integrating such lines of investigation into a general model of fan stratigraphy is hampered also by inherent problems of scale; many studies may not be directly compared and integrated because, by their nature, different allogenic factors act over variable time scales.

Recently, the effects of local geology on alluvial fan development have also been considered (Leeder *et al.*, 1996; Stokes & Mather, 2000; Went, 2005; Nichols & Thompson, 2005; Mack & Stout, 2005). Fan catchments, in particular, exert a strong influence on sedimentation through their lithology, hydrology and evolving morphology, adding an important complication to the variable fan dynamics reported in the literature. Most such studies have focused on Quaternary and especially Recent systems (Harvey, 1990; Church & Ryder, 1972; Kostaschuk *et al.*, 1986; Blair, 1999a, 2003; Webb & Fielding, 1999; Moscariello *et al.*, 2002), probably due to the presence of still accessible fan catchments, of which evidence is commonly not preserved in the stratigraphy of subaerial basin margins. In the ancient stratigraphic record, variation in the petrographic composition of sediments has been the most commonly observed signature of unroofing in relief sources or of drainage adjustments in catchment areas (e.g. Heward, 1978; DeCelles *et al.*, 1987; Nichols, 1987; Flint & Turner, 1988; Crews & Ethridge, 1993; Lloyd *et al.*, 1998). Exceptions are represented by two studies of

comparative fan sedimentology from the Miocene of Spain and Austria (Nichols & Thompson, 2005; Wagreich & Strauss, 2005), which show different depositional trends between adjacent, coeval fans to be linked to contrasting bedrock lithologies in the drainage areas.

Here, a case study is presented from the western margin of the Teruel Basin (central Spain), where proximal coarse-clastic systems developed during alternating phases of tectonism and quiescence from the late Oligocene to the Pleistocene. Extensive exposures allow complete examination of the sedimentology and architecture of a Late Miocene alluvial fan from proximal to distal segments. Exposures of the adjacent basement consent to relate unroofing of the local Mesozoic stratigraphy to the complex evolution of sediment transport processes and the development of a distinctly bipartite architecture within a single alluvial-fan system.

5.2. GEOLOGICAL SETTING

5.2.1. Teruel Basin and study area

The Iberian Chain is a mountain range in the central-eastern interior of the Iberian Peninsula. After a prolonged Mesozoic history of rifting and subsidence, with alternating continental (Triassic and Early Cretaceous) and shallow-marine deposition (Jurassic and Late Cretaceous) (Salas & Casas, 1993; Aurell *et al.*, 2002; Martín-Chivelet, 2002), the area was subjected to late Eocene-Oligocene deformation and uplift during the convergence of Africa and Europe. Several intermontane basins finally formed over the Iberian Chain during a Neogene-Quaternary phase of ESE extension, related to the opening of the western Mediterranean and of the Valencia Trough (Vegas, 1992; Anadón & Roca, 1996).

The Teruel Basin (Fig. 1) is formed by interconnected, *en-echelon* half-grabens trending NNE-SSW with an overall length of ~115 km and a maximum width of ~15 km. The depositional history started in the late Oligocene - early Miocene, and is represented by mudstones, continental limestones and evaporites of mudflat to shallow lacustrine environments in the central domains, and by coarse-clastic sediments from alluvial fans and ephemeral fluvial systems along the basin margins (Broekman, 1983; Anadón *et al.*, 1989, 2000; Alonso-Zarza & Calvo, 2000; Abels *et al.*, 2009a; Ventra, 2009). Essentially continuous deposition took place in a topographically enclosed, internally drained basin until the late Pliocene - Early Pleistocene (Adrover *et al.*, 1978; Broekman, 1983), when opening of a topographic threshold in the south connected the internal drainage to the Mediterranean. The drop in internal base level triggered a dominant erosional regime, still active with deep incision of the basin's stratigraphy by the present-day axial river (Rio Turia) and its tributaries. Climate in the Teruel Basin remained semiarid during most of the Neogene to the Quaternary (Alcalá *et al.*, 2000; Van Dam, 2006), with frequent fluctuations between relatively humid and dry conditions, mostly related to astronomical forcing (Abels *et al.*, 2009a,b).

The study area (Fig. 2) is situated ~12 km southwest of Teruel, close to the normal Teruel Fault, which marks the western boundary of the central basin segment (Fig. 1). Coarse-grained deposits form prominent topographic highs to the south and southwest of the village of Villastar (Fig. 2), with extensive outcrops on hillsides and in steep gorges incised by the Rio Turia and its ephemeral tributaries. Dip-parallel and strike-oriented exposures consent a full access to the stratigraphy, from proximal to distal domains. The system is

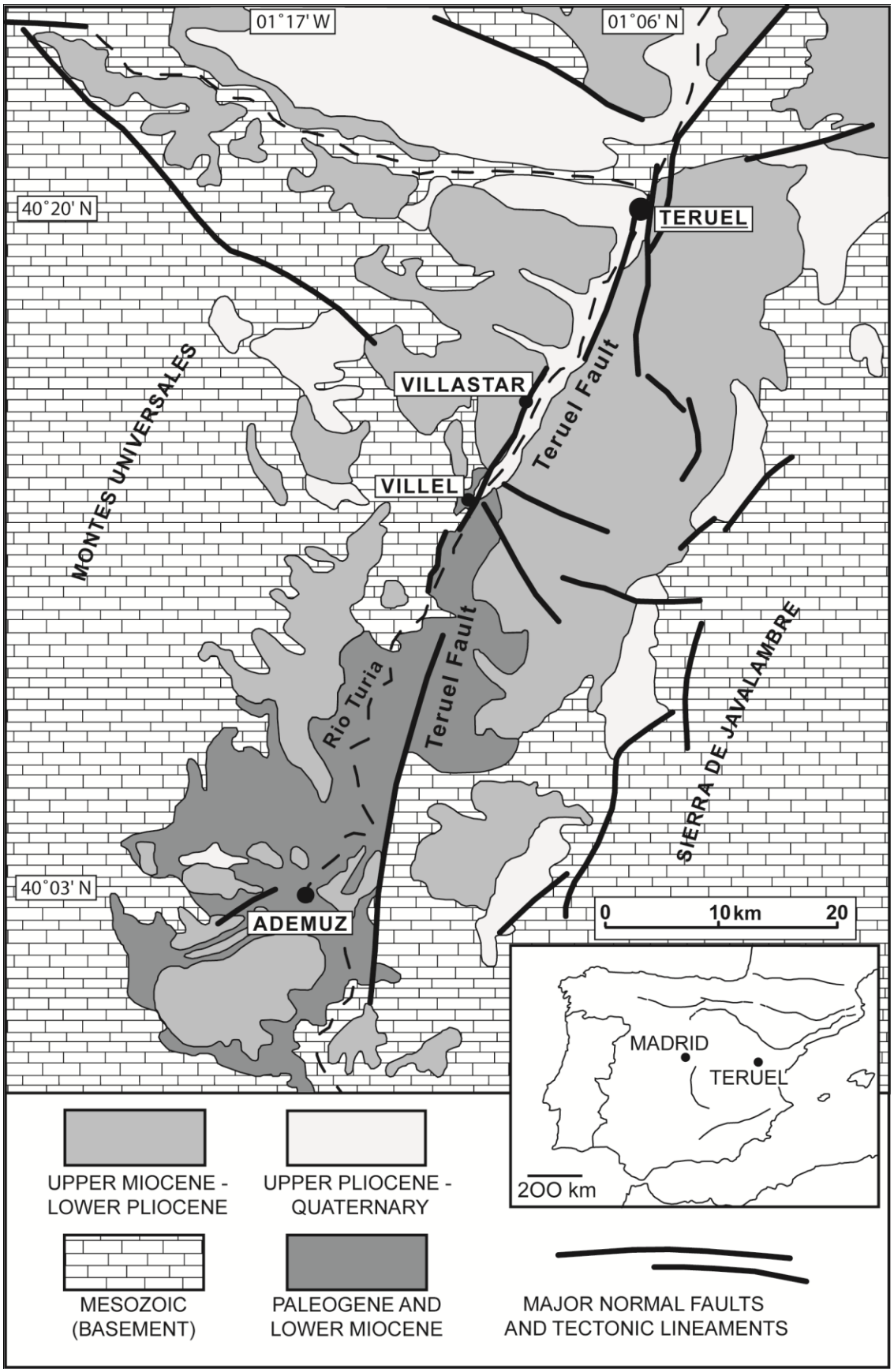

Figure 1 *- Geological map of the Teruel Basin (central Spain); the study area (see Fig. 2) extends between the villages of Villastar and Villel.*

interpreted as a typical, high-gradient, piedmont alluvial fan in view of the dominant coarse deposits, radial paleocurrent trends, relatively limited radial extent and development along the local boundary fault zone (*Teruel Fault*) (Blair & McPherson, 1994). The Villastar fan prograded toward SE with a minimum radial extent of ~4 km, and its exposed stratigraphic thickness reaches over 150 m in proximal exposures. The proximal portions are partly onlapped by Tortonian and Messinian deposits, but are well exposed in steep cliffs and canyons immediately SSW of Villastar on the northern side of the Rio Turia (Fig. 2), along the N-330 provincial road. The unconformable contact with the Mesozoic basement is visible at a few locations in the westernmost outcrops. Distal fan terminations outcrop in the badlands of the Prado area (Fig. 2), south of Villastar, which host a stratigraphically continuous Miocene succession of mudflat to shallow-lacustrine mudstones and carbonates (*Prado Section*; Abels *et al.*, 2009b). Astronomical tuning of facies cycles in the Prado Section, independently dated by biostratigraphy and high-resolution magnetostratigraphy, consented to relate them to orbital climate forcing (Abels *et al.*, 2009b). Conglomerate and sandstone beds from the highest stratigraphic levels of the alluvial fan interfinger with the lowermost cycles of the Prado Section, indicating a lower Tortonian age (~11 Ma) for the youngest fan units. The stratigraphic extent of the system below such units however implies that the fan aggraded mostly during the Serravallian age.

5.2.2. Local basement stratigraphy

Most of the basement in the area has been eroded or onlapped by Neogene deposits during internal basin aggradation, but extensive Mesozoic outcrops are accessible south-west of Villastar, directly adjacent to the fan system, along and above the road N-330 (Figs. 2 and 3). The local Mesozoic stratigraphy (Fig. 4) consists of partly deformed Triassic and Cretaceous allochtonous units separated by thrust faults.

The basal unit consists of gently folded, Late Triassic formations. The *Arcillas de Cofrentes* (Carnian; over 50 m in the study area) are a thick formation of stratified to massive red claystones with rare intercalations of thin marlstone beds, deposited in distal floodplains. This formation belongs to the Intermediate Detrital Series in the old Keuper lithostratigraphy of the Iberian Chain (Gabaldón, 1983). It is overlain by the thinner *Arcillas Yesiferas de Quesa* (late Carnian to possibly Norian; ~10-15 m), which consist of reddish to grey, massive claystones and siltstones comprising a minor, discontinuous evaporite member (mainly nodular to laminar gypsum and epsomite) toward the top. This formation belongs to the Upper Evaporite Series in the old Keuper lithostratigraphy (Gabaldón, 1983), and was deposited in distal floodplains and coastal sabkhas in a major transgressive cycle of the Iberian Basin (Sopeña *et al.*, 1988; Arche & López-Gómez, 1996; Arche *et al.*, 2002).

This thick pelitic interval probably acted as the favourable decollément level for a local thrust fault which unconformably superposes Early Cretaceous continental formations on the Triassic units. The *El Collado Formation* (Hauterivian-Barremian; ~80 m) is a thick succession of red claystones with subordinate lenticular interbeds of feldspathic and quartzo-feldspathic fine to medium sandstones, deposited in low-gradient fluvial environments. A depositional hiatus forms the unconformable contact with the overlying *Utrillas Formation* (Albian to lower Cenomanian; ~45 m; Fig. 3C), which in the area consists of thick, purple to red, unstratified claystones capped by a laterally extensive interval (~5-8 m thick) of tabular quartzo-

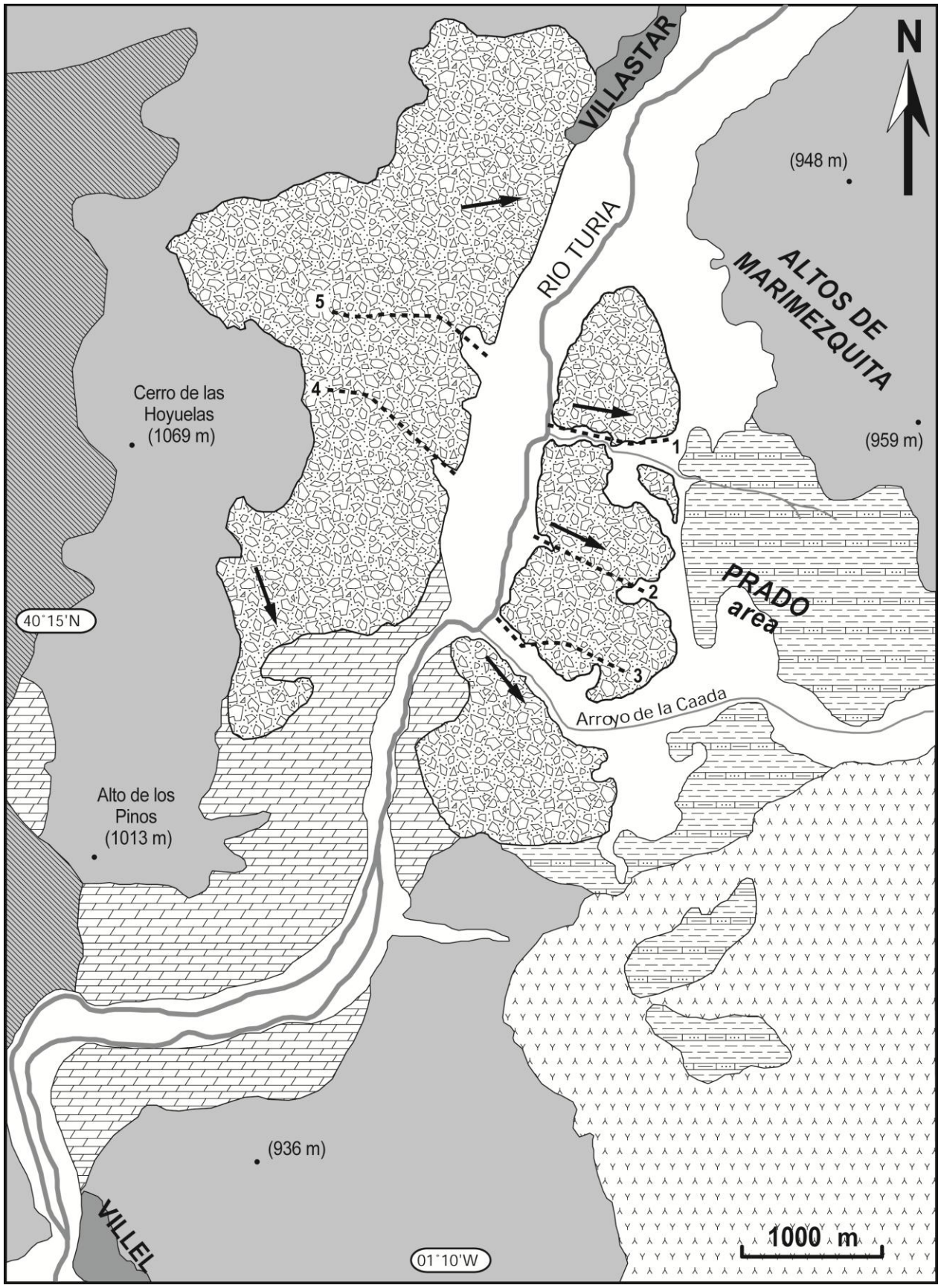

Figure 2 *- Geological map of the study area (front page). Mesozoic rocks are mapped according to a chronostratigraphic criterion (modified from Gabaldón, 1983); Cenozoic deposits are mapped according to their facies domains and age.*

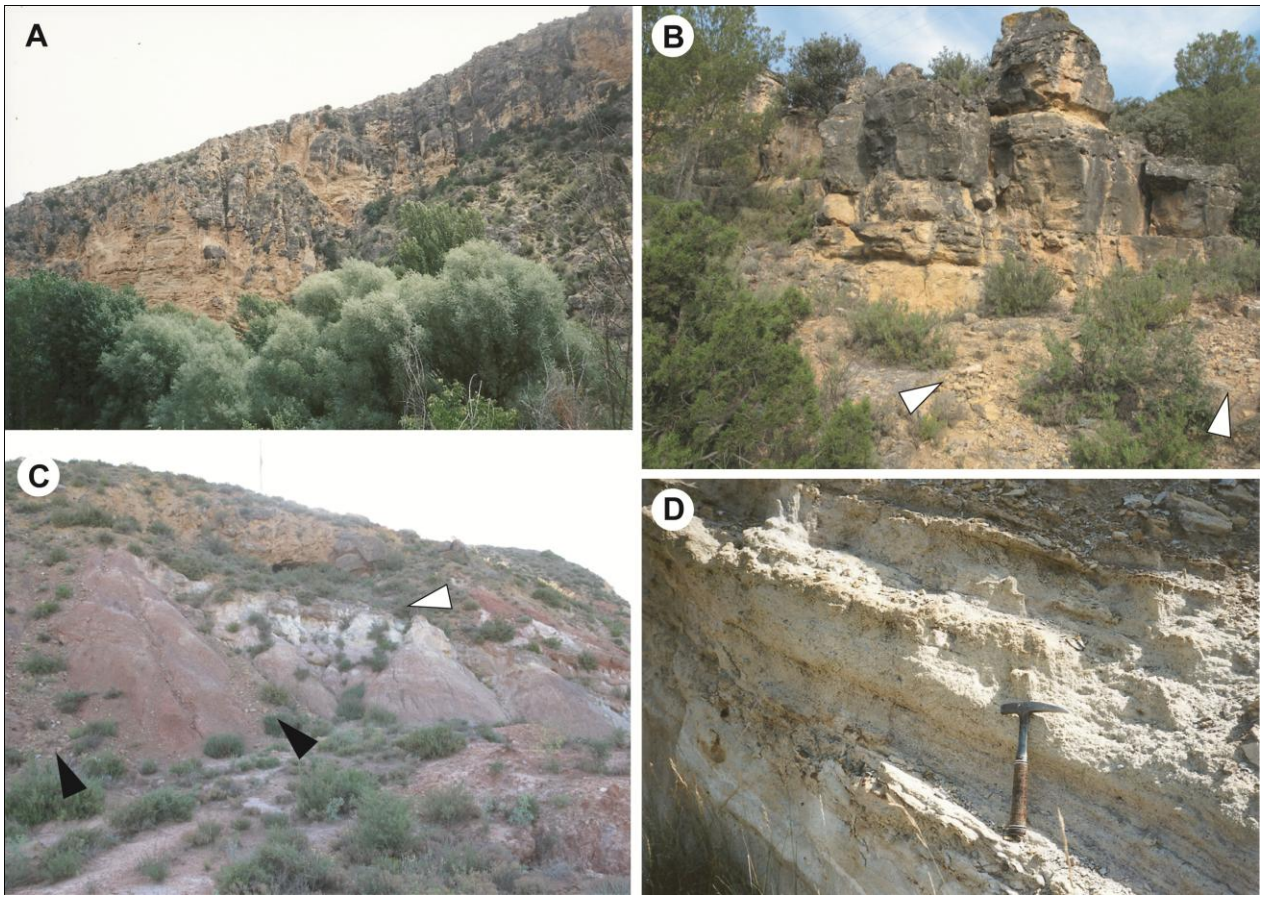

Figure 3 *- Basement outcrops in proximity of the Villastar fan. (A) Gradual stratigraphic transition between the well-stratified Alatoz Formation and the more massive and resistant dolostones of the Villa de Vés Formation. (B) Crudely bedded dolostones of the Villa de Vés Formation; note local regolith consisting mainly of granule to cobble gravel (white pointers). (C) Tectonic contact between Utrillas Formation (bottom, red mudstones) and Alatoz Formation (top, grey to light brown). Compare small talus tongues extending from the Alatoz Formation (mainly gravel, black pointers) with the smoother, compacted surface of mud-rich colluvium over the Utrillas Formation. Note also upper interval of the Utrillas Formation with light-toned, bedded sandstones (white pointer). (D) Bedded sandstones and siltstones at the top of the Utrillas Formation; hammer is 32 cm long.*

lithic, fine to medium sandstones and granule conglomerates, plane- to cross-bedded, intercalated by levels of massive kaolinitic sandstones and siltstones (Fig. 3D). These Cretaceous units have been related to the onset of a vast alluvial-aeolian system along the eastern margin of the Iberian Basin prior to the onset of the Cenomanian transgression (Elízaga, 1980; Arnaiz *et al.*, 1991; Martín-Chivelet, 2002; Rodríguez-López *et al.*, 2008).

The Early-Cretaceous formations dip uniformly toward the northeast, forming the limb of a wide-amplitude fold that is tectonically truncated by the Late Cretaceous allochtonous unit (Fig. 3C), which comprises two thick carbonate formations in the area. The *Alatoz Formation* (middle Cenomanian; ~120 m; Figs. 3A and C) is a thick, heterogeneous unit of well-stratified, fine-grained dolostones, interbedded with non-dolomitized bioclastic calcarenites with frequent fossils, rare micritic limestones and rare dolomitic marlstones. A gradual stratigraphic transition leads upward to the *Villa de Vés Formation* (also known as *Dolomías Tableadas de Villa de Vés*; late Cenomanian to Turonian; ~90 m; Figs. 3A and B), which is composed of thickly bedded dolostones with a coarse crystalline texture. These formations were deposited as inner-

platform, shallow-water to littoral carbonate bodies during an early Late Cretaceous highstand (Carenas *et al.*, 1989; Martín-Chivelet, 2002). The successive development of this shallow-water platform led to the deposition of other Late-Cretaceous carbonate formations (Gabaldón, 1983, 1985) which are not found in the local basement near Villastar, but could have been orginally present and subsequently eroded.

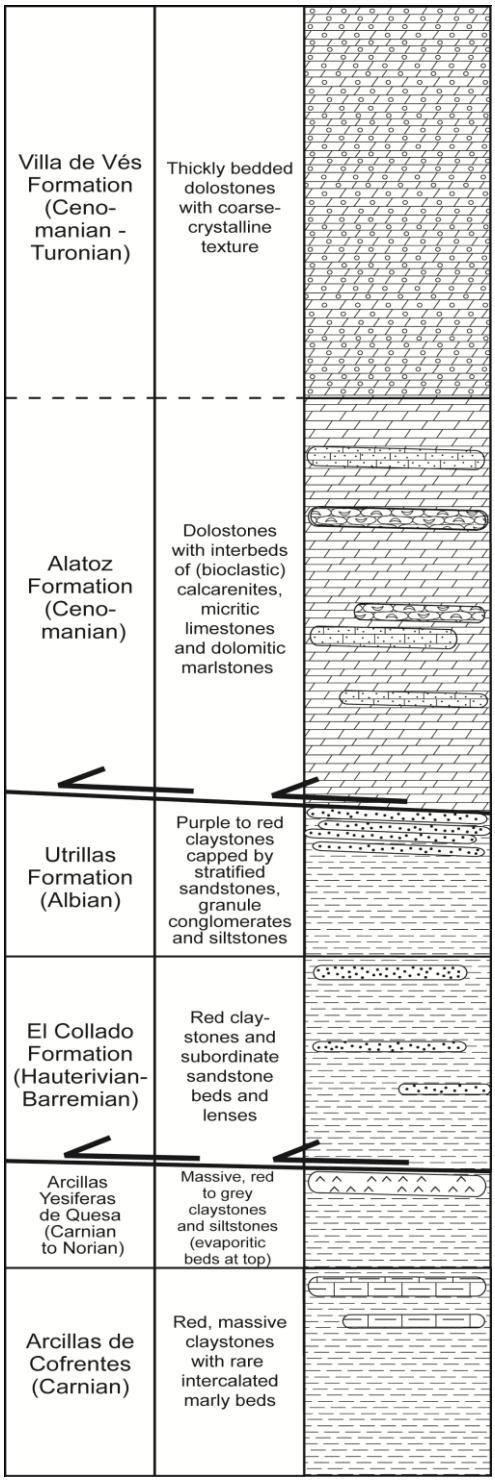

Figure 4 *- Mesozoic stratigraphy in basement outcrops west and southwest of the Villastar fan; vertical extent not to scale (see text for thickness of single formations). Continuous horizontal lines indicate sharp stratigraphic transitions; dashed lines indicate gradual transitions; thick lines with arrows indicate tectonic contact.*

SECTION 1

log 6

st.1 - VV 24%
ALA 69%
UTR 4%
JUR 2%
ind. 1%

st.2 - VV 28%
ALA 61%
UTR 2%
JUR 4%
ind. 5%

st.3 - VV 49%
ALA 35%
UTR 8%
ind. 8%

st.4 - VV 59%
ALA 32%
ind. 9%

log 5

st.1 - VV 6%
ALA 82%
UTR 2%
JUR 6%
ind. 4%

st.2 - VV 8%
ALA 80%
UTR 4%
JUR 5%
ind. 3%

st.3 - VV 49%
ALA 40%
UTR 4%
ind. 7%

log 2

st.1 - VV 8%
ALA 81%
UTR 4%
JUR 2%
ind. 5%

st.2 - VV 27%
ALA 60%
UTR 2%
JUR 3%
ind. 08%

SECTION 2

log 3

st.1 - VV 8%
ALA 86%
UTR 1%
JUR 5%

st.2 - VV 10%
ALA 82%
UTR 2%
JUR 6%

st.3 - VV 51%
ALA 39%
UTR 3%
ind. 7%

st.4 - VV 68%
ALA 30%
ind. 2%

log 4

st.1 - VV 4%
ALA 86%
UTR 1%
JUR 9%

st.2 - VV 7%
ALA 91%
JUR 2%

st.3 - VV 39%
ALA 45%
UTR 8%
ind. 8%

st.4 - VV 65%
ALA 31%
UTR 2%
ind. 2%

SECTION 5

log 2

st.1 - VV 8%
ALA 80%
UTR 2%
JUR 6%
ind. 4%

st.2 - VV 18%
ALA 65%
UTR 2%
JUR 7%
ind. 8%

st.3 - VV 35%
ALA 55%
UTR 2%
ind. 8%

st.4 - VV 48%
ALA 38%
UTR 4%
ind. 10%

st.5 - VV 59%
ALA 33%
UTR 6%
ind. 2%

st.6 - VV 68%
ALA 30%
ind. 2%

SECTION 4

log 1

st.1 - VV 20%
ALA 65%
UTR 4%
JUR 6%
ind. 5%

st.2 - VV 43%
ALA 43%
UTR 5%
JUR 8%
ind. 1%

st.3 - VV 56%
ALA 35%
UTR 3%
ind. 6%

st.4 - VV 66%
ALA 32%
ind. 2%

st.5 - VV 70%
ALA 34%
ind. 6%

Table 1 *- Clast counts from conglomerates along selected stratigraphic logs (see red numbering along logs in figures 6, 7 and 8 for stratigraphic positions), showing percent composition in terms of individual clast lithology and attribution to Mesozoic formation. VV = Villa de Vés Formation; ALA = Alatoz Formation; UTR = Utrillas Formation; JUR = Jurassic lithologies; ind. = undetermined lithologies.*

5.3 METHODS

Fifteen stratigraphic sections were logged in detail along five principal transects (sections 1 to 5; Figs. 2, 5, 6, 7 and 8) in proximal to distal fan domains, accompanied by facies analysis for the characterization of sedimentary processes. Seventy-two bedding measurements were taken by standard compass techniques and corrected for uniform post-depositional tilting (azimuth 20°/ dip 6°) in the area to derive the original

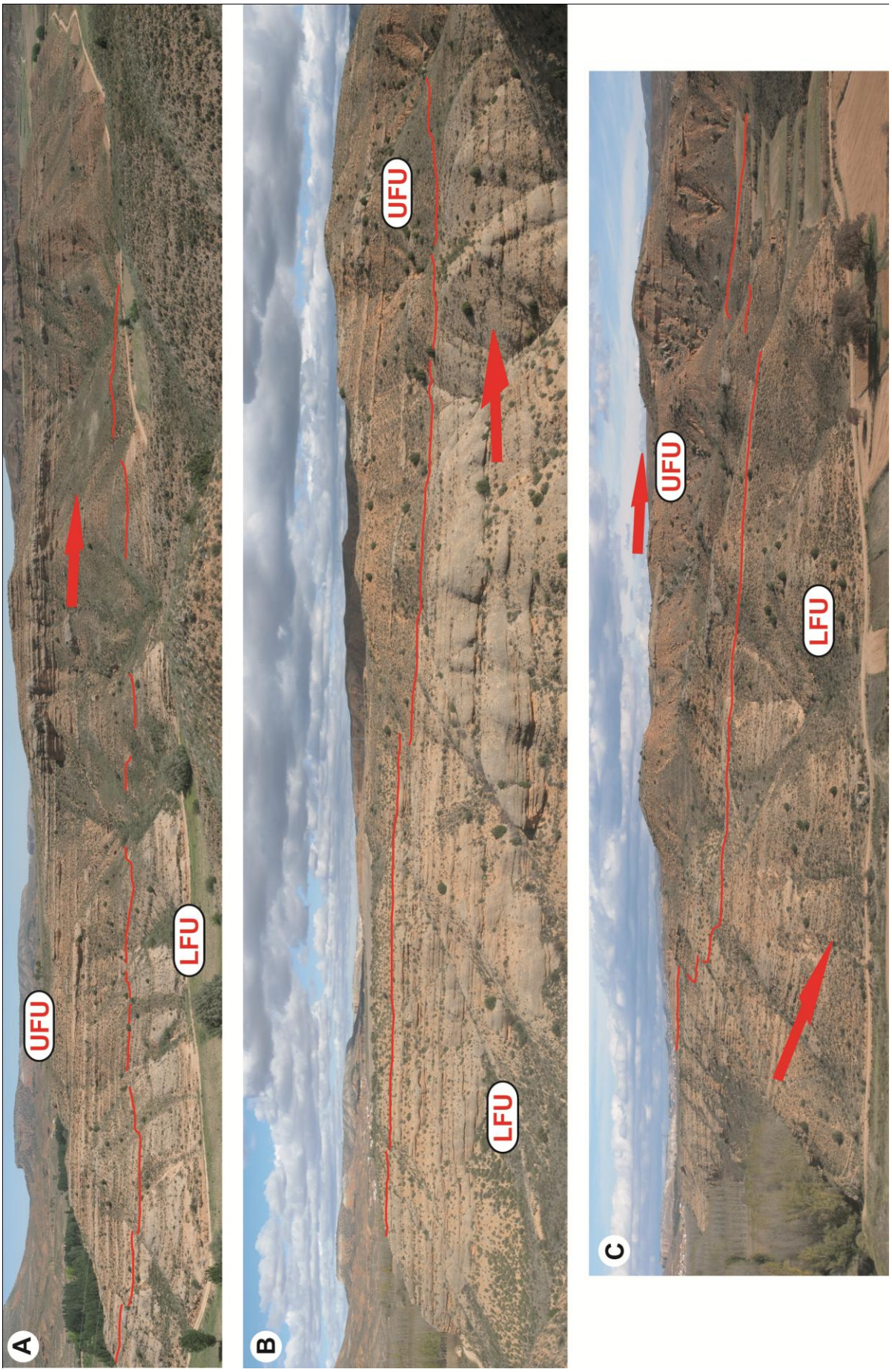
A
UFU
LFU
B
UFU
LFU
C
UFU
LFU

Figure 5 *(opposite page) - Panoramic views of the three most continuous, radially oriented exposures in medial-to-distal fan deposits; see Fig. 2 for location. Red arrows indicate approximate transport directions; red lines trace the transition between Lower and Upper Fan Units. (A) Section 1, nearly complete view. (B) Section 2, partial view of midfan domain; the canyon continues southeastward (to the right) into the distal fan domain. (C) Section 3, midfan domain for LFU, which dips under local ground level, and medial to distal domains for UFU (exposed in the distance).*

dip and orientation of depositional fan surfaces. Surveys were conducted also on the relief to the west and southwest of fan exposures, in order to assess the stratigraphy of the local Mesozoic basement. Characterization of the lithological composition of fan conglomerates (Table 1) was conducted at thirty-nine stations on clasts coarser than fine pebbles within one hammer radius (32 cm) from a point randomly chosen over the bed surface. Clasts coarser than medium cobbles were avoided, since they would significantly reduce the number of countable elements.

Textural analyses were performed on present-day colluvium along major Mesozoic outcrops, in order to ascertain the fines content of weathered regolith from the different basement lithologies (Fig. 9). Samples were collected from the topmost levels below the surface of unvegetated slopes, in order to analyze primary weathering products without biases from incipient pedogenesis and organic contamination. Sampled material was dry-sieved to eliminate particles coarser than granules (4 mm). Sand granulometries were separated by standard sieving (McCave & Syvitski, 1991). Residual fines were quantified with the classical settling-pipette method, since the more rapid, automated laser diffractometry is known to underestimate clay content (McCave *et al.*, 1986; Konert & Vanderberghe, 1997).

Textural terminology for gravel-sized particles follows Blair & McPherson's (1999) extension to the classical granulometric scale (Folk, 1954). Clast fabrics are described following Harm *et al.*'s (1975) notation, with long and intermediate clast axes referred to respectively as *a* and *b*; indices (*p*), (*t*) and (*i*) indicate respectively parallel and transverse orientations to flow and axis imbrication.

Hereafter, the Villastar fan is divided into a stratigraphically Lower Fan Unit (LFU) and an Upper Fan Unit (UFU), which are separately discussed in terms of facies analysis and stratal architectures. A comparative summary of both units and a general overview of identified controls on their development are provided in a final discussion.

5.4 LOWER FAN UNIT (LFU)

5.4.1. Facies analysis

Facies Gs (Planar-stratified conglomerates)

Facies Gs constitutes the great majority of gravelly deposits in the Lower Fan Unit (LFU), giving it a distinctly stratified appearance (Figs. 5 and 10A). This facies commonly consists of superposed gravelly divisions distinguishable by texture and fabric (Figs. 11A to C); two or more divisions were sequentially deposited to form a single bed (*sensu* Campbell, 1967) during a single sedimentation event with evolving conditions. Beds are commonly planar, ~20-110 cm thick, laterally continuous at outcrop over metres to a few tens of metres, and broadly lenticular where traceable along the depositional strike. Basal contacts are

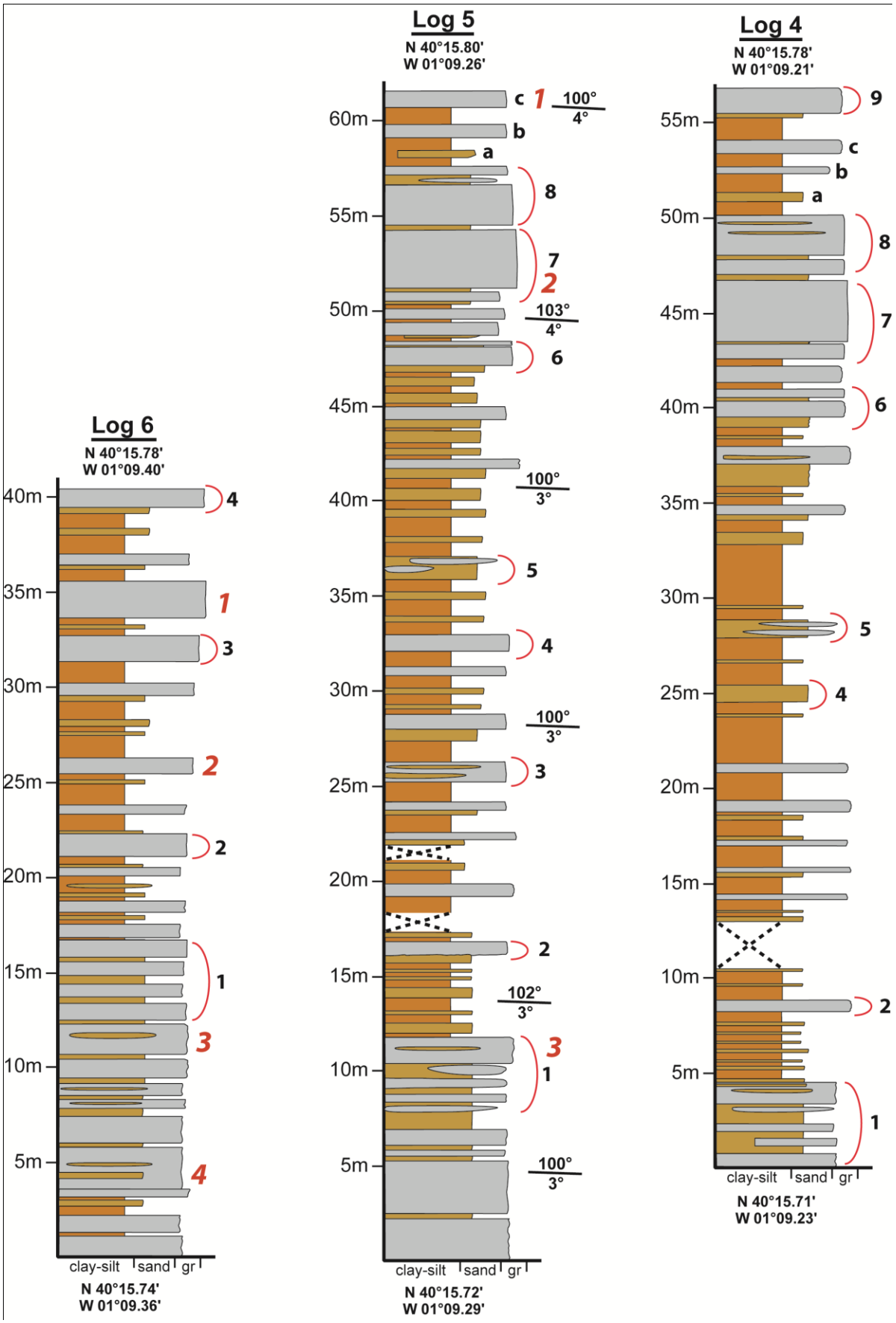
Log 6
N 40°15.78'
W 01°09.40'
40m
35m
30m
25m
20m
15m
10m
5m
4
1
3
2
2
1
3
4
clay-silt
sand
gr
N 40°15.74'
W 01°09.36'
Log 5
N 40°15.80'
W 01°09.26'
60m
55m
50m
45m
40m
35m
30m
25m
20m
15m
10m
5m
c
b
a
1
100°
4°
8
7
2
103°
4°
6
100°
3°
5
4
100°
3°
3
2
102°
3°
3
1
100°
3°
clay-silt
sand
gr
N 40°15.72'
W 01°09.29'
Log 4
N 40°15.78'
W 01°09.21'
55m
50m
45m
40m
35m
30m
25m
20m
15m
10m
5m
9
c
b
a
8
7
6
5
4
2
1
clay-silt
sand
gr
N 40°15.71'
W 01°09.23'

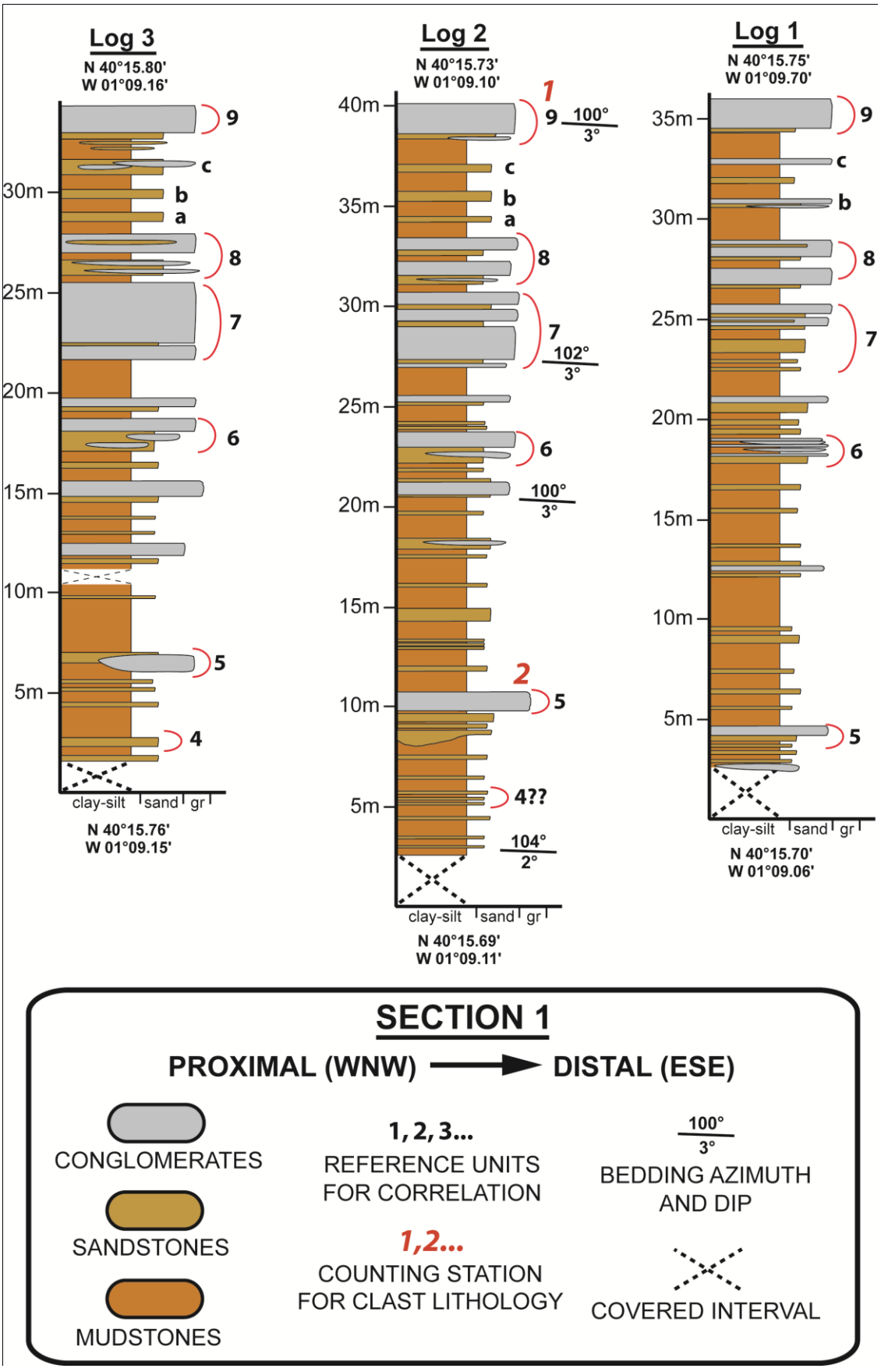

Figure 6 *- Six stratigraphic logs of section 1, medial to distal fan deposits (see Figure 2 for location); all logs are closely aligned along the main section line, except for log 3, which is a few tens of metres off-axis and therefore not exactly correlatable. Logs not aligned in exact height position due to graphic limitations.*

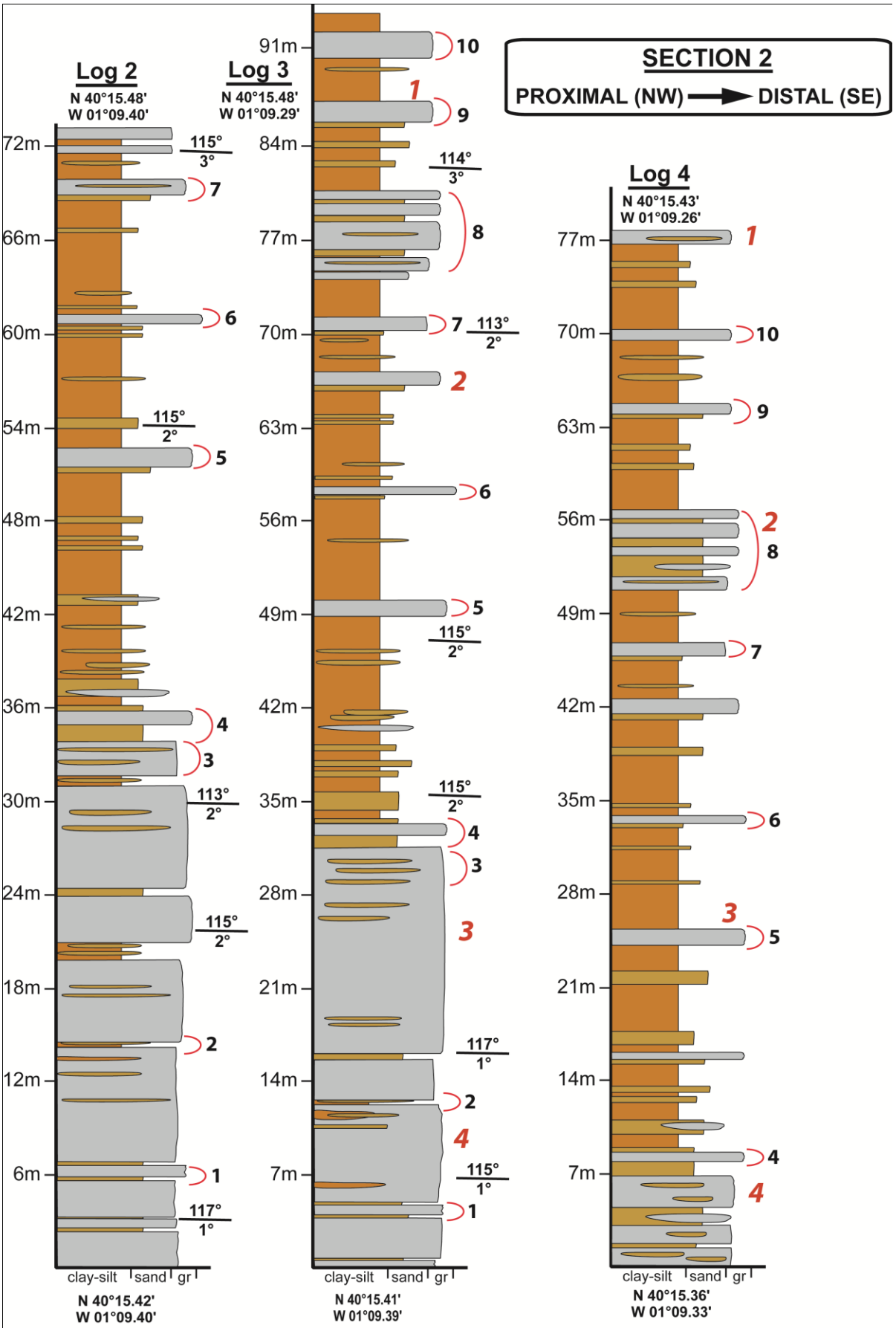

Figure 7 *- Selected stratigraphic logs in medial fan deposits, section 2 (see Figure 2 for location); graphic conventions applied as in fig. 4. Logs not aligned in exact height position due to graphic limitations.*

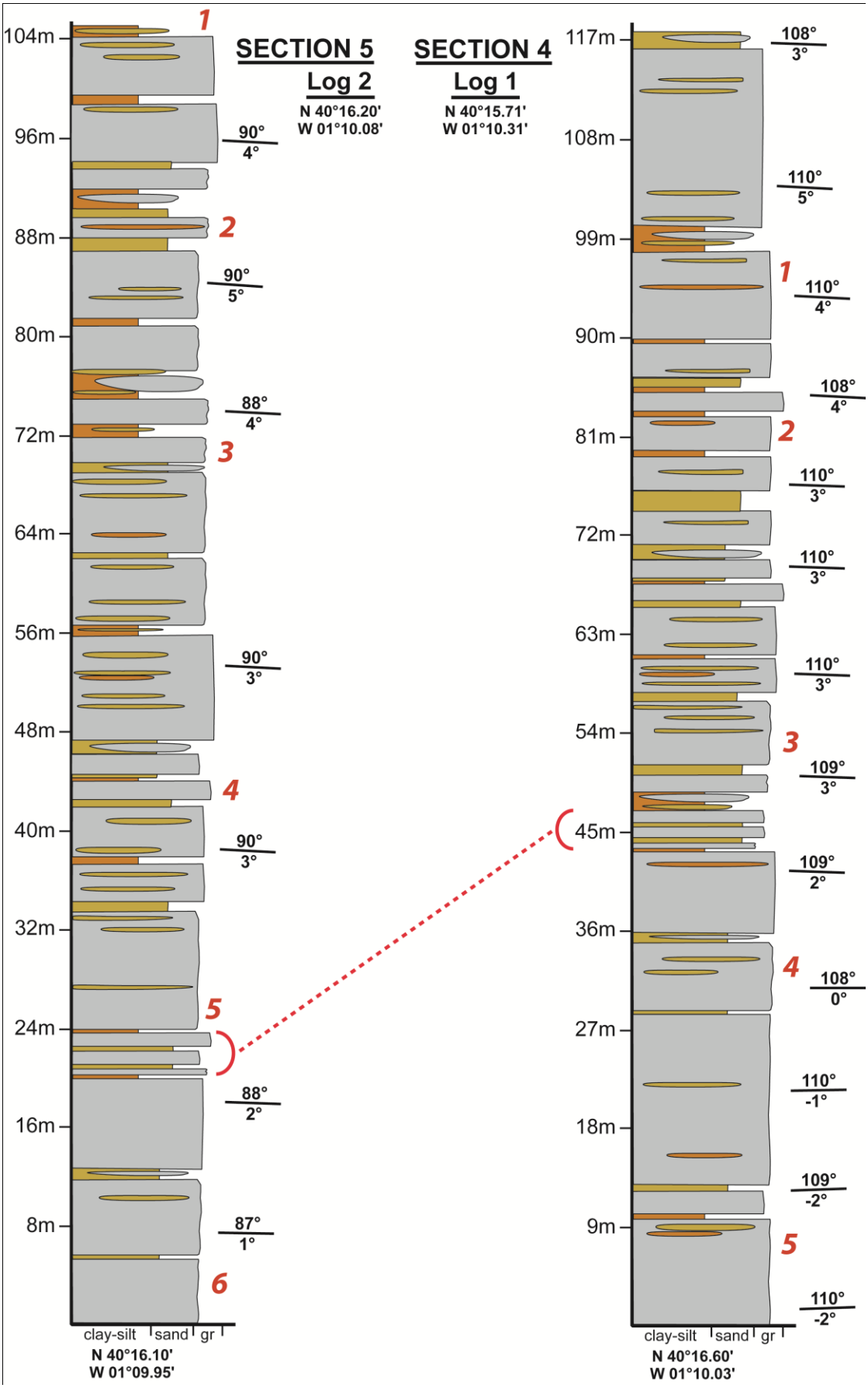

Figure 8 *- Representative logs for proximal sections 4 and 5 (see Figure 2 for location); graphic conventions applied as in Figure 4.*

weakly to sharply erosive with centimetric relief. The local degree of textural heterogeneity between divisions controls the relatively massive or layered appearance of Gs strata (Figs. 10B, C and 11A).

Coarser-grained, basal divisions (facies *Gs1*; Figs. 11A to C) consist of moderately to well-sorted coarse pebbles to fine cobbles, clast-supported to rarely matrix-supported, with common crude to well-developed normal grading, and moderately to very well-developed *a(p)* or *a(p)b(i)* fabrics with upcurrent imbrication (Figs. 11C and D). When not pervasively obliterated by carbonate cement, the abundant matrix consists of a massive, poorly to moderately sorted mixture of sand, granules and silt. Outsized cobbles within *Gs1* divisions or along their upper surfaces commonly have with *a(t)* or *a(t)b(i)* fabrics. Rare boulders lie with horizontal *ab* planes within the deposit or along its upper surface (Fig. 11E). The frequency of outsized clasts, however, decreases considerably from proximal to distal fan domains. Upward transitions are gradual or abrupt to a finer division (*Gs2*; Figs. 11A to C)) of matrix-rich, clast-supported fine to coarse or very coarse pebbles, in which grading and fabric characters are analogue to those in the underlying *Gs1* except for a common prevalence of flow-parallel *a(p)* orientations and horizontal *ab* planes for oblate pebbles. Outsized cobbles in this division lie with horizontal *ab* planes, or are weakly imbricated upstream. The facies sequence is topped by a final *Gs3* division (Figs. 11A, B and D), which consists of clast-supported granule to fine pebble gravel with distinct normal grading and analogue fabrics to *Gs2*; outsized cobbles are rare in these divisions, and have a horizontal position or are weakly imbricated upstream.

The number of divisions within one bed is variable, and some beds are homogeneous (Figs. 11E and F). The general trend however is always fining upward, starting from basal *Gs1* or *Gs2* divisions (Figs. 11A to D). Individual divisions vary in thickness from a few centimetres up to a few decimetres, and their transitions are commonly planar and weakly erosive or non-erosive.

This composite facies was deposited from heavily sediment-laden sheetfloods. The laterally extensive beds with prevalent fining-upward trends indicate progressive deposition from waning unconfined flows. Erosive features along basal surfaces, also in underlying conglomerates, indicate initial stages of great turbulence and potential for sediment bulking from the fan surface. However, poor sorting, frequent flow-parallel fabrics, absence of tractive structures and great volume of unsorted, unstratified coarse matrix imply that final deposition took place rapidly from highly concentrated clast dispersions which imposed strong particle interactions and prevented traction. Hyperconcentrated, mobile dispersions of coarse clasts can develop at the base of fast water flows carrying heterogeneous sediment mixtures due to internal gravity transformation (Fisher, 1983; Nemec & Muszynski, 1982; Sohn, 1997; Benvenuti & Martini, 2002; Manville & White, 2003). In the absence of clay, which may provide cohesion, a non-Newtonian rheology in the concentrated basal layer is attained through interparticle friction and impacts (Pierson & Costa, 1987; Coussot & Ancey, 1999). Clasts in these hyperconcentrated basal layers can be supported over great distances on high-gradients due to the shear imposed by the overriding turbulent flow, hindered settling, buoyancy from abundant suspended fines, and clast collisions. Deposition occurs by progressive aggradation at the base of the concentrated dispersion, whereas sediment supply and transport are maintained along its upper interface via a continuous sediment flux from the parent flow (Sohn, 1997; Benvenuti & Martini, 2002). The variable development of normal grading throughout beds and the thickness of single divisions

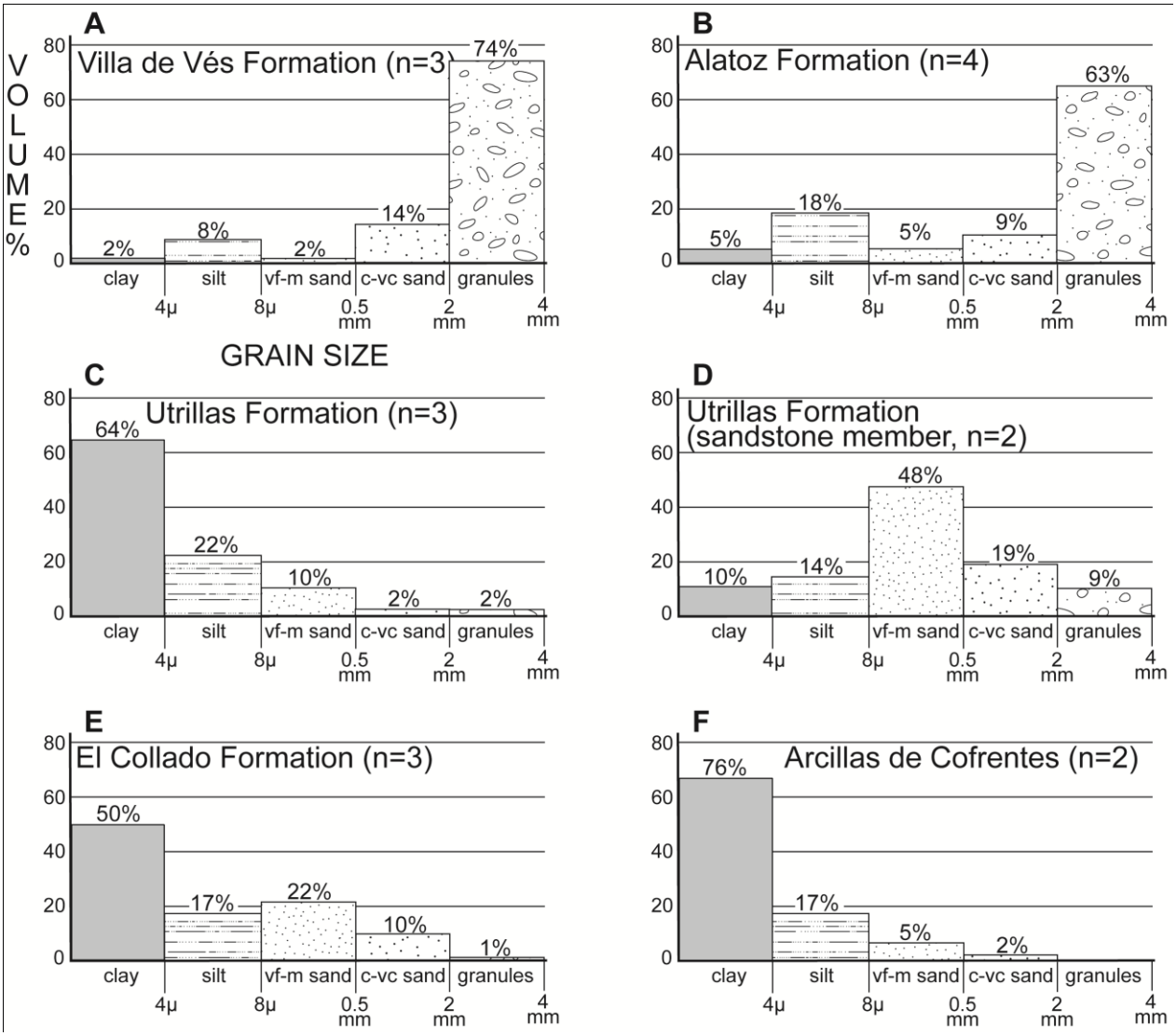

Figure 9 *- Relative volumes of clay to granule fractions in loose colluvial material of local Mesozoic outcrops; average values from analyses performed on 'n' samples of material finer than 4 mm.*

are thus related to progressive waning of the parent flow, and to the duration of successive flow stages with different capacity and competence. Outsized cobbles and boulders must have been transported for limited distances during the highest flow stages by traction and shear effects along the aggrading depositional interface (Sohn, 1997; Manville & White, 2003), in analogy to the mechanism in high-density turbidity currents (e.g. Postma *et al.*, 1988; Chun & Chough, 1992).

Facies Gmc (Massive clast-supported conglomerates)

This facies comprises a much lower volume of deposits than stratified *Gs* gravels, and is distributed almost exclusively in proximal fan outcrops west of the Rio Turia. It consists of very poorly sorted clast-supported to matrix-supported, fine pebbles to coarse cobbles in structureless beds or lenses, a few decimetres thick (Fig. 12A), with a maximum width (where observable in cross-fan exposures) of ~4-6 m. Basal contacts are typically planar and non-erosive, and lateral bed terminations are abrupt (Figs. 12B and C). Clasts are angular to subrounded and commonly form a close framework with abundant interstitial matrix, but matrix-

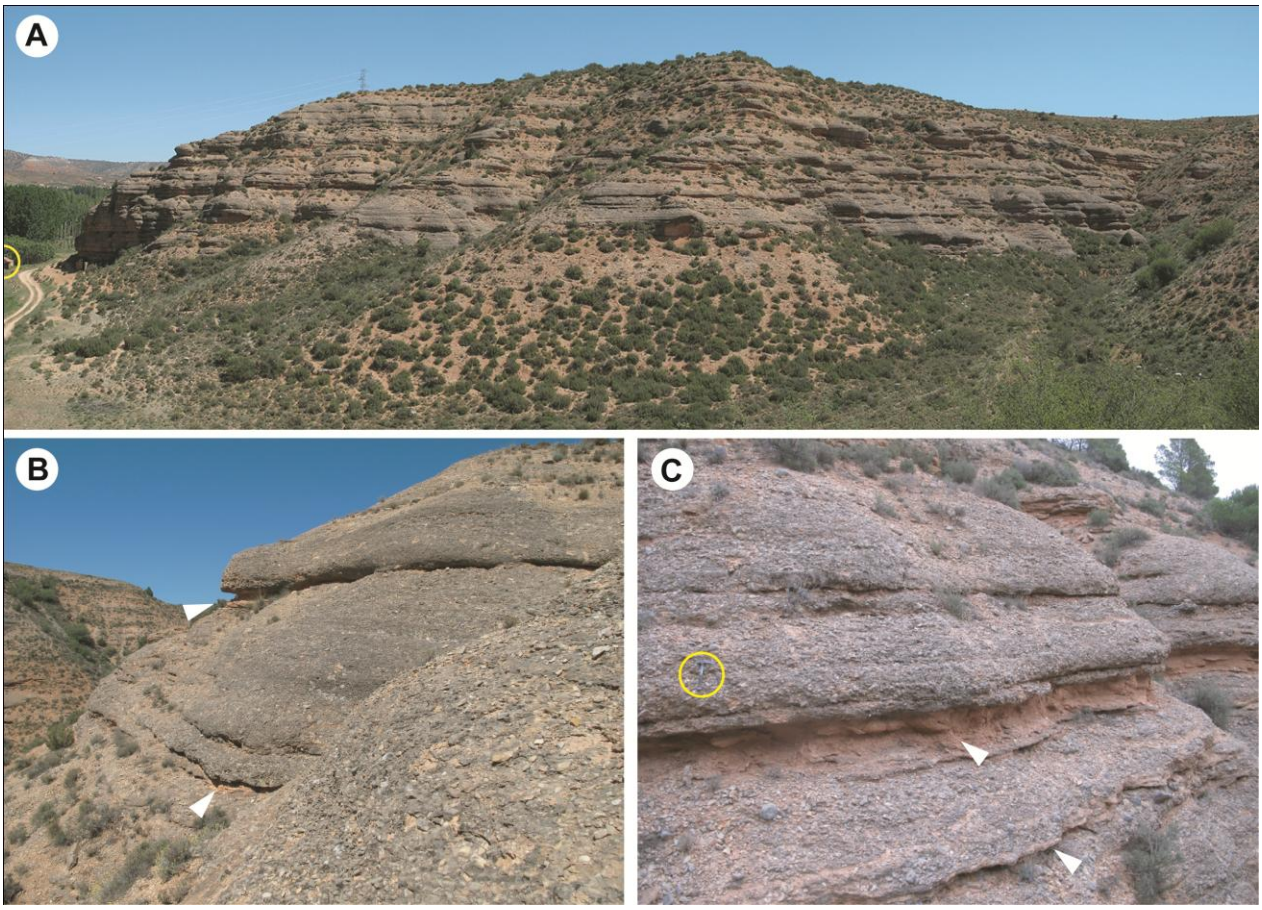

Figure 10 *- Outcrop views of the Lower Fan Unit. (A) Outcrop corner at the northwestern end of section 2, showing cross-fan (left side) and downdip (right side) lateral continuity of conglomerate strata (facies Gs); house for scale (circled in yellow) at the left margin. (B) Amalgamated conglomerates of facies Gs, with minor, fine-grained interbeds (white pointers); section 2, medial fan domain. (C) Downcurrent view of stratified conglomerates (facies Gs) in proximal outcrops, section 4; hammer for scale (circled in yellow). Note interbedded massive mudstones (facies Mm; white pointers) comprising one sandstone bed (facies Sl).*

supported domains are locally present. Where not obscured by carbonate cementation, the matrix is seen to consist of a poorly sorted, massive mixture of granules, sand and silt. Several beds show coarse-tail inverse grading, with cobbles protruding from the bed top (Fig. 12C), or basal inverse grading. Equant clasts are randomly oriented, whereas platy and discoidal clasts are frequently aligned horizontally within beds, and rare rod shaped clasts assume *a(p)* fabrics. Lateral bed terminations are often associated with chaotic concentrations of coarse pebbles to fine cobbles, typically a few clasts thick (Fig. 12B).

Facies characters are typical of deposition from cohesive debrisflows (in accordance with the terminological proposal of Blikra & Nemec, 1998) (Johnson, 1970; Fisher, 1971; Hooke, 1987; Hubert & Filipov, 1989; Blair & McPherson, 1994, 1998; Blikra & Nemec, 1998; Major & Iverson, 1999). Poorly sorted debris mixtures were transported over the proximal fan slopes in laminar flows. The gravel fraction was mainly supported by matrix strength and buoyancy as well as transient excess pore pressures (Johnson, 1970; Rodine & Johnson, 1976; Major & Iverson, 1999). Flow-parallel fabrics are due to internal shearing within the dense flowing mixture and to reciprocal clast interactions (Rees, 1968; Major, 1998). Basal inverse grading in matrix-rich units is due to the highest shear in the lowest flow levels, with resultant loss of matrix competence

(Hampton, 1975; Naylor, 1980; Hubert & Filipov, 1989), whereas in clast-rich beds it is probably related to the higher angular momentum imparted to coarser particles in the sheared granular mixture, and consequent 'climbing' of large clasts over smaller ones (Iverson & Denlinger, 1987). Coarse gravel concentrations at bed terminations inidicate a high level of flow organization, with frontal and lateral clast segregation forming typical debrisflow levees and snouts (Sharp, 1942; Johnson, 1970; Hubert & Filipov, 1989; Blair & McPherson, 1998) in which frictional clast interactions dominated over matrix-mediated effects of buoyancy and interstitial pressure, contributing to flow halting (Iverson & Denlinger, 1987; Major & Iverson, 1999).

Facies Sl (Laminated sandstones)

This facies is second in abundance within the LFU. It consists of moderately to well-sorted, light brown to buff, fine to medium sandstones in isolated or amalgamated centimetric units varying from laterally extensive, irregular beds to isolated lenses a few decimetres wide. Extensive beds frequently have a pinch-and-swell, discontinuous geometry controlled by the topography of underlying conglomerates, and weakly erosive planar bases over finer-grained sediments of facies Mm. Narrower sandstone lenses within mudstone partings show concave basal scours. Sandstones are frequently characterized by mm-thick plane-parallel lamination (Fig. 13A) and, very rarely, ripple cross-lamination. Grading is commonly absent.

Bed geometries and primary sedimentary structures indicate localized sand deposition from shallow waterflows which frequently attained supercritical conditions over the high-gradient fan surface, forming upper-stage plane beds or low-amplitude migrating bedforms (Cheel, 1990; Best & Bridge, 1992). Ripple lamination indicates bedload deposition in subcritical conditions at flow recession (Hubert & Hyde, 1982; Tunbridge, 1984). Its very rare preservation, together with absence of internal grading, suggests that waning stages were short, due probably to rapid flow expansion and water infiltration. Flow pathways were commonly influenced by the depositional topography of widespread conglomerate sheets, but could locally incise shallow gullies in finer-grained deposits. Sandstone interbeds associated with facies *Gs* and *Gmc* may represent the waning stages of higher-energy floods.

Facies Mm (Massive mudstones)

This facies represents a minor volume of LFU sediments, and consists of reddish brown to light brown massive mudstones (silty claystones to sandy siltstones), interbedded to dominant conglomeratic deposits (Fig. 10C) as lenses of a few centimetres, rarely up to 30-40 cm thick, and a few decimetres, rarely up to a few metres wide. Basal contacts are irregular and coincide with the undisturbed topography of underlying coarse-grained beds, whereas the tops are commonly subplanar and erosively truncated. This facies is commonly featureless, but minor pedogenic modification is rarely present in the form of red mottling, carbonate glaebules and crude blocky structures.

These thin mudstone interbeds are interpreted as deposition from low-energy sheetflows (cf. Hogg, 1982) with probably limited competence to transport only the finest-grained fractions of material available in the catchment (Smoot, 1982; Hubert & Hyde, 1982). Deposition took place mainly along rills and local surface hollows between coarser conglomerate sheets and lobes, followed by desiccation and incipient pedogenic

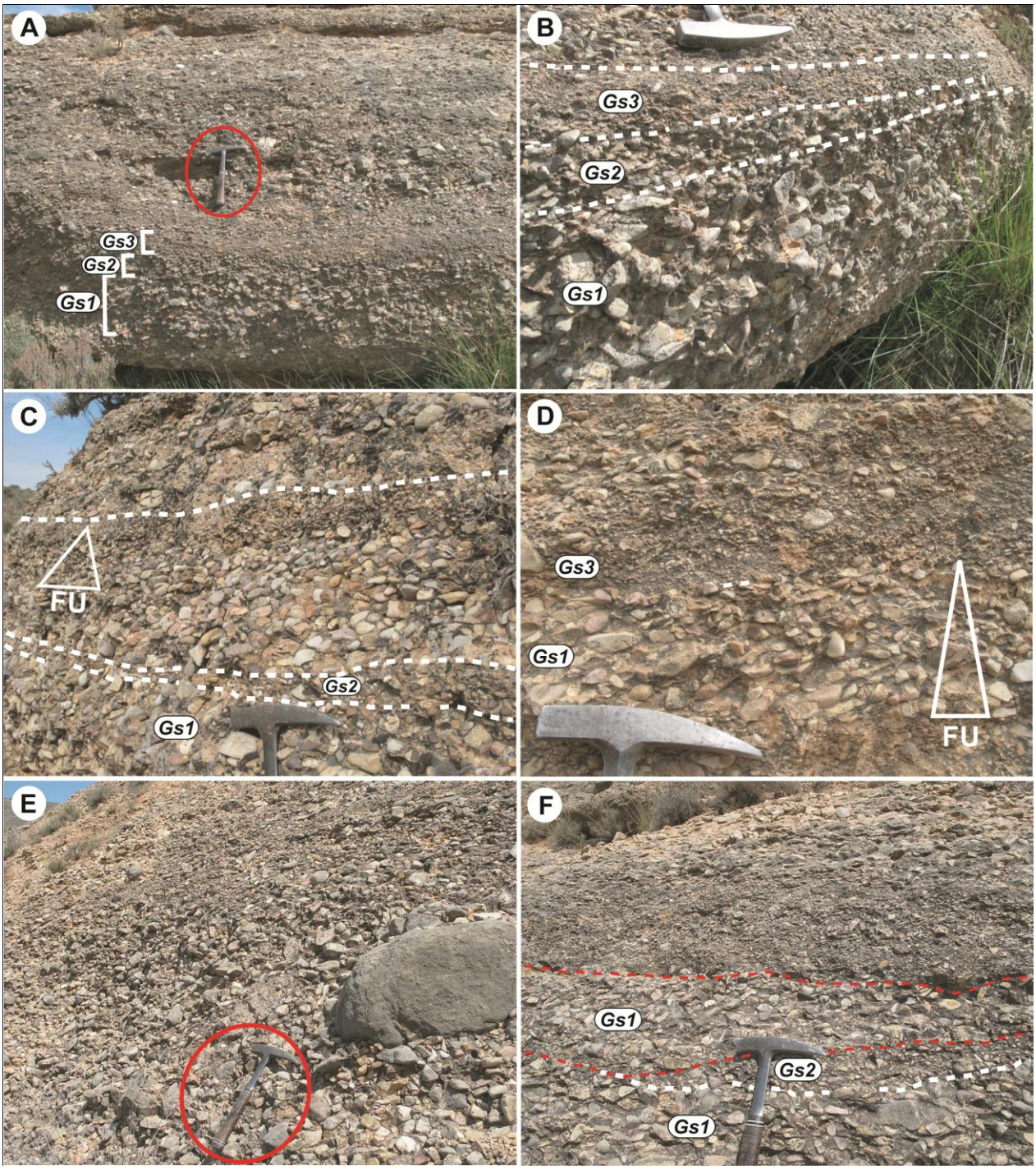

Figure 11 *- Well-stratified conglomerates from hyperconcentrated bedload deposition (facies Gs sheetflood deposits), proximal and distal LFU outcrops. Hammer for scale is 32 cm long and points toward general paleocurrent direction. (A) Planar amalgamated strata, with a distinct tripartite bed (divisions Gs1, Gs2 and Gs3). (B) Close-up of the tripartite bed in A; note fining-upward, clast-supported, matrix-rich fabric, with moderate to good imbrication, and gradual transition between divisions Gs1 and Gs2, and abrupt transition between Gs2 and Gs3. (C) Erosive contact between two beds; lower one has distinct bipartite structure, whereas the upper one presents a more gradual fining-upward trend. (D) Two superposed divisions Gs1 (note very good clast imbrication) and Gs3 with very abrupt contact; possibly related to distinct events (therefore to be interpreted as two distinct beds). (E) Outsized boulder lying flat within a homogeneous bed. (F) View partially cross-fan, showing erosive contact and lensing relationships between two beds.*

modification during surface inactivity. Such events probably could also partly rework the fine matrix of debrisflow and sheetflood deposits, but the rarity of clast-supported gravel lags (see facies *Gmo* below) suggests that surface winnowing was infrequent.

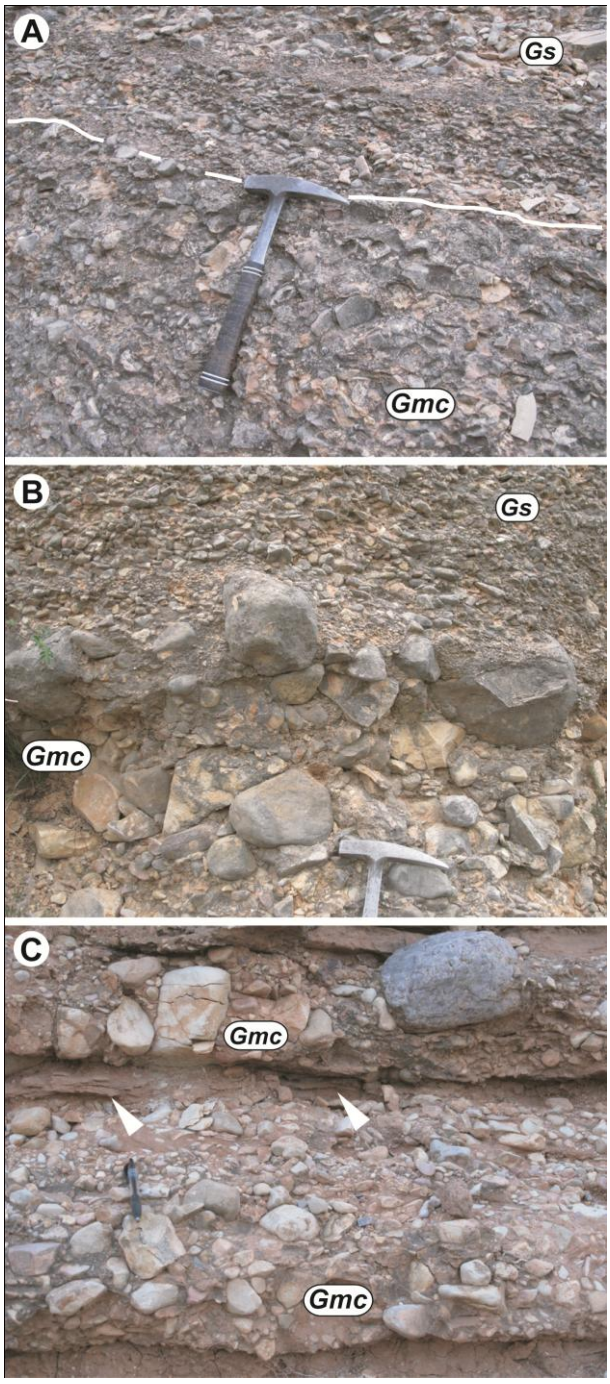

Figure 12 *- Debrisflow deposits in proximal LFU outcrops (facies Gmc); hammer for scale is 32 cm long; pen is 15 cm long. (A) Poorly sorted, massive, matrix-rich to matrix-supported debrisflow bed overlain by stratified sheetflood conglomerates (facies Gs). (B) Concentration of cobbles at the lateral margin of a debrisflow lens, indicating probable preservation of a lateral levee; flow direction to the left and towards the reader. (C) Massive, poorly sorted debrisflow beds in proximal outcrops of section 5, along the transition between LFU and UFU; note the abundance of fine-grained matrix, probably indicating initial supply of mud-sized sediment to the fan, and discontinuous, amalgamated, thin sandstone beds (facies Sm; white pointers).*

Facies Gmo (Openwork massive conglomerates)

This facies consists of rare isolated lenses of clast-supported, fine pebble to coarse cobble gravel, variable in thickness from a few clasts up to ~20 cm, and a few dm up to a couple of metres in width (Figs. 13B and C). Basal surfaces are commonly irregular and cut into underlying deposits. Openwork fabrics are common in predominantly cobbly units, whereas pebbly units sometimes contain a patchy granule to sandy matrix. Crude to distinct normal grading and a moderate *a(t)b(i)* imbrication upslope are present especially in coarser-grained units.

The sedimentology and geometry of this facies point to the action of sediment-deficient water flows in winnowing the fine matrix of mass-flow and hyperconcentrated-flow deposits (Blair & McPherson, 1994; Blair, 1999b; Moscariello *et al.* 2002). Ephemeral runoff was generally confined to small, shallow gullies and rills that extended downfan, as indicated by the cross-fan orientation of gravel lenses at outcrop. Gravel fractions beyond flow competence were partly reoriented or intermittently transported over short distances; the patchy, coarse-grained matrix probably results from inflitration during flow recession. Most of these deposits represent secondary processes that did not contribute to fan aggradation, but coarser-grained, dominantly cobbly lenses with normal grading and good imbrication might have resulted from active bedload deposition in energetic runoff events.

5.4.2. Stratigraphic architecture

Lower fan strata are characterized by prevalenct gravelly deposits and subordinate sandstones (facies *Gs* and *Sl*) from poorly confined to unconfined water flows with variable sediment concentrations. The architecture of the system in this lower stratigraphic interval consists of vertically aggrading, conformably stacked strata without major scours, channel bodies or large-scale inset geometries (Figs. 5, 10A,B and 14A). Superposed on this general trend are a poor facies organization and a recognizable tectonic signal at system scale. These features are consistently observable in both proximal and distal fan domains. However, the most distal 200-300 m of the fan have not been exposed by erosion to the west and south of the Prado area; the transition from distal fan to floodbasin is thus not observable for the LFU.

The greatest volume of coarse-grained deposits is represented by facies *Gs* conglomerates, in plane to broadly lenticular strata inclined according to the gradient of the depositional surface, as typical for alluvial fans (Blair & McPherson, 1994). The lack of distinct, medium- to large-scale erosive surfaces and channel bodies, and the laterally extensive geometry of most conglomerate beds, together indicate prevailing transport and deposition from shallow sheetfloods. Each flash-flood involved broad fan sectors and deposited gravel sheets and thin sand layers. Bedding discontinuities and cross-cutting relationships are recognizable in cross-fan exposures and were probably controlled by the irregular fan topography (cm- to dm-scale) due to dishomogeneous gravel deposition and grain-size contrasts. Most floods tended to follow deeper pathways around previously deposited gravel sheets and away from the coarsest deposits, which offered higher resistance to flow. Sedimentation focused along flow pathways and evened out the surface, filling topographic lows.

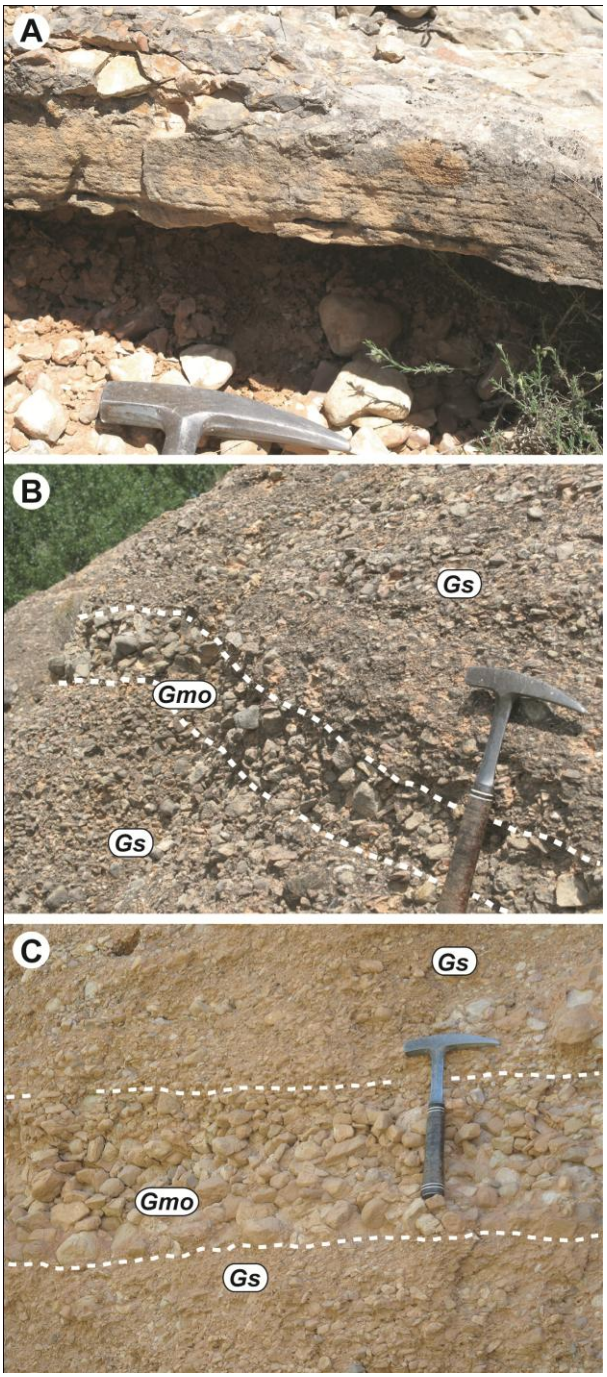

Figure 13 *- Facies related to reworking and deposition by secondary, low-discharge flood events in the LFU; hammer for scale is 32 cm long. (A) Close up of plane-laminated sandstones (facies Sl). (B) and (C) Views partially cross-fan (paleocurrents away from observer, to the right) of clast-supported, openwork, well-sorted pebble to cobble lenses (facies Gmo).*

The lack of tractive fabrics and structures in facies *Gs*, and prevalent features indicating deposition from highly concentrated clast dispersions at basal flow-layers, suggest that fan aggradation occurred only during very energetic, sediment-laden floods. These occurred with a long enough periodicity to consent catchment recharge with coarse regolith, which was bulked by exceptional runoff events over the steep highland slopes (e.g. Meyer & Wells, 1997; Moscariello *et al.*, 2002). The general lack of erosion is probably related also to high sediment concentrations, close to the capacity limit of most flows. The subordinate occurrence of

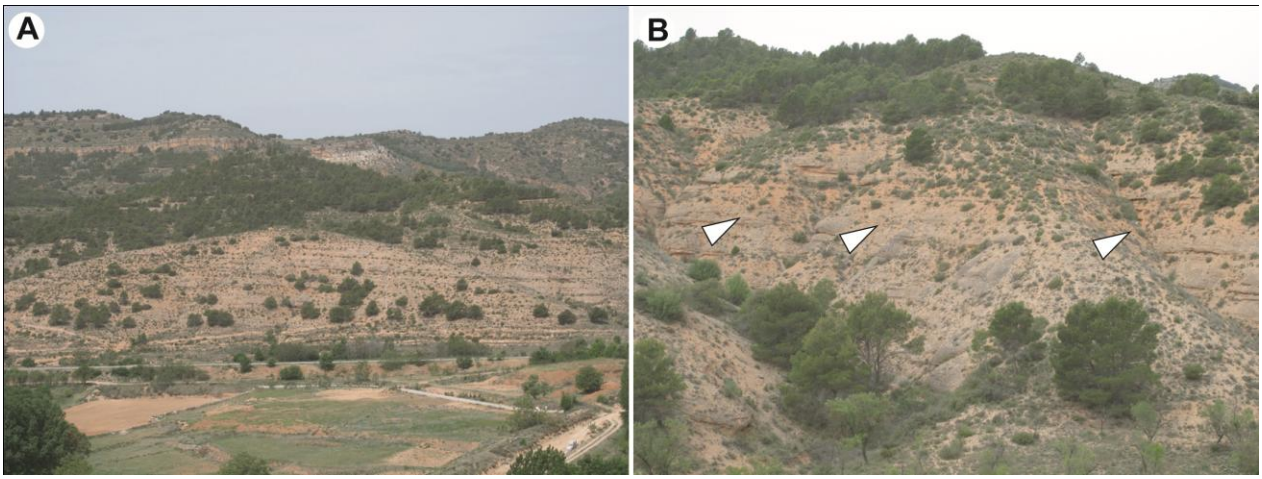

Figure 14 *- Views of proximal fan outcrops, west of the Rio Turia. (A) Cross-fan view of fan proximal LFU strata along the road N-313 to Villel, showing lateral continuity and the absence of incised channels; note the upward increase in arboreal vegetation, into the stratigraphic domain of the fine-rich surfaces of the UFU. (B) Section 4, transitional interval between LFU and UFU (white pointers) with gradual increase in fine-clastic component.*

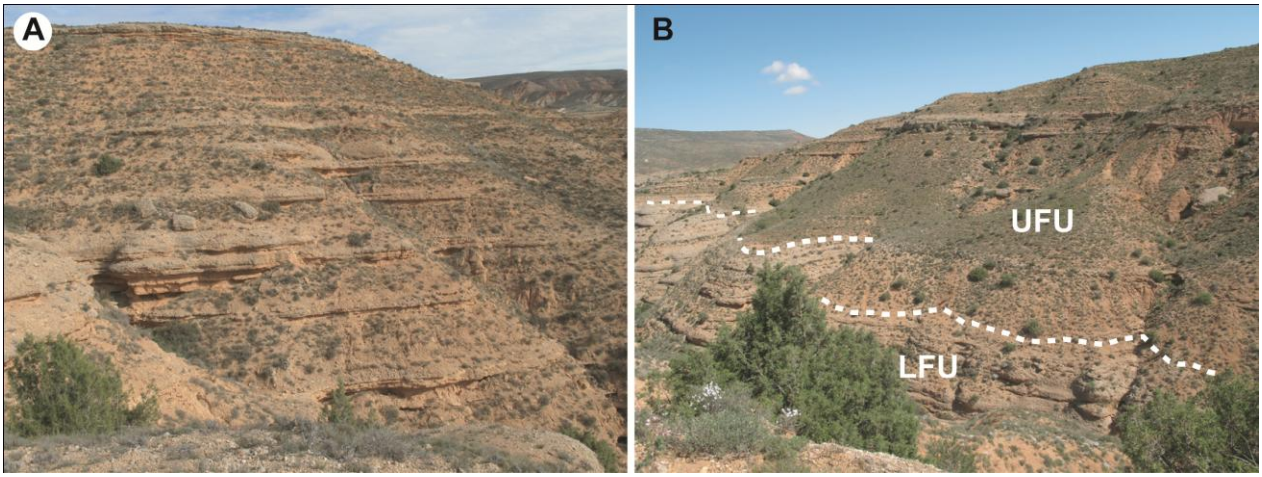

Figure 15 *- View of UFU outcrops; in both photos, paleotransport downfan is towards the right. (A) Top, distal portion of section 1; note regular alternation of thick, mudstone packages (mostly vegetated) and relatively thinner, conglomerate and sandstone packages. (B) Medial outcrops of section 2, north face; white stippled line traces the sharp stratigraphic transition between the gravel-dominated LFU and the mud-dominated UFU.*

openwork conglomerate lenses (facies *Gmo*) and plane-laminated sandstones (facies *Sl*) indicates that floods with lower discharge and sediment loads could extend up to the distal fan surface, but did not play a significant role in fan aggradation.

The generally planar, conformable stratal architecture with laterally extensive stratification is recognizable also in proximal fan outcrops west of the Rio Turia (Figs. 14A,B and 21C). No large-scale inset geometries or channel fills are observed, nor laterally confined facies associations. Such features would be indicative of incised channels extending onto the fanhead area (Bull, 1977; Blair & McPherson, 1994; Blair, 1999b; Went, 2005; Harvey, 2011). Their absence implies that sediment transport was not focused over restricted fan sectors, since main floods were not channelled within a proximal incised channel but expanded over a relatively wide surface directly from the catchment outlet. This inference is supported by the dominance of

sheetflood deposits, and explains the lateral invariance of stratal patterns in medial and distal outcrops. Alluvial-fan systems similar to the LFU in sedimentology and architecture have been reported from the rock record by Allen (1981), Ballance (1984), Wells (1984) and Flint and Turner (1988).

The minor presence of debrisflow deposits in the LFU suggests that sediment evacuation from the catchment by cohesive mass flows was infrequent at this stage of fan evolution. Their limited occurrence to the proximal fan domain and their absence in distal outcrops indicate that occasional debrisflows involved only low sediment volumes, since debrisflows are frequently observed to attain runouts of several kilometers over modern fans, contributing to aggradation also in medial and distal segments (Sharp & Nobles, 1953; Jackson et al., 1987; Hubert & Filipov, 1989; Blair & McPherson, 1994, 1998; Matthews et al., 1999; Moscariello & Deganutti, 2007).

On a large scale, the stratal architecture in the LFU is characterized by a gradual change in average bed dips, most evident along proximal outcrops, which expose the thickest stratigraphic successions belonging to the LFU phase. Over a stratigraphic interval of ~60 m in the lowest accessible deposits, dips reverse from a subtle inclination (~1-2°) to the northwest, in the direction of the bounding Teruel Fault, to an inclination of ~4-5° toward the distal fan domain and the Prado area, in the east and southeast. The latter value remains constant in the uppermost LFU and in the basal levels of the Upper Fan Unit. This fanning out of dip values towards the source area is consistently measurable in proximal sections (Fig. 8) and clearly points to syndepositional tectonic tilting of the active fan surface (*growth strata*; Anadón et al., 1986; Burbank *et al.*, 1996; Aschoff & Schmitt, 2008), probably due to dip-slip dislocation of the boundary fault zone and hanging-wall-block rotation along the adjacent basin margin.

5.5. UPPER FAN UNIT (UFU)

5.5.1. Facies analysis

Facies Mc (Clayey mudstones)

This mudstone facies comprises approximately half the volume of medial and distal domains of the Upper Fan Unit (UFU), and is a subordinate but widespread component of proximal outcrops (Figs. 14B and 15). It consists of red to light brown sandy, silty claystones in massive, laterally continuous units, from 10 cm to over 1 m thick, internally featureless with the exception of sparse, centimetric to decimetric rhizoliths and drab haloes, orange to light brown mottling, and blocky fracture patterns (Fig 16A). Upper and lower stratigraphic contacts follow the geometry of coarser-grained strata. Thick mudstone units can comprise discontinuous stringers of weakly to well imbricated pebbles, concordant with the general fan dip (Figs. 16B and 20A), and lenticular segregations of massive, sand-rich clay.

These abundant sediments are interpreted as deposition from mud-laden, mainly shallow, unconfined sheetwash events (Sohn *et al.*, 1999; Nakayama, 1999). The abundance of clay and the relatively steep fan gradients suggest probable bedload transport of mud aggregates (Wright & Marriott, 2007) rather than suspension settling from ponded waters. Clear evidence for runoff processes is provided by interlayered lenticular segregations of sand-rich mud and by imbricated pebble alignments, formed by events which

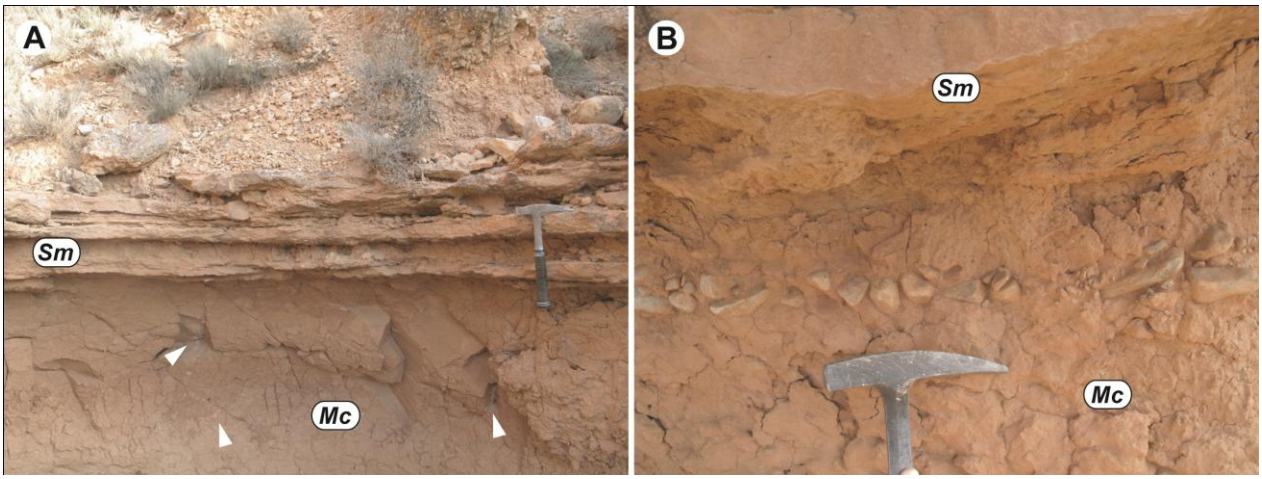

Figure 16 *- Thick mudstone units in the UFU (facies Mc); hammer for scale is 32 cm long. (A) Massive clayey mudstones overlain by amalgamated sandstone beds (facies Sm), section 1, medial domain; note blocky structure and small rhizoconcretions (white pointers). (B) Massive mudstone with a level of well-sorted, imbricated pebbles (above hammer head).*

carried coarser bedload. Vertic processes and pedogenic modification of the clay-rich mass amalgamated the deposits and overprinted them with a blocky ped structure (Retallack, 2001; Driese & Ober, 2005; Kraus & Hasiotis, 2006). The colours of the sediment ground mass and of mottling features suggest well-drained conditions (Kraus & Hasiotis, 2006), probably related to the fan gradient which did not retain water at the surface and to the clay-dominated, poorly permeable texture of the deposits.

Facies Gmm (Massive matrix-supported conglomerates)

This is the dominant coarse-grained facies in the Upper Fan Unit. It composes most of the outcrops in the proximal domain, but it occurs only as extensive coarse-clastic associations in the medial and distal domains (Fig. 17A), alternating to facies *Mc* mudstone units (Figs. 5 and 15). Extensive beds are 10-15 up to 90-120 cm thick, commonly amalgamated into packages of matrix-supported to locally clast-supported pebble to fine boulder conglomerates, varying in thickness from a few decimetres to several metres. Beds have weakly erosive to non-erosive bases. Internally, they are commonly ungraded or coarse-tail inversely graded, and clast fabrics are random, except for frequent subhorizontal *ab* planes of oblate clasts (Figs. 17B to E). The matrix is a red, massive, sandy, granule-bearing clay (Figs. 17C to E). Single beds are laterally continuous over distances from tens to a few hundred metres at outcrop; clast-supported segregations of cobbles or boulders are infrequent (Fig. 17A). Some of these conglomerates extend distally into the Prado area, where they abruptly pinch out within mudflat deposits (Abels *et al.*, 2009b), fining out as massive pebbly sandstones.

By analogy with facies *Gmc*, this facies is interpreted as deposition from cohesive debrisflows (Johnson, 1970; Hubert & Filipov, 1989; Blair & McPherson, 1994). The differences with facies Gmc are given by consistently higher volumes of clay-rich matrix, which confers the deposits a distinct red colour internally, and by the notable lateral continuity of beds. These features indicate that most flows probably had a rheology close to Bingham-plastic models, where the matrix played an important role in clast support, and that single events

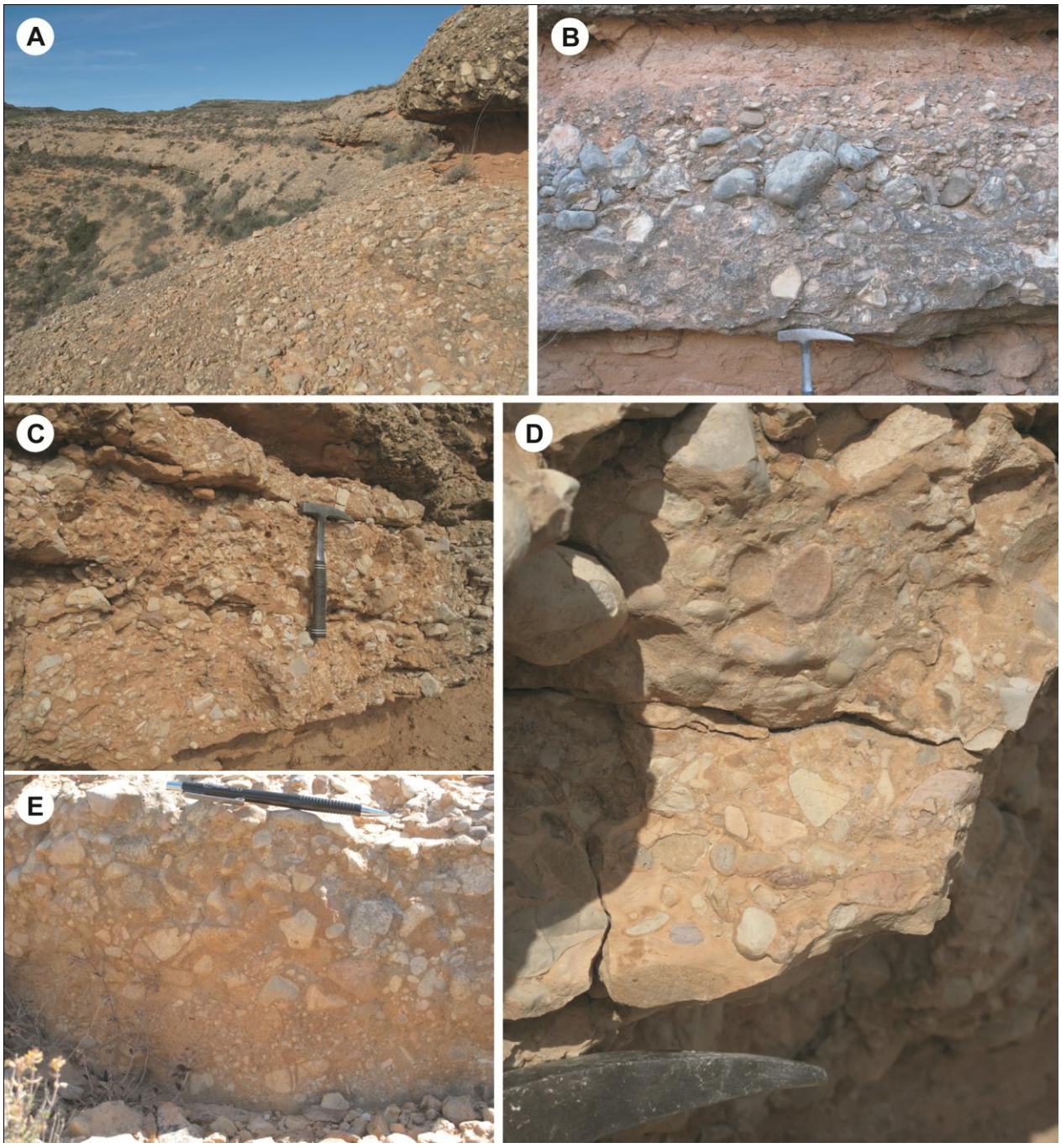

Figure 17 *- Debrisflow deposits of the UFU (facies Gmm); hammer for scale is 32 cm long; pencil is 14 cm long. (A) Section 1, medial fan domain; laterally continuous, amalgamated debrisflow deposits in thick units separated by thick mudstone units (highlighted by vegetation). (B) Detail of an isolated debrisflow bed, section 3, distal domain; note non-erosive base, inverse grading and floating cobbles at bed top. (C) Internal view of beds shown in A; note poorly sorted clasts supported by a clayey matrix and showing random orientations. (D) Detail of basal inverse grading and matrix-support. (E) Section 2, medial sector; thin debrisflow beds with crude inverse grading at the base and matrix support.*

involved much greater sediment volumes, with runout extending over vast sectors of the fan and occasionally over the distal mudflat, where they were halted by the drop in topographic gradient.

Facies Sm (Massive sandstones)

Facies *Sm* appears in a stratigraphic interval of ~8-10 m thickness at the transition between the LFU and the UFU, where it is relatively abundant (Figs. 12C and 18A), and is variously distributed in the upper-fan succession both within thick mudstone packages and in association with conglomerate deposits. It is more abundant within medial to distal outcrops, and subordinate in the proximal fan domain.

It consists of extensive beds and thin, broad lenses of massive, reddish to light brown, pebbly, clayey, medium-fine to rarely coarse sandstones, moderately to poorly sorted, comprising an abundant clay matrix with a distinctive red-brown colour. Beds are never thicker than a few centimetres, and occur in isolation or associated into sandstone packages 20-30 cm thick, rarely up to 100-150 cm (Figs. 18A and B). Basal surfaces are commonly non-erosive or weakly erosive. Sedimentary structures or diffuse internal banding are invariably absent, but these massive sandstones present varieties recognizable by differences in grading and in the distribution of the coarse-tail fractions (Figs. 18C to E). Some beds comprise minor to significant amounts of granules to fine pebble clasts, either concentrated along the basal surface and/or dispersed within the top part of the bed. Besides a coarse-tail normal or crude inverse grading, these beds have a homogeneous, ungraded clayey sand texture. By contrast, sandstones with no dispersed coarse fraction are commonly characterized by crude to well developed normal grading, from medium-coarse sand at the base to fine sand towards the top.

By analogy with facies *Sl* in the LFU, the general traits of facies *Sm* indicate deposition from shallow sheetfloods and poorly confined flows over wide sectors of the fan surface (Tunbridge, 1984; Blair & McPherson, 1994; Blair, 1999b). The complete absence of sedimentary structures and the poorly sorted, matrix-rich textures suggest rapid flow expansion and sediment deposition from highly concentrated dispersions in which bulk particle volumes and interactions damped turbulence and prevented bedload traction (Lowe, 1988; Arnott & Hand, 1989; Benvenuti & Martini, 2002). High amounts of associated clay would have favoured this depositional dynamics. As observed in studies of hyperconcentrated flows in alluvial settings (e.g. Beverage & Culbertson, 1964; Bradley & McCutcheon, 1987), elevated volumes of suspended fines severely damp turbulence in water flows and favour deposition of massive, poorly sorted beds. Recent experiments have demonstrated the role of clay in modifying the vertical structure of initially turbulent water flows (Wang & Larsen, 1994; Li & Gust, 2000; Baas & Best, 2002; Winterwerp, 2006), producing flow dynamics and depositional properties intermediate between those of Newtonian water flows and denser mudflows. Clay-rich flows develop a spectrum of vertical structures and turbulence distributions modulated by clay concentration, flow velocity and the size distribution of the noncohesive sediment fraction (Baas & Best, 2002; Baas *et al.*, 2009). Variable interactions between such factors may thus explain the observed sandstone types. Depending on the initial flow composition and on velocity and internal shear rate prior to deposition (Baas & Best, 2002), some clay-rich flows could have easily supported outsized granules and pebbles through the development of a cohesive, laminar 'plug' above a turbulent basal layer

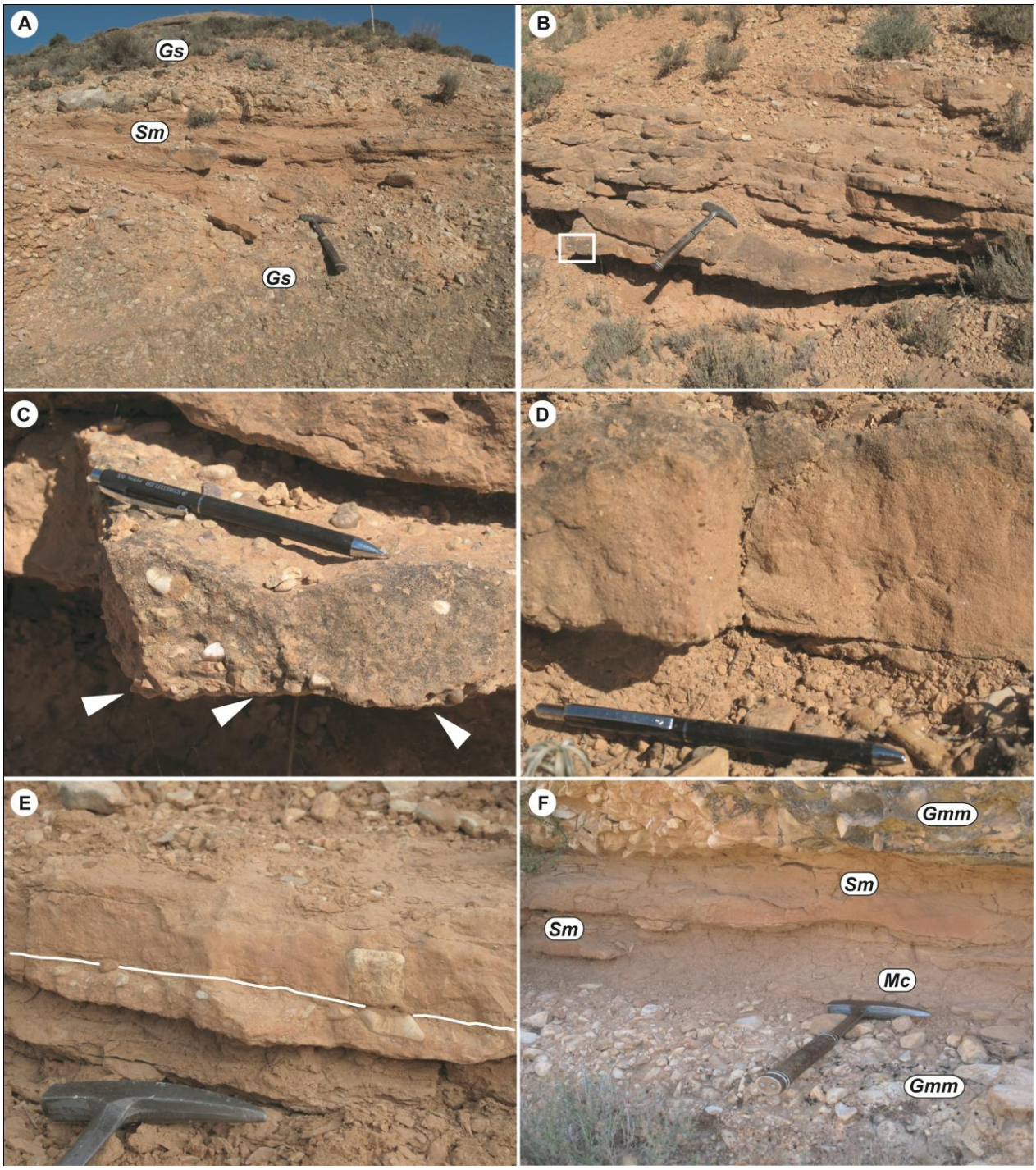

Figure 18 *- Massive sandstones (facies Sm) in the Upper Fan Unit. Hammer for scale is 32 cm long; pencil is 14 cm. (A) Thick association of amalgamated sandstone beds close to the stratigraphic transition between LFU and UFU, section 1, medial domain; vegetation at top outcrop coincides with the base of the first thick mudstone in the UFU. (B) Well-stratified, massive sandstones at the base of the UFU, section 3, medial domain. White inset indicates position of (C) close-up of a thin, massive sandstone bed, with fine-medium pebbles and granules within the basal centimetre (white pointers) and coarse pebbles floating higher within the bed. (D) Massive, normally graded sandstone bed with medium-coarse sand at the base to medium-fine sand at top; note the perfectly planar basal contact. (E) Two thin, amalgamated sandstone beds with floating pebbles at the top (lower bed) and a very coarse pebble (upper bed); both beds probably were deposited by mudflows. (F) Sandstone beds at the base of a cohesive debrisflow (facies Gmm), proximal fan outcrops, section 5; the upper sandstone bed(s) probably deposited by diluted flows surging ahead of the main, concentrated debrisflow body. Note continuous mudstone unit at the base of the coarse-clastic association.*

(*transitional* to *quasi-laminar plug flows* of Baas *et al.*, 2009). Slightly lower clay concentrations and/or higher flow velocities would have prevented the formation of a cohesive layer of relatively high competence, and would have enhanced turbulence along the basal flow layer, leading to a normal vertical distribution of grain sizes in the flow and a non-stratified, but normally graded deposit (*turbulent flows* to *turbulence-enhanced transitional flows* of Baas *et al.*, 2009). On the other hand, some flows with particularly high initial clay contents would have developed a plastic rheology controlled by matrix strength and viscosity, and would have behaved as typical debrisflows (Pierson & Costa, 1987; Major & Pierson, 1992; Fig. 18E). In fact, sandstone beds immediately underlying or overlying debrisflow conglomerates of facies *Gmm* may have been related to the development of fluidal, hyperconcentrated-flow phases in the longitudinal development of the flood (Pierson, 1986; Sohn *et al.*, 1999; Fig. 18F).

Facies Gmg (Massive, normally graded, matrix-rich conglomerates)

Facies *Gmg* is represented by matrix-rich to matrix-supported, fine pebble to coarse cobble conglomerates, commonly associated to facies *Gmm* or *Sm* as broad, erosively based lenses with thickness ranging from 10-15 cm up to ~50 cm. Internally, beds lack sedimentary structures and are commonly graded, with coarser cobbles and pebbles segregated along the basal surface. Coarse clasts frequently float in the matrix and are imbricated upstream with good *a(p)(b(i)* or *a(t)b(i)* fabrics (Fig. 19). The matrix consists of a massive, unstratified granule-bearing, sandy, clay mud or muddy sand. Basal surfaces are strongly erosive when cutting mudstone or sandstone beds (Fig. 19), but weakly erosive over conglomerates.

This facies presents strong analogies with debrisflow deposits (see facies *Gmm*), from which it differs because of very well developed normal grading and imbricated clast fabrics, strongly erosive bases, and a lack of outsized cobbles or boulders. These features indicate significant residual turbulence and a lower strength and viscosity of the matrix, with limited competence and a tendency for coarser clasts to be rolled or dragged along the lower flow boundary. Such flows probably exhibited a pseudoplastic rheology, with viscosity decreasing as shear rates increased. During active flow, the coarser bedload was not fully supported by the matrix and became concentrated toward the base, were it was transported by partial traction. As flows decelerated, turbulence was quickly suppressed and the flow halted also by gradual acquisition of strength thanks to the abundant clay in the mixture, as testified by pebbles and granules dispersed within the matrix. Similar deposits can thus be attributed to suspension-dominated hyperconcentrated flows. They have been described from ancient and modern alluvial, proglacial and volcanic settings (e.g. Bluck, 1967; Lawson, 1982; Shultz, 1984; Pierson, 1985; Bøe & Sturt, 1991; Fielding & Webb, 1995), and are commonly interpreted as water-diluted, fluidal varieties of debrisflows ('*fluidal sediment flows*' of Nemec & Steel, 1984).

Facies Gs

Facies *Gs* conglomerates are present in subordinate volumes in the UFU, commonly as shallow gully fills (Fig. 20A) and occasionally interbedded with debrisflow deposits (Fig. 20B), both in proximal and distal outcrops. Compared to its occurrence in the LFU, facies *Gs* here is not characterized by the superposition of fining-upward divisions into composite beds, but by homogeneous beds of poorly to moderately sorted,

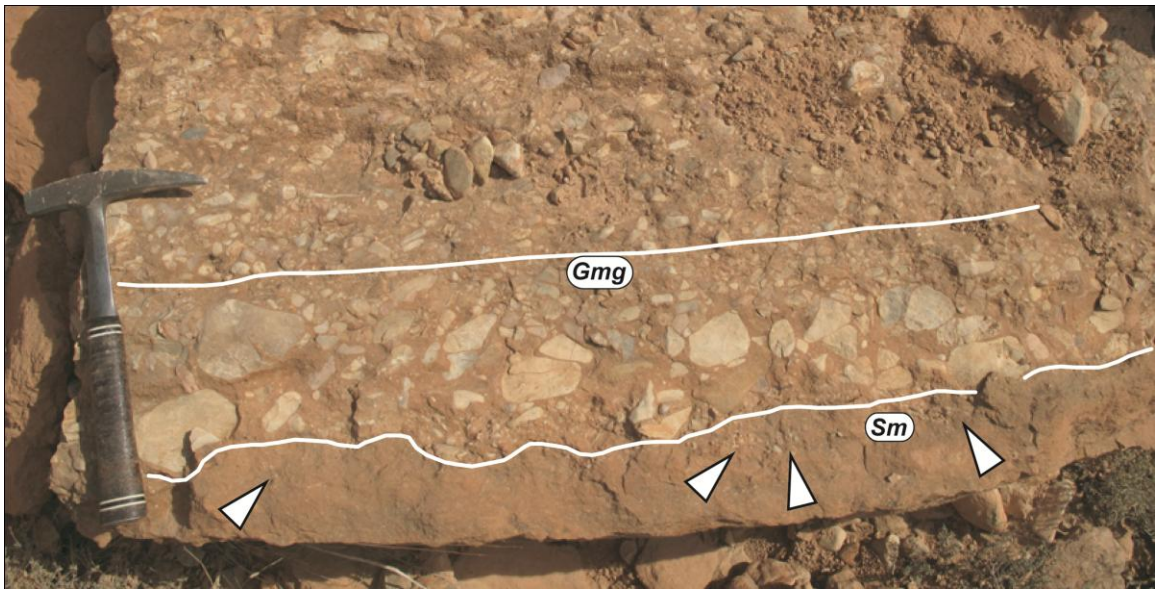

Figure 19 *- Facies Gmg matrix- to clast-supported conglomerates from probable hyperconcentrated flows, section 1, medial domain; hammer is 32 cm long. Note the basal erosive surface, coarse-tail normal grading, high-angle clast imbrication indicating a dense fluid medium, and clay-rich matrix. Note also underlying massive sandstone (facies Sm) with dispersed pebbles towards the top (white pointers).*

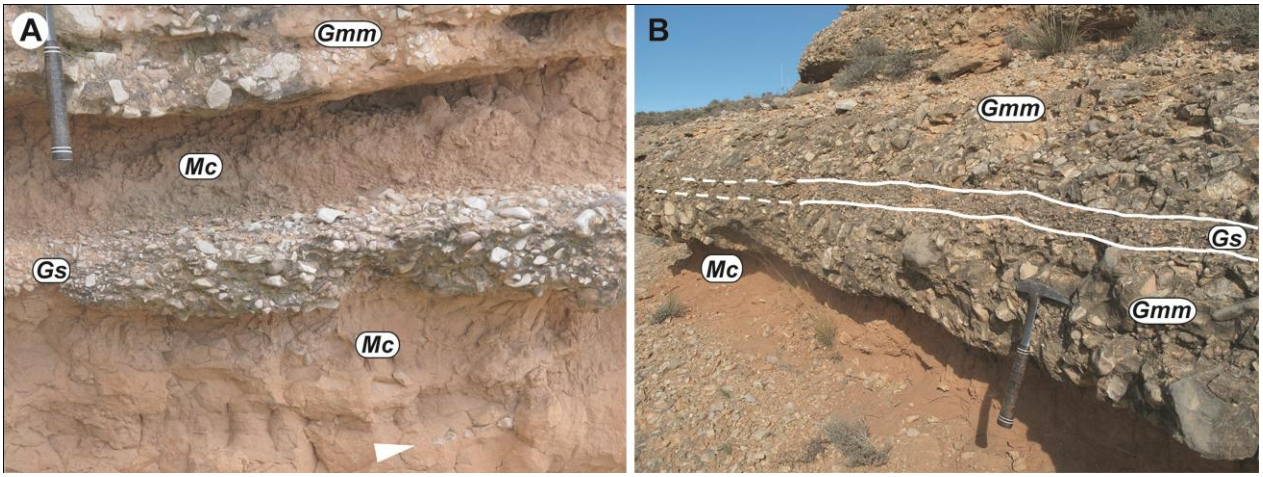

Figure 20 *- Facies Gs clast-supported, well-organized conglomerates in the UFU; hammer is 32 cm long. (A) Isolated gully fills forming gravel lenses within a thick mudstone unit of facies Mc, section 1, distal domain; note pebble alignment within the mudstone (white pointer). (B) Hyperconcentrated-flow deposits interbedded to debrisflow deposits; section 1, medial domain.*

clast-supported granule to fine cobble gravel with a clayey to sandy matrix. Well developed *a(p)* or *a(p)(b(i)* imbrication and the absence of tractive structures imply very rapid deposition from highly concentrated, shearing sediment dispersions (Rees, 1968; Lowe, 1988; Benvenuti & Martini, 2002). The minor volumes and lower clast sizes compared to the same facies in the LFU indicate that the magnitude of the relative floods was much reduced in this phase, and deposition was mainly limited to small gully fills. More extensive, thin beds associated with *Gmm* deposits probably represent hyperconcentrated, fluidal phases accompanying major debrisflow events (e.g. Scott, 1988; Sohn *et al.*, 1999; Cronin *et al.*, 2000).

5.5.2. Stratigraphic architecture

The medial and distal portions of the UFU present an unusually organized architecture for alluvial fans, with a vertical alternation of distinct, fine- and coarse-grained clastic packages, varying in thickness from ~1 to 5 m, laterally correlatable over hundreds of meters downdip and between different outcrops across fan (Figs. 5, 15 and 17A). Facies are differently distributed among these units. Fine-grained packages are composed mainly of facies *Mc* mudstones, with minor sandstone and conglomerate interbeds (facies *Sm* and *Gs*). Coarse-grained units consist mainly of facies *Gmm* conglomerates, with associated *Gmg*, *Gs* and *Sm* interbeds. At outcrop, the UFU is clearly distinguishable from the LFU because of its dominant clay-rich deposits, which confer a general reddish color, a recessional topography (Figs. 5 and 15B), and a stepped appearance due to the interlayered conglomerate packages. Muddy units are also easily colonized by seasonal vegetation (Figs. 15A and 17A), whereas conglomerates of the LFU form steep barren surfaces (Figs. 5 and 10A).

Proximal outcrops of the UFU are more uniformly dominated by coarse-grained debrisflow and hyperconcentrated flow deposits (facies *Gmm*, *Gmg* and *Gs*), and thus less well distinguishable from proximal units of the LFU (F9g. 14B). However, greater volumes of interbedded sandstones and especially mudstones (facies *Sm* and *Mc*) are present also in the proximal UFU compared to the LFU, and give it a clearly bipartite sediment distribution.

The abrupt stratigraphic transition from the LFU to the UFU, especially in medial and distal strata, is a laterally traceable surface dipping toward the east and southeast in conformity with fan strata (Figs. 5 and 15B). In proximal outcrops the distinction is less well visible due to the dominant coarse textures of proximal deposits. Next to the very evident increase in clayey sediments, the transition between the two fan units is accompanied by an increase in the volume of sandstones. Whereas the LFU presents only rare sandstone interbeds, these are a secondary but common element to the coarse-clastic packages of the UFU, and occur as broad lenses or amalgamated beds also within muddy units. Sandstone abundance increases over a stratigraphic interval of ~8-12 m thickness, recognizable in all proximal and distal sections, characterized in particular by the occurrence of relatively thick (~60-70 to 150 cm) associations of massive sandstones (facies *Sm*; Fig. 18A). This stands in sharp contrast with the rare, well-laminated sandstones of the LFU (facies *Sl*).

No fining- or coarsening-upward trends are superposed to these alternations of coarse and fine clastic facies in ther UFU. As mentioned, the only notable textural trend is radial, with lower volumes of sandstones and especially claystones in proximal sections. Facies analysis reveals the fundamental role played by clay also in the mechanics and extent of gravel transport. Debrisflow beds are characterized by matrix-support and great extent over vast fan sectors; the thickest units are correlatable between different sections. This suggests that debrisflows originated from catchment floods which bulked elevated volumes of fines. Flows attained great runout up to (and occasionally beyond) the distal fan domain because they were supplied with abundant fines, thus maintaining sufficient thickness and inertia over long distances (Moscariello *et al.*, 2002; Blair, 2003). The volumetric dominance of fine matrix tended to prevent frictional clast interlocking at flow margins, and thus enhanced the runout potential (Blair & McPherson, 1998; Blair, 2003). The role of abundant clay in governing sedimentary processes is evident also in the type of hyperconcentrated-flow

facies of the UFU (*Sm* and *Gmg*), deposited by dense, suspension-dominated, clay-rich viscous slurries probably transitional to fluidal debrisflows.

Corrected dip measurements show that fan strata maintain an inclination of 4-5° at the base of the UFU, conformable with the upper portion of the LFU. Dip values gradually decrease to ~2-3° towards the top of the succession, and consistently less in the most distal outcrops, where the concave fan profile lost gradient (Blair & McPherson, 1994; Harvey, 1990). Debrisflow beds which interfinger with distal mudflat strata of the Prado Section have bedding attitudes of 20°/6°, consistent with the local tilting of the hanging-wall block. This confirms the presence of a flat, distal floodbasin where high-volume flows halted after a final runout of a few hundred metres.

As in the LFU, there are no apparent unconformities in the UFU, nor is there any evidence for large-scale channel incision or inset architectures in proximal and medial domains (Figs. 5 and 14B). Clastic packages are vertically stacked into planar, laterally continuous units dipping downfan over the entire system. Limited evidence for incision on decimetre to metre scale is given only by a few small gully fills with granule to pebble conglomerates of facies *Gs* in medial and distal outcrops. This implies that a proximal feeder channel and midfan incision did not develop during this late phase of fan aggradation.

5.6. DISCUSSION

5.6.1. Bipartite system architecture

Alluvial-fan catchments are characterized by high relief, limited extent and poorly integrated drainage (Blair & McPherson, 1994). As a consequence, they generate flash-floods with sharp discharge peaks and commonly overloaded by high amounts of debris. Fan construction thus occurs mainly through mass flows, hyperconcentrated flows and ephemeral sheetfloods which tend to produce poorly sorted, spatially disorganized deposits. The well-known poor architectural organization of alluvial fans stands in typical contrast to the high complexity of sediment distribution within river systems (Blair & McPherson, 1994; Smith, 2000; Moscariello, 2005). The Villastar fan, on the other hand, presents an unusual, bipartite stratigraphic architecture and facies distribution (Fig. 5).

The older Lower Fan Unit is dominated by coarse-grained facies, especially gravel sheets (facies *Gs*) deposited from sediment-laden sheetfloods and poorly confined water flows. Associated sandstones and openwork conglomerates (facies *Sl* and *Gmo*) imply occasional reworking by water flows with minor sediment load. Debrisflow deposits (facies *Gmc*) are significant only in proximal fan outcrops, within a radius of ~1.5 km from the estimated apex area. They consist of thin beds with reduced lateral extent, implying that cohesive mass-flows did not reach volumes sufficient to extend their runout over wider, more distal fan sectors, and contributed little to aggradation during this phase. Rare mudstone lenses and interbeds indicate the presence of fines within the catchment. Their scarcity in medial and distal outcrops, however, suggests a low availability of mud to the system, rather than bypass to distal fan surfaces. Coarse deposits of the LFU form a clastic wedge in which stratification and subtle facies distinctions are very well developed on scales from decimetres to metres, due to the complex depositional dynamics of sheetfloods.

However, on a larger scale, conglomerates uniformly compose the outcrops and are only irregularly interbedded by matrix-rich debrisflows proximally, and by sandstones and rare mudstones distally.

The sharp transition to the Upper Fan Unit (Fig. 5) takes place over ~8-10 m in stratigraphy and is marked by a concentration of sandstone beds not observed in other intervals. The Upper Fan Unit presents an uncommon degree of facies organization for alluvial fans, with alternating, conformably stacking, planar coarse- and fine-clastic stratasets, most of them laterally continuous over the whole system. A notable increase in the volume of clay characterizes all facies in the UFU. Most conglomerates were deposited by processes varying from cohesive debrisflows to suspension-dominated, clay-modulated hyperconcentrated flows. The importance of clay is therefore evident in its control on the mechanics of sedimentary processes and on the types of coarse-clastic facies.

Corrected bedding measures show a gradual vertical change in dip trends within the LFU, from a few degrees tilting toward the boundary fault zone in the northwest, up to ~4-5° dips towards southeast at the transition with the UFU. The upper fan strata maintain this inclination, except for a slight dip reduction towards the top of the unit. Both fan units, however, present no detectable unconformities, nor evidence for large-scale incised channels or erosional features, except for a few small gully fills in the medial and distal portions of the UFU.

5.6.2. Controls on alluvial-fan sedimentation

Variations in vertical dip of alluvial-fan strata indicate syndepositional tectonics and the formation of growth strata through dip-slip activation of the Teruel Fault zone. Classic examples of contemporaneous deposition and tectonic deformation in alluvial fans have been described from thrust-faulted margins of foreland basins (Anadón *et al.*, 1986; Nichols, 1987; DeCelles *et al.*, 1987; Leleu *et al.*, 2009). In foreland settings, progressive accommodation loss is caused by basement uplift and increased proximal-fan gradients, and generates series of erosive surfaces radiating away from the tectonic hinge zone (*progressive unconformity*; Riba, 1976; Anadón *et al.*, 1986; Aschoff & Schmitt, 2008). In the case of the normal Teruel Fault, active tectonics generated local accommodation, and uplift enhanced sediment yield and transport potential (Allen & Densmore, 2000). Steady sediment supply and preservation potential over the gradually back-tilted fan surface maintained aggradation during fault activity, and counteracted the formation of angular unconformities (Patton, 2004; Aschoff & Schmitt, 2008).

Catchment incision and progressive basement denudation accompany long-term aggradation of alluvial fans at extensional tectonic margins (Jackson & Leeder, 1994; Allen & Densmore, 2000; Gawthorpe & Leeder, 2000). The Villastar Fan preserves clear evidence of basement unroofing as a vertical change in the petrographic composition of conglomerates (Table 1), but especially in the evolution of its general architecture and of sedimentary processes. The topmost 200 m of basement relief consist of Late-Cretaceous dolostones of the Alatoz and Villa de Vés Formations; minor volumes of calcarenites, micritic limestones and dolomitic marlstones are interbedded mainly in the upper part of the Alatoz Formation (Figs. 4A and B). Clast counts show a prevalence of coarse-crystalline dolostones in the lower strata of the LFU, followed by a progressive upward increase in fine-grained dolostones and limestones and of bioclastic calcarenites.

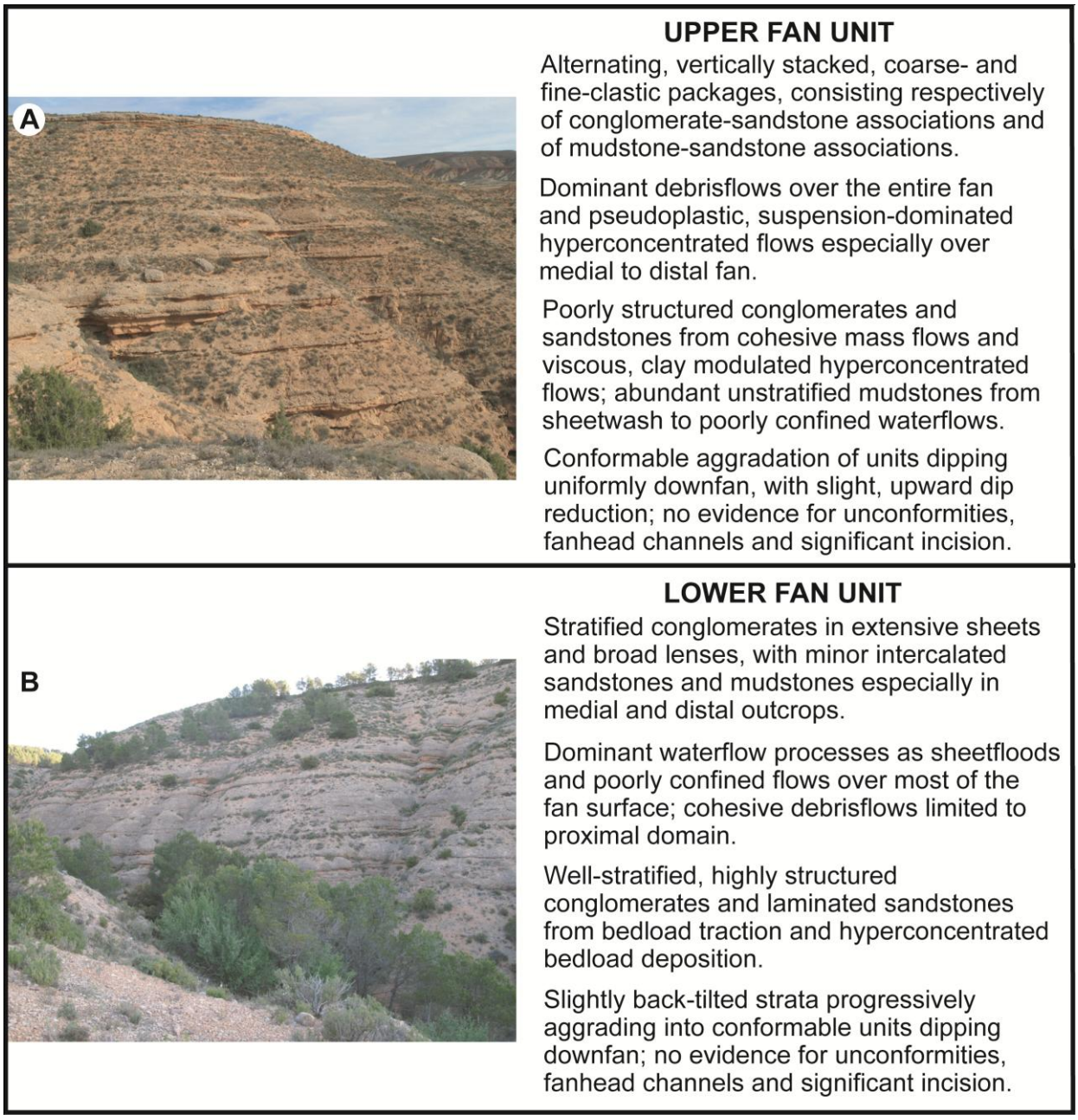

Figure 21 *- Comparative overviews of Lower Fan Unit and Upper Fan Unit. (A) Downdip view of distal outcrops, section 1. (B) Strike-oriented view of stratified sheetflood conglomerates, proximal outcrop to the west of Rio Turia.*

On the other hand, dolomitic marlstones from the upper Alatoz Formation represent only a minor clast percentage in LFU conglomerates. As confirmed by surveys (Figs. 4B and C) and grain-size analyses of colluvium from the corresponding outcrops (Figs. 9A and B), these carbonate lithologies produce mainly coarse gravelly debris upon weathering. The fine-grained fractions of the surficial colluvium consists mainly of granules and coarse sand (*grus*), probably from disaggregation of calcarenites in the Alatoz Formation and of crystalline dolostones in the Villa de Vés Formation. However, sand constitutes only a secondary fraction of the colluvium, because of rapid dissolution of small carbonate particles. A minor amount of silt was generated probably by disaggregation and decementation of marlstones and micritic limestones in the Alatoz Formation. The measured clay content is negligible.

The sedimentology of the Lower Fan Unit thus reflects catchment evolution at times when incision of the local basement exposed only Cretaceous carbonates. The great availability of carbonate gravel and the subordinate abundance of sand- and mud-grade material in the colluvium match the relative abundances of conglomerates, sandstones and mudstones in the LFU. Sedimentary events were triggered by floods which bulked mainly heterometric coarse debris. Deposition took place from high-concentration gravel dispersions and sand traction in sheetfloods, which implies bedload segregation and traction in clear-water flows of various discharge and competence. High-discharge floods deposited broad cobble sheets but could not bulk significant amounts of fines. This is confirmed also by the low volume of coeval debrisflow deposits restricted to the proximal domain: scarcity of matrix-grade material reduced the potential to trigger cohesive mass-flows and to sustain them over significant distances.

The abundance of sandstones at the transition between LFU and UFU indicates a sudden availability of sand sources as catchment incision progressively exposed the poorly cemented, fine to medium sandstones of the upper Utrillas Formation (Figs. 4C,D and 9D). Interbedded sandstones in the underlying, Early-Cretaceous El Collado Formation probably also contributed a relatively steady supply of sand, which explains the diffuse sandstone beds in the UFU. This is confirmed by the significant sand fraction in colluvial samples from outcrops of these formations (Fig. 9E). However, the most important change in sediment supply consisted in the great availability of mud during aggradation of the UFU. While Cretaceous formations continued to supply carbonate gravel, catchment incision exposed the whole suite of Early-Cretaceous and Late-Triassic mudstone formations (Utrillas and El Collado formations, Arcillas de Cofrentes and Arcillas Yesiferas de Quesa), mainly composed of silt and clay (Fig. 9C to F). From this point in catchment evolution, sedimentary processes on the fan are essentially controlled by the high amounts of clay mobilized probably by every flood, as observed also at present in proximity of Triassic outcrops. Thick claystone units of the UFU indicate deposition by shallow sheetwash events with limited competence. By contrast, most runoff events with low discharge could not leave any sedimentological signature during the LFU phase, except for rare siltstone lenses and drapes, because of the reduced availability of mud in carbonate formations of the basement. During the development of the UFU, major floods with the competence to entrain gravel were prone to generare large, cohesive debrisflows and a variety of suspension-dominated hyperconcentrated flows with transitional rheologies (Figs. 18 and 19), thanks to high volumes of mixed clay. Even at moderate concentrations, clays have the property to modify the structure and rheology of turbulent flows through the formation of electrostatic particle networks (Rodine & Johnson, 1976; Pierson & Costa, 1987; Major & Pierson, 1992). Depending on concentration and shear rate, clay-rich flows can acquire and maintain viscosity, buoyancy and incipient strength, thus gaining capacity for coarser suspended load and higher competence at lower flow layers (Beverage & Culbertson, 1964; Baas & Best, 2002; Manville & White, 2003). The transition from biphase hyperconcentrated flows to monodisperse debrisflows is controlled by the amount and composition of fines in the parent flow.

The vertical change of dominant processes and sediments in the Villastar fan is accompanied by a change in radial facies distribution. Whereas massive debrisflow deposits are limited to the proximal domain in the LFU, their fan-wide distribution and correlatability in the UFU are due to the enhanced runout and

expansion fed by large volumes of fines (Iverson *et al.*, 1998; Blair, 2003). Coarse-grained hyperconcentrated flows from high-discharge floods also distributed high volumes of poorly sorted sediment over broad fans sectors. Finer, sandy hyperconcentrated flows are generally not correlatable between different outcrops. Their lower thickness and competence are probably related to floods of lower discharge which could not affect large fan sectors. Mudstones could be transported over the whole distal fan surface and form the highest volume of deposits in the UFU; their reduced volume in proximal sections is probably related to bypassing of the steeper fan surfaces by shallow water flows. Although alluvial fans are typically made of coarse- to very coarse-grained deposits (Blair & McPherson, 1994), the occurrence of mud-dominated fans is reported from both present and ancient systems (Legget *et al.*, 1968; Wasson, 1977; Nakayama, 1999) where mud production reflects particular weathering conditions or the direct mobilization of pelitic sedimentary rocks.

The almost constant dip in UFU strata suggests either a reduction in tectonic activity or a marked increase in sedimentation rate to keep pace with accommodation creation during development of the UFU (Patton, 2004). The first hypothesis is favoured here, in view of the slight upward reduction in the dip of UFU strata, which indicates basin-margin onlap by progressively less steep fan surfaces and probably distal aggradation forced by base-leve rise in an endorheic setting (Anderson & Cross, 2001; Nichols, 2004, 2005). However, catchment expansion continued, as indicated by new clasts of micritic limestones, marlstones and purple cherts in the uppermost conglomerates of the Upper Fan Unit. These lithologies were sourced by Jurassic carbonates exposed immediately northwest of Triassic outcrops.

The vertical succession of facies produces an overall fining-upward trend in the stratigraphy of the Villastar fan. This has generally been interpreted as a result of variable subsidence-uplift patterns during fan aggradation in the literature, with the generation of classical 'fan megasequence' models related to palaeotectonics at basin margins (Heward, 1978; Steel et al., 1977; Crews & Ethridge, 1993). However, in view of what has been discussed above, a cautionary note is warranted to consider basement geology as an alternative interpretation to large-scale lithological trends in alluvial-fan successions.

Finally, the striking lateral continuity of fan strata and the absence of large-scale incisions and fanhead channels (Figs. 5, 10, 14 and 15), imply a mechanism capable of sustaining system-wide aggradation over long times. Reduced incision is related to extensive aggradation by debrisflows and sheetfloods, since the presence of an incised fanhead channel would normally focus transport and deposition only over limited fan sectors (Blair & McPherson, 1994; Dühnforth *et al.*, 2007). Regardless of variable tectonic activity, alluvial fans are subject to autogenic cycles of trenching and aggradation related to intrinsic slope-transport thresholds, also when developing under steady conditions (Schumm *et al.*, 1987; Van Dijk, 2009; Clarke *et al.*, 2010). During the Late Miocene, the Teruel Basin was topographically isolated and internally drained. Steady aggradation and essentially complete preservation of alluvial and lacustrine deposits are typical of closed continental basins, because of the continuously rising depositional surface and associated base level (e.g. Soria *et al.*, 1998; Lowenstein *et al.*, 2003; Nichols, 2005; Carroll *et al.*, 2010). Alluvial fans in similar basinal settings are also characterized by uniform aggradational patterns and great stratal continuity, accumulating essentially continuous sedimentary records (Anderson & Cross, 2001; Nichols, 2004, 2005).

5.7. CONCLUSIONS

Research on alluvial fans has highlighted the importance of catchment geology to understanding sedimentary dynamics, especially in consideration of the role that variable source lithologies may have on regulating sediment transport and composition. Most such studies have been carried out on Quaternary and presently active systems (Harvey, 1990; Kostaschuk *et al.*, 1986; Blair, 1999a; Webb & Fielding, 1999; Moscariello *et al.*, 2002). Only a few examples from the ancient rock record validate the inference that even coeval fans developing along the same tectonic margin could develop contrasting sedimentological characters if supplied by different sources (Nichols & Thompson, 2005; Wagreich & Strauss, 2005). An understanding of relations between catchment geology and alluvial-fan stratigraphy has important implications for subsurface exploration and for revisiting classical models of tectonically or climatically controlled fan evolution.

Thanks to excellent exposures in the Teruel Basin, this study demonstrated the relationship between the long-term sedimentary evolution of a Miocene alluvial fan and the geology of its catchment area. The clearly bipartite stratigraphy of the catchment determined an initial phase of abundant gravel supply from Late Cretaceous carbonate rocks, which corresponded to fan aggradation through bedload deposition from hyperconcentrated sheetfloods and minor, shallow-water flows. As catchment incision affected Early-Cretaceous and Triassic mudstones and subordinate sandstones, the great availability of clay-rich fines triggered an abrupt change in sediment transport by cohesive debrisflows and suspension-dominated, non-Newtonian hyperconcentrated flows. The vertical shift in facies abundance is accompanied by a change in the range of downfan facies distribution, controlled by the different runout potential of transport processes. In spite of evidence for active tectonics along the adjacent basin margin, the essentially complete preservation of sedimentary record in the fan has been granted by dominant aggradation in an endorheic setting, which prevented proximal incision and autogenic reworking.

ACKNOWLEDGEMENTS

This research was funded by grant ALW 815.01.012 of NWO (National Science Foundation, the Netherlands). Poppe L. de Boer is gratefully acknowledged for editorial advice and suggestions on field methods. Jan van Dam, Hemmo A. Abels and José P. Calvo are thanked for discussions on regional geology. I am grateful to Marco G. Benvenuti for initiating me to the complexities of hyperconcentrated flows many years ago.

REFERENCES

Abels, H.A., Abdul Aziz, H., Calvo, J.P. and **Tuenter, E.** (2009a) Shallow lacustrine carbonate microfacies document orbitally paced lake-level history in the Miocene Teruel Basin (Northeast Spain). *Sedimentology*, **56**, 399-419.

Abels, H.A., Abdul Aziz, H., Ventra, D. and **Hilgen, F.J.** (2009b) Orbital climate forcing in mudflat to marginal lacustrine deposits in the Miocene Teruel Basin (northeast Spain). *Journal of Sedimentary Research*, **79**, 831-847.

Adrover, R., Mein, P. and **Moissenet, E.** (1978) Nuevos datos sobre la edad de las formationes continentales neogenas de los alrededores de Teruel. *Estudios Geologicos*, **34**, 204-214.

Alcalá, L., Alonso-Zarza, A.M., Alvarez Sierra, M.A., Azanza, B., Calvo, J.P., Van Dam, J.A., Garcés, M., Van Der Meulen, A.J., Morales, J., Pérez González, A., Sancho, R. and **Sanz Rubio, E.** (2000) El registro sedimentario y faunístico de las cuencas de Calatayud-Daroca y Teruel. Evolución paleoambiental y paleoclimática durante el Neógeno. *Revista de la Sociedad Geológica de España*, **13**, 323-343.

Allen, P.A. (1981) Sediments and processes on a small stream-flow dominated, Devonian alluvial fan, Shetland Islands. *Sedimentary Geology*, **29**, 31-66.

Allen, P.A. (2008) Time scales of tectonic landscapes and their sediment routing systems. In: *Landscape Evolution: Denudation, Climate and Tectonics Over Different Time and Space Scales* (Eds. K. Gallagher, S.J. Jones, and J. Wainwright), Geological Society of London Special Publication, **296**, 7-28.

Allen, P.A. and **Densmore, A.L.** (2000) Sediment flux from an uplifting fault block. *Basin Research*, **8**, 367-380.

Allen, P.A. and **Hovius, N.** (1998) Sediment supply from landslide-dominated catchments: implications for basin-margin fans. *Basin Research*, **10**, 19-35.

Alonso-Zarza, A.M. and **Calvo, J.P.** (2000) Palustrine sedimentation in an episodically subsiding basin: the Miocene of the northern Teruel Graben (Spain). *Palaeogeography, Palaeoclimatology, Palaeoecology*, **160**, 1-21.

Anadón, P. and **Roca, E.** (1996) Geological setting of the Tertiary basins of Northeast Spain. In: *Tertiary Basins of Spain – The Stratigraphic Record of Crustal Kinematics* (Eds. P.F. Friend and C.J. Dabrio), pp. 43-48, Cambridge University Press, UK.

Anadón, P., Ortí, F. and **Rosell., L.** (2000) Neogene Lacustrine Systems of the Southern Teruel Graben (Spain). In: *Lake Basins Through Space and Time* (Eds. Gierlowski-Kordesch, E.H. and Kelts, K.R.), AAPG Studies in Geology, **46**, 497-504.

Anadón, P., Cabrera, L., Colombo, F., Marzo, M. and **Riba, O.** (1986) Syntectonic intraformational unconformities in alluvial fan deposits, eastern Ebro Basin margins (NE Spain). In: *Foreland Basins* (Eds. P.A. Allen and P. Homewood), IAS Special Publication, **8**, 259-271.

Anadón, P., Cabrera, L., Juliá, R., Roca, E. and **Rosell, L.** (1989) Lacustrine oil-shale basins in Tertiary grabens from NE Spain (Western European Rift System). *Palaeogeography, Palaeoclimatology, Palaeoecology*, **70**, 7-28.

Anderson, D.S. and **Cross, T.A.** (2001) Large-scale cycle architecture in continental strata, Hornelen Basin (Devonian), Norway. *Journal of Sedimentary Research*, **71**, 255-271.

Arche, A. and **López-Gómez, J.** (1996) Origin of the Permian and Triassic Iberian Basin. *Tectonophysics*, **266**, 443-464.

Arche, A., López-Gómez, J. and **García-Hidalgo, J.F.** (2002) Control climático, tectónico y eustático en depósitos del Carniense (Triásico Superior) del SE de la Península Ibérica. *Journal of Iberian Geology*, **28**, 13-30.

Arnaiz, I., Robles, S. and **Pujalte, V.** (1991) Correlación entre registro de sondeos y series de superficie del Aptiense-Albiense continental del extremo SW de la Cuenca Vascocantábrica y su aplicación a la identificación de zonas lignitíferas. *Geogaceta*, **10**, 65-68.

Arnott, R.W.C. and **Hand, B.M.** (1989) Bedforms, primary structures and grain fabric in the presence of suspended sediment rain. *Journal of Sedimentary Petrology*, **59**, 1062-1069.

Aschoff, J.L. and **Schmitt, J.G.** (2008) Distinguishing syntectonic unconformity types to enhance analysis of growth strata: an example from the Cretaceous southeastern Nevada, U.S.A. *Journal of Sedimentary Research*, **78**, 608-623.

Aurell, M., Meléndez, G. and **Olóriz F.** (coordinators) (2002) Jurassic. In: *The Geology of Spain* (Eds. W. Gibbons and T. Moreno), pp. 213-253, The Geological Society, London, UK.

Baas, J.H. and **Best, J.L.** (2002) Turbulence modulation in clay-rich sediment-laden flows and some implications for sediment deposition. *Journal of Sedimentary Research*, **72**, 336-340.

Baas, J.H., Best, J.L., Peakall, J. and **Wang, M.** (2009) A phase diagram for turbulent, transitional, and laminar clay suspension flows. *Journal of Sedimentary Research*, **79**, 162-183.

Ballance, P.F. (1984) Sheet-flow-dominated gravel fans of the non-marine middle Cenozoic Simmler Formation, central California. *Sedimentary Geology*, **38**, 337-359.

Beaty, C.B. (1961) Topographic effects of faulting: Death Valley, California. *Annals of the American Association of Geographers*, **51**, 234-240.

Benvenuti, M. and **Martini, I.P.** (2002) Analysis of terrestrial hyperconcentrated flows and their deposits. In: *Flood and Megaflood Processes and Deposits: Recent and Ancient Examples* (Eds. I.P. Martini, V. R. Baker and G. Garzón), IAS Special Publication, **32**, 167-193.

Best, J. and **Bridge, J.** (1992) The morphology and dynamics of low-amplitude bedwaves upon upper-stage plane beds and the preservation of planar laminae. *Sedimentology*, **39**, 737-752.

Beverage, J.P. and **Culbertson, J.K.** (1964) Hyperconcentrations of suspended sediment. *Journal of Hydraulic Engineering*, **90**, 117-128.

Blair, T.C. (1999a) Cause of dominance by sheetflood vs. debris-flow processes on two adjoining alluvial fans, Death Valley, California. *Sedimentology*, **46**, 1015-1028.

Blair, T.C. (1999b) Sedimentary processes and facies of the waterlaid Anvil Spring Canyon alluvial fan, Death Valley, California. *Sedimentology*, **46**, 913-940.

Blair, T.C. (2003) Features and origin of the giant Cucomungo Canyon alluvial fan, Eureka Valley, California. In: *Extreme Depositional Environments: Mega End Members in Geologic Time* (Eds. M.A. Chan and A.W. Archer), Geological Society of America Special Paper, **370**, 105-126.

Blair, T.C. and **McPherson, J.G.** (1994) Alluvial fans and their natural distinction from rivers based on morphology, hydraulic processes, sedimentary processes, and facies assemblages. *Journal of Sedimentary Research*, **A64**, 450-489.

Blair, T.C. and **McPherson, J.G.** (1998) Recent debris-flow processes and resultant form and facies of the Dolomite alluvial fan, Owens Valley, California. *Journal of Sedimentary Research*, **68**, 800-818.

Blair, T.C. and **McPherson, J.G.** (1999) Grain-size and textural classification of coarse sedimentary particles. *Journal of Sedimentary Research*, **69**, 6-19.

Blikra, L.H. and **Nemec, W.** (1998) Postglacial colluvium in western Norway: depositional processes, facies and palaeoclimatic record. *Sedimentology*, **45**, 909-959.

Bluck, B.J. (1967) Deposition of some Upper Old Red Sandstone conglomerates in the Clyde area: a study in the significance of bedding. Scot. *Journal of Geology*, **3**, 139-167.

Bradley, J.B. and **McCutcheon, S.C.** (1987) Influence of Large Suspended-sediment Concentrations in Rivers. In: *Sediment Transport in Gravel-Bed Rivers* (Eds. C.R. Thorne, J.C. Bathurst and R.D. Hey), pp. 645-689, John Wiley & Sons Ltd.

Broekman, J.A. (1983) Environments of deposition, sequences and history of Tertiary continental sedimentation in the Basin of Teruel-Ademuz (Spain). *Proceedings Koninklijke Nederlandse Akademie van Wetenschappen*, **B86**, 25-37.

Bull, W.B. (1972) Recognition of Alluvial-Fan Deposits in the Stratigraphic Record. In: *Recognition of Ancient Sedimentary Environments* (Eds. J.K. Rigby and W.K. Hamblin), SEPM Special Publication, **16**, 63-83.

Bull, W.B. (1977) The alluvial-fan environment. *Progress in Physical Geography*, **1**, 222-270.

Burbank, D, Meigs, A. and **Brozovic, N.** (1996) Interactions of growing folds and coeval depositional systems. *Basin Research*, **8**, 199-223.

Bøe, R. and **Sturt, B.A.** (1991) Textural responses to evolving mass-flows: an example from the Devonian Asen Formation, central Norway. *Geological Magazine*, **128**, 99-109.

Campbell, C.V. (1967) Lamina, laminaset, bed and bedset. *Sedimentology*, **8**, 7-26.

Carenas, B., García, A., Calonge, A., Perez, P. and **Segura, M.** (1989) Middle Cretaceous (Upper Albian-Turonian) in the central sector of the Iberian Ranges (Spain). In: *Cretaceous of the Western Tethys* (Ed. J. Wiedmann), pp. 265-279, E. Schweizerbartsche Verlagsbuchandlung, Stuttgart.

Carroll, A.R., Graham, S.A. and **Smith, M.E.** (2010) Walled sedimentary basins in China. *Basin Research*, **22**, 17-32.

Cheel, R.J. (1990) Horizontal lamination and the sequence of bed phases and stratification under upper-flow-regime conditions. *Sedimentology*, **37**, 517-529.

Chun, S.S. and **Chough, S.K.** (1992) Depositional sequences from high-concentration turbidity currents, Cretaceous Uhangri Formation (SW Korea). *Sedimentary Geology*, **77**, 225-233.

Church, M. and **Ryder, J.M.** (1972) Paraglacial Sedimentation: A Consideration of Fluvial Processes Conditioned by Glaciation. *Geological Society of America Bulletin*, **83**, 3059-3072.

Clarke, L., Quine, T.A. and **Nicholas, A.** (2010) An experimental investigation of autogenic behaviour during alluvial fan evolution. *Geomorphology*, **115**, 278-285.

Clevis, Q., De Jager, G., Nijman, W. and **De Boer, P.L.** (2004) Stratigraphic signatures of translation of thrust-sheet top basins over low-angle detachment faults. *Basin Research*, **16**, 145-163.

Coussot, P. and **Ancey, C.** (1999) Rheophysical classification of concentrated suspensions and granular pastes. *Physical Reviews E*, **59**, 4445-4457.

Crews, S.G. and **Ethridge, F.G.** (1993) Laramide tectonics and humid alluvial fan sedimentation, NE Uinta Uplift, Utah nd Wyoming. *Journal of Sedimentary Petrology*, **63**, 420-436.

Cronin, S.J., Lecointre, J.A., Palmer, A.S. and **Neall, V.E.** (2000) Transformation, internal stratification, and depositional processes within a channelised, multi-peaked lahar flow. *New Zealand Journal of Geology and Geophysics*, **43**, 117-128.

DeCelles, P.G., Tolson, R.B., Graham, S.A., Smith, G.A., Ingersoll, R.V., White, J., Schmidt, C.J., Rice, R., Moxon, I., Lemke, L., Handschy, J.W., Follo, M.F., Edwards, D.P., Cavazza, W., Caldwell. M. and **Bargar, E.** (1987) Laramide Thrust-Generated Alluvial-Fan Sedimentation, Sphinx Conglomerate, Southwestern Montana. *AAPG Bulletin*, **71**, 135-155.

Dorn, R.I. (2009) The Role of Climatic Change in Alluvial Fan Development. In: *Geomorphology of Desert Environments* (Eds. A.J. Parsons and A.D. Abrahams), pp. 723-741, Springer Science, Berlin.

Driese, S.G. and **Ober, E.G.** (2005) Paleopedologic and paleohydrologic records of precipitation seasonality from early Pennsylvanian "underclay" paleosols, U.S.A. *Journal of Sedimentary Research*, **75**, 997-1010.

Dühnforth, M., Densmore, A.L., Ivy-Ochs, S., Allen, P.A. and **Kubik, P.W.** (2007) Timing and patterns of debrisflow deposition on Shpherd and Symmes creek fans, Owens Valley, California, deduced from cosmogenic 10Be. *Journal of Geophysical Research*, **112**, F03S15, doi: 10.1029/2006JF000562.

Elízaga, E. (1980) Los sedimentos terrígenos del Cretacíco Medio del sur de la meseta y el norte del Prebético externo. Hypótesis sedímentologicas. *Boletín Geológico y Minero*, **91**, 619-638.

Fielding, C.R. and **Webb, J.A.** (1995) Sedimentology of the Permian Radok Conglomerate in the Beaver Lake area of MacRobertson Land, East Antarctica. *Geological Magazine*, **132**, 51-63.

Fisher, R.V. (1971) Features of coarse-grained, high-concentration fluids and their deposits. *Journal of Sedimentary Petrology*, **41**, 916-927.

Fisher, R.V. (1983) Flow transformations in sediment gravity flows. *Geology*, **11**, 273-274.

Flint, S. and **Turner, P.** (1988) Alluvial fan and fan-delta sedimentation in a forearc extensional setting: the Cretaceous Coloso Basin of northern Chile In: *Fan Deltas: Sedimentology and Tectonic Settings* (Eds. W. Nemec and R.J. Steel), pp. 387-399, Blackie & Son, Glasgow.

Folk, R.L. (1954) The distinction between grain size and mineral composition in sedimentary-rock nomenclature. *Journal of Geology*, **62**, 344-359.

Frostick, L.E. and **Jones, S.J.** (2002) Impact of periodicity on sediment flux in alluvial systems: grain to basin scale. In: *Sediment Flux to Basins: Causes, Controls and Consequences* (Eds. S.J. Jones and L.E. Frostick), Geological Society of London Special Publication, **191**, 81-95.

Gabaldón, V. (1983) Explanatory notes to *Map 590 – 27-23 (1:50.000), La Puebla de Valverde, Mapa Geologico de España*. Instituto Géologico y Minero de España, Madrid.

Gabaldón, V. (1985) Explanatory notes to *Map 47 – 7-6 (1:200.000), Teruel, Mapa Geologico de España*. Instituto Géologico y Minero de España, Madrid.

García, A.F. and **Stokes. M.** (2006) Late Pleistocene highstand and recession of a small, high-altitude pluvial lake, Jakes Valley, central Great Basin, USA. *Quaternary Research*, **65**, 179-186.

Gawthorphe, R.L. and **Leeder, M.R.** (2000) Tectono-sedimentary evolution of active extensional basins. *Basin Research*, **12**, 195-218.

Harms, J.C., Southard, J.B., Spearing, D.R. and **Walker, R.G.** (1975) *Depositional Environments as Interpreted from Primary Sedimentary Structures and Stratification Sequences.* SEPM Short Course Lecture Notes, **2**, Tulsa (OK).

Hartley, A.J., Mather, A.E., Jolley, E. and **Turner, P.** (2005) Climatic controls on alluvial-fan activity, Coastal Cordillera, northern Chile. In: *Alluvial Fans: Geomorphology, Sedimentology, Dynamics* (Eds. A.M. Harvey, A.E. Mather and M. Stokes), Geological Society of London Special Publication, **251**, 95-115.

Harvey, A.M. (1990) Factors influencing Quaternary fan development in southeast Spain. In: *Alluvial Fans – A Field Approach* (Eds. A.H. Rachocki and M. Church), pp. 247-270, John Wiley & Sons, New York.

Harvey, A.M. (1996)The role of alluvial fans in the mountain fluvial systems of southeast Spain: implications of climatic change. *Earth Surface Processes and Landforms*, **21**, 543-553.

Harvey. A.M. (2002) The role of base-level change in the dissection of alluvial fans: case studies from southeast Spain and Nevada. *Geomorphology*, **45**, 67-87.

Harvey, A.M. (2010) Local Buffers to the Sediment Cascade: Debris Cones and Alluvial Fans. In: *Sediment Cascades: An Integrated Approach* (Eds. T. Burt and R. Allison), pp. 153-180, John Wiley & Sons, New York.

Harvey, A.M. (2011) Dryland alluvial fans. In: *Arid Zone Geomorphology: Process, Form and Change in Drylands*, 3rd Ed. (Ed. D.S.G. Thomas), pp. 333-371, John Wiley & Sons, New York.

Harvey, A.M., Silva, P.G., Mather, A.E., Goy, J.L., Stokes, M. and **Zazo, C.** (1999) The impact of Quaternary sea-level and climatic change on coastal alluvial fans in the Cabo de Gata ranges, southeast Spain. *Geomorphology*, **28**, 1-22.

Heward, A.P. (1978) Alluvial fan sequence and megasequence models. In: *Fluvial Sedimentology* (Ed A.D. Miall), Canadian Society of Petroleum Geology Memoir, **5**, 669-702.

Hogg, S.E. (1982) Sheerfloods, sheetwash, sheetflow, or...? *Earth Science Reviews*, **18**, 59-76.

Hooke, R.LeB. (1972) Geomorphic Evidence for Late-Wisconsin and Holocene Tectonic Deformation, Death Valley, California. *Geological Society of America Bulletin*, **83**, 2073-2098.

Hooke, R. LeB. (1987) Mass Movement in Semi-Arid Environments and the Morphology of Alluvial Fans. In: *Slope Stability* (Eds. M.G. Anderson and K.S. Richards), pp. 505-529, John Wiley & Sons, New York.

Hubert, J.F. and **Filipov, A.J.** (1989) Debris-flow deposits in alluvial fans on the west flank of the White Mountains, Owens Valley, California, U.S.A. *Sedimentary Geology*, **61**, 177-205.

Hubert, J.F. and **Hyde, M.G.** (1982) Sheet-flow deposits of graded beds and mudstones on an alluvial-sandflat-playa system: Upper triassic Blomidon redbeds, St Mary's Bay, Nova Scotia. *Sedimentology*, **29**, 457-474.

Iverson, R.M. and **Denlinger, R.P.** (1987) The physics of debris flows – a conceptual assessment. In: *Erosion and Sedimentation in the Pacific Rim* (Ed. R.L. Beschta), *International Association of Hydrologists Publication*, **165**, 155-165.

Iverson, R.M. Schilling, S.P. and **Vallance, J.W.** (1998) Objective delineation of lahar-inundation hazard zones. *Geological Society of America Bulletin*, **110**, 972-984.

Jackson, J. and **Leeder, M.** (1994) Drainage systems and the development of normal faults: an example from Pleasant Valley, Nevada. *Journal of Structural Geology*, **16**, 1041-1059.

Jackson, L.E., Jr., Kostaschuk, R.A. and **MacDonald, G.M.** (1987) Identification of debris flow hazard on alluvial fans in the Canadian Rocky Mountains. In: *Debris Flows / Avalanches: Process, Recognition and Mitigation* (Eds. J.E. Costa and G.F. Wieczorek), Geological Society of America Reviews in Engineering Geology, **7**, 115-124.

Johnson, A.M. (1970) *Physical Processes in Geology*. Freeman, Cooper & Co., San Francisco, 577 p.

Konert, M. and **Vandenberghe, J.** (1997) Comparison of laser grain-size analysis with pipette and sieve analysis: a solution for the underestimation of the clay fraction. *Sedimentology,* **44**, 523-535.

Kostaschuk, R.A., MacDonald, G.M. and **Putnam, P.E.** (1986) Depositional process and alluvial fan-drainage morphometric relationships near Banff, Alberta, Canada. *Earth Surface Processes and Landforms*, **11**, 471-484.

Kraus, M.J. and **Hasiotis, S.T.** (2006) Significance of different modes of rhizolith preservation to interpreting paleoenvironmental and paleohydrologic settings: examples from Paleogene paleosols, Bighorn Basin, Wyoming, U.S.A. *Journal of Sedimentary Research*, **76**, 633-646.

Lawson, D.E. (1982) Mobilization, movement and deposition of active subaerial sediment flows, Matanuska Glacier, Alaska. *Journal of Geology*, **90**, 279-300.

Leeder, M.R., Mack, G.H. and **Salyards, S.L.** (1996) Axial-transverse fluvial interactions in half-graben: Plio-Pleistocene Palomas Basin, southern Rio Grande Rift, New Mexico, USA. *Basin Research*, **12**, 225-241.

Legget, R.F., Brown, R.J.E. and **Johnston, G.H.** (1968) Alluvial fan formation near Aklavik, Northwest Territories, Canada. *Geological Society of America Bulletin*, **77**, 15-30.

Leleu, S., Ghienne, J.-F. and **Manatschal, G.** (2009) Alluvial fan development and morphotectonic evolution in response to contractional fault reactivation (Late Cretaceous-Palaeocene), Provence, France. *Basin Research*, **21**, 157-187.

Li, M.Z. and **Gust, G.** (2000) Boundary layer dynamics and drag reduction in flows of high cohesive sediment suspensions. *Sedimentology*, **47**, 71-86.

Lloyd, M.J., Nichols, G.J. and **Friend, P.F.** (1998) Oligo-Miocene alluvial-fan evolution at the southern Pyrenean thrust front, Spain. *Journal of Sedimentary Research*, **68**, 869-878.

Lowe, D.R. (1988) Suspended-load fallout rate as an independent variable in the analysis of current structures. *Sedimentology*, **35**, 765-776.

Lowenstein, T.K., Hein, M.C., Bobst, A.L., Jordan, T.E., Ku, T.-L. and **Luo, S.** (2003) An assessment of stratigraphic completeness in climate-sensitive closed-basin lake sediments: Salar de Atacama, Chile. *Journal of Sedimentary Research.*, **73**, 91-104.

Mack, G.H. and **Stout, D.M.** (2005) Unconventional distribution of facies in a continental rift basin: the Pliocene-Pleistocene Mangas Basin, southwestern New Mexico, USA. *Sedimentology*, **52**, 1187-1205.

Major, J.J. (1998) Pebble orientation on large, experimental debris-flow deposits. *Sedimentary Geology*, **117**, 151-164.

Major, J.J. and **Pierson, T.C.** (1992) Debris flow rheology: experimental analysis of fine-grained slurries. *Water Resources Research*, **28**, 841-857.

Major, J.J. and **Iverson, R.M.** (1999) Debris-flow deposition: effects of pore-fluid pressure and friction concentrated at flow margins. *Geological Society of America Bulletin*, **111**, 1424-1434.

Manville, V. and **White, J.D.L.** (2003) Incipient granular mass flows at the base of sediment-laden floods, and the roles of flow competence and flow capacity in the deposition of stratified bouldery sands. *Sedimentary Geology*, **155**, 157-173.

Martín-Chivelet, J. (coordinator) (2002) *Cretaceous*. In: *The Geology of Spain* (Eds. W. Gibbons and T. Moreno), pp. 255-292, The Geological Society, London, UK.

Matthews, J.A., Shakesby, R.A., McEwen, L.J., Berrisford, M.S., Owen, G. and **Bevan, P.** (1999) Alpine debris-flows in Leirdalen, Jotunheimen, Norway, with particular reference to distal fans, intermediate-type deposits, and flow types. *Arctic and Alpine Research*, **31**, 421-435.

McCave, I.N. and **Syvitski, J.P.N.** (1991) Principles and methods of geological particle size analysis. In: *Principles, Methods and Application of Particle Size Analysis* (Ed. J.P.N. Syvitski), pp. 3-21, Cambridge University Press, Cambridge, UK.

McCave, I.N., Bryant, R.J., Cook, H.F. and **Coughanowr, C.A.** (1986) Evaluation of a laser-diffraction-size analyzer for use with natural sediments. *Journal of Sedimentary Petrology*, **56**, 561-564.

Meyer, G.A. and **Wells, S.G.** (1997) Fire-related sedimentation events on alluvial fans, Yellowstone National Park, U.S.A.. *Journal of Sedimentary Research*, **67A**, 776-791.

Moscariello, A. (2005) Exploration potential of the mature Southern North Sea basin margins: some unconventional plays based on alluvial and fluvial fan sedimentation models. In: *Petroleum Geology: North-West Europe and Global Perspectives – Proceedings of the 6th Petroleum Geology Conference* (Eds. A.G. Doré and B.A. Vining), pp. 595-605, Petroleum Geology Conferences Ltd., London.

Moscariello, A. and **Deganutti, A.M.** (2007) Hydrological and sedimentary processes related to a high intensity debris-flow catchment in the Dolomites (Italian Alps). In: *Debris-Flow Hazards Mitigation: Mechanics, Preciction and Assessment* (Eds. C.L. Chen and J.J. Major), pp. 340-351, Millpress Science Publishers, Amsterdam.

Moscariello, A., Marchi, L., Maraga, F. and **Mortara, G.** (2002) Alluvial fans in the Italian Alps: sedimentary facies and processes. In: *Flood and Megaflood Processes and Deposits: Recent and Ancient Examples* (Eds. I.P. Martini, V.R. Baker and G. Garzón), IAS Special Publication, **32,** 141-166.

Nakayama, K. (1999) Sand- and mud-dominated alluvial-fan deposits of the Miocene Seto Porcelain Clay Formation, Japan. In: *Fluvial Sedimentology VI* (Eds. N.D. Smith and J. Rogers), IAS Special Publication, **28**, 393-407.

Naylor, M.A. (1980) The origin of inverse grading in muddy debris flow deposits – a review. *Journal of Sedimentary Petrology*, **50**, 1111-1116.

Nemec, W. and **Muszynski, A.** (1982) Volcaniclastic alluvial aprons in the Tertiary of Sofia district (Bulgaria). *Acta Geologica Polonica*, **52**, 239-303.

Nemec, W. and **Steel, R.J.** (1984) Alluvial and coastal conglomerates: their significant features and some comments on gravelly mass-flow deposits. In: *Sedimentology of Gravels and Conglomerates* (Eds. E.H. Koster and R.J. Steel), Canadian Society of Petroleum Geologists Memoir, **10**, 1-31.

Nemec, W. and **Postma, G.** (1993) Quaternary alluvial fans in southwestern Crete: sedimentation processes and geomorphic evolution. In: *Alluvial Sedimentation* (Eds. M. Marzo and C. Puigdefabregas), IAS Special Publication, **17**, 235-276.

Nichols, G.J. (1987) Syntectonic alluvial fan sedimentation, southern Pyrenees. *Geological Magazine*, **124**, 121-133.

Nichols, G.J. (2004) Sedimentation and base level in an endorheic basin: the early Miocene of the Ebro Basin, Spain. *Boletín Geológico y Minero*, **115**, 427-438.

Nichols, G.J. (2005) Tertiary alluvial fans at the northern margin of the Ebro Basin: a review. In: *Alluvial Fans: Geomorphology, Sedimentology, Dynamics* (Eds. A.M. Harvey, A.E. Mather and M. Stokes), Geological Society of London Special Publication, **251**, 187-206.

Nichols, G. and **Thompson, B.** (2005) Bedrock lithology control on contemporaneous alluvial fan facies, Oligo-Miocene, southern Pyrenees, Spain. *Sedimentology*, **52**, 571-585.

Nilsen, T.H. (1982) Alluvial Fan Deposits. In: *Sandstone Depositional Environments* (Eds. P.A. Scholle and D. Spearing), AAPG Memoir, **31**, 49-86.

Patton, T.L. (2004) Numerical models of growth-sediment development above an active monocline. *Basin Research*, **16**, 25-39.

Pierson, T.C. (1985) Initiation and flow behavior of the 1980 Pine Creek and Muddy River lahars, Mount St. Helens, Washington. *Geological Society of America Bulletin*, **96**, 1056-1069.

Pierson, T.C. (1986) Flow behavior of channelized debris flows, Mount St. Helens, Washington. In: *Hillslope processes* (Ed. A.D. Abrahams), pp. 269-296, Allen & Unwin, London.

Pierson, T.C. and **Costa, J.E.** (1987) A rheologic classification of subaerial sediment-water flows. In: *Debris Flows/Avalanches: Processes, Recognition and Mitigation* (Eds. J.E. Costa and J.F. Wieczorek), Geological Society of America Reviews in Engineering Geology, **7**, 1-12.

Postma, G., Nemec, W. and **Kleinspehn, K.** (1988) Large floating clasts in turbidites: a mechanism for their emplacement. *Sedimentary Geology*, **58**, 47-61.

Rees, A.I. (1968) The production of preferred orientation in a concentrated dispersion of elongated and flattened grains. *Journal of Geology*, **76**, 457-465.

Reheis, M.C., Slate, J.L., Throckmorton, C.K., McGeehin, J.P., Sarna-Wojcicki, A.M. and **Dengler, L.** (1996) Late Quaternary sedimentation on the Leidy Creek fan, Nevada-California: geomorphic responses to climate change. *Basin Research*, **12**, 279-299.

Retallack, G.J. (2001) *Soils of the Past: An Introduction to Paleopedology*, 2nd Ed., Wiley-Blackwell, 512 p.

Riba, O. (1976) Syntectonic unconformities of the Alto Cardener, Spanish Pyrenees: a genetic interpretation. *Sedimentary Geology*, **15**, 213-233.

Ritter, J.B., Miller, J.R. and **Husek-Wulforst, J.** (2000) Enviromental controls on the evolution of alluvial fans in Buena Vista Valley, North Central Nevada, during late Quaternary time. *Geomorphology*, **36**, 63-87.

Rodine, J.D. and **Johnson, A.M.** (1976) The ability of debris, heavility freighted with coarse clastic materials, to flow on gentle slopes. *Sedimentology*, **23**, 213-234.

Ródriguez-López, J.P., Meléndez, N., De Boer, P.L. and **Soria, A.R.** (2008) Aeolian sand sea development along the mid-Cretaceous western Tethyan margin (Spain) erg sedimentology and palaeoclimate implications. *Sedimentology*, **55**, 1253-1292.

Rust, B.R. (1979) Coarse Alluvial Deposits. In: *Facies Models* (Ed. R.G.Walker), *Geoscience Canada Reprint Series*, **1**, 9-21.

Salas, R. and **Casas, A.** (1993) Mesozoic extensional tectonics, stratigraphy and crustal evolution during the Alpine cycle of the eastern Iberian Basin. *Tectonophysics*, **228**, 33-55.

Scott, K.M. (1988) Origins, behavior and sedimentology of lahars and lahar-runout flows in the Toutle-Cowlitz river system. USGS Professional Paper, **1447A**, 74 p.

Schumm, S.A., Mosley, M.P. and **Weaver, W.E.** (1987) *Experimental Fluvial Geomorphology*. John Wiley & Sons, New York.

Sharp, R.P. (1942) Mudflow levees. *Journal of Geomorphology*, **5**, 222-227.

Sharp, R.P. and **Nobles, L.H.** (1953) Mudflow of 1941 at Wrightwood, southern California. *Geological Society of America Bulletin*, **64**, 547-560.

Shultz, A.W. (1984) Subaerial debris-flow deposition in the upper Paleozoic Cutler Formation, western Colorado. *Journal of Sedimentary Petrology.*, **54**, 759-772.

Smith, G.A. (2000) Recognition and significance of streamflow-dominated piedmont facies in extensional basins. *Basin Research*, **12**, 399-411.

Smoot, J.P. (1983) Depositional subenvironments in an arid closed basin; the Wilkins Peak Member of the Green River Formation (Eocene), Wyoming, U.S.A. *Sedimentology*, **30**, 801-827.

Sohn, Y.K. (1997) On traction-carpet sedimentation. *Journal of Sedimentary Research.*, **67**, 502-509.

Sohn, Y.K., Rhee, C.W. and **Kim, B.C.** (1999) Debris flow and hyperconcentrated flood-flow deposits in an alluvial fan, northwestern part of the Cretaceous Yongdong Basin, central Korea. *Journal of Geology*, **107**, 111-132.

Sopeña, A., López-Gómez, J., Arche, A., Pérez-Arlucea, M., Ramos, A., Virgili, C. and **Hernándo, S.** (1988) Permian and Triassic of the Iberian Peninsula. In: *Triassic-Jurassic Rifting – Continental Breakup and the Origin of the Atlantic Ocean and Passive Margins* (Ed. W. Manspeizer), Developments in Geotectonics, **22B**, Elsevier, Amsterdam, 757-786.

Soria, J.M., Viseras, C. and **Fernández, J.** (1998) Late Miocece-Pleistocene tectono-sedimentary evolution and subsidence history of the central Betic Cordillera (Spain): a case study in the Guadix intramontane basin. *Geological Magazine*, **135**, 565-574.

Steel, R.J. (1974) New Red Sandstone floodplain and piedmont sedimentation in the Hebridean Province, Scotland. *Journal of Sedimentary Petrology*, **44**, 336-357.

Steel, R.J., Mæhle, S., Nilsen, H., Røe, S.L. and **Spinnangr Å.** (1977) Coarsening-upward cycles in the alluvium of Hornelen Basin (Devonian), Norway. *Geological Society of America Bulletin*, **88**, 1124-1134.

Stokes, M. and **García, A.F.** (2009) Late Quaternary landscape development along the Rancho Marino coastal range front (south-central Pacific Coast Ranges, California, USA). *Journal of Quaternary Science*, **24**, 728-746.

Stokes, M. and **Mather, A.E.** (2000) Response of Plio-Pleistocene alluvial systems to tectonically induced base-level changes, Vera Basin, SE Spain. *Journal of the Geological Society of London*, **157**, 303-316.

Tunbridge, I.P. (1984) Facies model for a sandy ephemeral stream and clay playa complex; the Middle Devonian Trentishoe Formation of North Devon, U.K. *Sedimentology*, **31**, 697-715.

Van Dam, J.A. (2006) Geographic and temporal patterns in the late Neogene (12-3 Ma) aridification of Europe: The use of small mammals as paleoprecipitation proxies. *Palaeogeography, Palaeoclimatology, Palaeoecology*, **238**, 190-218.

Van Dijk, M. (2009) *Autocylic Behaviour of Alluvial and Deltaic Systems*. PhD thesis, Geologica Ultraiectina, **306**, 128 p.

Vegas, R. (1992) The Valencia Trough and the origin of the western Mediterranean basins. *Tectonophysics*, **203**, 249-261.

Ventra, D. (2009) Ephemeral alluvial systems of the Teruel Basin (Miocene, Spain): Basinal and climatic controls. *Acta Geologica Lilloana*, **21**, 67-68.

Viseras, C., Calvache, M.L., Soria, J.M. and **Fernández, J.** (2003) Differential features of alluvial fans controlled by tectonic or eustatic accommodation space. Examples from the Betic Cordillera, Spain. *Geomorphology*, **50**, 181-202.

Wagreich, M. and **Strauss, P.E.** (2005) Source area and tectonic control on alluvial-fan development in the Miocene Fohnsdorf intramontane basin, Austria. In: *Alluvial Fans: Geomorphology, Sedimentology, Dynamics* (Eds. A.M. Harvey, A.E. Mather and M. Stokes), Geological Society of London Special Publication, **251**, 207-216.

Wang, Z. and **Larsen, P.** (1994) Turbulent structure of water and clay suspensions with bed load. *Journal of Hydraulic Engineering*, **120**, 577-600.

Wasson, R.J. (1977a) Catchment processes and the evolution of alluvial fans in the lower Derwent Valley, Tasmania. *Zeitschrift für Geomorphologie*, **21**, 147-168.

Wasson, R.J. (1977b) Last-glacial alluvial fan sedimentation in the Lower Derwent Valley, Tasmania. *Sedimentology*, **24**, 781-799.

Wasson, R.J. (1979) Sedimentation history of the Mundi Mundi alluvial fans, western New South Wales. *Sedimentary Geology*, **22**, 21-51.

Webb, J.A. and **Fielding, C.R.** (1999) Debris Flow and Sheetflood Fans of the Northern Prince Charles Mountains, East Antarctica. In: *Varieties of Fluvial Form* (Eds. A.J. Miller and A. Gupta), pp. 317-341, John Wiley & Sons Ltd.

Wells, N.A. (1984) Sheet debris flow and sheetflood conglomerates in Cretaceous cool-maritime alluvial fans, South Orkney Islands, Antarctica. In: *Sedimentology of Gravels and Conglomerates* (Eds. E.H. Koster and R.J. Steel), Canadian Society of Petroleum Geologists Memoir, **10**, 133-145.

Went, D.J. (2005) Pre-vegetation alluvial fan facies and processes: an example from the Cambro-Ordovician Rozel Conglomerate Formation, Jersey, Channel Islands. *Sedimentology*, **52**, 693-713.

Wright, V.P. and **Marriott, S.B.** (2007) The dangers of taking mud for granted: lessons from Lower Old Red Sandstone dryland river systems of South Wales. *Sedimentary Geology*, **195**, 91-100.

"*It is to fossils alone that we owe the commencement of even a Theory of the Earth... By them we are enabled to ascertain, with the utmost certainty, that our Earth has not always been covered over by the same external crust, because we are thoroughly assured that the organized bodies to which these fossil remains belong must have lived upon the surface before they came to be buried, as they now are, at a great depth.* "

Baron Georges Cuvier
Recherches sur les Ossemens Fossiles, 1812

Chapter 6

Pleistocene debrisflow deposition of the Collecurti bonebed (Macerata, central Italy): taphonomic and paleoenvironmental analysis

P.P.A. Mazza & D. Ventra

ABSTRACT

An integrated taphonomic-sedimentological study provides insight into the origin, preservation biases and paleobiological significance of the latest Early/earliest Middle Pleistocene bonebed of Collecurti, near Colfiorito (Macerata, central Italy), which represents an important benchmark in the European biochronological scale. Sedimentological evidence indicates that the bonebed is hosted in a debrisflow deposit which was emplaced in a shallow lacustrine setting. Geologic and geomorphic controls on sedimentation in the intermontane Colfiorito Basin provided an ideal setting for the development of cohesive mass flows, due to high-relief and poorly integrated catchments along the basin margin, and the abundance of detrital fines yielded by Mesozoic sedimentary rocks of the local basement. The fossil assemblage includes 496 bones, with a minimum of 24 individuals representing 9 species and 8 genera, dominated by *Hippopotamus antiquus*. The hippopotamus remains include partially articulated carcass parts as well as closely associated elements. Few disarticulated elements, which are bones that can be more easily transported hydraulically, were involved in pre-debrisflow winnowing and sorting, and then entrained by the debris flows in nearby uplands, transported a short distance down into a shallow pond or lake margin, where the flow buried hippopotamus carcasses that had accumulated in the pond/lake. The hippopotamus carcasses were in an advanced state of decomposition when the debris flow entrained them. Their bones show no evidence of weathering, trampling, scavenging, sorting or transportation prior to debrisflow reworking, which indicates that the animals were probably lying on the bottom of the pond where they lived, or were already partially buried in mud. Previous palynological investigations have shown that the strata of interest at Collecurti were deposited during a climatic trend towards ever increasing cooler conditions. The low richness of the fauna confirms long exposure to harsh climatic and environmental conditions. Two are the plausible causes of the death of the Collecurti animals, i.e., severe cold and/or drought. Taphonomic attributes rule out drought, indicating that the assemblage accumulated in a short time as the result of a mass mortality event, possibly due to a cold snap.

There are no other reported examples of Quaternary debris-flow-hosted bonebeds in Europe, probably because this agent of taphonomic accumulation is rarely investigated in high-energy paleogeomorphic settings. It is likely that more such sedimentary events took place in the area, and that similar fossil sites await to be discovered.

6.1. INTRODUCTION

The locality of Collecurti (Colfiorito Basin, central Italy) has been known to yield mammal fossils since the 1990s. The site is situated near Voltellina, approximately 56 km SW of Macerata (coordinates: 42°57'48"N, 12°55'20"E), at 840 m above sea level (Fig. 1). The areal extent of the bone accumulation comprises about 235 m^2 (Fig. 2). Although relatively limited, the exposed outcrop is amazingly rich in well preserved vertebrate fossils.

The multi-individual bonebed of Collecurti has been dated at around 1 Ma by biochronology and paleomagnetism (Gliozzi *et al.,* 1997; Coltorti *et al.*, 1998). It therefore yields insights into the spectacular faunal turnover that occurred in the Epivillafranchian (Kahlke, 1997; Kahlke *et al.*, 2010), and provides significant new information on the climatic conditions that accompanied this unique bioevent.

Collecurti represents a Faunal Unit of fundamental importance in the European biochronological scale of Plio-Pleistocene Land Mammal Ages (Gliozzi *et al.*, 1997; Montuire & Marcolini, 2002, and references therein). Although the site has been subject of several studies and cited countless times (e.g., Borselli *et al.*, 1988; Ficcarelli & Mazza, 1990; Ficcarelli *et al.*, 1990; Ficcarelli *et al.*, 1996; Ficcarelli & Silvestrini, 1991; Gliozzi *et al.,* 1997; Coltorti *et al.*, 1998; Montuire & Marcolini, 2002; Palombo & Mussi, 2006; Raia *et al.*, 2006), the causes of mortality and the biostratinomic history of its faunas have not yet been ascertained. This paper presents an integrated taphonomic and sedimentological analysis aiming to unravel the physical origin of the Collecurti bonebed and better constrain the unusual mechanism of final deposition.

The evidence points to the role of a subaqueous debris flow in causing the early burial of mammal remains in the Collecurti bonebed, as well as their spatial distribution. Debris flows have recently been recognized as effective biostratinomic agents for vertebrate fossil assemblages, but few studies have provided detailed sedimentological information to support interpretations of depositional processes (Sachse, 2005; Britt *et al.*, 2009). Almost all reported studies concern events in subaerial settings and in the pre-Quaternary record (e.g., Fastovsky *et al.*, 1995; Loope *et al.*, 1998; Van Itterbeeck *et al.*, 2005; Eberth *et al.*, 2006; Lauters *et al.*, 2008; Britt *et al.*, 2009), whereas the Collecurti site offers a Pleistocene example of bone transport and preservation by mass flow in a shallow-freshwater environment.

6.2. GEOLOGICAL AND PALEOENVIRONMENTAL SETTING

The Colfiorito intermontane basin is located in the Umbria-Marche Apennines, an eastward verging fold-and-thrust belt that represents the eastern segment of the Italian Northern Apennines (Fig. 1). The Umbro-Marchean tectonic belt was formed during Mio-Pliocene compression along the northern Apennine arc (Bally *et al.*, 1986; Calamita *et al.*, 1994), followed by a prolonged Plio-Quaternary extensional phase that

Figure 1 *- Location of the Collecurti site in the Colfiorito Basin, central Italy.*

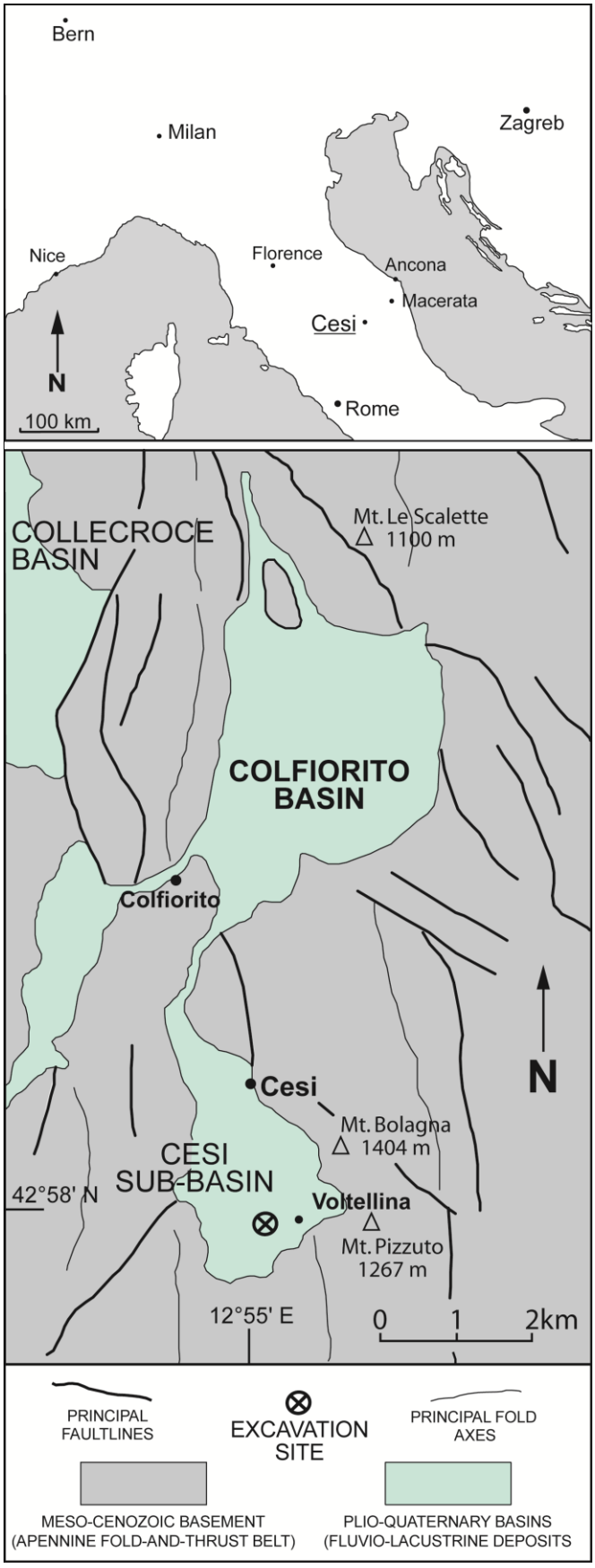

triggered the development of a series of intermontane depressions (Ambrosetti *et al.*, 1978; Calamita *et al.*, 1994). Paleodrainage pathways and local accommodation were strongly controlled by the main fault systems, several of which are still active (Di Giulio *et al.*, 2003; Mirabella *et al.*, 2005). The Quaternary basin fill of the Colfiorito area is up to 120 m thick (Messina *et al.*, 1999) and consists of unlithified continental clastics representing high-energy alluvial-fluvial systems at basin margins, and extensive lacustrine environments occupying the central basinal paleotopography (Ficcarelli & Mazza, 1990; Coltorti *et al.*, 1998; Di Giulio *et al.*, 2003). The deposits occur in two sub-basins connected by a tectonically controlled corridor (Fig. 1); the southern one, the Cesi sub-basin, comprises the bonebed locality. The local basement consists mainly of limestones and marlstones of the Umbria-Marche Meso-Cenozoic succession.

Coltorti *et al.* (1998) described the stratigraphic interval that comprises the bonebed and discussed its chronology. Further detailed observations on basin stratigraphy have been carried out for the present study. The paleontological site of Collecurti lies in close proximity to the eastern tectonic boundary of the Colfiorito Basin. The local sedimentary column comprises approximately 100 m of clastics (Fig. 3). The basal 20 m of the succession are characterized by poorly sorted, matrix-rich, structureless to plane bedded, often amalgamated pebble to cobble gravel, interpreted as deposits of unconfined

hyperconcentrated flows and debris flows from an alluvial fan or ephemeral fluvial system issuing from the nearby uplands. This coarse package is gradually transitional to an interval approximately 40 m thick, dominated by massive to horizontally bedded clay and silt, comprising peat layers and a few organic-rich and fossiliferous interbeds (including the Collecurti bonebed). This interval corresponds to the establishment of a relatively extensive, shallow freshwater body with abundant fine sedimentation, subject to periodic reductions in extent and establishment of marginal, vegetated swamp or wetland conditions. The lower half of this fines-dominated interval presents several gravelly interbeds, separated by a few meters of clay and silts. These probably indicate the activation of colluvial and fan systems during occasional floods or snowmelt events, and ephemeral transport of debris from the steep, adjacent hinterland into the lower-energy basinal setting. Coarse-clastic supply was progressively reduced through time, and the upper half of the fine-dominated interval is almost completely devoid of gravelly event-beds.

The upper strata at Collecurti are characterized by an abrupt transition from the fine clastic package to an overlying, coarse-clastic interval with variable thickness of 20 to over 30 m. The transition is represented by an erosional unconformity, probably related to a reduction in local base level due to renewed tectonic activity and/or reconfiguration of drainage systems between the two sub-basins. The upper clastic package aggrading over the basal unconformity comprises structured gravelly and sandy deposits, with small bar remnants and channel fills, and associated silts, clays, peats and pedogenic levels. This succession probably points to reestablishment of long-lasting subaerial conditions in the Recent history of the Colfiorito Basin, with a well-developed alluvial system and interchannel areas.

Paleomagnetic data (Coltorti *et al.*, 1998) show that the fossiliferous bed occurs within the base of a 5 m stratigraphic interval attributed to the normal polarity Jaramillo subchron (C1r.1n), and its age is therefore approximately 1.05 Ma (late Early Pleistocene; Singer *et al.*, 1999; Guo *et al.*, 2002). Confirmation of this age was obtained by $^{40}Ar/^{39}Ar$ dating of a volcaniclastic layer contained in the upper beds at Collecurti, with an age of 430 ka (Middle Pleistocene; Coltorti *et al.*, 1998). The Collecurti succession in fact correlates with the Marine Isotope Stages (MIS) 31 to 26 (Suc & Popescu, 2005).

Fourty palynological samples (Coltorti *et al.*, 1998) indicated four paleoecological zones in the Collecurti section, with distinct alternations between times of prevalent open vegetation, dominated by Asteraceae, Cichorioidae, Poaceae and Cyperaceae, and times of montane coniferous forest, dominanted by *the* arboreal taxa *Tsuga* and *Cedrus*. Interpretations of paleoclimate based on these floras indicate repeated alternation of relatively warm and more humid intervals (forested zones I and III; Coltorti *et al.*, 1998) to colder, drier conditions (open vegetated zones II and IV). The Collecurti bonebed fauna, which is dominated by hippopotamus and cervids, indicates a wet climate with mild winter temperatures. On the other hand, pollen evidence from the immediately overlying stratigraphic interval is indicative of a dramatic climate change, with significantly colder, drier spells. The paleoenvironmental indications given by the palynological analyses seem to rule out the generally very warm MIS 31 period, confining the bonebed within the more restricted MIS 30 to 26 span.

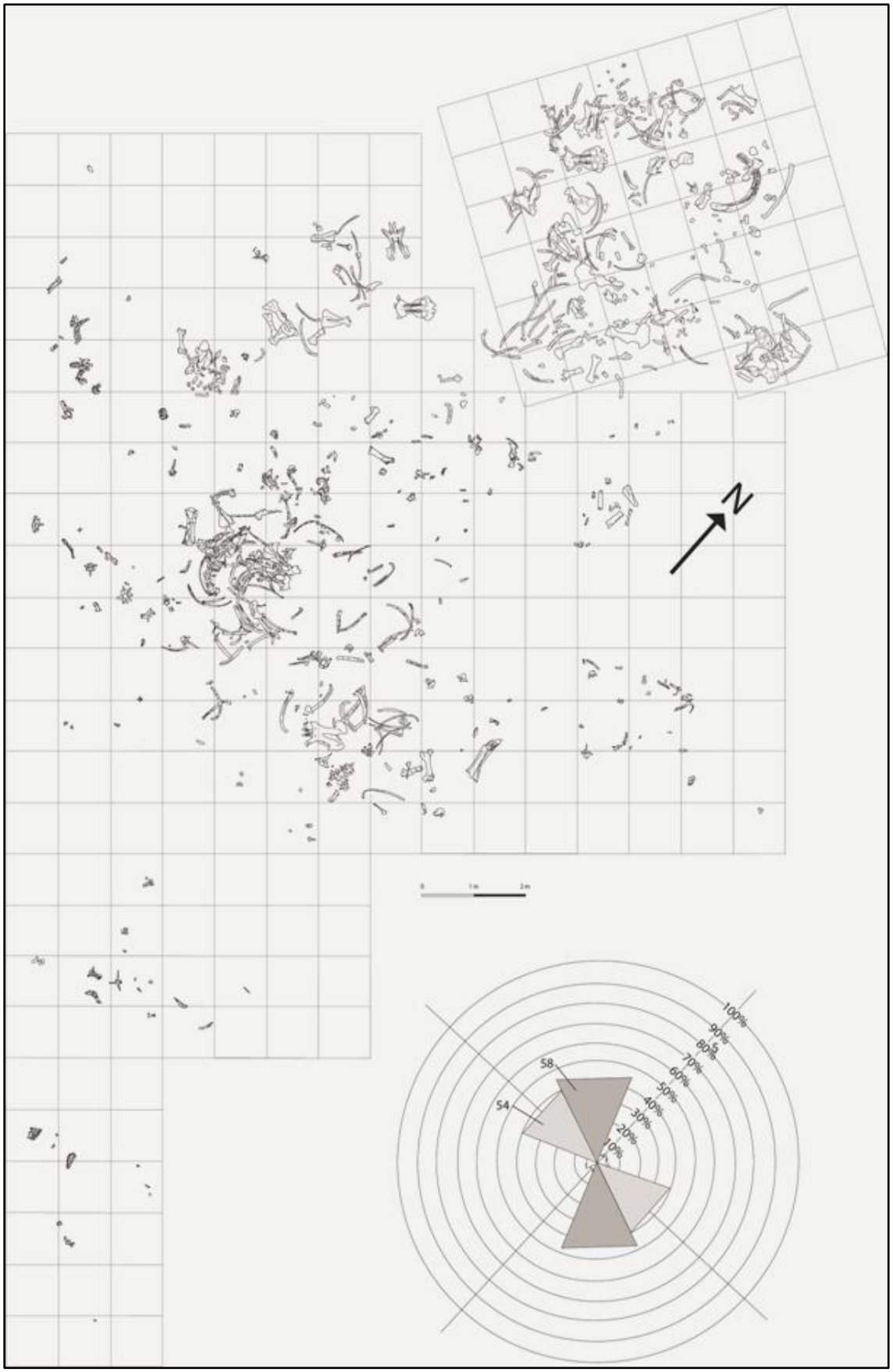

Figure 2 *- Collecurti quarry map.Bidirectional rose diagram shows orientation of 136 long bones or elongated fragments (e.g., ribs, vertebral spinous processes, etc.). Numbers in rose diagram indicate the absolute amount of bones aligned in the two principal orientations.*

6.3. SEDIMENTOLOGY

6.3.1. Methods

The excavation site is located at shallow depth beneath crop terrain on a hilltop in direct proximity to the village of Voltellina (Fig. 1). Extensive trenching during paleontological work allowed sedimentological observations of the whole stratigraphic interval comprising the Collecurti bonebed by means of standard facies analysis (Fig. 4). The detailed stratigraphy was obtained by integrating observations along trenches accessed at different times over several years. Six stratigraphic units were consistently recognizable in the trench logs (Fig. 5).

Besides facies analysis at outcrop, standard sieve-pipette grain-size analyses (following McCave & Syvitski, 1991) were carried out on four bulk samples (~300 to 400 g) of fine deposits (lacustrine mud and fine matrix of conglomerates), the texture and composition of which would be impossible to quantify in the field. Each sample was divided into three subsamples, one of ~20 g for estimates of total organic carbon content (TOC), and two for cross-checked granulometric analyses.

For standard semi-quantitative TOC determination (Dean, 1974; Schumacher, 2002), subsamples were disaggregated, treated in weak acid for elimination of carbonate, and subjected to prolonged heating (80°C) to eliminate residual moisture. Successively, they were weighed and then gradually brought up to ignition at 500°C for 1 h, in order to estimate percent dry weight loss after heated destruction of dispersed organic matter.

Subsamples for granulometry were first put through a 0.5 mm sieve to separate all coarse sand fractions from medium-fine sand and mud. The residual, mud-dominated fraction was brought up to 1000 ml with distilled water in a measuring cylinder, and mass percentages of silt and clay were successively measured by separation of three grain-size classes (> 62 μm, medium to fine sand; 62-8 μm, coarse to fine silt;
< 8 μm, very fine silt to clay) from the settling suspension. The 8-μm parameter, discriminating fine from very fine silt, was chosen in order to sum up quantities of very fine silt and clay within the sediment, since the aggregate properties of both grain-size classes contribute to cohesiveness and plastic rheology in granular mixtures (see below). Obtained mass fractions were converted into volume ratios by direct density measurement of each fraction. This is because the volume of a certain grain-size fraction within a clastic mixture is the relevant parameter to evaluate that fraction's contribution to mixture rheology, which depends on direct physical interactions between adjacent sediment particles (e.g., Major & Pierson, 1992; Coussot & Ancey, 1999). On the other hand, weight values for different grain-size fractions are too strictly dependent on variable mineralogical compositions. Since clay is highly effective in imparting complex rheology to water-particle mixtures (Howard, 1963; Coussot, 1995), the classical settling-pipette method was preferred over more rapid, automated laser diffractometry, as the latter technology is known to underestimate the clay content in samples (McCave *et al.*, 1986; Konert & Vandenberghe, 1997).

6.3.2. Description

The lowermost stratigraphic unit 6 (U6) has an undetermined thickness because only its upper part has been exposed by trenching. It consists of structureless, matrix-supported, granule to pebble gravel within a

brown to light brown, sandy, silty clay matrix. Clasts reach up to 4-5 cm in diameter, are angular to subrounded, floating in the matrix and locally aggregated in clusters, and consist primarily of limestone and marlstone from the adjacent basement, with evident signs of surface chemical alteration. A secondary component in gravel composition is given by pebbles of dark grey to reddish chert.

The transition to overlying unit 5 (U5) is indicated by a sharp reduction in coarse clastic content and sand fraction and a marked change to a darker color. Unit 5 consists of dark brown, massive, silty clay (clay content by volume ~65%; Fig. 5A), with variable thickness reaching a maximum of ~30 cm. Rare chert and carbonate clasts of granule to fine pebble size are scattered within the muddy bed. A few organic-rich interbeds are indicated by mm-thick layers of darker clayey mud characterized by the presence of black organic coatings; such layers are correlatable at outcrop in spite of centimetric lateral discontinuities along the bed. TOC in a bulk sample of U5 shows a relatively high value of ~2.7% by weight; the most significant contribution is probably given by concentrated organic matter along the dark, millimetric horizons.

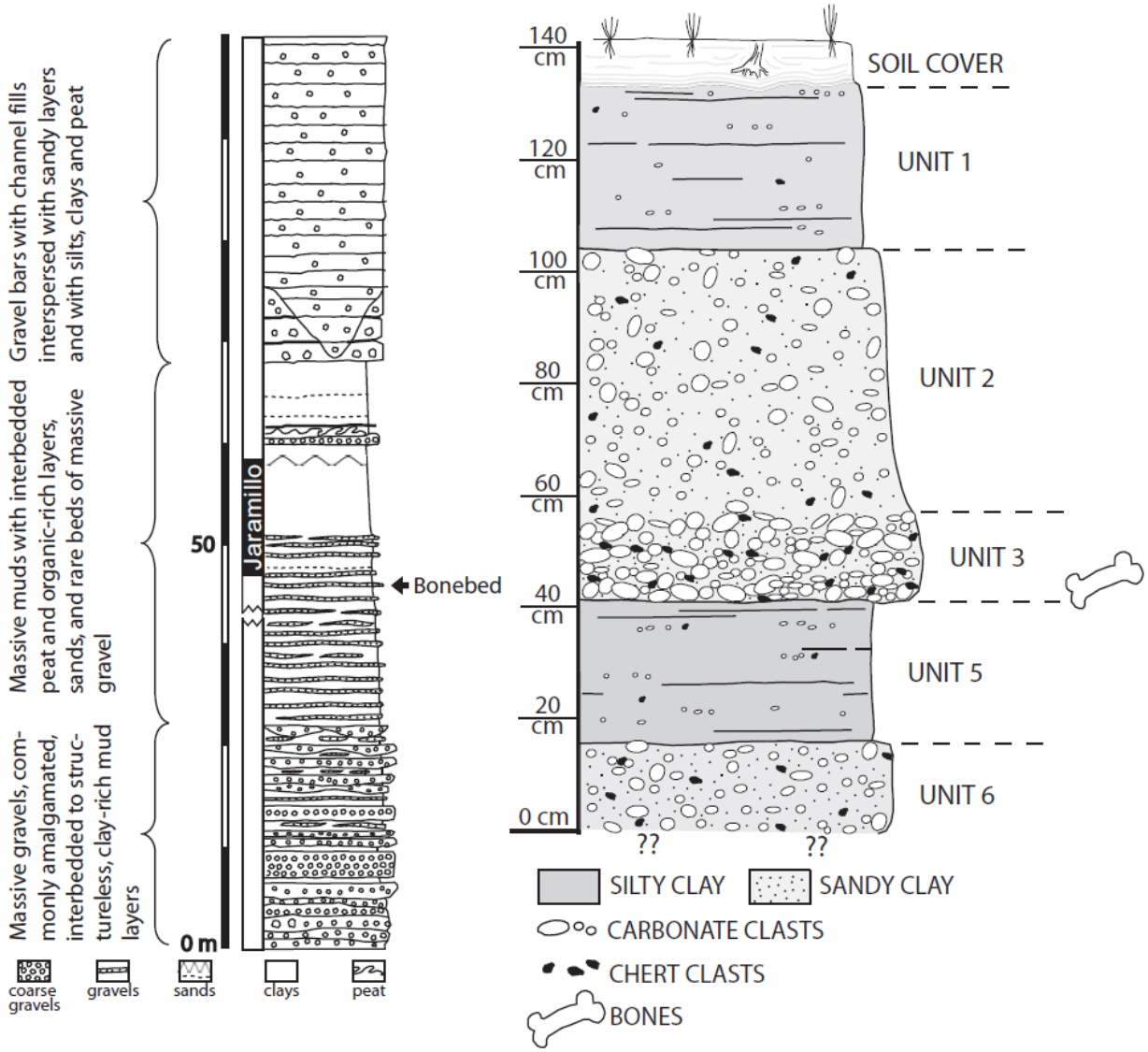

Figure 3 *- Generalized stratigraphic column of the sedimentary succession at Collecurti (left column for the entire basin fill, modified from Coltorti et al., 1998).*

Stratigraphic unit 4 (U4) is an elongate, lensoidal lithosome only a few square meters in size that is limited to the SW margin of the excavation. It is ~30 cm thick and a few dm wide, incised into U5, and consists of structureless, clast-supported, granule to medium pebble gravel with densely packed carbonate clasts and a scarce matrix of silty sand. One of the pebble-sized clasts has been identified as a polished antler fragment of *Praemegaceros verticornis*.

The overlying stratigraphic unit 3 (U3) contains the great majority of vertebrate remains and represents the principal bonebed at the Collecurti site. It is a variably thin (10-15 cm) bed of clast-supported to locally matrix-supported, pebble to coarse cobble gravel with a sandy, silty clay matrix. Lithic clasts represent approximately 60-70% of the unit by volume, clustered in clast-rich domains with long axes parallel or perpendicular to paleoflow, and less commonly isolated within matrix-rich domains. Carbonate pebbles to fine cobbles can reach up to 10-15 cm in diameter, angular to subrounded, whereas chert clasts are angular and distinctly smaller.

Unit 3 presents a gradual, indistinct transition upwards to unit 2 (U2), which consists of a continuous bed up to 50 cm thick of light-brown, massive, matrix-supported granule to small pebble conglomerate. Carbonate and minor chert clasts represent ~30% of the sediment by volume, are homogeneously dispersed in a thick, relatively sand-rich, silty clay matrix (sand content by volume ~20-24%; clay content by volume ~36-39%; Figs. 5B, C), and present no evident gradation or fabric. The modal grain size of dispersed pebbles is distinctly finer than that of the underlying U3, but the few fine cobbles present (up to ~10 cm) occur in the topmost 5-10 cm of the bed. A minor fraction of coarse clasts in U2 is represented by sparse, isolated bones and bone fragments showing no preferential orientation. TOC estimates for two samples of muddy matrix of U2 revealed a low to very low content of dispersed organic matter, ~0.4% and ~0.2% by weight.

The sharp, laterally continuous transition to the overlying stratigraphic unit 1 (U1) is recognizable at outcrop by the darker brown color of the fine fraction and the drastic reduction in volume of the coarse clastic fraction in U1. With a variable thickness from 10 to ~30 cm, this unit is directly overlain by the recent soil and agrarian terrain of the Collecurti hilltop. It is therefore deeply disrupted at its top (and locally over its entire thickness, down to U2) by arboreal rhizoturbation, fracturation and vertic phenomena related to Holocene and recent pedogenesis. Unit 1 is a massive, silty clay (clay content by volume ~62%; Figs. 5A, B, C) with rare, scattered granules and fine pebbles and very low sand content (~7% by volume; Figs. 5A, B, C). No preferential fabric or gradation is observed in the coarse clastic content of the unit. TOC estimate for U1, 1.2% by weight, is based on a sample taken from an undisturbed location within the bed. Given the stratigraphic position of this unit immediately underlying recent pedogenic horizons, the TOC results may not be representative of the original composition, since most of the original organic content may have been oxidized by vadose waters, and recent organic matter illuviated from vegetated soils above. The majority of bones from the Collecurti fossil assemblage were found within U3, mainly concentrated along two elongated alignments of coarse debris, trending EW and NS (Figs. 2, 5), and subordinately in U2. Bones in U3 were buried with intermediate and long axes lying horizontally or subhorizontally, parallel therefore to the depositional interface, whereas a few massive and elongated ones (isolated elephant bones, e.g., a tusk, some

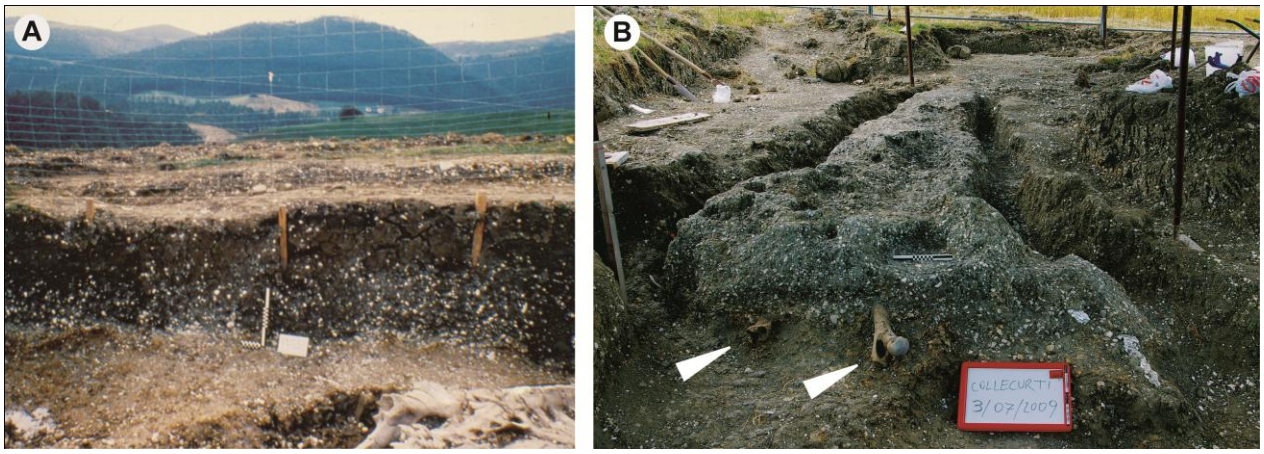

Figure 4 *- Overview of Collecurti excavation. (A) View toward ESE at an early stage of excavation; the bottom of the trench wall follows the contact between stratigraphic U2 (light brown, with abundant carbonate clasts) and the overlying U1 (dark brown, dominant fines with minor gravel content); in foreground, lower right corner, a partial skeleton of a hippopotamus is visible within U3. (B) Advanced stage of excavation, with intersecting trenches mainly terminating along the U5-U3 stratigraphic contact; white pointers show hippopotamus bones, a right tibia on the left, and a right femur on the right, still encased by sediment.*

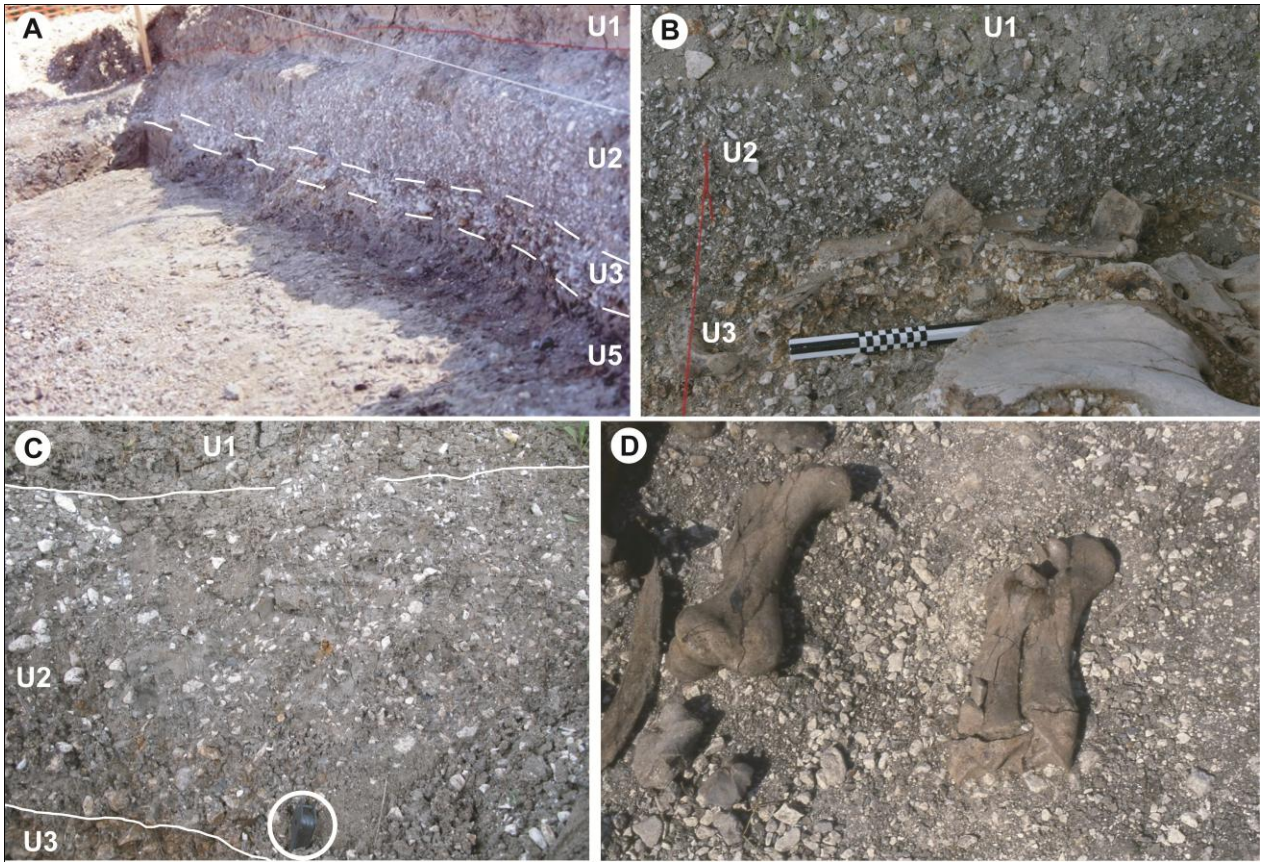

Figure 5 *- Sedimentology of the Collecurti site. (A) Deep trench exposing almost the whole stratigraphic interval comprising the bonebed, from U5 to U1; note the planar, non-erosive contact of the debris-flow (U3-U2) over the U5 lacustrine deposits, and the irregular contact between U2 and U1, marking fine lacustrine deposits aggrading over the mesotopography of the debris-flow lobe. (B), (C) Details of the upper strata, showing lithological transitions between U3, U2 and U1. (D) Orientation of elongated bones within U3.*

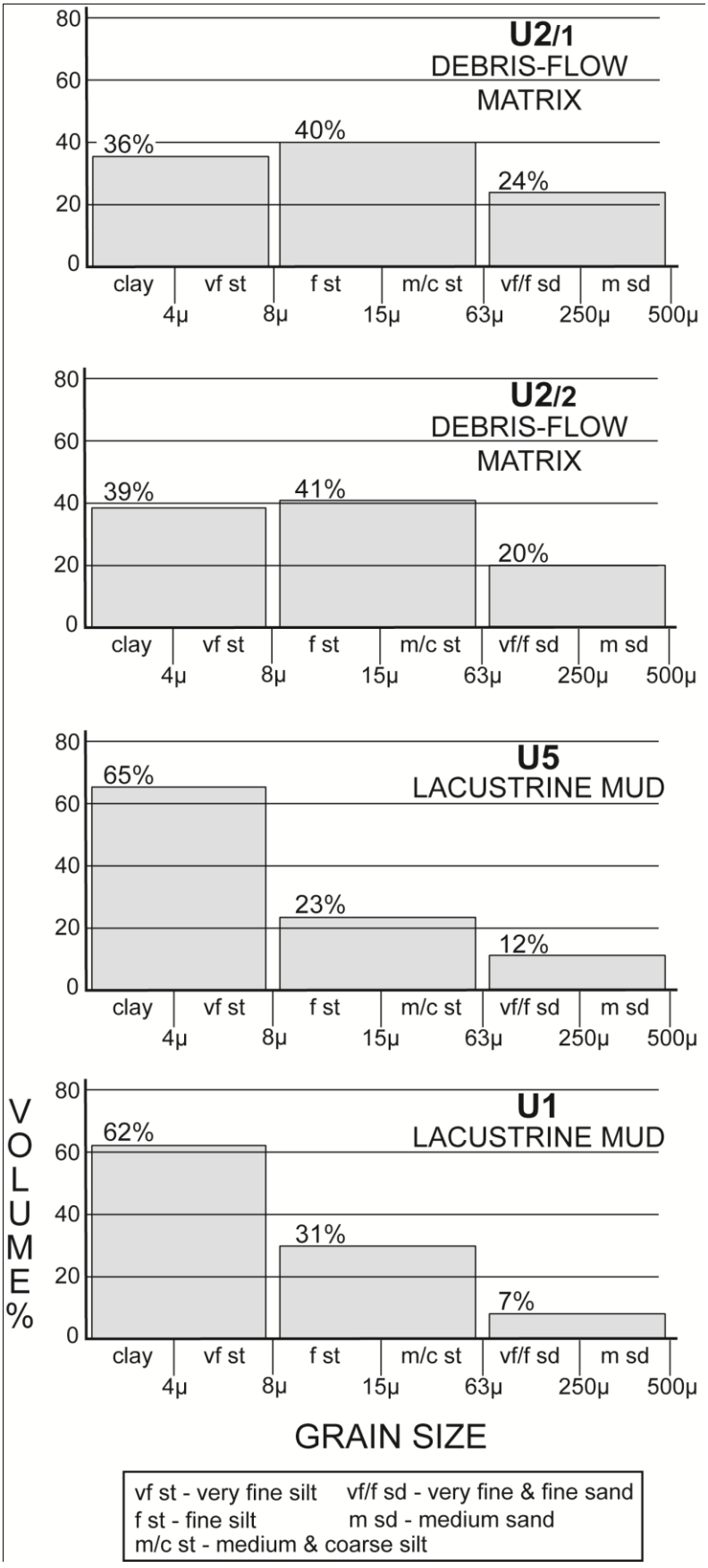

Figure 6 *- Representative grain-size diagrams for fine sediment fractions of U1, U2 and U3; for discussion, see text.*

rib fragments) were found with one extremity penetrating the topmost levels of the underlying U5. Fossil elements within U2 instead have horizontal to subhorizontal orientation, but no preferred fabric.

Clast lithologies in the coarse-grained fractions of sediments at Collecurti reflect provenance from nearby sources along the eastern basin margin. Prevalent limestone and marlstone clasts in the conglomerate beds were sourced by the Upper Jurassic to Eocene carbonate formations still extensively outcropping in the proximal hinterland (Calcare Massiccio, Calcare Rupestre, Scaglia Rossa and Marne a Fucoidi; Moretti, 1969). The latter three formations are also characterized by abundant dark-grey to reddish chert nodules, which represent the second most abundant gravel component by volume at the Collecurti site. The high volumes of clay that characterize the Colfiorito Basin fill, and sediments at Collecurti, were likely derived from marlstones of the Marne a Fucoidi and Scaglia Rossa formations, which are characterized by very high detrital clay contents (Moretti, 1969). The notable scarce volumes of fine to coarse sand reflects the paucity of sand-sized clasts produced by weathering and erosion of micritic carbonates, marlstones and cherts.

6.3.3. Interpretation

The 90 m succession of fluvio-lacustrine sediments at Collecurti comprises about 33 m of lacustrine sediments sandwiched between alluvial gravels in both its lower and upper part (Coltorti *et al.,* 1998). In particular, the stratigraphic interval of the bonebed presents interbedded lacustrine and alluvial mass-flow deposits. This facies association characterizes the early paleoenvironmental evolution of the Colfiorito Basin (Coltorti *et al*., 1998; see Section 2 and Fig. 3), where high-gradient streams and small alluvial fans issued from the basin margins supplying water and sediment into a wider, shallow-gradient basinal setting that was at times occupied by a lake.

Units 1 and 5 are dominated by clay-rich, structureless muds, with a very subordinate content of scattered granules and fine pebbles. Fine, organic-rich laminae within U5 present a subhorizontal attitude that traces the low topographic gradient of the original depositional interface. These features collectively represent undisturbed sedimentation in a low-energy, probably shallow lacustrine environment, at a sufficient distance from the paleocoastline to allow dominant suspension settling of clay and silt (Picard & High, 1972; Fouch & Dean, 1982; Hamblin, 1992). Fine sediment was probably supplied into the lake by periodic surface plumes of tributary streams and small fan deltas along highlands at the basin margin. The significant organic content in the U5 sample probably reveals abundant supply of organic debris from subaerial sources, since the scarcity of aquatic fossils suggests low local organic productivity. The lateral continuity of thin organic-rich laminae also points to quiet bottom waters. Given the relatively small areal extent of the basin, wave effects at the depositional interface must have been minimal or absent (Sly, 1994). Coarse-clastic deposition was limited to lake margins, and the scattered fine gravel within muddy facies were deposited during severe flood events.

Stratigraphic unit 4 is difficult to interpret due to its limited exposure, but it indicates energetic transport conditions along a shallow, well-delimited subaqueous channel, or possible alluvial incision and sedimentation during temporary lowstand and exposure of the lake bottom. The well-sorted, clast-supported fine gravel with poorly sorted, non-layered, sandy interstitial matrix and absence of tractive

structures indicate possible transport by the distal head of a hyperconcentrated flow, where high sediment load and rapid deposition would have prevented deposit organization (Arnott & Hand, 1989; Smith & Lowe, 1991). Flow propagation into the shallow waterbody and along the low-gradient bottom would have favored rapid loss of momentum and slowed the current, with consequent sudden bedload deposition. Given the absence of any other channelized alluvial deposits within the stratigraphic interval examined, this isolated lens probably represents an uncommon event. Similar poorly structured, coarse-grained deposits are common in distal alluvial-fan and fan-delta settings (e.g., Wells & Harvey, 1987; Kim *et al.*, 1997; Lowey, 2002), including the Quaternary stratigraphic record of Apennine intermontane basins (Benvenuti, 2003; Zembo, 2010).

Units 6, 3 and 2 are characterized by high volumes of poorly-sorted gravel up to cobble size (~10-15 cm) supported by a matrix with very high clay content, a total absence of sedimentary structures reflecting unidirectional flows, and a general absence of organized fabrics. In particular, the relatively clast-rich U3 presents a gradual transition to the overlying U2, and mantles the underlying depositional topography defined by U5 and U4 through a sharp, nonerosive contact. These characters point to transport and deposition by debris flows, which are highly concentrated slurries of sediment and water flowing as a single phase with non-Newtonian, plastic behavior (Nemec & Steel, 1984; Pierson & Costa, 1987; Major, 2003). The clay-rich matrix, which constitutes the bulk of the unit, provided high viscosity, preventing turbulence along the basal flow interface and thus preventing significant erosional scour. Next to the elevated viscosity, very high clay content provided also cohesion and maintainence of excess pore pressure within the flow body, allowing sufficient competence for debris flows to carry gravel distally along the shallow lake bottom (Pierson & Costa, 1987; Major & Iverson, 1999). High cohesiveness further prevented significant mixing and entrainment of ambient water at flow head and consequent dilution into a transitional or fully Newtonian sediment-gravity flow (Hampton, 1972; Weirich, 1989; Sletten *et aI.*, 2003; Sachse, 2005), which would have induced dumping of coarse load in the proximal lake realm. Recent experimental evidence (Marr *et al.*, 2001; Ilstad *et al.*, 2004) in fact shows that clay-rich debris flows (defined as > 25-33% clay by weight) can attain a strongly coherent behavior and advance in subaqueous environments while undergoing minimal mixing with ambient water.

Absence of sorting in U2 and of preferential fabrics in its gravel fraction are ascribed to typically high flow viscosity and lack of turbulence during cohesive debris-flow transport ('plug flow'), which prevented bedload traction and the attainment of hydrodynamically stable clast orientations. The relatively high content of very coarse sand particles scattered within the matrix also points to rapid mass transport without hydraulic selection, contrary to the finer, silty clayey distal lacustrine U5 and U1. The associated bones within U3 and U2 were transported as coarse, oversized clasts (Eberth *et al.*, 2006). The horizontal position of elongated bone fragments in U3 is due to laminar shear along the basal layers of debris-flow bodies during transport (Lindsey, 1968; Enos, 1977; Lewis *et al.*, 1980; Nemec & Steel, 1984; Hubert & Filipov, 1989).

An alternative interpretation could possibly be represented by deposition from a subaerial hyperconcentrated flow entering the lake margin. Hyperconcentrated flows are high-concentration sediment dispersions (~20-45 vol.%; Beverage & Culbertson, 1964; Costa, 1988), commonly characterized by

Newtonian to transitional rheology and dynamic separation of sediment and water as two distinct phases. A potentially very heterogeneous range of grain sizes is partly supported by particle interactions and buoyancy in the dense dispersion, but traction and clast segregation are commonly observed, due to the still prevalent action of the fluid phase. However, common characteristics of hyperconcentrated-flow deposits, such as distribution grading, internal structures and basal scouring due to residual turbulence (Smith & Lowe, 1991; Sohn *et al.*, 1999; Benvenuti & Martini, 2002) are not observed in U3 and U2. Irrespective of the possible sediment concentration, the elevated volume of clay in the original flow would have severely dampened turbulence (Coussot, 1995; Baas & Best, 2002) and forced rheology into the plastic to pseudo-plastic range of typical debris flows.

Debris flows are a frequent phenomenon in intermontane basins of the Apennine orogen (Guzzetti & Cardinali, 1991; Benvenuti, 2003) due to high relief and abundant clay- and silt-sized colluvium sourced from shale and marlstone Meso-Cenozoic formations and trapped in steep, immature catchments. These combined factors lead to high slope instability and sharp peaks in surface hydrological activity, especially during prolonged rain or exceptional snowmelt events. The geology of small catchments in highland settings is therefore instrumental in controlling the frequency and mechanics of resedimentation, and basements with high production of fines are very effective in triggering debris-flows (Blair, 1999; Moscariello *et al.*, 2002; Wagreich & Strauss, 2005). The markedly low TOC contents of U2 with respect to the underlying lacustrine U5 also supports a subaerial origin from colluvial sources (e.g., Sletten *et al.*, 2003) which included relatively little preserved organic matter.

Clast-rich U3 represents a concentrated segregation of coarse gravel and bones directly below the basal surface of U2, but as mentioned in the previous section, bones and coarser clasts are not uniformly distributed within U3. One major concentration is given by an elongated belt of coarse pebble to fine cobble gravel and bones, approximately 2 m wide and oriented EW along the southern portion of the excavated site (Fig. 2). The other important concentration of coarse clastic and fossil elements has a roughly perpendicular orientation to the first one, extending along an arch oriented approximately NS-NNE (Fig. 2) at the northern and western margins of the site.

The overall geometry of the two linear accumulations of coarse gravel and vertebrate remains within U3 suggests that their final distribution is related to mechanical effects of the advancing debris flow at its late stages. Strain distribution within moving debris-flows commonly segregates larger clasts towards the top and front, forming a coarse frontal “snout” with distinctly frictional behavior with respect to the slurry-like, fine-dominated flow body trailing behind it (Major, 1998; Major & Iverson, 1999; Parsons *et al.*, 2001). The frontal snout provides resistance to the advancing flow due to coarse-clast inertia and interlocking, and is intermittently sheared aside and partly overrun by the main flow body advancing behind it. This coupled mechanism of spatial clast segregation and intermittent flow surging produces characteristically elongated coarse lateral levees along the path of debris flows that carry heterometric sediment loads (Sharp, 1942; Johnson, 1970), as well as a frontal of coarse material upon final deposition (e.g., Pierson, 1986; Blair & McPherson, 1998). Furthermore, coarse clasts concentrated within lateral levees and along the frontal snout of debris flows may carry well-developed fabrics parallel to debris-flow margins, and thus respectively

parallel and transverse to the general flow direction (Bertran *et al.*, 1997; Major, 1998; Blair & McPherson, 1998). Clast-rich U3, underlying and gradually transitional to finer-grained, matrix-rich U2, is thus interpreted as the deposit of the coarse debris-flow front, progressively overrun and forced sideways by the advancing flow body (U2), and amalgamated at its base. The possible hypothesis that such a vertical facies distribution be due to debris-flow mixing with water and partial loss of capacity (i.e., incipient flow transformation into a high-density turbidity current) can be discounted because the "plug-flow unit" (U2), which represents most of the flow volume, does not present any evidence of partial dilution and internal gradation or reorganization.

The preferential distribution of mammal bones and coarser gravel along two elongated belts, therefore, represents the depositional signature of coarse clast segregation to the debris-flow snout and to the left (southern) lateral levee. Considering the orientation and proximity of highlands (Fig. 1) along the eastern basin margin, the overall evidence suggests debris-flow propagation toward W or WNW. Based on this evidence, we predict that another bone concentration could be revealed by extending future excavations towards NE; if confirmed, this second bone accumulation would represent the right (northern) debris-flow levee.

6.4. PALEONTOLOGY OF THE COLLECURTI BONEBED

6.4.1. Material and methods

Standard techniques have been used for field and quarry mapping, as well as for excavating and preparing the bones (Leiggi *et al.*, 1994). A meter grid system was employed to map the specimens (Figs. 2, 7A). All bones, identifiable to element or not, were mapped. Scale profile drawings of the stratification of the sidewalls of the excavation were obtained marking boundaries between layers with strings held in place with nails. Bones and rock particles above the size of gravels have been mapped.

Taphonomic data recorded in the field include specimen orientation , i.e., horizontal long-axis alignment and plunge data (obtained by compass and clinometer). These quarry data were essential for assessing patterns and causes of breakage, as well as sorting. Other taphonomic information has been collected in the laboratory. In fact, assemblage data, i.e., taxonomic and anatomical identification, quantification of the individuals, relative amounts of the different taxa, age spectrum, body size, degree of articulation and selection, and bone modification data, i.e., breakage, weathering, abrasion/polishing, surface marks (Beherensmeyer, 1991), have been obtained after preparation. Quarry data, and more specifically orientation trends and the relative position of the elements, have been completed in the laboratory from the maps. Specimens have been taxonomically and anatomically identified by comparison with others in the collections of the Museum of Natural History of the University of Florence. Standard taphonomic parameters have been used to categorize the specimens (Munthe & McLeod, 1975; Behrensmeyer, 1991; Lyman, 1994; Rogers, 1994; Eberth *et al.*, 2007; Britt *et al.*, 2009). The calculated NISP (number of identified specimens, in which "identified" is intended here to mean to taxon or only to skeletal element), MNI (minimum number of individuals), and MNE (minimum number of elements) values are reported in Table 1. These values are summarized in Table 2, where the number of non-determined specimens are added. The

MNI was obtained once the specimens had been attributed to single individuals by side-matching, taking into account size, proportions, degree of ossification, age, as well as state of preservation. The paleontological context had no effect on the estimation of the MNI, because all the specimens come from a single depositional unit and from a relatively confined area. Moreover, by analyzing the entire Collecurti faunal sample, the effects of aggregation on the MNI counts were avoided (Brewer, 1992; Grayson, 1978, 1984). Because most of the identified elements of Collecurti are complete the risk of significantly overestimating MNI by counting multiple specimens from the same element is minimal. The frequencies of element portions have also been tallied to calculate the MNE, accounting for age, size, and, where possible, sex.

Collecurti is characterized by a low overall number of species, as opposed to an unusually high concentration of hippopotamus carcasses. Biodiversity was assessed using Shannon and Weaver's (1949) measure of heterogeneity H' [H' = $\Sigma(ni/N)\ln(ni/N)$ where: N = total MNI, *ni* = MNI of (*i*)-species] and index of evenness J [J = H'/Hmax where: Hmax = ln s where s = number of species of the community] based on estimates obtained using the jack-knife technique (Kaufman, 1998). Shannon and Weaver's (1949) evenness index has the advantage of preventing the skewing by rare species of the H' index.

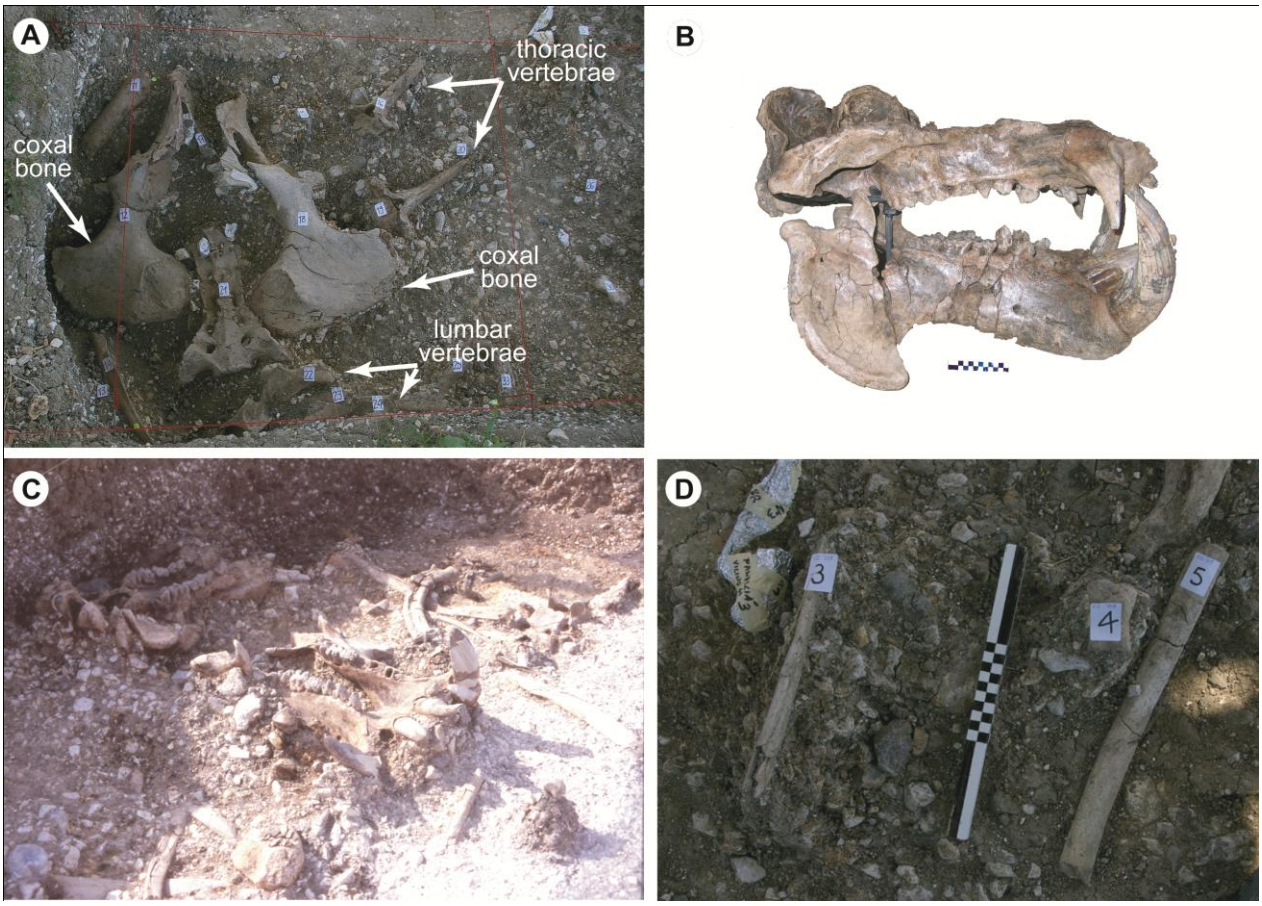

Figure 7 *- Examples of recovered fossils at the Collecurti bonebed. (A) View of the north-eastern sector of the excavation. (B) Right lateral view of adult skull of male hippopotamus (MNSUC 52486) from Collecurti, mounted with its mandible (MNSUC 52487). (C) Northern sector of the excavation. Overturned hippopotamus skull and mandible at upper left and at the center, respectively. (D) Northern sector of the excavation, showing hippopotamus ribs and phalanges.*

Exploring the origin of the bone accumulation prompts the question, What happened to all the hippopotamuses? Arguably the answer hinges upon what caused their death. Our taphonomic inquiry therefore aimed preferentially at this major target.

The distance between a fossil assemblage and its original living counterpart depends on how intensely the taphonomic processes and time-averaging effects have modified the composition of living communities. To detect and evaluate taphonomic biases we used Damuth's (1982) size-abundance relation [$Log\ A = \alpha+\beta\ (Log\ W)$], where A = taxon abundance and W=body weight). In an ideal, unbiased mammal assemblage, the slope of the logarithm of the number of individuals upon that of body weight approximates -105 ± 0.25 (95% confidence interval). The overall weight represented in the Collecurti bone assemblage is given by the average sum of the estimated body weights. To remove the bias of differential bone destruction (Behrensmeyer *et al*., 1979; Behrensmeyer & Boaz, 1980; Damuth, 1982), Damuth's (1982) correction factor ([$d_i = 0.68(log\ W_L — log\ W_i)$], where W_L is the body weight of the largest taxon in the assemblage and W_i is the weight of the "i"taxon) was added to each species abundance ($Log\ A_{corr} = \alpha+\beta\ [Log\ W]$, where Log A_{corr} = Log (A_i + d_i). Individual weights have been obtained by plotting dental measurements of the Collecurti specimens on Janis's (1990) equations and employing Prange *et al*.'s (1979), Schmidt-Nielsen's (1984), Reitz and Quitmyer's (1988) allometric scaling with the sizes of specific postcranial elements. In particular, the weights of the Collecurti hippopotamuses have been assessed by referring to Pienaar *et al*.'s (1966) body length and weight data for present-day *Hippopotamus amphibius*, cross-comparing them with the weights obtained by allometric scaling recalculated explicitly for the Collecurti hippopotamuses [e.g., in the femur: Log Y= 2,31+1,2 Log X, where X is the depth of the femur head (DC), and Y is the estimated body weight] using Mazza's (1995) osteometrical data.

Age mortality profiles can be most useful for the interpretation of death scenarios (Kahlke & Gaudzinski, 2005). Death patterns are age frequency distributions, obtained by plotting minimum numbers of individuals against age classes on a histogram. The ontogenetic ages have been obtained by referencing to Laws's (1968) age-scoring for *H. amphibius*, in the assumption that *H. antiquus* wore its teeth at a similar rate. Sudden death events normally give L-shaped death patterns, in which frequencies regularly decrease from younger to older age classes. In the hypothesis that the hippopotamuses of Collecurti were struck by some calamitous circumstance, the death rate of these pachyderms was calculated using Raup and Stanley's (1971) dynamic procedure and then compared with that of living hippopotamuses (Miller, 1988; Nowak, 1999; Morgan Ernest, 2003; see also http://genomics.senescence.info/species/). Alternatively, if the Collecurti hippopotamuses were killed through time, mortality diagrams are expected to show U-shaped patterns, as a result of attritional accumulation through time of carcasses of young and very old individuals, which are the two age classes especially exposed to risk of death under normal conditions.

Juveniles would be a fundamental source of information. The age at death of juvenile individuals may indicate if the deaths were concentrated in a particular period of the year - thus revealing a potential catastrophic mass death event -, or spread throughout. Unfortunately though, at Collecurti juveniles are rare.

Hippopotamus skeletons are protected by large amounts of flesh and fat, and their elements are held together by very tough connective tissues and organs. The degree of bone weathering matched with the percentage of disarticulation gave an estimate of the degrees of soft-tissue removal and bone scattering.

The absence of bites, gnaw marks, coprolites, and any other evidence of carnivore intervention rules out the possibility that carnivores had a role in the formation of the bone assemblage. Hence, tests specifically devised to detect and explore carnivore ravaging have not been used. On the contrary, because of the particular nature of the bone-bearing sediments, we explored the role that a-biotic agents had in the formation of the assemblage. The susceptibility of the Collecurti bones to fluvial transport was evaluated using different methods, above all Voorhies' approach (Voorhies, 1969; Behrensmeyer, 1975) and Frostick and Reid's (1983) classification of bones. Where possible, Binford's (1978) normalized MAU values, i.e., %MAU, which are obtained by dividing every single MAU value by the maximum MAU value, have been compared with Frison and Todd's (1986) saturated weight index (SWI) values, to see how much the weight of fresh bones affects their clustering. Behrensmeyer's (1975) tooth/vertebra ratio was yet another possible means to establish the susceptibility of the Collecurti bones to fluvial transport. The low number of isolated teeth (9) and vertebrae (46), however, prevented its use.Degree of articulation and selection, and bone modification data, i.e., breakage, weathering, abrasion/polishing, surface marks (Behrensmeyer, 1991), have been obtained after preparation.

Quarry data, and more specifically orientation trends and relative position of the elements, have been completed in the laboratory from the maps. Maps and excavation reports are archived at the Soprintendenza per i Beni Archeologici per le Marche, which supervised and financed the excavations, whereas the Collecurti specimens are stored at the Museum of Natural Sciences at the University of Camerino (MNSUC).

6.4.2. Fauna

The site yielded 496 unevenly distributed and mostly subhorizontally oriented bones (Figs. 2, 7). Of the total NISP, 2 (0,4%) have been identified only anatomically and 441 (99,6%) both anatomically and taxonomically, for a total of 9 species and 8 genera; the unidentified specimens sum up to 53 (Tabs. 1,2). The NISP counts of hippopotamus remains add up to 402, representing 90,7% of the total NISP. There are at least 11 individuals (MNI), including 3 senile individuals, 2 adults, 4 prime adults (around 20-25 years of age), 2 juveniles (under 10 years of age), and one fetus (which indicates the presence of a pregnant female). *Mammuthus meridionalis* is represented by 9 elements, belonging to 3 individuals: an adult, a prime or subadult, and a juvenile. There are 3 remains of *Stephanorhinus* cf. *hundsheimensis*, representing 2 elements of a single individual. *Pseudodama* ex gr. *nestii* counts 12 specimens of a minimum of 7 elements, representing 2 adults of slightly different age. *Praemegaceros verticornis* is present with 9 specimens of 7 elements which belong to at least 2 adults. Three remains belong to *Leptobos* sp., representing 3 elements all of a single adult individual. Each of the three carnivores, *Ursus* sp., *Canis arnesis* and *C.* (*Xenocyon*) *falconeri*, is represented by one specimen.

Collecurti includes a relatively low number of species [9; Shannon and Weaver's (1949) H' = 1,68], rather evenly represented (evenness J = 0.76) and with a wide spectrum of body sizes (~20 to ~9000 kg). This

suggests that the Collecurti assemblage may provide a fair picture of the local mammalian community. If so, its scarce richness may indicate that the region had long been exposed to stressed climatic and environmental conditions.

The result of the size-abundance analysis is shown in Figure 8. The logarithm of raw abundances regresses positively on the body mass logarithm [*Log A* = 1,9472 + 2,2915 (± 0,21) *Log W*], with a fairly dispersed correlation (r = + 0,69) as well as a fit that is statistically significant (rs =0,75; *p>0.05*). The corrected abundances logarithm, which should eliminate taphonomic biases, also regresses positively on the body-mass logarithm [Log A_{corr} = 0,3322 + 0,0435 (± 0,16) Log W] (Fig. 8B) with a much more dispersed correlation (r = + 0,24) but with a fit that is very significant statistically (rs = 0,91; *p>>0.01*). Hence, abundance and weight of the Collecurti animals are correlated rather positively, than negatively as imposed by Damuth's (1982) model - a result indicating that the accumulation is definitively biased.

Among living hippopotamuses sexes are readily distinguished by relative body size, although dimensional differences are not so clear-cut to prevent very large females to attain the size of small males. Needless to say, sexing hippopotamus bones is even more complicate. Nonetheless, females normally bear smaller and proportionally more slender canines compared to males. Accordingly, the alveoli of these ever-growing tusks give wider and more powerful rostral fans in males as opposed to females. Based on this and also on Laws' (1968) age-scoring, the Collecurti hippopotamus sample includes a ~33-year-old male (skull 52486 and mandible 52487), two ~24-year-old females (skull 21 and mandible 20, and skull 602107 and mandible 632007), and a ~35-year-old female (right upper canine 82147, left upper canine 52671, and mandible 52697).

The aging of these as well as of other skull and jawbone remains permitted the construction of a mortality diagram of the hippopotamus community (Fig. 9). The mortality pattern shows a census profile of a living community of hippopotamuses. Modern hippopotamuses have a low mortality rate (initial mortality rate: 0.01/year; mortality rate doubling time: 7 years; Weigl, 2005), they live around 40 years, reproduce into old age, and cows usually have their first calf at about 10 years of age (Finch, 1990). After a gestation of 227-240 days cows give birth to a single young. Weaning lasts around a year, although lactation can extend for 18 months. Living hippopotamus groups therefore have an overturned-L-shaped structure, with a number of individuals growing in parallel with ageing, in line with what is expected in populations of megaherbivores in which juveniles sum up to 6 to 14% (Norman Owen-Smith, 1992). If *H. antiquus* had lifespan, ageing, and history traits similar to those of living hippopotamuses, the mortality diagram in Figure 9 is that of a group (family?) of hippopotamuses killed simultaneously.

6.4.3. Taphonomy

Bone accumulations formed by a-biotic agents are usually characterized by low amounts of articulated bones. With the exception of a rear half of a hippopotamus axial skeleton, including two thoracical vertebrae, 4 lumbar vertebrae, the sacrum, pelvis and 10 caudal vertebrae, all lying in a single plane, the Collecurti bone assemblage is entirely composed of disarticulated specimens. Though disarticulated, most of the bones of the different hippopotamus skeletons have been found in close association within the excavated area.

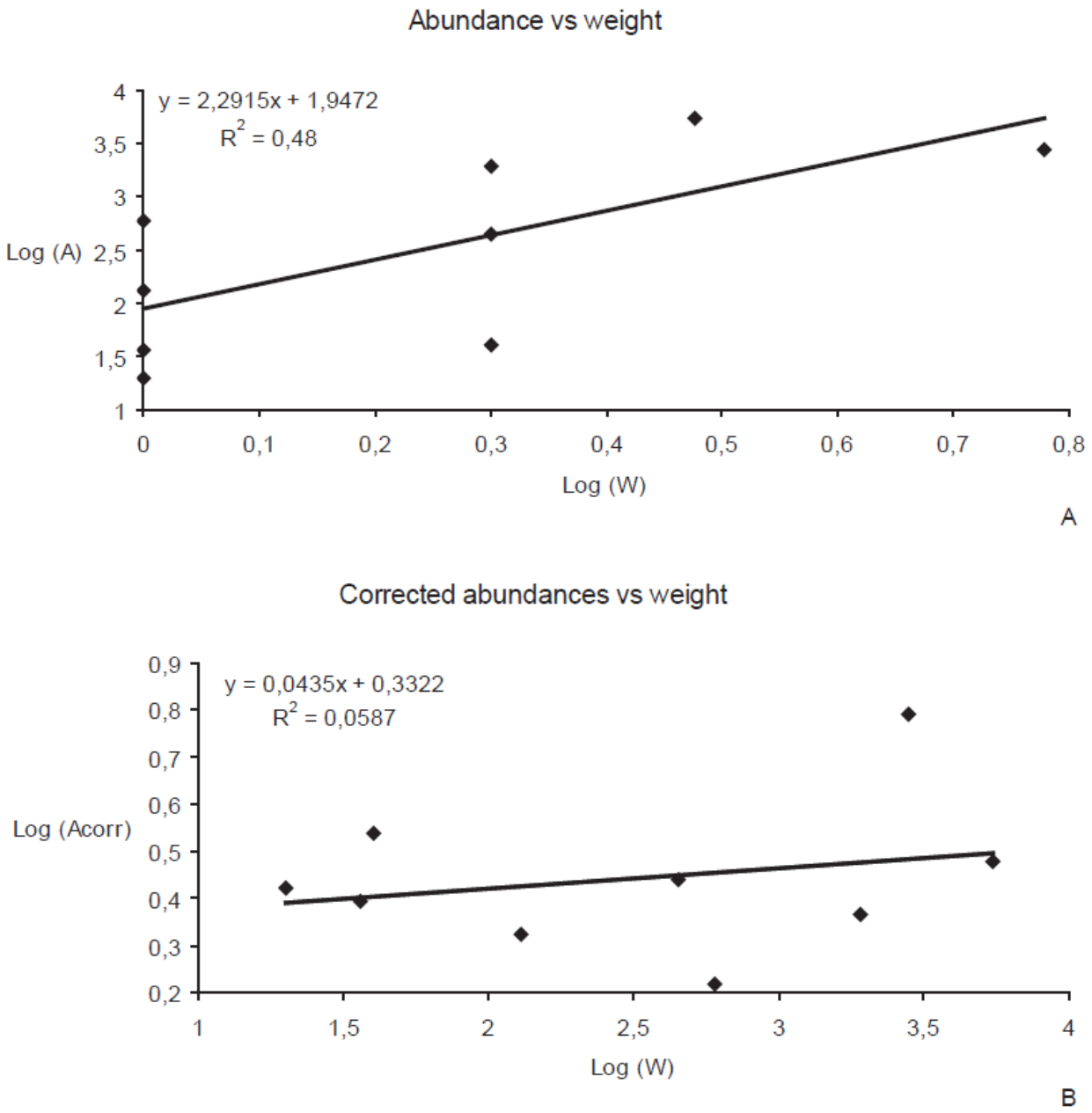

Figure 8 *- Abundance–size relation in the Collecurti assemblage. (A) Abundance (A)-size (W) relation; the relative abundance of a species is a function of both its population density and turnover rate, which in turn are inversely related to body weight. (B) Modified abundance (Acorr)-size (W) relation in the Collecurti assemblage corrected for bone size bias, following Damuth (1982). Abundance and weight of the Collecurti animals correlate positively, indicating that the accumulation preferentially preserved large bones.*

As noted above, the bones are largely concentrated along the northeastern, western and southern sectors of the excavated area, and most Collecurti elements were found oriented with horizontal to subhorizontal long axes; only a few bones (~ 4%) were lying with a modest (~ 5°) dip. The rose diagram depicting trends in long axis orientation of 136 long bones or elongated fragments (Fig. 2) shows bimodally distributed specimens, with 43% oriented NW–SE, and 40% E–W. All other bones show random orientations. More specifically, most thoracical vertebrae of the hippopotamus bones have the spinal process pointing WNW, long bones are often oriented NNW-SSE, and ribs E-W. The convexity of an elephant tusk fragment was oriented

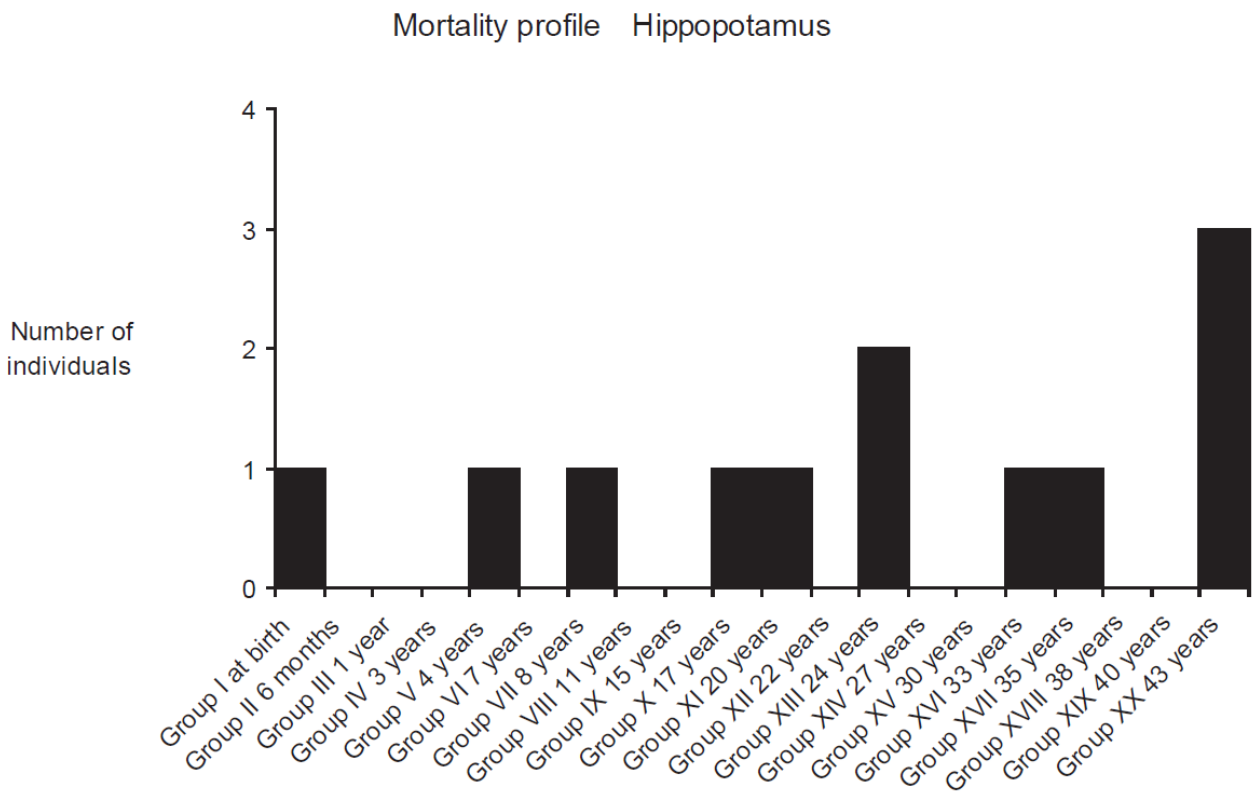

Figure 9 *- Mortality profile showing the population structure for Hippopotamus antiquus. The mortality pattern is similar to a census profile of a living community of hippopotamuses, suggesting the animals preserved at Collecurti were killed simultaneously.*

eastward. Many of the determined specimens have a size far exceeding the granulometry of the hosting sediment, and even the grainsize of the associated gravel. In other words, there is little hydraulic equivalence between skeletal elements and embedding sediments.

The hippopotamus bones are practically unaffected by abrasion/polishing (only 0.7% of all hippopotamus remains and 0.4% of the total Collecurti bone sample shows this kind of alteration).The bones of all other taxa, on the contrary, are isolated elements. Almost 10% of them are abraded/polished, and ~12% shows evidence of subaerial exposure (weathering ranging from stage 1 to 3). Using Frostick and Reid's (1983) classification, 7% of the hippopotamus bones from Collecurti can be classified as disks, 24% as spheres, 26% as rods, and 43% as blades. Comparing these percentages with those of an unaltered hippopotamus skeleton (disks 3%, rods 27%, spheres 45%, and blades 25%) we notice that at Collecurti there is a significant increase in blades, spheres are half as much, disks show a very modest increase, whereas rods are present in a virtually equivalent amount. If we classify the bones of all other taxa at Collecurti we find a prevalence of rods (55%) and spheres (26%), blades sum up to 19% and disks reach merely 6%. Frostick and Reid (1983) state that blades and disks are less likely to be removed, as opposed to rods and spheres, which can be more easily dispersed by fluvial action. Hence, at Collecurti hippopotamuses are represented by a comparatively higher amount of less easily removable bones than all other taxa. Similar results are obtained analyzing the proportions of Voorhies Groups present in the site. In fact, hippopotamus shows 46% of Group I bones (most easily removable), 34% of Group II, and equivalent amounts (10% each) of Group I and II (fairly easy

to remove) and Group III bones (least easy to remove). Compared to an unaltered hippopotamus skeleton (Group I: 44%; IandII: 37%; II: 18%; III: 1%) at Collecurti we see a significant increase in Group II and Group III bones, and a drop in Group I and II bones, whereas Group I show virtually constant proportions. As for the rest of the assemblage, most easily removed bones sum up to 40%, Group II bones reach 54%, whereas less easily removable elements total 6%. Compared to hippopotamus, all other taxa at Collecurti are represented by bones that are most to moderately subjected to fluvial transport.

The %MAU values of *Mammuthus meridionalis*, the only taxon of the Collecurti assemblage relatively close to the present-day Indian elephant for which Frison and Todd (1986) had provided the SWI values, do not correlate significantly with Frison and Todd's data (r_s=0,825, p < 0,1). Hence, the weight due to saturation had very little or no influence on the accumulation of the bones. Moreover, virtually all the elephant bones are skeletal elements with FTI values exceeding 50, and some (i.e., thoracic vertebrae) even over 75, which Frison and Todd say are similar to Voorhies Group I and Group II bones, respectively.

Weathering is virtually absent at Collecurti. Extremely rare (~2%) evidence of exposure, not greater than Behrensmeyer's (1978) stage 3, which indicates a span of at most 15 years of exposure to weathering agents, has been observed almost only on remains of *Mammuthus*, *Pseudodama*, and *Praemegaceros*. Hippopotamus bones and teeth are practically unaffected by this kind of alteration, if we exclude a patella showing weathering stage 1 fissures at its proximal end.

There is no evidence of carnivore ravaging, as mentioned above, nor of trampling. Long bones are extensively broken by transverse fractures, most of which faulted. Adopting Villa and Mahieu's (1991) categories to determine if the hardparts were crushed fresh or dry, all the fracture characteristics prove that the bones were broken in a dehydrated state. Sometimes fractured elongate elements (e.g., ribs) conformed to the surface upon which they were deposited. Skulls, mandibles, and coxals are damaged by vertical compression. The Collecurti bones therefore suffered the effects of dynamic efforts in post-depositional circumstances, likely during advanced stages of burial diagenesis, due to sediment load and possibly also tectonic stress.

Debrisflows tend to form poorly-sorted deposits. As for sedimentary particles, debrisflows are expected to be effective at removing and dispersing skeletal remains, but ineffective at sorting them (Johnson, 1970; Dasgupta, 2003). Therefore, although skeletal representation in debrisflow deposits can generally expected to be low, it should roughly reflect the original skeletal completeness. At Collecurti all taxa are actually unsorted. Yet, hippopotamus is much better represented than all other taxa: virtually every bone type of hippopotamus has been found, other taxa are most scantily represented (Fig. 10). Assuming that the debrisflow entrained all the bones on its path, the hippopotamus skeletons were far more complete and far less disarticulated, winnowed, and altered than the skeletons of all other components in the assemblage.

6.4.4 Interpretation

Based on taphonomic evidence that (1) the Collecurti assemblage is formed by a large number of disarticulated elements from all taxa; (2) that all taxa, except hippopotamus, are represented by isolated remains; and (3) that the latter are often polished and weathered, we conclude that a debrisflow ran into,

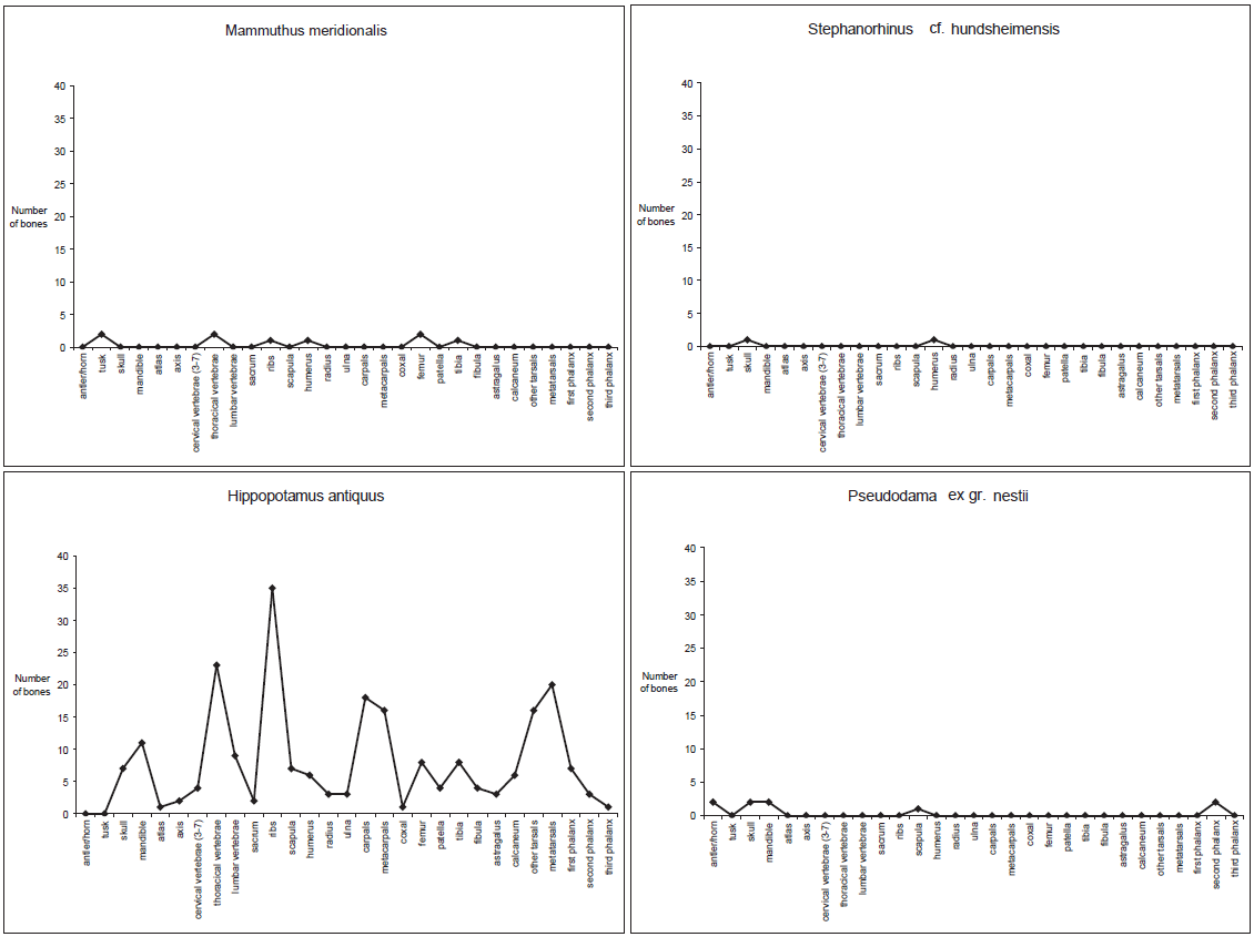

Figure 10 *- Relative abundances of the different skeletal elements in each species. Hippopotamus is by far the best represented genus at Collecurti (continues on opposite page).*

entrained and buried, the hippopotamus carcasses which were already in an advanced state of decomposition, while adding to this death assemblage bones from disarticulated skeletons which had been lying exposed uphill. The picture that looms out is that the remains of elephants and cervids, on the one hand, and those of hippopotamuses, on the other, reflect two different taphonomic histories. The former were exposed for some time at an upslope location and probably fluvially reworked, and later entrained by the debrisflow. Transported downslope, into the area of present-day excavations, they mixed up and were finally buried with the carcasses of hippopotamuses. The latter, in contrast, lied long enough to be skeletonised and disarticulated, but their bones were not exposed to weathering agents, nor to scavengers; only fractions of easily transported elements of their skeletons were removed by hydraulic winnowing. Their corpses therefore must have lied decomposing in a quiet waterbody.

These inferences are consistent with the sedimentological evidence reported in section 3.2, which points to a mass flow origin for U3 and U2. Viewing the skeletal elements as sediment, the shape and size of most of them would imply poor mobility and no hydraulic equivalence with respect to the hosting bed. This supports the role of a debrisflow as main agent of transport and burial, with high competence and a poor tendency to select its entrained load. The absence of significant impact marks and bone breakage in the assemblage relate to the plastic flow rheology, with the high volume of cohesive muddy matrix reducing mechanical interactions between coarse clasts (Nemec & Steel, 1984; Major & Pierson, 1992).

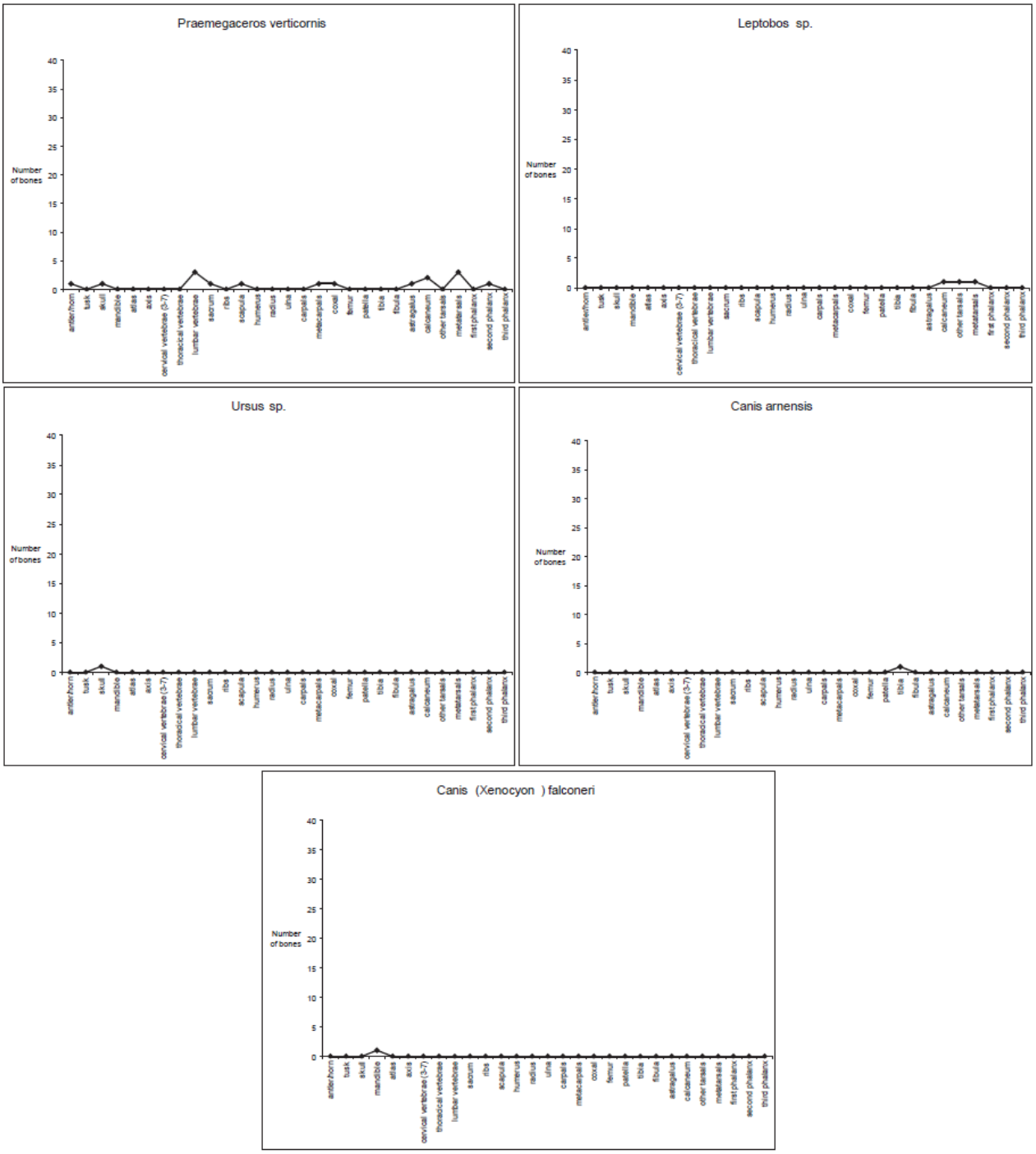

Figure 10 *- (continued from previous page)*

Furthermore, the evidence on the sedimentological behavior of fossil material at Collecurti matches the few detailed sedimentological observations in the literature on fossil preservation by debrisflows. Most such works (e.g., Van Itterbeeck *et al.*, 2005; Eberth *et al.*, 2006; Lauters *et al.*, 2008; Britt *et al.*, 2009) report a general horizontal to subhorizontal orientation of elongate bone elements, as well as a preferential concentration along or slightly above the basal surfaces of the event beds. Whereas many studies do not describe any preferential orientations of elongate fossil elements in plan view, the assemblage at Collecurti features two dominant modes with EW and SE-NW orientations (Fig. 2), interpreted as coarse-clast

alignments with the lateral and frontal frictional margins of the active flow. A similar interpretation has been offered by Eberth *et al.* (2006) for the distribution of dinosaur bones in a debrisflow-hosted Cretaceous bonebeds.

Abundant debrisflow deposits in the stratigraphic column at Colfiorito suggest significant topographic relief at basin margin throughout the Quaternary, as still evident in the present-day physiography, linked to Apennine tectonics and uplift (Ambrosetti *et al.*, 1978; Cantalamessa *et al.*, 1986; Coltorti *et al.*, 1991). Debrisflows have been interpreted as indicators of nearby relief also in recent works on the taphonomy of Mesozoic bonebeds (Eberth *et al.*, 2006; Britt *et al.*, 2009).

But how long had the hippopotamus corpses been dead? We can only conjecture from the state of the carcasses. Decay and disarticulation follow a predictable course. In subaerial conditions, limbs disarticulate more or less proximally to distally, whereas the opposite occurs in water (Hill, 1979). A carcass predictably loses ever more integrity with increasing time since death. Ligaments, tendons and muscles gradually rotten to the point that a skeleton will disarticulate after a certain period since death, and it will fall apart much faster if it is disturbed in any way. Strong ligaments, however, such as those of the lumbar area, are expected to resist longer holding together some of the vertebrae. This is exactly what was found at Collecurti: the only articulated part that was recovered at the site is a section of backbone consisting of the last two thoracical vertebrae, the four lumbar vertebrae, the sacrum, and the pelvis. Moreover, this is a part of the skeleton which is expected to be the last to fall apart according to the patterns of disarticulation for carcasses decaying in water (Hill, 1979).

Environmental conditions play an important role in the rate of decomposition. Rain and snow, sunlight, plant growth, summer heat and winter cold, water, insects and insect larvae impact on decomposition. All other things being equal, the hotter the weather, the faster a carcass decomposes. Immersion in water notoriously delays the process of decay, and the rate of decay declines with increasing water depth (Gunn, 2006). Hippopotamuses, however, prefer rather shallow water, about 1.5 m deep, just enough to walk on the bottom (Eltringham, 1999). The amphibian habits of hippopotamuses, matched to the absence of weathering or carnivore ravaging on the hippopotamus bones at Collecurti, indicates that these carcasses accumulated and decayed in water in a reasonably short period of time, or that they were rapidly subtracted from carnivores' access by sediment burial.

Large carcasses reach complete disarticulation in subaerial conditions after more than one year of exposure (Hill & Behrensmeyer, 1984). This likely occurred to the carcasses of the other, non-hippopotamus taxa of the site: the weathered and polished conditions of the isolated bones of these animals indicate that their corpses lied exposed possibly for longer than a year, anyhow long enough to skeletonise, fall apart, and be winnowed prior to debrisflow entrainment. This is confirmed by the sedimentological evidence of U3-U2 mass-flow deposits, which points to an origin from colluvial settings external to the lacustrine environment of final deposition. In very dry circumstances the body fluids readily evaporate leading to mummification of the whole body (Galloway *et al.*, 1989; Mann, Bass & Meadows, 1990; Lee Goff, 2009; Noto, 2011). This prevents disarticulation and scattering. Because the other, non-hippopotamus taxa are represented only by scattered, isolated elements, we infer that their carcasses skeletonised under moist conditions. Moreover,

Hill (1979) observed that bones that are less susceptible to transport by running water disarticulate more easily, whereas bones more exposed to winnowing detach later from the skeleton. At Collecurti, the non-hippopotamus taxa are largely represented by bones that disarticulate fairly late and that are not so easily transported by flowing water. These specimens are also the most weathered and abraded/polished of the whole bone assemblage. In sum, the debrisflow caught up bones scattered from skeletons that had been lying for a certain while in a fairly moist environment.

The taphonomic analysis ascertained that 1) hippopotamuses died all together; 2) all the carcasses represented at the site decayed long enough to skeletonise and be disarticulated; 3) some bones lied exposed long enough to reach weathering stage 3, and also be transported by running water prior to final reworking and debrisflow transport; 4) the debrisflow ran into the almost entirely skeletonised hippopotamus carcasses, completing the discarticulation and adding allochthonous bones reworked from uphill areas. In spite of animal carcasses decomposing uphill and hippopotamus corpses decaying at the margins of a shallow lake, there is no evidence of carnivore ravaging. What kept carnivores away from all this potential food source? The hippopotamus carcasses were presumably lying underwater, and therefore far from the reach of scavengers, but what protected the corpses of other animals uphill from carnivores? Perhaps what prevented carnivores from having access to the carcasses is the same that killed the animals in the first place. Because the eleven hippopotamuses died simultaneously, we can involve also the other taxa in the same death event, configuring a generalized catastrophic occurrence in the area. The taphonomic signatures distinguishing hippopotamuses from other animals do not exclude this option, because they may reflect preservational biases due to the different conditions (i.e., underwater as opposed to sub-aerial) under which they had developed. The disarticulate state of all skeletons rules out the hypothesis that the animals were caught up and killed by the debrisflow itself.

The assemblage data from the site adds an important paleobiologic clue to our hunt for the killer: the low level of diversification of the fauna. Low richness is likely to result from long exposure to harsh climatic and environmental conditions. Coltorti *et al.* (1998) and Bertini (2000) have shown that the strata of interest at Collecurti were deposited during a climatic trend towards ever increasing cooler conditions. Stadial/glacial cycles are known to turn progressively cooler and drier throughout the Pleistocene (Suc *et al.*, 1995; Bertini, 2000). Hence, freezing cold and/or drought are the most likely causes of the death of the Collecurti animals. There are lines of evidence, however, working against drought: 1) no mudcracks nor evaporitic minerals have been found anywhere and at any level in the excavated area; 2) all bones other than those of hippopotamus are largely elements that detach fairly late from the skeleton: hence, their carcasses had not mummified; 3) the rapid drying of exposed bones would have produced far more extensive weathering alterations; 4) drought alone would not have prevented carnivores from ravaging the carcasses. On the contrary, drought can offer carnivores ready and easy access to large amounts of resources (e.g., Poggio Rosso, Tuscany: Mazza, Bertini & Magi, 2004; Mazza, 2006). But another important clue comes from the pregnancy of one of the female hippopotamuses. Extant hippopotamus is capable of breeding year round, but it experiences seasonal breeding peaks from March to June (Pienaar et al., 1966). Moreover, cubs are born in months of peak rainfall, i.e., October and March (Smuts & Whyte, 1981). Breeding thus seems to be somewhat

correlated with rainfall (Laws & Clough, 1966). Assuming that the same occurred also in the even more amphibian *H. antiquus* (Mazza, 1995), the pregnant female indicates that the Collecurti community was not killed in a dry season of the year, but rather in a period of the year when precipitation was most likely. Drought, therefore, seems a fairly improbable cause of death at Collecurti. Sudden cold, in contrast, is much more probable. It could not only simultaneously kill many animals and keep away predators, but also turn rainfall into snowfall in months of peak precipitation. The fact that hippopotamuses can stand short periods of frost (Kahlke 1997, p. 367, and references therein), as long as their water places do not frost, imposes that there was a very intense cold snap beyond their thermal tolerance limits, and too sudden to flee from. In this reconstruction of hypothetical events, after the fauna's annihilation as temperatures grew the carcasses of the hippopotamus family lied rotting under water, whereas those of other individuals skeletonised uphill, falling apart and providing bones to stream catchments. When snow/ice started melting extensively, available runoff favored hillslope instability and the generation of a debrisflow, which swept bones from the disarticulated skeletons along the way and surged downhill into the lake, where it ran into decaying hippopotamus corpses.

6.5. CONCLUSIONS

Pleistocene lacustrine sediments of the Colfiorito Basin present repeated intercalations of debrisflow and hyperconcentrated flow deposits, due to adjacent high-relief catchments, slope instability, and recurrent exceptional hydrological events that mobilized colluvial material in mass flows from the hinterland. The frequent occurrence of subaerial sediment gravity flows played a fundamental role in the assemblage and preservation of the Collecurti bonebed, which represents an important element in the European biochronological scale. In the proposed sedimentological-taphonomic reconstruction, a debrisflow was triggered in upland areas at basin margins, where it swept away bones from disarticulated skeletons which had been lying exposed. The flow successively reached a lake basin at the base of local highlands, and entrained several hippopotamus carcasses that were lying in advanced decomposition. The spatial pattern of bone distribution suggests a direct control by debrisflow dynamics, with frontal and lateral concentration of a significant number of large bones and carcasses due to the development of debrisflow levees and snout. The exceptional preservation is tied to the essentially instantaneous entombment of animal remains within a relatively thick and uniform body of cohesive sediment as the debrisflow froze to a halt over the low-gradient, shallow lake bottom.

We hypothesise that a sudden, very cold episode may have killed the animals, both those inhabiting the hinterland and the hippopotamuses that lived in the lake basin. The taphonomic attributes of Collecurti's mammal assemblage, palynological analyses (Coltorti *et al.*, 1998), and the characteristics of its debrisflow deposits support a link with a phase of climate instability connected with the onset of one of the cold cycles of the MIS 30 to 26 span, characterized by increasing rain/snowfall and sudden, intense cold snaps.

To the authors' knowledge, mammalian bonebeds preserved in well documented debrisflow deposits are extremely rare and unreported in the Quaternary of Europe, the only other Quaternary case being the one studied by Rossetti *et al.* (2004) from the Pleistocene of the Amazon Basin, Brazil. Given the geological

context of the Colfiorito intermontane basin, it is very likely that more bone accumulations have been preserved by mass-flow deposits in small basins along the Apennine orogen. These results show the strength of combined taphonomy and sedimentology in providing a paleoenvironmental, process-oriented context for unravelling the origin of subaerial fossil assemblages.

ACKNOWLEDGEMENTS

We thank Mr. Mauro Magnatti (University of Camerino), who discovered the site of Collecurti at the end of the 1980s, and everyone who took part in the subsequent excavations. We are also grateful to Dr. Mara Silvestrini (Inspector of the Soprintendenza per i Beni Archeologici, Regione Marche) for granting us access to the site and to the fossil material. We extend our gratitude to Dr. Chiara Invernizzi, Dr. Maria Luisa Magnoni, but most of all to Dr. Alessandro Blasetti (University of Camerino) for his help and support during our visits and field work. Poppe L. de Boer (Utrecht University) provided insightful editorial comments on a first draft. Reviewers R.-D. Kahlke and A. Brooks provided interesting discussion points. Part of this study was funded by ex 60% MIUR (Ministry of Education, University and Research) grants to P. Mazza. D. Ventra was financially supported by NWO (National Science Foundation, the Netherlands, research grant NWO-ALW 815.01.012).

REFERENCES

Ambrosetti, P., Carboni, M.G., Conti, M.A., Constantini, A., Esu., D., Gandin, A., Girotti, O., Lazzarotto, A., Mazzanti, R., Nicosia, U., Parisi, G. and **Sandrelli, F.** (1978) Evoluzione paleogeografica e tettonica nei bacini tosco-umbro-laziali nel Pliocene e nel Pleistocene inferiore. *Memorie della Societá Geologica Italiana*, **19**, 573-580.

Arnott, R.W.C. and **Hand, B.M.** (1989) Bedforms, primary structures and grain fabric in the presence of suspended sediment rain. *Journal of Sedimentary Petrology*, **59**, 1062-1069.

Baas, J.H. and **Best, J.L.** (2002) Turbulence modulation in clay-rich sediment-laden flows and some implications for sediment deposition. *Journal of Sedimentary Research*, **72**, 336-340.

Bally, A.W., Burbi, L., Cooper, C. and **Ghelardoni, R.** (1986) Balanced sections and seismic reflection profiles across the central Apennines. *Memorie della Societá Geologica Italiana*, **35**, 257-310.

Behrensmeyer, A.K. (1975) The taphonomy and paleoecology of Plio-Pleistocene vertebrate assemblages east of Lake Rudolf, Kenya. *Bulletin of the Museum of Comparative Zoology, Harvard*, **146**, 473-578.

Behrensmeyer, A.K. (1978) Taphonomic and ecological information from bone weathering. *Paleobiology*, **4**, 150-162.

Behrensmeyer, A.K. (1991) Terrestrial vertebrate accumulations. In: *Taphonomy: Releasing the Data Locked in the Fossil Record* (Eds. P.A. Allison and D.E.G. Briggs), pp. 291-335, Plenum Press, New York.

Behrensmeyer, A.K. and **Boaz, D.E.D**. (1980) The recent bones of Amboseli National Park, Kenya in relation to East African paleoecology. In: *Fossils in the Making: Vertebrate Taphonomy and Paleoecology* (Eds. A.K. Behrensmeyer and A.P. Hill), pp. 72-92, University of Chicago Press, Chicago.

Behrensmeyer, A.K., Western, D. and **Boaz, D.E.D.** (1979) New perspectives in vertebrate paleoecology from a recent bone assemblage. *Paleobiology*, **5**, 12-21.

Benvenuti, M. (2003) Facies analysis and tectonic significance of lacustrine fan-deltaic successions in the Pliocene-Pleistocene Mugello Basin, Central Italy. *Sedimentary Geology*, **157**, 197-234.

Benvenuti, M. and **Martini, I.P.** (2002) Analysis of terrestrial hyperconcentrated flows and their deposits. In: *Flood and Megaflood Processes and Deposits* (Eds. I.P. Martini, V.R. Baker and G. GarzÒn), IAS Special Publication, **32**, 167-193.

Bertini, A. (2000) Pollen record from Colle Curti and Cesi: Early and Middle Pleistocene mammal sites in the Umbro-Marchean Apennine Mountains (central Italy). *Journal of Quaternary Sciences*, **15**, 825-840.

Bertran, P., Hétu, B., Texier, J.-P. and **Van Steijn, H.** (1997). Fabric characteristic of subaerial slope deposits. *Sedimentology*, **44**, 1-16.

Beverage, J.P. and **Culbertson, J.K.** (1964) Hyperconcentrations of suspended sediment. American Society of Civil Engineers, *Journal of the Hydraulic Division*, **90, HY6**, 117-128.

Blair, T.C. (1999). Cause of dominance by sheetflood vs. debris-flow processes on two adjoining alluvial fans, Death Valley, California. *Sedimentology*, **46**, 1015-1028.

Blair, T.C. and **McPherson, J.G.** (1998) Recent debris-flow processes and resultant form and facies of the Dolomite alluvial fan, Owens Valley, California. *Journal of Sedimentary Research*, **68**, 800-818.

Borselli V., Ficcarelli G., Landucci, F..Magnatti, M., Napoleone G. and **Pambianchi G.** (1988) Segnalazione di mammiferi pleistocenici nell'area di Colfiorito (Appennino umbro-marchigiano) e valutazione della potenzialità del giacirnento con metodi geofisici. *Bollettino della Societá Paleontologica Italiana*, **27**, 253-257.

Brewer, D. (1992) Zooarchaeology: method, theory, and goals. *Archaeological Method and Theory*, **4**, 195–244.

Britt, B.B., Eberth, D.A., Scheetz, R.D., Greenhalgh, B.W. and **Stadtman, K.L.** (2009) Taphonomy of debris-flow hosted dinosaur bonebeds at Dalton Wells, Utah (Lower Cretaceous, Cedar Mountain Formation, USA). *Palaeogeography, Palaeoclimatology, Palaeoecology*, **280**, 1-22.

Calamita, F., Cello, G. and **Deiana, G.** (1994) Structural styles, chronology rates of deformations, and time-space relationships in the Umbria-Marche thrust system (central Apennines, Italy). *Tectonics*, **13**, 873-881.

Cantalamessa G., Centamore E., Chiocchini U., Colalongo M. L., Micarelli A., Nanni T., Pasini G., Potetti G., Potetti M. and **Ricci Lucchi F.** (1986) Il Plio-Pleistocene nelle Marche. In: Studi Geologici Camerti, volume speciale, *La Geologia delle Marche*, pp. 61-81.

Coltorti M., Consoli M., Dramis F., Gentili B. and **Pambianchi G.** (1991) Evoluzione geomorfica delle piane alluvionali delle Marche centro-meridionali. *Geografia fisica e Dinamica Quaternaria*, **14**, 73-86.

Coltorti, M., Albianelli, A., Bertini, A., Ficcarelli, G., Laurenzi, M.A., Napoleone, G. and **Torre, D.** (1998). The Colle Curti mammal site in the Colfiorito area (Umbria-Marchean Apennine, Italy): geomorphology,stratigraphy, paleomagnetism and palynology. *Quaternary International*, **47/48**, 107-116.

Costa, J.E. (1988) Rheologic, geomorphic and sedimentologic differentiation of water floods, hyperconcentrated flows, and debris flows. In: *Flood Geomorphology* (Eds. V.R. Baker, R.C. Kochel and P.C. Patton), pp. 113-122, John Wiley & Sons, New York.

Coussot, P. (1995) Structural similarity and transition from Newtonian to non-Newtonian bahavior for water-clay suspensions. *Physical Reviews Letters*, **74**, 3971-3974.

Coussot, P. and **Ancey, C.** (1999) Rheophysical classification of concentrated suspensions and granular pastes. *Physical Review*, **E 59**, 4445-4457.

Damuth, J. (1982) Analysis of the preservation of community structure in assemblages of fossil mammals. *Paleobiology*, **8**, 434-446.

Dasgupta, P. (2003) Sediment gravity flow—the conceptual problems. *Earth Science Reviews*, **62**, 265-281.

Dean, W.E. (1974) Determination of carbonate and organic matter in calcareous sediments and sedimentary rocks by loss on ignition: comparison with other methods. *Journal of Sedimentary Petrology*, **44**, 242-248.

Di Giulio, G., Rovelli, A., Cara, F., Azzara, R.M.., Marra, F., Basili, R. and **Caserta, A.** (2003) Long-duration asynchrononous ground motions in the Colfiorito plain, central Italy, observed on a two-dimensional dense array. *Journal of Geophysical Research*, **108(B10)**, doi:10.1029/2002JB002367.

Eberth, D.A., Britt, B.B., Scheetz, R., Stadtman, K.L. and **Brinkman, D.B.** (2006) Dalton Wells: geology and significance of debris-flow-hosted dinosaur bonebeds in the Cedar Mountain Formation (Lower Cretaceous) of eastern Utah, USA. *Palaeogeography, Palaeoclimatology, Palaeoecology*, **236**, 217-245.

Eberth, D.A., Rogers, R.R. and **Fiorillo, A.P.** (2007) A practical approach to the study of bonebeds. In: *Bonebeds: Genesis, Analysis, and Paleobiological Significance* (Eds. R.R. Rogers, D.A. Eberth and A.P. Fiorillo), pp. 265-331, University of Chicago Press, Chicago.

Eltringham, S. K. (1999) *The Hippos: natural history and conservation*. Cambridge University Press, Cambridge, UK. 184 p.

Enos, P. (1977) Flow regimes in debris flows. *Sedimentology*, **24**, 133-142.

Fastovsky, D.E., Clark, J.M., Strater, N.H., Montellano, M.R., Hernandez, R. and **Hopson, J.A.** (1995) Depositional environments of a Middle Jurassic terrestrial vertebrate assemblage, Huizachal Canyon, Mexico. *Journal of Vertebrate Paleontology*, **15**, 561-575.

Ficcarelli, G., Magnatti, M. and **Mazza, P.** (1990) Occurrence of *Microtus* (*Allophaiomys*) gr. *pliocaenicus* in the Pleistocene lacustrine basin of Colfiorito (Umbria-Marchean Apennine, Central Italy). *Bollettino della Società Paleontologica Italiana*, **29**, 89-90.

Ficcarelli, G. and **Mazza, P.** (1990) New fossil findings from the Colfiorito basin (Umbria-Marchean Apennine). *Bollettino della Società Paleontologica Italiana*, **29**, 245-247.

Ficcarelli, G., Masini, F., Mazza, P. and **Torre, D.** (1996) The mammals of the latest Villafranchian in Italy. In: *The Early Middle Pleistocene in Europe* (Ed. C. Turner), pp. 263-272, Balkema, Rotterdam.

Ficcarelli, G. and **Silvestrini, M.** (1991) Biochronologic remarks on the Local Fauna of Colle Curti (Colfiorito basin, Umbria-Marchean Apennine, Central Italy). *Bollettino della Società Paleontologica Italiana*, **30**, 197-200.

Finch, C.E. (1990) *Longevity, Senescence, and the Genome*. University of Chicago Press, Chicago. 938 p.

Fouch, T.F. and **Dean, W.E.** (1982) Lacustrine and associated clastic depositional environments. In: *Sandstone Depositional Environments* (Eds. P.A. Scholle and D.R. Spearing), AAPG Memoir, **31**, 87-114.

Frison, G.C. and **Todd, L.C.** (1986) *The Colby Mammoth Site: Taphonomy and Archaeology of a Clovis Kill in Northern Wyoming*. University of New Mexico Press, Albuquerque, 230 p.

Frostick, L. and **Reid, I.** (1983) Taphonomic significance of sub-aerial transport of vertebrate fossils on steep semi-arid slopes. *Lethaia*, **16**, 157–164.

Galloway A., Birkby, W.H., Jones A.M., Henry, T.E. and **Parks, B.O.** (1989) Decay rates of human remains in an arid environment. *Journal of Forensic Science*, **34**, 607-616.

Gliozzi, E., Abbazzi, L., Argenti, P., Azzaroli, A., Caloi, L., Capasso Barbato, L., Di Stefano, G., Esu, D., Ficcarelli, G., Girotti, O., Kotsakis, T., Masini, F., Mazza, P., Mezzabotta, C., Palombo, M.R., Petronio, C., Rook, L., Sala, B., Sardella, R., Zanalda, E. and **Torre, D.** (1997) Biochronology of selected mammals, molluscs and ostracods from the Middle Pliocene to the Late Pleistocene in Italy. The state of the art. *Rivista Italiana di Paleontologia e Stratigrafia*, **103**, 369-388

Grayson, D.K. (1978) Minimum numbers and sample size in vertebrate faunal analysis. *American Antiquity*, **43**, 53–65.

Grayson, D.K. (1984) *Quantitative Zooarchaeology - Topics in the Analysis of Archaeological Faunas*. Academic Press, San Diego, 202 p.

Gunn, A. (2006) *Essential Forensic Biology*. John Wiley and Sons Ltd, Chichester, UK, 440 p.

Guo, B., Zhu, R., Florindo, F., Ding, Z. and **Sun, J.** (2002) A short, reverse polarity interval within the Jaramillo subchron: Evidence from the Jingbian section, northern Chinese Loess Plateau. *Journal of Geophysical Research*, **107(B6)**, DOI 10.1029/2001JB000706.

Guzzetti, F. and **Cardinali, M.** (1991) Debris-flow phenomena in the Central Appennines of Italy. *Terra Nova*, **3**, 619-627.

Hamblin, A.P. (1992) Half-graben lacustrine sedimentary rocks of the lower Carboniferous Strathlorne Formation, Horton Group, Cape Breton Island, Nova Scotia, Canada. *Sedimentology*, **39**, 263-384.

Hampton, M.A. (1972) The role of subaqueous debris flow in generating turbidity currents. *Journal of Sedimentary Petrology*, **42**, 775-793.

Hill A. (1979) Disarticulation and Scattering of Mammal Skeletons. *Paleobiology*, **5**, 261-274.

Hill, A. and **Behrensmeyer, A. K.** (1984) Disarticulation patterns of East African ungulates. *Paleobiology*, **10**, 366-376.

Howard, C.D.D. (1963) Flow of clay-water suspensions. *Journal of the Hydraulics Division*, *American Society of Civil Engineers*, **5**, 89-97.

Hubert, J.F. and **Filipov, A.J.** (1989) Debris-flow deposits in alluvial fans on the west flank of the White Mountains, Owens Valley, California, U.S.A. *Sedimentary Geology*, **61**, 177-205.

Ilstad, T., Elverhøi, A., Issler, D. and **Marr, J.G.** (2004) Subaqueous debris flow behaviour and its dependence on the sand-clay ratio: a laboratory study using particle tracking. *Marine Geology*, **213**, 415-438.

Janis, C.M. (1990) Correlation of cranial and dental variables with body size in ungulates and macropodoids. In: *Body Size in Mammalian Paleobiology: Estimation and Biological Implications* (Eds. J. Damuth and B.J. MacFadden), pp. 255-299, Cambridge University Press, Cambridge, UK.

Johnson, A.M. (1970) Formation of debris flow deposits. In: *Physical Processes in Geology*, Johnson, A.M., pp. 433-448, W.H. Freeman, San Francisco.

Kahlke, R.-D. (1997) Die *Hippopotamus*-Reste aus dem Unterpleistozän von Untermaßfeld. In: *Das Pleistozän von Untermaßfeld bei Meiningen (Thüringen), Teil 1* (Ed. R.-D. Kahlke), Monographien des Römisch-Germanischen Zentralmuseums **40, 1,** Habelt, Bonn, 277-374.

Kahlke, R.-D. (2007) Late Early Pleistocene European large mammals and the concept of an Epivillafranchian biochron. *Courier Forschungsinstitut Senckenberg*, **259**, 265-278.

Kahlke, R.-D., García, N., Kostopoulos, D.S., Lacombat, F., Lister, A.M., Mazza, P.P.A., Spassov, N. and **Titov, V.V.** (2010) Western Palaearctic palaeoenvironmental conditions during the Early and early Middle Pleistocene inferred from large mammal communities, and implications for hominin dispersal in Europe. *Quaternary Science Reviews*, **89,** 1-28.

Kahlke, R.-D. and **Gaudzinski, S.** (2005) The blessing of a great flood: differentiation of mortality patterns in the large mammal record of the Lower Pleistocene fluvial site of Untermassfeld (Germany) and its relevance for the interpretation of faunal assemblages from archaeological sites. *Journal of Archaeological Science*, **32**, 1202-1222.

Kaufman, D. (1998). Measuring archaeological diversity: an application of the jackknife technique. *American Antiquity*, **63**, 73-85.

Kim, B.C., Yu, K.M., Chun, H.Y., Choi, S.J. and **Kim, Y.B.** (1997) The southeastern margin of the Cretaceous Yongdong Basin, Korea: a lacustrine fan-delta system. *Geoscience Journal*, **1**, 61-74.

Konert, M. and **Vandenberghe, J.** (1997) Comparison of laser grain-size analysis with pipette and sieve analysis: a solution for the underestimation of the clay fraction. *Sedimentology*, **44**, 523-535.

Lauters, P., Bolotsky, Y.L., Van Itterbeeck, J. and **Godefroit, P.** (2008) Taphonomy and age profile of a latest Cretaceous dinosaur bonebed in far eastern Russia. *Palaios*, **23**, 153-162.

Laws, R. M. (1968) Dentition and ageing of the hippopotamus. *African Journal of Ecology*, **6**, 19-52.

Laws, R. M. and **Clough, G.** (1966) Observation of reproduction in the hippopotamus (*Hippopotamus amphibius*). *Symposium of the Zoological Society of London*, **15**, 117-140.

Lee Goff, M. (2009) Early post-mortem changes and stages of decomposition in exposed cadavers. *Experimental and Applied Acarology*, **49**, 21-36.

Leiggi, P., Schaff, C.R. and **May, P.** (1994) Macrovertebrate collecting. In: *Vertebrate Paleontological Techniques* (Eds. P. Leiggi and P. May), pp. 59-92, Cambridge University Press, Cambridge, UK.

Lewis, D.W., Laird, M.G. and **Powell, R.D.** (1980) Debris flow deposits of early Miocene age, Deadman Stream, Marlborough, New Zealand. *Sedimentary Geology*, **27**, 83-118.

Lindsey, J.F. (1968) The development of clast fabric in mudflows. *Journal of Sedimentary Petrology*, **38**, 1242-1253.

Loope, D.B., Dingus, L., Swisher III, C.C. and **Minjin, C.** (1998) Life and death in a Late Cretaceous dune field, Nemegt Basin, Mongolia. *Geology*, **26**, 27-30.

Lowey, G.W. (2002) Sedimentary processes of the Kusawa Lake torrent system, Yukon, Canada, as revealed by the September 16, 1982 flood event. *Sedimentary Geology*, **151**, 293-312.

Lyman, R.L. (1994) *Vertebrate Taphonomy*. Cambridge University Press, Cambridge, UK, 524 p.

Major, J.J. (1998) Pebble orientation on large, experimental debris-flow deposits. *Sedimentary Geology*, **117**, 151-164.

Major, J.J. (2003) Debris flow. In: *Encyclopaedia of Sediments and Sedimentary Rocks* (Ed. G.V. Middleton), pp. 186-188, Kluwer Academic Publishers, Dordrecht, The Netherlands.

Major, J.J. and **Iverson, R.M.** (1999) Debris-flow deposition: effects of pore-fluid pressure and friction concentrated at flow margins. *Geological Society of America Bulletin*, **111**, 1424-1434.

Major, J.J. and **Pierson, T.C.** (1992) Debris Flow Rheology: Experimental Analysis of Fine-grained Slurries. *Water Resources Research*, **28**, 841-857.

Mann, R.W., Bass, W.M. and **Meadows, L.** (1990) Time since death and decomposition of the human body: variables and observations in case and experimental field studies. *Journal of Forensic Science*, **35**, 103-111.

Marr, J.G., Harff, P.A., Shanmugam, G. and **Parker, G.** (2001) Experiments on subaqueous sandy gravity flows: The role of clay and water content in flow dynamics and depositional structures. *Geological Society of America Bulletin*, **113**, 1377-1386.

Mazza, P. (1995) New evidence on the Pleistocene hippopotami of western Europe. *Geologica Romana*, **31**, 61-241.

Mazza, P. (2006) Poggio Rosso (Upper Valdarno, Central Italy), A window on latest Pliocene wildlife. *Palaios*, **21**, 493-498.

Mazza, P., Bertini, A. and **Magi, M.** (2004) The Late Pliocene Site Of Poggio Rosso (Central Italy): Taphonomy And Paleoenvironment. *Palaios*, **19**, 227-248.

McCave, I.N. and **Syvitski, J.P.N.** (1991) Principles and methods of geological particle size analysis. In: *Principles, Methods and Applications of Particle Size Analysis* (Ed. J.P.M. Syvitski), pp. 3-21, Cambridge University Press, Cambridge, UK.

McCave, I.N., Bryant, R.J., Cook, H.F. and **Coughanowr, C.A.** (1986) Evaluation of a laser-diffraction-size analyzer for use with natural sediments. *Journal of Sedimentary Petrology*, **56**, 561-564.

Messina, P., Galadini, F., Galli, P. and **Sposato, A.** (1999) Evoluzione a lungo termine e caratteristiche della tettonica attiva nell'area Umbro-Marchigiana colpita dalla sequenza sismica del 1997-98 (Italia Centrale). In: *Progetto MISHA – Metodi Innovativi per la Stima dell'Hazard: Applicatione all'Italia Centrale.* (Ed. L. Peruzza), pp. 39-42, CNR-GNDT, Roma, Italy.

Miller, A.R. (1988) A set of test life tables for theoretical gerontology. *Journal of Gerontology*, **43**, B43-B49.

Mirabella, F., Boccali, V. and **Barchi M.R.** (2005) Segmentation and interaction of normal faults within the Colfiorito fault system (central Italy). In: *Deformation Mechanisms, Rheology and Tectonics: from Minerals to the Lithosphere* (Eds D. Gapais, J.P. Brun and P.R. Cobbold), *Geological Society of London Special Publication*, **243**, 25-36.

Montuire, S. and **Marcolini, F.** (2002) Palaeonvironmental significance of the mammalian faunas of Italy since the Pliocene. *Journal of Quaternary Science*, **17**, 87-96.

Moretti A. (1969) *Note illustrative della Carta Geologica d'Italia alla scala 1:100.000. Foglio 124 "Macerata"*. Servizio Geologico d'Italia, Roma.

Morgan Ernest, S.K. (2003) Life history characteristics of placental non-volant mammals. *Ecology*, **84**, 3402-3402.

Moscariello, A., Marchi, L., Maraga, F. and **Mortara, G.** (2002) Alluvial fans in the Italian Alps: sedimentary facies and processes. In: *Flood and Megaflood Processes and Deposits: Recent and Ancient Examples* (Eds. I.P. Martini, V.R. Baker and G. GarzÒn), IAS Special Publication, **32**, 141-166.

Munthe, K. and **McLeod, S.A.** (1975) Collection of taphonomic information from fossil and recent vertebrate specimens with a selected bibliography. *Paleobios*, **19**, 1-12.

Nemec, W. and **Steel, R.J.** (1984) Alluvial and coastal conglomerates: their significant features and some comments on gravelly mass flow deposits. In: *Sedimentology of Gravels and Conglomerates* (Eds. E.H. Koster and R.J. Steel), Canadian Society of Petroleum Geologists Memoir, **10**, 1-31.

Norman Owen-Smith, R. (1992) *Megaherbivores: the influence of very large body size on ecology*. Cambridge University Press, Cambridge, UK, 369 p.

Noto, C.R. (2011) Hierarchical Control of Terrestrial Vertebrate Taphonomy Over Space and Time: Discussion of Mechanisms and Implications for Vertebrate Paleobiology. *Topics in Geobiology*, **32**, 287-336.

Nowak R.M. (1999) *Walker's Mammals of the World.* Johns Hopkins University Press, Baltimore, 926 p.

Palombo, M. R. and **Mussi, M.** (2006) Large mammal guilds at the time of the first human colonization of Europe: The case of the Italian Pleistocene record. *Quaternary International*, **149**, 94-103.

Parsons, J.D., Whipple, K.X. and **Simoni, A.** (2001) Experimental study of the grain-flow, fluid-mud transition in debris flows. *Journal of Geology*, **109**, 427-447.

Picard, M.D. and **High, L.R.** (1972) Criteria for recognizing lacustrine rocks. In: *Recognition of Ancient Sedimentary Environments* (Eds. J.K. Rigby and W.K. Hamblin), SEPM, Special Publication, **16**, 108-145.

Pienaar U. De V., Van Wyk, P. and **Fairall, N.** (1966) An experimental cropping scheme of hippopotami in the Letaba River of the Kruger National Park. *Koedoe*, **9**, 1-33.

Pierson, T.C. (1986) Flow behaviour of channelized debris flows, Mount St Helens, Washington. In: *Hillslope Processes* (Ed. A.D. Abrahams), pp. 269-296, Allen and Unwin, Boston.

Pierson, T.C. and **Costa, J.E.** (1987) A rheologic classification of subaerial sediment-water flows. In: *Debris Flows/Avalanches: Process, Recognition, and Mitigation* (Eds. J.E. Costa and G.F. Wieczorek), Geological Society of America Reviews in Engineering Geology, **7**, 1-12.

Prange, H.D., Anderson, J.F. and **Rahn, H.** (1979) Scaling of skeletal mass to body mass in birds and mammals. *American Naturalist*, **113**, 103-122.

Raia, P., Piras, P. and **Kotsakis, T.** (2006) Detection of Plio-Quaternary large mammal communities of Italy. An integration of fossil faunas biochronology and similarity. *Quaternary Science Reviews*, **25**, 846-854.

Raup, D.M. and **Stanley, S.M.** (1971) *Principles of paleontology*. W.H. Freeman and Co., San Francisco 388 p.

Reitz, E.J. and **Quitmyer, I.R.** (1988). Faunal remains from two coastal Georgia Swift Creek sites. *Southern Archaeology*, **7**, 95-108.

Rogers, R.R. (1994) Collecting taphonomic data from vertebrate localities. In: *Vertebrate Paleontological Techniques* (Eds. P. Leiggi, P. and P. May), pp. 47-58, Cambridge University Press, Cambridge, UK.

Rossetti, D.d.F., Mann de Toledo, P., Moraes-Santos, H.M. and **Santos, A.E.d.A.** (2004) Reconstructing habitats in central Amazonia using megafauna, sedimentology, radiocarbon, and isotope analyses. *Quaternary Research*, **61**, 289-300.

Sachse, M. (2005) A remarkable fossiliferous mass flow deposit in the Eocene Eckfeld Maar (Germany) – sedimentological, taphonomical, and palaeoecological considerations. *Facies*, **51**, 173-184.

Schmidt-Nielsen, K. (1984) *Scaling: Why is Animal Size so Important?* Cambridge University Press, Cambridge, 241 p.

Schumacher, B.A. (2002) *Methods for the Determination of Total Organic Carbon (TOC) in Soils and Sediments*. United States Environmental Protection Agency, occasional publication, http://www.epa.gov/esd/cmb/research/papers/bs116.pdf (last accessed online, November 2010).

Shannon, C.E. and **Weaver, W.** (1949) The Mathematical Theory of Communication. University of Illinois Press, Urbana, IL, 144 p.

Sharp, R.P. (1942) Mudflow levees. *Journal of Geomorphology*, **5**, 222-227.

Singer, B.S., Hoffman, K., Chauvin, A., Coe, R.S. and **Pringle, M.S.** (1999) Dating transitionally magnetized lavas of the late Matuyama Chron: Toward a new $^{40}Ar/^{39}Ar$ timescale of reversals and events. *Journal of Geophysical Research*, **104**, 679-693.

Sletten, K., Blikra, L.H., Ballantyne, C.K., Neske, A. and **Dahl, S.O.** (2003) Holocene debris flows recognized in a lacustrine sedimentary succession: sedimentology, chronostratigraphy and cause of triggering. *The Holocene*, **13**, 907-920

Sly, P.G. (1994) Sedimentary processes in lakes. In: *Sediment Transport and Depositional Processes* (Ed. K. Pye), pp. 157-191, Blackwell Scientific Publications, Oxford, UK.

Smith, G.A. and **Lowe, D.R.** (1991). Lahars: volcano-hydrologic events and deposition in the debris flow – hyperconcentrated flow continuum. In: *Sedimentation in Volcanic Settings* (Eds. R.V. Fisher and G.A. Smith), SEPM Special Publication, **45**, 59-70.

Smuts, G.L. and **Whyte, I.J.** (1981) Relationships between reproduction and environment in the hippopotamus *Hippopotamus amphibius* in the Kruger National Park. *Koedoe*, **24**, 169-185.

Sohn, Y.K., Rhee, C.W. and **Kim, B.C.** (1999) Debris flow and hyperconcentrated flood-flow deposits in an alluvial fan, northwestern part of the Cretaceous Yongdong Basin, central Korea. *Journal of Geology*, **107**, 111-132.

Suc, J.-P., Bertini, A., Combourieu Nebout, N., Diniz, F., Leroy, S., Russo-Ermolli, E., Zheng, Z., Bessais, R. and **E., Ferrier, J.** (1995) Structure of West Mediterranean vegetation and climate since 5.3 ma. Acta Zoologica Cracoviensia, **38**, 3–16.

Suc, J.-P. and **Popescu, S.-M.** (2005) Pollen records and climatic cycles in the North Mediterranean region since 2.7 Ma. In: *Early-Middle Pleistocene Transitions: The Land-Ocean Evidence* (Eds. M.J. Head and P.L. Gibbard), Geological Society of London Special Publication, **247**, 147-158.

Van Itterbeeck, J., Boltsky, Y., Bulytynck, P. and **Godefroit, P.** (2005) Stratigraphy, sedimentology and palaeoecology of the dinosaur-bearing Kundur section (Zeya-Bureya Basin, Amur Region, far eastern Russia). *Geological Magazine*, **142**, 735-750.

Villa, P. and **Mahieu, E.** (1991) Breakage patterns of human long bones. *Journal of Human Evolution*, **21**, 27–48.

Voorhies, M. (1969) Taphonomy and Population Dynamics of an Early Pliocene Vertebrate Fauna, Knox County, Nebraska: Contributions to Geology. *University of Wyoming Special Paper*, **1**, 69 p.

Wagreich, M. and **Strauss, P.E.** (2005) Source area and tectonic control on alluvial-fan development in the Miocene Fohnsdorf intramontane basin, Austria. In: *Alluvial Fans: Geomorphology, Sedimentology, Dynamics* (Eds. A.M. Harvey, A.E. Mather and M. Stokes), Geological Society of London Special Publication, **251**, 207-216.

Weigl R. (2005) Longevity of mammals in captivity; from the Living Collections of the world. A list of mammalian longevity in captivity. *Kleine Senckenberg-Reihe Band*, **48**, Stuttgart, Germany, 214 p.

Weirich, F.H. (1989) The generation of turbidity currents by subaerial debris flows, California. *Geological Society of America Bulletin*, **101**, 278-291.

Wells, S.G. and **Harvey, A.M.** (1987) Sedimentologic and geomorphic variations in storm-generated alluvial fans, Howgill Fells, northwest England. *Geological Society of America Bulletin*, **98**, 182-198.

Zembo, I. (2010) Stratigraphic architecture and Quaternary evolution of the Val d'Agri intermontane basin (Southern Apennines, Italy). *Sedimentary Geology*, **223**, 206-234.

"*We live in a society exquisitely dependent on science and technology, in which hardly anyone knows anything about science and technology.*"

Carl Sagan, 1995
The Demon-Haunted World: Science as a Candle in the Dark

Chapter 7
Synthesis and conclusions

7.1 SYNTHESIS

This thesis discussed the sedimentology and dynamics of selected clastic depositional systems at subaerial basin margins. The focus on single depositional systems has provided the opportunity to pay particular attention to sedimentary processes and their interactions on the basis of field observations. A recent research emphasis on modelling, geophysical- and space-based remote sensing, and on basin-scale analysis has been spurred by advances in computing and technology, in the theoretical quantification of sedimentary systems (scaling, sediment transport equations, geomorphic parameterization, etc.), and especially by the advent of sequence stratigraphy. Whereas models and abstractions provide rapid access to large amounts of conceptual data, it is increasingly asserted that the ultimate test to validate all predictions (and retrodictions) still lies in field-based work.

Facies analysis has been one of the most successful approaches in bringing sedimentary geology to a mature stage, and it remains the basic approach to acquire information on sedimentary environments, both present and fossil. Whereas several authors have been involved in controversies on the meaning and applicability of '*facies models*' in the past (Anderton, 1985; Bridge, 1993; Miall, 1995, 1999; Mutti *et al.*, 1999), it is nowadays clear that 'generally applicable' models of sediment transport and depositional environments do not always provide an adequate picture of reality. Simplified models are adequate for the elaboration of large amounts of data, and for rapid decision-making in industry and public institutions, but from a scientific perspective these advantages come to the cost of gradually losing touch with how things really work in nature.

The results of this thesis demonstrate that common generalizations in the analysis of depositional processes and systems stand corrected in the face of information gathered directly in the field. The general picture that one obtains of sedimentation is somewhat more complicated, but probably more reliable. Proximal depositional settings at basin margins are particularly apt to restate the importance of the field approach, since various research questions on these systems remain open and long-standing misconceptions in the literature are recently under reconsideration (see sections 1.2, 1.3 and 1.4).

Chapter 2 discusses the sedimentology and stratigraphy of mudflat to shallow-lacustrine deposits in the Late Miocene Prado Section of the central Teruel Basin (Spain). In spite of the direct proximity to an active tectonic margin, an unequivocal climate signal is evident from comparison of facies patterns with insolation curves and with the periodicity of astronomically induced variations in the Earth's orbit. No known tectonic or autogenic mechanisms produce facies stacking patterns coincident with the long-term interference of precession, obliquity and eccentricity cycles. The proposed phase relationship between Milankovitch-controlled insolation parameters and facies transitions allows to interpret sedimentary processes and thus

environmental dynamics in terms of long-term climate change. Counter to common assumptions, it has been established that deposition of pedogenic carbonates and incipient calcretization coincided with relatively humid periods coincident with precessional minima, during which the hydrological cycle was more active and abundant surface runoff could efficiently mobilize solutes.

Palaeoenvironmental information and process models gained from the Prado Section have been instrumental for **chapter 3**, centered on the hypothesis that Milankovitch-forced climate cyclicity may have influenced alluvial-fan dynamics. The relationship between climate change and alluvial-fan sedimentation remains difficult to ascertain the pre-Quaternary record. This is due to inherent difficulties in high-resolution dating of fan deposits, and due to the stochastic nature of catastrophic processes on alluvial fans, which are mainly related to high-energy hydrologic events not univocally attributable to a specific climate phase. In particular, the idea that orbital climate change might have played a role in driving fan evolution has been proposed in a very few works only for Quaternary systems (Mack & Leeder, 1999; Waters *et al*., 2010), but not formally demonstrated through the analysis of orbitally tuned stratigraphic sections.
The opportunity to investigate this problem has been taken along the western margin of the study area examined in chapter 2, where distal coarse-clastic strata of alluvial-fan provenance interfinger with the lower interval of the Prado Section. Debrisflow beds that extend beyond the main fan body into the distal floodbasin represent events that mobilized particularly great sediment volumes. They are regularly traceable in correspondence of Ca-rich pedogenic horizons or incipient calcretes. Considering the phase relationships discussed in the previous chapter for sedimentation in the Prado Section, it is possible to relate the occurrence of high-volume mass flows with arid-humid climate transitions that directly preceded the onset of effective Ca mobilization and redeposition at the surface.
Although a detailed magnetostratigraphic correlation between mudflat and alluvial-fan strata has not been successful, the stratigraphic architecture of fan strata in the medial to distal domain presents an unusual degree of organization into alternating coarse- and fine-grained clastic packages, laterally continuous over hundreds of metres. This confirms that large-scale patterns of fan deposition responded to a cyclic control which could not be related to tectonics at basin margins, given the ascertained regularity and time scale of facies relations with the Prado Section. Autogenic processes can also be excluded on grounds that forced fan aggradation in the endorheic Teruel Basin dampened incision-aggradation autocycles, as noted in other fan systems of internally drained basins (Anderson, & Cross, 2001, in the Devonian Hornelen Basin of Norway; Nichols, 2004, in the Cenozoic Ebro Basin of Spain). This demonstrates that cyclostratigraphy can be a reliable method of investigation also in proximal depositional settings, in the presence of high-energy processes and concomitant tectonic control. Although high-resolution chronologies are hard to constrain in such depositional systems, the possibility to directly compare their records with those of adjacent environments is a valid test to verify climate-related hypotheses.

Figure 1 *- Where not to build your home: suburbs climbing up onto an active alluvial fan (aerial photograph of an unspecified location in Nevada; USGS photo-archives).*

Chapter 4 presents a detailed discussion of the geomorphology and sedimentology of an active piedmont setting along the northern Pacific coast south of Antofagasta, in the Atacama Desert (Chile). The opportunity to study this colluvial depositional system is provided by an abandoned roadcut which extends over several kilometres in the area, offering full accessibility and continuous stratigraphic exposures. Coupled observations of active surfaces and corresponding stratigraphy consented to divide the study area into five distinct sectors, characterized by well-differentiated processes and facies associations.

Recent sedimentological studies on colluvial systems focused on alpine to periglacial 'cold' settings, and on the significance of colluvium as a potential stratigraphic proxy for Quaternary palaeoclimatology. This study offers an alternative perspective from a slope system developed in a hyperarid tropical setting, and highlights the role of variable piedmont geomorphology and hydrology in producing highly differentiated depositional signatures, and in controlling the preservation potential of the deposits. For example, it has been possible to ascertain that different slope profiles and exposure to dominant winds directly influence not only the distribution of aeolian facies, but through the latter they also control the type and location of mass flows. Slope sectors entirely dominated by aeolian deposition at the surface can actually lose this process signature in their stratigraphic records if positioned at favourable locations for the occurrence of exceptional runoff. In studies of ancient slope systems, the abundance of waterlain facies would not immediately suggest a hyperarid climate setting, whereas the importance and climatic significance of aeolian deposition would be lost along with the deposits. Although relief configuration is an intuitively fundamental factor in driving slope processes, its importance has often been downplayed in the literature, especially because the large-scale geomorphic context commonly cannot be reconstructed in studies of ancient colluvium. This raises a cautionary note for numerous studies that associate regional palaeoclimate evolution with the architecture of slope deposits, since a broad set of different depositional styles for coeval colluvial successions has been observed along a single active piedmont system over a distance of only ~5 km.

Chapter 5 examines the overall sedimentological and stratigraphic evolution of the alluvial fan whose distal segments were examined in chapter 3. Whereas interfingering with the Prado Section extends over a limited stratigraphic interval, excellent outcrops towards the basin margin show a much longer and complex history for this depositional system. The original Mesozoic basement, consisting of deformed Triassic and Cretaceous mudstones and carbonates, is still accessible in proximity of the study area. The alluvial fan presents a distinct bipartite architecture, comprising a lower gravel-dominated unit in which deposition was prevalently by unconfined waterflows and bedload-dominated hyperconcentrated flows, and an upper unit with alternating mudstone and conglomerate packages, in which sedimentation took place mainly by cohesive debris flows and a spectrum of clay-modulated, suspension-dominated hyperconcentrated flows. Progressive unroofing of the Mesozoic basement changed the available source lithologies in the catchment through time. This is reflected not only in the provenance signal of fan sediments, but especially by the chronological succession of depositional processes and stratal geometries. In alluvial-fan settings, a fundamental distinction can be made between primary sedimentary processes, which are commonly high-magnitude events effectively contributing to fan construction and aggradation, and secondary processes that essentially only rework fan deposits. The distinction between these two categories is made evident by the chronological evolution of process associations in the studied fan. Besides a clear chronological and spatial variation in the occurrence of cohesive debris flows, detailed facies analysis demonstrated that the onset of clay availability has influenced the typology of hyperconcentrated-flow deposits. Deposition from traction carpets under bedload-dominated sheetfloods was replaced by sedimentation from fine-rich, suspension-dominated hyperconcentrated flows. This study thus adds a possible criterion to enhance stratigraphic

facies predictivity in alluvial fans and along subaerial basin margins, showing that the catchment geology can be intimately linked to the nature and even to the distribution of processes and deposits. Wheras classical studies of alluvial-fan successions attributed coarsening or fining 'megasequences' to palaeotectonic control, it is evident that alternative hypotheses could consider local climate and catchment lithologies as likely sources for the stacking of different sediments in aggrading fan bodies.

A combined sedimentological-taphonomic study is the object of **chapter 6**. The Collecurti bonebed comprises an unusual accumulation of Pleistocene fossil vertebrates along the eastern tectonic margin of the intermontane Colfiorito Basin (central Apennines, Italy). This fossil assemblage played a significant role for paleontologists and Quaternary scientists to unravel the climatic deterioration and faunistic turnover of the Middle Pleistocene in the Mediterranean region. The succession comprising the bonebed consists of shallow-lacustrine muds and organic-rich interbeds. Detailed sedimentological analysis reveals that the exact mechanism of deposition for the fossil assemblage was related to the emplacement of a debrisflow sourced from the adjacent highlands. The areal distribution of fossil specimens closely recalls the spatial flow organization of a cohesive mass flow, with coarse clast segregation into lateral levees and a frontal snout. The largest bone elements and partly disarticulated carcasses thus behaved as sedimentary particles, and their position and orientation in the excavated area are better explained (and most important, predicted) applying basic insights from physical sedimentology.
The classical interpretation of this fossil concentration relied on the permanence of a low-energy lacustrine environment where carcasses lied protected from large scavengers and physical disturbance (Ficcarelli *et al*., 1997; Coltorti *et al*., 1998), in line with general biostratinomic and taphonomic models. The evidence from this study demonstrates that the bonebed is actually related to a high-energy, infrequent process of resedimentation which supplied specimens from the nearby highland, and entrained several carcasses that were already lying in place at the margins of a standing waterbody. All animal remains were instantly buried within a clay-rich plug, enhancing their preservation. This has important implications for the paleontological analysis of the faunistic association and for its validation as a palaeoclimatic indicator, since instant mass-flow deposition prevented the effects of time averaging and granted unbiased preservation of the entire assemblage.

7.2 CONCLUSIONS

A common thread in the results of each chapter is the apparently inescapable influence of basement and catchment geology on the dynamics of alluvial fans and subaerial slope systems. Although an initial emphasis was given to climatic inferences in the research goals, field observations constantly brought forward the realization that whatever happened in these depositional settings was mediated by the input signal of clastic sources, on process to system scales. The alluvial fan studied in the Teruel Basin offered an excellent opportunity to explore hypotheses on allogenic controls, thanks to extensive 3D exposures and the partial preservation of a complete lithological suite from the adjacent basin margin. As discussed in chapters 2 and 3, this semiarid area is close to hydrological and geomorphic thresholds which make it very sensitive

to environmental changes forced by climate fluctuations. The effects of long-term, Milankovitch-scale climate change are especially evident in the stratigraphic records of several localities within the same basin and other basins in the region. The recurrent facies relationships between distal-fan deposits and cycles of the Prado Section show that a climate signal is recognizable also in process patterns of fan deposition, and by inference also in the geomorphic and hydrological dynamics of the original highland catchment.

However, zooming out from detailed facies relationships with the Prado Section to the scale of the whole depositional system, an overriding control appears to have been exerted by the geology of the basin margin. Comparing the evidence from chapters 3 and 5, it appears that as long as sediment sources lied in Cretaceous carbonate formations, characterized by a relative lithological uniformity, no significant diversification occurred in alluvial-fan processes and especially in the resultant stratigraphy. Ephemeral sheetfloods expelled most of the catchment debris onto the fan, stacking a monotonous succession of tabular stratified conglomerates. Basement uplift and catchment incision into an underlying suite of Early-Cretaceous and Triassic mudstone-dominated rocks triggered a complete shift in sedimentation patterns. The availability of abundant mudrock sources implied a change from sheetflood-dominated to debrisflow-dominated processes, and a clear differentiation between the stratigraphic effects of low- and high-magnitude floods from the catchment, represented by thick mud-dominated packages alternating with coarse-clastic units. The latter lithological association (designated as Upper Fan Unit in chapter 5) is the one studied in its distal relationships with the Prado Section in chapter 3. This suggests that long-term climate variability, although probably occurring throughout the whole fan development, translated into a detectable sedimentological signal only when the catchment expanded to comprise a broader suite of rock sources and associated colluvial covers, characterized by distinct sediment yields and erosion thresholds.

The diversity of sedimentary processes and architectures in relation to substrate geomorphology is even more evident in the piedmont system analyzed in chapter 4. The salient points are given by the spatially heterogeneous distribution of waterlaid and aeolian deposits, influenced by the geometry of upslope relief and the exposure to dominant winds. The local geomorphic context is often quickly modifed in highland settings and potentially lost when dealing with pre-Quaternary rock records. It is clear that palaeoclimatic inferences based on colluvial deposition must be measured against the added complications of differential process distributions on, and across, slopes.

Three general conclusions are extracted from the observations reported in this thesis.

1) Various conceptual models have been proposed on the relationships between allogenic controls and the evolution of proximal depositional systems in subaerial settings. Whereas base-level changes apply more specifically in proximity of large waterbodies and along axial fluvial valleys, tectonics and climate have been the default choices for geologists to frame their observations, interpretations and predictions. Many valuable and still valid contributions have been made to the literature following either the climate or tectonic approach, although an integration between the two lines of research remains difficult, also because of different methodological perspectives and scales of analysis. However, the geomorphic and geologic nature of the substrate at basin margins plays an equally important role in driving the evolution of alluvial fans and

Figure 2 *- Incised fan channel, showing the record of recent high-magnitude events; note dimensions of transported blocks at middle outcrop (black pointer) (coastal fan near Michilla, northern Chile; P.L. de Boer for scale).*

colluvial systems. In fact, the presence and detectability of tectonic, but especially climatic signals in proximal sedimentary successions may be related to geomorphic thresholds controlled by catchment/slope lithology, hydrology and morphology. The recognition of this 'fourth player' in the field may have broader implications for our understanding of timing and rates of sediment supply to continental basins.

2) Irrespective of whether or not we can identify dominant allogenic controls on sedimentation along certain piedmont tracts, it is quite evident that depositional systems in proximal continental settings present a strong individuality. Their fundamental dependence on very local geologic and geomorphic context (at scales of a few square kilometres or even less) makes these systems difficult to generalize under broadly applicable stratigraphic models. The apparent impossibility to derive a general 'theory of alluvial fans' (Lecce, 1990) after several decades of research is most likely tied to the spatial and genetic variability of such systems at small geographic scales. This obviously poses a big challenge to predictive approaches. Nonetheless, rather than an obstacle to further advances in the field, this realization can be considered fundamental to formulate and assess new research strategies for the future.

3) Depending on the geologic context, sedimentary systems along basin margins can represent valuable repositories for ore resources, significant elements of petroleum systems, aquifers or aquicludes of local to regional importance, very hazardous locations for settlements and infrastructure (Fig. 1), and beautiful

natural landscapes for recreational activities. Although an understanding of their geomorphology and stratigraphy has value in and of itself, it is crucial for prediction of surface processes and of subsurface geology. Of all the possible factors controlling the dynamics of slope systems and alluvial fans, piedmont geology and geomorphology are the most easily observable and measurable in present-day, active settings. Engineers and geomorphologists have long tried to refine their knowledge and parameterization of catchments in order to predict geohazard. The long-term perspective (on decadal to centennial time scales) can be offered by sedimentological analysis of local stratigraphic records, where available (Fig. 2). In terms of larger-scale stratigraphic prediction, however, such as in exploration for economic resources, a modest knowledge of 'basement' geology and an approximate palaeoclimate context might go a long way to inform reasonable expectations on what deposits could be encountered along the marginal basin domain in exploration. The necessary tools for a preliminary assessment of this kind (some geological maps, scientific literature and a quiet place to read it all through) will be much cheaper than a geophysical exploration campaign.

REFERENCES

Anderson, D.S. and **Cross, T.A.** (2001) Large-scale cycle architecture in continental strata, Hornelen Basin (Devonian), Norway. *Journal of Sedimentary Research*, **71**, 255-271.

Anderton, R. (1985) Clastic facies models and facies analysis. In: *Sedimentology: Recent Developments and Applied Aspects* (Eds. P.J. Brenchley and B.P.J. Williams), pp. 31-47, Blackwell Scientific Publications, Oxford.

Bridge, J.S. (1993) Description and interpretation of fluvial deposits: a critical perspective. *Sedimentology*, **40**, 801-810.

Coltorti, M., Albianelli, A., Bertini, A., Ficcarelli, G., Laurenzi, M.A., Napoleone, G. and **Torre, D.** (1998) The Colle Curti mammal site in the Colfiorito area (Umbria-Marchean Apennine, Italy): geomorphology, stratigraphy, paleomagnetism and palynology. *Quaternary International*, **47/48**, 107-116.

Ficcarelli, G., Abbazzi, L., Albianelli, A., Bertini, A., Coltorti, M., Magnatti, M., Masini, F., Mazza, P., Mezzabotta, C., Napoleone, G., Rook, L., Rustioni, M. and **Torre, D.** (1997) Cesi, an early Middle Pleistocene site in the Colfiorito Basin (Umbro-Marchean Apennine), central Italy. *Journal of Quaternary Science*, **12**, 507-518.

Lecce, S.A. (1990) The Alluvial Fan Problem. In: *Alluvial Fans: A Field Approach* (Eds. A.H. Rachocki and M. Church), pp. 3-24, John Wiley & Sons, New York.

Mack, G.H. and **Leeder, M.R.** (1999) Climatic and tectonic controls on alluvial-fan and axial-fluvial sedimentation in the Plio-Pleistocene Palomas half graben, southern Rio Grande rift. *Journal of Sedimentary Research*, **69**, 635-652.

Miall, A.D. (1995) Description and interpretation of fluvial deposits: a critical perspective – Discussion. *Sedimentology*, **42**, 379-384.

Miall, A.D. (1999) In defense of facies classifications and models. *Journal of Sedimentary Research*, **69**, 2-5.

Mutti, E., Tinterri, R., Remacha, E., Mavilla, N., Angella, S. and **Fava, L.** (1999) *An Introduction to the Analysis of Ancient Turbidite Basins from an Outcrop Perspective*. AAPG Course Note Series, 39.

Nichols, G.J. (2004) Sedimentation and base level in an endorheic basin: the early Miocene of the Ebro Basin, Spain. *Boletín Geologico y Minero*, **115**, 427-438.

Waters, J.V., Jones, S.J. and **Armstrong, H.A.** (2010) Climatic controls on late Pleistocene alluvial fans, Cyprus. *Geomorphology*, **115**, 228-251.

Samenvatting

Gebergten staan bloot aan geleidelijke erosie door fysische en chemische processen. Water en wind, zwaartekracht en de activiteit van gletsjers spelen daarbij een rol. Het gesteente wordt geleidelijk afgebroken. Daarbij worden in de loop van de tijd grote hoeveelheden los gesteente geproduceerd. Dat noemen we '*sediment*'. Sediment varieert in grootte van microscopisch kleine kleideeltjes tot zand en grind zoals we dat tegenkomen op het strand en in droge rivierbeddingen. Deze sedimenten worden voortdurend getransporteerd naar laag gelegen gebieden, door water en door de zwaartekracht, en in droge gebieden in belangrijke mate ook door de wind. Het sediment wordt afgezet tot op grote afstanden. Vaak is dat de zeebodem, die in het algemeen wordt gekenmerkt door een relatief lage energie.

Voor veel sediment duurt de reis naar zee of naar de laagste delen van sedimentaire bekkens op het continent lang, vaak vele miljoenen jaren. Op (geologisch) kortere tijdschalen wordt een deel van het grovere sediment tijdelijk dicht bij de gebergten opgeslagen. Daar kan het de hellingen van het gebergte bedekken als '*colluvium*' of het vormt puinwaaiers (of '*alluvial fans*') met veel grof sediment, die uitbouwen vanaf het gebergte. Aangezien complete dorpen en steden op dergelijke puinwaaiers zijn gebouwd en omdat er water en bouwmaterialen uit kunnen worden gewonnen, is het belangrijk te begrijpen hoe dergelijke accumulaties van sediment worden gevormd en hoe ze zich gedragen. Catastrofale gebeurtenissen zoals aardverschuivingen en modderstromen zijn de natuurlijke processen waardoor puinwaaiers worden opgebouwd en daarmee vormen ze ook een risico voor grote rampen wanneer mensen in dergelijke gebieden wonen.

Fossiele equivalenten van puinwaaiers, begraven in de ondergrond en verhard tot '*sedimentaire gesteenten*', zoals zandsteen en conglomeraat, kunnen grote hoeveelheden water, olie en gas herbergen, die wij nodig hebben voor onze moderne maatschappij. Het kennen en herkennen van de interne organisatie van puinwaaiers is van essentieel belang om op de goede plaatsen boringen te doen voor de winning van water, olie en gas uit soortgelijke systemen die miljoenen jaren geleden zijn gevormd en nu diep in de ondergrond zijn begraven.

Het onderzoek dat in dit proefschrift wordt beschreven gaat over voorbeelden van colluvium en puinwaaiers en de wijze waarop we de processen die tot hun vorming leiden

kunnen begrijpen. De eigenschappen van fossiele systemen worden gedeeltelijk bepaald door veranderingen van het klimaat in het verre verleden, aangezien klimaat van invloed is op de hoeveelheid neerslag en daarmee de vegetatie en ook bepalend is voor de verdeling van neerslag over het jaar en voor het optreden van extreme regenval. Het laatste is gewoonlijk de belangrijkste oorzaak van het optreden van aardverschuivingen en modderstromen.

Daarnaast bepaalt het soort gesteente in het gebergte van waaruit het sediment wordt aangevoerd de aard van het sediment, bijvoorbeeld modder of zeer grof materiaal. Verschillende soorten sediment die over de helling van puinwaaiers worden getransporteerd gedragen zich op geheel verschillende wijze. Des te beter we dit begrijpen, des te beter kunnen we voorspellen wat het risico is van natuurrampen en ook hoe de ruimtelijke verdeling van verschillende gesteente soorten in de ondergrond is om daar onze grondstoffen uit te kunnen winnen.

Riassunto

Tutte le forme di rilievo della superficie terrestre sono soggette a graduale erosione ad opera di svariati processi fisici e chimici, innescati per esempio dagli agenti atmosferici, da acque di scorrimento superficiale e di infiltrazione, dai ghiacciai, o direttamente per instabilitá dovuta alla forza di gravitá. Via via che i rilievi rocciosi vengono progressivamente distrutti, si creano grandi volumi di detrito che chiamiamo '*sedimenti*'. Questi materiali variano in dimensioni dalle finissime particelle argillose che costituiscono il fango, su fino alle piú grossolane sabbie e ghiaie con cui abbiamo comunemente a che fare lungo l'alveo di un torrente o durante una giornata in spiaggia. Questi sedimenti sono continuamente in trasporto attivo o latente verso ambienti topograficamente ribassati (e perció a minore energia potenziale) da parte di acqua, vento in regioni particolarmente aride, o per azione diretta della gravitá. Le dsetinazioni finali di questo trasporto possono trovarsi anche a distanze molto grandi dalle aree di origine. In principio, i collettori terminali per la maggiorparte di questo materiale sono rappresentati dai fondali marini, che costituiscono gli elementi topograficamente piú ribassati della superficie terrestre e sono spesso caratterizzati da condizioni ambientali di relativamente bassa energia.

Comunque, il viaggio verso i mari o verso i piú grandi bacini continentali puó essere molto lungo per la maggiorparte del detrito, comunemente nell'ordine di molti milioni di anni. Per intervalli temporali piú brevi (alla scale dei tempi geologici!), parte del detrito piú grossolano, come le ghiaie, viene temporaneamente accumulata nelle vicinanze dei rilievi originari, dove puó ricoprire i versanti (formando depositi che chiamiamo '*colluvio*') o formare estese rampe inclinate di detrito sciolto che si accrescono a distanza dai margini montuosi (e che chiamiamo '*conoidi alluvionali*' o piú semplicemente '*conoidi*'). Comprendere la genesi, le caratteristiche e la dinamica di questi vasti accumuli di sabbia e ghiaia é molto importante perché la gente tende a costruire interi villaggi e cittá su di essi, e ad estrarne risorse come acqua e materiali da costruzione. Violenti eventi che mobilizzano grandi quantitá di sedimenti, come frane e colate di fango, fanno parte dei processi piú tipici di questi ambienti ad alta energia, ma rappresentano anche grandi rischi potenziali per le popolazioni che li colonizzano.

Inoltre, gli antichi equivalenti di queste forme di rilievo, oggi sepolti nel sottosuolo profondo e trasformati in roccia ('*roccia sedimentaria*', come le arenarie e i conglomerati) possono contenere elevati volumi di olio e gas necessari per il sostentamento delle nostre frenetiche attivitá quotidiane e per il nostro lussuoso stile di vita. Una conoscenza dell'organizzazione interna dei sistemi attuali e della distribuzione spaziale dei sedimenti in essi é fondamentale per predire dove perforare per l'estrazione di fluidi in sistemi analoghi formatisi molti milioni di anni fa, oggi sepolti in profonditá.

Le ricerche qui discusse presentano alcuni esempi di come possiamo interpretare i processi di formazione per colluvi e conoidi sia moderni che antichi, studiando i loro depositi. Le caratteristiche di questi sistemi sedimentari sono state in parte controllate da antichi cambiamenti climatici; il clima determina la quantitá di precipitazioni e la vegetazione in una data regione, o la stagionalitá e il verificarsi di eventi meteorologici estremi, che sono solitamente il principale fattore scatenante di frane, colate di fango e alluvioni. Ad ogni modo, i tipi di roccia nel substrato montuoso da cui questi sistemi si formano esercitano un controllo altrettanto importante sul genere di sedimenti disponibili (as esempio, fanghi finissimi, o materiale ghiaioso molto grossolano). Una volta in movimento sulla superficie, diversi tipi di sedimento assumono proprietá dinamiche differenti e danno luogo a processi ben distinti. Quanto meglio siamo in grado di comprendere queste complesse associazioni di processi superficiali e i relativi controlli geologici e climatici, tanto meglio potremo predire il verificarsi di eventi potenzialmente disastrosi in ambienti attuali, o predire la natura e distribuzione di rocce da cui estraiamo le nostre risorse.

Something more than just…

…Acknowledgements

Doing science is a thing, but gaining your PhD is a completely different story… That (and more) should be made clear at the outset to all those venturesome enough to embark upon such a project for several years. No general advice exists, I guess, because the people, the places, the situations, the goals, and the sheer amount of nerdness it takes to get through this, all differ from case to case… One thing is clear though. You don't get to do it by yourself, forget about it. Science as a lonesome enterprise started and stopped with Newton, or maybe one of his contemporaries. Once this cultural machine was set into full motion, it became a very social thing. And luckily so, because rocks are fun, but the real fun is only when you deal with other geofolks to make something interesting out of it all. Whether you're right or wrong always matters, but what matters more is that at least you gained some very personal, inner reward from what you've done. If you didn't, then you were in the wrong place, and you shouldn't have been doing science…

And so it was that the first time I was in Teruel with **Poppe**, back when we were exploring for some more alluvial fans to study within and outside the basin, we really couldn't find any in the end, but we had lots of fun through freak Spanish snowstorms, driving down thickly wooded slopes because the main road should have been somewhere down there (but it never was…), and drinking coffee in forlorn villages. Me, actually, a coke… I should truly keep it to myself, but this is the right point to let him know I called him 'Ome Poppe' all these years, because he's been the wise old friend behind all my work, more than a supervisor. Thanks, for the fun trips to the other end of the world, and especially for the seriously endless patience, 'cause I know I'm a little(!) eigenwijs, but somehow you made it work out.

However I am not yet entirely convinced of this thing of the 'English teacher and the teacher of English'!

Frits once sent me an e-mail, while I was starting six oily months at Shell, asking me to drive along with one Hemmo (about whom more later…) to some obscure place in Spain. I think that was March or April 2004. No thanks, got to leave to Assen now, was my answer… Maybe another time? Well, thanks to Frits for still remembering about 'another time' after a few months, because that's how the adventure started. I owe you a big apology, because I know you intended for this to become one more Milankovitch-centered project, and instead you tripped into someone who was all into catastrophic sediment transport and comparative facies analysis. Thanks for showing me what it really takes to go that extra mile in the field and in teaching… (But next time we warn you about 'the bastards', do wear longer pants!)

Oh yes, then there's **Hemmo** (**aka** '**Mootje**'), the tallest stratigrapher around. As geology had it, every time together each one of us wanted to spend time and energy exactly at the opposite sedimentological ends of the basin, in the muds him, in the coarse stuff me ('…die troep.'). Distant in facies, but united in the eternal war against 'the bastards', we always agreed on the patatas bravas, jamon y queso y costillas del diablo that prepared us for the day after. **Hayfaa** shared our muddy, fly-ridden, ham-fed destinies with stoical resolution during the first year, and being the one with the most experience, knew to allay my initial fears in the face of endless calcretes and sandy silty claystones… (Or clayey siltstones… Or whatever…) Thanks guys for the company in the field!

Once back to the office, good ol' **Maurits** (**aka** '**Maukje**'), the dutchest Dutchman in Dutchland, provided the right mix of music and company, as well as intriguing examples of Dutch lexicon during his animated fights with the computer. In case of need, you always knew there was plenty of food in his drawers (although you couldn't exactly tell how old it was…), precious advice about anything Dutch I hadn't yet learned, and plenty of tolerance for the inordinate amounts of kwark I introduced into the room. Unfortunately we never got to do much fieldwork together, but thanks for loads of fun during our geotraverse of Canada, our first exploration of Chile and the many Belgian trips, 'cause those were the best!

Matthieu (**aka** '**die Matthieu**') is an engineer, but that's not his fault… He calculates, builds, repairs, measures, and other complicated stuff that geologists usually won't do. When he arrived he couldn't tell a feldspar from a radiolarian. Mind you, he probably still can't… And yet, out of nothing, little by little, a great sedimentologist was born! Thanks for your questions, as they always made me see things from interesting new perspectives, for the many pizzas during which 'the long paper' quickly faded in the background of assorted nonsense (think of it, that paper has been 'almost finished' for about five months now… we have redefined 'almost'!), but especially for countless breaks on 'the bench', accompanied by some wisdom (let's face it, rarely) and lots of laughs (plenty of those).

João Trabucho Alexandre Coutiño Fonseca Medeiros da Silva quinto (**aka as just João**) is the most talkative Portuguese I ever got to know, and that'll undoubtedly stay so even if I ever were to move to Portugal. His encyclopaedic knowledge about <u>everything</u> is second only to his uncanny ability to use it on any occasion, in any language, and probably also talking backwards (although we didn't test this option yet…), for the force is strong in him. The obvious advantage is that once you're fed up with sedimentology for the day, the guy provides unlimited possibilities for animated discourse on topics ranging from avionics (no kidding, just try him…) to politics in eastern Europe! Thanks for the incessant entertainment and for sharing our southern-Europeanness in a life suddenly turned Dutch.

Germari is no longer very convincing as a South African after the 1249 times she exclaimed 'Cacchio!' in the field with a faultless northern Italian accent, probably gained from her famous husband Filippo (of whose family I now know nearly everything!). She combines an odd propensity for all things Martian with a predictable obsession for early-morning rugby on television, a rare mix that makes for unusual dinner talks. Thanks for providing me with another excuse for fieldwork in the Atacama, and for putting up with my sedimentological overconfidence sometimes… (And of course, for those birthday cookies!)

Joris used to be a hard-working student when I arrived here, and is now bravely running the Eurotank from project to project, working even harder than before. After weeks of exhausting fieldwork and teaching, he usually leaving the damp Netherlands to dedicate himself to sun-bathed pastimes in tropical resorts, such as camping in Norway, running in Scotland and hiking in Wales. But only when it rains… Thanks for the razor-sharp humour (when you're not overwhelmed…), the cynical jokes, and the mutual support when we got stranded eight days in Houston because of the stupid volcano. We made it man, we're out of the Marriott Hotel! ("Please hold on to the handrails…")

Given his characteristic English demeanour, it was to be expected that **Henk Kombrink** would some day make his move to Great Britain. In spite of an inexplicable nostalgia for Carboniferous times, his friendly humour has always stayed very much in the present. The first days teaching for the 3rd-year course on the North Sea would have been an unmitigated disaster without his assistance and dedication: thanks for letting it work a lot better…

Frank was somebody who should have originally belonged to room N308, but wisely knew to stay out of it, since geology (he claims while driving minicars along sun-scorched roads in Spain…) is not the most important thing after all. And there might be some truth in it. But offer him some fieldwork in the coal measures of Pennsylvania, and he's out there in no time… Thanks for a memorable trip to the amazing outcrops at the margins of the Ebro Basin!

George Postma is the only one who survived a 'Discussion & Reply' with my favourite author, the fearful Terence Blair, and even ended up being right. The guy obviously means business… Enthusiastic in class and skillful in the field, he's always sailing offshore in the North Sea when you look for him, only to pop up at lunchtime when you were just about to give up. He provided unsolicited inspiration, sedimentological reassurance at times, abundant food for thought at others, and stupendous amounts of student practicals to correct each year, for all of which I'm grateful (builds experience…), as well as the nickname 'the crazy Italian', about which by now you might agree with him…

Jan van Dam (**aka** '**Jantjevandampje**') is an adventurous palaeontologist with a keen passion for music, and an even more serious interest for the astronomically controlled variation of oxygen isotopic compositions in mammalian teeth

(about which he luckily doesn't talk at dinner). His knowledge of Spanish geology made me discover some great new outcrops, and his social network in Teruel has earned me a few hundred croquetas caseras (prepared by his trusted friend **Alberto**, who by now has generously fed a lot of Utrecht geologists!). Thanks a lot for your generous help in those long days sampling for the magstrat, for natafelen in the evenings, and because you always bring good mood…

By the way, about that magstrat… Turns out, if you want to do cyclostratigraphy you also have to do magnetostratigraphy. It's a dirty job (and very literally so), made possible only through the advice of a group of world-class professionals that are kept locked in Fort Hoofddijk to prevent them from drilling holes into pretty much anything they spot. Thanks to the sapient **Mark Dekkers** for guiding me through the whole procedure of preparing and measuring samples; to the amazing **Tom Mullender**, whose unlimited technical genius (a mild understatement…) made it possible to repair any software or hardware malfunction within no time, and build machines that can do most of the work for you (but obviously didn't do it for me…); to the cheerful **Wout Krijgsman**, who finally told me, with the seasoned smile of one who has seen it all too often, that a couple of months of field and lab work were completely worthless; and to the perennially smiling **Arjan**, the resourceful **Maud,** and last but not least Silja Huesing for teaching me pretty much anything that the others couldn't. (Including that next time I need magstrat I'd better ask somebody else! Saves trouble…)

Silja (**aka** '**Silly**'), like so many other Germans born in New Zealand, is an insatiable globe-trotter, a convinced vegetarian and a fine expert of anything regarding bunnies (but most regrettably not of good ways to cook them). She's recently become the mother of a cute little boy that she'll raise with the help of her world-wise husband **Phil** (**aka** '**Mr Phil**') and of course of **Ina**, the fat bunny with black shorts! Thanks for being friends since the very first day we set foot in this department, back when we knew all about the Newark Basin…

Peter (**aka** '**Pietje**' or '**the bastard**') (the second option strictly reserved only to people from room N308) has been one of my best friends since short after I arrived in Utrecht. I think I learned more about Dutch habits and ways of thinking from him than anybody else before or after, although I guess he really just wanted to get some greasy pizzas and watch movies and football matches together on a sagging couch, without particular intercultural ambitions. In return, I showed him how to bake the best home-made Italian pizzas, for which he keeps thanking me all the time (admit it, you do…). A hard worker and severe perfectionist (at times too much, but hey, that's Dutch too), he's now rebuilding his new home, where I hope a new couch will appear for more sagging into it…

Aart Peter (**aka** '**AP**') is the guy who used to sit at my place before I took over in room N308. I always thought he was tailor-made for an academic career in sedimentary geology, but then he moved to the oil industry and became a geophysicist (although he will loudly deny that!) and rich, so there you go… His passion for science, South Park, the Happy Tree Friends and weird music made for real fun dinner talk, until he decided to leave to Germany for even more geophysics, so there you go again… In the hope he'll some day return to the Netherlands and stop eating quiche, I expect him for more dinners and nonsensical wisdom!

And of course no day goes by in the northern wing of the third floor without the pleasantly chaotic, multilingual chit-chat of the famous 'Strat-Pal people'. Somehow I was always too busy writing something or reading something else to get to know them better, but they don't know it's fun to feel them all around. If our rooms were trees, they would be the birds… (Of course I am the bear sleeping underneath!). You knew that **Lucy** was in every morning because of her unmistakable laugh; she provided me with daily updates on weather, traffic and the state of public transport. **Kees** showed me what happens to you during the last year of your Phd, but I was fooled by his unflagging cool temper into believing it'd be much easier. The guy has got character! The other wonder-boy of cyclostratigraphy, **Luc** never knew that his providential scanner saved my day right before leaving to Chile, when I suddenly realized the last figures had to be made with old photos on paper! **Christian** makes his own bread and knows everything about Kazakhstan, and is

getting a bit edgy about his deadline: well, by how hard I see you working, you'll obviously make it... I learned more about **Mariëtte** when she asked me to write holiday sentences for an Italian journey; her encouragement towards the end, in May, has helped in the couple of months that followed more than I ever told her (so I am actually telling you now!). **Albert** has always been generous with his anecdotes about past fieldwork in Italy and greeted me with an impeccable 'Buongiorno!' in the hallways every morning... Thanks also to **Martin**, **Karoliina**, **Ivo**, **Anja**, **Erik** (and his old scanner), **Wilma**, **Hans** and **Willem-Jan** for the atmosphere, the smiles and an Easter lunch together when inexplicably the Paashaas hopped onto my leg... (It's caught on photo!)

Over these years more people quickly visited our research group than I can probably remember. My thanks go to **Sebastien Rohais**, the quiet Frenchman of the big fan deltas, who wanted to numerically model everything I saw in the field, and he might be relieved to know that now I finally have time to do it! And to the volcanic **Daniel Mikes**, who started from the microscopic processes of flocculation and zoomed out to describe sequence stratigraphy in the complicated language of logic... And **Manuela Chamizo Borreguero** (**aka 'Manolita'**), who just couldn't get used to Dutch lunch times (me neither, for that matter...) and has been a fun companion on geotrips from Belgium to Argentina. And to **Juan Pedro Rodríguez-López** (**aka 'Juampe'** or **'el eolianero'**), who taught the whole of geological Spain that talking about Mesozoic ergs in the middle of Iberia was not just, well, wind, and is the next promise of aeolian sedimentology. And **Erin Kraal**, the Texan geomorphologist (and mam, not to forget) who magically appeared at my door one morning, on a late November, to propose we go to the Atacama Desert and check out alluvial fans there (and I truly did since then!). And to **Jochem Bijkerk**, who as a student often asked those annoyingly difficult questions that suggested he had talent, and is now coming all the way from Leeds to be the last one in a series of brave strugglers with the Eurotank! (Thanks for pdf's, by the way...)

Several people from our sister Faculty of Geography ('the other side') have provided company and different perspectives on geology during my visits to their building and especially during a few conferences and a memorable geotrip to northern Germany. My salute goes to **Esther Stouthamer**, **Kim Cohen**, **Freek Busschers**, **Sanneke van Asselen**, **Marc Hijma, Maarten Kleinhans** and **Wytze van de Lageweg**, the first one to actually introduce gardening to the Eurotank! (He is actually spending more time 'on this side' now, with us...).

Thanks also to **Jacqueline Landsheer**, who deals with my administrative incompetence with smiling efficiency; to **Ton Zalm**, master of labs, whose grain-size measurements of aeolian sands from Chile made it all clear; to **Henk van der Meer**, who's actually taking care more of my other colleagues, but brings abundant gezelligheid in the process; to **Maarten Zeylmans van Emmickhoven**, resourceful GIS advisor; to **Theo van Zessen** and **Mark van Alphen**, who promptly dealt with digital crises; and to **Roy** (**aka 'Opa'**) and **Ronald**, without whom the whole building would have collapsed into chaos. Special acknowledgements to the omniscience of **Kabir Roy Chowdury**, the only seismologist who can confidently discuss biology, sociology, psychology, philosophy; and to the patiently analytical **Paul Meijer**, who promptly helped to find the actual physical meaning in a bundle of fundamental (at least, they were for me...) differential equations.

Last, but very much not least, my particular gratitude goes to our superefficient team of librarians, who make it possible to obtain vital information in spite of all the obstacles, limitations and restrictions that the administration recently poses to them. **Anne van Weerden** (who's actually a quantum physicist and cosmologist disguised as a librarian), **Jan Jansen** (who regularly knew what I needed and where it was before I even entered the library... talk about a professional!), **Lidy Jansen**, **Wim van Hattem** and **Jeroen Bosman** provided quick assistance with any requests, whether digital or paper-bound, and found pretty much anything I looked for. All the more reason to come up soon with even more difficult requests...

Outside the university tribe, a completely different bunch of people kept me entertained, fed, sane, occasionally insane, and generally happy. However, the transition from geologists to non-geologists is best made gradual starting with the hyperactive **Andrea** (**aka 'Ingegnere'**). Alluvial fans were the reason why we got to know each other on a sleepy conference afternoon in Delft, and the fun of being Italians together was simply the reason why it turned into a solid friendship, leaving real geology very far behind. Through innumerable messy dinners and long discussions with plenty of humour and no meaning at all, accompanied by his enthusiastic, noisy, unpredictable wife **Fiammetta** (if I had a nickname for you it would still not be of the kind allowed on a PhD thesis…), somehow they adopted me as what in Italy is called 'il terzo incomodo', and Holland is a lot emptier now that they've left. Thanks for academic advice, for the bed on the second floor, for the couch on the first floor, for the kitchen at the ground floor, for the laughs and the madness, and especially for making me realize it's so much cooler to be a sedimentologist than a metamorphic geologist!

Michele (**aka 'Panza'**) and I have been friends since much longer ago, when we spent summers in the same village in southern Italy. He used to be a world-acclaimed expert of something obscure called *Semantic Web*, back when he studied in Delft, but has now moved to a promising, rampant career in a mysterious profession called 'o'managgerre', and more notably as a father, supported by **Carmensita**, a brave girl of typically Irish looks and Spanish name (but actually Calabrian descent…) who follows him everywhere to make sure he doesn't get into trouble. Their presence in Holland provides me with a taste of my past, but happily for me not only they also belong to my present.

Nicole (**aka 'Cooltje'**) has been my faithful shoulder and virtual sister for years now. Accompanied by her psychologically complex cats, **Shakira** and **Olivier**, and occasionally by her sisters **Hellen** and **Ingrid** and her adventurous nephew **Louis** (**aka 'Louitje'**), she has provided listening ears, warm meals (best kippetje ever…), sunny trips to the Posbank, Sanadome, Rijkerswoerd, a lot of adventure on the road with the ANWB, and a robust dose of interminable discussions between a scientist and an alternative philosopher! We never managed to establish who was right and who was wrong in those discussions, but I hope we both gained something in the process, if nothing else an even closer friendship… And I catch the occasion here to thank **Rinie and Silvia** for their hospitality in Oss and a serious lot of food on every occasion!

Birgit (**aka 'Dautzie'**, or **'Lei'** for the Italians) was my first smily introduction to the reality of life in Utrecht in the old days when I never even suspected to come and live here for real! She offered me a place to stay during my holidays in the 90's and in my first two months in Utrecht when I came to change my fortunes, although it turned out we could see each other more often when we lived in different countries than when we lived under the same roof… (Now, how's that?) I am grateful for the many times she would have killed me, but didn't, and for being still there, after all these years, a firm reference point, inoxidable as the good old Acaciastraat where I once arrived on bike, and that still represents my first mental image if anybody mention Holland to me…

Thanks also to **Maarten**, **Martijn** and **Richard** for company at the gym! To the inarrestable **Jeanet** (**aka 'J'**), who just can't stop running, for sharing my greed for books and for our distant friendship that doesn't break in spite of sometimes almost years passing by without seeing each other. To **Margot** (**aga 'Go'**) for her patience through the years in listening to all my geology stuff while I was munching on double uitsmijters, when she actually would have preferred to illuminate me about art critique and other humanistic disciplines more sophisticated than just plain rocks! And **Elisa** (**aka 'la Contessa Guasti'**), who makes the best pesto you can find to the north of the Alps! And to **Ruben**, best landlord ever and consummate philosopher of the quiet life on the garden-side of the Adelaarstraat, who knows to keep everything in working order while we still try to mess it up for him on a daily basis…

Down south, where the sun doesn't shine as often as the Dutchies seem to believe, my old friends and family have been and are the reason why I can enjoy my life today as it is. The people you grow up with and that somehow make you who you are. Would be too long to celebrate them as they deserve, so that I'll keep for back in Florence when we spend time

in our own way... That's the only proper way to do it. **Niccoló** (**aka 'Nicco'**) grew up with me from middle school to high school to university to Africa to Holland to wherever else we'll happen to go together. His letter convinced me to kiss chemistry goodbye and go back to the old idea of studying geology... So he's the guy to blame for all that happened afterwards! He still can't find the Pratomagno after all these years, but we know to find each other with one look in a crowd, and that's what counts... We met **Christian** (**aka 'Pupo'**) when he was still a baby during the second year at Earth Science in Florence, and since then he has grown up a lot, but always with us. Were it not for his resolute wife **Nathaly** (**aka 'Nathyda'**) he'd have been through a lot more trouble than just working until three a.m. every night! I can recommend his guidance in learning Adobe Illustrator, you won't regret... **Simona** (**aka 'Ciuffy'**) has become an expert in seismology and geothermics and works all around the world nowadays, but always looking forward to get back home soon because, well, just ask her... When not holidaying at her office, she'll preferably be on Elba, the biggest island offshore Tuscany, together with her **Marco** (**aka 'Ca'**), who will be easier to find somewhere at hypoabyssal depths than on the beach... Together with **Samuele** (**aka 'Zio Samu'**), **Donata** (**aka 'Onorevole Bianchi'**), **Filippo** (**aka 'lo Sborci'**), **Rocco** (**aka 'Rokko'**) (...vediamo di darli questi esami!) and **Lucia** (alla quale colgo l'occasione per porgere, come sempre, i miei piú cordiali saluti...), these people form a solid core of generally deranged but trusted individuals that make for fun dinners and much more. That's not supposed to be important to you, but luckily it's been important to me throughout all these years, and that's no small thing.

Roberto (**aka 'Fatilla'**) drove me and an undetermined amount of books to the north one summer night when life turned, from Italian, Dutch. From elementary school to the years of 'the gym', we still find each other and retain the bond of those who learned to write together back then, and have done too much to write about it today. He still dreams of settling in California some day, but secretly I hope his new girlfriend will take that out of his mind, because we still need to see more years together, if only when he gets a free day!

Thanks to my old high-school mates, **Alberto** (**aka 'l'Ortolani'**), **Lucia** (**aka 'Lucilla'**), **Chiara** and her husband **Alessio,** the chemically savant **Marco** (**aka 'Von Thany'**) and his girlfriend **Francesca**, for bringing me back to the old times every time we meet and do pretty much the very same things that we did back then, except for studying mathematics for the day after, 'cause that's apparently not needed anymore (but only apparently...). E ai ragazzi della palestra, **Filippo** (**'Filippo il bello'**), **Simone**, **Saverio** (**'il merdillone'**), **Giacomo** (**'Giacomino'**), e l'inossidabile **Panconesi**, per anni di scemenze fra le sei e le sette e mezza di mattina sollevando pesi semplicemente perche' ci piaceva. Avrei voluto in qualche modo che anche il nostro **Fabio** (**'il Maestro'**) sapesse che alla fine ce l'ho fatta a restare in Olanda, ma lui non c'é piú. And to **Paul** (**...Peter Anthony, aka ' il Mazza'**, but today you'll have to call him '**Professor Mazza**'...) and **Marco** (**'il bestia'**), once teachers of palaeontology and fieldwork instructors, nowadays friends, thanks for the memorable trips to the south, digging out bones by day and kicking up a mess by night at the mountain refuge. In you I first saw what it's like to do research because it's a part of yourself, not because of any other reasons.

Sul fronte della mia numerosa e turbolenta famiglia, tanto per fare una minima selezione, grazie per il sostegno e l'affetto a **Miacugggina** (**'Barbara'**), che ha partecipato con generoso interesse e travolgente chiacchiera (spesso io appoggio il telefono e dico sí ogni cento secondi, sappilo...) alle mie vicende olandesi sin da quando venne a trovarmi ad Assen un bel po' di tempo addietro, accompagnata dall' invincibile, imponente, bronzodiriaceo **Graziano** (**'Grasianó'**); a **Monica**, che vedo purtroppo molto meno spesso, e che un tempo, a sua insaputa, mi accese le prime curiositá per il Nord Europa con le sue descrizioni della Crande Cermania (in altre parole, é colpa tua); a **ZIO Guido**, per l'entusiastico incoraggiamento e per le animate discussioni su aspetti fra i piú coloriti della vita; e a **Christine** (**'Titine'**), che é diventata ramo belga della famiglia dopo essere sopravvissuta per anni alle vicende varie dei Ventra e degli Imparato; e ovviamente a **Zia Carla**, seconda mamma, che mi sa che alla fine non verrá, perché probabilmente ha paura di perdere

come sempre a scopa (Arriviamo a 100? Ma quando la rifacciamo?); e al buon vecchio (il 'vecchio' ce lo mette sempre lui) **Zio Alberto**, eterna presenza fiorentina, per l'arcigno affetto e le battute frequenti e taglienti...

Unexpectedly, over the last year and a half, it seems I also acquired another family in the Netherlands, and a lot of it! There's truth in saying that Brabanders enjoy life and partying and all that, 'cause this is quite a restless bunch, it's often just like being with my old family from southern Italy. **Hermine** and **Peter** (**aka** '**Ma & Pa Erken**') have opened their door to me with a warmth I did not hope on the first time, and incomprehensibly they still do so even after getting to know me better! When they're not working in their little shop, they walk and bike for hundreds of kilometres around Europe, they make movies, they study Italian, they go skiing, they go skating, they tend to the most beautiful garden, they chase wild pigs in the woods and generally can't sit still. (A habit, unfortunately, they passed to their children...) You can have lots of fun with them, but apparently you can't have meat! **Hugo & Marieke are** more or less the same, but more extreme. There are curious records of them hanging from trees in Indonesia (or was it Cambodia...), sleeping on the Himalayas of Nepal and more such exotic localities. Hugo has gained his PhD in economics by day while living the wild life of the drummer by night, so you might think the guy knows his stuff, but in fact most of this is possible because little Marieke wisely takes care of him (and soon also of a new little Erkentje... Congratulations!). And then there's the rest of the tribe, cheerful, restless people with funny names starting with **Tante (...Mech, Marjon..)** and **Ome (Geert, Hein, Syl, Kees, Jos..)**. A very few others have real names (**Monique, Matthijs, Marga, Jose...**), but it's always the tante's and the ome's that decide what goes on, especially on dangerous occasions called 'familieweekend'. Given the nature of this book, a special acknowledgement here goes to **Ome Hein**, who is a real geologist, having learned everything about the territory of his country just by exploring it in the field, by himself, seeing things that many of us have only seen in the books. I still hope he will teach me something more one day!

Olga (**aka 'loefje'**) (I am not allowed to reveal others...) is the reason why I got involved with all the ome's and tante's. She likes Alfa Romeo's, volcanoes, the Alps, olives, pasta, pizza, Rome, Sicily, Italian beaches, the Italian language, the Italian countryside, Italian cities, Italian movies, Laura Pausini (confess, you do...), and besides all that, I am not sure why, she seems to like me too. To her dismay, but much to my luck, she was born in the wrong country and so it was that I ran into her at Janskerkhof on a hot summer afternoon, in which she'd make me walk the whole city without rest (being the proud daughter of Hermine and Peter). Since then, anything I did in Holland (and a few things I did in Switzerland too) I could do thanks to her. Finishing my research would not have been possible without her patience and support. I hope one day I'll be able to do even more, and still have a chance to be thankful for her love and support.

Ai miei genitori, **Moms** e **Ciccio**, non sono mai riuscito pienamente a spiegare perché me ne dovevo assolutamente andare via dall'Italia, e perché non posso neanche pensare di tornare, almeno per ora. In questo libro possono vedere uno dei motivi che mi hanno tenuto lontano, quello forse di valore piú tangibile. Non immagino che ne capiscano i contenuti per ora (ma sono pronto a spiegare il tutto nel minimo dettaglio), ma so che sentiranno l'entusiasmo e la felicitá che tutto questo mi ha portato (in fondo, ognuno é contento a modo suo...), e che nella speranza di andare avanti in tutto ció, sono contento giá solo per aver realizzato qualcosa che sin da piccolo ritenevo fondamentale nelle mie ambizioni, ammesso che di ambizioni si potesse parlare, ma troppo distante. Perché certe cose chiamandole 'sogni' a volte diventano automaticamente lontane, inaccessibili. Ora so che lo potevo fare. Grazie anche a come mi avete cresciuto e alle possibilitá che ho avuto da voi. Probabilmente non sempre meritate, ma finalmente messe a frutto, anche se sembra solo un sacco di sabbia e ghiaia... Per questo, e per tutto quello che c'é stato prima, e per fortuna c'é ancora, grazie.

The author

Dario Ventra was born in San Paolo Belsito (Napoli) on August 6th, 1969. From a birthplace dangerously close to the pyroclastic antics of the Vesuvius, his parents brought him to Firenze, where the floods of the rivers Arno, Mugnone and Terzolle were even more frequent. There, he studied at the Liceo Scientifico Leonardo da Vinci, with too much latin and philosophy to really satisfy his childhood interest for paleontology and zoology. After a somewhat bored attempt at chemistry at the Universitá degli Studi di Firenze, he moved to study Earth science within the same university. With a resolute intention to finally make his chance into vertebrate paleontology and all things fossilized, he firmly declared, during his second year, he'd never even take a course in sedimentology... Only to find himself sitting at a course of sedimentary petrology during the third year... Grudgingly admitting to himself that there might have been something interesting about sand after all, he joined the course in sedimentology during the fourth year and it was love. An MSc thesis on the Quaternary sequence stratigraphy of Lake Shala, in the Ethiopian Rift, didn't help to prevent some turbulent years of slightly too lively social life in a Florence neighbourhood, exploration of northern and eastern Europe, and long work as a translator. After all of which, he finally graduated and moved to his beloved Holland, intending to stay. But that's when they started sending him out again to Spain and Chile... For next year, he's planning to explore monumental outcrops of ephemeral fluvial systems in the Argentinian foreland and the intricacies of hyperconcentrated sediment transport in Dutch flumes and Spanish exposures, but he's now prepared to expect the unexpected. As long as his friends and fabulous girlfriend will be with him, everything should work out just fine...

Figure 1 *- Sedimentological inclinations through time. (A) Early experiences on fine- to medium-grained, well sorted backshore sands… (summer 1970(?), southern Italy; Moms for scale is ~160 cm; photo by Ciccio); (B) …but coarse-grained deposits of proximal fluvial systems are decidedly more interesting to play with (May 2008, Teruel Basin; photo by Mootje Abels; hammer for scale is 32 cm).*

Printed by *Wöhrmann Print Service*,
Zutphen (the Netherlands)